ISSN 2307-8960 (online)

World Journal of *Clinical Cases*

World J Clin Cases 2023 April 16; 11(11): 2363-2581

Published by Baishideng Publishing Group Inc

World Journal of Clinical Cases

Contents

Thrice Monthly Volume 11 Number 11 April 16, 2023

REVIEW

MINIREVIEWS

ORIGINAL ARTICLE

Retrospective Study

Observational Study

CASE REPORT

World Journal of Clinical Cases

Thrice Monthly Volume 11 Number 11 April 16, 2023

Contents

World Journal of Clinical Cases

Thrice Monthly Volume 11 Number 11 April 16, 2023

Contents

ABOUT COVER

Editorial Board Member of *World Journal of Clinical Cases*, Farooq Shahzad, FACS, MBBS, MS, Assistant Professor, Plastic Surgery Service, Department of Surgery, Memorial Sloan-Kettering Cancer Center, New York, NY 10065, United States. fooqs@hotmail.com

AIMS AND SCOPE

The primary aim of *World Journal of Clinical Cases* (*WJCC*, *World J Clin Cases*) is to provide scholars and readers from various fields of clinical medicine with a platform to publish high-quality clinical research articles and communicate their research findings online.

WJCC mainly publishes articles reporting research results and findings obtained in the field of clinical medicine and covering a wide range of topics, including case control studies, retrospective cohort studies, retrospective studies, clinical trials studies, observational studies, prospective studies, randomized controlled trials, randomized clinical trials, systematic reviews, meta-analysis, and case reports.

INDEXING/ABSTRACTING

The *WJCC* is now abstracted and indexed in Science Citation Index Expanded (SCIE, also known as SciSearch®), Journal Citation Reports/Science Edition, Current Contents®/Clinical Medicine, PubMed, PubMed Central, Scopus, Reference Citation Analysis, China National Knowledge Infrastructure, China Science and Technology Journal Database, and Superstar Journals Database. The 2022 Edition of Journal Citation Reports® cites the 2021 impact factor (IF) for *WJCC* as 1.534; IF without journal self cites: 1.491; 5-year IF: 1.599; Journal Citation Indicator: 0.28; Ranking: 135 among 172 journals in medicine, general and internal; and Quartile category: Q4. The *WJCC*'s CiteScore for 2021 is 1.2 and Scopus CiteScore rank 2021: General Medicine is 443/826.

RESPONSIBLE EDITORS FOR THIS ISSUE

NAME OF JOURNAL
World Journal of Clinical Cases

ISSN
ISSN 2307-8960 (online)

LAUNCH DATE
April 16, 2013

FREQUENCY
Thrice Monthly

PUBLICATION DATE
April 16, 2023

World Journal of Clinical Cases

Submit a Manuscript: https://www.f6publishing.com

World J Clin Cases 2023 April 16; 11(11): 2363-2373

DOI: 10.12998/wjcc.v11.i11.2363

ISSN 2307-8960 (online)

REVIEW

Presbyphagia: Dysphagia in the elderly

Hai-Yang Feng, Ping-Ping Zhang, Xiao-Wen Wang

Specialty type: Medicine, research and experimental

Provenance and peer review: Unsolicited article; Externally peer reviewed.

Peer-review model: Single blind

Peer-review report's scientific quality classification

Grade A (Excellent): 0
Grade B (Very good): B
Grade C (Good): C, C
Grade D (Fair): 0
Grade E (Poor): 0

P-Reviewer: Byeon H, South Korea; Huang Y, China; Liao Z, Singapore

Received: January 17, 2023
Peer-review started: January 17, 2023
First decision: January 31, 2023
Revised: February 8, 2023
Accepted: March 22, 2023
Article in press: March 22, 2023
Published online: April 16, 2023

Hai-Yang Feng, Ping-Ping Zhang, Xiao-Wen Wang, School of Rehabilitation Medicine, Weifang Medical University, Weifang 261021, Shandong Province, China

Corresponding author: Xiao-Wen Wang, PhD, Additional Professor, School of Rehabilitation Medicine, Weifang Medical University, No. 7166 Baotong West Street, Weifang 261021, Shandong Province, China. 1832770656@qq.com

Abstract

Dysphagia has been classified as a "geriatric syndrome" and can lead to serious complications that result in a tremendous burden on population health and healthcare resources worldwide. A characteristic age-related change in swallowing is defined as "presbyphagia." Medical imaging has shown some changes that seriously affect the safety and efficacy of swallowing. However, there is a general lack of awareness of the effects of aging on swallowing function and a belief that these changes are part of normal aging. Our review provides an overview of presbyphagia, which has been a neglected health problem for a long time. Attention and awareness of dysphagia in the elderly population should be strengthened, and targeted intervention measures should be actively implemented.

Key Words: Aging; Dysphagia; Presbyphagia; Geriatric syndromes; Swallowing

Core Tip: Dysphagia in older people is unfortunately considered a part of aging. Many factors contribute, such as decreased cognitive function, loss of teeth, reduced muscle strength, decreased taste and olfaction, altered salivary secretion, impaired cough and swallowing reflexes, altered hyoid bone and larynx position, reduced laryngeal adductor reflex, decreased tongue root retraction, incomplete esophageal sphincter opening, reduced pharyngeal constriction and sensation, reduced breathing and swallowing coordination, and decreased esophageal motility. Several may be amenable to therapeutic strategies, including rehabilitation, to improve, and even restore swallowing function at the anatomical and physiological levels. Improved screening, clinical assessment, and diagnostic procedures are needed.

Citation: Feng HY, Zhang PP, Wang XW. Presbyphagia: Dysphagia in the elderly. *World J Clin Cases* 2023; 11(11): 2363-2373
URL: https://www.wjgnet.com/2307-8960/full/v11/i11/2363.htm
DOI: https://dx.doi.org/10.12998/wjcc.v11.i11.2363

INTRODUCTION

The effects of aging on swallowing are multifaceted, insidious, and frequently considered a natural part of aging. Older adults gradually develop characteristic changes in swallowing during aging; this phenomenon is called "presbyphagia"[1]. Dysphagia can affect the safety and effectiveness of swallowing, causing severe complications, and affect social interactions, quality of life, and mental health due to fear and anxiety about eating[2,3]. It also increases the financial burden on patients and the healthcare system. Bonilha *et al*[4] observed that yearly medical costs for patients with dysphagia were $4510 higher than those for patients without dysphagia.

However, the problem of presbyphagia continues to be overlooked by most patients, families, and medical practitioners due to the perception that these physiological changes constitute a part of aging. This review aims to raise awareness and understanding of presbyphagia as a critical health problem, improve the diagnostic criteria for presbyphagia, guide interventions, and enhance prevention and treatment performance.

EFFECTS OF AGING ON SWALLOWING FUNCTION

During aging, physiological functions continue to decline and gradually lose their integrity. This deterioration process is also a major contributor to the risk of dysphagia. Functional degradation is mediated by characteristic molecular and cellular phenomena associated with normal aging. These phenomena can be divided into three categories: Primary, antagonistic, and integrative hallmarks[5]. When environmental homeostasis mechanisms within the tissue cannot compensate for the cumulative damage caused by primary and antagonistic hallmarks, the integrative hallmarks arise and ultimately lead to age-related functional decline[5,6].

Nervous system changes

Changes in neural structure, brain chemistry, and related functions occur and accumulate with age, making aging a major risk factor for neurodegeneration. Malandraki *et al*[7] used functional magnetic resonance imaging to compare sites of central nervous activation during swallowing in healthy older adults with those in younger adults. They found that activation of the areas corresponding to sensory processing, sensorimotor integration, and motor coordination and control is diminished in healthy older adults compared to younger adults. The cerebral blood flow is reduced, the cortical sulcus is widened, and the ventricles are enlarged. Furthermore, the volume of some nuclei is reduced, and the ability to process neural information is diminished[8]. The functional and electrophysiological properties of the peripheral nervous system are affected by aging, manifesting as decreased nerve conduction velocity, autonomic responses, endoneurial blood flow, and sensory discrimination[9,10].

Skeletal changes

Cellular senescence increases with age, and senescent chondrocytes accumulate and produce a factor that inhibits cartilage regeneration[11-13]. Epiglottis and paired arytenoid cartilages play an important role in preventing aspiration. Aged cartilage changes shape and becomes less elastic, weakening the protective capacity of the airway. More than 75% of adults aged > 65 years suffer from degenerative changes in the cervical spine; cervical osteophytosis affects swallowing in older adults through various mechanisms, causing frequent coughing and choking[14,15].

Muscle changes

Research has shown that total muscle mass in older adults decreases by 0.5%–1.0% per year, with a cumulative decrease of 30%–50% by 80 years of age[16,17]. Forty muscles are involved in the complex physiological activity of swallowing[2,18,19]. The strength of muscle contraction decreases with age [20]. The tendon transmits the force of the muscle fiber contraction to the bone. During aging, the water and proteoglycan content of tendons decreases, while calcification and fat accumulation increases, leading to decreased tensile strength and stiffness in the tendons, impaired flexibility and coordination of physiological activities required for swallowing, and increased risk of serious complications in older adults[21-23].

Respiratory function

The number of lung epithelial cells gradually decreases with aging, the proportion of fibroblasts increases, and surfactant secretion is impaired, leading to a decline in lung volume and elasticity[24]. The change in thoracic shape serves to reduce chest wall compliance, as shown by altered spinal physiological curvature, increased sternal curvature, and thinning of chest wall muscles[25-27]. Significantly reduced pulmonary function and chest wall compliance decrease the ability of older adults to clear respiratory residue and increase the risk of food entering the respiratory tract.

Overall situation

Older adults are more susceptible to weight loss and malnutrition due to a diminished sense of smell and taste, which affects their appetite and dietary preferences[28,29]. Simultaneously, cortical decompensation reduces physiological sensitivity to osmotic pressure and volume stimuli in older adults, diminishes self-perception of thirst, causes defects in fluid regulation, and tends to result in dehydration[30]. Weakness and aging go hand in hand, manifesting as a weakening of the body's ability to resist and adapt[31]. Dehydration and malnutrition can worsen weakness and lead to muscle atrophy, decreased immunity, and reduced functional reserve. Weakness can, in turn, contribute to the deterioration of swallowing function, reducing the safety of swallowing and increasing the risk of aspiration.

STAGES OF PRESBYPHAGIA

Oral preparatory stage

The oral preparatory stage is controlled by human will (*i.e.*, food is placed in the mouth, stirred, chewed, and processed into a bolus) (Figure 1A). The main changes occurring during this stage are as follows.

Decreased cognitive function: Overall, the brain's weight and cortical surface area decrease with age; a rigorous survey demonstrated that 40% of older adults show symptoms of cognitive impairment[32]. Compared with younger adults, hemispheric specialization is reduced or altered in older adults, necessitating the recruitment of a higher volume of brain areas to compensate for the increased task demands during swallowing[33,34]. The main manifestation of this stage is a cognitive bias regarding the texture, quantity, temperature, taste, and smell of food. Affected individuals may also show the following symptomology: Difficulty concentrating, lower responsivity, impaired casual eating movements, poor coordination, lack of flexibility in adjusting the speed of eating and food intake, and inability to judge in advance how the food will be handled in the mouth[35].

Decreased number of teeth: A controlled trial conducted by Yurkstas *et al*[36] found that individuals with a greater number of teeth (within an age-matched group of older individuals) chewed more efficiently than those with a smaller number of teeth. Missing teeth reduced masticatory efficiency (16%–50%), prolonged the residence time of food in the mouth, and affected older people's choice of food. The prevalence of root caries in people aged > 60 years is twice as high as in young people, and 64% and 96% of people aged > 80 years have root and crown caries, respectively[37,38]. When the neurovascular structures in the dental pulp are involved, the teeth may become sensitive, painful, and even infected (*i.e.*, bacteremia)[39]. This may lead to a reduced intake of vegetables, fruits, and nuts, thus affecting nutritional status. Hence, people without teeth are more likely to suffer from weight loss and malnutrition[37,40].

Reduced muscle strength: Reduced contraction of the orbicularis oris muscle frequently occurs during aging–approximately 20% of older adults are unable to keep their lips closed while swallowing, and food and liquids flow out of their mouths[41]. The cross-sectional area of the masticatory muscles (*i.e.*, the masseterica, temporalis, pterygoideus medialis, pterygoideus lateralis, buccinator, zygomaticus, and mentalis) decreases during the aging process, resulting in a decrease in the force of muscle contraction. The tongue muscles show muscle atrophy and increased connective tissue, reduced muscle strength and range of motion, and decreased flexibility[1,42,43]. Moreover, older adults have a decreased swallowing pressure reserve and lower maximum tongue pressure compared to younger adults[44]. Hence, food spreads in the mouth and stays longer.

Decreased taste and olfaction: The number of nerve fibers and receptors on the olfactory bulb decreases significantly with age. Olfactory function deteriorates progressively with aging such that > 34.5% of older adults have olfactory impairment[45]. Older adults have thinner oral mucosa, weaker secretion, fewer chemoreceptors, and reduced taste perception[46]. During the oral preparation period, olfactory and gustatory information converges on specific brain neurons, activating the amygdala, insular cortex, and anterior cingulate cortex regions; reduced olfaction and gustation can lead to reduced appetite[47]. Compared to younger adults, older adults need two to three times the salt concentration to experience the same saltiness in their food. Older adults prefer sweet and salty foods due to a diminished sense of taste; this increases their risk of obesity, cardiovascular disease, and metabolic disorders[48,49].

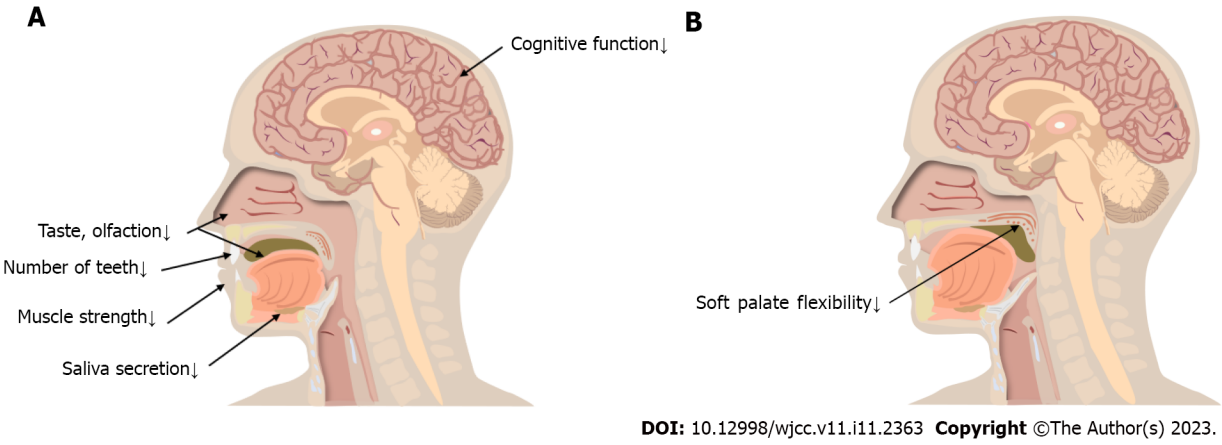

DOI: 10.12998/wjcc.v11.i11.2363

Figure 1 Oral preparatory and transport stage changes. A: Oral preparatory stage changes; B: Oral transport stage changes.

Therefore, nutritional problems are important complications of olfactory and gustatory disorders. A 5-year follow-up study[50] showed that a reduced sense of taste and smell affects the quality of life of older persons and is detrimental to their mental health.

Altered salivary secretion: The prevalence of xerostomia increases with age, affecting approximately 30% of the population aged ³65 years[51,52]. Aging affects salivary gland secretion and decreases inorganic ion concentrations, thereby increasing the threshold for eliciting taste sensations. Further, the number of salivary secretory cells decreases with age, causing diminished sensitivity in taste receptor cells and affecting taste perception[53]. Reduced saliva production also affects the forward movement of food in the mouth, increases oropharyngeal residue, aggravates xerostomia, and increases the risk of poor oral hygiene in older adults.

Oral transport stage

The tongue pushes the bolus backward towards the pharynx in a process termed the oral transport stage. The soft palate plays an important role in this stage: It hangs between the oropharynx and nasopharynx, preventing food from falling into the pharynx prematurely and/or flowing backward into the nasopharynx during swallowing[47] (Figure 1B).

Diminished flexibility tension in the soft palate: The soft palate is composed of connective tissue and muscle. Muscle fiber number, length, and cross-sectional area all decrease due to aging, and increased connective tissue and lipid deposition in the soft palate reduce its flexibility and range of motion[54-56]. When the closure of the tongue and soft palate is inadequate, food can fall into the pharynx and the open expiratory pathways before the swallowing response is triggered, leading to pre-swallowing aspiration[57]. Aerodynamic studies have shown that older speakers exhibit a similar nasal airflow and air volume compared to younger speakers and that velopharyngeal function does not deteriorate with age[58].

Pharyngeal stage

The pharyngeal stage represents the period when the bolus enters the pharynx and reaches the esophagus through the open upper esophageal sphincter (UES) (Figure 2A). Physiological activity during this period is rapid and complex. In a previous study, videofluoroscopic swallowing studies (VFSSs) were performed on 56 healthy older people, and only 16% of them had normal swallowing function[59]. Pharyngeal residue was the most frequent phenomenon during imaging, though it did not cause significant clinical symptoms in most cases[59-61]. Increased pharyngeal residue is usually associated with weak tongue extrusion and diminished pharyngeal clearance[62]. VFSSs revealed that frail older individuals had severely impaired swallowing and coughing reflexes. Up to 55% of older adults show fluid penetration into the laryngeal vestibule during swallowing; approximately 15% show fluid crossing the vocal cords to reach the trachea and bronchi, which eventually causes aspiration[41]. Studies[63-67] have also shown physiological changes in older adults, such as delayed swallowing response, altered distance and time with respect to hyoid and laryngeal elevation, delayed laryngeal closure, and incomplete opening of the UES. These age-related changes result in a higher incidence of permeation and aspiration, significantly reducing the safety of swallowing in older adults (Figure 2B).

Impaired cough and swallowing reflexes: The airway protective reflexes include coughing and swallowing reflexes, which are important for preventing aspiration pneumonia[68]. Tracy *et al*[69] measured the initiation time of the swallowing reflex in different age groups; they found that the

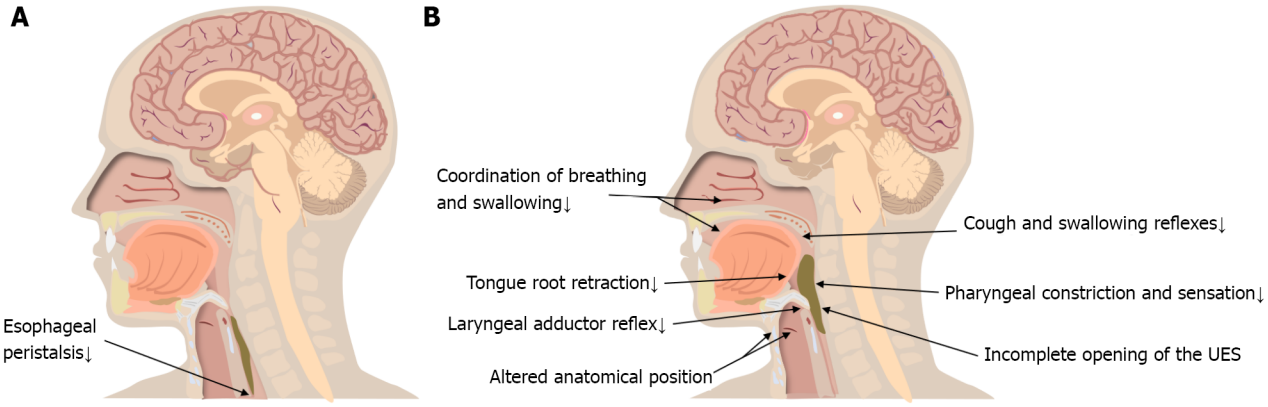

DOI: 10.12998/wjcc.v11.i11.2363

Figure 2 Esophageal and pharyngeal stage changes. A: Esophageal stage changes; B: Pharyngeal stage changes. UES: Upper esophageal sphincter.

swallowing response initiation time was on average 0.4 s longer and the sensitivity of the swallowing reflex area was reduced in older adults. The decrease in the number of myelin sheaths with age leads to reduced sensory input, and older adults require a larger bolus volume to elicit a swallowing reflex[70-72]. Frequently, the bolus has fallen into the pharynx by the time older adults begin swallowing. Most older adults with impaired swallowing reflexes also have impaired cough reflexes. The cough reflex is significantly weakened and suppressed in older patients with aspiration pneumonia; this may be related to the disruption of the cortical facilitation pathway and the medullary reflex pathway of cough caused by aging[73,74].

Altered anatomical position of the hyoid bone and larynx: The anatomical positions of the hyoid bone and larynx are altered in older persons due to changes in spinal morphology and reduced muscle tone. Additionally, the larynx descends to a position close to C7 in older persons aged > 70 years. However, the distance traversed by the larynx during swallowing does not decrease[43]. Accordingly, older individuals need more time to complete the movement that mediates laryngeal elevation[75]. Functional reserve describes the difference between a maximal effort and a normal swallowing task[76]. Aging decreases the speed of hyoid bone and laryngeal elevation, reducing the functional reserve in older adults and increasing the risk of swallowing problems[66,75]. Changes in the anatomical positions weaken the protective mechanisms of the respiratory tract and affect the duration and degree of opening of the UES, hence preventing the smooth passage of the bolus from the pharynx into the esophagus[47,77,78]. The hyoid bone is connected to the larynx through the thyroid hyoid membrane; the movement of the hyoid bone generates a pulling force on the larynx, which is then transmitted to the UES by means of the cricoid cartilage. This is the initial force that causes the cricopharyngeal muscle to open by approximately 8 mm[75,79-81].

Reduced laryngeal adductor reflex: Superior laryngeal nerves play an important role in sensation and autonomic innervation. Mortelliti *et al*[82] used electron-microscopic morphometric techniques to observe the difference between the superior laryngeal nerves of older adults and younger people. They showed that the myelinated nerve fiber count in older people decreased by 31% compared to that in younger people (P = 0.032). The ammonia concentration required to trigger laryngeal closure is six times higher in older adults than in younger adults[83]. The occurrence of silent aspiration is not only related to motor abnormalities, but is also largely influenced by sensory abnormalities[84]. Randomized controlled trials have shown that patients with laryngopharyngeal sensory deficits have difficulty inducing the laryngeal adductor reflex (even under intense stimulation) and a significantly higher risk of penetration and aspiration than controls[85]. Patients lacking the laryngeal adductor reflex have a 6.8 times increased risk of pneumonia (odds ratio: 6.75; 95% confidence interval: 1.76–25.96)[86].

Decreased tongue root retraction: Retraction of the tongue root is one of the main driving forces on the bolus during the pharyngeal stage and is especially important for the smooth entry of the bolus into the pharynx. Cook *et al*[87] found that aging causes a decrease in tongue root retraction. It is speculated that this is a compensatory mechanism due to the increased threshold of the swallowing reflex in older persons; reductions in tongue root retraction movement can increase the accumulation of food in the oropharynx, making it easier to trigger pharyngeal-stage swallowing. On the other hand, the reduced retraction of the tongue root weakens its ability to remove food from the pharynx, resulting in increased pharyngeal residue[88,89].

Incomplete opening of the UES: The resting pressure of the UES in older persons is 43 ± 5 mmHg, which is significantly lower than that in younger persons (71 ± 8 mmHg; P < 0.05)[90]. With aging, the

number of UES muscle fibers decreases, and the excitatory impulses that maintain cricopharyngeal tension also gradually reduce[91]. An inadequate UES pressure decrease during swallowing was observed in 15.4% of older adults aged 60–69 years and 30.4% of older adults aged 70–83 years, while 39% had inadequate UES opening[59,92]. The UES pressure decreased more slowly in older adults, and there was a delayed opening time and significantly fewer UES openings than in younger adults[92-94]. Aging increases muscle connective tissue, which results in a decrease in the elasticity and compliance of the UES[94]. The degree and duration of UES opening are abnormal, increasing the risk of pharyngeal residual and aspiration.

Reduced pharyngeal constriction and sensation: There is prolonged bolus passage through the pharynx when healthy older adults swallow their food[92]. The pharyngeal sensation is significantly reduced in older adults compared to younger adults. A disrupted pattern of cortical activation is observed in older adults, and their ability to find and remove residual food from the pharynx is reduced [90,95,96]. Increased pharyngeal residue is the most common imaging sign in older adults, and the amount of pharyngeal residue is positively correlated with age[87,89]. Reginelli *et al*[97] conducted a VFSS study on older adults and observed that they had a higher prevalence of post-swallowing aspiration than younger adults–this is usually caused by foods remaining in the pharynx.

Reduced coordination of breathing and swallowing: Swallowing and breathing share a common anatomy; hence, food and liquids must be secured as they enter the digestive tract by ensuring that the respiratory tract is closed. Shaker *et al*[98] reported reduced coordination between swallowing and breathing in older persons and found that aging leads to substantially longer pauses in breathing during swallowing. Older adults take longer to return to normal tidal breathing than young individuals[47]. Aging also reduces respiratory function and weakens airway clearance[24].

Esophageal stage

The esophageal stage begins at the tip of the esophagus. The bolus passes through the esophagus under peristaltic contraction and gravity, the lower esophageal sphincter opens, and the bolus enters the stomach (Figure 2A).

Decreased esophageal motility: Myenteric neurons in the esophagus steadily decline with age, causing dysmotility associated with denervation[99]. Secondary esophageal peristalsis removes refluxed contents from the esophagus and is one of the airway protective mechanisms[100]. Mei *et al*[101] found a reduced incidence of secondary esophageal peristalsis and a decreased esophageal response to low-volume ultra-slow reflux in older adults. In the absence of secondary peristalsis of the esophagus, reflux containing gastric acid will stay in the esophagus for a longer time and easily cause reflux esophagitis [102]. Biomechanical changes in the esophagus during aging were observed: The esophageal wall changed in stiffness, circumferentially and longitudinally, with age ($P < 0.05$ and $P < 0.01$, respectively) [103]. Although the percentage of muscle fiber types in the esophagus does not change meaningfully in older persons, a prior study demonstrated a statistically significant increase in muscle fiber diameter due to atrophy and compensatory hypertrophy[104].

INTERVENTION MEASURES

Rehabilitation education

Rather than directly improving the physiological function of swallowing in older adults, rehabilitation education minimizes or eliminates the symptoms of swallowing dysfunction and reduces the occurrence of adverse events. These include postural adjustment, adjustment of eating strategies, use of assistive devices, and periodic oral care[105,106]. Swallowing forcefully in older adults can help to increase pharyngeal pressure, and the downward swallowing position of the lower jaw can change the biomechanical relationship during swallowing and reduce the occurrence of aspiration[106]. Adjustments to diet and eating strategies are the most common compensatory methods. For example, older people should eat slowly, not eat while watching TV, not talk while eating, avoid eating when tired or in a hurry, avoid taking too much in one bite, and avoid swallowing mixed foods and liquids. Single texture foods are easier to swallow. Foods that are relatively viscous and easy to form are also easier to swallow. Assistive devices, such as those used for placing, guiding and controlling food or fluids during swallowing, can increase or prolong eating independence. Paying attention to oral hygiene can also reduce the risk of developing aspiration pneumonia in older people with dysphagia.

Rehabilitation therapy

Rehabilitation training can improve the physiological function of swallowing and reduce the risk of complications[105], and ageing-induced muscle weakness can be improved by rehabilitation training. In a study involving older people, isometric resistance training of the buccal surface, lips, tongue and related oropharyngeal muscles for 8 wk significantly improved swallowing function[107]. In another

study, ice stimulation improved sensitivity of the soft palate and pharynx, increased sensory input, excited neurons in the motor pathway and promoted axonal regeneration of neurons[108]. Additionally, respiratory training improved the coordination of swallowing and breathing and enhanced the ability of the respiratory tract to clear foreign bodies[109]. Finally, simple shaker training in older people improved cricopharyngeal opening, prolonged its opening time, and improved the strength of the supraglottis muscle group and the thyrohyoid muscle[105].

CONCLUSION

Many people, including healthcare practitioners, assume that some age-related changes in swallowing are part of natural aging. However, imaging signs show that some changes may affect the effectiveness and safety of swallowing and lead to severe complications[41,64,89]. Presbyphagia is a common and dangerous, but widely neglected health problem. First, improving the awareness of presbyphagia among medical staff is necessary. We need to understand the mechanisms through which aging affects swallowing function, as well as improve our ability to recognize presbyphagia and its manifestations. Second, screening and assessment of high-risk groups should be performed as early as possible. However, the current screening and clinical assessment process for dysphagia in older adults is not standardized. Further research is needed to improve and standardize screening tools, clinical assessments, and instrumental diagnostic procedures. Finally, it has been well documented that rehabilitation therapy positively affects the anatomical structures and sensory-cortical-motor circuits related to swallowing. Additionally, it can directly and effectively improve and restore swallowing function at the anatomical and physiological levels[105,110-112]. In recent years, non-invasive brain stimulation has been shown to induce plasticity changes in the swallowing motor cortex, resulting in increased cortical excitability and ultimately improving swallowing disorders in older adults[113,114]. Taste[115], olfaction[116], and vision[117] can also alter cortical excitability or activate the swallowing motor cortex. However, there is no standard intervention at present to manage dysphagia in older adults. Further clinical research is required to facilitate the development of clear guidelines to address this issue.

FOOTNOTES

Author contributions: Feng HY wrote the manuscript; Zhang PP and Wang XW modified the manuscript; The corresponding author, Wang XW, guarantees that all descriptions are accurate and that all authors have agreed to the submission of the present manuscript.

Supported by 2021 China Disabled Persons' Federation to Fund Projects, No. 2021CDPFAT-45.

Conflict-of-interest statement: Wang Xiaowen has received research funding from China Disabled Persons' Federation.

Country/Territory of origin: China

ORCID number: Hai-Yang Feng 0000-0003-4212-9964; Xiao-Wen Wang 0000-0002-0594-4401.

S-Editor: Fan JR
L-Editor: A
P-Editor: Fan JR

REFERENCES

1 **Robbins J**, Hamilton JW, Lof GL, Kempster GB. Oropharyngeal swallowing in normal adults of different ages. *Gastroenterology* 1992; **103**: 823-829 [PMID: 1499933 DOI: 10.1016/0016-5085(92)90013-o]
2 **Baijens LW**, Clavé P, Cras P, Ekberg O, Forster A, Kolb GF, Leners JC, Masiero S, Mateos-Nozal J, Ortega O, Smithard DG, Speyer R, Walshe M. European Society for Swallowing Disorders - European Union Geriatric Medicine Society white paper: oropharyngeal dysphagia as a geriatric syndrome. *Clin Interv Aging* 2016; **11**: 1403-1428 [PMID: 27785002 DOI: 10.2147/cia.S107750]
3 **Gellrich D**, Wechtenbruch J, Echternach M. [Swallowing disorders in the elderly]. *MMW Fortschr Med* 2019; **161**: 45-48

[PMID: 31587201 DOI: 10.1007/s15006-019-0961-2]
4 **Bonilha HS**, Simpson AN, Ellis C, Mauldin P, Martin-Harris B, Simpson K. The one-year attributable cost of post-stroke dysphagia. *Dysphagia* 2014; **29**: 545-552 [PMID: 24948438 DOI: 10.1007/s00455-014-9543-8]
5 **López-Otín C**, Blasco MA, Partridge L, Serrano M, Kroemer G. The hallmarks of aging. *Cell* 2013; **153**: 1194-1217 [PMID: 23746838 DOI: 10.1016/j.cell.2013.05.039]
6 **Hou Y**, Dan X, Babbar M, Wei Y, Hasselbalch SG, Croteau DL, Bohr VA. Ageing as a risk factor for neurodegenerative disease. *Nat Rev Neurol* 2019; **15**: 565-581 [PMID: 31501588 DOI: 10.1038/s41582-019-0244-7]
7 **Malandraki GA**, Perlman AL, Karampinos DC, Sutton BP. Reduced somatosensory activations in swallowing with age. *Hum Brain Mapp* 2011; **32**: 730-743 [PMID: 20960572 DOI: 10.1002/hbm.21062]
8 **Bertoni-Freddari C**, Fattoretti P, Paoloni R, Caselli U, Galeazzi L, Meier-Ruge W. Synaptic structural dynamics and aging. *Gerontology* 1996; **42**: 170-180 [PMID: 8796376 DOI: 10.1159/000213789]
9 **Adinolfi AM**, Yamuy J, Morales FR, Chase MH. Segmental demyelination in peripheral nerves of old cats. *Neurobiol Aging* 1991; **12**: 175-179 [PMID: 2052131]
10 **Verdú E**, Ceballos D, Vilches JJ, Navarro X. Influence of aging on peripheral nerve function and regeneration. *J Peripher Nerv Syst* 2000; **5**: 191-208 [PMID: 11151980 DOI: 10.1046/j.1529-8027.2000.00026.x]
11 **Williams PD**, Day T. Antagonistic pleiotropy, mortality source interactions, and the evolutionary theory of senescence. *Evolution* 2003; **57**: 1478-1488 [PMID: 12940353 DOI: 10.1111/j.0014-3820.2003.tb00356.x]
12 **Wang C**, Jurk D, Maddick M, Nelson G, Martin-Ruiz C, von Zglinicki T. DNA damage response and cellular senescence in tissues of aging mice. *Aging Cell* 2009; **8**: 311-323 [PMID: 19627270 DOI: 10.1111/j.1474-9726.2009.00481.x]
13 **Carlo MD Jr**, Loeser RF. Increased oxidative stress with aging reduces chondrocyte survival: correlation with intracellular glutathione levels. *Arthritis Rheum* 2003; **48**: 3419-3430 [PMID: 14673993 DOI: 10.1002/art.11338]
14 **Chen YR**, Sung K, Tharin S. Symptomatic Anterior Cervical Osteophyte Causing Dysphagia: Case Report, Imaging, and Review of the Literature. *Cureus* 2016; **8**: e473 [PMID: 27004150 DOI: 10.7759/cureus.473]
15 **Abdel-Aziz M**, Azab N, El-Badrawy A. Cervical osteophytosis and spine posture: contribution to swallow disorders and symptoms. *Curr Opin Otolaryngol Head Neck Surg* 2018; **26**: 375-381 [PMID: 30234660 DOI: 10.1097/MOO.0000000000000488]
16 **Siparsky PN**, Kirkendall DT, Garrett WE Jr. Muscle changes in aging: understanding sarcopenia. *Sports Health* 2014; **6**: 36-40 [PMID: 24427440 DOI: 10.1177/1941738113502296]
17 **Baker DJ**, Childs BG, Durik M, Wijers ME, Sieben CJ, Zhong J, Saltness RA, Jeganathan KB, Verzosa GC, Pezeshki A, Khazaie K, Miller JD, van Deursen JM. Naturally occurring p16(Ink4a)-positive cells shorten healthy lifespan. *Nature* 2016; **530**: 184-189 [PMID: 26840489 DOI: 10.1038/nature16932]
18 **Kahrilas PJ**, Lin S, Chen J, Logemann JA. Oropharyngeal accommodation to swallow volume. *Gastroenterology* 1996; **111**: 297-306 [PMID: 8690194 DOI: 10.1053/gast.1996.v111.pm8690194]
19 **Suzuki M**, Asada Y, Ito J, Hayashi K, Inoue H, Kitano H. Activation of cerebellum and basal ganglia on volitional swallowing detected by functional magnetic resonance imaging. *Dysphagia* 2003; **18**: 71-77 [PMID: 12825899 DOI: 10.1007/s00455-002-0088-x]
20 **Carnio S**, LoVerso F, Baraibar MA, Longa E, Khan MM, Maffei M, Reischl M, Canepari M, Loefler S, Kern H, Blaauw B, Friguet B, Bottinelli R, Rudolf R, Sandri M. Autophagy impairment in muscle induces neuromuscular junction degeneration and precocious aging. *Cell Rep* 2014; **8**: 1509-1521 [PMID: 25176656 DOI: 10.1016/j.celrep.2014.07.061]
21 **Vafek EC**, Plate JF, Friedman E, Mannava S, Scott AT, Danelson KA. The effect of strain and age on the mechanical properties of rat Achilles tendons. *Muscles Ligaments Tendons J* 2017; **7**: 548-553 [PMID: 29387650 DOI: 10.11138/mltj/2017.7.3.548]
22 **Thornton GM**, Lemmex DB, Ono Y, Beach CJ, Reno CR, Hart DA, Lo IK. Aging affects mechanical properties and lubricin/PRG4 gene expression in normal ligaments. *J Biomech* 2015; **48**: 3306-3311 [PMID: 26163751 DOI: 10.1016/j.jbiomech.2015.06.005]
23 **Peffers MJ**, Thorpe CT, Collins JA, Eong R, Wei TK, Screen HR, Clegg PD. Proteomic analysis reveals age-related changes in tendon matrix composition, with age- and injury-specific matrix fragmentation. *J Biol Chem* 2014; **289**: 25867-25878 [PMID: 25077967 DOI: 10.1074/jbc.M114.566554]
24 **Lee S**, Islam MN, Boostanpour K, Aran D, Jin G, Christenson S, Matthay MA, Eckalbar WL, DePianto DJ, Arron JR, Magee L, Bhattacharya S, Matsumoto R, Kubota M, Farber DL, Bhattacharya J, Wolters PJ, Bhattacharya M. Molecular programs of fibrotic change in aging human lung. *Nat Commun* 2021; **12**: 6309 [PMID: 34728633 DOI: 10.1038/s41467-021-26603-2]
25 **Miller MR**. Structural and physiological age-associated changes in aging lungs. *Semin Respir Crit Care Med* 2010; **31**: 521-527 [PMID: 20941653 DOI: 10.1055/s-0030-1265893]
26 **Kado DM**, Prenovost K, Crandall C. Narrative review: hyperkyphosis in older persons. *Ann Intern Med* 2007; **147**: 330-338 [PMID: 17785488 DOI: 10.7326/0003-4819-147-5-200709040-00008]
27 **Hochhegger B**, Meirelles GS, Irion K, Zanetti G, Garcia E, Moreira J, Marchiori E. The chest and aging: radiological findings. *J Bras Pneumol* 2012; **38**: 656-665 [PMID: 23147059 DOI: 10.1590/s1806-37132012000500016]
28 **Wysocki CJ**, Pelchat ML. The effects of aging on the human sense of smell and its relationship to food choice. *Crit Rev Food Sci Nutr* 1993; **33**: 63-82 [PMID: 8424856 DOI: 10.1080/10408399309527613]
29 **Ahmed T**, Haboubi N. Assessment and management of nutrition in older people and its importance to health. *Clin Interv Aging* 2010; **5**: 207-216 [PMID: 20711440 DOI: 10.2147/cia.s9664]
30 **Phillips PA**, Rolls BJ, Ledingham JG, Forsling ML, Morton JJ, Crowe MJ, Wollner L. Reduced thirst after water deprivation in healthy elderly men. *N Engl J Med* 1984; **311**: 753-759 [PMID: 6472364 DOI: 10.1056/NEJM198409203111202]
31 **Xu M**, Pirtskhalava T, Farr JN, Weigand BM, Palmer AK, Weivoda MM, Inman CL, Ogrodnik MB, Hachfeld CM, Fraser DG, Onken JL, Johnson KO, Verzosa GC, Langhi LGP, Weigl M, Giorgadze N, LeBrasseur NK, Miller JD, Jurk D, Singh RJ, Allison DB, Ejima K, Hubbard GB, Ikeno Y, Cubro H, Garovic VD, Hou X, Weroha SJ, Robbins PD, Niedernhofer LJ, Khosla S, Tchkonia T, Kirkland JL. Senolytics improve physical function and increase lifespan in old age. *Nat Med*

2018; **24**: 1246-1256 [PMID: 29988130 DOI: 10.1038/s41591-018-0092-9]
32 **Vanguilder HD**, Freeman WM. The hippocampal neuroproteome with aging and cognitive decline: past progress and future directions. *Front Aging Neurosci* 2011; **3**: 8 [PMID: 21647399 DOI: 10.3389/fnagi.2011.00008]
33 **Dziewas R**, Sörös P, Ishii R, Chau W, Henningsen H, Ringelstein EB, Knecht S, Pantev C. Neuroimaging evidence for cortical involvement in the preparation and in the act of swallowing. *Neuroimage* 2003; **20**: 135-144 [PMID: 14527576]
34 **Teismann IK**, Steinstraeter O, Schwindt W, Ringelstein EB, Pantev C, Dziewas R. Age-related changes in cortical swallowing processing. *Neurobiol Aging* 2010; **31**: 1044-1050 [PMID: 18715676 DOI: 10.1016/j.neurobiolaging.2008.07.001]
35 **Michel A**, Verin E, Hansen K, Chassagne P, Roca F. Buccofacial Apraxia, Oropharyngeal Dysphagia, and Dementia Severity in Community-Dwelling Elderly Patients. *J Geriatr Psychiatry Neurol* 2021; **34**: 150-155 [PMID: 32292086 DOI: 10.1177/0891988720915519]
36 **Yurkstas A**, Emerson WH. Dietary selections of persons with natural and artificial teeth. *J Prosthet Dent* 1964; **14**: 695-697 [DOI: 10.1016/0022-3913(64)90204-5]
37 **Heath MR**. The effect of maximum biting force and bone loss upon masticatory function and dietary selection of the elderly. *Int Dent J* 1982; **32**: 345-356 [PMID: 6761273]
38 **MacDonald DE**. Principles of geriatric dentistry and their application to the older adult with a physical disability. *Clin Geriatr Med* 2006; **22**: 413-34; x [PMID: 16627086 DOI: 10.1016/j.cger.2005.12.009]
39 **Hahn CL**, Liewehr FR. Innate immune responses of the dental pulp to caries. *J Endod* 2007; **33**: 643-651 [PMID: 17509400 DOI: 10.1016/j.joen.2007.01.001]
40 **Amella EJ**. Feeding and hydration issues for older adults with dementia. *Nurs Clin North Am* 2004; **39**: 607-623 [PMID: 15331305 DOI: 10.1016/j.cnur.2004.02.014]
41 **Rofes L**, Arreola V, Romea M, Palomera E, Almirall J, Cabré M, Serra-Prat M, Clavé P. Pathophysiology of oropharyngeal dysphagia in the frail elderly. *Neurogastroenterol Motil* 2010; **22**: 851-858, e230 [PMID: 20529208 DOI: 10.1111/j.1365-2982.2010.01521.x]
42 **Robbins J**, Humpal NS, Banaszynski K, Hind J, Rogus-Pulia N. Age-Related Differences in Pressures Generated During Isometric Presses and Swallows by Healthy Adults. *Dysphagia* 2016; **31**: 90-96 [PMID: 26525059 DOI: 10.1007/s00455-015-9662-x]
43 **Logemann JA**, Pauloski BR, Rademaker AW, Colangelo LA, Kahrilas PJ, Smith CH. Temporal and biomechanical characteristics of oropharyngeal swallow in younger and older men. *J Speech Lang Hear Res* 2000; **43**: 1264-1274 [PMID: 11063246 DOI: 10.1044/jslhr.4305.1264]
44 **Pitts LL**, Stierwalt JAG, Hageman CF, LaPointe LL. The Influence of Oropalatal Dimensions on the Measurement of Tongue Strength. *Dysphagia* 2017; **32**: 759-766 [PMID: 28687869 DOI: 10.1007/s00455-017-9820-4]
45 **Desiato VM**, Levy DA, Byun YJ, Nguyen SA, Soler ZM, Schlosser RJ. The Prevalence of Olfactory Dysfunction in the General Population: A Systematic Review and Meta-analysis. *Am J Rhinol Allergy* 2021; **35**: 195-205 [PMID: 32746612 DOI: 10.1177/1945892420946254]
46 **Krull IS**, Mazzeo JR. Capillary electrophoresis: the promise and the practice. *Nature* 1992; **357**: 92-94 [PMID: 1574129 DOI: 10.1093/gerona/60.1.109]
47 **Ekberg O**, Editor. Dysphagia Diagnosis and Treatment. 2nd ed. Berlin: Springer International Publishing, 2019: 247-267
48 **O'Keeffe M**, Kelly M, O'Herlihy E, O'Toole PW, Kearney PM, Timmons S, O'Shea E, Stanton C, Hickson M, Rolland Y, Sulmont Rossé C, Issanchou S, Maitre I, Stelmach-Mardas M, Nagel G, Flechtner-Mors M, Wolters M, Hebestreit A, De Groot LCPGM, van de Rest O, Teh R, Peyron MA, Dardevet D, Papet I, Schindler K, Streicher M, Torbahn G, Kiesswetter E, Visser M, Volkert D, O'Connor EM; MaNuEL consortium. Potentially modifiable determinants of malnutrition in older adults: A systematic review. *Clin Nutr* 2019; **38**: 2477-2498 [PMID: 30685297 DOI: 10.1016/j.clnu.2018.12.007]
49 **Imoscopi A**, Inelmen EM, Sergi G, Miotto F, Manzato E. Taste loss in the elderly: epidemiology, causes and consequences. *Aging Clin Exp Res* 2012; **24**: 570-579 [PMID: 22828477 DOI: 10.3275/8520]
50 **Gopinath B**, Russell J, Flood VM, Burlutsky G, Mitchell P. Adherence to dietary guidelines positively affects quality of life and functional status of older adults. *J Acad Nutr Diet* 2014; **114**: 220-229 [PMID: 24239401 DOI: 10.1016/j.jand.2013.09.001]
51 **Rhodus NL**, Moller K, Colby S, Bereuter J. Dysphagia in patients with three different etiologies of salivary gland dysfunction. *Ear Nose Throat J* 1995; **74**: 39-42, 45 [PMID: 7867530]
52 **Ship JA**, Pillemer SR, Baum BJ. Xerostomia and the geriatric patient. *J Am Geriatr Soc* 2002; **50**: 535-543 [PMID: 11943053 DOI: 10.1046/j.1532-5415.2002.50123.x]
53 **Xu F**, Laguna L, Sarkar A. Aging-related changes in quantity and quality of saliva: Where do we stand in our understanding? *J Texture Stud* 2019; **50**: 27-35 [PMID: 30091142 DOI: 10.1111/jtxs.12356]
54 **Veldi M**, Vasar V, Hion T, Kull M, Vain A. Ageing, soft-palate tone and sleep-related breathing disorders. *Clin Physiol* 2001; **21**: 358-364 [PMID: 11380536 DOI: 10.1046/j.1365-2281.2001.00339.x]
55 **Michalowski R**, Chibowska M. Lipid deposition in soft palate of man and its relation to aging. *Pol Med Sci Hist Bull* 1965; **8**: 141-144 [PMID: 5857855]
56 **Faulkner JA**, Larkin LM, Claflin DR, Brooks SV. Age-related changes in the structure and function of skeletal muscles. *Clin Exp Pharmacol Physiol* 2007; **34**: 1091-1096 [PMID: 17880359 DOI: 10.1111/j.1440-1681.2007.04752.x]
57 **Ortega O**, Martín A, Clavé P. Diagnosis and Management of Oropharyngeal Dysphagia Among Older Persons, State of the Art. *J Am Med Dir Assoc* 2017; **18**: 576-582 [PMID: 28412164 DOI: 10.1016/j.jamda.2017.02.015]
58 **Zajac DJ**. Velopharyngeal function in young and older adult speakers: evidence from aerodynamic studies. *J Acoust Soc Am* 1997; **102**: 1846-1852 [PMID: 9301062 DOI: 10.1121/1.420091]
59 **Ekberg O**, Feinberg MJ. Altered swallowing function in elderly patients without dysphagia: radiologic findings in 56 cases. *AJR Am J Roentgenol* 1991; **156**: 1181-1184 [PMID: 2028863 DOI: 10.2214/ajr.156.6.2028863]
60 **Kendall KA**, Leonard RJ, McKenzie S. Common medical conditions in the elderly: impact on pharyngeal bolus transit.

Dysphagia 2004; **19**: 71-77 [PMID: 15382793 DOI: 10.1007/s00455-003-0502-z]
61 **Clavé P**, Rofes L, Carrión S, Ortega O, Cabré M, Serra-Prat M, Arreola V. Pathophysiology, relevance and natural history of oropharyngeal dysphagia among older people. *Nestle Nutr Inst Workshop Ser* 2012; **72**: 57-66 [PMID: 23052001 DOI: 10.1159/000339986]
62 **Cook IJ**. Oropharyngeal dysphagia. *Gastroenterol Clin North Am* 2009; **38**: 411-431 [PMID: 19699405 DOI: 10.1016/j.gtc.2009.06.003]
63 **Nawaz S**, Tulunay-Ugur OE. Dysphagia in the Older Patient. *Otolaryngol Clin North Am* 2018; **51**: 769-777 [PMID: 29779617 DOI: 10.1016/j.otc.2018.03.006]
64 **Robbins J**. Normal swallowing and aging. *Semin Neurol* 1996; **16**: 309-317 [PMID: 9112310 DOI: 10.1055/s-2008-1040989]
65 **Namasivayam-MacDonald AM**, Barbon CEA, Steele CM. A review of swallow timing in the elderly. *Physiol Behav* 2018; **184**: 12-26 [PMID: 29101012 DOI: 10.1016/j.physbeh.2017.10.023]
66 **Kendall KA**, Leonard RJ. Pharyngeal constriction in elderly dysphagic patients compared with young and elderly nondysphagic controls. *Dysphagia* 2001; **16**: 272-278 [PMID: 11720403 DOI: 10.1007/s00455-001-0086-4]
67 **Aviv JE**. Effects of aging on sensitivity of the pharyngeal and supraglottic areas. *Am J Med* 1997; **103**: 74S-76S [PMID: 9422628 DOI: 10.1016/s0002-9343(97)00327-6]
68 **Pitts T**. Airway protective mechanisms. *Lung* 2014; **192**: 27-31 [PMID: 24297325 DOI: 10.1007/s00408-013-9540-y]
69 **Tracy JF**, Logemann JA, Kahrilas PJ, Jacob P, Kobara M, Krugler C. Preliminary observations on the effects of age on oropharyngeal deglutition. *Dysphagia* 1989; **4**: 90-94 [PMID: 2640185 DOI: 10.1007/BF02407151]
70 **Ebihara S**, Ebihara T, Kohzuki M. Effect of aging on cough and swallowing reflexes: implications for preventing aspiration pneumonia. *Lung* 2012; **190**: 29-33 [PMID: 22033612 DOI: 10.1007/s00408-011-9334-z]
71 **Nakajima J**, Karaho T, Kawahara K, Hayashi Y, Nakamura M, Matsuura N, Kohno N. Latent changes in the pharyngeal stage of swallowing in non-aspirating older adults. *Eur Geriatr Med* 2022; **13**: 655-661 [PMID: 35091892 DOI: 10.1007/s41999-021-00604-2]
72 **Ebihara S**, Ebihara T. Cough in the elderly: a novel strategy for preventing aspiration pneumonia. *Pulm Pharmacol Ther* 2011; **24**: 318-323 [PMID: 20937403 DOI: 10.1016/j.pupt.2010.10.003]
73 **Yamanda S**, Ebihara S, Ebihara T, Yamasaki M, Asamura T, Asada M, Une K, Arai H. Impaired urge-to-cough in elderly patients with aspiration pneumonia. *Cough* 2008; **4**: 11 [PMID: 19019213 DOI: 10.1186/1745-9974-4-11]
74 **Sekizawa K**, Ujiie Y, Itabashi S, Sasaki H, Takishima T. Lack of cough reflex in aspiration pneumonia. *Lancet* 1990; **335**: 1228-1229 [PMID: 1971077 DOI: 10.1016/0140-6736(90)92758-a]
75 **Yokoyama M**, Mitomi N, Tetsuka K, Tayama N, Niimi S. Role of laryngeal movement and effect of aging on swallowing pressure in the pharynx and upper esophageal sphincter. *Laryngoscope* 2000; **110**: 434-439 [PMID: 10718434 DOI: 10.1097/00005537-200003000-00021]
76 **Jones CA**, Colletti CM. Age-Related Functional Reserve Decline Is Not Seen in Pharyngeal Swallowing Pressures. *J Speech Lang Hear Res* 2021; **64**: 3734-3741 [PMID: 34525307 DOI: 10.1044/2021_JSLHR-21-00164]
77 **Kletzien H**, Cullins MJ, Connor NP. Age-related alterations in swallowing biomechanics. *Exp Gerontol* 2019; **118**: 45-50 [PMID: 30633957 DOI: 10.1016/j.exger.2019.01.006]
78 **Grote C**, Reinhardt D, Zhang M, Wang J. Regulatory mechanisms and clinical manifestations of musculoskeletal aging. *J Orthop Res* 2019; **37**: 1475-1488 [PMID: 30919498 DOI: 10.1002/jor.24292]
79 **Leonard R**, Kendall K, McKenzie S. UES opening and cricopharyngeal bar in nondysphagic elderly and nonelderly adults. *Dysphagia* 2004; **19**: 182-191 [PMID: 15383948 DOI: 10.1007/s00455-004-0005-6]
80 **Im I**, Kim Y, Oommen E, Kim H, Ko MH. The Effects of Bolus Consistency in Pharyngeal Transit Duration during Normal Swallowing. *Ann Rehabil Med* 2012; **36**: 220-225 [PMID: 22639746 DOI: 10.5535/arm.2012.36.2.220]
81 **Mendell DA**, Logemann JA. Temporal sequence of swallow events during the oropharyngeal swallow. *J Speech Lang Hear Res* 2007; **50**: 1256-1271 [PMID: 17905910 DOI: 10.1044/1092-4388(2007/088)]
82 **Mortelliti AJ**, Malmgren LT, Gacek RR. Ultrastructural changes with age in the human superior laryngeal nerve. *Arch Otolaryngol Head Neck Surg* 1990; **116**: 1062-1069 [PMID: 2200442 DOI: 10.1001/archotol.1990.01870090078013]
83 **Bartlett JG**, Gorbach SL. The triple threat of aspiration pneumonia. *Chest* 1975; **68**: 560-566 [PMID: 1175415 DOI: 10.1378/chest.68.4.560]
84 **Kikuchi R**, Watabe N, Konno T, Mishina N, Sekizawa K, Sasaki H. High incidence of silent aspiration in elderly patients with community-acquired pneumonia. *Am J Respir Crit Care Med* 1994; **150**: 251-253 [PMID: 8025758 DOI: 10.1164/ajrccm.150.1.8025758]
85 **Aviv JE**, Spitzer J, Cohen M, Ma G, Belafsky P, Close LG. Laryngeal adductor reflex and pharyngeal squeeze as predictors of laryngeal penetration and aspiration. *Laryngoscope* 2002; **112**: 338-341 [PMID: 11889394 DOI: 10.1097/00005537-200202000-00025]
86 **Kaneoka A**, Pisegna JM, Inokuchi H, Ueha R, Goto T, Nito T, Stepp CE, LaValley MP, Haga N, Langmore SE. Relationship Between Laryngeal Sensory Deficits, Aspiration, and Pneumonia in Patients with Dysphagia. *Dysphagia* 2018; **33**: 192-199 [PMID: 28866750 DOI: 10.1007/s00455-017-9845-8]
87 **Cook IJ**, Weltman MD, Wallace K, Shaw DW, McKay E, Smart RC, Butler SP. Influence of aging on oral-pharyngeal bolus transit and clearance during swallowing: scintigraphic study. *Am J Physiol* 1994; **266**: G972-G977 [PMID: 8023945 DOI: 10.1152/ajpgi.1994.266.6.G972]
88 **Hosseini P**, Tadavarthi Y, Martin-Harris B, Pearson WG Jr. Functional Modules of Pharyngeal Swallowing Mechanics. *Laryngoscope Investig Otolaryngol* 2019; **4**: 341-346 [PMID: 31236469 DOI: 10.1002/lio2.273]
89 **Mehraban-Far S**, Alrassi J, Patel R, Ahmad V, Browne N, Lam W, Jiang Y, Barber N, Mortensen M. Dysphagia in the elderly population: A Videofluoroscopic study. *Am J Otolaryngol* 2021; **42**: 102854 [PMID: 33482586 DOI: 10.1016/j.amjoto.2020.102854]
90 **Shaker R**, Ren J, Podvrsan B, Dodds WJ, Hogan WJ, Kern M, Hoffmann R, Hintz J. Effect of aging and bolus variables on pharyngeal and upper esophageal sphincter motor function. *Am J Physiol* 1993; **264**: G427-G432 [PMID: 8460698 DOI: 10.1152/ajpgi.1993.264.3.G427]

91 **Shaker R**, Lang IM. Effect of aging on the deglutitive oral, pharyngeal, and esophageal motor function. *Dysphagia* 1994; **9**: 221-228 [PMID: 7805420 DOI: 10.1007/bf00301914]

92 **Nishikubo K**, Mise K, Ameya M, Hirose K, Kobayashi T, Hyodo M. Quantitative evaluation of age-related alteration of swallowing function: Videofluoroscopic and manometric studies. *Auris Nasus Larynx* 2015; **42**: 134-138 [PMID: 25199737 DOI: 10.1016/j.anl.2014.07.002]

93 **Fulp SR**, Dalton CB, Castell JA, Castell DO. Aging-related alterations in human upper esophageal sphincter function. *Am J Gastroenterol* 1990; **85**: 1569-1572 [PMID: 2252018]

94 **Shaw DW**, Cook IJ, Gabb M, Holloway RH, Simula ME, Panagopoulos V, Dent J. Influence of normal aging on oral-pharyngeal and upper esophageal sphincter function during swallowing. *Am J Physiol* 1995; **268**: G389-G396 [PMID: 7900799 DOI: 10.1152/ajpgi.1995.268.3.G389]

95 **Aviv JE**, Martin JH, Sacco RL, Zagar D, Diamond B, Keen MS, Blitzer A. Supraglottic and pharyngeal sensory abnormalities in stroke patients with dysphagia. *Ann Otol Rhinol Laryngol* 1996; **105**: 92-97 [PMID: 8659942 DOI: 10.1177/000348949610500202]

96 **Jean A**. Control of the central swallowing program by inputs from the peripheral receptors. A review. *J Auton Nerv Syst* 1984; **10**: 225-233 [PMID: 6384335 DOI: 10.1016/0165-1838(84)90017-1]

97 **Reginelli A**, D'Amora M, Del Vecchio L, Monaco L, Barillari MR, Di Martino N, Barillari U, Motta G, Cappabianca S, Grassi R. Videofluoroscopy and oropharyngeal manometry for evaluation of swallowing in elderly patients. *Int J Surg* 2016; **33** Suppl 1: S154-S158 [PMID: 27392720 DOI: 10.1016/j.ijsu.2016.06.017]

98 **Shaker R**, Li Q, Ren J, Townsend WF, Dodds WJ, Martin BJ, Kern MK, Rynders A. Coordination of deglutition and phases of respiration: effect of aging, tachypnea, bolus volume, and chronic obstructive pulmonary disease. *Am J Physiol* 1992; **263**: G750-G755 [PMID: 1443150 DOI: 10.1152/ajpgi.1992.263.5.G750]

99 **Eckardt VF**, LeCompte PM. Esophageal ganglia and smooth muscle in the elderly. *Am J Dig Dis* 1978; **23**: 443-448 [PMID: 677096 DOI: 10.1007/bf01072928]

100 **Shaker R**. Airway protective mechanisms: current concepts. *Dysphagia* 1995; **10**: 216-227 [PMID: 7493501 DOI: 10.1007/bf00431413]

101 **Mei L**, Dua A, Kern M, Gao S, Edeani F, Dua K, Wilson A, Lynch S, Sanvanson P, Shaker R. Older Age Reduces Upper Esophageal Sphincter and Esophageal Body Responses to Simulated Slow and Ultraslow Reflux Events and Post-Reflux Residue. *Gastroenterology* 2018; **155**: 760-770.e1 [PMID: 29803837 DOI: 10.1053/j.gastro.2018.05.036]

102 **Kawami N**, Iwakiri K, Sano H, Tanaka Y, Sakamoto C. Effects of aging and acid reflux on esophageal motility. *Digestion* 2015; **91**: 181-186 [PMID: 25765546 DOI: 10.1159/000367650]

103 **Zhao J**, Gregersen H. Esophageal morphometric and biomechanical changes during aging in rats. *Neurogastroenterol Motil* 2015; **27**: 1638-1647 [PMID: 26303784 DOI: 10.1111/nmo.12661]

104 **Leese G**, Hopwood D. Muscle fibre typing in the human pharyngeal constrictors and oesophagus: the effect of ageing. *Acta Anat (Basel)* 1986; **127**: 77-80 [PMID: 3788449 DOI: 10.1159/000146241]

105 **Ney DM**, Weiss JM, Kind AJ, Robbins J. Senescent swallowing: impact, strategies, and interventions. *Nutr Clin Pract* 2009; **24**: 395-413 [PMID: 19483069 DOI: 10.1177/0884533609332005]

106 **Christmas C**, Rogus-Pulia N. Swallowing Disorders in the Older Population. *J Am Geriatr Soc* 2019; **67**: 2643-2649 [PMID: 31430395 DOI: 10.1111/jgs.16137]

107 **Sanders DS**, Carter MJ, D'Silva J, James G, Bolton RP, Willemse PJ, Bardhan KD. Percutaneous endoscopic gastrostomy: a prospective audit of the impact of guidelines in two district general hospitals in the United Kingdom. *Am J Gastroenterol* 2002; **97**: 2239-2245 [PMID: 12358239 DOI: 10.1016/S0002-9270(02)04134-5]

108 **Adeyemo BO**, Simis M, Macea DD, Fregni F. Systematic review of parameters of stimulation, clinical trial design characteristics, and motor outcomes in non-invasive brain stimulation in stroke. *Front Psychiatry* 2012; **3**: 88 [PMID: 23162477 DOI: 10.3389/fpsyt.2012.00088]

109 **Ghannouchi I**, Speyer R, Doma K, Cordier R, Verin E. Swallowing function and chronic respiratory diseases: Systematic review. *Respir Med* 2016; **117**: 54-64 [PMID: 27492514 DOI: 10.1016/j.rmed.2016.05.024]

110 **Marik PE**, Kaplan D. Aspiration pneumonia and dysphagia in the elderly. *Chest* 2003; **124**: 328-336 [PMID: 12853541 DOI: 10.1378/chest.124.1.328]

111 **Hasten DL**, Pak-Loduca J, Obert KA, Yarasheski KE. Resistance exercise acutely increases MHC and mixed muscle protein synthesis rates in 78-84 and 23-32 yr olds. *Am J Physiol Endocrinol Metab* 2000; **278**: E620-E626 [PMID: 10751194 DOI: 10.1152/ajpendo.2000.278.4.E620]

112 **Schulte JN**, Yarasheski KE. Effects of resistance training on the rate of muscle protein synthesis in frail elderly people. *Int J Sport Nutr Exerc Metab* 2001; **11** Suppl: S111-S118 [PMID: 11915909 DOI: 10.1123/ijsnem.11.s1.s111]

113 **Pisegna JM**, Kaneoka A, Pearson WG Jr, Kumar S, Langmore SE. Effects of non-invasive brain stimulation on post-stroke dysphagia: A systematic review and meta-analysis of randomized controlled trials. *Clin Neurophysiol* 2016; **127**: 956-968 [PMID: 26070517 DOI: 10.1016/j.clinph.2015.04.069]

114 **Chiang CF**, Lin MT, Hsiao MY, Yeh YC, Liang YC, Wang TG. Comparative Efficacy of Noninvasive Neurostimulation Therapies for Acute and Subacute Poststroke Dysphagia: A Systematic Review and Network Meta-analysis. *Arch Phys Med Rehabil* 2019; **100**: 739-750.e4 [PMID: 30352222 DOI: 10.1016/j.apmr.2018.09.117]

115 **Mistry S**, Rothwell JC, Thompson DG, Hamdy S. Modulation of human cortical swallowing motor pathways after pleasant and aversive taste stimuli. *Am J Physiol Gastrointest Liver Physiol* 2006; **291**: G666-G671 [PMID: 16728724 DOI: 10.1152/ajpgi.00573.2005]

116 **Ebihara T**, Ebihara S, Maruyama M, Kobayashi M, Itou A, Arai H, Sasaki H. A randomized trial of olfactory stimulation using black pepper oil in older people with swallowing dysfunction. *J Am Geriatr Soc* 2006; **54**: 1401-1406 [PMID: 16970649 DOI: 10.1111/j.1532-5415.2006.00840.x]

117 **Vicario CM**, Rafal RD, Borgomaneri S, Paracampo R, Kritikos A, Avenanti A. Pictures of disgusting foods and disgusted facial expressions suppress the tongue motor cortex. *Soc Cogn Affect Neurosci* 2017; **12**: 352-362 [PMID: 27614770 DOI: 10.1093/scan/nsw129]

World Journal of Clinical Cases

Submit a Manuscript: https://www.f6publishing.com

World J Clin Cases 2023 April 16; 11(11): 2374-2385

DOI: 10.12998/wjcc.v11.i11.2374

ISSN 2307-8960 (online)

MINIREVIEWS

Narrative minireview of the spatial epidemiology of substance use disorder in the United States: Who is at risk and where?

Diego F Cuadros, Adam J Branscum, Claudia M Moreno, Neil J MacKinnon

Specialty type: Medicine, research and experimental

Provenance and peer review: Invited article; Externally peer reviewed.

Peer-review model: Single blind

Peer-review report's scientific quality classification

Grade A (Excellent): A, A
Grade B (Very good): B
Grade C (Good): C
Grade D (Fair): 0
Grade E (Poor): 0

P-Reviewer: Long X, China; Wang T, China; Welter J, Switzerland

Received: November 28, 2022
Peer-review started: November 28, 2022
First decision: January 19, 2023
Revised: January 31, 2023
Accepted: March 20, 2023
Article in press: March 20, 2023
Published online: April 16, 2023

Diego F Cuadros, Digital Futures, University of Cincinnati, Cincinnati, OH 45206, United States

Adam J Branscum, Department of Biostatistics, Oregon State University, Corvallis, OR 97331, United States

Claudia M Moreno, Department of Physiology and Biophysics, University of Washington, Seattle, WA 98195, United States

Neil J MacKinnon, Department of Population Health Sciences, Augusta University, Augusta, GA 30912, United States

Corresponding author: Diego F Cuadros, PhD, Associate Professor, Digital Futures, University of Cincinnati, 3080 Exploration Ave, Cincinnati, OH 45206, United States.
diego.cuadros@uc.edu

Abstract

Drug overdose is the leading cause of death by injury in the United States. The incidence of substance use disorder (SUD) in the United States has increased steadily over the past two decades, becoming a major public health problem for the country. The drivers of the SUD epidemic in the United States have changed over time, characterized by an initial heroin outbreak between 1970 and 1999, followed by a painkiller outbreak, and finally by an ongoing synthetic opioid outbreak. The nature and sources of these abused substances reveal striking differences in the socioeconomic and behavioral factors that shape the drug epidemic. Moreover, the geospatial distribution of the SUD epidemic is not homogeneous. The United States has specific locations where vulnerable communities at high risk of SUD are concentrated, reaffirming the multifactorial socioeconomic nature of this epidemic. A better understanding of the SUD epidemic under a spatial epidemiology framework is necessary to determine the factors that have shaped its spread and how these patterns can be used to predict new outbreaks and create effective mitigation policies. This narrative minireview summarizes the current records of the spatial distribution of the SUD epidemic in the United States across different periods, revealing some spatiotemporal patterns that have preceded the occurrence of outbreaks. By analyzing the epidemic of SUD-related deaths, we also describe the epidemic behavior in areas with high incidence of cases. Finally, we describe public health interventions that can be effective for demographic groups, and we discuss future challenges in the study and control of the SUD epidemic in the country.

Key Words: Substance use disorder; Spatial epidemiology; Risk factors; Spatial statistics; Disease mapping

Core Tip: A comprehensive geographical analysis of the substance use disorder (SUD) epidemic is fundamental to understanding the dynamics of the epidemic and to identifying important factors associated with the spatial dynamics of the disease. The SUD epidemic is not uniformly distributed within the United States. The epidemic is characterized by the emergence of several micro-epidemics of different intensities across demographic groups and geographical locations across the country. Micro-targeting strategies based on understanding the spatial structure and the multifactorial nature of the addiction epidemic would facilitate the design of integrated preventive strategies for substance use in vulnerable populations in the United States.

Citation: Cuadros DF, Branscum AJ, Moreno CM, MacKinnon NJ. Narrative minireview of the spatial epidemiology of substance use disorder in the United States: Who is at risk and where? *World J Clin Cases* 2023; 11(11): 2374-2385
URL: https://www.wjgnet.com/2307-8960/full/v11/i11/2374.htm
DOI: https://dx.doi.org/10.12998/wjcc.v11.i11.2374

INTRODUCTION

Substance use disorder (SUD) is a mental disorder that affects nearly 20.4 million Americans[1]. SUD is defined as the inability of a person to control their use of substances such as legal or illegal drugs or medications[2]. Among the 20.4 million people with SUD, 40.7% have illicit drug disorder. Illicit drug overdoses have increased steadily in the last three decades, claiming over 900000 lives in the United States since 1999[3]. In 2020 alone, 92000 people died from illicit drug overdose in the country. Thus, SUD has been acknowledged as one of the public health priorities in the United States Opioids have recently been the largest contributor to SUD-related mortality in the country, accounting for about 75% of all drug overdose deaths in 2020[4]. Collectively, these finds make the study of the opioid epidemic a priority.

National data on SUD show that the epidemic is not homogenously distributed within the country. Overdose rates are highest and have increased in specific regions of the country, particularly in Appalachia, New England, Florida, eastern Kentucky, and the Southwest[5,6]. The type of substance contributing to most deaths also varies across the United States, with a large share of drug overdoses in the Northeast attributed to synthetic opioids (fentanyl), whereas heroin overdoses are most prevalent in New Mexico and the Midwest[7,8]. Several studies examining the attributes of the addiction epidemic in the United States have described significant demographic and spatial heterogeneities[9]. These heterogeneities have been partially attributed to the concomitant spatial heterogeneity that the United States exhibits for socioeconomic status, race and ethnicity, and comorbidities[9]. The reasons behind the geospatial heterogeneity of SUD incidence in the United States, however, are still not completely understood[10].

Socioeconomic status, accessibility to primary and mental health care, unemployment rate, urbanicity, and availability of substances have been proposed to be some of the main drivers of this heterogeneity[11-13]. In addition, rates of prescribing patterns and the accessibility of treatments to reverse overdose episodes (*e.g.*, naloxone) have been identified as important factors associated with the uneven spatial and demographical distributions of SUD-related mortality[14-16]. Furthermore, the epidemiological attributes of the SUD public health emergency remain understudied. There is little information about where (location) and who (demographic groups) are at higher risk of developing SUD and dying of related overdoses[17]. In this perspective, spatial statistics and geospatial epidemiological models are key tools for recognizing the temporal and geographical dynamics of the epidemic [18]. The identification of the key spatiotemporal dynamics of the SUD challenge will provide significant information to identify geographic areas where vulnerable populations are located as well as potential socioeconomic drivers of the epidemic. Geospatial statistical and spatial epidemiological models can be used to develop strategies for mitigating the SUD crisis in the most affected areas and preventing future outbreaks in vulnerable communities.

This narrative minireview aims to summarize and discuss the advances in the study of the spatial distribution of the SUD epidemic in the United States. Geospatial analyses have been foundational to the study and management of many global epidemics [*e.g.*, human immunodeficiency virus (HIV)]. However, the use of geospatial analysis to aid in the study of the SUD crisis has been limited. This minireview begins with a concise summary of the general concepts and advances in the use of

geospatial methods applied in epidemiology. Then, we discuss the spatial structure of the SUD epidemic in the United States, with a detailed emphasis on Ohio because it is one of the most affected states in the country. Finally, we discuss the challenges and the future of the implementation of spatial epidemiology in the study of the SUD epidemic.

GEOGRAPHICAL INFORMATION SYSTEMS IN EPIDEMIOLOGY

Epidemiology entails the study of the distribution and determinants of health challenges in populations. Epidemiological studies have centered on recognizing the type and extent of diseases affecting human health and identifying the causes associated to disease incidence[19]. In epidemiology, it is common to assess the associations that arise among the host, the agent, and the environment (the epidemiologic triangle) to identify the primary triggers of the health challenge and produce strategies for control and prevention[20]. Conventional epidemiology has traditionally centered on persons and time, and less on place[21]. Not long ago, the spatial place at which epidemics emerge and disperse has become a critical element for understanding the dynamics of an epidemic. As a result, the interconnected fields of spatial epidemiology and health geography, which focus on explaining spatial heterogeneity of diseases by examining spatially explicit health outcomes and predictors, have emerged as novel approaches for the understanding and controlling epidemics.

The ability to understand and study the function of geographical places in health outcome dynamics has significantly improved in the past several years. This progress is mainly associated to innovations in geospatial methods such as spatial analysis and Geographical Information Systems (GIS)[22]. Together with the fast development of geospatial tools such as spatial analysis and GIS, vast quantities of spatial social, environmental and health data are currently available[23,24]. Geospatial analysis can be used to identify spatial information by recognizing relationships and drivers of disease distribution.

Epidemiological research has been fundamental for understanding health disparities and preventing an increasing incidence of major diseases. In epidemiological research, GIS has been used to study basic health and epidemiological indicators and tendencies among populations and regions. Such information is used for planning, implementation, and monitoring targeted health interventions[25,26]. GIS can also assess changes in resource allocation or environmental exposures in addition to mapping epidemiological measures such as incidence, prevalence and mortality, as well as risk factors and treatment options[26]. GIS can identify trends in access and uptake of healthcare interventions; it can also reveal unanticipated factors impacting vulnerable populations. Consequently, GIS identifies healthcare disparities and aids in equitable resource reallocation[27], and it is also used to characterize health-related economic and behavioral traits in specific populations to design geographically targeted interventions[28].

Spatial analysis in epidemiological research and disease surveillance has become a critical component of the decision-making process in the design and implementation of control interventions and prevention programs[29]. Spatial epidemiology has been used mostly for studying communicable, and relatively indirectly, non-communicable diseases. However, recently, its application has been expanded to study other public health and social issues, such as suicide and sexual violence[30-32].

EXAMPLES OF THE IMPLEMENTATION OF SPATIAL EPIDEMIOLOGY TO STUDY DISEASE BURDEN

Spatial epidemiology is now a critical tool in the battle against harmful epidemics such as HIV and malaria. The quantitative methods for assessing the impact of geographical hotspots (areas suffering an excessively large burden of the health challenge) and determinants of the ecological and individual-level transmission have facilitated the control of these diseases[33]. The detection of these areas can reveal the locations of high-risk populations in addition to exposing the causes that enable the spread and persistence of epidemics[34].

One of the most successful examples of the implementation of spatial epidemiology and GIS is the Malaria Atlas Project (MAP)[35], a project funded by the Bill and Melinda Gates Foundation and developed by Oxford University. MAP has focused on understanding the spatial distribution of malaria, particularly in sub-Saharan Africa (SSA). Using spatial epidemiology and disease mapping techniques, MAP has uncovered the spatial distribution of malaria with a high level of detail. The spatial information provided by MAP has become a key tool in the fight against malaria in SSA identifying geographical regions that should be targeted through control efforts. Similarly, successful approaches like the "Know your epidemic, know your response"; a framework implemented for counteracting HIV epidemics in the world[36], have centered on the development of targeted prevention strategies based on detailed knowledge of the spatial dynamics of the epidemic. Healthcare providers have developed and used high-resolution maps of the HIV distribution in SSA to implement geographically-targeted, cost-effective interventions[37,38].

SPATIAL EPIDEMIOLOGY OF SUD

Despite spatial epidemiology's positive impact, there is limited research focused on how it can be used to manage the SUD epidemic in the United States. Unlike the previous examples of malaria and HIV, SUD is not an infectious disease. However, the incidence of SUD is dependent on several socioeconomic and demographic health determinants such as gender, age, income, education, and access to healthcare among others, factors that are strongly connected to the geographical location of individuals and communities[39]. In this context, geographical place provides a foundation for understanding how substance use-related behaviors, treatment, and prevention relate to spatial features that compose the geographical space, from the individual to the community and regional scale. Within this framework, SUD is a negative health behavior shaped by a spatial context that includes local access and cost of substances, access to resources and services, emerging social networks, economic conditions and cultural norms, and other specific socioeconomic characteristics that either enhance or reduce the exposure to substance use in a given geographical place[40]. Moreover, the intensity and effectiveness of treatment and prevention strategies for SUD vary from place to place, reflecting social, economic, and political factors that intersect around the community environment. Thus, spatial research on SUD requires analysis in a geographical context at different scales.

GIS and geospatial analyses can be used as powerful tools in the study of the SUD epidemic. For example, the place of prescribing and dispensing opioids can be mapped and spatially analyzed, though illicit substance distribution is more complex as drugs can be transported between areas. Still, both licit and illicit distribution and demand can be locally defined, and thus could exhibit specific spatial patterns[41]. The location of identified harms can be used as a sign of where substances are used, which can be linked to the location of the markets. Such information can be used to identify flows of the substances from the moment of dispensing to the point of use. Some studies have mapped the locations of such harms[42], as well as to find spatial hotspots of harms[43], how these harms diffuse in space[44] and their relationships with several individual and area-level predictors[45]. Analyzing changes in the spatial patterns of SUD dynamics over time is also important for understanding the impact of policy adjustments on substance use. For example, how is SUD-related mortality linked to environmental and social risk factors? How do social and economic factors influence the prevalence of drug users? Are rates of specific drug use elevated around drug production markets? These fundamental inquiries about the epidemiology of SUD can be addressed using a spatial epidemiology approach. For example, this approach was implemented in a report from North Carolina that observed an ecological correlation between rates of admission to Emergency Departments from opioid overdoses and rates of opioid sales [45].

The common understanding that addiction does not discriminate and everyone is at risk ignores the fact that the frequency of SUD cases varies significantly in space and that cases are commonly clustered in places characterized by specific socioeconomic and demographic factors such as income, education, crime levels, access to care, drug availability among others. Thus, while the underlying physiological processes linked to addiction may not discriminate, several socioeconomic and environmental factors that expose individuals and communities to increased risk of substance use are not spatially random. Therefore, the identification of vulnerable populations and locations at higher risk of SUD, as well as the drivers of SUD epidemics, are key to improving health policies and developing effective spatially-targeted prevention strategies.

SPATIAL EPIDEMIOLOGY OF SUD IN THE UNITED STATES

The United States is the country with the highest incidence of SUD and the highest burden of opioid overdose-related mortality in the world (Figure 1). As a result, SUD has been declared a top public health priority in the country[46]. In an attempt to understand the reasons behind this burden, numerous studies have investigated multiple attributes of the SUD epidemic in the United States. A growing body of evidence has shown associations between demographic and socioeconomic factors with SUD outcomes[47-49]. Other studies have found a strong connection between drug supply and a rise in drug mortality rates. These data suggest that the SUD crisis in the United States has been driven by changes in the dynamics of drug supply, availability, and distribution. For example, the opioids overdose crisis can be explained by the rise in prescription opioids in the late 1990s and 2000s, more than by social or economic conditions[8,50]. As a result, policymakers in the United States have applied several strategies to reduce SUD-related mortality levels. These measures have focused on restrictions to drug availability, including regulating the prescription of opioids, attempts to restrict the influx of illicit opioids, and increasing access to naloxone, a medicine that rapidly reverses an opioid overdose[51-54]. Although these efforts have been moderately effective in reducing SUD-related mortality rates in general, other strategies like identifying the areas and vulnerable populations that are suffering the highest burden of the epidemic in the United States would improve the capacity to implement prevention strategies, which have been shown to be more effective in controlling other diseases than coercive intervention strategies alone[36].

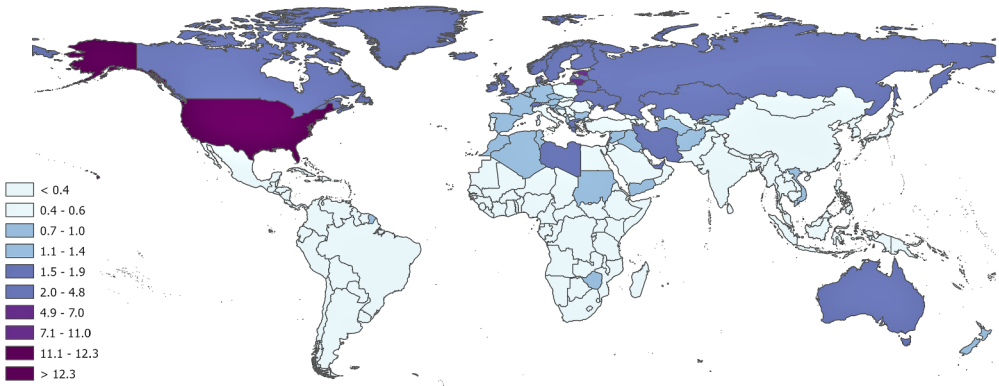

DOI: 10.12998/wjcc.v11.i11.2374

Figure 1 Death rates (number of deaths per 100000 individuals in 2019) from opioid overdoses in the world. Source: IHME, Global Burden of Disease, 2019 (https://www.healthdata.org/gbd/2019). Maps were generated using ArcGIS Pro. 2.8[86].

National data on SUD-related mortality have shown that the epidemic is not uniformly distributed within the United States[55]. The reasons behind the heterogeneous spatial distribution of the SUD epidemic within the country are relatively unknown. Although a link between illegal and prescription drug availability and SUD-related deaths has been described, the major reasons behind the sharp increase in the epidemic in specific areas remain incomplete[10]. In addition, the epidemiological characteristics of the SUD epidemic remain underexplored, what factors are boosting the epidemic, and where and what demographical groups are at higher risk in recent years[17,18], particularly at the local level[56,57]. Understanding the geographical distribution of SUD at this level of specificity may enable the implementation of public health intervention strategies and elucidate geographically specific risk management responses. It also facilitates the identification of contextual factors that contribute to and may increase the risk of drug misuse, including health-related, economic, socio-cultural, and local policy-relevant attributes. Geospatial analyses at this more granular local level could contextualize these individual and community factors linked to SUD and other risk behaviors[43].

Aligned with the "Know your epidemic, know your response" approach that has been successfully implemented to tackle the HIV epidemic[36], we previously conducted a detailed spatial analysis to identify the vulnerable populations and locations at higher risk of SUD-related mortality as well as the drivers of the current SUD epidemic in the United States[58]. Using a repertoire of interdisciplinary methods, including spatial epidemiology, disease mapping, and statistical modeling, we examined data provided by the Centers for Disease Control and Prevention on more than 22 million deaths from 2005 to 2017[59]. We obtained information about drug overdose deaths for persons aged five to 84 years to estimate SUD mortality rates in the United States. These rates included deaths caused by heroin, methadone, cocaine, opioids, synthetic narcotics, and unspecified narcotics. The main finding of this study is that the SUD epidemic in the United States is typified by the occurrence of several micro-epidemics of distinct intensities across geographical locations and demographic groups within the country. We found that White males, particularly those aged 25-34 years, had the highest risk of SUD-related death. Recently, there has been a rapid rise of the SUD epidemic in the Black male population, with a rapid increase in the SUD-related mortality rate in this group since 2014, reaching a death rate similar to that for White males in 2017. The temporal dynamics of the epidemic can be the result of changes in the substances driving the epidemic, switching from prescription opioids mostly affecting the White male population to more readily available synthetic opioids leading to the latest phase of the epidemic and affecting the Black male population.

The notable disparity among gender and racial groups could be associated with the temporal trend associated with three different waves in the SUD epidemic[60]. Briefly, the first epidemic wave from 1970 to 1999 was driven by heroin overdoses, which affected the Black population at higher rates than other racial populations. Prescription opioids frequently used for pain management therapy served as the primary driver of the second wave, which spanned the years from 1999 to 2010 and caused a more pronounced rise in death rates among White people[61,62]. The emergence of synthetic opioids and the combination of prescription opioids are primarily blamed for the third and most current wave[63]. This most recent wave has revealed a comparable increase in both racial groupings across the country (White and Black)[61].

Further analysis revealed that the epidemic is concentrated in specific geographic areas located in the West and Midwest regions (Figure 2A). The majority of SUD-related deaths occurred in regions of the Midwest around the tri-state border of Kentucky, Ohio, and West Virginia. Southern Pacific and mountain states, including California, Colorado, Nevada, New Mexico, and Utah, are other regions with a high proportion of SUD-related mortality. The spatial structure of the epidemic in the White population had a similar pattern as observed for the general population (Figure 2B). In contrast, the

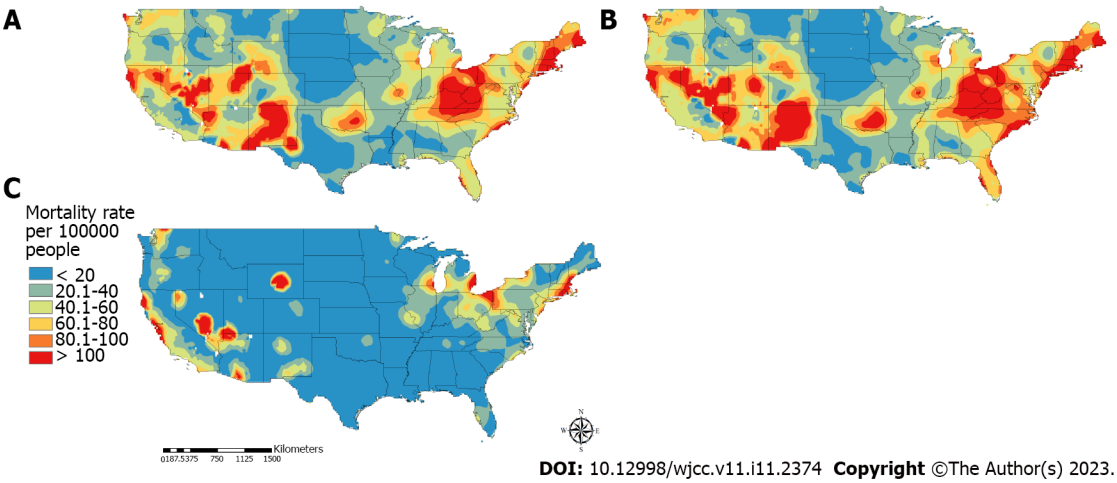

DOI: 10.12998/wjcc.v11.i11.2374

Figure 2 Spatial distribution of the substance use disorder related mortality. A: The general population; B: White population; C: Black population in the contiguous United States. Maps were generated using ArcGIS Pro. 2.8[86].

epidemic in the Black population was concentrated in the mid-Atlantic and Northeast (*e.g.*, Connecticut, Rhode Island, Massachusetts, and New Hampshire) and the West (*e.g.*, California, Nevada, and Arizona) (Figure 2C).

It is important to note that, as the United States Department of Health and Human Services declared in 2018[64], overdoses caused by synthetic opioids (such as fentanyl and analogs) are developing into a nationwide public health disaster. Opioid overdose deaths frequently result from prior drug use, which frequently starts between the ages of 18 and 25[63]. Teenagers who have a history of substance abuse are 10 times more likely than other teenagers to have drug use disorders in the future[60]. People between the ages of 25 and 44 may start taking opioids for recreational or therapeutic purposes before switching to more affordable drugs like fentanyl[65]. Our findings, which indicate that the young adult population (25–39 years) was bearing the greatest burden of opioid overdose deaths and was likely in the latter stage of an opioid use disorder history, are consistent with this early onset of substance addiction.

These comprehensive geographical and epidemiological descriptions of the vulnerable populations at high risk of the SUD epidemic in the United States can be applied to generate spatially targeted prevention strategies and intervention campaigns. Geospatial approaches and data visualization technologies (*e.g.*, GIS maps) generate unique opportunities for the early detection of the impacts of highly affected areas and then assess, diagnose, and treat those vulnerable communities affected by this health challenge. Geospatial data acquired from GIS maps support the visualization of SUD events that can be rapidly analyzed, permitting the detection of patterns and the creation of plans to monitor trends in data and co-locate needs and resources[66]. The development of targeted, integrated, preventive strategies for the early identification of substance use in the vulnerable populations nationwide would be made possible by micro-targeting strategies based on an understanding of the spatial assembly and the multifactorial characterization of the addiction epidemic[6,67]. Such strategies have been shown to be successful in areas in New York City and Cambridge, MA, that are highly affected by SUD. In these areas, geospatial analyses have been used to identify priority targets for the deployment of naloxone as a key element of their SUD intervention programs[68,69].

GEOGRAPHICAL PROFILE OF THE OPIOID OVERDOSE EPIDEMIC IN OHIO

Spatial variation of health outcomes occurs at different scales, from a large national level to a local scale. Similarly, the drivers of disease distribution can influence the spatial structure of epidemics at different scales. As we have shown in the previous section, the SUD crisis in the United States is not homogeneously distributed across the country. For example, national data on SUD overdose mortality rates have shown that 20 states and the District of Columbia have reported SUD-related mortality rates that are statistically higher than the national rate. In particular, West Virginia (57.8 SUD-related deaths per 100000 persons), Ohio (46.3), Pennsylvania (44.3), the District of Columbia (44.0), and Kentucky (37.2) experienced the highest death rates in 2017[70]. Therefore, a more detailed local description of the epidemic can uncover local drivers of the epidemic in each of these affected areas. As a result, a more thorough local description of the epidemic can reveal the outbreak's regional causes in each of these impacted locations. As previously indicated, opioids are the leading cause of SUD-related mortality in the nation, accounting for over 75% of all drug overdose deaths in 2020[4]. Ohio is one of eight states where the opioid mortality rate doubled between 1999 and 2019, with data being released every three

years. Unintentional drug overdose deaths in Ohio have reached record highs, especially those caused by synthetic opioids[7,71].

In a previous study[72], we analyzed the geographical and temporal dynamics of the opioid overdose epidemic in Ohio using data from the Ohio Department of Health. We examined data on more than 11000 opioid related death cases in Ohio occurring from 2010 to 2016. We found that the opioid overdose epidemic in Ohio was located in specific areas (hotspots) and affected limited demographic groups during this time period. There was a fast surge in prescription opioid death rates among the White male population aged 30-39 years and a rise of the epidemic in the Black male population. White males had the highest mortality rate caused by opioid overdose deaths with 43.7 deaths/100000 persons, followed by Black males with 27.3 deaths/100000 persons, and in general, the opioid overdose mortality rate was exponentially increasing in all of these groups from 2010 to 2016 (Figure 3).

The geospatial analysis conducted suggested that most of the deaths were geographically clustered within the Ohio counties of Butler, Clark, Clermont, Cuyahoga, Franklin, Hamilton, Marion, and Montgomery (Figure 4A), where the average mortality rate caused by opioid overdose was more than eight times higher (199/100000 persons) than the state average (29/100000 persons). These results support our observations that, comparable to the national patterns observed, the opioid overdose epidemic in Ohio is concentrated in geographic hotspot areas and vulnerable populations at risk of opioid overdose. Figure 4A also illustrates the distribution of pharmacies that dispense naloxone in Ohio. There is a high density of pharmacies in the main cities and metropolitan areas of Cincinnati, Columbus, and Cleveland. In further analyses, we found that the average distance between opioid overdose death locations and the nearest pharmacy dispensing naloxone was 3.15 km (1.96 mi). We estimated that in 14% of Ohio, the nearest pharmacy with an established protocol for naloxone dispensing was located more than 10 km (6.2 mi) away from the location of the opioid overdose death. We also identified counties (*e.g.*, Ross, Hocking, Pike, Jackson, Vinton, and Gallia) that had high mortality rates but low density of pharmacies (Figure 4B). These results identified specific underserved areas for naloxone distribution characterized by high SUD mortality rates that would benefit from an increase in the response capacity for these areas.

Overall, these findings highlight the necessity of concentrating local public health initiatives on vulnerable populations and high-risk locations in order to not only contain the current SUD epidemic in Ohio but also to educate other states across the nation experiencing comparable local epidemics. It's possible that the opioid overdose epidemic will keep growing. Therefore, to combat the epidemic's present rising phase, it is essential to recognize economic, social, and health determinants[73]. The opioid crisis is a complicated epidemic that may have been started by unchecked prescribing of painkillers. Nevertheless, it has also recently been fueled by the introduction of synthetic opioids intended for recreational use, particularly fentanyl and its analogs. It's important to emphasize that in order to highlight the local spatial differences of the SUD epidemic, we only included data from January 2011 to December 2016 in the instances presented here. According to reports, there was a decline in opioid overdose deaths in Ohio beginning in the final semester of 2017 and early 2018, followed by a rebound in 2019 and 2020. This is thought to be due to the availability of more potent drugs such as carfentanyl on the state's and the nation's black market[74,75].

CONCLUSION

The role of spatial epidemiology and geographic methods for the study of drug abuse continues to grow. The combination of geographical and epidemiological research methods focused on human and social environment interactions is essential to gain a better understanding of drug use issues and their inherent complexities. The use of geospatial analysis to target areas with high SUD risk can allow for a more comprehensive understanding of the socioeconomic and demographic drivers of the SUD epidemic in the United States. While the SUD epidemic still disproportionately affects higher-poverty areas and racial minorities, SUD-associated deaths have become more dispersed across broader geographic areas and sociodemographic groups.

In this narrative minireview, we summarized current research that applied geospatial techniques to the study of the ongoing SUD epidemic in the United States. SUD rates may continue to increase over time, and different areas and populations are affected with different intensities by this epidemic in the country. While socioeconomic or geographic characteristics of specific neighborhoods can contribute to the impact of the SUD epidemic in vulnerable communities in the country at different intensities[42,76,77], specific social, geographical, and economic determinants are numerous and the ability to isolate one variable is still challenging[77-79]. Therefore, identifying who is most likely to be affected and where they are located is critical to effectively confront this epidemic[73].

Strategies to tackle the SUD epidemic include identifying the demographic and socioeconomic drivers of the epidemic and targeting improved interventions and access to them (*e.g.*, access to naloxone). Furthermore, the establishment of safe places for regulated drug use can help to prevent death and avoid the spread of other diseases[73,80]. There are several challenges, however, such as the constrained geography of most of the studies: Most have been conducted in major metropolitan areas,

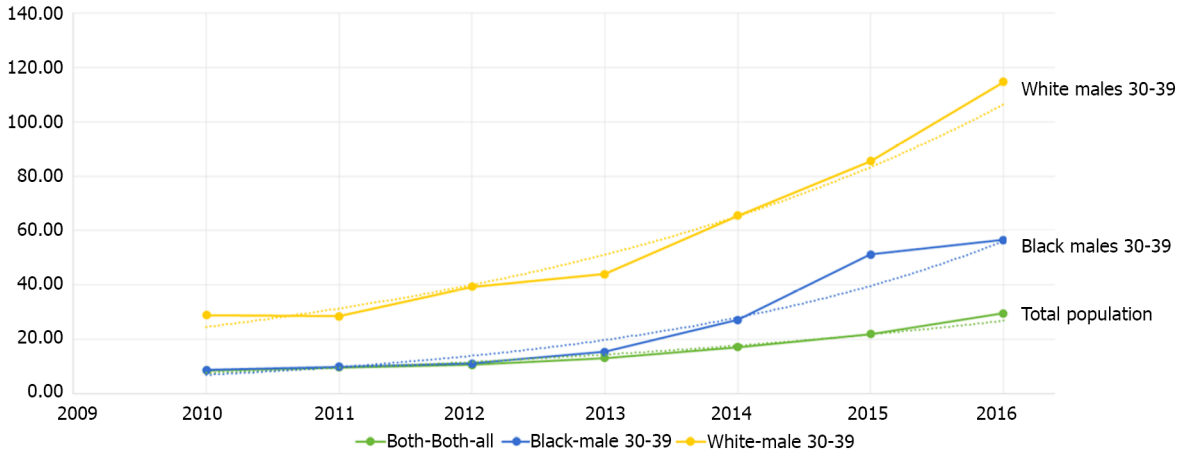

DOI: 10.12998/wjcc.v11.i11.2374

Figure 3 Temporal dynamics of the opioids overdose epidemic in Ohio (2010–2016) in the total population and in the most affected populations. The highest prescription opioid overdose mortality rates were found in the White male population aged 30-39 years, with 125 deaths/100000 persons, followed by Black males of same age, with 57 deaths/100000 persons compared to the 29 deaths/100000 persons for the total population in 2016. Dashed lines illustrated the fitted exponential curve for each growth rate. Plot was created using the software environment R[87].

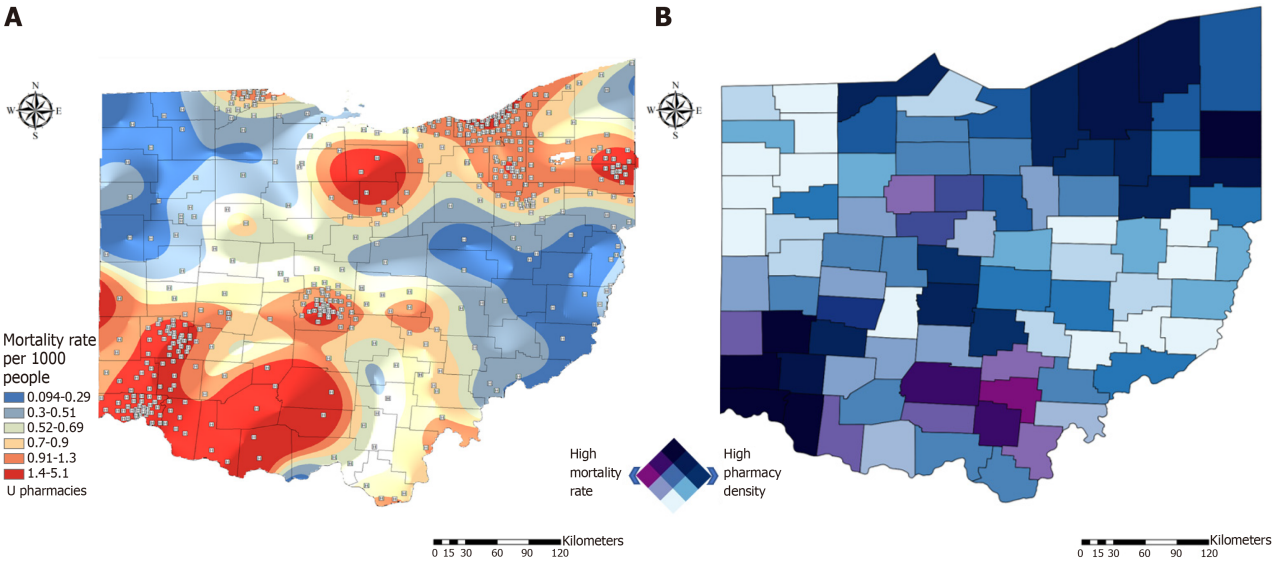

DOI: 10.12998/wjcc.v11.i11.2374

Figure 4 Spatial distribution of the opioid overdose epidemic in Ohio. A: Spatial distribution of opioids overdose mortality rate in Ohio; B: Bivariate map illustrating counties with high opioid overdose mortality rate (purple) and high density of pharmacies (blue). Counties in dark color have both high opioids overdose mortality and density of pharmacies dispensing naloxone. Maps were generated using ArcGIS Pro. 2.8[86].

which have been heavily affected by the epidemic. Still, substance abuse is certainly not limited to these places. The impact of the SUD epidemic in small towns and rural areas is understudied. Spatial techniques such as GIS are needed to learn more about these areas[81]. Measuring the SUD epidemic at the local level is a challenge that has significant consequences on resource allocation.

Furthermore, geospatial analyses are usually ecologic studies that cannot account for decedent characteristics, including duration of county residence, and data aggregation precludes the inclusion of information such as race/ethnicity, sex, and age and the subsequent identification of important demographic variation in the epidemic[82]. Associations between the risk factors and SUD-related mortality rates may vary across groups[83]. Likewise, adults and adolescents may display distinct spatial trends and need unique interventions and resources, making it important to examine the problem at different demographic scales[84]. Promising advances in geospatial methods are making this possible, but more work is necessary to identify the methods and to analyze the results of their applications.

The federal, state, and local governments in the United States have implemented a number of intervention strategies to lower the mortality rates associated with SUD, including initiatives to reduce the flow of illegal opioids, restrictions on the prescription of opioids, and increased access to naloxone.

While efforts like these and others have been somewhat successful in lowering overdose mortality rates overall, pinpointing the regions and populations most vulnerable to the various sub-epidemics would make it easier to plan prevention and control campaigns, which have been shown to be more successful in combating other diseases than broad intervention strategies alone[36]. Furthermore, identifying the extent to which geographical factors and social context are interrelated is a key step to generate a more comprehensive understanding of the SUD epidemic. All domains of the SUD epidemic including demand, supply, harms and harm reduction, can have a distinct geographic dimension[41]. As a result, the geographical and epidemiological identification of vulnerable groups in the United States at high risk of SUD-related mortality presented in this minireview can be used to develop geotargeted preventative strategies and intervention initiatives. Targeted tactics based on a knowledge of the geographical structure and multidimensional character of the addiction epidemic would aid in the development of coherent preventive treatments for early diagnosis in the young adult population[6,67,85,86]. Nonetheless, there is an undeniable need for more comprehensive initiatives targeted at understanding the epidemic, such as a focus on possible disparities among demographic groups and locations with vulnerable populations at high risk of drug use.

FOOTNOTES

Author contributions: Cuadros DF contribute to the conceptual idea and wrote the first draft of the paper; Branscum AJ, Moreno CM, and MacKinnon NJ contributed to the conceptual idea and helped to write the manuscript.

Conflict-of-interest statement: All the authors report no relevant conflicts of interest for this article.

Country/Territory of origin: United States

ORCID number: Diego F Cuadros 0000-0001-7060-4203.

S-Editor: Fan JR
L-Editor: A
P-Editor: Fan JR

REFERENCES

1 **Chen S**, Ma Y, Cai W, Moretta T, Wang X, Liu T, Potenza MN. Factorial validity of a substance-use stigma scale in methamphetamine-using adults in China. *Drug Alcohol Depend* 2020; **206**: 107677 [PMID: 31732296 DOI: 10.1016/j.drugalcdep.2019.107677]
2 **American Society of Addiction Medicine (ASAM)**. Public Policy Statement: Long Definition of Addiction, 2019. Available from: https://academic.oup.com/book/29516/chapter-abstract/248088740?redirectedFrom=fulltext
3 **CDC**. National Center for Health Statistics Mortality Data on CDC WONDER. 2022. Available from: https://wonder.cdc.gov/Deaths-by-Underlying-Cause.html
4 **NIH**. Overdose Death Rates. 2022. Available from: https://www.nih.gov/
5 **Olfson M**, Rossen LM, Wall MM, Houry D, Blanco C. Trends in Intentional and Unintentional Opioid Overdose Deaths in the United States, 2000-2017. *JAMA* 2019; **322**: 2340-2342 [PMID: 31846008 DOI: 10.1001/jama.2019.16566]
6 **Rigg KK**, Monnat SM, Chavez MN. Opioid-related mortality in rural America: Geographic heterogeneity and intervention strategies. *Int J Drug Policy* 2018; **57**: 119-129 [PMID: 29754032 DOI: 10.1016/j.drugpo.2018.04.011]
7 **Kiang MV**, Basu S, Chen J, Alexander MJ. Assessment of Changes in the Geographical Distribution of Opioid-Related Mortality Across the United States by Opioid Type, 1999-2016. *JAMA Netw Open* 2019; **2**: e190040 [PMID: 30794299 DOI: 10.1001/jamanetworkopen.2019.0040]
8 **Ruhm CJ**. Geographic Variation in Opioid and Heroin Involved Drug Poisoning Mortality Rates. *Am J Prev Med* 2017; **53**: 745-753 [PMID: 28797652 DOI: 10.1016/j.amepre.2017.06.009]
9 **Unick GJ**, Ciccarone D. US regional and demographic differences in prescription opioid and heroin-related overdose hospitalizations. *Int J Drug Policy* 2017; **46**: 112-119 [PMID: 28688539 DOI: 10.1016/j.drugpo.2017.06.003]
10 **Stopka TJ**, Amaravadi H, Kaplan AR, Hoh R, Bernson D, Chui KKH, Land T, Walley AY, LaRochelle MR, Rose AJ. Opioid overdose deaths and potentially inappropriate opioid prescribing practices (PIP): A spatial epidemiological study. *Int J Drug Policy* 2019; **68**: 37-45 [PMID: 30981166 DOI: 10.1016/j.drugpo.2019.03.024]
11 **Compton WM**, Gfroerer J, Conway KP, Finger MS. Unemployment and substance outcomes in the United States 2002-2010. *Drug Alcohol Depend* 2014; **142**: 350-353 [PMID: 25042761 DOI: 10.1016/j.drugalcdep.2014.06.012]
12 **Langabeer JR**, Chambers KA, Cardenas-Turanzas M, Champagne-Langabeer T. County-level factors underlying opioid

mortality in the United States. *Subst Abus* 2022; **43**: 76-82 [PMID: 32186475 DOI: 10.1080/08897077.2020.1740379]
13 **Acharya A**, Izquierdo AM, Gonçalves SF, Bates RA, Taxman FS, Slawski MP, Rangwala HS, Sikdar S. Exploring county-level spatio-temporal patterns in opioid overdose related emergency department visits. *PLoS One* 2022; **17**: e0269509 [PMID: 36584000 DOI: 10.1371/journal.pone.0269509]
14 **Schoenfeld ER**, Leibowitz GS, Wang Y, Chen X, Hou W, Rashidian S, Saltz MM, Saltz JH, Wang F. Geographic, Temporal, and Sociodemographic Differences in Opioid Poisoning. *Am J Prev Med* 2019; **57**: 153-164 [PMID: 31227281 DOI: 10.1016/j.amepre.2019.03.020]
15 **Dean A**, Kimmel S. Free trade and opioid overdose death in the United States. *SSM Popul Health* 2019; **8**: 100409 [PMID: 31309136 DOI: 10.1016/j.ssmph.2019.100409]
16 **Haffajee RL**, Lin LA, Bohnert ASB, Goldstick JE. Characteristics of US Counties With High Opioid Overdose Mortality and Low Capacity to Deliver Medications for Opioid Use Disorder. *JAMA Netw Open* 2019; **2**: e196373 [PMID: 31251376 DOI: 10.1001/jamanetworkopen.2019.6373]
17 **James K**, Jordan A. The Opioid Crisis in Black Communities. *J Law Med Ethics* 2018; **46**: 404-421 [PMID: 30146996 DOI: 10.1177/1073110518782949]
18 **Blangiardo M**, Cameletti M, Baio G, Rue H. Spatial and spatio-temporal models with R-INLA. *Spat Spatiotemporal Epidemiol* 2013; **4**: 33-49 [PMID: 23481252 DOI: 10.1016/j.sste.2012.12.001]
19 **Krieger N**. Epidemiology and the people's health: theory and context. Oxford University Press, 2011
20 **Mcanally HB**. Opioid dependence: a clinical and epidemiologic approach. *Springer* 2017 [DOI: 10.1007/978-3-319-47497-7_1]
21 **Moore DA**, Carpenter TE. Spatial analytical methods and geographic information systems: use in health research and epidemiology. *Epidemiol Rev* 1999; **21**: 143-161 [PMID: 10682254 DOI: 10.1093/oxfordjournals.epirev.a017993]
22 **Rushton G**. Public health, GIS, and spatial analytic tools. *Annu Rev Public Health* 2003; **24**: 43-56 [PMID: 12471269 DOI: 10.1146/annurev.publhealth.24.012902.140843]
23 **Nykiforuk CI**, Flaman LM. Geographic information systems (GIS) for Health Promotion and Public Health: a review. *Health Promot Pract* 2011; **12**: 63-73 [PMID: 19546198 DOI: 10.1177/1524839909334624]
24 **Thomas YF**, Richardson D, Cheung I. Geography and drug addiction. New York: Springer Science and Business Media, 2008
25 **Musa GJ**, Chiang PH, Sylk T, Bavley R, Keating W, Lakew B, Tsou HC, Hoven CW. Use of GIS Mapping as a Public Health Tool-From Cholera to Cancer. *Health Serv Insights* 2013; **6**: 111-116 [PMID: 25114567 DOI: 10.4137/HSI.S10471]
26 **Higgs G**. A literature review of the use of GIS-based measures of access to health care services. *Health Serv Outcomes Res Methodol* 2004; **5**: 119-139 [DOI: 10.1007/s10742-005-4304-7]
27 **Jones AP**, Haynes R, Sauerzapf V, Crawford SM, Zhao H, Forman D. Travel time to hospital and treatment for breast, colon, rectum, lung, ovary and prostate cancer. *Eur J Cancer* 2008; **44**: 992-999 [PMID: 18375117 DOI: 10.1016/j.ejca.2008.02.001]
28 **Dermatis Z**, Tsoromokos D, Gozadinos F, Lazakidou A. The utilization of geographic information systems in healthcare. *Int J Health Res Innov* 2016; **4** [DOI: 10.1007/978-3-319-23341-3_4]
29 **Rytkönen MJ**. Not all maps are equal: GIS and spatial analysis in epidemiology. *Int J Circumpolar Health* 2004; **63**: 9-24 [PMID: 15139238 DOI: 10.3402/ijch.v63i1.17642]
30 **Fontanella CA**, Saman DM, Campo JV, Hiance-Steelesmith DL, Bridge JA, Sweeney HA, Root ED. Mapping suicide mortality in Ohio: A spatial epidemiological analysis of suicide clusters and area level correlates. *Prev Med* 2018; **106**: 177-184 [PMID: 29133266 DOI: 10.1016/j.ypmed.2017.10.033]
31 **Kelling C**, Graif C, Korkmaz G, Haran M. Modeling the Social and Spatial Proximity of Crime: Domestic and Sexual Violence Across Neighborhoods. *J Quant Criminol* 2021; **37**: 481-516 [PMID: 34149156 DOI: 10.1007/s10940-020-09454-w]
32 **Tomita A**, Cuadros DF, Gibbs A. Syndemics of intimate partner violence among women in HIV endemic South Africa: geospatial analysis of nationally representative data. *Sci Rep* 2022; **12**: 18083 [PMID: 36302814 DOI: 10.1038/s41598-022-20230-7]
33 **Cuadros DF**, Awad SF, Abu-Raddad LJ. Mapping HIV clustering: a strategy for identifying populations at high risk of HIV infection in sub-Saharan Africa. *Int J Health Geogr* 2013; **12**: 28 [PMID: 23692994 DOI: 10.1186/1476-072X-12-28]
34 **Ostfeld RS**, Glass GE, Keesing F. Spatial epidemiology: an emerging (or re-emerging) discipline. *Trends Ecol Evol* 2005; **20**: 328-336 [PMID: 16701389 DOI: 10.1016/j.tree.2005.03.009]
35 **Hay SI**, Snow RW. The malaria Atlas Project: developing global maps of malaria risk. *PLoS Med* 2006; **3**: e473 [PMID: 17147467 DOI: 10.1371/journal.pmed.0030473]
36 **Wilson D**, Halperin DT. "Know your epidemic, know your response": a useful approach, if we get it right. *Lancet* 2008; **372**: 423-426 [PMID: 18687462 DOI: 10.1016/S0140-6736(08)60883-1]
37 **Cuadros DF**, Li J, Branscum AJ, Akullian A, Jia P, Mziray EN, Tanser F. Mapping the spatial variability of HIV infection in Sub-Saharan Africa: Effective information for localized HIV prevention and control. *Sci Rep* 2017; **7**: 9093 [PMID: 28831171 DOI: 10.1038/s41598-017-09464-y]
38 **Dwyer-Lindgren L**, Cork MA, Sligar A, Steuben KM, Wilson KF, Provost NR, Mayala BK, VanderHeide JD, Collison ML, Hall JB, Biehl MH, Carter A, Frank T, Douwes-Schultz D, Burstein R, Casey DC, Deshpande A, Earl L, El Bcheraoui C, Farag TH, Henry NJ, Kinyoki D, Marczak LB, Nixon MR, Osgood-Zimmerman A, Pigott D, Reiner RC Jr, Ross JM, Schaeffer LE, Smith DL, Davis Weaver N, Wiens KE, Eaton JW, Justman JE, Opio A, Sartorius B, Tanser F, Wabiri N, Piot P, Murray CJL, Hay SI. Mapping HIV prevalence in sub-Saharan Africa between 2000 and 2017. *Nature* 2019; **570**: 189-193 [PMID: 31092927 DOI: 10.1038/s41586-019-1200-9]
39 **Dijkstra A**, Hak E, Janssen F. A systematic review of the application of spatial analysis in pharmacoepidemiologic research. *Ann Epidemiol* 2013; **23**: 504-514 [PMID: 23830932 DOI: 10.1016/j.annepidem.2013.05.015]
40 **Merikangas KR**, McClair VL. Epidemiology of substance use disorders. *Hum Genet* 2012; **131**: 779-789 [PMID: 22543841 DOI: 10.1007/s00439-012-1168-0]

41 **Mazumdar S**, Mcrae IS, Islam MM. How Can Geographical Information Systems and Spatial Analysis Inform a Response to Prescription Opioid Misuse? *Curr Drug Abuse Rev* 2015; **8**: 104-110 [PMID: 26452451 DOI: 10.2174/1874473708021509281853 02]

42 **Cerdá M**, Ransome Y, Keyes KM, Koenen KC, Tracy M, Tardiff KJ, Vlahov D, Galea S. Prescription opioid mortality trends in New York City, 1990-2006: examining the emergence of an epidemic. *Drug Alcohol Depend* 2013; **132**: 53-62 [PMID: 23357743 DOI: 10.1016/j.drugalcdep.2012.12.027]

43 **Brownstein JS**, Green TC, Cassidy TA, Butler SF. Geographic information systems and pharmacoepidemiology: using spatial cluster detection to monitor local patterns of prescription opioid abuse. *Pharmacoepidemiol Drug Saf* 2010; **19**: 627-637 [PMID: 20535759 DOI: 10.1002/pds.1939]

44 **Frischer M**, Anderson S, Hickman M, Heatlie H. Diffusion of drug misuse in Scotland: Findings from the 1993 and 1996 Scottish Crime Surveys. *Addict Res Theory* 2002; **10**: 83-96 [DOI: 10.1046/j.1360-0443.2001.9610146510.x]

45 **Modarai F**, Mack K, Hicks P, Benoit S, Park S, Jones C, Proescholdbell S, Ising A, Paulozzi L. Relationship of opioid prescription sales and overdoses, North Carolina. *Drug Alcohol Depend* 2013; **132**: 81-86 [PMID: 23399467 DOI: 10.1016/j.drugalcdep.2013.01.006]

46 **Schulden JD**, Thomas YF, Compton WM. Substance abuse in the United States: findings from recent epidemiologic studies. *Curr Psychiatry Rep* 2009; **11**: 353-359 [PMID: 19785975 DOI: 10.1007/s11920-009-0053-6]

47 **Frasquilho D**, Matos MG, Salonna F, Guerreiro D, Storti CC, Gaspar T, Caldas-de-Almeida JM. Mental health outcomes in times of economic recession: a systematic literature review. *BMC Public Health* 2016; **16**: 115 [PMID: 26847554 DOI: 10.1186/s12889-016-2720-y]

48 **Hempstead KA**, Phillips JA. Rising suicide among adults aged 40-64 years: the role of job and financial circumstances. *Am J Prev Med* 2015; **48**: 491-500 [PMID: 25736978 DOI: 10.1016/j.amepre.2014.11.006]

49 **Kerr WC**, Kaplan MS, Huguet N, Caetano R, Giesbrecht N, McFarland BH. Economic Recession, Alcohol, and Suicide Rates: Comparative Effects of Poverty, Foreclosure, and Job Loss. *Am J Prev Med* 2017; **52**: 469-475 [PMID: 27856114 DOI: 10.1016/j.amepre.2016.09.021]

50 **Masters RK**, Tilstra AM, Simon DH. Mortality from Suicide, Chronic Liver Disease, and Drug Poisonings among Middle-Aged U.S. White Men and Women, 1980-2013. *Biodemography Soc Biol* 2017; **63**: 31-37 [PMID: 28287304 DOI: 10.1080/19485565.2016.1248892]

51 **Sugarman OK**, Bachhuber MA, Wennerstrom A, Bruno T, Springgate BF. Interventions for incarcerated adults with opioid use disorder in the United States: A systematic review with a focus on social determinants of health. *PLoS One* 2020; **15**: e0227968 [PMID: 31961908 DOI: 10.1371/journal.pone.0227968]

52 **Timko C**, Valenstein H, Lin PY, Moos RH, Stuart GL, Cronkite RC. Addressing substance abuse and violence in substance use disorder treatment and batterer intervention programs. *Subst Abuse Treat Prev Policy* 2012; **7**: 37 [PMID: 22958624 DOI: 10.1186/1747-597X-7-37]

53 **MacCoun R**, Reuter P. Drug control. Stanford: The handbook of crime and punishment, 1998: 207-238

54 **Sacks DW**, Hollingsworth A, Nguyen T, Simon K. Can policy affect initiation of addictive substance use? *J Health Econ* 2021; **76**: 102397 [PMID: 33383263 DOI: 10.1016/j.jhealeco.2020.102397]

55 **Jalal H**, Buchanich JM, Roberts MS, Balmert LC, Zhang K, Burke DS. Changing dynamics of the drug overdose epidemic in the United States from 1979 through 2016. *Science* 2018; **361** [PMID: 30237320 DOI: 10.1126/science.aau1184]

56 **Forrester MB**. Oxycodone abuse in Texas, 1998-2004. *J Toxicol Environ Health A* 2007; **70**: 534-538 [PMID: 17365606 DOI: 10.1080/15287390600870924]

57 **Havens JR**, Talbert JC, Walker R, Leedham C, Leukefeld CG. Trends in controlled-release oxycodone (OxyContin) prescribing among Medicaid recipients in Kentucky, 1998-2002. *J Rural Health* 2006; **22**: 276-278 [PMID: 16824176 DOI: 10.1111/j.1748-0361.2006.00046.x]

58 **Hernández A**, Lan M, MacKinnon NJ, Branscum AJ, Cuadros DF. "Know your epidemic, know your response": Epidemiological assessment of the substance use disorder crisis in the United States. *PLoS One* 2021; **16**: e0251502 [PMID: 34038441 DOI: 10.1371/journal.pone.0251502]

59 **National Center for Health**. Mortality Multiple Cause Data Files. In: Centers for Disease Control and Prevention, US Department of Health and Human Services, editors. United States, 2005-2017

60 **Mohammad JS**, Botticelli M, Hwang R, Koh HK, McHugh RK. The Opioid Crisis: A Contextual Framework and Call for Systems Science Research. Working paper. Available from: https://scholar.harvard.edu/files/jalali/files/the_opioid_crisis_preprint.pdf

61 **Alexander MJ**, Kiang MV, Barbieri M. Trends in Black and White Opioid Mortality in the United States, 1979-2015. *Epidemiology* 2018; **29**: 707-715 [PMID: 29847496 DOI: 10.1097/EDE.0000000000000858]

62 **Hadland SE**, Rivera-Aguirre A, Marshall BDL, Cerdá M. Association of Pharmaceutical Industry Marketing of Opioid Products With Mortality From Opioid-Related Overdoses. *JAMA Netw Open* 2019; **2**: e186007 [PMID: 30657529 DOI: 10.1001/jamanetworkopen.2018.6007]

63 **Ciccarone D**. The triple wave epidemic: Supply and demand drivers of the US opioid overdose crisis. *Int J Drug Policy* 2019; **71**: 183-188 [PMID: 30718120 DOI: 10.1016/j.drugpo.2019.01.010]

64 **The White House**. Ending Americas Opioid Crisis. 2018 Available from: https://academic.oup.com/book/32440/chapter-abstract/268773308?redirectedFrom=fulltext

65 **Spencer MR**, Warner M, Bastian BA, Trinidad JP, Hedegaard H. Drug Overdose Deaths Involving Fentanyl, 2011-2016. *Natl Vital Stat Rep* 2019; **68**: 1-19 [PMID: 31112123]

66 **Anwar T**, Duever M, Jayawardhana J. Access to methadone clinics and opioid overdose deaths in Georgia: A geospatial analysis. *Drug Alcohol Depend* 2022; **238**: 109565 [PMID: 35839618 DOI: 10.1016/j.drugalcdep.2022.109565]

67 **Holmes CB**, Rabkin M, Ford N, Preko P, Rosen S, Ellman T, Ehrenkranz P. Tailored HIV programmes and universal health coverage. *Bull World Health Organ* 2020; **98**: 87-94 [PMID: 32015578 DOI: 10.2471/BLT.18.223495]

68 **Hallas D**, Klar RT, Baldyga JA, Rattner I, Waingortin R, Fletcher J. Traditional and Nontraditional Collaborations to Improve Population Health Using Geospatial Information SystemMaps: Analysis of the Opioid Crisis. *J Pediatr Health Care* 2019; **33**: 309-322 [PMID: 30902507 DOI: 10.1016/j.pedhc.2018.10.006]

69 **Dworkis DA**, Weiner SG, Liao VT, Rabickow D, Goldberg SA. Geospatial Clustering of Opioid-Related Emergency Medical Services Runs for Public Deployment of Naloxone. *West J Emerg Med* 2018; **19**: 641-648 [PMID: 30013698 DOI: 10.5811/westjem.2018.4.37054]

70 **Hedegaard H**, Miniño AM, Warner M. Drug Overdose Deaths in the United States, 1999–2017. NCHS Data Brief: National Center for Health Statistics, 2018. Available from: https://stacks.cdc.gov/view/cdc/112340

71 **Ohio Opioid Summary (March 2019)**. National Institute on Drug Abuse (NIDA), 2019. Available from: https://nida.nih.gov/drug-topics/publications/drug-facts

72 **Hernandez A**, Branscum AJ, Li J, MacKinnon NJ, Hincapie AL, Cuadros DF. Epidemiological and geospatial profile of the prescription opioid crisis in Ohio, United States. *Sci Rep* 2020; **10**: 4341 [PMID: 32152360 DOI: 10.1038/s41598-020-61281-y]

73 **Feinberg J**. Tackle the epidemic, not the opioids. *Nature* 2019; **573**: 165 [PMID: 31501585 DOI: 10.1038/d41586-019-02671-9]

74 **Goodnough A**. This City's Overdose Deaths Have Plunged. Can Others Learn From It? *New York Times* 2018 [DOI: 10.1002/catl.30440]

75 **Guy GJ**, Haegerich T, Evans M, Losby J, Young R, Jones C. Vital Signs: Pharmacy-Based Naloxone Dispensing — United States, 2012–2018. *MMWR Morb Mortal Wkly Rep* 2019; 2019 [DOI: 10.15585/mmwr.mm6831e1]

76 **Visconti AJ**, Santos GM, Lemos NP, Burke C, Coffin PO. Opioid Overdose Deaths in the City and County of San Francisco: Prevalence, Distribution, and Disparities. *J Urban Health* 2015; **92**: 758-772 [PMID: 26077643 DOI: 10.1007/s11524-015-9967-y]

77 **Cerdá M**, Ransome Y, Keyes KM, Koenen KC, Tardiff K, Vlahov D, Galea S. Revisiting the role of the urban environment in substance use: the case of analgesic overdose fatalities. *Am J Public Health* 2013; **103**: 2252-2260 [PMID: 24134362 DOI: 10.2105/AJPH.2013.301347]

78 **Green CR**, Ndao-Brumblay SK, West B, Washington T. Differences in prescription opioid analgesic availability: comparing minority and white pharmacies across Michigan. *J Pain* 2005; **6**: 689-699 [PMID: 16202962 DOI: 10.1016/j.jpain.2005.06.002]

79 **Burgess DJ**, Phelan S, Workman M, Hagel E, Nelson DB, Fu SS, Widome R, van Ryn M. The effect of cognitive load and patient race on physicians' decisions to prescribe opioids for chronic low back pain: a randomized trial. *Pain Med* 2014; **15**: 965-974 [PMID: 24506332 DOI: 10.1111/pme.12378]

80 **Humphreys K**. Avoiding globalisation of the prescription opioid epidemic. *Lancet* 2017; **390**: 437-439 [PMID: 28792397 DOI: 10.1016/S0140-6736(17)31918-9]

81 **VanGeest JB**, Johnson TP, Alemagno SA. Research methods in the study of substance abuse. New York: Springer, 2017

82 **Monnat SM**. Drugs, alcohol, and suicide represent growing share of US mortality. 2017. Available from: https://scholars.unh.edu/carsey/292/

83 **Monnat SM**. Factors Associated With County-Level Differences in U.S. Drug-Related Mortality Rates. *Am J Prev Med* 2018; **54**: 611-619 [PMID: 29598858 DOI: 10.1016/j.amepre.2018.01.040]

84 **Cobert J**, Lantos PM, Janko MM, Williams DGA, Raghunathan K, Krishnamoorthy V, JohnBull EA, Barbeito A, Gulur P. Geospatial Variations and Neighborhood Deprivation in Drug-Related Admissions and Overdoses. *J Urban Health* 2020; **97**: 814-822 [PMID: 32367203 DOI: 10.1007/s11524-020-00436-8]

85 **Penm J**, MacKinnon NJ, Boone JM, Ciaccia A, McNamee C, Winstanley EL. Strategies and policies to address the opioid epidemic: A case study of Ohio. *J Am Pharm Assoc (2003)* 2017; **57**: S148-S153 [PMID: 28189539 DOI: 10.1016/j.japh.2017.01.001]

86 **ESRI**. ArcGIS Pro.x. Redlands. CA, USA: ESRI Press, 2020: 427

87 **R Development Core Team**. R: A Language and Environment for Statistical Computing 2008. Available from: https://peerj.com/preprints/26489v1/#supp-2

World Journal of Clinical Cases

Submit a Manuscript: https://www.f6publishing.com

World J Clin Cases 2023 April 16; 11(11): 2386-2395

DOI: 10.12998/wjcc.v11.i11.2386

ISSN 2307-8960 (online)

MINIREVIEWS

Pyroptosis and its role in cancer

Shi-Wei Liu, Wen-Jing Song, Gui-Kai Ma, Hui Wang, Liang Yang

Specialty type: Oncology

Provenance and peer review: Unsolicited article; Externally peer reviewed.

Peer-review model: Single blind

Peer-review report's scientific quality classification

Grade A (Excellent): 0
Grade B (Very good): B
Grade C (Good): 0
Grade D (Fair): D
Grade E (Poor): 0

P-Reviewer: Arslan M, Turkey; Portillo R, Czech Republic

Received: December 26, 2022
Peer-review started: December 26, 2022
First decision: February 8, 2023
Revised: February 23, 2023
Accepted: March 14, 2023
Article in press: March 14, 2023
Published online: April 16, 2023

Shi-Wei Liu, Department of Joint Surgery, Dalian Medical University, Dalian 116044, Liaoning Province, China

Wen-Jing Song, Gui-Kai Ma, Hui Wang, Department of Oncology, The First Affiliated Hospital of Weifang Medical University, Weifang 261000, Shandong Province, China

Liang Yang, Department of Joint Surgery, The Second Hospital of Dalian Medical University, Dalian 116023, Liaoning Province, China

Corresponding author: Liang Yang, MD, PhD, Chief Physician, Department of Joint Surgery, The Second Hospital of Dalian Medical University, No. 467 Zhongshan Road, Shahekou District, Dalian 116023, Liaoning Province, China. 18863031115@sohu.com

Abstract

Programmed cell death (PCD) is mediated by specific genes that encode signals. It can balance cell survival and death. Pyroptosis is a type of inflammatory, caspase-dependent PCD mediated by gasdermin proteins, which function in pore formation, cell expansion, and plasma membrane rupture, followed by the release of intracellular contents. Pyroptosis is mediated by caspase-1/3/4/5/11 and is primarily divided into the classical pathway, which is dependent on caspase-1, and the non-classical pathway, which is dependent on caspase-4/5/11. Inflammasomes play a vital role in these processes. The various components of the pyroptosis pathway are related to the occurrence, invasion, and metastasis of tumors. Research on pyroptosis has revealed new options for tumor treatment. This article summarizes the recent research progress on the molecular mechanism of pyroptosis, the relationship between the various components of the pyroptosis pathway and cancer, and the applications and prospects of pyroptosis in anticancer therapy.

Key Words: Pyroptosis; Caspase-1/3/4/5/11; Gasdermin family; Cancer

Core Tip: Pyroptosis is a type of inflammatory caspase-dependent programmed cell death mediated by gasdermin proteins, which function in pore formation, cell swelling, and cell membrane rupture. This review discusses the classical and non-classical pathways of pyroptosis and the recent research progress on the molecular mechanisms of pyroptosis. We also review the relationship between various pyroptosis pathway components and different cancers, including nucleotide-binding oligomerization domain-like receptor thermal protein domain associated protein 3 inflammasomes, interleukin (IL)-18, IL-1β, and absent in melanoma 2. The potential applications of this form of cell death as a cancer treatment approach are also explored.

Citation: Liu SW, Song WJ, Ma GK, Wang H, Yang L. Pyroptosis and its role in cancer. *World J Clin Cases* 2023; 11(11): 2386-2395
URL: https://www.wjgnet.com/2307-8960/full/v11/i11/2386.htm
DOI: https://dx.doi.org/10.12998/wjcc.v11.i11.2386

INTRODUCTION

The dynamic balance among cell death, proliferation, and differentiation sustains individual development, homeostasis, and pathological processes in humans. Many disease states are associated with cell death. Programmed cell death (PCD) is regulated by specific cellular mechanisms, and some signaling pathways are activated in these processes[1]. Autophagy, apoptosis, and programmed necrosis are the three main types of PCD[2], and together, they may affect the fate of cancer cells. Apoptosis is a type of PCD that involves cell self-destruction controlled by genes. In apoptosis, the cell membrane remains intact, and inflammation usually does not occur[3]. Necrosis is a passive cell death process caused by pathological stimuli. The permeability of the cell membrane of necrotic cells increases, which causes the cells to swell and finally break down and release their contents. This leads to an inflammatory reaction[3]. Pyroptosis is a form of programmed necrosis, which is PCD induced by gasdermin-mediated.

Pyroptosis was first described in myeloid cells infected by pathogens in 1992[4-6]. It is believed that by clearing intracellular replication niches and improving the defensive responses of the host, pyroptosis plays a vital role in clearing various bacterial and viral infections[7]. The activation of pyroptosis may promote cell death and exert anticancer effects[8]. Pyroptosis has attracted increased attention because it is related to innate immunity and disease. The research status of the relationship between pyroptosis and various cancers is shown in Figure 1, according to publications in PubMed. Emerging evidence has demonstrated the importance of pyroptosis in cancer. Recently, more and more studies have shown that pyroptosis has become a new research topic in cancer, because it may affect the process of cancer. In this review, we outline the molecular mechanism of pyroptosis and highlight its differences from apoptosis. The importance of the various components of the pyroptosis pathway in cancer and its application prospects in antitumor therapy are also discussed.

THE MECHANISM OF PYROPTOSIS

Pyroptosis is also called gasdermin-mediated PCD. The gasdermin family has regulatory functions in normal cell proliferation and differentiation; it includes gasdermin A (GSDMA), gasdermin B (GSDMB), gasdermin C (GSDMC), gasdermin D (GSDMD), gasdermin E (GSDME) (also known as DFNA5, [Deafness, Autosomal Dominant Nonsyndromic Sensorineural 5]), and DFNB59 (Autosomal Recessive Deafness Type 59 Protein)[9-13]. Among them, GSDMD and GSDME have been extensively studied in pyroptosis. These proteins have inherent necrotic activity in their gasdermin-N domain, which is usually masked by their gasdermin-C domain[14-16]. Pyroptosis is activated by various stimuli and inflammatory caspases, which induce the cleavage of proteins in the gasdermin family and release its N-terminal effector and C-terminal inhibitory domains. The necrotic gasdermin-N domain is then transferred to the plasma membrane, forming oligomers[14-19]. These oligomers form transmembrane pores that disrupt the osmotic potential, which results in rapid plasma membrane rupture, causing the cells to release their intracellular contents and pro-inflammatory mediators, such as interleukin (IL)-1β and IL-18[20].

Of the proteins in the gasdermin family, GSDMA, GSDMB, and GSDMC proteins possess a pore-forming gasdermin-N domain. However, they are not cleaved to form functional pores in response to physiological or pathological stimuli[14,21]. Only GSDMD and GSDME are cleaved by caspases between their gasdermin-N and gasdermin-C domains to form membrane pores[11,14,21-23]. Typically, GSDMD, the downstream effector of inflammasome activation, is cleaved by inflammatory caspases (caspase-1/4/5/11) to induce pyroptosis. However, GSDME is cleaved by an apoptotic caspase

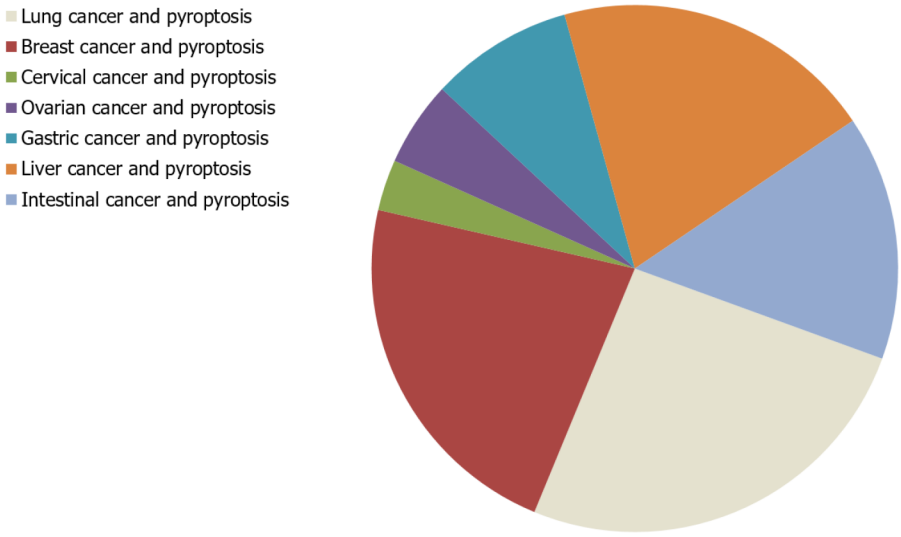

DOI: 10.12998/wjcc.v11.i11.2386

Figure 1 PubMed-searchable publications on pyroptosis and various cancers. Publications were displayed through a search using "pyroptosis and various cancers" on October 7, 2022.

(caspase-3), which causes pyroptotic death[14]. Different molecular patterns are activated depending on the specific signaling pathway and cell type to induce pyroptosis[24]. The role of each component in the gasdermin family is described in Supplementary Table 1.

Pyroptosis belongs to the inflammatory cell death pathway. According to its activation mechanism, pyroptosis can be divided into the classical pathway, which is dependent on caspase-1, and the non-classical pathway, which is dependent on caspase-4, 5, and 11. These pathways are shown in Figure 2. Both pathways are formed by the cleavage of GSDMD, which forms a free N-terminal peptide; this peptide induces cells to form pores and rupture, which causes the release of cytoplasmic components. Both pathways can simultaneously induce the cleavage of IL-1β and IL-18 precursors to form mature IL-1β and IL-18. The difference between the two is whether caspase-1 is directly activated. (1) The classical pathway of pyroptosis[21,25]: Inflammasomes are multimolecular complexes that contain pattern-recognition receptors (PRRs). The PRR series usually contains Toll-like receptors, intracellular nucleotide-binding oligomerization domain (NOD)-like receptors, and absent in melanoma-like receptors. PRRs can recognize pathogen-associated and damage-associated molecular patterns, and can sense the presence of risk factors, such as infection and injury. PRRs can also recruit the adaptor protein containing the caspase recruitment domain [apoptosis-associated speck-like protein containing a caspase recruitment domain (ASC)] and activate caspase-1 through the adaptor protein ASC and pro-caspase-1 binding. On the one hand, the activated caspase-1 cleaves GSDMD to form the GSDMD-N and GSDMD-C domains. The GSDMD-N domain combines with phospholipid proteins on the cell membrane to form holes, after which contents are released, and pyroptosis is induced. On the other hand, the activated caspase-1 cleaves IL-1β and IL-18 precursors to form active IL-1β and IL-18, which are released outside the cell, causing inflammation; and (2) Non-classical pathways that depend on caspase-4, 5, and 11[21,25]. Taking the inflammatory stimulating factor lipopolysaccharide (LPS) as an example, it directly enters the cytoplasm, although not through the receptor, where it activates other caspases, such as caspase-4, 5, and 11, which cleave GSDMD to induce pyroptosis. A new pathway known to cause pyroptosis is caspase-3/GSDME[11,26]. Caspase-3 can be activated by death receptors and mitochondrial pathways. Mature caspase-3 cleaves GSDME to produce GSDME N-fragments. It participates in pore formation in the plasma membrane, resulting in cell swelling and pyroptosis.

THE RELATIONSHIP BETWEEN VARIOUS COMPONENTS IN THE PYROPTOSIS PATHWAY AND CANCER

Pyroptosis is an important natural immune response of the body. It plays a vital role in antagonizing infection and endogenous danger signals. Pyroptosis is widely involved in the occurrence and development of infectious, nervous system-related, and atherosclerotic diseases. In-depth research on pyroptosis has implicated its role in the occurrence, development, and outcome of related diseases and has provided new ideas for clinical prevention and treatment. In recent years, research interest in pyroptosis has increased significantly as it has successful attracted the attention of scientists and has become a popular research topic. For tumors, pyroptosis is a double-edged sword. On the one hand, as

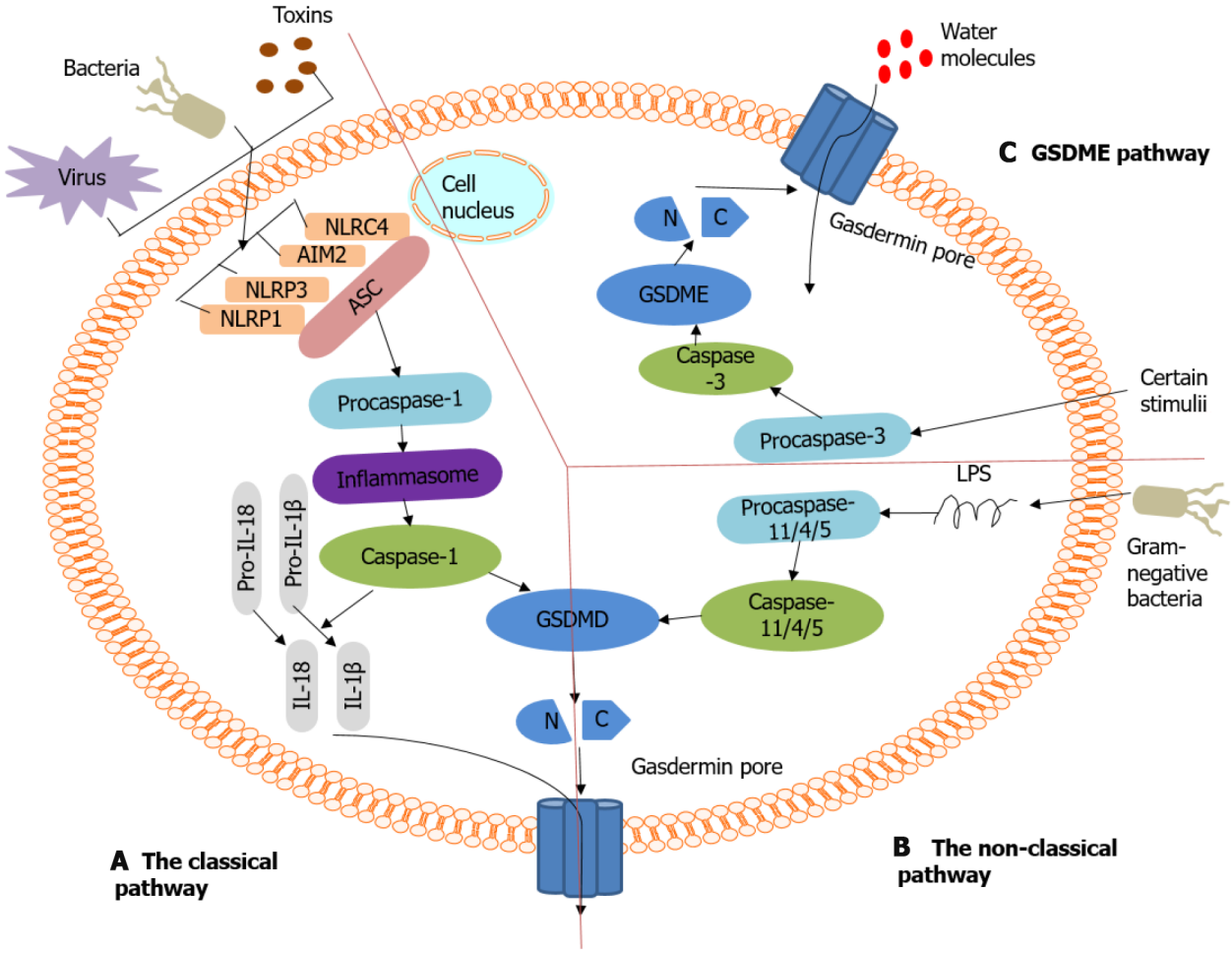

DOI: 10.12998/wjcc.v11.i11.2386

Figure 2 Molecular mechanism of pyroptosis. Pyroptosis belongs to the inflammatory death pathway. It can be divided into the classical pathway, which is dependent on caspase-1, and the non-classical pathway, which is dependent on caspase-4, 5, and 11. A: The classical pyroptosis pathway: Upon sensing pathogen-associated molecular patterns, damage-associated molecular patterns, or other cytosolic disturbances, caspase-1 is activated *via* the recruitment of ASC. Caspase-1 successively promotes the maturation of pro-IL-18/1β and cleaves GSDMD to form GSDMD-N and GSDMD-C domains. The GSDMD-N domain interacts with phospholipid proteins on the cell membrane to form holes, leading to the secretion of IL-1β/18 and water influx and causing cell swelling and osmotic lysis; B: The non-classical pathway that depends on caspase-4, 5, and 11: When lipopolysaccharide derived from bacteria recognizes and activates caspase-11/4/5, it can also cause pyroptosis by cleavage of GSDMD; C: A new pathway to cause pyroptosis is caspase-3/GSDME. Caspase-3 can be activated by the death receptor and mitochondrial pathway. Mature caspase-3 cleaves GSDME to produce GSDME N-fragments and participates in pore formation in the plasma membrane, which results in cell swelling and pyroptosis. ASC: Apoptosis-associated speck-like protein containing a caspase recruitment domain; IL: Interleukin, GSDMD: Gasdermin D; GSDME: Gasdermin E; NLRP1: NOD-like receptor protein 1; NLRP3: NOD-like receptor protein 3; AIM2: Absent in melanoma 2; NLRC4: NLR family CARD domain-containing protein 4; LPS: Lipopolysaccharide.

an innate immune mechanism, pyroptosis can inhibit the occurrence and development of tumors. On the other hand, as a mechanism of pro-inflammatory cell death, pyroptosis provides a suitable microenvironment for tumor growth. The key components of the pyroptosis pathway, inflammasomes, gasdermin proteins, and pro-inflammatory cytokines, are all related to tumor occurrence, invasion, and metastasis[27].

GSDMD AND CANCER

Many molecules that participate in the pyroptosis process are closely related to the occurrence and development of lung cancer. Studies have confirmed that the expression level of GSDMD in non-small cell lung cancer is significantly higher than in surrounding lung tissues. Moreover, the GSDMD expression is related to the tumor size, tumor–node–metastasis stage, and high aggressive characteristics[28]. In addition, GSDMD is considered to be an independent prognostic marker of lung adenocarcinoma[28]. Studies have found that GSDMD in gastric cancer was downregulated and led to the occurrence and spread of this cancer type[29]. The low level of GSDMD in gastric cancer cells may be associated with the acceleration of the cell cycle S/G2 transition; GSDMD also inhibits the signal transducer and activator of transcription 3, extracellular signal-regulated kinase (ERK), and

phosphatidylinositol 3-kinase/protein kinase B (PI3K/AKT) in gastric cancer. These data indicate the tumor-suppressive effect of GSDMD in gastric cancer. However, whether GSDMD plays a tumor-suppressive or cancer-promoting role in breast and colorectal cancers and other cancers is unknown. Therefore, this will be the focus of future research.

GSDME AND CANCER

In lung cancer, the deletion of the *DFNA5/GSDME* gene promotes drug resistance, whereas the overexpression of *DFNA5/GSDME* can result in increased drug sensitivity[30]. Both cisplatin and paclitaxel can induce pyroptosis through caspase-3/GSDME activation. However, in A549 Lung cancer cells, cisplatin is more effective than paclitaxel in triggering pyroptosis[31]. According to several studies, the expression of DFNA5/GSDME in hepatocellular carcinoma (HCC) cells was significantly reduced compared to that in normal cells. Furthermore, the upregulation of the *DFNA5/GSDME* expression inhibited cell proliferation, which suggests that *DFNA5/GSDME* may be an anticancer gene[10,32]. Studies have found that GSDME knockout can significantly inhibit breast cancer (BC) cell pyroptosis and reduce the sensitivity of cancer cells to paclitaxel. In addition, GSDME methylation can increase the risk of BC lymph node metastasis, which suggests that GSDME exerts anticancer effects. Recent studies have suggested that chemotherapeutics can convert caspase-3-dependent apoptosis into pyroptosis *via* DFNA5/GSDME, which may be downregulated because of promoter methylation[33]. Treatment with decitabine can induce *DFNA5/GSDME* up-regulation in cancer cells, which causes pyroptosis and increases the sensitivity of these cells to chemotherapeutics[11,34].

NOD-LIKE RECEPTOR PROTEIN 3 AND CANCER

Studies have reported that stimulating the formation of NOD-like receptor protein 3 (NLRP3) inflammasomes in A549 lung cancer cells with LPS and adenosine triphosphate can activate AKT, ERK1/2, and cyclic adenosine monophosphate response element binding protein. Moreover, it can upregulate the transcription factor Snail and downregulate E-cadherin, which confirms that the NLRP3 inflammasome can promote lung cancer cell proliferation and migration[35]. In BC, the production of NLRP3 inflammasomes and IL-1β promote the infiltration of bone marrow cells, such as tumor-associated macrophages and myeloid-derived suppressor cells, which provide an inflammatory microenvironment that promotes BC progression[36]. Furthermore, NLRP3 inflammasomes in fibroblasts are associated with progression and metastasis[37]. The NLRP3 inflammasome appears to be an effector that promotes lymphatic system metastasis and BC development[38]. Various components involved in pyroptosis are closely related to digestive system tumors. Studies have found that the NLRP3 expression in HCC is significantly downregulated or even absent and that its expression is negatively correlated with the clinical stage and pathological grade. This suggests that the NLRP3 inflammasome participates in developing HCC[39]. Furthermore, the NLRP3 inflammasome participates in the innate immune response to cervical cancer, and its expression is widely present in tumor cells[40,41]. The NLRP3 inflammasome activation can be achieved through lysosomal rupture, hemi-ion channels, and reactive oxygen species (ROS). In cervical cancer, the NLRP3 inflammasome is mainly activated by ROS to induce pyroptosis. In most of the cited reports, evidence on the role of NLRP3 in tumors is still in the preliminary stage, and further confirmation is needed to determine the potential therapeutic role of NLRP3 inflammasomes in human malignancies.

IL-18 AND CANCER

IL-18 plays an immunomodulatory role in the occurrence of esophageal squamous cell carcinoma (ESCC)[42,43]. IL-18 can induce $CD8^+$ T cells and natural killer cells to produce interferon-γ, improve anticancer immunity, and inhibit cancer cell proliferation and metastasis[42]. Exogenous IL-18 is expected to be a new approach for treating ESCC. In one study, the vascular endothelial growth factor stimulated the production, processing, and secretion of IL-18 in gastric cancer cells. IL-18 promotes cell migration through actin polymerization and tensin down-regulation. Therefore, IL-18 may amplify the angiogenesis, migration, and progression of gastric cancer cells[44,45]. In addition to the angiogenic and invasive properties of IL-18, this cytokine can also induce the expression of protease inhibitor 9 and granzyme B inhibitor in gastric cancer cells, which reduces their sensitivity to lymphocyte-mediated cytotoxicity[46]. Recent data indicate that the NLRP3 inflammatory body inhibitor thymoquinone and resveratrol inhibit the metastases of murine melanoma cells by inhibiting the IL-18-mediated vascular cell adhesion molecule 1 expression and IL-18 secretion[47,48]. Different studies have reported the association between polymorphisms in the IL-18 gene promoter (-137 G>C and -607 C>A) and the development of different human cancers. A meta-analysis showed that the -137 G>C polymorphism is

associated with an increased risk of nasopharyngeal carcinoma (NPC) in Asian populations but not in Caucasian populations[49]. Another meta-analysis showed that the -607 C>A polymorphism is connected with an increase in the overall cancer risk, especially for esophageal cancer and NPC, in Asian populations[50]. Recently, the discovery of IL-18-binding protein (IL-18BP) as a physiological inhibitor of IL-18 has suggested that this cytokine may be an attractive target. Its advantages and disadvantages in treating various diseases are currently being investigated[51,52]. In some types of tumors, the tumor-promoting effect of IL-18 is dominant, and IL-18BP may be beneficial. Therefore, any potential IL-18 treatment should be considered with caution.

IL-1B AND CANCER

IL-1β can promote epithelial–mesenchymal transition (EMT) in ESCC, colorectal carcinoma (CRC), and HCC, and it can promote the migration and invasiveness of cancer cells[53-56]. Multiple studies have found that IL-1β is a crucial cytokine related to BC. IL-1β can induce the EMT process in BC, increase tumor malignancy, and increase the resistance of BC to cisplatin by upregulating resistance-related genes. IL-1β can also promote the expression of the oncogene baculoviral inhibitor of apoptosis repeat-containing 3 to decrease the resistance of BC to doxorubicin[56]. Moreover, other studies have reported that IL-1β can induce tamoxifen resistance in BC by downregulating estrogen receptor-α[57]. In response to the cancer-promoting effect of IL-1β, Tulotta *et al*[53] used anakinra and kanazumab to block the IL-1β signaling pathway. They found that the body's anticancer immunity was enhanced, the number of cancer cells entering the circulation was decreased, and the metastasis of BC was suppressed. In the future, it is hoped that antitumor drugs that target IL-1β will become novel cancer therapies.

AIM2 (ABSENT IN MELANOMA 2) AND CANCER

AIM2 is a cytoplasmic sensor that recognizes double-stranded DNA (dsDNA) released during cellular perturbation and pathogenic assault[58]. Upon binding to dsDNA, AIM2 assembles a multiprotein complex termed the inflammasome, which drives IL-1β and IL-18 secretion and pyroptosis[59]. Several studies observed a decreased AIM2 expression in HCC tissues but not in normal tissues. The AIM2 expression was negatively correlated with tumor progression[60,61]. Additionally, AIM2 deficiency enhanced EMT and fibronectin-1 expression, which may be related to HCC metastasis[60]. In human papillomavirus-infected cervical cancer cells, AIM2 can exert a tumor-inhibitory effect by stimulating pyroptosis[62]. The AIM2 gene contains a microsatellite instability site, leading to frequent gene mutations in CRC and small intestine cancer[63,64]. Two independent studies have shown that AIM2 can inhibit CRC development[65,66]; AIM2 inhibits the proliferation of colonic stem cells and facilitates cell death by inhibiting the PI3K/AKT signaling pathway[65,66]. In addition, studies have shown that AIM2 inhibits the proliferation of colon cancer cells in the G2/M phase by inducing cell cycle arrest[67]. Furthermore, the release of IL-18 mediated by the AIM2 inflammasome triggers the up-regulation of IL-22 binding protein and antimicrobial peptides that regulate intestinal homeostasis[68]. A high AIM2 expression is associated with the increased survival rate of patients with Epstein–Barr virus-associated NPC. The function of AIM2 in NPC may involve IL-1β and the recruitment of immunostimulatory neutrophils into tumor masses, which can mediate antitumor activity[69]. Depending on cancer, AIM2 plays different roles; for example, AIM2 functions as a tumor suppressor in CRC and HCC but as a tumor promoter in skin carcinoma[70]. The AIM2 expression is moderate in skin squamous cell carcinoma, whereas its expression is low or absent in normal skin. The knockdown of AIM2 also leads to the reduced invasiveness of skin squamous cell carcinoma cells. It can inhibit the growth and vascularization of skin squamous cell carcinoma *in vivo*[70]. Further research on AIM2 will help us better understand the role of AIM2 in cancer and to develop new antitumor drugs.

CONCLUSION

Pyroptosis is a type of inflammatory PCD characterized by cell swelling and lysis that is mediated by various inflammasomes, which can discern danger signals and activate the secretion of pro-inflammatory cytokines (such as IL-18 and IL-1β). Pyroptosis can regulate cell proliferation, infiltration, migration, chemotherapy resistance, and other malignant phenotypes through various cell signaling pathways, thereby affecting tumor progression. The various components of the pyroptosis pathway are involved in almost all aspects of tumor development. They play either a tumor-suppressive or a pro-tumorigenic role. Therefore, research on the characteristics and mechanisms of pyroptosis and its relationship with cancer can provide novel ideas and effective drug targets for disease prevention and treatment.

FOOTNOTES

Author contributions: Song WJ and Yang L contributed to conceptualization; Ma GK and Wang H contributed to data collection and analysis; Liu SW, Song WJ, and Ma GK contributed to manuscript writing; Yang L contributed to final approval of manuscript; All authors contributed to the article and approved the submitted version.

Conflict-of-interest statement: All the authors report no conflict of interest in this work.

Country/Territory of origin: China

ORCID number: Wen-Jing Song 0000-0003-2583-4362; Liang Yang 0000-0002-9099-1738.

S-Editor: Liu JH
L-Editor: A
P-Editor: Liu JH

REFERENCES

1 **Andón FT**, Fadeel B. Programmed cell death: molecular mechanisms and implications for safety assessment of nanomaterials. *Acc Chem Res* 2013; **46**: 733-742 [PMID: 22720979 DOI: 10.1021/ar300020b]
2 **Ouyang L**, Shi Z, Zhao S, Wang FT, Zhou TT, Liu B, Bao JK. Programmed cell death pathways in cancer: a review of apoptosis, autophagy and programmed necrosis. *Cell Prolif* 2012; **45**: 487-498 [PMID: 23030059 DOI: 10.1111/j.1365-2184.2012.00845.x]
3 **Fink SL**, Cookson BT. Apoptosis, pyroptosis, and necrosis: mechanistic description of dead and dying eukaryotic cells. *Infect Immun* 2005; **73**: 1907-1916 [PMID: 15784530 DOI: 10.1128/iai.73.4.1907-1916.2005]
4 **Wallach D**, Kang TB, Dillon CP, Green DR. Programmed necrosis in inflammation: Toward identification of the effector molecules. *Science* 2016; **352**: aaf2154 [PMID: 27034377 DOI: 10.1126/science.aaf2154]
5 **Shi J**, Gao W, Shao F. Pyroptosis: Gasdermin-Mediated Programmed Necrotic Cell Death. *Trends Biochem Sci* 2017; **42**: 245-254 [PMID: 27932073 DOI: 10.1016/j.tibs.2016.10.004]
6 **Zychlinsky A**, Prevost MC, Sansonetti PJ. Shigella flexneri induces apoptosis in infected macrophages. *Nature* 1992; **358**: 167-169 [PMID: 1614548 DOI: 10.1038/358167a0]
7 **Jorgensen I**, Miao EA. Pyroptotic cell death defends against intracellular pathogens. *Immunol Rev* 2015; **265**: 130-142 [PMID: 25879289 DOI: 10.1111/imr.12287]
8 **Li L**, Li Y, Bai Y. Role of GSDMB in Pyroptosis and Cancer. *Cancer Manag Res* 2020; **12**: 3033-3043 [PMID: 32431546 DOI: 10.2147/CMAR.S246948]
9 **Burgener SS**, Leborgne NGF, Snipas SJ, Salvesen GS, Bird PI, Benarafa C. Cathepsin G Inhibition by Serpinb1 and Serpinb6 Prevents Programmed Necrosis in Neutrophils and Monocytes and Reduces GSDMD-Driven Inflammation. *Cell Rep* 2019; **27**: 3646-3656.e5 [PMID: 31216481 DOI: 10.1016/j.celrep.2019.05.065]
10 **Wang CJ**, Tang L, Shen DW, Wang C, Yuan QY, Gao W, Wang YK, Xu RH, Zhang H. The expression and regulation of DFNA5 in human hepatocellular carcinoma DFNA5 in hepatocellular carcinoma. *Mol Biol Rep* 2013; **40**: 6525-6531 [PMID: 24154762 DOI: 10.1007/s11033-013-2581-8]
11 **Wang Y**, Gao W, Shi X, Ding J, Liu W, He H, Wang K, Shao F. Chemotherapy drugs induce pyroptosis through caspase-3 cleavage of a gasdermin. *Nature* 2017; **547**: 99-103 [PMID: 28459430 DOI: 10.1038/nature22393]
12 **Tamura M**, Tanaka S, Fujii T, Aoki A, Komiyama H, Ezawa K, Sumiyama K, Sagai T, Shiroishi T. Members of a novel gene family, Gsdm, are expressed exclusively in the epithelium of the skin and gastrointestinal tract in a highly tissue-specific manner. *Genomics* 2007; **89**: 618-629 [PMID: 17350798 DOI: 10.1016/j.ygeno.2007.01.003]
13 **Wei Q**, Zhu R, Zhu J, Zhao R, Li M. E2-Induced Activation of the NLRP3 Inflammasome Triggers Pyroptosis and Inhibits Autophagy in HCC Cells. *Oncol Res* 2019; **27**: 827-834 [PMID: 30940293 DOI: 10.3727/096504018X15462920753012]
14 **Ding J**, Wang K, Liu W, She Y, Sun Q, Shi J, Sun H, Wang DC, Shao F. Pore-forming activity and structural autoinhibition of the gasdermin family. *Nature* 2016; **535**: 111-116 [PMID: 27281216 DOI: 10.1038/nature18590]
15 **Rogers C**, Fernandes-Alnemri T, Mayes L, Alnemri D, Cingolani G, Alnemri ES. Cleavage of DFNA5 by caspase-3 during apoptosis mediates progression to secondary necrotic/pyroptotic cell death. *Nat Commun* 2017; **8**: 14128 [PMID: 28045099 DOI: 10.1038/ncomms14128]
16 **Liu X**, Zhang Z, Ruan J, Pan Y, Magupalli VG, Wu H, Lieberman J. Inflammasome-activated gasdermin D causes pyroptosis by forming membrane pores. *Nature* 2016; **535**: 153-158 [PMID: 27383986 DOI: 10.1038/nature18629]
17 **Aglietti RA**, Estevez A, Gupta A, Ramirez MG, Liu PS, Kayagaki N, Ciferri C, Dixit VM, Dueber EC. GsdmD p30 elicited by caspase-11 during pyroptosis forms pores in membranes. *Proc Natl Acad Sci U S A* 2016; **113**: 7858-7863 [PMID: 27339137 DOI: 10.1073/pnas.1607769113]
18 **Russo HM**, Rathkey J, Boyd-Tressler A, Katsnelson MA, Abbott DW, Dubyak GR. Active Caspase-1 Induces Plasma Membrane Pores That Precede Pyroptotic Lysis and Are Blocked by Lanthanides. *J Immunol* 2016; **197**: 1353-1367

[PMID: 27385778 DOI: 10.4049/jimmunol.1600699]
19 **Sborgi L**, Rühl S, Mulvihill E, Pipercevic J, Heilig R, Stahlberg H, Farady CJ, Müller DJ, Broz P, Hiller S. GSDMD membrane pore formation constitutes the mechanism of pyroptotic cell death. *EMBO J* 2016; **35**: 1766-1778 [PMID: 27418190 DOI: 10.15252/embj.201694696]
20 **Pizato N**, Luzete BC, Kiffer LFMV, Corrêa LH, de Oliveira Santos I, Assumpção JAF, Ito MK, Magalhães KG. Omega-3 docosahexaenoic acid induces pyroptosis cell death in triple-negative breast cancer cells. *Sci Rep* 2018; **8**: 1952 [PMID: 29386662 DOI: 10.1038/s41598-018-20422-0]
21 **Shi J**, Zhao Y, Wang K, Shi X, Wang Y, Huang H, Zhuang Y, Cai T, Wang F, Shao F. Cleavage of GSDMD by inflammatory caspases determines pyroptotic cell death. *Nature* 2015; **526**: 660-665 [PMID: 26375003 DOI: 10.1038/nature15514]
22 **He WT**, Wan H, Hu L, Chen P, Wang X, Huang Z, Yang ZH, Zhong CQ, Han J. Gasdermin D is an executor of pyroptosis and required for interleukin-1β secretion. *Cell Res* 2015; **25**: 1285-1298 [PMID: 26611636 DOI: 10.1038/cr.2015.139]
23 **Kayagaki N**, Stowe IB, Lee BL, O'Rourke K, Anderson K, Warming S, Cuellar T, Haley B, Roose-Girma M, Phung QT, Liu PS, Lill JR, Li H, Wu J, Kummerfeld S, Zhang J, Lee WP, Snipas SJ, Salvesen GS, Morris LX, Fitzgerald L, Zhang Y, Bertram EM, Goodnow CC, Dixit VM. Caspase-11 cleaves gasdermin D for non-canonical inflammasome signalling. *Nature* 2015; **526**: 666-671 [PMID: 26375259 DOI: 10.1038/nature15541]
24 **Wimmer K**, Sachet M, Oehler R. Circulating biomarkers of cell death. *Clin Chim Acta* 2020; **500**: 87-97 [PMID: 31655053 DOI: 10.1016/j.cca.2019.10.003]
25 **Ding J**, Wang K, Liu W, She Y, Sun Q, Shi J, Sun H, Wang DC, Shao F. Erratum: Pore-forming activity and structural autoinhibition of the gasdermin family. *Nature* 2016; **540**: 150 [PMID: 27706141 DOI: 10.1038/nature20106]
26 **Zhang Z**, Zhang H, Li D, Zhou X, Qin Q, Zhang Q. Caspase-3-mediated GSDME induced Pyroptosis in breast cancer cells through the ROS/JNK signalling pathway. *J Cell Mol Med* 2021; **25**: 8159-8168 [PMID: 34369076 DOI: 10.1111/jcmm.16574]
27 **Kolb R**, Liu GH, Janowski AM, Sutterwala FS, Zhang W. Inflammasomes in cancer: a double-edged sword. *Protein Cell* 2014; **5**: 12-20 [PMID: 24474192 DOI: 10.1007/s13238-013-0001-4]
28 **Gao J**, Qiu X, Xi G, Liu H, Zhang F, Lv T, Song Y. Downregulation of GSDMD attenuates tumor proliferation *via* the intrinsic mitochondrial apoptotic pathway and inhibition of EGFR/Akt signaling and predicts a good prognosis in nonsmall cell lung cancer. *Oncol Rep* 2018; **40**: 1971-1984 [PMID: 30106450 DOI: 10.3892/or.2018.6634]
29 **Wang WJ**, Chen D, Jiang MZ, Xu B, Li XW, Chu Y, Zhang YJ, Mao R, Liang J, Fan DM. Downregulation of gasdermin D promotes gastric cancer proliferation by regulating cell cycle-related proteins. *J Dig Dis* 2018; **19**: 74-83 [PMID: 29314754 DOI: 10.1111/1751-2980.12576]
30 **Lu H**, Zhang S, Wu J, Chen M, Cai MC, Fu Y, Li W, Wang J, Zhao X, Yu Z, Ma P, Zhuang G. Molecular Targeted Therapies Elicit Concurrent Apoptotic and GSDME-Dependent Pyroptotic Tumor Cell Death. *Clin Cancer Res* 2018; **24**: 6066-6077 [PMID: 30061362 DOI: 10.1158/1078-0432.CCR-18-1478]
31 **Zhang CC**, Li CG, Wang YF, Xu LH, He XH, Zeng QZ, Zeng CY, Mai FY, Hu B, Ouyang DY. Chemotherapeutic paclitaxel and cisplatin differentially induce pyroptosis in A549 lung cancer cells *via* caspase-3/GSDME activation. *Apoptosis* 2019; **24**: 312-325 [PMID: 30710195 DOI: 10.1007/s10495-019-01515-1]
32 **Sharma D**, Malik A, Guy CS, Karki R, Vogel P, Kanneganti TD. Pyrin Inflammasome Regulates Tight Junction Integrity to Restrict Colitis and Tumorigenesis. *Gastroenterology* 2018; **154**: 948-964.e8 [PMID: 29203393 DOI: 10.1053/j.gastro.2017.11.276]
33 **Wang Y**, Yin B, Li D, Wang G, Han X, Sun X. GSDME mediates caspase-3-dependent pyroptosis in gastric cancer. *Biochem Biophys Res Commun* 2018; **495**: 1418-1425 [PMID: 29183726 DOI: 10.1016/j.bbrc.2017.11.156]
34 **Feng S**, Fox D, Man SM. Mechanisms of Gasdermin Family Members in Inflammasome Signaling and Cell Death. *J Mol Biol* 2018; **430**: 3068-3080 [PMID: 29990470 DOI: 10.1016/j.jmb.2018.07.002]
35 **Wang Y**, Kong H, Zeng X, Liu W, Wang Z, Yan X, Wang H, Xie W. Activation of NLRP3 inflammasome enhances the proliferation and migration of A549 lung cancer cells. *Oncol Rep* 2016; **35**: 2053-2064 [PMID: 26782741 DOI: 10.3892/or.2016.4569]
36 **Guo B**, Fu S, Zhang J, Liu B, Li Z. Targeting inflammasome/IL-1 pathways for cancer immunotherapy. *Sci Rep* 2016; **6**: 36107 [PMID: 27786298 DOI: 10.1038/srep36107]
37 **Ershaid N**, Sharon Y, Doron H, Raz Y, Shani O, Cohen N, Monteran L, Leider-Trejo L, Ben-Shmuel A, Yassin M, Gerlic M, Ben-Baruch A, Pasmanik-Chor M, Apte R, Erez N. NLRP3 inflammasome in fibroblasts links tissue damage with inflammation in breast cancer progression and metastasis. *Nat Commun* 2019; **10**: 4375 [PMID: 31558756 DOI: 10.1038/s41467-019-12370-8]
38 **Weichand B**, Popp R, Dziumbla S, Mora J, Strack E, Elwakeel E, Frank AC, Scholich K, Pierre S, Syed SN, Olesch C, Ringleb J, Ören B, Döring C, Savai R, Jung M, von Knethen A, Levkau B, Fleming I, Weigert A, Brüne B. S1PR1 on tumor-associated macrophages promotes lymphangiogenesis and metastasis *via* NLRP3/IL-1β. *J Exp Med* 2017; **214**: 2695-2713 [PMID: 28739604 DOI: 10.1084/jem.20160392]
39 **Wei Q**, Mu K, Li T, Zhang Y, Yang Z, Jia X, Zhao W, Huai W, Guo P, Han L. Deregulation of the NLRP3 inflammasome in hepatic parenchymal cells during liver cancer progression. *Lab Invest* 2014; **94**: 52-62 [PMID: 24166187 DOI: 10.1038/labinvest.2013.126]
40 **Zhang H**, Li L, Liu L. FcγRI (CD64) contributes to the severity of immune inflammation through regulating NF-κB/NLRP3 inflammasome pathway. *Life Sci* 2018; **207**: 296-303 [PMID: 29920250 DOI: 10.1016/j.lfs.2018.06.015]
41 **Hoseini Z**, Sepahvand F, Rashidi B, Sahebkar A, Masoudifar A, Mirzaei H. NLRP3 inflammasome: Its regulation and involvement in atherosclerosis. *J Cell Physiol* 2018; **233**: 2116-2132 [PMID: 28345767 DOI: 10.1002/jcp.25930]
42 **Li J**, Qiu G, Fang B, Dai X, Cai J. Deficiency of IL-18 Aggravates Esophageal Carcinoma Through Inhibiting IFN-γ Production by CD8(+)T Cells and NK Cells. *Inflammation* 2018; **41**: 667-676 [PMID: 29264744 DOI: 10.1007/s10753-017-0721-3]
43 **Wei YS**, Lan Y, Liu YG, Tang H, Tang RG, Wang JC. Interleukin-18 gene promoter polymorphisms and the risk of esophageal squamous cell carcinoma. *Acta Oncol* 2007; **46**: 1090-1096 [PMID: 17851835 DOI:

10.1080/02841860701373595]
44 **Kim KE**, Song H, Kim TS, Yoon D, Kim CW, Bang SI, Hur DY, Park H, Cho DH. Interleukin-18 is a critical factor for vascular endothelial growth factor-enhanced migration in human gastric cancer cell lines. *Oncogene* 2007; **26**: 1468-1476 [PMID: 17001321 DOI: 10.1038/sj.onc.1209926]
45 **Kim KE**, Song H, Hahm C, Yoon SY, Park S, Lee HR, Hur DY, Kim T, Kim CH, Bang SI, Bang JW, Park H, Cho DH. Expression of ADAM33 is a novel regulatory mechanism in IL-18-secreted process in gastric cancer. *J Immunol* 2009; **182**: 3548-3555 [PMID: 19265133 DOI: 10.4049/jimmunol.0801695]
46 **Majima T**, Ichikura T, Chochi K, Kawabata T, Tsujimoto H, Sugasawa H, Kuranaga N, Takayama E, Kinoshita M, Hiraide H, Seki S, Mochizuki H. Exploitation of interleukin-18 by gastric cancers for their growth and evasion of host immunity. *Int J Cancer* 2006; **118**: 388-395 [PMID: 16049975 DOI: 10.1002/ijc.21334]
47 **Ahmad I**, Muneer KM, Tamimi IA, Chang ME, Ata MO, Yusuf N. Thymoquinone suppresses metastasis of melanoma cells by inhibition of NLRP3 inflammasome. *Toxicol Appl Pharmacol* 2013; **270**: 70-76 [PMID: 23583630 DOI: 10.1016/j.taap.2013.03.027]
48 **Salado C**, Olaso E, Gallot N, Valcarcel M, Egilegor E, Mendoza L, Vidal-Vanaclocha F. Resveratrol prevents inflammation-dependent hepatic melanoma metastasis by inhibiting the secretion and effects of interleukin-18. *J Transl Med* 2011; **9**: 59 [PMID: 21569399 DOI: 10.1186/1479-5876-9-59]
49 **Yang X**, Qiu MT, Hu JW, Jiang F, Li M, Wang J, Zhang Q, Yin R, Xu L. Association of interleukin-18 gene promoter -607 C>A and -137G>C polymorphisms with cancer risk: a meta-analysis of 26 studies. *PLoS One* 2013; **8**: e73671 [PMID: 24066061 DOI: 10.1371/journal.pone.0073671]
50 **Wang M**, Zhu XY, Wang L, Lin Y. The -607C/A polymorphisms in interleukin-18 gene promoter contributes to cancer risk: evidence from a meta-analysis of 22 case-control studies. *PLoS One* 2013; **8**: e76915 [PMID: 24130810 DOI: 10.1371/journal.pone.0076915]
51 **Esmailbeig M**, Ghaderi A. Interleukin-18: a regulator of cancer and autoimmune diseases. *Eur Cytokine Netw* 2017; **28**: 127-140 [PMID: 29478963 DOI: 10.1684/ecn.2018.0401]
52 **Fabbi M**, Carbotti G, Ferrini S. Context-dependent role of IL-18 in cancer biology and counter-regulation by IL-18BP. *J Leukoc Biol* 2015; **97**: 665-675 [PMID: 25548255 DOI: 10.1189/jlb.5RU0714-360RR]
53 **Tulotta C**, Lefley DV, Freeman K, Gregory WM, Hanby AM, Heath PR, Nutter F, Wilkinson JM, Spicer-Hadlington AR, Liu X, Bradbury SMJ, Hambley L, Cookson V, Allocca G, Kruithof de Julio M, Coleman RE, Brown JE, Holen I, Ottewell PD. Endogenous Production of IL1B by Breast Cancer Cells Drives Metastasis and Colonization of the Bone Microenvironment. *Clin Cancer Res* 2019; **25**: 2769-2782 [PMID: 30670488 DOI: 10.1158/1078-0432.CCR-18-2202]
54 **Yu Q**, Zhang M, Ying Q, Xie X, Yue S, Tong B, Wei Q, Bai Z, Ma L. Decrease of AIM2 mediated by luteolin contributes to non-small cell lung cancer treatment. *Cell Death Dis* 2019; **10**: 218 [PMID: 30833546 DOI: 10.1038/s41419-019-1447-y]
55 **Chen L**, Weng B, Li H, Wang H, Li Q, Wei X, Deng H, Wang S, Jiang C, Lin R, Wu J. A thiopyran derivative with low murine toxicity with therapeutic potential on lung cancer acting through a NF-κB mediated apoptosis-to-pyroptosis switch. *Apoptosis* 2019; **24**: 74-82 [PMID: 30519834 DOI: 10.1007/s10495-018-1499-y]
56 **Storr SJ**, Safuan S, Ahmad N, El-Refaee M, Jackson AM, Martin SG. Macrophage-derived interleukin-1beta promotes human breast cancer cell migration and lymphatic adhesion in vitro. *Cancer Immunol Immunother* 2017; **66**: 1287-1294 [PMID: 28551814 DOI: 10.1007/s00262-017-2020-0]
57 **Jiménez-Garduño AM**, Mendoza-Rodríguez MG, Urrutia-Cabrera D, Domínguez-Robles MC, Pérez-Yépez EA, Ayala-Sumuano JT, Meza I. IL-1β induced methylation of the estrogen receptor ERα gene correlates with EMT and chemoresistance in breast cancer cells. *Biochem Biophys Res Commun* 2017; **490**: 780-785 [PMID: 28645612 DOI: 10.1016/j.bbrc.2017.06.117]
58 **Sharma BR**, Karki R, Kanneganti TD. Role of AIM2 inflammasome in inflammatory diseases, cancer and infection. *Eur J Immunol* 2019; **49**: 1998-2011 [PMID: 31372985 DOI: 10.1002/eji.201848070]
59 **Man SM**, Karki R, Kanneganti TD. AIM2 inflammasome in infection, cancer, and autoimmunity: Role in DNA sensing, inflammation, and innate immunity. *Eur J Immunol* 2016; **46**: 269-280 [PMID: 26626159 DOI: 10.1002/eji.201545839]
60 **Chen SL**, Liu LL, Lu SX, Luo RZ, Wang CH, Wang H, Cai SH, Yang X, Xie D, Zhang CZ, Yun JP. HBx-mediated decrease of AIM2 contributes to hepatocellular carcinoma metastasis. *Mol Oncol* 2017; **11**: 1225-1240 [PMID: 28580773 DOI: 10.1002/1878-0261.12090]
61 **Ma X**, Guo P, Qiu Y, Mu K, Zhu L, Zhao W, Li T, Han L. Loss of AIM2 expression promotes hepatocarcinoma progression through activation of mTOR-S6K1 pathway. *Oncotarget* 2016; **7**: 36185-36197 [PMID: 27167192 DOI: 10.18632/oncotarget.9154]
62 **So D**, Shin HW, Kim J, Lee M, Myeong J, Chun YS, Park JW. Cervical cancer is addicted to SIRT1 disarming the AIM2 antiviral defense. *Oncogene* 2018; **37**: 5191-5204 [PMID: 29844574 DOI: 10.1038/s41388-018-0339-4]
63 **Mori Y**, Yin J, Rashid A, Leggett BA, Young J, Simms L, Kuehl PM, Langenberg P, Meltzer SJ, Stine OC. Instabilotyping: comprehensive identification of frameshift mutations caused by coding region microsatellite instability. *Cancer Res* 2001; **61**: 6046-6049 [PMID: 11507051]
64 **Schulmann K**, Brasch FE, Kunstmann E, Engel C, Pagenstecher C, Vogelsang H, Krüger S, Vogel T, Knaebel HP, Rüschoff J, Hahn SA, Knebel-Doeberitz MV, Moeslein G, Meltzer SJ, Schackert HK, Tympner C, Mangold E, Schmiegel W; German HNPCC Consortium. HNPCC-associated small bowel cancer: clinical and molecular characteristics. *Gastroenterology* 2005; **128**: 590-599 [PMID: 15765394 DOI: 10.1053/j.gastro.2004.12.051]
65 **Wilson JE**, Petrucelli AS, Chen L, Koblansky AA, Truax AD, Oyama Y, Rogers AB, Brickey WJ, Wang Y, Schneider M, Mühlbauer M, Chou WC, Barker BR, Jobin C, Allbritton NL, Ramsden DA, Davis BK, Ting JP. Inflammasome-independent role of AIM2 in suppressing colon tumorigenesis *via* DNA-PK and Akt. *Nat Med* 2015; **21**: 906-913 [PMID: 26107252 DOI: 10.1038/nm.3908]
66 **Man SM**, Zhu Q, Zhu L, Liu Z, Karki R, Malik A, Sharma D, Li L, Malireddi RK, Gurung P, Neale G, Olsen SR, Carter RA, McGoldrick DJ, Wu G, Finkelstein D, Vogel P, Gilbertson RJ, Kanneganti TD. Critical Role for the DNA Sensor AIM2 in Stem Cell Proliferation and Cancer. *Cell* 2015; **162**: 45-58 [PMID: 26095253 DOI: 10.1016/j.cell.2015.06.001]

67 **Patsos G**, Germann A, Gebert J, Dihlmann S. Restoration of absent in melanoma 2 (AIM2) induces G2/M cell cycle arrest and promotes invasion of colorectal cancer cells. *Int J Cancer* 2010; **126**: 1838-1849 [PMID: 19795419 DOI: 10.1002/ijc.24905]

68 **Ratsimandresey RA**, Indramohan M, Dorfleutner A, Stehlik C. The AIM2 inflammasome is a central regulator of intestinal homeostasis through the IL-18/IL-22/STAT3 pathway. *Cell Mol Immunol* 2017; **14**: 127-142 [PMID: 27524110 DOI: 10.1038/cmi.2016.35]

69 **Chen LC**, Wang LJ, Tsang NM, Ojcius DM, Chen CC, Ouyang CN, Hsueh C, Liang Y, Chang KP, Chang YS. Tumour inflammasome-derived IL-1β recruits neutrophils and improves local recurrence-free survival in EBV-induced nasopharyngeal carcinoma. *EMBO Mol Med* 2012; **4**: 1276-1293 [PMID: 23065753 DOI: 10.1002/emmm.201201569]

70 **Farshchian M**, Nissinen L, Siljamäki E, Riihilä P, Piipponen M, Kivisaari A, Kallajoki M, Grénman R, Peltonen J, Peltonen S, Quint KD, Bavinck JNB, Kähäri VM. Tumor cell-specific AIM2 regulates growth and invasion of cutaneous squamous cell carcinoma. *Oncotarget* 2017; **8**: 45825-45836 [PMID: 28526809 DOI: 10.18632/oncotarget.17573]

World Journal of Clinical Cases

Submit a Manuscript: https://www.f6publishing.com

World J Clin Cases 2023 April 16; 11(11): 2396-2404

DOI: 10.12998/wjcc.v11.i11.2396

ISSN 2307-8960 (online)

MINIREVIEWS

Platelet rich fibrin is not a barrier membrane! Or is it?

Amit Arvind Agrawal

Specialty type: Dentistry, oral surgery and medicine

Provenance and peer review: Invited article; Externally peer reviewed.

Peer-review model: Single blind

Peer-review report's scientific quality classification

Grade A (Excellent): 0
Grade B (Very good): B
Grade C (Good): C
Grade D (Fair): 0
Grade E (Poor): 0

P-Reviewer: Grawish ME, Egypt; Navarro-Alvarez N, Mexico

Received: January 1, 2023
Peer-review started: January 1, 2023
First decision: January 20, 2023
Revised: January 27, 2023
Accepted: March 17, 2023
Article in press: March 17, 2023
Published online: April 16, 2023

Amit Arvind Agrawal, Department of Periodontology and Implantology, Mahatma Gandhi Vidyamandir's Karmaveer Bhausaheb Hiray Dental College and Hospital, Nasik 422003, India

Corresponding author: Amit Arvind Agrawal, MDS, MPhil, Doctor, Professor, Department of Peridontology and Implantology, Mahatma Gandhi Vidyamandir's Karmaveer Bhausaheb Hiray Dental College and Hospital, Mumbai-Agra Road, Panchavati, Near Kannamwar Bridge, Nasik 422003, India. agrodent@rediffmail.com

Abstract

Platelet-rich fibrin (PRF) is widely used in dentistry and other fields of medicine, and its use has become popular in dental implantology. In several published studies, PRF has been used as a barrier membrane. A barrier membrane is a sheet of a certain material that acts as a biological and mechanical barrier against the invasion of cells that are not involved in bone formation, such as epithelial cells. Among the basic requirements of a 'barrier membrane, occlusivity, stiffness, and space maintenance are the criteria that PRF primarily lacks; therefore, it does not fall under the category of barrier membranes. However, there is evidence that PRF membranes are useful in significantly improving wound healing. Does the PRF membrane act as a barrier? Should we think of adding or subtracting some points from the ideal requirements of a barrier membrane, or should we coin a new term or concept for PRF that will incorporate some features of a barrier membrane and be a combination of tissue engineering and biotechnology? This review is aimed at answering the basic question of whether the PRF membrane should be considered a barrier membrane or whether it is something more beyond the boundaries of a barrier membrane.

Key Words: Platelet rich fibrin; Platelet rich plasma; Barrier membrane; Guided tissue regeneration; Guided bone regeneration

Core Tip: Barrier membranes are an important aspect of guided bone and tissue regeneration in periodontics and implant dentistry. Extensive research has been conducted on barrier membranes; however, no single ideal barrier membrane available. Platelet-rich fibrin (PRF) is increasingly becoming popular in dentistry due to its growth factor-secreting properties and is also known to enhance wound healing and soft tissue thickness at the surgical site. However, PRF membranes are labelled as barrier membranes, although they do not fulfil the basic requirements of a barrier membrane.

Citation: Agrawal AA. Platelet rich fibrin is not a barrier membrane! Or is it? *World J Clin Cases* 2023; 11(11): 2396-2404
URL: https://www.wjgnet.com/2307-8960/full/v11/i11/2396.htm
DOI: https://dx.doi.org/10.12998/wjcc.v11.i11.2396

INTRODUCTION

Before discussing whether platelet-rich fibrin (PRF) is a barrier membrane, let us understand what PRF is, along with the concept of a barrier membrane. PRF, as the name suggests, contains a high number of platelets and leukocytes, in addition to a dense fibrin matrix. It is produced by the slow centrifugation of the patient's blood as a chair-side procedure. The fibrin matrix and platelets contribute to wound healing, whereas leukocytes contribute to the antibacterial effects. PRF clots are formed after the termination of the centrifugation cycle in the upper layer of the centrifuge tubes. Following their removal, they can be used in different modalities by either compression or using an extraction socket. They can be cut into small fragments and mixed with bone graft materials. Alternatively, they can be flattened to produce a membrane called the PRF membrane for eventual use in guided tissue regeneration (GTR) or guided bone regeneration (GBR) procedures. PRF exhibits a slow and sustained release of growth factors, such as transforming growth factor-beta1, platelet-derived growth factor, and vascular endothelial growth factor, all of which have been proven to promote wound healing and tissue regeneration[1,2].

A barrier membrane is a sheet of a certain material, which acts as a biological and mechanical barrier against the invasion of cells not involved in bone formation, such as epithelial cells, and allows for the migration of slow-migrating bone-forming cells into the defect sites[3]. In simple terms, as bone defects heal, there is competition between soft tissue and bone-forming cells to invade the surgical site. In general, soft tissue cells migrate at a much faster rate than bone-forming cells. Therefore, the primary goal of barrier membranes is to allow for selective cell repopulation and guide the proliferation of various tissues during the healing process[4]. Regeneration occurs below the membrane and involves angiogenesis and migration of osteogenic cells. The initial blood clot is replaced by woven bone after vascular ingrowth, which is later transformed into a load-bearing lamellar bone. This ultimately supports hard- and soft tissue regeneration[5]. If a barrier membrane is not utilised, the lack of space maintenance will result in soft tissue integration and compromised bone growth.

Literature has laid out various aspects of an ideal barrier membrane, including biocompatibility, the ability to create space, cell occlusiveness, tissue integration and handling, and resorption time. A membrane should be stiff and biocompatible enough to avoid soft tissue penetration or collapse into the regeneration area[6]. This stiffness is required because successful bone regeneration requires bone defects to be isolated from the soft tissues, permitting bone growth, which takes a minimum of 4-6 wk for periodontal tissues and 16-24 wk for bones[7,8]. Lee *et al*[6] reported that non-resorbable membranes are the best barrier membranes; although they do not require a second surgery, they have a low tensile strength, which can be a limitation when compared with expanded polytetrafluoroethylene membranes or a titanium mesh, thereby lowering their ability to maintain space.

Caballé-Serrano *et al*[7] performed a systematic review with a primary research question, 'which main criteria should a barrier membrane fulfil?' They concluded that an ideal membrane should maintain its barrier function for enough time for new bone formation and, if possible, should be resorbable so that a second surgery would not be needed, thereby reducing morbidity. With reference to degradation properties, porcine natural collagen membranes are the fastest to resorb (4-8 wk), whereas cross-linked membranes and bone lamina membranes offer more margins in terms of resorption (4-6 mo and 5-8 mo, respectively)[8].

In the context of resorbable membranes, Zellin *et al*[9] stated that even if resorbable barrier membranes can initially maintain space, they generally lose strength, collapse into the space, and lead to failed reconstruction. In contrast, PRF membranes are unable to maintain space even at placement; therefore, technically, when it comes to the space maintenance criterion, the PRF score is 0.

THE BIG QUESTION?

Having understood the basics of PRF and PRF membranes, and the ideal requirements of a barrier membrane, let us focus on the question, 'should PRF membranes be considered as a barrier membrane?' This question is important because there are thousands of articles published in literature in which the title itself mentions 'PRF used as barrier membrane'; there could be lakhs more where not in title *per se* but clinical studies, care series, case reports, *etc.* have included 'PRF was used in patient as a barrier membrane'. However, there is still much debate on whether PRF acts as a barrier membrane. This question should be answered because the literature needs to be evidence based. It is possible that PRF is a barrier membrane in some way or may be used as a barrier membrane, although it does not fulfil the criteria for a barrier membrane, and thus labels it incorrectly. This article discusses the available literature both as evidence against the belief that PRF is a barrier membrane and evidence in support of it. Finally, let the individual reader decide what is true: Should we continue to label PRF as a 'barrier membrane' or should we find other terminologies that are more relevant and appropriate? Table 1 Lists all the terms related to membranes (in the context of dentistry) and their meanings for a basic understanding of different terms.

EVIDENCE AGAINST PRF AS BARRIER MEMBRANE

Wang *et al*[10] laid the 'PASS' criteria for ideal regenerative procedure, wherein 'P' stands for primary, non-tension wound closure that enables healing by primary intention; 'A' for angiogenesis to promote blood supply to the regenerative area; 'S' for stability of clot to allow development and proliferation of osteogenic cell; and 'S' for space maintenance for undifferentiated mesenchymal cells platform. Dimitriou *et al*[11] performed an extensive review of barrier membranes and highlighted the importance of variability and the lack of control over the rate of resorption of commercially available resorbable membranes, which are influenced by factors such as the local pH and material composition. They also listed the requirements for desirable membrane pore size, topography, soft tissue ingrowth capacity, and mechanical stability. There was no mention of PRF membranes in any of the inclusions of the various barrier membranes. The pore size of a barrier membrane is crucial for preventing excessive penetration of fibrous tissue (soft tissue) into the bone defect while simultaneously allowing neovascularisation and bone formation. Different intensities of bone regeneration can be observed depending on the variability in pore size[12]. Pores in excess of 100 μm are required for the rapid penetration of highly vascular connective tissue, and small pores tend to become filled with more avascular tissue[13] because they are not adequate for the penetration of capillaries[14]. A pore size of 50-100 μm allows bone ingrowth, whereas a size > 150 μm is required for osteon formation[15,16]. As much variability has been reported in the preparation of PRF based on patient age, sex, time of blood aspiration, and type of centrifuge, there is no consensus regarding the pore size of a PRF membrane. In addition to porosity, the three-dimensional topography of the membrane with interconnecting pores and channels is important, as it can alter the cell occlusion properties and biological responses of different cell types to the membrane[17]. However, there is no strong literature on the internal topography of a PRF membrane; hence, the fulfilment of this parameter is questionable. In terms of membrane stability, micromovements between the bone and any implanted material prevent bone formation. These micromovements may result in the development of fibrous tissue[18,19]. Therefore, adequate stability and minimal stress on the graft site are required to allow early tissue infiltration through the pores to differentiate into bone by direct or appositional bone formation[20]. Membrane-fixing pins are generally recommended to achieve higher membrane stability. Bone formation is significantly enhanced when the resorbable membrane is tightly attached and immobilised on the bone surface[21]. The PRF membrane is extremely flexible; although heating or double heating of the PRF membranes is recommended to increase their tensile strength[22], there has been no evidence that any modification or treatment of the PRF membrane increases its stiffness or has been used along with fixation pins or tack pins for GBR procedures. In terms of space maintenance, the implanted barrier membrane is expected to provide a shielding effect for up to 6 wk for periodontal tissue regeneration and for approximately 24 wk for bone augmentation therapy[8,23,24]. As PRF membranes degrade in < 6 wk[25], their role in the shielding effect seems questionable.

In their review article, Rakhmatia *et al*[26] summarised more than 30 articles (between 1994 and 2012) on current barrier membranes, but did not include articles on PRF. Soheilifar *et al*[27] conducted an extensive review of barrier membranes and assessed articles published from 1982 to 2013; they highlighted the importance of space maintenance and specified that a particular barrier membrane should primarily act as a 'barrier'. However, their review did not include any articles on PRF or its variants. In a systematic review by Miron *et al*[28], the authors evaluated approximately 35 articles and concluded that the literature supports the use of PRF for periodontal and soft tissue repair; however, well-conducted studies demonstrating the role of PRF in hard tissue bone regeneration are lacking. Similarly, in a systematic review on the search for a barrier membrane, Caballé-Serrano *et al*[7] analysed 22 articles, none of which were related to PRF. Rodriguez *et al*[29], in their review article on barrier

Table 1 Different names/terminologies related to membrane and their meanings

Sr. No.	Terminologies	Meanings/definition
1	Membranes	A thin pliable sheet of material or tissue forming a barrier or lining.
2	Resorbable membranes	Membranes that are biocompatible and are metabolised by hydrolysis or enzymatic activity over the course of time.
3	Non-resorbable membranes	Membranes that are bio-inert and require a second surgical procedure to remove after bone regeneration is complete.
4	Barrier membranes	A barrier membrane is a device used in oral surgery and periodontal surgery to prevent epithelium, which regenerates relatively quickly, from growing into an area in which another more slowly growing tissue type, such as bone, is desired.
5	Collagen membranes	Membranes made of collagen (mostly type-1 collagen) that are fabricated in different shapes and sizes and used in oral surgical procedures for bone and tissue regeneration.
6	Collagen barrier membranes	Selective collagen membranes that can act as barrier membrane for bone and tissue regeneration.
7	Natural membranes	Membranes made from natural materials or sources, such as collagen, dermis, tendons, sclera, amnion, pericardium, chorion, and silk.
8	Synthetic membranes	Membranes made from synthetic materials, such as polytetrafluroethylene, titanium, and ceramic.
9	GTR membranes	Barrier membranes used for regeneration of lost PDL, cementum, and bone.
10	GBR membranes	Barrier membranes used for bone regeneration.
11	PRF membranes	Autologous membrane made *via* blood centrifugation followed by compression of clot to the desired thickness.
12	Multiphasic membranes	Multiphasic membranes that are designed in phases (or layers) to meet the various criteria of the periodontal tissue types.
13	3D-printed membranes	Customised zirconia printed *via* the CAD CAM technology to serve as new-generation barrier membranes.
14	Functional membranes	Membranes that are not passive barriers but are actively functioning in supporting the regeneration process.
15	Bioactive membranes	Membranes that are loaded with different biological activities, which are timed to play a role in different stages of bone healing and mimic the natural osteogenesis process.
16	Antimicrobial membranes	Barrier membranes loaded with antimicrobial components such as antibiotics, silver ion coating, PEG, superhydrophobic and structural coating.
17	Structurally layered membranes	Multiple layered membrane that are structurally engineered so that each layer has a different biological characteristic.
18	Polymer barrier membranes	Membranes made from polymers such as polylactic acid, polyglycolic acid, collagen, and alginate.

GTR: Guided tissue regeneration; PDL: Periodontal ligament; GBR: Guided bone regeneration; PRF: Platelet-rich fibrin; CAD CAM: Computer-aided design computer-aided manufacturing.

membranes used in dentistry, not only included almost all resorbable and non-resorbable membranes but also mentioned upcoming potential membranes such as BioXclude, hybrid and multiphasic barrier membranes, anti-infective membranes, and novel manuka honey advancement of membranes. However, no platelet concentrates, including PRF, were included in this study. On thermal manipulation of PRF membrane and using single syringe closed system, Kardos *et al*[22] found significant improvement in tensile strength, significantly higher cell adhesion, and lower degradation rate. Despite this, they advocated the use of PRF as an autologous biocompatible membrane for tissue regeneration and did not claim its use as a barrier membrane.

PRF membranes typically have very short resorption times, ranging from a 10- to 28-d period[25]. However, during their limited resorption time, a slow and gradual release of growth factors is observed within the PRF matrix[30]. This release of growth factors is higher than that of platelet-rich plasma. Miron *et al*[31], in one of their review articles, highlighted the question, 'Can we use PRF alone as a replacement to collagen barrier membranes?' However, they added that barrier membranes, in general, were developed to prevent fast-growing soft tissues from entering the slow-growing compartment containing bone. Therefore, the role of PRF remains controversial. They concluded that PRF membranes can be placed around the implant collars to facilitate more rapid soft tissue healing without utilising a collagen barrier membrane. They added that PRF can also be utilised in a 'poncho' technique and wrapped around the healing cap to favour soft tissue attachment and prevent infection. However, in both of these applications, the PRF membrane is not utilised as a barrier membrane but as a sheet of autologous fibrin intended to assist and improve soft tissue healing and thickness. The authors concluded that during GBR procedures (most notably during extensive GBR cases), PRF membranes

should be combined with either a collagen barrier membrane or titanium/titanium-reinforced membranes, further proving that PRF alone cannot be considered or should not be used as a barrier membrane'. In this context, PRF membranes can be placed over or under the barrier membrane. As PRF is known to rapidly promote greater soft tissue wound healing, its biological use involves contact with soft tissues on the outer surface of barrier membranes. However, it would be advantageous to place the PRF membrane under a non-resorbable membrane as the periosteum would not be able to supply angiogenesis through this membrane, and PRF placed under this membrane can supply the early growth factors responsible for new blood vessel formation within the underlying bone augmentation procedure. Therefore, PRF should be placed above or under the barrier membrane but should not be used as a barrier membrane by itself. Furthermore, Omar *et al*[32] presented a comprehensive narrative review and up-to-date survey of the available literature on in-vivo biological mechanisms related to GBR and the potential active role of the membrane. They summarised numerous membranes under various headings and subheadings but did not mention PRF anywhere. In their article, Higuchi *et al*[33] suggested that the current trend of designing membranes should focus not only on biodegradability or compatible growth for cells but also on additional functions such as bone stimulating or antibacterial properties. However, there was no mention of PRF in their description.

In their review article, Sasaki *et al*[34] summarised the fundamental characteristics of barrier membranes based on their components and provided an update from the material point of view; PRF was not included in the list of biodegradable and non-degradable membranes. In a recent narrative review by Alauddin *et al*[35], the authors summarised recent biomaterials and contemporary membranes utilised in periodontal regeneration and implant therapy in the market. Although the title was 'Barrier membranes in regenerative therapy', their aim was to evaluate all biological membranes and not just barrier membranes. Hence, PRF must have found its place in this review. However, in their description of autologous platelet concentrates (APCs), they concluded that in their literature search, APCs alone, as a barrier membrane, are lacking and, therefore, are recommended for future studies. Kim *et al*[36] reviewed various coated barrier membranes and reported that PRF-coated collagen membranes increased gingival thickness[37]. In another recent review on advances in barrier membranes by Yang *et al*[38], the authors summarised and described the ideal requirements of a barrier membrane. They also added notes on functional membranes, bioactive membranes, antimicrobial membranes, and structurally layered membranes. However, PRF was not mentioned under any heading or subheading of barrier membranes. Ren *et al*[39] mentioned PRF but specified that PRF should be used as a bioactive molecule as an adjunct to barrier membranes.

LITERATURE ADVOCATING PRF AS BARRIER MEMBRANE

Kawase *et al*[40] conducted a study on heat compression of PRF membranes and concluded that heat-compressed PRF membranes can be easily prepared on the chair-side and applied as a barrier membrane in the GTR procedure. However, in their in-vitro and in-vivo animal studies, they only evaluated the degradation rate of conventional gauze-pressed PRF against heat-compressed PRF. No other properties of barrier membranes have been studied; therefore, based on their observation, claiming that heat-compressed PRF can be used as a 'barrier membrane' does not seem justified. Isobe *et al*[41] studied the mechanical properties of fibrin membranes and associated them with their degradability compared with advance PRF, concentrated growth factors (CGFs), and platelet-poor plasma-derived fibrin membranes. They concluded that all three membranes were tough enough to serve as barrier membranes. Their statement was based on the evaluation of 'toughness as mechanical strength', but they evaluated the tensile strength of the membranes. Based on this, it can be concluded that certain membranes are mechanically resistant to stretching; however, their study did not provide any data on their space-maintaining capacity, stiffness, or delayed degradation time. Increased tensile strength of a membrane is useful for its ability to be sutured without tearing, as reported by Kardos *et al*[22].

A further extensive review by Aprile *et al*[42] presented the latest advancements in GBR membranes and described the process leading to the industrial development of materials for such biomedical applications. Among the exhaustive list, there was only a single sentence that mentioned PRF without any clear specification on whether PRF can be used as a barrier membrane. In another summary of barrier membranes[43], the authors particularly included PRF under the subheading of resorbable membranes but added that PRF should be used with other membranes where bone growth factors are indicated. Yu *et al*[44] demonstrated that double heating of a PRF membrane at 90°C for 10 s significantly improved its mechanical and degradation properties but decreased cell viability and fibroblast proliferation activity. Surmeli Baran *et al*[45] demonstrated that photobiomodulation of L-PRF resulted in better results than L-PRF alone (although not statistically significant) when used as a barrier membrane in animal studies. However, their study also included a collagen membrane group, which showed significantly improved results compared with all other study groups. In addition, the study was performed for 1 mo, which is too short to evaluate the regeneration and degradation of a membrane, and the defects were filled with bone substitutes, which again ruled out the stiffness or space-maintaining capacity of the membrane. In a recent descriptive review by Solomon *et al*[46] on identifying the perfect membrane, the authors

Table 2 List of review articles on barrier membranes

Sr. No.	Ref.	Was PRF included in the list of barrier membranes?
1	Dimitriou *et al*[11], 2012	No
2	Rakhmatia *et al*[26], 2013	No
3	Soheilifar *et al*[27], 2014	No
4	Lee *et al*[6], 2014	No
5	Rodriguez *et al*[29], 2018	No
6	Caballé-Serrano *et al*[7], 2018	No
7	Omar *et al*[32], 2019	No
8	Higuchi *et al*[33], 2019	No
9	Caballé-Serrano *et al*[47], 2019	No
10	Aprile *et al*[42], 2020	Yes (only mentioned)
11	Sasaki *et al*[34], 2021	No
12	Ren *et al*[39], 2022	Yes (as a supportive bioactive molecule to other barrier membranes)
13	Yang *et al*[38], 2022	No
14	Alauddin *et al*[35], 2022	Yes (as a supportive membrane)
15	Solomon *et al*[46], 2022	Yes (for increasing the soft tissue thickness)

PRF: Platelet-rich fibrin.

included PRF under the subheading of trends in the development of barrier membranes. However, all studies supported either mixing bone grafts with PRF for better regeneration, management of gingival recession, or improvement in the thickness of soft tissue due to PRF. There was no evidence or justification for including PRF in the category of barrier membranes[47]. A summary of different review articles on barrier membranes is presented in Table 2, with a mention of whether they included PRF in their list of barrier membranes.

FUTURE POTENTIAL OF USING PRF MEMBRANE AS A BARRIER MEMBRANE

Wong *et al*[48] enlarged the pores in the structures of PRFs by repeated freeze-drying and used Mg rings to create a scaffold. They found that the use of an Mg ring enhanced the osteogenic ability and migration capacity of Mg ions during degradation. Although they did not study any property fulfilling it to be a barrier membrane, the concept of modifying the pore size and incorporating Mg rings might be a potential area of future research to study its ability to improve the space-maintaining capacity, delay degradation time, and potentially increase the stiffness of PRF membranes. CGF, developed by Sacco, produces an autologous membrane that is thicker, denser, and more durable than conventional PRF [49]. Future research on the potential use of CGFs, rather than PRF, as barrier membranes should also be explored.

CONCLUSION

Although PRF can mimic and be handled like a GTR membrane, its main disadvantage is that it resorbs within approximately 7 d[5] to 28 d[25], which is substantially shorter than the 4-6 wk required for most periodontal regeneration applications. In addition, owing to its high resorption rate, its ability to maintain space is compromised. The quest for an ideal barrier membrane depends on the operator's preference, skills, and experience rather than specific guidelines implemented for bone and tissue generation. The incorporation of metal ions and nanoparticles to improve the stiffness and space-maintaining properties of PRF may be useful as a barrier membrane and can potentially be used alone. Thus, it is better to label PRF membranes as a supportive, revitalising, rejuvenating, biological, autologous, or biocompatible membrane for tissue regeneration.

FOOTNOTES

Author contributions: Agrawal AA has solely contributed to the manuscript.

Conflict-of-interest statement: The author declared no conflict of interest related to this manuscript.

Country/Territory of origin: India

ORCID number: Amit Arvind Agrawal 0000-0002-2235-7305.

Corresponding Author's Membership in Professional Societies: Indian Dental Association, No. 51827; Indian Society of Periodontology, No. A25-621.

S-Editor: Zhang H
L-Editor: A
P-Editor: Zhang H

REFERENCES

1 **Dohan Ehrenfest DM**, Bielecki T, Mishra A, Borzini P, Inchingolo F, Sammartino G, Rasmusson L, Everts PA. In search of a consensus terminology in the field of platelet concentrates for surgical use: platelet-rich plasma (PRP), platelet-rich fibrin (PRF), fibrin gel polymerization and leukocytes. *Curr Pharm Biotechnol* 2012; **13**: 1131-1137 [PMID: 21740379 DOI: 10.2174/138920112800624328]
2 **Dvorak HF**, Harvey VS, Estrella P, Brown LF, McDonagh J, Dvorak AM. Fibrin containing gels induce angiogenesis. Implications for tumor stroma generation and wound healing. *Lab Invest* 1987; **57**: 673-686 [PMID: 2447383]
3 **Chou AH**, LeGeros RZ, Chen Z, Li Y. Antibacterial effect of zinc phosphate mineralized guided bone regeneration membranes. *Implant Dent* 2007; **16**: 89-100 [PMID: 17356375 DOI: 10.1097/ID.0b013e318031224a]
4 **Nishibori M**, Betts NJ, Salama H, Listgarten MA. Short-term healing of autogenous and allogeneic bone grafts after sinus augmentation: a report of 2 cases. *J Periodontol* 1994; **65**: 958-966 [PMID: 7823278 DOI: 10.1902/jop.1994.65.10.958]
5 **Lekovic V**, Milinkovic I, Aleksic Z, Jankovic S, Stankovic P, Kenney EB, Camargo PM. Platelet-rich fibrin and bovine porous bone mineral vs. platelet-rich fibrin in the treatment of intrabony periodontal defects. *J Periodontal Res* 2012; **47**: 409-417 [PMID: 22126591 DOI: 10.1111/j.1600-0765.2011.01446.x]
6 **Lee SW**, Kim SG. Membranes for the Guided Bone Regeneration. *Maxillofac Plast Reconstr Surg* 2014; **36**: 239-246 [PMID: 27489841 DOI: 10.14402/jkamprs.2014.36.6.239]
7 **Caballé-Serrano J**, Munar-Frau A, Ortiz-Puigpelat O, Soto-Penaloza D, Peñarrocha M, Hernández-Alfaro F. On the search of the ideal barrier membrane for guided bone regeneration. *J Clin Exp Dent* 2018; **10**: e477-e483 [PMID: 29849973 DOI: 10.4317/jced.54767]
8 **Hoornaert A**, d'Arros C, Heymann MF, Layrolle P. Biocompatibility, resorption and biofunctionality of a new synthetic biodegradable membrane for guided bone regeneration. *Biomed Mater* 2016; **11**: 045012 [PMID: 27509180 DOI: 10.1088/1748-6041/11/4/045012]
9 **Zellin G**, Gritli-Linde A, Linde A. Healing of mandibular defects with different biodegradable and non-biodegradable membranes: an experimental study in rats. *Biomaterials* 1995; **16**: 601-609 [PMID: 7548610 DOI: 10.1016/0142-9612(95)93857-a]
10 **Wang HL**, Boyapati L. "PASS" principles for predictable bone regeneration. *Implant Dent* 2006; **15**: 8-17 [PMID: 16569956 DOI: 10.1097/01.id.0000204762.39826.0f]
11 **Dimitriou R**, Mataliotakis GI, Calori GM, Giannoudis PV. The role of barrier membranes for guided bone regeneration and restoration of large bone defects: current experimental and clinical evidence. *BMC Med* 2012; **10**: 81 [PMID: 22834465 DOI: 10.1186/1741-7015-10-81]
12 **Pineda LM**, Büsing M, Meinig RP, Gogolewski S. Bone regeneration with resorbable polymeric membranes. III. Effect of poly(L-lactide) membrane pore size on the bone healing process in large defects. *J Biomed Mater Res* 1996; **31**: 385-394 [PMID: 8806065 DOI: 10.1002/(SICI)1097-4636(199607)31:3<385::AID-JBM13>3.0.CO;2-I]
13 **Chvapil M**, Holusa R, Kliment K, Stoll M. Some chemical and biological characteristics of a new collagen-polymer compound material. *J Biomed Mater Res* 1969; **3**: 315-332 [PMID: 5793837 DOI: 10.1002/jbm.820030211]
14 **Taylor DF**, Smith FB. Porous methyl methacrylate as an implant material. *J Biomed Mater Res* 1972; **6**: 467-479 [PMID: 5014905 DOI: 10.1002/jbm.820060112]
15 **Klawitter JJ**, Bagwell JG, Weinstein AM, Sauer BW. An evaluation of bone growth into porous high density polyethylene. *J Biomed Mater Res* 1976; **10**: 311-323 [PMID: 1254618 DOI: 10.1002/jbm.820100212]
16 **Spector M**, Flemming WR, Kreutner A. Bone growth into porous high-density polyethylene. *J Biomed Mater Res* 1976; **10**: 595-603 [PMID: 947921 DOI: 10.1002/jbm.820100416]
17 **de Santana RB**, de Mattos CM, Francischone CE, Van Dyke T. Superficial topography and porosity of an absorbable

barrier membrane impacts soft tissue response in guided bone regeneration. *J Periodontol* 2010; **81**: 926-933 [PMID: 20380512 DOI: 10.1902/jop.2010.090592]

18 **Ducheyne P**, De Meester P, Aernoudt E. Influence of a functional dynamic loading on bone ingrowth into surface pores of orthopedic implants. *J Biomed Mater Res* 1977; **11**: 811-838 [PMID: 591524 DOI: 10.1002/jbm.820110603]

19 **Heck DA**, Nakajima I, Kelly PJ, Chao EY. The effect of load alteration on the biological and biomechanical performance of a titanium fiber-metal segmental prosthesis. *J Bone Joint Surg Am* 1986; **68**: 118-126 [PMID: 3941113]

20 **Gutta R**, Baker RA, Bartolucci AA, Louis PJ. Barrier membranes used for ridge augmentation: is there an optimal pore size? *J Oral Maxillofac Surg* 2009; **67**: 1218-1225 [PMID: 19446207 DOI: 10.1016/j.joms.2008.11.022]

21 **Amano Y**, Ota M, Sekiguchi K, Shibukawa Y, Yamada S. Evaluation of a poly-l-lactic acid membrane and membrane fixing pin for guided tissue regeneration on bone defects in dogs. *Oral Surg Oral Med Oral Pathol Oral Radiol Endod* 2004; **97**: 155-163 [PMID: 14970774 DOI: 10.1016/j.tripleo.2003.09.009]

22 **Kardos D**, Hornyák I, Simon M, Hinsenkamp A, Marschall B, Várdai R, Kállay-Menyhárd A, Pinke B, Mészáros L, Kuten O, Nehrer S, Lacza Z. Biological and Mechanical Properties of Platelet-Rich Fibrin Membranes after Thermal Manipulation and Preparation in a Single-Syringe Closed System. *Int J Mol Sci* 2018; **19** [PMID: 30388866 DOI: 10.3390/ijms19113433]

23 **Caballé-Serrano J**, Sawada K, Miron RJ, Bosshardt DD, Buser D, Gruber R. Collagen barrier membranes adsorb growth factors liberated from autogenous bone chips. *Clin Oral Implants Res* 2017; **28**: 236-241 [PMID: 26818588 DOI: 10.1111/clr.12789]

24 **Huang HL**, Ma YH, Tu CC, Chang PC. Radiographic Evaluation of Regeneration Strategies for the Treatment of Advanced Mandibular Furcation Defects: A Retrospective Study. *Membranes (Basel)* 2022; **12** [PMID: 35207140 DOI: 10.3390/membranes12020219]

25 **Yamashita Y**, Chen K, Kuroda S, Kasugai S. Stability of platelet-rich fibrin in vivo: histological study in rats. *Jr Oral Tissue Eng* 2016; **14**: 83-90 [DOI: 10.11223/JARDE.14.83]

26 **Rakhmatia YD**, Ayukawa Y, Furuhashi A, Koyano K. Current barrier membranes: titanium mesh and other membranes for guided bone regeneration in dental applications. *J Prosthodont Res* 2013; **57**: 3-14 [PMID: 23347794 DOI: 10.1016/j.jpor.2012.12.001]

27 **Soheilifar S**, Soheilifar S, Bidgoli M, Torkzaban P. Barrier Membrane, a Device for Regeneration: Properties and Applications. *Avicenna J Dent Res* 2014; **6**: e21343 [DOI: 10.17795/ajdr-21343]

28 **Miron RJ**, Zucchelli G, Pikos MA, Salama M, Lee S, Guillemette V, Fujioka-Kobayashi M, Bishara M, Zhang Y, Wang HL, Chandad F, Nacopoulos C, Simonpieri A, Aalam AA, Felice P, Sammartino G, Ghanaati S, Hernandez MA, Choukroun J. Use of platelet-rich fibrin in regenerative dentistry: a systematic review. *Clin Oral Investig* 2017; **21**: 1913-1927 [PMID: 28551729 DOI: 10.1007/s00784-017-2133-z]

29 **Rodriguez IA**, Selders GS, Fetz AE, Gehrmann CJ, Stein SH, Evensky JA, Green MS, Bowlin GL. Barrier membranes for dental applications: A review and sweet advancement in membrane developments. *Mouth Teeth* 2018; **2**: 6-9 [DOI: 10.15761/MTJ.1000108]

30 **Kobayashi E**, Flückiger L, Fujioka-Kobayashi M, Sawada K, Sculean A, Schaller B, Miron RJ. Comparative release of growth factors from PRP, PRF, and advanced-PRF. *Clin Oral Investig* 2016; **20**: 2353-2360 [PMID: 26809431 DOI: 10.1007/s00784-016-1719-1]

31 **Miron RJ**, Picos MA. PRF as a Barrier Membrane in Guided Bone Regeneration. [cited 25 December 2022]. In: Dentalcetoday.com [Internet]. Available from: https://www.dentalcetoday.com/wp-content/uploads/2018/06/1217_Miron_CE_216.pdf

32 **Omar O**, Elgali I, Dahlin C, Thomsen P. Barrier membranes: More than the barrier effect? *J Clin Periodontol* 2019; **46** Suppl 21: 103-123 [PMID: 30667525 DOI: 10.1111/jcpe.13068]

33 **Higuchi J**, Woźniak B, Chodara A, Fortunato G, Łojkowski W. Recent Advances In GTR/GBR Barrier Membranes Design for Periodontal Regeneration. *Biomed J Sci & Tech Res* 2019; **16** [DOI: 10.26717/BJSTR.2019.16.002807]

34 **Sasaki JI**, Abe GL, Li A, Thongthai P, Tsuboi R, Kohno T, Imazato S. Barrier membranes for tissue regeneration in dentistry. *Biomater Investig Dent* 2021; **8**: 54-63 [PMID: 34104896 DOI: 10.1080/26415275.2021.1925556]

35 **Alauddin MS**, Abdul Hayei NA, Sabarudin MA, Mat Baharin NH. Barrier Membrane in Regenerative Therapy: A Narrative Review. *Membranes (Basel)* 2022; **12** [PMID: 35629770 DOI: 10.3390/membranes12050444]

36 **Kim JY**, Park JB. Various Coated Barrier Membranes for Better Guided Bone Regeneration: A Review. *Coatings* 2022; **12**: 1059 [DOI: 10.3390/coatings12081059]

37 **Kapa BP**, N K S, G V G, Mehta DS. Coronally Advanced Flap Combined With Sticky Bone and i-PRF-Coated Collagen Membrane to Treat Single Maxillary Gingival Recessions: Case Series. *Clin Adv Periodontics* 2022; **12**: 147-151 [PMID: 33938633 DOI: 10.1002/cap.10164]

38 **Yang Z**, Wu C, Shi H, Luo X, Sun H, Wang Q, Zhang D. Advances in Barrier Membranes for Guided Bone Regeneration Techniques. *Front Bioeng Biotechnol* 2022; **10**: 921576 [PMID: 35814003 DOI: 10.3389/fbioe.2022.921576]

39 **Ren Y**, Fan L, Alkildani S, Liu L, Emmert S, Najman S, Rimashevskiy D, Schnettler R, Jung O, Xiong X, Barbeck M. Barrier Membranes for Guided Bone Regeneration (GBR): A Focus on Recent Advances in Collagen Membranes. *Int J Mol Sci* 2022; **23** [PMID: 36499315 DOI: 10.3390/ijms232314987]

40 **Kawase T**, Kamiya M, Kobayashi M, Tanaka T, Okuda K, Wolff LF, Yoshie H. The heat-compression technique for the conversion of platelet-rich fibrin preparation to a barrier membrane with a reduced rate of biodegradation. *J Biomed Mater Res B Appl Biomater* 2015; **103**: 825-831 [PMID: 25132655 DOI: 10.1002/jbm.b.33262]

41 **Isobe K**, Watanebe T, Kawabata H, Kitamura Y, Okudera T, Okudera H, Uematsu K, Okuda K, Nakata K, Tanaka T, Kawase T. Mechanical and degradation properties of advanced platelet-rich fibrin (A-PRF), concentrated growth factors (CGF), and platelet-poor plasma-derived fibrin (PPTF). *Int J Implant Dent* 2017; **3**: 17 [PMID: 28466249 DOI: 10.1186/s40729-017-0081-7]

42 **Aprile P**, Letourneur D, Simon-Yarza T. Membranes for Guided Bone Regeneration: A Road from Bench to Bedside. *Adv Healthc Mater* 2020; **9**: e2000707 [PMID: 32864879 DOI: 10.1002/adhm.202000707]

43 **Resnik RR**. The Use of Barrier Membranes in Implant Dentistry. *Chairside Magazine* 2018; **13**

44 **Yu S**, Wang Y, Miron RJ, Zhang Y. Structure, Barrier Function, and Bioactivity of Platelet-Rich Fibrin Following Thermal Processing. *Tissue Eng Part C Methods* 2021; **27**: 605-615 [PMID: 34714157 DOI: 10.1089/ten.TEC.2021.0177]

45 **Surmeli Baran S**, Temmerman A, Salimov F, Ucak Turer O, Sapmaz T, Haytac MC, Ozcan M. The Effects of Photobiomodulation on Leukocyte and Platelet-Rich Fibrin as Barrier Membrane on Bone Regeneration: An Experimental Animal Study. *Photobiomodul Photomed Laser Surg* 2021; **39**: 245-253 [PMID: 33434103 DOI: 10.1089/photob.2020.4943]

46 **Solomon SM**, Sufaru IG, Teslaru S, Ghiciuc CM, Stafie CS. Finding the Perfect Membrane: Current Knowledge on Barrier Membranes in Regenerative Procedures: A Descriptive Review. *Appl Sci* 2022; **12**: 1042 [DOI: 10.3390/app12031042]

47 **Caballé-Serrano J**, Munar-Frau A, Delgado L, Pérez R, Hernández-Alfaro F. Physicochemical characterization of barrier membranes for bone regeneration. *J Mech Behav Biomed Mater* 2019; **97**: 13-20 [PMID: 31085456 DOI: 10.1016/j.jmbbm.2019.04.053]

48 **Wong PC**, Wang CY, Jang JS, Lee CH, Wu JL. Large-Pore Platelet-Rich Fibrin with a Mg Ring to Allow MC3T3-E1 Preosteoblast Migration and to Improve Osteogenic Ability for Bone Defect Repair. *Int J Mol Sci* 2021; **22** [PMID: 33919677 DOI: 10.3390/ijms22084022]

49 **Rodella LF**, Favero G, Boninsegna R, Buffoli B, Labanca M, Scarì G, Sacco L, Batani T, Rezzani R. Growth factors, CD34 positive cells, and fibrin network analysis in concentrated growth factors fraction. *Microsc Res Tech* 2011; **74**: 772-777 [PMID: 21780251 DOI: 10.1002/jemt.20968]

World Journal of Clinical Cases

Submit a Manuscript: https://www.f6publishing.com

World J Clin Cases 2023 April 16; 11(11): 2405-2411

DOI: 10.12998/wjcc.v11.i11.2405

ISSN 2307-8960 (online)

MINIREVIEWS

Advances in translational therapy for locally advanced gastric cancer

Kai Zhao, Ying Na, Hui-Min Xu

Specialty type: Oncology

Provenance and peer review: Invited article; Externally peer reviewed.

Peer-review model: Single blind

Peer-review report's scientific quality classification

Grade A (Excellent): 0
Grade B (Very good): B, B
Grade C (Good): C, C, C
Grade D (Fair): 0
Grade E (Poor): 0

P-Reviewer: Kanaoujiya R, India; Kinami S, Japan; Preziosi F, Italy; Yuan X, China

Received: January 2, 2023
Peer-review started: January 2, 2023
First decision: January 20, 2023
Revised: February 2, 2023
Accepted: March 17, 2023
Article in press: March 17, 2023
Published online: April 16, 2023

Kai Zhao, Ying Na, Hui-Min Xu, Department of General Surgery, Weifang People's Hospital, Weifang 261041, Shandong Province, China

Corresponding author: Hui-Min Xu, MD, Chief Physician, Department of General Surgery, Weifang People's Hospital, No. 151 Guangwen Street, Kuiwen District, Weifang 261041, Shandong Province, China. xhm001@126.com

Abstract

Translational therapy refers to a combination of chemotherapy, radiotherapy, targeted therapy, and immunotherapy for patients with advanced gastric cancer who are initially unable to undergo R0 resection. This treatment can achieve partial or complete remission of the unresectable tumors to meet the criteria for R0 resection, thus enabling the patients to prolong their survival time and improve their quality of life. In gastric cancer, translational therapy has been tried and improved. At present, there are a large number of patients with locally advanced gastric cancer in China, and the selection of suitable patients for translational therapy to prolong objective survival and improve survival quality is one of the hot spots in the field of gastric cancer research.

Key Words: Translational therapy; Locally advanced; Gastric cancer; Chemotherapy; Radiotherapy treatment; Targeted therapy

Core Tip: In general, for patients with locally advanced gastric cancer, translational therapy can achieve different levels of survival benefit. Immunohistochemistry and genetic testing should be performed before treatment to select a more optimal comprehensive treatment strategy. For patients with locally advanced gastric cancer that is difficult to be resected at the initial stage, translational therapy followed by surgery can improve the survival benefit of patients.

Citation: Zhao K, Na Y, Xu HM. Advances in translational therapy for locally advanced gastric cancer. *World J Clin Cases* 2023; 11(11): 2405-2411
URL: https://www.wjgnet.com/2307-8960/full/v11/i11/2405.htm
DOI: https://dx.doi.org/10.12998/wjcc.v11.i11.2405

INTRODUCTION

The incidence and mortality rates of gastric cancer are among the highest in China and around the world[1]. As early gastroenteroscopy is not performed in all medical centers, the proportion of patients with advanced gastric cancer is high, and locally advanced gastric cancer accounts for 10%-35%. R0 resection cannot be performed due to severe invasion by the tumor, which cannot be separated from surrounding normal tissues or may be wrapped around large vessels, metastasized to regional lymph nodes, and fused into clusters. Yoshida *et al*[2] proposed that advanced gastric cancer can be divided into four categories: Class I, metastases are technically resectable, including single liver metastases, and 16a2, b1 lymph node metastases; Class II, patients with resectable metastases, accompanied by multiple liver metastases, intrahepatic metastases larger than 5 cm, or accompanied by No. 16a1, b2, or mediastinal lymph node metastases; Class III is only peritoneal metastases visible to the naked eye; Class IV refers to the combination of other distant metastases in addition to peritoneal metastases[2]. Several national and international studies[3-5] have shown that D2 Lymph node dissection should be the first treatment option for advanced gastric cancer, and there is little difference between open surgery and laparoscopic surgery[6]. The treatment model has changed from a single D2 lymph node dissection to a multidisciplinary and comprehensive treatment based on surgery for patients with locally advanced cancer. The integrated treatment model can further improve the survival quality of patients compared to traditional radical surgery combined with postoperative chemotherapy. For patients with locally advanced cancer, attention is focused on the examination of comprehensive treatment options and reducing the proportion of perioperative recurrence and achieving partial or full remission of unresectable factors by translational therapy, which has become one of the hot spots of research. Based on existing national and international research results[7,8], the current translational therapy for locally advanced gastric cancer generally includes the following: postoperative adjuvant chemotherapy and chemoradiotherapy, targeted therapy and immunotherapy. Neoadjuvant therapy refers to the preoperative administration of chemotherapy or radiotherapy to lower tumor stage, increase R0 resection rate and pathological remission, and improve patient prognosis. Neoadjuvant chemotherapy has potential advantages such as elimination of small metastases and reduction of postoperative recurrence. Preoperative tumor vessels are more abundant, and the drug can enter the tumor *via* blood vessels more easily, which increases the sensitivity of radiotherapy. A series of studies have been conducted on preoperative neoadjuvant chemoradiotherapy[9].

POSTOPERATIVE ADJUVANT CHEMOTHERAPY

The ACTS-GC study in Japan in 2011 included a total of 1059 patients with stage II and III gastric cancer after radical D2 surgery in a controlled study, with the experimental group (n = 529) given S-1 monotherapy postoperatively and the control group (n = 530) undergoing surgery only. The results showed that the 5-year progression-free survival (PFS) rate of patients in the experimental group (65.4% *vs* 53.1%, HR = 0.65, 95%CI: 0.54-0.80) was significantly higher, and the analysis showed that postoperative S-1 monotherapy provided benefit in patients with stage II and IIIA gastric cancer, but did not improve the survival of patients with stage IIIB disease[10]. Due to the difference in pharmacokinetics between Caucasians and Xanthoderms, and the fact that D0-D1 surgery for gastric cancer was mostly performed in Europe and America at that time, while D2 surgery was performed in Japan, the ACTS-GC study was not directly extended to the postoperative adjuvant treatment of gastric cancer in Europe and America. Furthermore, the JACCRO GC-07 study conducted in Japan treated advanced gastric cancer patients with either S-1 monotherapy or S-1 combined with docetaxel chemotherapy. The 3-year disease recurrence-free survival (RFS) rate (67.7% *vs* 57.4%, P = 0.0008) and 3-year overall survival (OS) rate (77.7% *vs* 71.2%, P = 0.007) were significantly improved in the combination treatment group[11]. In order to determine the optimal adjuvant treatment protocol for advanced gastric cancer, the CLASSIC study by Korean and Chinese researchers included 1035 patients with gastric cancer who underwent stage II-IIIb radical D2 surgery, and were randomly divided into the experimental group (520 cases) and the observational group (515 cases), and the experimental group was treated with the XELOX regimen (oxaliplatin and capecitabine) for 6 mo. The 5-year follow-up results showed that the XELOX regimen improved disease-free survival (DFS) (68% *vs* 53%, P < 0.0001) and OS (78% *vs* 69%, P < 0.0015), suggesting that the XELOX regimen can be used as the standard adjuvant chemotherapy regimen after D2 radical surgery for stage II-IIIb gastric cancer[12,13]. Based on the ACTS-GC and CLASSIC studies, it was determined that postoperative adjuvant chemotherapy may be the standard treatment strategy after radical D2 surgery for gastric cancer.

POSTOPERATIVE ADJUVANT RADIOTHERAPY

As mentioned above, due to the different surgical protocols for gastric cancer used in Europe and America, postoperative chemotherapy is mostly combined with radiotherapy. A total of 559 patients

with T3-T4 stage surgically resectable gastric cancer were included in the study by Smalley *et al*[14] in 2012. These patients were randomly assigned to the surgery group or the surgery combined with postoperative radiotherapy group, and the results showed that patients in the surgery combined with postoperative radiotherapy group had a longer 3-year median RFS (27 mo *vs* 19 mo, $P < 0.001$) and 3-year median OS (35 mo *vs* 27 mo, $P = 0.0046$) than those in the surgery-only group[14], which provided the basis for the subsequent NCCN gastric cancer guidelines. The ARTIST and ARTIST-II studies were conducted in Korea to determine whether the addition of radiotherapy to combination chemotherapy after radical surgery for D2 lymph node dissection improves patient survival[15,16]. The studies showed that the addition of radiotherapy to D2 Lymph node dissection plus two-drug adjuvant chemotherapy did not improve patient survival. According to the results of several randomized controlled studies in patients with locally advanced gastric cancer, combination chemotherapy after D2 radical surgery can improve patient survival. For patients with stage III gastric cancer after D2 radical surgery, two-drug combination is more effective than single-drug chemotherapy and the addition of radiotherapy to chemotherapy can improve the survival of patients with D0 or D1 lymph node dissection but cannot improve the survival of patients after D2 radical surgery.

Based on the results of a number of large randomized controlled studies (Table 1), for patients with locally advanced gastric cancer, adjuvant chemotherapy S-1, S-1 + docetaxel, SOX and XELOX are all optional chemotherapy regimens after radical D2 treatment which can significantly improve survival. For stage III gastric cancer patients after D2 radical resection, two-drug chemotherapy is more effective than single-drug chemotherapy. At present, all major guidelines recommend postoperative adjuvant therapy for locally advanced gastric cancer. Adding radiotherapy to postoperative chemotherapy could improve the survival rate of patients in the D1 or D0 clearance range, but could not further improve the survival rate of patients after D2 radical resection.

TARGETED THERAPY

Progress is slow in targeted therapy research for gastric cancer, and overexpression of human epidermal growth factor receptor 2 (HER-2) may be an independent factor in the poor prognosis of gastric cancer. The T0GA study published in 2010 confirmed, for the first time, the effectiveness of trastuzumab in the treatment of advanced gastric cancer, opening the era of targeted therapy for advanced gastric cancer [17]. Currently, there are more drugs and studies targeting HER-2, vascular endothelial growth factor (VEGF), epidermal growth factor receptor (EGFR)-1, the hepatocyte growth factor (HGF)/tyrosine protein kinase Met (c-MET) signaling pathway, immune checkpoints and other related pathways and targets.

Anti-HER-2-targeted drugs

HER-2 is a member of the epidermal growth factor family, which accelerates tumor cell growth and invasion by activating the RAS-RAF-MRK-MAPK pathway, PI3K-AKT and other pathways. The T0GA trial confirmed that trastuzumab combined with cisplatin-based chemotherapy can prolong OS in patients with locally advanced gastric cancer by approximately 1.2 mo[17]. The 2011 NCCN guidelines recommend first-line trastuzumab in combination with platinum-based chemotherapy for eligible patients with advanced gastric cancer, and clinical trials such as JFMC45-1102 showed that in patients with advanced gastric cancer who have not previously been treated with anti-HER2-directed agents, trastuzumab is beneficial as a second- or super-second-line agent[18]. Clinical trials such as HER-FLOT [19] have also shown that trastuzumab plays a role in the preoperative translational therapy and neoadjuvant therapy of locally advanced gastric cancer.

Anti-angiogenesis-related targeted drugs

The VEGF family accelerates the formation of neovascularization in the tumor through a series of cellular pathways to provide sufficient blood supply and nutrition for tumor cells, and the current anti-angiogenesis-targeted drugs for locally advanced gastric cancer include monoclonal antibodies, tyrosine kinase inhibitors, *etc*. As monoclonal antibodies have more adverse effects and unsatisfactory clinical trial results, most of the drugs have not entered the clinic. Tyrosine kinase inhibitors mainly inhibit tumor angiogenesis by binding to the VEGFR and can selectively inhibit tyrosine kinase activity to exert anti-tumor effects. A phase II clinical trial of apatinib in locally advanced gastric cancer patients after failure of second-line chemotherapy showed that a single agent could improve the survival of patients with locally advanced gastric cancer who had previously received ≥ 2 failed chemotherapy regimens [20]. Currently, it is mainly used in China for third-line and above treatment of locally advanced gastric cancer or esophagogastric junction cancer.

Anti-EGFR targeting drugs

The overexpression of EGFR in gastric cancer can reach 50%-63%, and its expression level is positively correlated with tumor aggressiveness and negatively correlated with differentiation degree and survival time, suggesting that EFGR may be a target in gastric cancer treatment. However, the clinical trial

Table 1 Research on postoperative chemotherapy and radiochemotherapy for locally advanced gastric cancer

Title of research study	Year	Country/district	Study design	Study assignment	Surgical procedure	Complete percentage	3-yr progression-free survival	Overall survival
ARTIST	2012	South Korea	Phase 3 randomized controlled study	Surgery + XP (228 cases); Surgery + XP + radiotherapy (230 cases)	D2	82%; 75%	74.2%; 78.2%	73%; 75%
INT-0116	2012	North America	Phase 3 randomized controlled study	Surgery (277 cases); R0 + radiotherapy/fluorouracil (282 cases)	D2	96%; 65%	-	-
CLASSIC	2014	Eastern Asia	Phase 3 randomized controlled study	Surgery (515 cases); Surgery + XELOX (520 cases)	D2	83%; 67%	59%; 74%	69%; 78%
RESOLVE	2021	China	Phase 3 randomized controlled study	Surgery + XELOX (364 cases); Surgery + SOX (364 cases); SOX + surgery + SOX\S-1 (365 cases)	D2	70%; 68%; 58%	51.1%; 56.5%; 59.4%	-
ARTIST II	2021	South Korea	Phase 3 randomized controlled study	Surgery + S-1; Surgery + SOX (181 cases); Surgery + SOX + radiotherapy (183 cases)	D2	71%; 85%; 83%	64.8%; 74.3%; 72.8%	-
JACCROGC-07	2022	Japan	Phase 3 randomized controlled study	Surgery + S-1; Surgery + S-1 + docetaxel (456 cases)	D2	80%; 40%	57.4%; 67.7%	71.2%; 77.7%

results of related targeting drugs have not met the clinical application requirements.

Targeted drugs of the HGF/c-MET signaling pathway

The HGF/c-MET signaling pathway is related to tumor cell migration, invasion and intra-tumor blood vessel formation. Also, 10%-15% of patients with advanced gastric cancer have amplification of MET, the gene encoding c-MET protein, and 30% of these patients have high expression of MET, and the expression level is negatively correlated with patient prognosis. However, the current clinical trial results of drugs targeting this pathway are unsatisfactory.

IMMUNOTHERAPY

Immune checkpoint inhibitors are used to inhibit tumor growth and invasion by restoring the immune killing effect of host T cells on tumor cells and weakening the immune escape of tumor cells. KEYNOTE-059 is a global phase II clinical trial of programmed cell death protein (PD)-1 inhibitors for gastric cancer or esophagogastric junction cancer, which has shown that immunosuppressants are effective and safe in the treatment of advanced gastric cancer or esophagogastric junction cancer[21]. The CHECKMATE-649 study showed that chemotherapy combined with nivolumab significantly improved OS in patients with a PD-ligand 1 (PD-L1) combined positive score (CPS) ≥ 5 compared to chemotherapy alone, and that combination therapy resulted in a statistically significant benefit in PFS in patients with CPS ≥1 and in all randomized patients with CPS ≥ 5[22]. Data analysis in the KEYNOTE-811 study of HER-2 positive patients showed that the experimental group (chemotherapy + trastuzumab + pembrolizumab) had a significantly improved objective remission rate (74.4% *vs* 51.9% P = 0.00006)[23]. The results of the ongoing ATTRACTION-05 study in Japan which is evaluating the efficacy and safety of adjuvant nivolumab in combination with SOX or XELOX regimens for stage III gastric or esophagogastric junction cancer after D2 radical surgery have not yet been published. The preliminary data of multiple phase II clinical trials of preoperative immunosuppressive agents combined with chemotherapy in the treatment of locally advanced gastric cancer presented at the 2021 ASCO Congress showed that the pathological complete response rate was 10%-30%[23-25]. At present, a number of multicenter, phase II, randomized controlled clinical trials of preoperative immunotherapy combined with neoadjuvant chemotherapy for the treatment of advanced gastric cancer (NICE study) are being conducted in China, and the results are expected to be announced.

CONCLUSION

In translational therapy of locally advanced gastric cancer, D2 lymph node dissection is the first standard surgical procedure, and D2 radical surgery + a postoperative adjuvant chemotherapy regimen has long been used as the main treatment regimen. When there is a bottleneck in the therapeutic effect, the emergence of neoadjuvant chemotherapy has improved the survival quality of patients, thus establishing the use of neoadjuvant chemotherapy. D1 radical surgery + postoperative radiotherapy in Europe and America showed improved survival, but the later regimen of D2 radical surgery + postoperative adjuvant chemotherapy + radiotherapy has not further improved survival, and the therapeutic effect of neoadjuvant radiotherapy is still being verified. In recent years, microsatellite instability and high-frequency tumor mutation antigens in Epstein-Barr virus-positive gastric cancer are expected to be potential targets for gastric cancer immunotherapy, and there are several phase III clinical trials underway. We look forward to the announcement of the results. Targeted therapies for gastric cancer are progressing slowly, and the currently available drugs for different targets are not effective in the treatment of locally advanced gastric cancer, but the combination of immunotherapy with targeted therapies is also in progress[26]. Nivolumab in combination with ipilimumab and pembrolizumab plus trastuzumab[27] can improve the survival of patients to some extent, but the combination of drugs leads to an increase in adverse effects, and further comprehensive assessment of the benefit is thus needed.

Challenges and opportunities

At present, with the continuous development of clinical research on translational therapy, its status in the treatment of locally advanced gastric cancer may be further improved, and immune and targeted therapies are also likely to make breakthroughs. Further refinement of treatment plans and models, identification of the best combination and treatment opportunities, and even the treatment sequence of immunotherapy and chemoradiotherapy are all future research directions. The heterogeneity of gastric cancer is strong, and the molecular characteristics of tumors are also important factors affecting treatment efficacy and prognosis of locally advanced gastric cancer. Future studies also need to be designed to stratify tumors more accurately. The author believes that with the rapid development of drug research and extensive clinical trials, the survival of patients with locally advanced gastric cancer is expected to be further improved.

FOOTNOTES

Author contributions: Zhao K, Na Y, and Xu HM designed the study; Zhao K, Na Y, and Xu HM wrote the manuscript; all authors have read and approve the final manuscript.

Conflict-of-interest statement: The authors declare that they have no conflicts of interest or financial interests with any organization involved in the research.

Country/Territory of origin: China

ORCID number: Kai Zhao 0000-0002-1773-4460; Ying Na 0000-0002-8356-9109; Hui-Min Xu 0000-0001-8896-571X.

S-Editor: Yan JP
L-Editor: A
P-Editor: Yan JP

REFERENCES

1 **Cao W**, Chen HD, Yu YW, Li N, Chen WQ. Changing profiles of cancer burden worldwide and in China: a secondary analysis of the global cancer statistics 2020. *Chin Med J (Engl)* 2021; **134**: 783-791 [PMID: 33734139 DOI: 10.1097/CM9.0000000000001474]

2 **Yoshida K**, Yamaguchi K, Okumura N, Tanahashi T, Kodera Y. Is conversion therapy possible in stage IV gastric cancer: the proposal of new biological categories of classification. *Gastric Cancer* 2016; **19**: 329-338 [PMID: 26643880 DOI: 10.1007/s10120-015-0575-z]

3 **Wang FH**, Zhang XT, Li YF, Tang L, Qu XJ, Ying JE, Zhang J, Sun LY, Lin RB, Qiu H, Wang C, Qiu MZ, Cai MY, Wu

Q, Liu H, Guan WL, Zhou AP, Zhang YJ, Liu TS, Bi F, Yuan XL, Rao SX, Xin Y, Sheng WQ, Xu HM, Li GX, Ji JF, Zhou ZW, Liang H, Zhang YQ, Jin J, Shen L, Li J, Xu RH. The Chinese Society of Clinical Oncology (CSCO): Clinical guidelines for the diagnosis and treatment of gastric cancer, 2021. *Cancer Commun (Lond)* 2021; **41**: 747-795 [PMID: 34197702 DOI: 10.1002/cac2.12193]

4 **Japanese Gastric Cancer Association**. Japanese gastric cancer treatment guidelines 2018 (5th edition). *Gastric Cancer* 2021; **24**: 1-21 [PMID: 32060757 DOI: 10.1007/s10120-020-01042-y]

5 **Adachi Y**, Mori M, Maehara Y, Matsumata T, Okudaira Y, Sugimachi K. Surgical results of perforated gastric carcinoma: an analysis of 155 Japanese patients. *Am J Gastroenterol* 1997; **92**: 516-518 [PMID: 9068483]

6 **Huang C**, Liu H, Hu Y, Sun Y, Su X, Cao H, Hu J, Wang K, Suo J, Tao K, He X, Wei H, Ying M, Hu W, Du X, Yu J, Zheng C, Liu F, Li Z, Zhao G, Zhang J, Chen P, Li G; Chinese Laparoscopic Gastrointestinal Surgery Study (CLASS) Group. Laparoscopic vs Open Distal Gastrectomy for Locally Advanced Gastric Cancer: Five-Year Outcomes From the CLASS-01 Randomized Clinical Trial. *JAMA Surg* 2022; **157**: 9-17 [PMID: 34668963 DOI: 10.1001/jamasurg.2021.5104]

7 **Sah BK**, Zhang B, Zhang H, Li J, Yuan F, Ma T, Shi M, Xu W, Zhu Z, Liu W, Yan C, Li C, Liu B, Yan M. Neoadjuvant FLOT versus SOX phase II randomized clinical trial for patients with locally advanced gastric cancer. *Nat Commun* 2020; **11**: 6093 [PMID: 33257672 DOI: 10.1038/s41467-020-19965-6]

8 **Satyananda V**, Gupta R, Hari DM, Yeh J, Chen KT. Advances in Translational Research and Clinical Care in Pancreatic Cancer: Where Are We Headed? *Gastroenterol Res Pract* 2019; **2019**: 7690528 [PMID: 30863442 DOI: 10.1155/2019/7690528]

9 **Yeoh KG**, Tan P. Mapping the genomic diaspora of gastric cancer. *Nat Rev Cancer* 2022; **22**: 71-84 [PMID: 34702982 DOI: 10.1038/s41568-021-00412-7]

10 **Sasako M**, Sakuramoto S, Katai H, Kinoshita T, Furukawa H, Yamaguchi T, Nashimoto A, Fujii M, Nakajima T, Ohashi Y. Five-year outcomes of a randomized phase III trial comparing adjuvant chemotherapy with S-1 versus surgery alone in stage II or III gastric cancer. *J Clin Oncol* 2011; **29**: 4387-4393 [PMID: 22010012 DOI: 10.1200/JCO.2011.36.5908]

11 **Kakeji Y**, Yoshida K, Kodera Y, Kochi M, Sano T, Ichikawa W, Lee SW, Shibahara K, Shikano T, Kataoka M, Ishiguro A, Ojima H, Sakai Y, Musha N, Takase T, Kimura T, Takeuchi M, Fujii M. Three-year outcomes of a randomized phase III trial comparing adjuvant chemotherapy with S-1 plus docetaxel versus S-1 alone in stage III gastric cancer: JACCRO GC-07. *Gastric Cancer* 2022; **25**: 188-196 [PMID: 34351555 DOI: 10.1007/s10120-021-01224-2]

12 **Bang YJ**, Kim YW, Yang HK, Chung HC, Park YK, Lee KH, Lee KW, Kim YH, Noh SI, Cho JY, Mok YJ, Ji J, Yeh TS, Button P, Sirzén F, Noh SH; CLASSIC trial investigators. Adjuvant capecitabine and oxaliplatin for gastric cancer after D2 gastrectomy (CLASSIC): a phase 3 open-label, randomised controlled trial. *Lancet* 2012; **379**: 315-321 [PMID: 22226517 DOI: 10.1016/S0140-6736(11)61873-4]

13 **Noh SH**, Park SR, Yang HK, Chung HC, Chung IJ, Kim SW, Kim HH, Choi JH, Kim HK, Yu W, Lee JI, Shin DB, Ji J, Chen JS, Lim Y, Ha S, Bang YJ; CLASSIC trial investigators. Adjuvant capecitabine plus oxaliplatin for gastric cancer after D2 gastrectomy (CLASSIC): 5-year follow-up of an open-label, randomised phase 3 trial. *Lancet Oncol* 2014; **15**: 1389-1396 [PMID: 25439693 DOI: 10.1016/S1470-2045(14)70473-5]

14 **Smalley SR**, Benedetti JK, Haller DG, Hundahl SA, Estes NC, Ajani JA, Gunderson LL, Goldman B, Martenson JA, Jessup JM, Stemmermann GN, Blanke CD, Macdonald JS. Updated analysis of SWOG-directed intergroup study 0116: a phase III trial of adjuvant radiochemotherapy versus observation after curative gastric cancer resection. *J Clin Oncol* 2012; **30**: 2327-2333 [PMID: 22585691 DOI: 10.1200/JCO.2011.36.7136]

15 **Lee J**, Lim DH, Kim S, Park SH, Park JO, Park YS, Lim HY, Choi MG, Sohn TS, Noh JH, Bae JM, Ahn YC, Sohn I, Jung SH, Park CK, Kim KM, Kang WK. Phase III trial comparing capecitabine plus cisplatin versus capecitabine plus cisplatin with concurrent capecitabine radiotherapy in completely resected gastric cancer with D2 lymph node dissection: the ARTIST trial. *J Clin Oncol* 2012; **30**: 268-273 [PMID: 22184384 DOI: 10.1200/JCO.2011.39.1953]

16 **Park SH**, Lim DH, Sohn TS, Lee J, Zang DY, Kim ST, Kang JH, Oh SY, Hwang IG, Ji JH, Shin DB, Yu JI, Kim KM, An JY, Choi MG, Lee JH, Kim S, Hong JY, Park JO, Park YS, Lim HY, Bae JM, Kang WK; ARTIST 2 investigators. A randomized phase III trial comparing adjuvant single-agent S1, S-1 with oxaliplatin, and postoperative chemoradiation with S-1 and oxaliplatin in patients with node-positive gastric cancer after D2 resection: the ARTIST 2 trial(☆). *Ann Oncol* 2021; **32**: 368-374 [PMID: 33278599 DOI: 10.1016/j.annonc.2020.11.017]

17 **Bang YJ**, Van Cutsem E, Feyereislova A, Chung HC, Shen L, Sawaki A, Lordick F, Ohtsu A, Omuro Y, Satoh T, Aprile G, Kulikov E, Hill J, Lehle M, Rüschoff J, Kang YK; ToGA Trial Investigators. Trastuzumab in combination with chemotherapy versus chemotherapy alone for treatment of HER2-positive advanced gastric or gastro-oesophageal junction cancer (ToGA): a phase 3, open-label, randomised controlled trial. *Lancet* 2010; **376**: 687-697 [PMID: 20728210 DOI: 10.1016/S0140-6736(10)61121-X]

18 **Mitsui Y**, Sato Y, Miyamoto H, Fujino Y, Takaoka T, Miyoshi J, Kagawa M, Ohnuma H, Hirakawa M, Kubo T, Osuga T, Sagawa T, Takahashi Y, Katsuki S, Okuda T, Takimoto R, Kobune M, Nobuoka T, Hirata K, Kato J, Takayama T. Trastuzumab in combination with docetaxel/cisplatin/S-1 (DCS) for patients with HER2-positive metastatic gastric cancer: feasibility and preliminary efficacy. *Cancer Chemother Pharmacol* 2015; **76**: 375-382 [PMID: 26099968 DOI: 10.1007/s00280-015-2807-7]

19 **Al-Batran SE**, Hozaeel W, Jäger E. Combination of trastuzumab and triple FLOT chemotherapy (5-fluorouracil/leucovorin, oxaliplatin, and docetaxel) in patients with HER2-positive metastatic gastric cancer: report of 3 cases. *Onkologie* 2012; **35**: 505-508 [PMID: 23007148 DOI: 10.1159/000341841]

20 **Li J**, Qin S, Xu J, Guo W, Xiong J, Bai Y, Sun G, Yang Y, Wang L, Xu N, Cheng Y, Wang Z, Zheng L, Tao M, Zhu X, Ji D, Liu X, Yu H. Apatinib for chemotherapy-refractory advanced metastatic gastric cancer: results from a randomized, placebo-controlled, parallel-arm, phase II trial. *J Clin Oncol* 2013; **31**: 3219-3225 [PMID: 23918952 DOI: 10.1200/JCO.2013.48.8585]

21 **Shitara K**, Van Cutsem E, Bang YJ, Fuchs C, Wyrwicz L, Lee KW, Kudaba I, Garrido M, Chung HC, Lee J, Castro HR, Mansoor W, Braghiroli MI, Karaseva N, Caglevic C, Villanueva L, Goekkurt E, Satake H, Enzinger P, Alsina M, Benson A, Chao J, Ko AH, Wainberg ZA, Kher U, Shah S, Kang SP, Tabernero J. Efficacy and Safety of Pembrolizumab or Pembrolizumab Plus Chemotherapy vs Chemotherapy Alone for Patients With First-line, Advanced Gastric Cancer: The

KEYNOTE-062 Phase 3 Randomized Clinical Trial. *JAMA Oncol* 2020; **6**: 1571-1580 [PMID: 32880601 DOI: 10.1001/jamaoncol.2020.3370]

22 **Janjigian YY**, Shitara K, Moehler M, Garrido M, Salman P, Shen L, Wyrwicz L, Yamaguchi K, Skoczylas T, Campos Bragagnoli A, Liu T, Schenker M, Yanez P, Tehfe M, Kowalyszyn R, Karamouzis MV, Bruges R, Zander T, Pazo-Cid R, Hitre E, Feeney K, Cleary JM, Poulart V, Cullen D, Lei M, Xiao H, Kondo K, Li M, Ajani JA. First-line nivolumab plus chemotherapy versus chemotherapy alone for advanced gastric, gastro-oesophageal junction, and oesophageal adenocarcinoma (CheckMate 649): a randomised, open-label, phase 3 trial. *Lancet* 2021; **398**: 27-40 [PMID: 34102137 DOI: 10.1016/S0140-6736(21)00797-2]

23 **Janjigian YY**, Kawazoe A, Yañez P, Li N, Lonardi S, Kolesnik O, Barajas O, Bai Y, Shen L, Tang Y, Wyrwicz LS, Xu J, Shitara K, Qin S, Van Cutsem E, Tabernero J, Li L, Shah S, Bhagia P, Chung HC. The KEYNOTE-811 trial of dual PD-1 and HER2 blockade in HER2-positive gastric cancer. *Nature* 2021; **600**: 727-730 [PMID: 34912120 DOI: 10.1038/s41586-021-04161-3]

24 **Bang YJ**, Van Cutsem E, Fuchs CS, Ohtsu A, Tabernero J, Ilson DH, Hyung WJ, Strong VE, Goetze TO, Yoshikawa T, Tang LH, Hwang PMT, Webb N, Adelberg D, Shitara K. KEYNOTE-585: Phase III study of perioperative chemotherapy with or without pembrolizumab for gastric cancer. *Future Oncol* 2019; **15**: 943-952 [PMID: 30777447 DOI: 10.2217/fon-2018-0581]

25 **Rivera F**, Izquierdo-Manuel M, García-Alfonso P, Martínez de Castro E, Gallego J, Limón ML, Alsina M, López L, Galán M, Falcó E, Manzano JL, González E, Muñoz-Unceta N, López C, Aranda E, Fernández E, Jorge M, Jiménez-Fonseca P. Perioperative trastuzumab, capecitabine and oxaliplatin in patients with HER2-positive resectable gastric or gastro-oesophageal junction adenocarcinoma: NEOHX phase II trial. *Eur J Cancer* 2021; **145**: 158-167 [PMID: 33485079 DOI: 10.1016/j.ejca.2020.12.005]

26 **Saito H**, Kuroda H, Matsunaga T, Osaki T, Ikeguchi M. Increased PD-1 expression on CD4+ and CD8+ T cells is involved in immune evasion in gastric cancer. *J Surg Oncol* 2013; **107**: 517-522 [PMID: 23129549 DOI: 10.1002/jso.23281]

27 **Janjigian YY**, Maron SB, Chatila WK, Millang B, Chavan SS, Alterman C, Chou JF, Segal MF, Simmons MZ, Momtaz P, Shcherba M, Ku GY, Zervoudakis A, Won ES, Kelsen DP, Ilson DH, Nagy RJ, Lanman RB, Ptashkin RN, Donoghue MTA, Capanu M, Taylor BS, Solit DB, Schultz N, Hechtman JF. First-line pembrolizumab and trastuzumab in HER2-positive oesophageal, gastric, or gastro-oesophageal junction cancer: an open-label, single-arm, phase 2 trial. *Lancet Oncol* 2020; **21**: 821-831 [PMID: 32437664 DOI: 10.1016/S1470-2045(20)30169-8]

World Journal of Clinical Cases

Submit a Manuscript: https://www.f6publishing.com

World J Clin Cases 2023 April 16; 11(11): 2412-2422

DOI: 10.12998/wjcc.v11.i11.2412

ISSN 2307-8960 (online)

ORIGINAL ARTICLE

Retrospective Study

Study of pathogenic genes in a pedigree with familial dilated cardiomyopathy

Xin-Ru Zhang, Hang Ren, Fang Yao, Yang Liu, Chun-Li Song

Specialty type: Cardiac and cardiovascular systems

Provenance and peer review: Unsolicited article; Externally peer reviewed.

Peer-review model: Single blind

Peer-review report's scientific quality classification

Grade A (Excellent): 0
Grade B (Very good): B
Grade C (Good): 0
Grade D (Fair): 0
Grade E (Poor): 0

P-Reviewer: Gupta P, United States

Received: November 12, 2022
Peer-review started: November 12, 2022
First decision: February 14, 2023
Revised: February 22, 2023
Accepted: March 15, 2023
Article in press: March 15, 2023
Published online: April 16, 2023

Xin-Ru Zhang, Department of Pharmacy, The Second Hospital of Jilin University, Changchun 130000, Jilin Province, China

Hang Ren, Fang Yao, Yang Liu, Chun-Li Song, Department of Cardiovascular Medicine, The Second Hospital of Jilin University, Changchun 130000, Jilin Province, China

Corresponding author: Chun-Li Song, MD, Chief Physician, Professor, Department of Cardiovascular Medicine, The Second Hospital of Jilin University, Ziqiang Street, Nanguan District, Changchun 130000, Jilin Province, China. songchunl@jlu.edu.cn

Abstract

BACKGROUND

Dilated cardiomyopathy (DCM) is a genetically heterogeneous cardiac disorder characterized by left ventricular dilation and contractile dysfunction. The substantial genetic heterogeneity evident in patients with DCM contributes to variable disease severity and complicates overall prognosis, which can be very poor.

AIM

To identify pathogenic genes in DCM through pedigree analysis.

METHODS

Our research team identified a patient with DCM in the clinic. Through investigation, we found that the family of this patient has a typical DCM pedigree. High-throughput sequencing technology, next-generation sequencing, was used to sequence the whole exomes of seven samples in the pedigree.

RESULTS

A novel and potentially pathogenic gene mutation-ANK2p.F3067L-was discovered. The mutation was completely consistent with the clinical information for this DCM pedigree. Sanger sequencing was used to further verify the locus of the mutation in pedigree samples. These results were consistent with those of high-throughput sequencing.

CONCLUSIONS

ANK2p.F3067L is considered a novel and potentially pathogenic gene mutation in DCM.

Key Words: Dilated cardiomyopathy; Gene mutation; Whole exomes sequencing; Sanger sequencing; ANK2p.F3067L; Potentially pathogenic gene

Core Tip: Our research team identified a typical dilated cardiomyopathy (DCM) pedigree clinically. High-throughput sequencing technology, namely second-generation sequencing, is used to sequence the entire exon group of seven samples in the pedigree. A new potential pathogenic gene mutation ANK2p.F3067L was found in DCM.

Citation: Zhang XR, Ren H, Yao F, Liu Y, Song CL. Study of pathogenic genes in a pedigree with familial dilated cardiomyopathy. *World J Clin Cases* 2023; 11(11): 2412-2422
URL: https://www.wjgnet.com/2307-8960/full/v11/i11/2412.htm
DOI: https://dx.doi.org/10.12998/wjcc.v11.i11.2412

INTRODUCTION

Dilated cardiomyopathy (DCM) is a type of genetically heterogeneous cardiomyopathy[1]. It is the primary cause of heart transplantation and the third most common cause of heart failure, malignant arrhythmia, and sudden death[2]. DCM has obvious genetic heterogeneity, with nearly 50% of DCM cases caused by genetic factors that are dominant in pathogenesis[3]. However, research on the pathogenic genes associated with DCM is lacking. With the development of next-generation sequencing technology, it has recently been found that DCM is related to variations in genes encoding sarcomeric, cytoskeletal, nuclear membrane, and desmosomal proteins such as TTN, MYH7, TNNT2, LMNA, and DSP[4,5]. However, only ~40% of familial DCM patients harbor known hereditary changes in pathogenic genes[6], while the etiology of the remaining 60% of familial DCM patients remains unclear. Therefore, the identification of pathogenic genes in DCM through pedigree analysis has become an ardent focus of current research.

We believe that our study makes a significant contribution to the literature and will be of interest to the readership of your journal because we discovered the rs764952487 (ANK2p.F3067L) locus-a novel mutation locus of pathogenic genes-in a DCM family characterized in this study. It would be useful for clinical implications of these results in medicine, especially general medicine.

Clinical presentation

The family with the DCM pedigree resides in Nongan, a county in Jilin Province. The patient's parents were cousins (both of his parents are deceased-his father having succumbed to DCM). There are five brothers and three sisters in his generation of the family pedigree. Among the eight siblings, six were DCM patients (five males and one female). Based on information from the patient, there are more than 30 living family members in his family. At the time of writing this manuscript, we have obtained 19 samples from this pedigree, including II-2, II-3 and his wife, II-4 and his wife, II-6, II-7, II-8, III-1, III-2 and his wife, III-3, III-4, IV-1, IV-2, IV-3, IV-4, IV-5, and IV-6. According to clinical tests on existing samples, the key clinical information confirmed that these patients are afflicted with DCM. The pedigree chart is presented in Figure 1, from which it may be inferred that DCM in the patient's pedigree may be autosomal dominant.

According to their chief complaints, clinical medical records, and electrocardiogram and echocardiogram results, seven patients were confirmed to have DCM in the pedigree. Among these seven patients, two (I-1, II-1) died of DCM. Four samples of surviving patients were collected (II-2, II-3, II-4, and II-7; sample II-5 was not collected). Although II-2 had no obvious clinical symptoms, echocardiography showed enlargement of the left ventricle. The proband II-3 was first diagnosed at the age of 47, presenting with chest tightness and shortness of breath when fatigued. At the age of 57, mild activity after a common viral illness lead to chest tightness, shortness of breath, cough, and phlegm. These symptoms prompted him to visit a doctor for the first time. Echocardiography revealed a left ventricular end-diastolic diameter of 67 mm and left ventricular ejection fraction (LVEF) of 23%. The results indicated that his heart was significantly enlarged and his LVEF reduced. Coronary angiography was performed, ruling out cardiac enlargement caused by coronary heart disease. The clinical diagnosis was DCM. In the past 5 years, the proband was admitted to the hospital more than 10 times due to heart failure. He was equipped with an implantable cardioverter defibrillator pacemaker at the age of 60. In addition, II-4 and II-7 were also diagnosed with DCM. They also underwent coronary angiography, again ruling out cardiac enlargement caused by coronary heart disease. The clinical characteristics of the

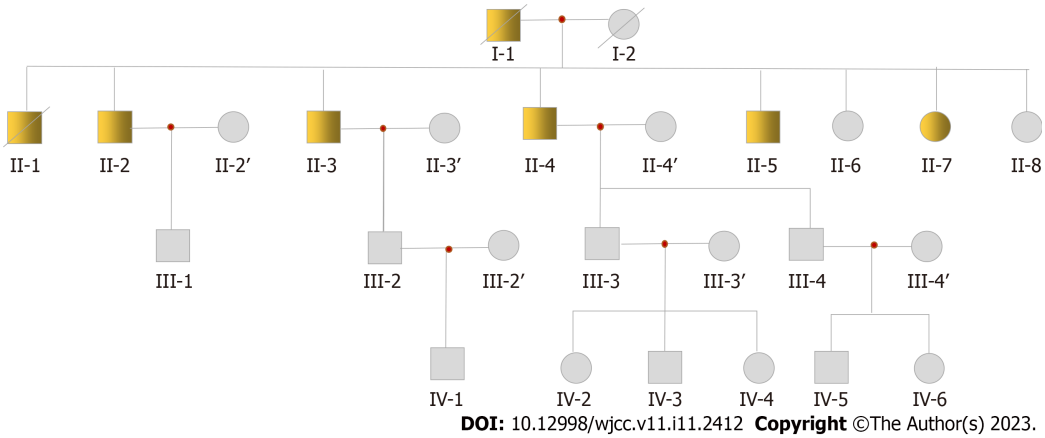

DOI: 10.12998/wjcc.v11.i11.2412

Figure 1 Dilated cardiomyopathy pedigree map.

patients with DCM in the pedigree are shown in Table 1.

METHODS AND MATERIALS

Subjects

The pedigree consisted of 26 family members (13 men and 13 women; Figure 1). They were diagnosed according to the World Health Organization 1995 diagnostic criteria (left ventricle end-diastolic diameter > 2.7 cm/m^2; fractional shortening < 25%).

Linkage analysis

Seven subjects were included in the linkage study. Genomic DNA was extracted from peripheral blood samples. Linkage analysis of the peripheral blood of seven family members was performed.

Exome sequencing

Five micrograms of DNA from each of the two affected male individuals was used to construct exome libraries using the Agilent SureSelect exome capture system (Agilent Technologies, Santa Clara, CA, United States). The libraries were sequenced on the Illumina Solexa GAIIx platform following the manufacturer's instructions (Illumina, San Diego, CA, United States). Raw image files were processed using the Illumina pipeline (version 1.3.4) for base calling and generating reads. Reads were aligned to the human reference genome (University of California Santa Cruz, UCSC hg19; Santa Cruz, CA, United States) using Burrows-Wheeler aligner (BWA, version 0.7.5a-r405) software[7]. Single nucleotide polymorphisms (SNPs) and indels (insertions and deletions) were identified using the genome analysis toolkit (GATK, version 4.1.4.1)[8]. SNPs from regions with read depth > 4 and quality scores > 20 (Q20 scores) were reserved for subsequent analysis. SNPs and indels were annotated using ANNOVAR (version 2017-07-17)[9]. Based on the SNP database (dbSNP) and 1000 genomes annotation with PolyPhen prediction, any non-synonymous variants not assigned a 'benign' prediction were considered damaging.

Identification of pathogenic genes

Whole-exome sequencing and analysis: To determine the pathogenic mutations of the DCM pedigree, we sequenced the whole exomes of seven samples (II-3, II-4 and his wife, II-7, II-8, III-3, and IV-2) and evaluated the data quality using FastQC (version 0.11.7)[10]. In addition, we removed adapter sequences and filtered low-quality sequences using Trimmomatic (version 0.39)[11]. The results of the filtered exome data are shown in Table 2. Then we aligned the paired-end sequences based on the human reference genome hg38 using BWA (version 0.7.5a-r405)[7]. The results for the comparative analysis of full exon data are presented in Table 3. To evaluate these results, we performed statistical analysis on the coverage of all exon regions. The average exon coverage for each sample was 106×–133× and approximately 95% of the regions reached 20× coverage. The read depth attained during sequencing was deemed sufficient for downstream data processing, with results listed in Table 4.

Identification of potentially pathogenic gene mutations: To identify potentially pathogenic gene mutations, we first identified sequence mutations using GATK software based on sequence alignment results. A total of 790998 sequence variation sites were obtained from seven samples. Subsequently, the sequence variations were annotated using ANNOVAR (version 2017-07-17)[9]. These annotations refer to a number of public databases, including RefSeq gene, cytoBand, phast ConsElements46way, genomic

Table 1 Clinical situation of dilated cardiomyopathy patients in the family

Pedigree number	Age	Gender	Age of first episode	LVDD (mm)	EF	Arrythmia
I-1	60 (death)	Male	-	-	-	-
II-1	63 (death)	Male	-	-	-	-
II-2	67	Male	-	57	74	Tachyarrhythmia
II-3	62	Male	47	67	23	Occasional premature beat
II-4	60	Male	53	72	46	Occasional premature beat
II-7	64	Female	58	60	45	Normal

Normal value of left ventricular diastolic dysfunction range: 45-55 mm (male), 35-50 mm (female). Normal value of ejection fraction range: 50%-70%. LVDD: Left ventricular diastolic dysfunction; EF: Ejection fraction.

Table 2 Results of full exon data filtering for 7 samples of the dilated cardiomyopathy pedigree

Sample	Total fragment	Both surviving read	Both surviving percent (%)	Forward surviving read	Forward surviving percent (%)	Reverse surviving read	Reverse surviving percent (%)
NKHS180096608-1A	46819669	44206494	94.42	1744245	3.73	479022	1.02
NKHS180096609-1A	49533235	46949404	94.78	1678343	3.39	520287	1.05
NKHS180096610-1A	48923103	46768485	95.60	1261086	2.58	556552	1.14
BDYE190000049-1A-A15-D709	40876211	38862445	95.07	1166146	2.85	500985	1.23
BDYE190000049-1A-A16-D712	41083445	37681342	91.72	2509536	6.11	328352	0.80
BDYE190000049-1A-A18-N710	48628579	45254586	93.06	2318870	4.77	604022	1.24
BDYE190000049-1A-A94-N709	40940470	38630007	94.36	1406632	3.44	533856	1.30

Table 3 Comparison results of full exon data in 7 samples of the dilated cardiomyopathy pedigree

Sample	Total read	Map read	Map percent (%)	Pair read	Pair percent (%)	Unmap read	Unmap percent (%)	Error rate	Insert size
NKHS180096608-1A	88412988	88409570	100.00	88406934	99.99	3418	0.00	1.423552e-03	240.0
NKHS180096609-1A	93898808	93894502	100.00	93891688	99.99	4306	0.00	1.443503e-03	251.1
NKHS180096610-1A	93536970	93533588	100.00	93530978	99.99	3382	0.00	1.420605e-03	263.9
BDYE190000049-1A-A15-D709	77724890	77721381	100.00	77719324	99.99	3509	0.00	1.472474e-03	268.5
BDYE190000049-1A-A16-D712	75362684	75358337	99.99	75354470	99.99	4347	0.01	1.745109e-03	242.0
BDYE190000049-1A-A18-N710	90509172	90505290	100.00	90502656	99.99	3882	0.00	1.417089e-03	228.7
BDYE190000049-1A-A94-N709	77260014	77257377	100.00	77255286	99.99	2637	0.00	1.423070e-03	247.2

Super Dups, gwas Catalog, avsnp147, cosmic70, esp6500siv2_all, nci60, exac03, 1000g2015aug_all, 1000g2015aug_afr, 1000g2015aug_amr, 1000g2015 aug_eur, 1000g2015aug_eas, 1000g2015aug_sas, dbSNP, SIFT, Polyphen2, LRT, Mutation Taster, Mutation Assessor, FATHMM, PROVEAN, VEST3, CADD, DANN, fath mm-MKL, Meta SVM, Meta LR, integrated fit Cons, integrated confidence,

Table 4 Comparison results of all exon coverage data in 7 samples of the dilated cardiomyopathy pedigree

Sample	Target length	Coverage length	Coverage ratio (%)	20× coverage length	20× coverage ratio (%)	Average coverage ratio
NKHS180096608-1A	60448148	60132794	99.48	57685743	95.43	120.31
NKHS180096609-1A	60448148	60141586	99.49	57964001	95.89	125.84
NKHS180096610-1A	60448148	60001829	99.26	57821317	95.65	121.60
BDYE190000049-1A-A15-D709	60448148	60134381	99.48	57334579	94.85	106.07
BDYE190000049-1A-A16-D712	60448148	60119415	99.46	57181880	94.60	109.16
BDYE190000049-1A-A18-N710	60448148	59997575	99.25	57728734	95.50	132.73
BDYE190000049-1A-A94-N709	60448148	59993121	99.25	57223253	94.67	110.74

GERP++_RS, phyloP7way_vertebrat, phyloP20way_mammalian, phastCons7way_vertebrate, phastCons20way_mammalian, SiPhy_29way_log Odds, and clinvar _20170130. Next, the sequence variations and annotation results were multilayer-filtered, based primarily on the allele frequency of the locus in the population [the locus with mutation allele frequency (MAF) ≥ 0.05 was filtered according to the MAF value of the site in sequence variation databases, such as esp6500siv2_all, ExAC ALL, ExAC_EAS, ExAC_SAS, 1000g2015aug_all, 1000g2015aug_eas, and 1000g2015aug_sas], locus annotation information, locus harmfulness prediction, clinical information, comparison of sample genotype, and comparison with the Online Mendelian Inheritance in Man database.

In addition, we identified CNVs using HMZDelFinder (version 2016)[12] and identified variations in chromosome structure using Meerkat. Finally, based on an investigation of the relevant literature and comprehensive analysis of the filtered mutation sites, rs764952487 (ANK2p.F3067L) emerged as a potential new DCM pathogenic gene mutation site.

RESULTS

Candidate variant analysis

The frequency of the rs764952487 mutation genotype in the population was less than 0.0001 (1/10000) in each public database. The mutation genotype is located in a conserved region of the genome. Its conservation score in the phastConsElements100way database is 499. It is predicted to be a harmful mutation by LRT, Mutation Taster, PROVEAN, MetaSVM, MetaLR, CAP, fathmm-MKL, and other software. This site is located in the 38th exon of the ankyrin-B gene (*ANK2*) (reference sequence NM_001148)-an arrhythmia pathogenic gene. The codon changes to c.T9199C and the amino acid changes to p.F3067L (phenylalanine mutates to leucine), characterized as non-synonymous mutations (missense mutations). Information on the mutation sites is shown in Table 5.

According to a study on the protein structure of the *ANK2* gene, rs764952487 is located on the helix of ZU5-ZU5-UPA-DD tandem, the neighbor of the death domain (DD). Studies have confirmed that the ZU5-ZU5-UPA domain can form a tightly packed structural supermodel, while DD can enter freely. The formation of the ZZU supermodel does not affect the spectral binding of the anchorin. However, it does change the interface mutation of the ZZU domain and further impairs the function of ankyrin-B, which has become the target of many pathogenic mutations.

Sequencing results for the mutation sites of potential pathogenic genes

To further determine the reliability of gene mutation identification, we obtained the sequence alignment results for rs764952487 in seven samples. As shown in Figure 2, mutations were detected in samples from all three afflicted patients (II-3, II-4, and II-7), while mutations were not detected in the other four samples. In all seven samples, the sequence coverage of the site location was greater than 100×, ensuring the accuracy of the identification of variant sites.

At the same time, we verified the locus of rs764952487 in all 19 samples, including the above seven samples, using Sanger sequencing. The Sanger sequencing results were consistent with the results for whole-exome sequencing. Moreover, the Sanger results for the rs764952487 Locus in all samples were consistent with the clinical information. This further indicated that the rs764952487 Locus may constitute a novel pathogenic gene mutation in DCM. The clinical information and mutation site genotype of the rs764952487 Locus in all samples are shown in Table 4. The Sanger sequencing results

Table 5 Mutation site information

Site	Mutation	Gene	Reference sequence	Gene subregion	Codon	Amino acid
Chr4: 113357817 (rs764952487)	T/C	*ANK2*	NM_001148	Exon38	c.T9199C	p.F3067L

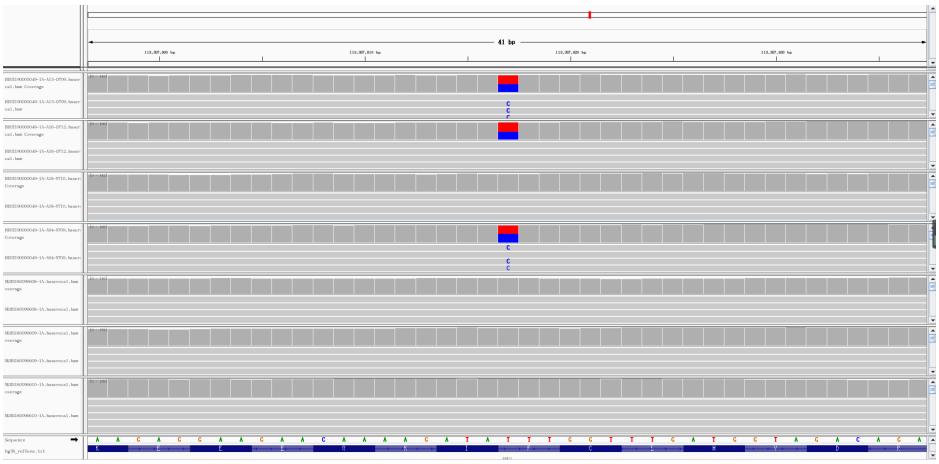

DOI: 10.12998/wjcc.v11.i11.2412

Figure 2 Sequence alignment results of rs764952487 in the 7 samples.

for some of the samples are shown in Figure 3. As shown in Figure 3A, the rs764952487 Locus for sample II-3 is a heterozygous mutant. As shown in Figure 3B, the rs764952487 Locus for sample III--3 is wild-type.

Table 6 shows that among the samples collected in the pedigree so far, all DCM patients carry the ANK2p.F3067L locus. No abnormalities were found in family members who did not carry ANK2p.F3067L. Younger participants carrying ANK2p.F3067L had not yet reported clinical symptoms or received abnormal ultrasound results. In summary, ANK2p.F3067L-a novel and potentially pathogenic mutation, was discovered by genetic investigation of this DCM pedigree. Considering the influence of ANK mutations on prolonged QT intervals, all DCM patients in the pedigree were reviewed. The mutation did not cause arrhythmia in patient II-3.

DISCUSSION

Ankyrin-B is a member of the anchor protein family. As a multifunctional membrane adapter, ankyrin-B is an important ion channel protein auxiliary. It is widely expressed in human tissues and highly expressed in cardiomyocytes, playing an important role in a variety of cardiac physiological functions. Ankyrin-B plays a vital role in the localization of ion transporters, ion channel localization, calcium homeostasis regulation, and membrane stability of cardiomyocytes (Figure 4). As shown in Figure 1, Na^+/K^+-ATPase, Na^+/Ca^{2+} exchanger (NCX1), and inositol 1,4,5-trisphosphate receptor in the sarcoplasmic reticulum and transverse tubules of cardiomyocytes, maintain normal contractile function and signal transduction function in cardiomyocytes[13]. The targeting and post-translational stability of NCX1 in cardiomyocytes depends on the expression of ankyrin-B, while elevated expression of NCX1 is directly related to myocardial contractile function[14]. The elevated expression of NCX1 leads to an imbalance in intracellular calcium homeostasis and activates calpains. The activation of calpains partially degrades contractile proteins and inhibits myocardial systolic function, resulting in cardiac enlargement and eventually leading to DCM[15,16]. Therefore, the expression of ankyrin-B is important for maintaining the normal contractile function of cardiomyocytes.

ANK2 is a gene coding for ankyrin-B. Its size is approximately 560 kb, consisting of 53 exons on human chromosome 4. In the present study, we found that *ANK2* is a common pathogenic gene in arrhythmia syndrome. Its genetic mutation can lead to a broad-spectrum arrhythmia phenotype called "anchor protein-B syndrome".

Although arrhythmia syndrome and hereditary cardiomyopathy are considered to be different genetic diseases, there is a significant phenotypic overlap between them. Clinically, cardiomyopathy is often associated with arrhythmias and abnormal cardiac conduction. Conversely, gene mutations associated with arrhythmia syndrome are also linked to morphological and structural abnormalities in certain types of cardiomyopathy[17-19]. It has been confirmed that common arrhythmia genes such as *PLN*, *SCN5A*, *KCNQ1*, *KCNH2*, and *KCNE2* are associated with hereditary cardiomyopathy[20]. Recent

Table 6 Clinical information and mutation site genotypes of the pedigree

Pedigree number	Gender	Age	DCM	*ANK2* (T>C)
II-2	Male	67	Yes	T/C
II-3	Male	62	Yes	T/C
II-4	Male	60	Yes	T/C
II-6	Female	71	No	T/T
II-7	Female	65	Yes	T/C
II-8	Female	56	No	T/T
II-3′	Female	56	No	T/T
II-4′	Female	55	No	T/T
III-1	Male	40	Unknow	T/T
III-2	Male	41	Unknow	T/C
III-3	Male	38	Unknow	T/T
III-4	Male	32	Unknow	T/C
III-3′	Female	37	No	T/T
IV-3	Female	15	Unknow	T/T
IV-4	Female	13	Unknow	T/T
IV-1	Male	11	Unknow	T/T
IV-2	Male	11	Unknow	T/T
IV-5	Male	6	Unknow	T/C
IV-6	Female	2	Unknow	T/T

DCM: Dilated cardiomyopathy.

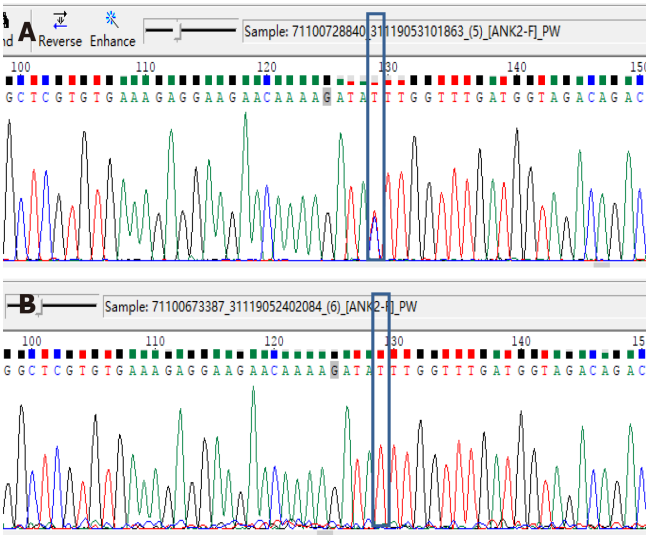

DOI: 10.12998/wjcc.v11.i11.2412

Figure 3 Sanger sequencing results. A: Sanger sequencing results of rs764952487 Locus of sample II-3; B: Sanger sequencing results of rs764952487 Locus of sample III-3.

studies have found that there are multiple co-pathogenic genes in arrhythmia syndrome and DCM (such as *ABCC9* and *SCN5A*)[18,21]. A number of researchers have found that variations in the *SCN5A* gene can cause calcium homeostasis imbalance, resulting in myocardial injury and cardiac enlargement. This eventually leads to DCM[19-23]. *In vitro* studies have shown that most *ANK2* gene mutations can cause abnormal expression and distribution of ankyrin-B and its binding proteins, resulting in an

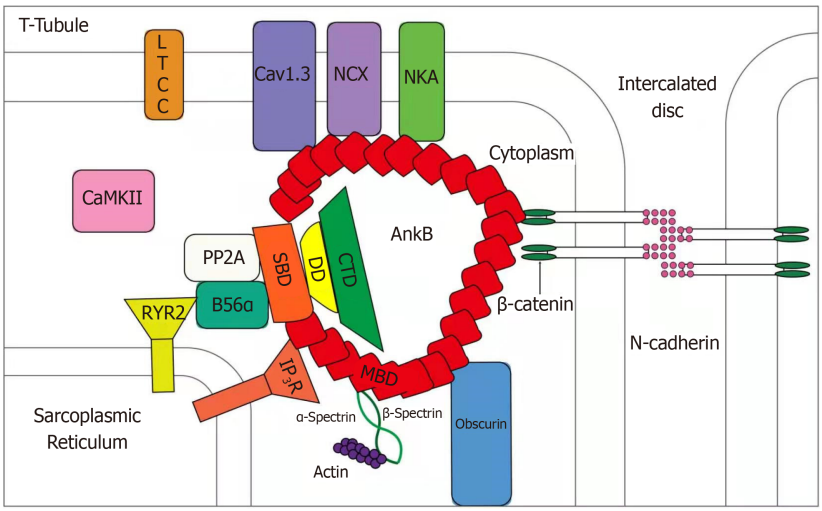

DOI: 10.12998/wjcc.v11.i11.2412

Figure 4 Role of ankyrin-B in cardiomyocytes.

imbalance of calcium homeostasis in cardiomyocytes[24,25].

In recent years, an increasing number of researchers have found that *ANK2* gene mutations not only cause arrhythmia syndrome but are also related to the occurrence of cardiomyopathy. As early as 2003, Mohler *et al*[26] found that ANK2+/- myocardial cells exhibited spontaneous contraction capacity decline and intracellular calcium dynamic disorder. In 2015, Lopes *et al*[20] found that mutations in *ANK2* can modify the phenotypic expression of hypertrophic cardiomyopathy. In 2017, Swayne *et al*[24] reported the case of a severe idiopathic DCM patient (sudden death at the age of 36) and a DCM patient with pulmonary hypertension. Both of these patients carried the *ANK2* gene mutation. In the same year, Forleo *et al*[27] also found *ANK2* gene variation in patients with DCM. Although there is a host of ankyrin-B isoforms in the heart, the primary isoform is canonical 220-kD ankyrin-B[28]. Ankyrin-B-188 and ankyrin-B-212 are two ankyrin-B isoforms present in the heart. Ankyrin-B-188 is expressed in human ventricular cardiomyocytes, which regulates NCX expression, whereas ankyrin-B-212 is expressed in cardiomyocytes and skeletal muscle, is localized to the M-line, and exclusively interacts with obscurin[29]. A cardiomyocyte-specific ankyrin-B-knockout mouse was designed (as ankyrin-B-null mice die shortly after birth) that developed a phenotype including dramatic structural abnormalities, biventricular dilation, reduced ejection fraction, cardiac fibrosis, premature death, and exercise-induced death[30].

In summary, our research team discovered the rs764952487 (ANK2p.F3067L) locus-a novel mutation locus of pathogenic genes-in the DCM family characterized in this study. The codon changes to c.T9199C and the amino acid changes to p.F3067L (phenylalanine mutates to leucine). It is a non-synonymous mutation (*i.e.*, missense mutation). The frequency of the rs764952487 mutation genotype in the population of each public database is less than 0.0001 (1/10 000). The mutation genotype is located in a conserved region of the genome. Its conservation score in the phastCons-Elements100way database is 499. It is predicted to be a harmful mutation by LRT, MutationTaster, PROVEAN, MetaSVM, MetaLR, CAP, fathmm-MKL, and other software. Sanger sequencing of the rs764952487 locus in 19 pedigrees was performed by our team to validate the whole-exome sequencing results. The clinical information of this DCM family is consistent with that of the former. Among all samples collected thus far, all DCM patients carried ANK2p.F3067L, while no abnormalities were found in non-ANK2p.F3067L carriers. Young people carrying ANK2p.F3067L did not report clinical symptoms or receive abnormal ultrasound results. This indicates that ANK2p.F3067L is likely a pathogenic gene mutation in DCM and that its influence on the onset of DCM is age-dependent. Our team will continue to monitor the pedigree, especially the young ANK2p.F3067L carriers who have not yet developed DCM. We will further verify the function of ANK2p.F3067L *in vitro* and *in vivo*, as a novel gene mutation in this pedigree.

CONCLUSION

In summary, ANK2p.F3067L is considered a novel and potentially pathogenic gene mutation in DCM.

ARTICLE HIGHLIGHTS

Research background

Dilated cardiomyopathy (DCM) is a type of genetically heterogeneous cardiomyopathy; it is the primary cause of heart transplantation and the third most common cause of heart failure, malignant arrhythmia, and sudden death. Although DCM has obvious genetic heterogeneity, with nearly 50% of DCM cases caused by genetic factors that are dominant in pathogenesis, research on the pathogenic genes associated with DCM is lacking.

Research motivation

With the development of next-generation sequencing technology, it has recently been found that DCM is related to variations in a number of genes encoding sarcomeric, cytoskeletal, nuclear membrane, and desmosomal proteins. However, only ~40% of familial DCM patients harbor known hereditary changes in pathogenic genes, while the etiology of the remaining 60% of familial DCM patients remains unclear. Therefore, the identification of pathogenic genes in DCM through pedigree analysis has become critical in the field of cardiovascular disease.

Research objectives

Our research team identified a typical DCM pedigree clinically. This study aimed to identify pathogenic genes in DCM through pedigree analysis.

Research methods

Our research team sequenced the whole exomes of seven samples in the pedigree using high-throughput sequencing technology, namely next-generation sequencing, and verified the potential candidate gene mutations in nineteen samples of the pedigree using Sanger sequencing. Then, we identified the sample sequence mutations using bioinformatics methods, and identified the family pathogenic gene mutations according to the family sample clinical information and gene variation annotation information.

Research results

A novel and potentially pathogenic gene mutation-ANK2p.F3067L-was discovered. The codon changes to c.T9199C and the amino acid changes to p.F3067L (phenylalanine mutates to leucine). It is a non-synonymous mutation (*i.e.*, missense mutation).

Research conclusions

The mutation-ANK2p.F3067L was completely consistent with the clinical information for this DCM pedigree. It is considered a novel and potentially pathogenic gene mutation in DCM.

Research perspectives

Our study adds new members to DCM pathogenic genes, and makes a significant contribution to the literature. It would be useful for clinical implications of these results in medicine, especially general medicine.

ACKNOWLEDGEMENTS

The authors thank those who contributed to this paper, as well as all participants and the reviewers for their careful reading and valuable.

FOOTNOTES

Author contributions: Zhang XR contributed to the concept, definition of intellectual content, literature search, clinical studies, statistical analysis, manuscript preparation and review; Song CL contributed to the design and manuscript editing; Liu Y contributed to the experimental studies; Yao F contributed to the data acquisition; Ren H contributed to the data analysis.

Supported by the Jilin Provincial Healthcare Talent Special Program, No. 2019SCZT08.

Institutional review board statement: The study was reviewed and approved by the Ethics Committee of The Second Hospital of Jilin University.

Informed consent statement: All study participants, or their legal guardian, provided informed written consent prior to study enrollment.

Conflict-of-interest statement: The authors have no conflicts of interest to declare.

Data sharing statement: No additional data are available.

Country/Territory of origin: China

ORCID number: Xin-Ru Zhang 0000-0001-5064-0362; Chun-Li Song 0000-0001-5028-5567.

S-Editor: Zhang H
L-Editor: A
P-Editor: Zhang H

REFERENCES

1 **Ramchand J**, Wallis M, Macciocca I, Lynch E, Farouque O, Martyn M, Phelan D, Chong B, Lockwood S, Weintraub R, Thompson T, Trainer A, Zentner D, Vohra J, Chetrit M, Hare DL, James P. Prospective Evaluation of the Utility of Whole Exome Sequencing in Dilated Cardiomyopathy. *J Am Heart Assoc* 2020; **9**: e013346 [PMID: 31931689 DOI: 10.1161/JAHA.119.013346]

2 **Liu X**, Yu H, Pei J, Chu J, Pu J, Zhang S. Clinical characteristics and long-term prognosis in patients with chronic heart failure and reduced ejection fraction in China. *Heart Lung Circ* 2014; **23**: 818-826 [PMID: 24881031 DOI: 10.1016/j.hlc.2014.02.022]

3 **McNally EM**, Golbus JR, Puckelwartz MJ. Genetic mutations and mechanisms in dilated cardiomyopathy. *J Clin Invest* 2013; **123**: 19-26 [PMID: 23281406 DOI: 10.1172/JCI62862]

4 **Zhao Y**, Feng Y, Zhang YM, Ding XX, Song YZ, Zhang AM, Liu L, Zhang H, Ding JH, Xia XS. Targeted next-generation sequencing of candidate genes reveals novel mutations in patients with dilated cardiomyopathy. *Int J Mol Med* 2015; **36**: 1479-1486 [PMID: 26458567 DOI: 10.3892/ijmm.2015.2361]

5 **Pérez-Serra A**, Toro R, Sarquella-Brugada G, de Gonzalo-Calvo D, Cesar S, Carro E, Llorente-Cortes V, Iglesias A, Brugada J, Brugada R, Campuzano O. Genetic basis of dilated cardiomyopathy. *Int J Cardiol* 2016; **224**: 461-472 [PMID: 27736720 DOI: 10.1016/j.ijcard.2016.09.068]

6 **Section of Precision Cardiovascular Medicine of Chinese Society of Cardiology**, Precision Cardiovascular Medicine Branch of China International Exchange; Promotive Association for Medical, Health Care Editorial Board of Chinese Journal of Cardiology. [Guideline for the genetic diagnosis of monogenic cardiovascular diseases]. *Zhonghua Xin Xue Guan Bing Za Zhi* 2019; **47**: 175-196 [PMID: 30897877 DOI: 10.3760/cma.j.issn.0253-3758.2019.03.003]

7 **Li H**, Durbin R. Fast and accurate long-read alignment with Burrows-Wheeler transform. *Bioinformatics* 2010; **26**: 589-595 [PMID: 20080505 DOI: 10.1093/bioinformatics/btp698]

8 **McKenna A**, Hanna M, Banks E, Sivachenko A, Cibulskis K, Kernytsky A, Garimella K, Altshuler D, Gabriel S, Daly M, DePristo MA. The Genome Analysis Toolkit: a MapReduce framework for analyzing next-generation DNA sequencing data. *Genome Res* 2010; **20**: 1297-1303 [PMID: 20644199 DOI: 10.1101/gr.107524.110]

9 **Wang K**, Li M, Hakonarson H. ANNOVAR: functional annotation of genetic variants from high-throughput sequencing data. *Nucleic Acids Res* 2010; **38**: e164 [PMID: 20601685 DOI: 10.1093/nar/gkq603]

10 **de Sena Brandine G**, Smith AD. Falco: high-speed FastQC emulation for quality control of sequencing data. *F1000Res* 2019; **8**: 1874 [PMID: 33552473 DOI: 10.12688/f1000research.21142.2]

11 **Bolger AM**, Lohse M, Usadel B. Trimmomatic: a flexible trimmer for Illumina sequence data. *Bioinformatics* 2014; **30**: 2114-2120 [PMID: 24695404 DOI: 10.1093/bioinformatics/btu170]

12 **Gambin T**, Akdemir ZC, Yuan B, Gu S, Chiang T, Carvalho CMB, Shaw C, Jhangiani S, Boone PM, Eldomery MK, Karaca E, Bayram Y, Stray-Pedersen A, Muzny D, Charng WL, Bahrambeigi V, Belmont JW, Boerwinkle E, Beaudet AL, Gibbs RA, Lupski JR. Homozygous and hemizygous CNV detection from exome sequencing data in a Mendelian disease cohort. *Nucleic Acids Res* 2017; **45**: 1633-1648 [PMID: 27980096 DOI: 10.1093/nar/gkw1237]

13 **Koenig SN**, Mohler PJ. The evolving role of ankyrin-B in cardiovascular disease. *Heart Rhythm* 2017; **14**: 1884-1889 [PMID: 28765088 DOI: 10.1016/j.hrthm.2017.07.032]

14 **Skogestad J**, Aronsen JM, Tovsrud N, Wanichawan P, Hougen K, Stokke MK, Carlson CR, Sjaastad I, Sejersted OM, Swift F. Coupling of the Na+/K+-ATPase to Ankyrin B controls Na+/Ca2+ exchanger activity in cardiomyocytes. *Cardiovasc Res* 2020; **116**: 78-90 [PMID: 30949686 DOI: 10.1093/cvr/cvz087]

15 **Primessnig U**, Bracic T, Levijoki J, Otsomaa L, Pollesello P, Falcke M, Pieske B, Heinzel FR. Long-term effects of Na(+) / Ca(2+) exchanger inhibition with ORM-11035 improves cardiac function and remodelling without lowering blood pressure in a model of heart failure with preserved ejection fraction. *Eur J Heart Fail* 2019; **21**: 1543-1552 [PMID: 31762174 DOI: 10.1002/ejhf.1619]

16 **Song SS**, Tang G, Tang LX, Si LY, Xiong W. NAKα2 inhibits fibrosis formation and protects against cardiomyocyte hypertrophy by suppressing hypertrophy associated molecules and activating LTCC/NCX signaling pathway. *Eur Rev Med Pharmacol Sci* 2019; **23**: 3021-3033 [PMID: 31002153 DOI: 10.26355/eurrev_201904_17584]

17 **Boczek NJ**, Ye D, Jin F, Tester DJ, Huseby A, Bos JM, Johnson AJ, Kanter R, Ackerman MJ. Identification and Functional Characterization of a Novel CACNA1C-Mediated Cardiac Disorder Characterized by Prolonged QT Intervals With Hypertrophic Cardiomyopathy, Congenital Heart Defects, and Sudden Cardiac Death. *Circ Arrhythm Electrophysiol* 2015; **8**: 1122-1132 [PMID: 26253506 DOI: 10.1161/CIRCEP.115.002745]

18 **Bienengraeber M**, Olson TM, Selivanov VA, Kathmann EC, O'Cochlain F, Gao F, Karger AB, Ballew JD, Hodgson DM, Zingman LV, Pang YP, Alekseev AE, Terzic A. ABCC9 mutations identified in human dilated cardiomyopathy disrupt catalytic KATP channel gating. *Nat Genet* 2004; **36**: 382-387 [PMID: 15034580 DOI: 10.1038/ng1329]

19 **Olson TM**, Michels VV, Ballew JD, Reyna SP, Karst ML, Herron KJ, Horton SC, Rodeheffer RJ, Anderson JL. Sodium channel mutations and susceptibility to heart failure and atrial fibrillation. *JAMA* 2005; **293**: 447-454 [PMID: 15671429 DOI: 10.1001/jama.293.4.447]

20 **Lopes LR**, Syrris P, Guttmann OP, O'Mahony C, Tang HC, Dalageorgou C, Jenkins S, Hubank M, Monserrat L, McKenna WJ, Plagnol V, Elliott PM. Novel genotype-phenotype associations demonstrated by high-throughput sequencing in patients with hypertrophic cardiomyopathy. *Heart* 2015; **101**: 294-301 [PMID: 25351510 DOI: 10.1136/heartjnl-2014-306387]

21 **McNair WP**, Ku L, Taylor MR, Fain PR, Dao D, Wolfel E, Mestroni L; Familial Cardiomyopathy Registry Research Group. SCN5A mutation associated with dilated cardiomyopathy, conduction disorder, and arrhythmia. *Circulation* 2004; **110**: 2163-2167 [PMID: 15466643 DOI: 10.1161/01.CIR.0000144458.58660.BB]

22 **Bezzina CR**, Lahrouchi N, Priori SG. Genetics of sudden cardiac death. *Circ Res* 2015; **116**: 1919-1936 [PMID: 26044248 DOI: 10.1161/CIRCRESAHA.116.304030]

23 **Ge J**, Sun A, Paajanen V, Wang S, Su C, Yang Z, Li Y, Jia J, Wang K, Zou Y, Gao L, Fan Z. Molecular and clinical characterization of a novel SCN5A mutation associated with atrioventricular block and dilated cardiomyopathy. *Circ Arrhythm Electrophysiol* 2008; **1**: 83-92 [PMID: 19808398 DOI: 10.1161/CIRCEP.107.750752]

24 **Swayne LA**, Murphy NP, Asuri S, Chen L, Xu X, McIntosh S, Wang C, Lancione PJ, Roberts JD, Kerr C, Sanatani S, Sherwin E, Kline CF, Zhang M, Mohler PJ, Arbour LT. Novel Variant in the ANK2 Membrane-Binding Domain Is Associated With Ankyrin-B Syndrome and Structural Heart Disease in a First Nations Population With a High Rate of Long QT Syndrome. *Circ Cardiovasc Genet* 2017; **10** [PMID: 28196901 DOI: 10.1161/CIRCGENETICS.116.001537]

25 **Choi CSW**, Souza IA, Sanchez-Arias JC, Zamponi GW, Arbour LT, Swayne LA. Ankyrin B and Ankyrin B variants differentially modulate intracellular and surface Cav2.1 levels. *Mol Brain* 2019; **12**: 75 [PMID: 31477143 DOI: 10.1186/s13041-019-0494-8]

26 **Mohler PJ**, Schott JJ, Gramolini AO, Dilly KW, Guatimosim S, duBell WH, Song LS, Haurogné K, Kyndt F, Ali ME, Rogers TB, Lederer WJ, Escande D, Le Marec H, Bennett V. Ankyrin-B mutation causes type 4 long-QT cardiac arrhythmia and sudden cardiac death. *Nature* 2003; **421**: 634-639 [PMID: 12571597 DOI: 10.1038/nature01335]

27 **Forleo C**, D'Erchia AM, Sorrentino S, Manzari C, Chiara M, Iacoviello M, Guaricci AI, De Santis D, Musci RL, La Spada A, Marangelli V, Pesole G, Favale S. Targeted next-generation sequencing detects novel gene-phenotype associations and expands the mutational spectrum in cardiomyopathies. *PLoS One* 2017; **12**: e0181842 [PMID: 28750076 DOI: 10.1371/journal.pone.0181842]

28 **Sucharski HC**, Dudley EK, Keith CBR, El Refaey M, Koenig SN, Mohler PJ. Mechanisms and Alterations of Cardiac Ion Channels Leading to Disease: Role of Ankyrin-B in Cardiac Function. *Biomolecules* 2020; **10** [PMID: 32023981 DOI: 10.3390/biom10020211]

29 **Wu HC**, Yamankurt G, Luo J, Subramaniam J, Hashmi SS, Hu H, Cunha SR. Identification and characterization of two ankyrin-B isoforms in mammalian heart. *Cardiovasc Res* 2015; **107**: 466-477 [PMID: 26109584 DOI: 10.1093/cvr/cvv184]

30 **Roberts JD**, Murphy NP, Hamilton RM, Lubbers ER, James CA, Kline CF, Gollob MH, Krahn AD, Sturm AC, Musa H, El-Refaey M, Koenig S, Aneq MÅ, Hoorntje ET, Graw SL, Davies RW, Rafiq MA, Koopmann TT, Aafaqi S, Fatah M, Chiasson DA, Taylor MR, Simmons SL, Han M, van Opbergen CJ, Wold LE, Sinagra G, Mittal K, Tichnell C, Murray B, Codima A, Nazer B, Nguyen DT, Marcus FI, Sobriera N, Lodder EM, van den Berg MP, Spears DA, Robinson JF, Ursell PC, Green AK, Skanes AC, Tang AS, Gardner MJ, Hegele RA, van Veen TA, Wilde AA, Healey JS, Janssen PM, Mestroni L, van Tintelen JP, Calkins H, Judge DP, Hund TJ, Scheinman MM, Mohler PJ. Ankyrin-B dysfunction predisposes to arrhythmogenic cardiomyopathy and is amenable to therapy. *J Clin Invest* 2019; **129**: 3171-3184 [PMID: 31264976 DOI: 10.1172/JCI125538]

World Journal of Clinical Cases

Submit a Manuscript: https://www.f6publishing.com

World J Clin Cases 2023 April 16; 11(11): 2423-2434

DOI: 10.12998/wjcc.v11.i11.2423

ISSN 2307-8960 (online)

ORIGINAL ARTICLE

Retrospective Study

Classification of hepatobiliary scintigraphy patterns in segmented gallbladder according to anatomical discordance

Yun-Chae Lee, Won-Sik Jung, Chang-Hun Lee, Seong-Hun Kim, Seung-Ok Lee

Specialty type: Medicine, research and experimental

Provenance and peer review: Unsolicited article; Externally peer reviewed.

Peer-review model: Single blind

Peer-review report's scientific quality classification

Grade A (Excellent): 0
Grade B (Very good): B, B
Grade C (Good): C, C
Grade D (Fair): D, D
Grade E (Poor): 0

P-Reviewer: Gupta R, India; Limaiem F, Tunisia; Wani I, India

Received: December 21, 2022
Peer-review started: December 21, 2022
First decision: January 11, 2023
Revised: January 25, 2023
Accepted: March 17, 2023
Article in press: March 17, 2023
Published online: April 16, 2023

Yun-Chae Lee, Won-Sik Jung, Chang-Hun Lee, Seong-Hun Kim, Seung-Ok Lee, Division of Gastroenterology, Department of Internal Medicine, Jeonbuk National University Medical School, Jeonju 54907, Jeonbuk, South Korea

Yun-Chae Lee, Won-Sik Jung, Chang-Hun Lee, Seong-Hun Kim, Seung-Ok Lee, Research Institute of Clinical Medicine of Jeonbuk National University-Biomedical Research Institute of Jeonbuk National University Hospital, Jeonju 54907, Jeonbuk, South Korea

Corresponding author: Seung-Ok Lee, MD, PhD, Professor, Division of Gastroenterology, Department of Internal Medicine, Jeonbuk National University Medical School, 20 Geonjiro, Dukjingu, Jeonju 54907, Jeonbuk, South Korea. solee@jbnu.ac.kr

Abstract

BACKGROUND

Hepatobiliary scintigraphy (HBS) is a useful diagnostic imaging technique that uses radiotracers to evaluate the function of the gallbladder (GB) and biliary system. In segmented GB, some HBS images reveal a discordant GB boundary as compared to anatomical images.

AIM

To evaluate the characteristics of HBS in segmented GB and determine the clinical relevance according to HBS characteristics.

METHODS

A total of 268 patients with chronic cholecystitis, gallstones, or biliary colic symptoms who underwent HBS between 2011 and 2020 were enrolled. Segmented GB was defined as segmental luminal narrowing of the GB body on computed tomography (CT) or magnetic resonance (MR) images, and HBS was examined 1 mo before or after CT or MR. Segmented GB was classified into 3 types based on the filling and emptying patterns of the proximal and distal segments according to the characteristics of HBS images, and GB ejection fraction (GBEF) was identified: Type 1 was defined as a normal filling and emptying pattern; Type 2 was defined as an emptying defect on the distal segment; and Type 3 was defined as a filling defect in the distal segment.

RESULTS

Segmented GB accounted for 63 cases (23.5%), including 36 patients (57.1%) with Type 1, 18 patients (28.6%) with Type 2, and 9 patients (14.3%) with Type 3

emptying pattern. Thus, approximately 43% of HBS images showed a discordant pattern as compared to anatomical imaging of segmented GB. Although there were no significant differences in clinical symptoms, rate of cholecystectomy, or pathological findings based on the type, most gallstones occurred in the distal segment. Reported GBEF was 62.50% ± 24.79% for Type 1, 75.89% ± 17.21% for Type 2, and 88.56% ± 7.20% for Type 3. Type 1 showed no difference in reported GBEF compared to the non-segmented GB group (62.50% ± 24.79% *vs* 67.40% ± 21.78%). In contrast, the reported GBEF was higher in Types 2 and 3 with defective emptying and filling when compared to Type 1 (80.11% ± 15.70% *vs* 62.57% ± 24.79%; $P = 0.001$).

CONCLUSION

In segmented GB, discordance in the filling patterns detected by HBS and anatomical imaging could lead to misinterpretation of GBEF. For this reason, clinicians should be cautious when interpreting HBS results in patients with segmented GB.

Key Words: Gallbladder; Segmented; Gallbladder emptying; Radionuclide imaging; Misdiagnosis; Cholecystitis

Core Tip: This retrospective study aimed to evaluate the clinical relevance of discrepancies between anatomical and hepatobiliary scintigraphy (HBS) images in patients with segmented gallbladder (GB). HBS images of segmented GB were classified according to filling and emptying patterns: Type 1 was a normal pattern; Type 2 was an emptying defect on the distal segment; and Type 3 was a filling defect in the distal segment. Types 2 and 3 had higher GB ejection fraction measurements than Type 1. Therefore, clinicians should be cautious when interpreting the results of HBS in patients with segmented GB.

Citation: Lee YC, Jung WS, Lee CH, Kim SH, Lee SO. Classification of hepatobiliary scintigraphy patterns in segmented gallbladder according to anatomical discordance. *World J Clin Cases* 2023; 11(11): 2423-2434
URL: https://www.wjgnet.com/2307-8960/full/v11/i11/2423.htm
DOI: https://dx.doi.org/10.12998/wjcc.v11.i11.2423

INTRODUCTION

The gallbladder (GB) is a single pear-shaped chamber mainly located in a shallow depression below the right lobe of the liver. The GB can be anatomically divided into 4 parts: Fundus, body, infundibulum, and neck. The neck is connected to the common bile duct *via* the cystic duct. The liver secretes approximately 600 mL of bile per day (0.4 mL/min)[1], a major portion of which enters the GB during fasting with the rest bypassing the GB and entering the duodenum. In the basal state, bile moves within the GB from the long central axis toward the periphery in a lamellar fashion within approximately 30 min[2].

A segmented GB refers to a hyperplastic condition of uncertain etiology in which the organ is divided into two chambers by a fold or septum[3,4]. Nevertheless, it is unknown how GB segmentation affects hepatic bile entry and exit from the two segments. Studies have demonstrated a relationship between segmented GB and the development of cholestasis[4]. A few studies have proposed a relationship between cholestasis and GB cancer[4-6]. Thus, it is hypothesized that segmented GB influences bile flow and as such may be associated with GB-related diseases. Therefore, cholecystectomy can be considered for the treatment of segmented GB.

Hepatobiliary scintigraphy (HBS) is a diagnostic technique used in nuclear medicine to continuously capture the pattern of radiotracers ingested by hepatocytes and secreted together with bile acid. The radiotracer is administered intravenously, bound to albumin, transported to the liver, and drained into the duodenum through the GB and bile ducts. Normal hepatobiliary findings are characterized by the presence of hepatic parenchyma and rapid clearance of cardiac hematologic activity, followed sequentially by activities in the intrahepatic and extrahepatic biliary ductal system, GB, and upper small bowel within approximately 1 h[7]. Abdominal ultrasonography (US), computed tomography (CT), or magnetic resonance cholangiopancreatography (MRCP) can provide morphological information to aid in the diagnosis of hepatobiliary disease, whereas HBS can be used to delineate hepatic and GB function and the degree of cholestasis by tracking radiotracers in the bilirubin metabolic pathway into the bile duct[8].

HBS is used to assess the adequacy of GB contraction and calculate the GB ejection fraction (GBEF) to determine the need for surgery in patients with chronic cholecystitis and GB dyskinesia, and also in

symptomatic patients without gallstones[8-11]. An absolute ejection fraction cutoff for surgery has not been definitively established, but has historically been suggested to be approximately 40%[10]. Because clinicians usually make the decision for surgery based on these results and patient symptoms, accurate measurement of GBEF is mandatory. However, it is generally accepted that scintigraphic findings are not always specific. Therefore, it is crucial to correlate HBS findings with clinical information and findings from other imaging modalities to arrive at optimal management strategy[7].

In segmented GB, changes in bile flow may affect HBS results. Some HBS images revealed discordant GB filling and emptying patterns when compared to anatomical images obtained using CT or MR techniques. Changes in these patterns may influence the interpretation of HBS findings and lead to miscalculation of GBEF. However, there are no studies on the clinical significance of HBS in segmented GB with a reasonable classification of the HBS pattern. Therefore, this study aimed to evaluate HBS image features in a segmented GB and determine the clinical impact of these features.

MATERIALS AND METHODS

Study population and clinical information

We performed a retrospective review of patients who underwent HBS at Jeonbuk National University Hospital from 2011 to 2020. Baseline demographic and clinical characteristics on biliary colic symptoms (right upper quadrant and epigastric pain or discomfort or postprandial discomfort) and atypical abdominal symptoms (dyspepsia or abdominal discomfort in an uncertain location) were obtained. In addition, the presence and location of any gallstones, sludge, or polyps was assessed. Laboratory testing [alkaline phosphatase, gamma (γ)-glutamyl transferase, aspartate aminotransferase, alanine aminotransferase, total bilirubin, direct bilirubin, carcinoembryonic antigen, and carbohydrate antigen 19-9] was performed near the date of HBS. Morphological characteristics of the GB were verified by CT or MRCP. The interval between CT or MRCP and HBS was no longer than 1 mo. GBEF and scanned images of the radiotracers were validated using HBS. This study was approved by the Institutional Review Board of Jeonbuk National University Hospital (IRB No. 2021-07-005).

Definition of segmented GB

A segmented GB was defined as segmental luminal narrowing of the GB body observed on CT or MR imaging. Segmented GB contains a fold or septum that divides the GB lumen into two or more interconnected compartments: A neck proximal to the stricture and a fundus distal to the stricture; determination of the presence of a septum and compartments is based on a review of CT or MR images. A new approach was proposed to define segmented GB (Figure 1). The segmented GB was first defined as:

$A + B > 3C$

where A and B denote the long axes of the outer lumen of the distal and proximal portions, respectively. C is defined as the diameter of luminal narrowing based on the outer lumen of the GB body. This calculation was made after observing a segmented GB on CT or MR images and HBS images of an enrolled patient and measuring each GB area of that patient.

Hepatobiliary scintigraphy

After a minimum of 6 h of fasting, each patient received ^{99m}Tc-mebrofenin intravenously while lying supine under a dual-head gamma camera fitted with a low-energy parallel-hole collimator, with a detector centered over the abdomen covering the region between the heart and pelvis in the field of view. GB phase images were obtained 60 min after ^{99m}Tc-mebrofenin injection. Following a fatty meal, GB phase images were obtained at 30 and 60 min. GBEF was measured using immediate pre- and post-fatty meal images, and the regions of interest were drawn around the GB (considering the patient's movement) and adjacent liver (background). The GBEF was calculated as the ratio of the difference between the maximum and minimum signals to the maximum signal and corrected for the background signal[7].

Classification of a segmented GB based on HBS

Baseline images used for classification were those obtained 60 min after ^{99m}Tc-mebrofenin injection and the GB phase obtained 30 min and 60 min after fatty meal intake. HBS images were compared with CT or MR images and classified into 3 groups according to the filling and emptying patterns according to the actual anatomical morphology of the GB. Type 1 was defined as a normal filling and emptying pattern, Type 2 was defined as an emptying defect on the distal segment, and Type 3 was defined as a filling defect in the distal segment (Figure 2). Figure 3 depicts the anatomical boundaries of segmented GB as shown in typical CT images, the scanned images of HBS in normal GB, and each segmented GB subtype classified according to the filling and emptying pattern.

Statistical analysis

Results were reported as numbers (percentages) or as mean ± standard deviation. Continuous variables

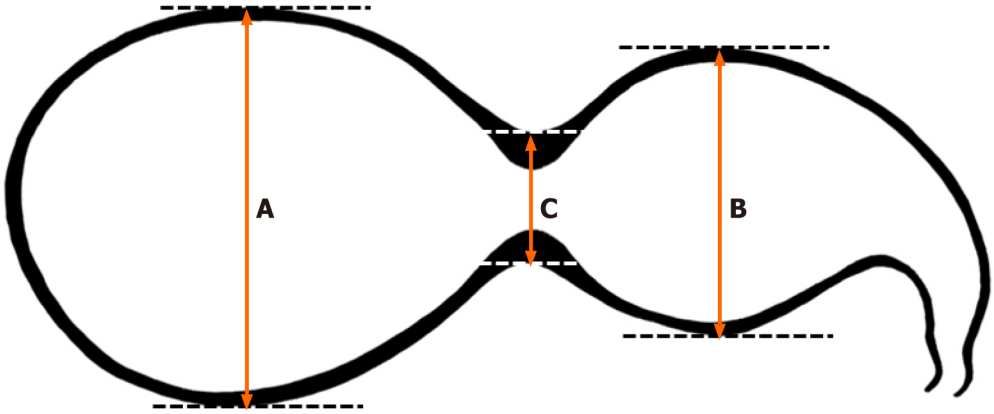

DOI: 10.12998/wjcc.v11.i11.2423

Figure 1 Schematic of the segmented gallbladder. A: Long axis of the distal segment; B: Long axis of the proximal segment; C: Segmental luminal narrowing of the gallbladder (GB) body. Segmented GB was diagnosed if the sum of A and B was greater than 3 times C.

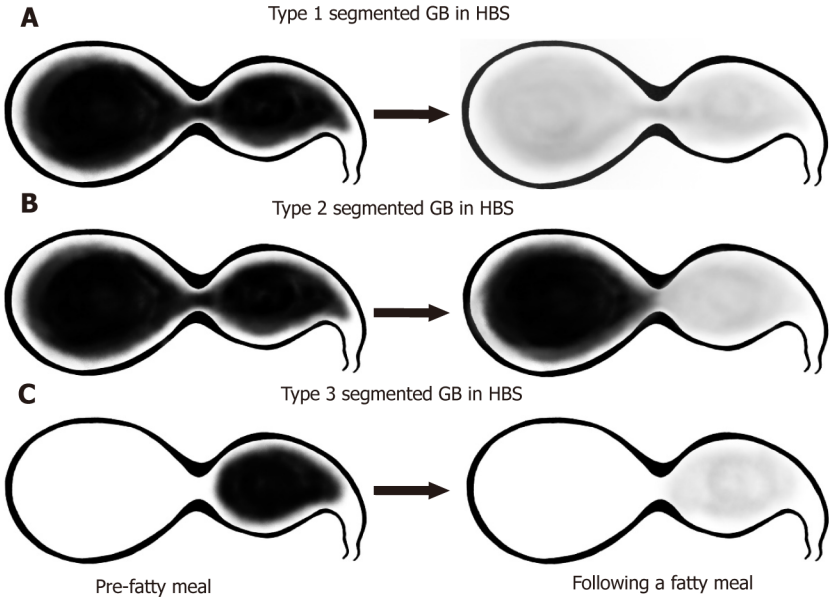

DOI: 10.12998/wjcc.v11.i11.2423

Figure 2 Schematic of the classification of filling and emptying patterns in segmented gallbladder as measured by hepatobiliary scintigraphy. A: Type 1 was defined as a normal filling and emptying pattern; B: Type 2 was defined as an emptying defect at the distal segment; C: Type 3 was defined as a filling defect at the distal segment. GB: gallbladder; HBS: Hepatobiliary scintigraphy.

were compared using the Student's *t*-test, and categorical data were compared using Pearson's chi-squared test and Fisher's exact test. Statistical significance was set at $P < 0.05$. Data were analyzed using SPSS software (version 25.0; IBM Corp., Armonk, NY, United States).

RESULTS

Baseline characteristics

A total of 268 adult patients 18 years or older underwent HBS for chronic cholecystitis, gallstones, or biliary colic. The patients' baseline characteristics are listed in Table 1. The mean age was 51.65 years ± 13.10 years and men constituted 43.2% of the study population. Approximately 20% of patients complained of biliary colic pain. Among these, 63 (23.51%) belonged to the segmented GB group. There were no differences in laboratory findings between the non-segmented and segmented GB groups. Based on radiological findings, adenomyomatosis and chronic cholecystitis were diagnosed more frequently in the segmented GB group (18/63, 28.6% and 45/63, 71.4%, respectively) than in the non-segmented GB group (12/205, 5.9% and 107/205, 52.2%, respectively) ($P < 0.001$ and $P = 0.009$, respectively). Reported GBEF was 68.01% ± 22.05%, and there was no difference between the two

Table 1 Comparison of baseline characteristics between patients of non-segmented and segmented gallbladder groups

Variables		Non-segmented GB, *n* = 205	Segmented GB, *n* = 63	*P* value
Age in year		51.8 ± 13.6	51.1 ± 11.3	0.664
Male		87 (42.4%)	29 (46.0%)	0.72
Atypical symptoms		52 (25.4%)	9 (14.3%)	0.085
Biliary colic pain		50 (24.4%)	10 (15.9%)	0.171
Laboratory findings				
	ALP in IU/L	67.6 ± 24.6	68.0 ± 20.5	0.911
	GGT in IU/L	37.1 ± 54.9	33.1 ± 28.4	0.58
	AST in IU/L	24.2 ± 8.7	26.3 ± 14.7	0.163
	ALT in IU/L	23.5 ± 12.7	26.3 ± 15.4	0.148
	Total bilirubin in mg/dL	1.05 ± 2.60	0.86 ± 0.41	0.583
	Direct bilirubin in mg/dL	0.31 ± 0.87	0.25 ± 0.12	0.59
	CEA in ng/mL	1.58 ± 1.31	1.35 ± 0.83	0.31
Radiologic findings				
	GB stone	110 (53.7%)	37 (58.7%)	0.563
	GB sludge	7 (3.4%)	2 (3.2%)	0.999
	GB polyp	14 (6.8%)	8 (12.7%)	0.186
	Adenomyomatosis	12 (5.9%)	18 (28.6%)	< 0.001
	Chronic cholecystitis	107 (52.2%)	45 (71.4%)	0.009
Reported GBEF, %		67.40 ± 21.78	70.05 ± 22.97	0.405
Cholecystectomy		73 (35.6%)	45 (71.4%)	< 0.001
Pathology[1]				
	Adenomyomatosis	3 (4.1%)	5 (11.1%)	0.257
	Chronic cholecystitis	68 (93.2%)	41 (91.1%)	0.73
	Cholesterol polyp	16 (21.9%)	7 (15.6%)	0.478

[1]Duplicate test results.

Data were expressed as *n* (percentage) or mean ± SD. Comparisons were performed using the Student's *t*-test, Pearson's chi-squared test, and Fisher's exact test. ALP: Alkaline phosphatase; ALT: Alanine aminotransferase; AST: Aspartate aminotransferase; CA19-9: Carbohydrate antigen 19-9; CEA: Carcinoembryonic antigen; GB: Gallbladder; GBEF: Gallbladder ejection fraction; GGT: Gamma (γ)-gamma-glutamyl transferase.

groups (61.70% ± 21.78% *vs* 70.05% ± 22.97%; $P = 0.405$). Cholecystectomy was performed more frequently in the segmented GB group (45/63, 71.4%) than in the non-segmented GB group (73/205, 35.6%; $P < 0.001$).

Clinical characteristics of variables according to the type of segmented GB

According to the HBS patterns defined for segmented GB, 36 patients (57.1%) with Type 1, 18 patients (28.6%) with Type 2, and 9 patients (14.3%) with Type 3 were identified. A comparison of variables according to the type of segmented GB is presented in Table 2. Demographic, radiological, and pathological findings did not differ according to the type of segmented GB. In addition, the rates of atypical symptoms and biliary colic pain did not differ between the groups. GB stones occurred more frequently in the distal segment in both groups; however, no significant intergroup difference was found. Type 1, with normal emptying and filling patterns, showed no difference in the reported GBEF compared to the non-segmented GB group. Interestingly, the reported GBEF was higher in Types 2 and 3 with defective emptying and filling than in Type 1 (80.11% ± 15.70% *vs* 62.57% ± 24.79%; $P = 0.001$).

The reported GBEF was 62.50% ± 24.79% for Type 1, 75.89% ± 17.21% for Type 2, and 88.56% ± 7.20% for Type 3 (Figure 4). Notably, a significant difference was observed between the reported GBEF of Types 1 and 3 ($P = 0.005$). The mean GBEF trended toward being higher in Type 2 than in Type 1, but the difference was not significant ($P = 0.082$).

Table 2 Comparison of variables according to type of segmented gallbladder

Variables			Type 1, *n* = 36	Types 2 & 3, *n* = 27	*P* value
Age in year			50.2 ± 9.6	52.3 ± 13.2	0.483
Male			14 (38.9%)	15 (55.6%)	0.212
Atypical symptoms			4 (11.1%)	5 (18.5%)	0.48
Biliary colic pain			7 (19.4%)	3 (11.1%)	0.494
Radiological findings					
	GB stone		22 (61.1%)	15 (55.6%)	0.797
	Location of GB stone				0.147
		Proximal	5 (22.7%)	0 (0.0%)	0.067
		Distal	15 (68.2%)	13 (86.7%)	0.262
		Both	2 (9.1%)	2 (13.3%)	0.999
	GB sludge		1 (2.8%)	1 (3.7%)	0.999
	GB polyp		5 (13.9%)	3 (11.1%)	0.999
	Adenomyomatosis		10 (27.8%)	8 (29.6%)	0.999
	Chronic cholecystitis		25 (69.4%)	20 (74.1%)	0.782
Reported GBEF, %			62.50 ± 24.79	80.11 ± 15.70	< 0.001
Cholecystectomy			26 (72.2%)	19 (70.4%)	0.999
Pathology[1]					
	Adenomyomatosis		3 (11.5%)	2 (10.5%)	0.999
	Chronic cholecystitis		24 (92.3%)	17 (89.5%)	0.999
	Cholesterol polyp		4 (15.4%)	3 (15.8%)	0.999

[1]Duplicate test results.

Data are expressed as number (percentage) or mean ± SD. GB: Gallbladder; GBEF: Gallbladder ejection fraction.

DISCUSSION

The segmentation of the GB into two chambers by a fold or septum is a hyperplastic condition of uncertain etiology[3,4]. GB segmentation in adults is often attributed to adenomyomatosis or congenital septa[12,13]. The term segmented GB is used in a broader fashion to include segmental adenomyosis of the GB. This term is not commonly used; however, GB segmentation without adenomyomatosis is often observed in imaging studies of patients of any age. Krishnamurthy *et al*[14] reported that microscopic examination of a segmented GB revealed chronic inflammatory changes, fibrosis, and wall thickening [14]. The strictures caused by the annular thickening of the GB wall may be narrow[2]. The anatomical stricture of a segmented GB leads to difficult bile movement and causes cholestasis, which may lead to chronic inflammatory changes, cholelithiasis, and tumorigenesis[4,5,13]. Therefore, clinical symptoms and the patient's physiological status should be considered; however, surgical treatment is recommended in the management of segmented GB.

Gallstones are one of the most common biliary tract diseases, and its prevalence is estimated at 5.9%-21.9% in the West and 3.1%-10.7% in Asia[15]. Diagnosis of gallstones is often incidental, and most patients remain asymptomatic throughout their lives. During a follow-up period of 10–15 years, symptoms appear in approximately 15%–25% of patients, and the risk of developing biliary pain due to complications is reported to be approximately 2%–3% annually[16-18]. Patients with symptomatic gallstones are at high risk of gallstone-related complications, and cholecystectomy is recommended in such cases[19]. In addition, cholecystectomy is recommended if there are risk factors for GB cancer [*e.g.*, anomalous pancreatic ductal drainage, GB adenoma, porcelain GB, or large gallstones (especially those larger than 3 cm)][20-22]. However, if a patient with gallstones has ambiguous symptoms, it is often difficult to distinguish gallstone-related symptoms; therefore, blood tests, ultrasound, HBS, and the patient's personal circumstances are considered to determine the need for surgery.

HBS is a radionuclide diagnostic imaging modality that is used to evaluate hepatocellular function and the biliary system by tracing the synthesis and flow of bile from the liver and its passage through the biliary system into the small intestine[7]. The technique assesses the function of hepatocytes, the

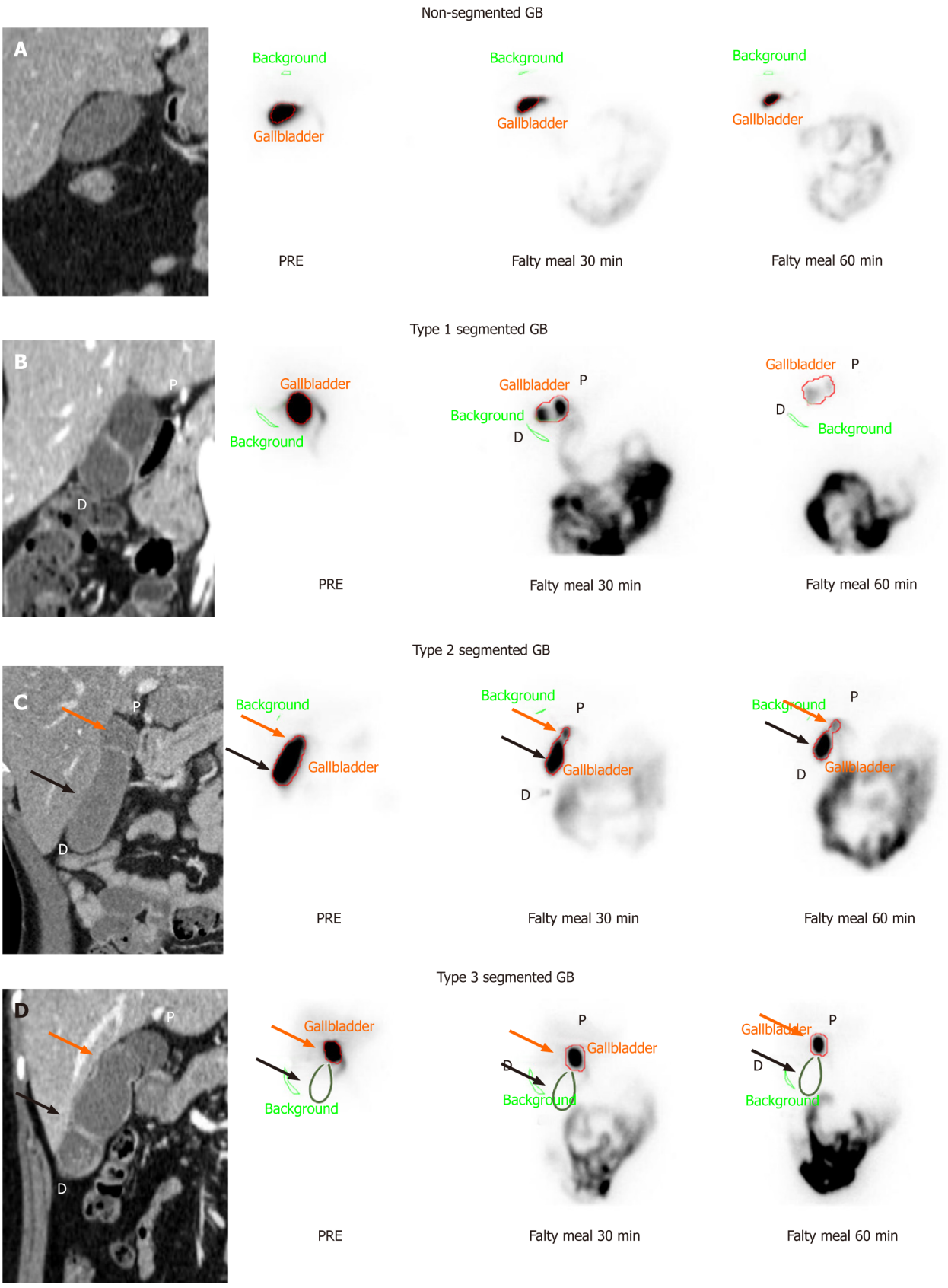

DOI: 10.12998/wjcc.v11.i11.2423

Figure 3 Typical images of computed tomography and hepatobiliary scintigraphy according to pattern in the normal and segmented gallbladder. A: Hepatobiliary scintigraphy (HBS) in non-segmented gallbladder (GB). Reported GB ejection fraction (GBEF) was 74%; B: Type 1, normal filling and emptying pattern on HBS. Reported GBEF (95%) was reflected in both segments; C: Type 2, emptying defect of the distal segment on HBS. After 60 min, the proximal segment showed normal emptying, but the distal segment showed poor emptying. Reported GBEF (87%) reflects proximal segmentation more than distal segmentation; D: Type 3, filling defect of the distal segment on HBS. As the distal segment is not observed in the scanned image, other radiological validation is

required. Reported GBEF (89%) reflects only proximal segmentation. The green line is a rough representation of the outline of the gallbladder per computed tomography. GB: gallbladder; P: Proximal segment (orange arrows); D: Distal segment (black arrows).

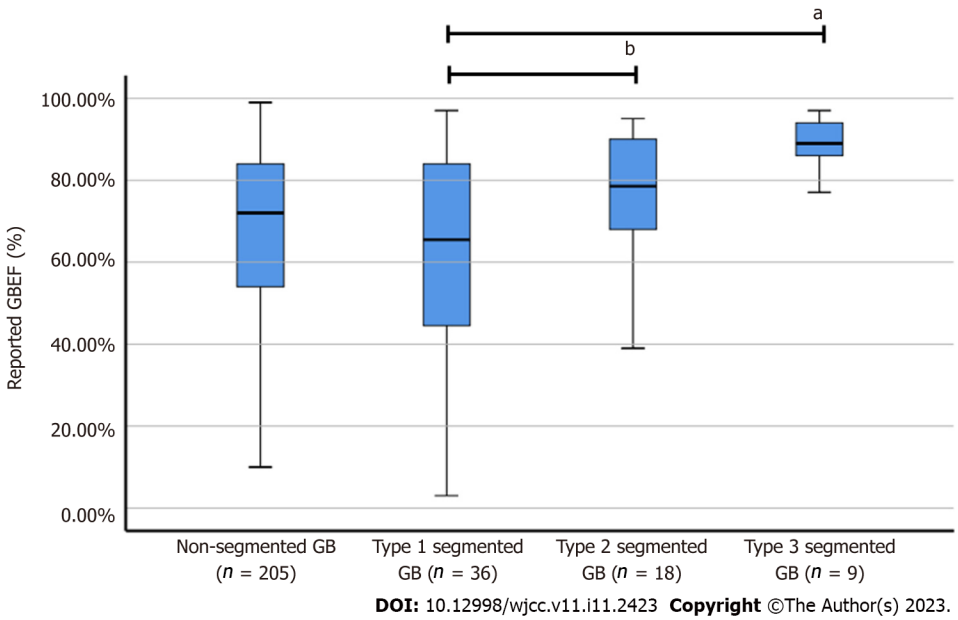

DOI: 10.12998/wjcc.v11.i11.2423

Figure 4 Gallbladder ejection fraction in non-segmented gallbladder and segmented gallbladder subtypes. Reported gallbladder ejection fraction (GBEF) in non-segmented gallbladder (GB) was 67.40% ± 21.78%, whereas that of segmented GB was 62.50% ± 24.79% for Type 1, 75.89% ± 17.21% for Type 2, and 88.56% ± 7.20% for Type 3. [a]There was a significant difference between reported GBEF of Types 1 and 3; [b]The difference in GBEF of Types 1 and 2 was not statistically significant (P = 0.082). GB: Gallbladder; GBEF: Gallbladder ejection fraction.

patency and integrity of the biliary ducts, GB contractility, and sphincter of Oddi function[23]. HBS has frequently been used to investigate the physiological parameters of the GB during emptying and filling [24]. A reduced GBEF is observed in calculous and acalculous biliary diseases, such as chronic acalculous cholecystitis, biliary dyskinesia, and sphincter of Oddi dysfunction. It may also be associated with various nonbiliary diseases and conditions as well as with the use of various medications (*e.g.*, morphine, atropine, calcium channel blockers, octreotide, *etc*)[7,25]. To this end, a meta-analysis concluded that the utility of a low GBEF in deciding whether to perform cholecystectomy in individuals with GB dyskinesia is still unclear[10]. However, the reduced GBEF in HBS has been advocated as a diagnostic parameter for the clinical evaluation of individuals presenting with suspected biliary pain or gallstones and altered GB morphology (such as segmented GB) in deciding whether to proceed with cholecystectomy.

The GBEF as evaluated in this study did not differ between patients with segmented or non-segmented GB. In a previous study, the GBEF measured in segmented GB was lower than that in non-segmented GB[14]. In this study, we observed the appearance of partial filling and emptying events in each lumen in segmented GB using HBS imaging. The anatomical features of annular strictures in segmented GB may alter the emptying of radiotracers without completely replenishing them. Defective HBS images in segmented GB have been reported[26]; however, they have never been classified according to filling and emptying patterns on scanned images. HBS images were divided into three categories. Type 1 was defined as a normal filling and emptying pattern. Type 2 was defined as emptying defects in the distal portion, and Type 3 was characterized by filling defects in the distal portion.

Furthermore, GBEF varied across segmented GB types depending on the HBS imaging pattern. We have described GBEF as "reported GBEF" because GBEF may be incorrectly measured depending on the type. We measured GBEF in Type 1 as 62.50%, with higher measured GBEF in Types 2 and 3 with defective filling or emptying (P = 0.001). Filling or emptying defects in HBS images of a segmented GB are attributable to the undesirable effects of bile flow. However, the higher GBEF of Types 2 and 3 compared with that of Type 1 renders the results unreliable and inconsistent with those of a previous study of 7 patients with segmented GB analyzed *via* HBS[14]. In this study, the total GBEF was determined by measuring the ejection fraction (EF) of the proximal and distal segments of the GB using HBS. Distal EF was lower in the segmented GB group than the proximal EF. The total EF in the segmented GB group was also lower than that in the non-segmented GB group. However, in the non-segmented GB group (n = 10), distal EF was higher than proximal EF. Decreased emptying (low EF) of the distal segment indicates that the septum acts as a one-way valve, allowing normal bile entry into the

distal segment, but does not allow an easy exit. However, the total GBEF of segmented GB measured in our hospital was often good, suggesting normal GB contractility. This phenomenon indicates that the measurement of total GBEF *via* HBS in segmented GB does not reflect the actual contractility of the organ. Total GBEF in Types 2 and 3 was primarily measured based on the contractility of the proximal part rather than the overall contractility as the GB boundary was not adequately demonstrated in the HBS images.

Changes in bile acid filling and emptying and the effect of the segmented GB on GBEF can be determined from the location of gallstones. GB stones were located mainly in the distal part and were related to the contraction and imbalance of the bile flow between the two segments. Nishimura *et al*[4] investigated the association between segmental adenomyomatosis of the GB and gallstones[4]. In addition, the contribution of gallstones to adenomyomatosis was investigated by examining their components. According to this study, the incidence of gallstones was higher in segmental adenomyomatosis than in fundal and diffuse adenomyomatosis, and distal compartment stones were detected in 80.6% (58/72). In our study, 75.7% (28/37) of stones were found in distal segments, 10.8% (4/37) in both segments, and only 13.5% (5/37) in the proximal segment of segmented GB. Although the size or composition of gallstones was not investigated in our study, the narrowed passageway was considered to obstruct the flow of bile and facilitate the production of gallstones at the distal part of the segmented GB.

The total GBEF (80.11% ± 15.70%) of the groups with defective filling or emptying (Types 2 and 3) suggested an overestimation of the proximal portion compared with the normal filling and emptying group (62.57% ± 24.79%). The difference between the groups underscores the need to interpret the HBS results in segmented GB in combination with GB morphology assessed by other imaging modalities (US, CT, or MRCP).

This study had some limitations. Our study was a relatively small, single-center cohort study. In addition, EFs of the proximal and distal GB were not investigated, which precluded the determination of the contribution of each GB part to total EF. The filling and emptying radiotracer volume of bile flow could not be confirmed; therefore, no quantitative results could be reported. However, quantitative studies require the use of single-photon emission CT. Lastly, non-specific fatty meals were used to stimulate GB contraction, as cholecystokinin (CCK) was unavailable for use at our institute. Although CCK would have offered a more reliable GB stimulus, a previous study did not show any significant difference between CCK and fatty meals in measuring GBEF[27].

Despite these limitations, our findings provide a better understanding of the results of HBS in segmented GB. Clinically, segmented GB is associated with a higher incidence of GB-related diseases than are other morphological features. Therefore, cholecystectomy is often indicated for the surgical treatment of segmented GB. In addition to the assessment of patient symptoms, reduced contractility in segmented GB measured by HBS is critical in determining the need for cholecystectomy. However, GBEF measurement in segmented GB may be misinterpreted depending on the type of HBS images. In particular, the GBEF in Type 2 and Type 3 HBS scans can be overestimated, which can complicate the development of an ideal treatment plan.

CONCLUSION

In segmented GB, discordance between HBS and anatomical imaging (CT or MR techniques) could lead to inaccurate estimation of GBEF. Therefore, clinicians should be cautious when interpreting GB contractility as measured by HBS in patients with segmented GB.

ARTICLE HIGHLIGHTS

Research background

Hepatobiliary scintigraphy (HBS) is a useful diagnostic imaging technique that uses radioactive tracers to evaluate the function of the gallbladder (GB) and biliary tract. In segmented GB, some HBS images show inconsistent GB boundaries as compared to anatomical imaging, limiting the evaluation of GB contractility through HBS.

Research motivation

Cholecystectomy is sometimes necessary in patients with gallstones or chronic cholecystitis. In addition, in the case of anatomically segmented GB, cholecystectomy is recommended due to the higher risk of future GB disease. Because there are patients who are reluctant to undergo cholecystectomy, cholecystectomy is recommended again if cholecystectomy decreases after evaluating the GB contractability using HBS. In previous studies, the GB ejection fraction (GBEF) was reduced in the case of segmental GB, but GBEF was often normal when measured in our study.

Research objectives

We evaluated the characteristics of HBS in segmented GB and investigated the effect of segmented GB on the measurement of GBEF using HBS.

Research methods

From a larger group of patients with chronic cholecystitis, gallstones, or biliary colic, those who underwent HBS were identified. Patients with segmented GB features with segmental lumen stricture were identified using computed tomography (CT) or magnetic resonance (MR) imaging. Patients were asked whether CT or MR was performed either 1 mo before or after HBS. Segmented GB was classified into 3 types based on the filling and emptying patterns of the proximal and distal segments according to the characteristics of HBS images, and GBEF was measured. Type 1 was defined as a normal filling and emptying pattern, Type 2 was defined as an emptying defect on the distal segment, and Type 3 was defined as a filling defect in the distal segment.

Research results

Segmented GB accounted for 63 cases (23.5%), including 36 patients (57.1%) with Type 1, 18 patients (28.6%) with Type 2, and 9 patients (14.3%) with Type 3. Thus, approximately 43% of segmented GB cases demonstrated discordance between HBS and anatomical imaging. Although there were no significant differences in clinical symptoms, rate of cholecystectomy, or pathological findings based on the type, most gallstones occurred in the distal segment. Reported GBEF was 62.50% ± 24.79% for Type 1, 75.89% ± 17.21% for Type 2, and 88.56% ± 7.20% for Type 3. Type 1 showed no difference in reported GBEF as compared to the non-segmented GB group (62.50% ± 24.79% *vs* 67.40 ± 21.78%). In contrast, the reported GBEF was higher in Types 2 and 3 with defective emptying and filling than in Type 1 (80.11% ± 15.70% *vs* 62.57% ± 24.79%; $P = 0.001$).

Research conclusions

In segmented GB, discordance between HBS and anatomical imaging (CT or MR) could lead to inaccurate estimation of GBEF. Therefore, clinicians should use caution when interpreting GB contractility through HBS in patients with segmented GB.

Research perspectives

Since the presence or absence of gallstones may affect HBS, additional studies may be conducted to examine the difference in GBEF according to the presence or absence of gallstones in patients with segmented GB. Further studies using single-photon emission CT to evaluate discrepancies between HBS and anatomical imaging are expected to help determine the need for cholecystectomy.

FOOTNOTES

Author contributions: Lee SO designed the study; Lee YC and Jung WS collected and analyzed the data; Lee YC, Lee CH, and Kim SH drafted the manuscript; Lee YC and Lee SO revised the manuscript; All authors reviewed the manuscript.

Institutional review board statement: The study was reviewed and approved by the Jeonbuk National University Hospital Institutional Review Board, No.2021-07-005.

Informed consent statement: This study was a retrospective mandatory records review study in patients who did not have additional in-hospital plans and could not obtain consent at this time; Even if consent is waived, the risk to the study subjects is extremely low. After review by the ethics committee, this study can exempt the respondent's consent.

Conflict-of-interest statement: All authors report no relevant conflicts of interest for this article.

Data sharing statement: Consent was not obtained but the presented data are anonymized, and risk of identification is low. No additional data are available.

Country/Territory of origin: South Korea

ORCID number: Yun-Chae Lee 0000-0003-4957-0226; Seung-Ok Lee 0000-0003-0243-215X.

S-Editor: Li L
L-Editor: Filipodia
P-Editor: Li L

REFERENCES

1 **Sherlock S**, Dooley J. Diseases of the Liver and Biliary System. 11th ed. New York: John Wiley & Sons, 2008 [DOI: 10.1002/9780470986820]
2 **Krishnamurthy GT**, Krishnamurthy S. Hepatic bile entry into and transit pattern within the gallbladder lumen: a new quantitative cholescintigraphic technique for measurement of its concentration function. *J Nucl Med* 2002; **43**: 901-908 [PMID: 12097460 DOI: 10.1007/s00259-006-0182-7]
3 **Golse N**, Lewin M, Rode A, Sebagh M, Mabrut JY. Gallbladder adenomyomatosis: Diagnosis and management. *J Visc Surg* 2017; **154**: 345-353 [PMID: 28844704 DOI: 10.1016/j.jviscsurg.2017.06.004]
4 **Nishimura A**, Shirai Y, Hatakeyama K. Segmental adenomyomatosis of the gallbladder predisposes to cholecystolithiasis. *J Hepatobiliary Pancreat Surg* 2004; **11**: 342-347 [PMID: 15549435 DOI: 10.1007/s00534-004-0911-x]
5 **Li T**, Apte U. Bile Acid Metabolism and Signaling in Cholestasis, Inflammation, and Cancer. *Adv Pharmacol* 2015; **74**: 263-302 [PMID: 26233910 DOI: 10.1016/bs.apha.2015.04.003]
6 **Ootani T**, Shirai Y, Tsukada K, Muto T. Relationship between gallbladder carcinoma and the segmental type of adenomyomatosis of the gallbladder. *Cancer* 1992; **69**: 2647-2652 [PMID: 1571894 DOI: 10.1002/1097-0142(19920601)69:11<2647::aid-cncr2820691105>3.0.co;2-0]
7 **Tulchinsky M**, Ciak BW, Delbeke D, Hilson A, Holes-Lewis KA, Stabin MG, Ziessman HA; Society of Nuclear Medicine. SNM practice guideline for hepatobiliary scintigraphy 4.0. *J Nucl Med Technol* 2010; **38**: 210-218 [PMID: 21078782 DOI: 10.2967/jnmt.110.082289]
8 **Snyder E**, Kashyap S, Lopez PP. Hepatobiliary Iminodiacetic Acid Scan. 2022 Jul 25. In: StatPearls [Internet]. Treasure Island (FL): StatPearls Publishing; 2022 Jan- [PMID: 30969603]
9 **Mahid SS**, Jafri NS, Brangers BC, Minor KS, Hornung CA, Galandiuk S. Meta-analysis of cholecystectomy in symptomatic patients with positive hepatobiliary iminodiacetic acid scan results without gallstones. *Arch Surg* 2009; **144**: 180-187 [PMID: 19221331 DOI: 10.1001/archsurg.2008.543]
10 **Gudsoorkar VS**, Oglat A, Jain A, Raza A, Quigley EMM. Systematic review with meta-analysis: cholecystectomy for biliary dyskinesia-what can the gallbladder ejection fraction tell us? *Aliment Pharmacol Ther* 2019; **49**: 654-663 [PMID: 30706496 DOI: 10.1111/apt.15128]
11 **Yap L**, Wycherley AG, Morphett AD, Toouli J. Acalculous biliary pain: cholecystectomy alleviates symptoms in patients with abnormal cholescintigraphy. *Gastroenterology* 1991; **101**: 786-793 [PMID: 1860640 DOI: 10.1016/0016-5085(91)90540-2]
12 **Aguirre JR**, Bohler RO, Guraieb S. Hyperplastic cholecystoses; a new contribution to the unitarian theory. *Am J Roentgenol Radium Ther Nucl Med* 1969; **107**: 1-13 [PMID: 5811558 DOI: 10.2214/ajr.107.1.1]
13 **Kramer EL**, Rumancik WM, Harkavy L, Tiu S, Banner HJ, Sanger JJ. Hepatobiliary scintigraphy of the compartmentalized gallbladder. *AJR Am J Roentgenol* 1985; **145**: 1205-1206 [PMID: 3877423 DOI: 10.2214/ajr.145.6.1205]
14 **Krishnamurthy GT**, Krishnamurthy S, Milleson T, Brown PH, Urstadt DS. Segmentation of the gallbladder: effect on bile entry and exit and its clinical relevance in a patient with abdominal pain. *Nucl Med Commun* 2007; **28**: 109-115 [PMID: 17198351 DOI: 10.1097/MNM.0b013e328013eb2f]
15 **Chuang SC**, Hsi E, Lee KT. Genetics of gallstone disease. *Adv Clin Chem* 2013; **60**: 143-185 [PMID: 23724744 DOI: 10.1016/b978-0-12-407681-5.00005-2]
16 **Shabanzadeh DM**, Sørensen LT, Jørgensen T. A Prediction Rule for Risk Stratification of Incidentally Discovered Gallstones: Results From a Large Cohort Study. *Gastroenterology* 2016; **150**: 156-167 e1 [PMID: 26375367 DOI: 10.1053/j.gastro.2015.09.002]
17 **Festi D**, Reggiani ML, Attili AF, Loria P, Pazzi P, Scaioli E, Capodicasa S, Romano F, Roda E, Colecchia A. Natural history of gallstone disease: Expectant management or active treatment? *J Gastroenterol Hepatol* 2010; **25**: 719-724 [PMID: 20492328 DOI: 10.1111/j.1440-1746.2009.06146.x]
18 **Lee SK**, Kim MH. Natural history of gallstone; an important and old issue, but still debatable. *J Gastroenterol Hepatol* 2010; **25**: 651-652 [PMID: 20492320 DOI: 10.1111/j.1440-1746.2010.06252.x]
19 **Friedman GD**, Raviola CA, Fireman B. Prognosis of gallstones with mild or no symptoms: 25 years of follow-up in a health maintenance organization. *J Clin Epidemiol* 1989; **42**: 127-136 [PMID: 2918322 DOI: 10.1016/0895-4356(89)90086-3]
20 **Leitzmann MF**, Rimm EB, Willett WC, Spiegelman D, Grodstein F, Stampfer MJ, Colditz GA, Giovannucci E. Recreational physical activity and the risk of cholecystectomy in women. *N Engl J Med* 1999; **341**: 777-784 [PMID: 10477775 DOI: 10.1056/NEJM199909093411101]
21 **Leitzmann MF**, Giovannucci EL, Rimm EB, Stampfer MJ, Spiegelman D, Wing AL, Willett WC. The relation of physical activity to risk for symptomatic gallstone disease in men. *Ann Intern Med* 1998; **128**: 417-425 [PMID: 9499324 DOI: 10.7326/0003-4819-128-6-199803150-00001]
22 **Diehl AK**. Gallstone size and the risk of gallbladder cancer. *JAMA* 1983; **250**: 2323-2326 [PMID: 6632129]
23 **Afzal M**, Ali SM, Khairy AT, Khattabi M, Shahid F, Ramzee AF, Ahmed K. Hepatobiliary scintigraphy and its clinical implications: mini review. International Surgery Journal 2021; 8: 766-770 [DOI: 10.18203/2349-2902.isj20210402]
24 **Ziessman HA**. Hepatobiliary scintigraphy in 2014. *J Nucl Med* 2014; **55**: 967-975 [PMID: 24744445 DOI: 10.2967/jnumed.113.131490]

25 **Richmond BK**, DiBaise J, Ziessman H. Utilization of cholecystokinin cholescintigraphy in clinical practice. *J Am Coll Surg* 2013; **217**: 317-323 [PMID: 23731969 DOI: 10.1016/j.jamcollsurg.2013.02.034]
26 **Won KY**, Kim C. Bicameral Gallbladder With Chronic Cholecystitis on Hepatobiliary Scintigraphy. *Clin Nucl Med* 2021; **46**: 78-80 [PMID: 33181736 DOI: 10.1097/RLU.0000000000003369]
27 **DeBruin A**, Ellefson K, Johnson C. Comparison of fatty meal interventional agents to CCK for GBEF studies. *Soc Nuclear Med* 2021; **62** (suppl 1): 157

World Journal of Clinical Cases

Submit a Manuscript: https://www.f6publishing.com

World J Clin Cases 2023 April 16; 11(11): 2435-2442

DOI: 10.12998/wjcc.v11.i11.2435

ISSN 2307-8960 (online)

ORIGINAL ARTICLE

Retrospective Study

Optimal laboratory testing protocol for patients with acne taking oral isotretinoin

Yu Jeong Park, Hui Young Shin, Woo Kyoung Choi, Ai-Young Lee, Seung Ho Lee, Jong Soo Hong

Specialty type: Dermatology

Provenance and peer review: Unsolicited article; Externally peer reviewed.

Peer-review model: Single blind

Peer-review report's scientific quality classification

Grade A (Excellent): 0
Grade B (Very good): B, B
Grade C (Good): 0
Grade D (Fair): D, D
Grade E (Poor): 0

P-Reviewer: Bugaj AM, Poland; Khamdan FA, Bahrain; Kutlubay Z, Turkey; Li CM, China

Received: January 5, 2023
Peer-review started: January 5, 2023
First decision: January 30, 2023
Revised: February 7, 2023
Accepted: March 23, 2023
Article in press: March 23, 2023
Published online: April 16, 2023

Yu Jeong Park, Hui Young Shin, Woo Kyoung Choi, Ai-Young Lee, Seung Ho Lee, Jong Soo Hong, Department of Dermatology, Dongguk University Ilsan Hospital, College of Medicine, Dongguk University, Goyang 10326, South Korea

Corresponding author: Jong Soo Hong, MD, PhD, Associate Professor, Department of Dermatology, Dongguk University Ilsan Hospital, College of Medicine, Dongguk University, 27, Dongguk-ro, Ilsandong-gu, Goyang-si, Gyeonggi-do, Goyang 10326, South Korea. jsttjstt@hanmail.net

Abstract

BACKGROUND

Isotretinoin is a widely prescribed drug for various dermatological conditions, especially acne. Blood tests are routinely performed to monitor its side effects. However, the optimal testing schedule remains controversial.

AIM

To evaluate the laboratory monitoring tests and schedules of patients with acne taking isotretinoin to determine the most efficient testing regimen.

METHODS

We retrospectively reviewed electronic medical records from the Dermatology Department of Dongguk University Ilsan Hospital from 2005 to 2020 for patients prescribed isotretinoin for acne who underwent monthly blood tests.

RESULTS

Aspartate aminotransferase (AST), alanine aminotransferase (ALT), and triglyceride (TG) levels significantly changed between 5 and 6 mo when the total prescription period and dose variables were considered altogether. The high-density lipoprotein level also significantly changed between 5 and 6 mo. However, low-density lipoprotein (LDL) and total cholesterol levels significantly changed between 1 and 2 mo.

CONCLUSION

We recommend testing AST, ALT, and TG levels once every 5 to 6 mo. We also suggest testing LDL and total cholesterol levels during the first and second months.

Key Words: Acne vulgaris; Isotretinoin; Clinical laboratory techniques; Vitamin A; Liver

function test; Lipid panel

Core Tip: Isotretinoin is a widely prescribed drug for various dermatological conditions, especially acne. Blood tests are routinely performed to monitor its side effects. However, the optimal testing schedule remains controversial. This study investigated the optimal blood test type and frequency for patients taking isotretinoin for acne. This article will contribute to Asian-specific isotretinoin laboratory guidelines and further studies.

Citation: Park YJ, Shin HY, Choi WK, Lee AY, Lee SH, Hong JS. Optimal laboratory testing protocol for patients with acne taking oral isotretinoin. *World J Clin Cases* 2023; 11(11): 2435-2442
URL: https://www.wjgnet.com/2307-8960/full/v11/i11/2435.htm
DOI: https://dx.doi.org/10.12998/wjcc.v11.i11.2435

INTRODUCTION

Oral isotretinoin is a natural vitamin A metabolite (a retinoid) approved for use in 1982 by the United States Food and Drug Administration to treat acne vulgaris[1-4]. Isotretinoin inhibits sebaceous cell proliferation, differentiation, and lipid synthesis *in vivo*[1]. It also suppresses acne by reducing inflammation caused by *Propionibacterium acnes* and hyperkeratosis of the hair follicle sebaceous gland system [1].

Isotretinoin is a very effective treatment for acne. However, side effects such as teratogenicity, hyperlipidemia, pancreatitis, and leukopenia are possible and require periodic laboratory monitoring[1-10]. The 2016 laboratory monitoring guidelines in the US do not recommend routine monitoring of the complete blood cell count (CBC) during oral isotretinoin administration for acne[1,5,6]. However, the United States and European guidelines recommend monitoring serum lipid profiles and liver function enzymes[1]. Specifically, they recommended performing a liver and lipid panel before treatment, 1 mo after treatment, and every 3 mo thereafter[1].

In Korea, isotretinoin doses and routine laboratory monitoring protocols vary, which has likely contributed to the increase in unnecessary hospital visits, thus increasing medical expenses, which is detrimental to the finances of the national health insurance. In Korea, although the adverse effects of isotretinoin therapy for acne are known, a cohort study analyzing laboratory changes at a single institution does not exist, nor do Asian-specific guidelines regarding isotretinoin dose and monitoring protocols.

This study retrospectively investigated hematological monitoring tests and intervals for patients taking isotretinoin for acne at a single institution to determine the most effective protocol.

MATERIALS AND METHODS

Study period and population

This retrospective study analyzed medical records obtained from Dongguk University Ilsan Hospital's electronic medical records database. We included patients who visited the dermatology outpatient department at this hospital from 2005 to 2020 and were prescribed isotretinoin for acne based on the Korean standard classification of disease codes L700 (acne vulgaris), L701 (acne conglobata), and L709 (acne, unspecified). Among them, patients who had not taken isotretinoin for > 1 mo or had irregular laboratory monitoring instead of terminating laboratory monitoring at 1-mo intervals because side effects were excluded from the analysis. For example, patients who underwent laboratory testing at 2 mo after the first dose, or those who underwent laboratory testing at 1st month and 4th month sporadically, rather than serial laboratory monitoring, were excluded.

Data on age, sex, prescription dose, prescription period, and underlying disease were collected. Patients who underwent monthly laboratory monitoring for aspartate aminotransferase (AST), alanine aminotransferase (ALT), triglyceride (TG), high-density lipoprotein (HDL), low-density lipoprotein (LDL), and total cholesterol levels were included. Meanwhile, patients with irregular laboratory testing intervals during isotretinoin administration were excluded from the study.

The Institutional Review Board of Dongguk University Ilsan Hospital approved this study (IRB No. DUIH 2022-05-002).

Blood testing

All blood tests were performed in US units. Normal AST levels were 10-40 units/L for men and 9-25 units/L for women. Normal ALT ranges were 10-55 units/L for men and 7-30 units/L for women. Furthermore, the normal range (men and women) for the TG level was 40-200 mg/dL. Finally, HDL levels ≥ 40 mg/dL, LDL levels ≤ 100 mg/dL, and total cholesterol levels < 200 mg/dL were considered normal.

Outcomes

Laboratory values for AST, ALT, TG, HDL, LDL, and total cholesterol levels were identified for each patient and were categorized by month of therapy for those performed while the patient was receiving isotretinoin. The tendency of the laboratory values to change was determined through the graph slope of the median value.

Statistical analyses

Independent variables (*e.g.*, sex, total prescription date and dose, daily average prescription dose, underlying disease type, and monthly interval per blood test) were analyzed by repeated-measures analysis of variance. Significance was set at $P < 0.05$.

RESULTS

Patient demographics

Among the 112 patients with acne, 30 were included in the analysis according to the exclusion criteria. Nineteen (63.3%) were male, and 11 (36.7%) were female. The average age was 22.8 years. The total number of prescription days was 60-180 d, with a mean of 140 d. The total prescribed dose was 600-3600 mg, with a mean total of 1825.4 mg. The lowest daily dose was 5 mg/d, and the highest daily dose was 20 mg/d; the average daily dose was 13.2 mg.

In total, 23 patients had no underlying diseases. However, one patient had androgenetic alopecia, one had asthma, one had Crohn's disease, one had ulcerative colitis, one had seborrheic dermatitis, and two had urticaria (Table 1).

Monthly blood test abnormalities

Blood tests were performed for 30 patients 1 mo after taking isotretinoin (Table 2). Overall, 2 (7%) patients had abnormal AST levels, 2 (7%) had abnormal HDL levels, 21 (70%) had abnormal LDL levels, and 6 (20%) had abnormal total cholesterol levels. All the patients had normal ALT and TG levels.

Blood tests were performed after 2 mo of isotretinoin administration (n = 26). Overall, 2 (8%), 1 (4%), 2 (8%), 19 (73%), and 4 (15%) patients had abnormal AST, ALT, HDL, LDL, and total cholesterol levels, respectively. All the patients had normal TG levels.

Blood tests were performed after 3 mo of isotretinoin administration (n = 21). Overall, 4 (19%), 1 (5%), 1 (5%), 14 (67%), and 5 (24%) patients had abnormal AST, ALT, HDL, LDL, and total cholesterol levels, respectively. One (5%) patient had an abnormal TG level.

Blood tests were performed 4 mo after isotretinoin administration (n = 20). Overall, 1 (5%), 1 (5%), 14 (70%), and 3 (15%) patients had abnormal AST, ALT, LDL, and total cholesterol levels, respectively. All the patients had normal HDL and TG levels.

Blood tests were performed after 5 mo of isotretinoin administration (n = 18). Overall, 1 (6%), 11 (61%), and 5 (28%) patients had abnormal HDL, LDL, and total cholesterol levels, respectively. All the patients had normal AST, ALT, and TG levels.

Blood tests were performed after 6 mo of isotretinoin administration (n = 10). Overall, 1 (8%), 1 (8%), 7 (54%), and 3 (23%) patients had abnormal AST, ALT, LDL, and total cholesterol levels, respectively. All the patients had normal HDL and TG levels.

Monthly changes per blood test

Table 3 and Figure 1 present the monthly changes per blood test in detail.

AST: The AST level did not change when only AST values were included in the analysis. However, the AST level significantly changed between 5 and 6 mo of isotretinoin use when the prescription period and dose were included in the analysis (Figure 1A).

ALT: Although Figure 1B indicates that the median value of ALT tended to increase over a longer period of use, no significant change in ALT levels was observed when only the blood test values were considered. However, significant changes were observed between 5 and 6 mo of isotretinoin administration when the prescription period and dose were included in the analysis.

TG: Figure 1C presents that the median value of TG tended to increase over a longer period of use; significant changes were observed between 5 and 6 mo of isotretinoin administration. Significant

Table 1 Overall patients' characteristics

Characteristics		Mean (min-max)	*n* (%)
Age		22.8 (15-38)	30 (100)
Sex	Male		19 (63)
	Female		11 (37)
	Total		30 (100)
Total prescription days		339.1 (230-1216)	
Total prescription dose (mg)		4029.7 (230-10495)	
Daily prescription dose (mg/d)		13.2 (8.01-20)	
Underlying disease	None		23 (77)
	Androgenetic alopecia		1 (3)
	Asthma		1 (3)
	Crohn's disease		1 (3)
	Ulcerative colitis		1 (3)
	Seborrheic dermatitis		1 (3)
	Urticaria		2 (6)

Table 2 Number of patients with a laboratory abnormality by month of therapy

Laboratory	Month 1 (total number: 30), *n* (%)	Month 2 (total number: 26), *n* (%)	Month 3 (total number: 21), *n* (%)	Month 4 (total number: 20), *n* (%)	Month 5 (total number: 18), *n* (%)	Month 6 (total number: 13), *n* (%)
AST	2 (7)	2 (8)	4 (19)	1 (5)	0 (0)	1 (8)
ALT	0 (0)	1 (4)	1 (5)	1 (5)	0 (0)	1 (8)
TG	0 (0)	0 (0)	1 (5)	0 (0)	0 (0)	0 (0)
HDL	2 (7)	2 (8)	1 (5)	0 (0)	1 (6)	0 (0)
LDL	21 (70)	19 (73)	14 (67)	14 (70)	11 (61)	7 (54)
Total cholesterol	6 (20)	4 (15)	5 (24)	3 (15)	5 (28)	3 (23)

AST: Aspartate aminotransferase; ALT: Alanine aminotransferase; TG: Triglycerides; HDL: High-density lipoprotein; LDL: Low-density lipoprotein.

changes in the prescription period and dose were also observed between 5 and 6 mo after including the dependent variable.

HDL: Generally, the median value of HDL in Figure 1D tended to decrease, and a significant change was observed between 5 and 6 mo of isotretinoin administration when only the blood test values were considered. However, this effect disappeared after including the dependent variable.

LDL: Although Figure 1E demonstrates that the median value of LDL tended to increase over a longer period of use, the LDL level did not change when we included only the LDL values in the analysis. However, the LDL level significantly changed between 1 and 2 mo of isotretinoin use when the prescription period and dose were included in the analysis.

Total cholesterol: Although Figure 1F presents that the median value of total cholesterol tends to increase over a longer period of use, the total cholesterol level did not change when we included only the blood test values in the analysis. However, a significant change was observed between 1 and 2 mo of isotretinoin use when the prescription period and dose were included in the analysis.

Table 3 Significant monthly change points for each blood test and their relationship to the dependent variable

Blood test	Variable	1-2 mo	2-3 mo	3-4 mo	4-5 mo	5-6 mo
AST	Sex	0.221	0.761	0.769	0.467	0.743
	Prescription days	0.721	0.341	0.584	0.777	0.020
	Prescription dose	0.588	0.310	0.369	0.980	0.029
	Total	0.523	0.434	0.868	0.311	0.153
ALT	Sex	0.296	0.362	0.174	0.912	0.927
	Prescription days	0.699	0.055	0.345	0.262	0.016
	Prescription dose	0.948	0.081	0.527	0.314	0.021
	Total	0.580	0.261	0.689	0.709	0.126
TG	Sex	0.818	0.357	0.538	0.858	0.313
	Prescription days	0.801	0.681	0.823	0.718	0.008
	Prescription dose	0.730	0.355	0.876	0.883	0.009
	Total	0.788	0.501	0.529	0.536	0.024
HDL	Sex	0.552	0.999	0.747	0.498	0.190
	Prescription days	0.475	0.227	0.579	0.922	0.323
	Prescription dose	0.632	0.190	0.528	0.950	0.083
	Total	0.521	0.232	0.716	0.611	0.018
LDL	Sex	0.464	0.524	0.510	0.715	0.445
	Prescription days	0.015	0.869	0.325	0.747	0.786
	Prescription dose	0.006	0.918	0.167	0.842	0.835
	Total	0.052	0.338	0.140	0.755	0.746
Total cholesterol	Sex	0.469	0.348	0.373	0.576	0.336
	Prescription days	0.066	0.761	0.310	0.869	0.761
	Prescription dose	0.019	0.576	0.095	0.925	0.710
	Total	0.104	0.228	0.076	0.698	0.427

P-values of < 0.05 were considered statistically significant. AST: Aspartate aminotransferase; ALT: Alanine aminotransferase; TG: Triglycerides; HDL: High-density lipoprotein; LDL: Low-density lipoprotein.

DISCUSSION

Oral isotretinoin has revolutionized acne treatment and has become the standard treatment[8]. However, it can cause systemic side effects, including leukopenia, hyperlipidemia, and hepatotoxicity[1-9]. Moreover, most patients require long-term use. Thus, periodic blood tests are necessary to ensure patient safety; however, no consensus on dose and frequency has been established to date[1-6,9].

Since 2006, many studies have argued that only few patients have abnormal laboratory test results[6]. Thus, the frequent monitoring of isotretinoin treatment has little value. For example, a 2016 retrospective study including 515 patients in the United States who received isotretinoin for acne treatment has reported that 2.4% of patients developed leukopenia but they did not require treatment discontinuation, and a clinically non-significant number of patients (1.6%) developed thrombocytopenia [2]. This evidence suggests that routine CBC tests are unnecessary, which has been supported by other authors, such as Barbieri*et al*[6]. Furthermore, Hansen *et al*[2] evaluated patients who received the maximum daily dose of isotretinoin, reporting that liver function and lipid profile monitoring was unnecessary unless the patient had specific risk factors. The 2016 United States and European guidelines also include these recommendations[1]. However, Barbieri *et al*[6]have reported that many clinicians still perform monthly blood tests, creating a cost burden for patients and the health insurance system.

Here, significant changes in AST, ALT, and TG levels in terms of total prescription period and isotretinoin dose were observed between 5 and 6 mo. Isotretinoin is metabolized in the liver and has an approximately 14 h half-life in the blood[8]. The primary metabolite 4-oxo-isotretinoin has a half-life of almost 28 h[8,10]. Therefore, it would take between 5 and 6 mo to significantly accumulate in the body

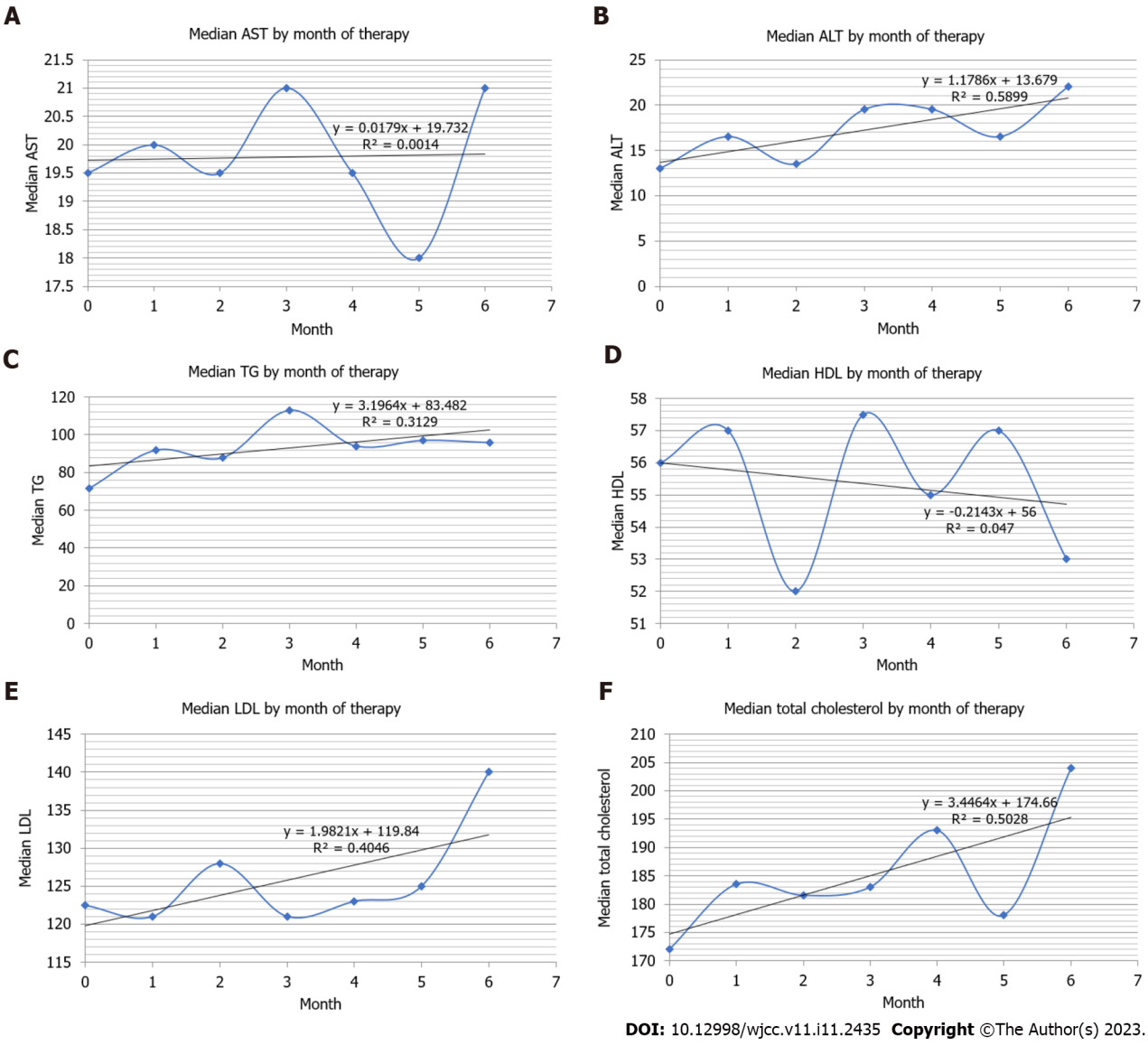

DOI: 10.12998/wjcc.v11.i11.2435

Figure 1 The tendency of blood test levels to change while taking isotretinoin. A: Aspartate aminotransferase; B: Alanine aminotransferase; C: Triglycerides; D: High-density lipoprotein; E: Low-density lipoprotein; F: Total cholesterol. AST: Aspartate aminotransferase; ALT: Alanine aminotransferase; TG: Triglycerides; HDL: High-density lipoprotein; LDL: Low-density lipoprotein.

and affect blood test results. This result is consistent with those of other previously reported studies[11, 12]. In addition to liver levels, vitamin A derivatives have the potential to increase lipid levels because they accumulate in fat[13]. As lipid accumulation and elimination take a long time, changes may occur between 5 and 6 mo. Therefore, the contraceptive period of another vitamin A derivative, alitretinoin, is 1-3 years because of this fat accumulation[13]. Therefore, we recommend testing LDL, total cholesterol, liver function, and lipid levels before treatment and 1-2 mo after starting isotretinoin. Subsequently, if no abnormalities are detected, monitoring every 6 mo is sufficient.

Shah *et al*[3] published a study in 2018 with a similar opinion to that in our study. They also argued that patients should be tested at baseline, 2-3 mo, and a few months after reaching the peak dose; such testing protocol would be cost-effective for patients and the national insurance system[3]. The total cost for patients who underwent baseline and monthly laboratory monitoring for 6 mo was approximately $525, compared with approximately $225 at baseline, after 1-2 mo, and after 6 mo, with estimated savings of $300[3].

In Korea, a liver + lipid panel (excluding direct bilirubin and gamma-glutamyl transferase tests) costs 91650 won, of which 65470 won are covered by insurance. If monthly monitoring is performed for 6 mo (including the baseline exam), the cost to the patient will be 641550 won, of which 458290 won is covered by insurance. However, testing only at the baseline, 1 mo, 2 mo, and 6 mo reduces the general rate to 366600 won, of which 261880 won is covered by insurance, which is a considerable reduction in cost.

Some studies, including those by Hansen *et al*[2] and Shah *et al*[3], have discouraged performing liver and lipid tests if the first 3 mo of monitoring indicate normal results. However, significant changes in liver function and lipid test results were observed. Furthermore, the European Medicines Agency, the United States, and other European guidelines recommend performing liver function and lipid tests (at different intervals)[1]. Therefore, minimal tests are necessary. Consequently, we recommend minimal periodic examinations once every 6 mo after reaching the peak isotretinoin dose.

Some limitations of this study are that we could not confirm isotretinoin compliance and that we only included few patients. Furthermore, if blood test abnormalities were detected, the drug may have been immediately stopped, and subsequent progress could not be confirmed.

CONCLUSION

This study investigated the optimal blood test type and frequency for patients taking isotretinoin for acne. Our results suggest performing a liver and lipid panel before beginning isotretinoin, 1 mo and 2 mo after administration, and every 6 mo thereafter if no abnormalities are detected, to save on costs. However, more frequent monitoring may be necessary if there is a family history of related adverse effects, such as hyperlipidemia, or if the patient has specific risk factors, such as obesity, viral hepatitis, and additional drug or alcohol intake. This article will contribute to Asian-specific isotretinoin laboratory guidelines and further studies.

ARTICLE HIGHLIGHTS

Research background

Isotretinoin is a widely prescribed medication for various dermatological conditions, particularly acne. Regular blood tests are performed to monitor its side effects. However, the optimal tests and their timing remain controversial.

Research motivation

Since 2006, many studies have reported that only a small proportion of patients taking isotretinoin have abnormal laboratory test results. Thus, frequent monitoring of isotretinoin treatment may be unnecessary.

Research objectives

This study aimed to evaluate the most efficient testing regimen for patients with acne taking isotretinoin.

Research methods

This retrospective study analyzed medical records obtained from Dongguk University Ilsan Hospital's electronic medical records database. Independent variables (*e.g.*, sex, total prescription date and dose, daily average prescription dose, underlying disease type, and monthly interval per blood test) were analyzed using repeated-measures analysis of variance.

Research results

Aspartate aminotransferase, alanine aminotransferase, and triglyceride levels significantly changed between 5 and 6 mo when the total prescription period and dose variables were considered altogether. High-density lipoprotein level also significantly changed between 5 and 6 mo. However, low-density lipoprotein and total cholesterol levels significantly changed between 1 and 2 mo.

Research conclusions

Liver and lipid panel should be performed before beginning isotretinoin administration, 1 and 2 mo after administration, and every 6 mo thereafter if no abnormalities are detected to save on costs.

Research perspectives

This article will contribute to Asian-specific isotretinoin laboratory guidelines and further studies.

FOOTNOTES

Author contributions: Park YJ, the first author, analyzed the data and wrote the manuscript; Shin HY and Choi WK participated in the data collection; Lee SH and Lee AY reviewed and edited the manuscript; Hong JS was the corresponding author and designed the study; all authors have read and approved the final manuscript.

Supported by the Dongguk University Research Program (2021).

Institutional review board statement: The Institutional Review Board of Dongguk University Ilsan Hospital approved this study (IRB No. DUIH 2022-05-002).

Informed consent statement: All study participants, or their legal guardian, provided informed written consent prior to study enrollment.

Conflict-of-interest statement: The authors have no conflicts of interest to declare.

Data sharing statement: All data related to this study are presented in this article.

Country/Territory of origin: South Korea

ORCID number: Yu Jeong Park 0000-0003-2462-5278; Hui Young Shin 0000-0003-2523-9504; Woo Kyoung Choi 0000-0003-1675-3720; Ai-Young Lee 0000-0001-7720-7833; Seung Ho Lee 0000-0001-5057-1379; Jong Soo Hong 0000-0003-3813-3055.

S-Editor: Yan JP
L-Editor: A
P-Editor: Wu RR

REFERENCES

1 **Dessinioti C**, Zouboulis CC, Bettoli V, Rigopoulos D. Comparison of guidelines and consensus articles on the management of patients with acne with oral isotretinoin. *J EurAcad Dermatol Venereol* 2020; **34**: 2229-2240 [PMID: 32277497 DOI: 10.1111/jdv.16430]
2 **Hansen TJ**, Lucking S, Miller JJ, Kirby JS, Thiboutot DM, Zaenglein AL. Standardized laboratory monitoring with use of isotretinoin in acne. *J Am Acad Dermatol* 2016; **75**: 323-328 [PMID: 27189824 DOI: 10.1016/j.jaad.2016.03.019]
3 **Shah R**, Kroshinsky D. Re-evaluating the need for routine laboratory monitoring in patients taking isotretinoin: A retrospective analysis. *J Am Acad Dermatol* 2021; **85**: 504-506 [PMID: 30315820 DOI: 10.1016/j.jaad.2018.10.005]
4 **Nazarian RS**, Zheng E, Halverstam C, Cohen SR, Wolkoff AW. Prolonged Serum Alanine Aminotransferase Elevation Associated with Isotretinoin Administration. *Case Reports Hepatol* 2019; **2019**: 9270827 [PMID: 31380129 DOI: 10.1155/2019/9270827]
5 **Ben-Shoshan D**, Gomolin A, Litvinov IV, Netchiporouk E. Time to Change Guidelines for Laboratory Monitoring During Isotretinoin Treatment. *J Cutan Med Surg* 2020; **24**: 92-93 [PMID: 31994935 DOI: 10.1177/1203475419879882]
6 **Barbieri JS**, Shin DB, Wang S, Margolis DJ, Takeshita J. The clinical utility of laboratory monitoring during isotretinoin therapy for acne and changes to monitoring practices over time. *J Am Acad Dermatol* 2020; **82**: 72-79 [PMID: 31228528 DOI: 10.1016/j.jaad.2019.06.025]
7 **Lee YH**, Scharnitz TP, Muscat J, Chen A, Gupta-Elera G, Kirby JS. Laboratory Monitoring During Isotretinoin Therapy for Acne: A Systematic Review and Meta-analysis. *JAMA Dermatol* 2016; **152**: 35-44 [PMID: 26630323 DOI: 10.1001/jamadermatol.2015.3091]
8 **Brzezinski P**, Borowska K, Chiriac A, Smigielski J. Adverse effects of isotretinoin: A large, retrospective review. *Dermatol Ther* 2017; **30** [PMID: 28295859 DOI: 10.1111/dth.12483]
9 **Öktem A**, Hayran Y, Arı E, Yalçın B. Minimize the regular laboratory monitoring during the systemic isotretinoin treatment: data of 704 patients with acne vulgaris. *J Dermatolog Treat* 2019; **30**: 813-817 [PMID: 30836808 DOI: 10.1080/09546634.2019.1591578]
10 **Almond-Roesler B**, Blume-Peytavi U, Bisson S, Krahn M, Rohloff E, Orfanos CE. Monitoring of isotretinoin therapy by measuring the plasma levels of isotretinoin and 4-oxo-isotretinoin. A useful tool for management of severe acne. *Dermatology* 1998; **196**: 176-181 [PMID: 9557257 DOI: 10.1159/000017856]
11 **Kızılyel O**, Metin MS, Elmas ÖF, Çayır Y, Aktaş A. Effects of oral isotretinoin on lipids and liver enzymes in acne patients. *Cutis* 2014; **94**: 234-238 [PMID: 25474452]
12 **Vieira AS**, Beijamini V, Melchiors AC. The effect of isotretinoin on triglycerides and liver aminotransferases. *An Bras Dermatol* 2012; **87**: 382-387 [PMID: 22714752 DOI: 10.1590/s0365-05962012000300005]
13 **Jeong JH**, Hyun GH, Park YJ, Kwon SW, Lee AY. Clinical Factors Affecting the Serum Retention of a Teratogenic Etretinate after the Acitretin Administration. *BiomolTher (Seoul)* 2022; **30**: 562-569 [PMID: 35871607 DOI: 10.4062/biomolther.2022.069]

World Journal of Clinical Cases

Submit a Manuscript: https://www.f6publishing.com

World J Clin Cases 2023 April 16; 11(11): 2443-2451

DOI: 10.12998/wjcc.v11.i11.2443

ISSN 2307-8960 (online)

ORIGINAL ARTICLE

Observational Study

Etiology analysis for term newborns with severe hyperbilirubinemia in eastern Guangdong of China

Jia-Xin Xu, Fen Lin, Yong-Hao Wu, Zi-Kai Chen, Yu-Bin Ma, Li-Ye Yang

Specialty type: Pediatrics

Provenance and peer review: Unsolicited article; Externally peer reviewed.

Peer-review model: Single blind

Peer-review report's scientific quality classification

Grade A (Excellent): 0
Grade B (Very good): 0
Grade C (Good): C, C
Grade D (Fair): 0
Grade E (Poor): 0

P-Reviewer: Ali A, Malaysia; Huang CS, Taiwan

Received: November 23, 2022
Peer-review started: November 23, 2022
First decision: February 2, 2023
Revised: February 9, 2023
Accepted: March 15, 2023
Article in press: March 15, 2023
Published online: April 16, 2023

Jia-Xin Xu, Fen Lin, Yong-Hao Wu, Precision Medical Center, Chaozhou Central Hospital, Chaozhou 521021, Guangdong Province, China

Zi-Kai Chen, School of Food Engineering and Biotechnology, Hanshan Normal University, Chaozhou 521021, Guangdong Province, China

Yu-Bin Ma, Department of Pediatrics, Chaozhou Central Hospital, Chaozhou 521021, Guangdong Province, China

Li-Ye Yang, Precision Medical Lab Center, People's Hospital of Yangjiang, Yangjiang 529500, Guangdong Province, China

Corresponding author: Li-Ye Yang, MD, PhD, Chief Doctor, Precision Medical Lab Center, People's Hospital of Yangjiang, No. 42 Dongshan Road, Jiangcheng District, Yangjiang 529500, Guangdong Province, China. yangleeyee@sina.com

Abstract

BACKGROUND

Neonatal hyperbilirubinemia is one of the common diseases of newborns that typically presents with yellow staining of skin, resulting in sequelaes such as hearing loss, motor and intellectual development disorders, and even death. The pathogenic factors of neonatal hyperbilirubinemia are complex. Different cases of hyperbilirubinemia may have a single or mixed etiology.

AIM

To explore the etiological characteristics of severe hyperbilirubinemia in term newborns of eastern Guangdong of China.

METHODS

Term newborns with severe hyperbilirubinemia in one hospital from January 2012 to December 2021 were retrospectively analyzed. The etiology was determined according to the laboratory results and clinical manifestations.

RESULTS

Among 1602 term newborns with hyperbilirubinemia in eastern Guangdong of China, 32.20% (580/1602) was severe hyperbilirubinemia. Among the causes of severe hyperbilirubinemia, neonatal hemolysis accounted for 15.17%, breast milk jaundice accounted for 12.09%, infection accounted for 10.17%, glucose-6-

phosphate dehydrogenase (G6PD) deficiency accounted for 9.14%, and the coexistence of multiple etiologies accounted for 6.55%, unknown etiology accounted for 41.72%. ABO hemolysis and G6PD deficiency were the most common causes in the 20 cases with bilirubin encephalopathy. 94 severe hyperbilirubinemia newborns were tested for uridine diphosphate glucuronosyl transferase 1A1 (UGT1A1)*6 variant (rs4148323, c.211G>A, p.Arg71Gly), 9 cases were 211 G to A homozygous variant, 37 cases were 211 G to A heterozygous variant, and 48 cases were wild genotypes.

CONCLUSION

The main cause for severe hyperbilirubinemia and bilirubin encephalopathy in eastern Guangdong of China were the hemolytic disease of the newborns, G6PD deficiency and infection. *UGT1A1* gene variant was also a high-risk factor for neonatal hyperbilirubinemia. Targeted prevention and treatment according to the etiology may reduce the occurrence of bilirubin encephalopathy and kernicterus.

Key Words: Severe hyperbilirubinemia; Term newborns; Etiology; Uridine diphosphate glucuronosyl transferase 1A1; Glucose-6-phosphate dehydrogenase deficiency

Core Tip: The main cause for severe hyperbilirubinemia and bilirubin encephalopathy in eastern Guangdong of China were the hemolytic disease of the newborns, glucose-6-phosphate dehydrogenase deficiency and infection. *UGT1A1* gene variant was also a high-risk factor for neonatal hyperbilirubinemia.

Citation: Xu JX, Lin F, Wu YH, Chen ZK, Ma YB, Yang LY. Etiology analysis for term newborns with severe hyperbilirubinemia in eastern Guangdong of China. *World J Clin Cases* 2023; 11(11): 2443-2451
URL: https://www.wjgnet.com/2307-8960/full/v11/i11/2443.htm
DOI: https://dx.doi.org/10.12998/wjcc.v11.i11.2443

INTRODUCTION

Neonatal hyperbilirubinemia is one of the common diseases of newborns, which is mainly caused by the imbalance between the production and elimination of bilirubin in the body[1]. It can be manifested as yellow staining of skin mucosa and sclera and usually resolves within 1 wk after birth, and most of neonates with jaundice have a good prognosis. However, if the total bilirubin level exceeds a certain threshold, it can lead to bilirubin encephalopathy, resulting in sequelaes such as hearing loss, motor and intellectual development disorders, and even death, which will bring a heavy burden to the society and family.

The pathogenic factors of neonatal hyperbilirubinemia are complex. Different cases of hyperbilirubinemia may have a single or mixed etiology. The etiological composition and related genetic variants of hyperbilirubinemia in different regions may be different, resulting in different degrees of hyperbilirubinemia in clinic. The American Academy of Pediatrics published the percentile curve of hourly total serum bilirubin (TSB) of newborns in venous blood, which defined bilirubin more than 95% percentile as hyperbilirubinemia and should be intervened[2]. According to the level of bilirubin and clinical symptoms, hyperbilirubinemia can be divided into significant hyperbilirubinemia (TSB < 342 μmol/L), severe hyperbilirubinemia (TSB ≥ 342 μmol/L), extreme hyperbilirubinemia (TSB ≥ 428 μmol/L), hazardous or critical hyperbilirubinemia (TSB ≥ 513 μmol/L), acute bilirubin encephalopathy, and kernicterus[3,4].

Glucose 6-phosphate dehydrogenase (G6PD) deficiency is one of the commonest human enzymopathies, with an estimated global prevalence of 4.9% that affects more than 500 million individuals worldwide[5]. The prevalence of G6PD deficiency in Chaozhou was 3.36%[6]. To date, 12 mutations have been reported in Chaozhou population, Canton (c.1376 G>T) and Kaiping (c.1388 G>A) were the most common variants[6]. Uridine diphosphate glucuronosyl transferase 1A1 (UGT1A1) is a rate-limiting enzyme in the process of bilirubin metabolism[7]. It catalyzes the glucuronic acid binding reaction and converts unconjugated bilirubin into conjugated bilirubin[8]. UGT1A1 (*UGT1A1**6, c.211G>A, p.Arg71Gly, rs4148323), one of the most common *UGT1A1* gene polymorphisms in the coding regions, was reported to be a risk factor for neonatal hyperbilirubinema[9].

Early detection of high-risk factors for severe hyperbilirubinemia and prompt treatment are crucial for the prevention of bilirubin encephalopathy. This study analyzed the clinical data of term newborns

with severe hyperbilirubinemia retrospectively, to explore the etiology and clinical characteristics of severe hyperbilirubinemia in term newborns in Chaozhou, eastern Guangdong province, and to provide basis for clinical prevention and early treatment of hyperbilirubinemia.

MATERIALS AND METHODS

Subjects

All of term newborns with hyperbilirubinemia (gestational age > 37 wk) admitted to neonatal intensive care unit of Chaozhou Central Hospital from January 2012 to December 2021 were selected. The age of admission was 1-28 d. Demographic and clinical data were collected from the medical records of the studied participants. Hyperbilirubinemia was defined for bilirubin more than 95% percentile and TSB ≥ 342 μmol/L was used as the diagnostic standard for severe hyperbilirubinemia[3,4].

This study was initially approved by the Ethics Committee of Chaozhou Central Hospital in 2011 (No. 2011021), and then the second ethical approval was obtained in 2015 (No. 2015001). The data was collected retrospectively, which did not require informed consent form.

Methods

General information including sex, gestational age, birth weight, admission age and weight, mode of delivery, feeding pattern, and treatment were collected. The major clinical etiologies included hemolytic disease of the newborn (HDN) (ABO hemolysis and Rh hemolysis), G6PD deficiency (G6PD enzyme activity ≤ 2500 U/L, Co-Heath Beijing Laboratories Co., Ltd.), infection (sepsis, pneumonia, urinary tract infection), extravascular hemorrhage (intracranial hematoma, scalp hematoma and other bleeding), polycythemia (venous red blood cells > 6×10^{12}/L, hemoglobin > 220 g/L, and hematocrit > 65%), congenital hypothyroidism (diagnosed by neonatal screening), insufficient breastfeeding (breastfeeding newborns with 10% birth weight loss after birth), and breast milk jaundice. Breast milk jaundice was diagnosed by exclusion. Therefore, it is not included in the combined factors. Prolonged jaundice was defined as jaundice persisting for more than 2 wk, with bilirubin level > 150 μmol/L. Bilirubin encephalopathy (hyperbilirubinemia and clinical symptoms of nervous system for encephalopathy), and blood exchange indications (blood exchange reference standard recommended by American Academy of Pediatrics in 2004.) were also recorded[2].

The whole blood samples of ethylenediamine tetraacetic acid anticoagulants in newborns with severe hyperbilirubinemia were prospectively collected after clinical diagnosis and stored at -40 °C in a biobank. The whole blood DNA extraction kit (Chaozhou Hybribio Co., Ltd.) was used to extract DNA according to the instructions of the kit, and then the DNA quantity and purity were tested (NanoDrop One, Thermo Fisher Scientific Co., Ltd.). MJ Mini Personal Thermal Cycler (Bio-Rad Company) was used for polymerase chain reaction amplification of *G6PD*, and then, *G6PD* gene variant was detected by reverse dot blot method (Chaozhou Hybribio Co., Ltd.) for 13 common G6PD mutation types c.95A>G (G6PD Gaohe), c.392G>T (G6PD Qing Yan), c.487G>A (G6PD Mahidol), c.493A>G (G6PD Taipei), c.592G>T (G6PD Coimbra), c.871G>A (G6PD Viangchan), c.1004C>T (G6PD Fushan), c.1024C>T (G6PD Chinese-5), c.1360C>T (G6PD Union), c.1376G>T (G6PD Canton), c.1387C>T (G6PD Keelung), c.1388G>A (G6PD Kaiping), c.1381G>A (G6PD Yunan) and one polymorphism c.1311C>T[10]. *UGT1A1* gene was amplified and sequenced (3500Dx, Life Technologies) to detect c.211G>A variant (*UGT1A1**6, rs4148323), which was specifically described in our previous study[10].

A total of 94 severe hyperbilirubinemia newborns were tested for *UGT1A1**6 variant (rs4148323). The control 65 newborns for *UGT1A1**6 test were the term newborns without hyperbilirubinemia, and with a TSB not requiring phototherapy, their clinical characteristics were described previously[11].

Statistical analysis

SPSS 20.0 was used for data analysis. The continuous variables in the data group were expressed as mean ± SD. Count data was described by frequency and percentage. The Pearson chi-square test was used, and $P < 0.05$ was considered as statistically significant.

RESULTS

General clinical characteristics

A total of 1602 newborns with hyperbilirubinemia (915 males and 687 females) were collected in this study, 580 newborns (346 males and 234 females) were severe hyperbilirubinemia (32.20%, 580/1602). In these 580 cases, birth weight was 2050-5500 g, with an average of 3211.6 ± 444.53 g, gestational age was 37-42 wk, with an average of 39.07 ± 1.10 wk; the age of the highest bilirubin value was 1-28 d, with an average of 8 ± 5 d; 315 cases were vaginal delivery, 265 cases were cesarean section; 174 cases were breastfeeding, 165 cases were formula feeding, 195 cases were mixed feeding and 46 cases were unknown. The peak value of TSB was 342.05-817.8 μmol/L, with an average of 398.07 ± 55.09 μmol/L.

Among them, 213 cases met the standard of blood exchange, 52 cases were prolonged jaundice (22 cases were breast feeding), and 20 cases were complicated with bilirubin encephalopathy (Table 1).

Etiology composition

Among the cases of severe hyperbilirubinemia with clear etiology, the most common was neonatal hemolysis (15.17%), followed by breast milk jaundice (12.09%), infection (10.17%), G6PD deficiency (9.14%), and combined factors (6.55%), the etiology for the remaining 41.72% (242/580) cases was not clear. Among combined factors, neonatal hemolysis combined with infection (36.84%) was the most common, followed by G6PD deficiency combined with infection (26.32%) and infection combined with vascular bleeding (13.16%). In all cases of neonatal hemolysis, one case of Rh hemolysis was identified, the other 106 cases were ABO hemolysis (Figure 1).

*G6PD genotype and UGT1A1*6 variant*

Among 580 cases of severe hyperbilirubinemia, 68 cases were G6PD deficient by enzyme activity test, and 43 newborns were tested for 13 common *G6PD* gene mutations in Chinese[10]. Gene mutations were found in 40 cases, including 1 case c.95A>G (G6PD Gaohe), 1 case c.1024C>T (G6PD Chinese-5), 14 cases c.1376G>T (G6PD Canton), 23 cases c.1388G>A (G6PD Kaiping), and 1 case of composite mutation c.1311C>T combined with c.871G>A (G6PD Viangchan). No mutation was detected in the remaining 3 cases.

A total of 94 neonates with severe hyperbilirubinemia were selected to detect *UGT1A1**6 variant (*UGT1A1**6, c.211G>A, p.Arg71Gly, rs4148323). 48 cases were wild type, 37 cases were heterozygous variants, and 9 cases of homozygous variants were detected, with a gene variant frequency of 48.94 % (46/94). Among that 94 cases, a total of 18 cases of G6PD deficiency combined with *UGT1A1* variants were found, including 2 cases of homozygous variants of *UGT1A1**6 with c.1376G>T, 2 cases of homozygous variants of *UGT1A1**6 with c.1388G>A, 4 cases of heterozygous variants of *UGT1A1**6 with c.1376G>T, 10 cases of heterozygous variants of *UGT1A1**6 with c.1388G>A (Table 2). Compared with our previous study on the *UGT1A1* c.211G>A variant in 65 full-term newborns with normal bilirubin (Table 3)[11]. The proportion of c.211G>A variant in newborns with severe hyperbilirubinemia was higher than that in term neonates with normal bilirubin ($P < 0.001$). ABO hemolysis occurred in 34 of these 94 cases, and 10 cases (10.64%, 10/94) were ABO hemolysis combined with *UGT1A1**6 variant.

Bilirubin encephalopathy

Among 580 cases of severe hyperbilirubinemia, 20 cases were bilirubin encephalopathy, including 11 cases of male and 9 cases of female, and TSB bilirubin level was 359-817.8 μmol/L, with an average of 480.21 ± 64.19 μmol/ L. The main causes of bilirubin encephalopathy were ABO hemolysis (6 cases), followed by infection (sepsis in 1 case, pneumonia in 4 cases), G6PD deficiency (4 cases), unknown causes (3 cases), one case was ABO hemolysis combined with infection, and one case was ABO hemolysis combined with G6PD deficiency and infection.

DISCUSSION

Neonatal hyperbilirubinemia is one of the common diseases in neonatal period. The pathogenesis of severe neonatal hyperbilirubinemia is often multifactorial. In recent years, there have been many studies on the etiology and related risk factors of neonatal hyperbilirubinemia in China and abroad[12-14]. However, the etiology of hyperbilirubinemia is easily affected by environment and other relative factors. Therefore, the analysis of the etiology of neonates with severe hyperbilirubinemia in eastern Guangdong is of great significance to reduce the incidence of severe hyperbilirubinemia and its serious complications in this region.

Our study found that 32.20% of the 1602 hospitalized newborns with hyperbilirubinemia were severe hyperbilirubinemia. HDN was the most common cause of severe hyperbilirubinemia in term newborns. ABO blood group incompatibility is one of the most common causes of HDN which often occurs in infants of blood type A or B with mothers of blood type O. The blood type antibody in mother combines with the corresponding antigen on the surface of fetal red blood cells during pregnancy. Macrophages and natural killer cells in newborn destroy sensitized red blood cells, resulting in hemolysis, jaundice and anemia after birth[15].

A total of 68 cases of G6PD deficiency was identified (11.72%, 68/580) in this study, 53 cases were single G6PD deficiency and 15 cases were combined factor with other causes. The incidence of G6PD deficiency was relatively high, which might be related to the geographical location of Chaozhou. The prevalence of G6PD deficiency in Chaozhou was 3.36%[6]. The prevalence of G6PD deficiency in severe hyperbilirubinemia group was higher than that of the general population. G6PD deficiency causes increased susceptibility of erythrocytes to H_2O_2 and other reactive oxygen species that can lead to hemolytic anemia, and in neonatal hyperbilirubinemia cases, it even results in neonatal kernicterus. G6PD deficiency is an important reason for severe hyperbilirubinemia in term newborns. Of the 68 cases

Table 1 Demographic and clinical characteristics of severe hyperbilirubinemia, *n* (%)

Basic data	Cases
Sex	
Male	346 (59.66)
Female	234 (40.34)
Delivery pattern	
Caesarean section	265 (45.69)
Vaginal delivery	315 (54.31)
Feeding pattern	
Breast feeding	174 (29.90)
Mixed feeding	195 (33.62)
Formula feeding	165 (28.45)
Unknown	46 (7.93)
Proportion of exchange transfusion level	213 (36.72)
Prolonged jaundice	52 (8.97)
Bilirubin encephalopathy	20 (3.45)

Table 2 UGT1A1*6 variant combination with glucose-6-phosphate dehydrogenase deficiency in 94 cases of severe neonatal hyperbilirubinemia

	G6PD deficiency	G6PD normal	Total	*P* value
G211A variation				
Wild type	16	32	48	0.787
c.211 hetereozygote	14	23	37	
c.211 homozygote	4	5	9	
Total	34	60	94	

G6PD: Glucose-6-phosphate dehydrogenase.

Table 3 Comparison of UGT1A1*6 variant between neonates with severe hyperbilirubinemia and the control group

	Case	Control[1]	*P* value
G211A variation			
Wild type	48	51	< 0.001
c.211 hetereozygote	37	13	
c.211 homozygote	9	1	
Total	94	65	

[1]Term newborns without major abnormality or illness, and with a total serum bilirubin not requiring phototherapy according to the updated clinical guidelines by the China Neonatal Association[11].

with G6PD deficiency, 11 cases were combined with infection. Infection was the main inducing cause of acute hemolysis in G6PD deficiency[16]. We performed gene analysis in 43 cases of G6PD deficiency and found that c.1388G>A and c.1376G>T were the most common variants in severe hyperbilirubinemia neonates. The bilirubin level in severe hyperbilirubinemia caused by hemolysis is high, and it occurs early and develops rapidly. In addition, neonatal blood-brain barrier is not fully matured, bilirubin encephalopathy and even death are prone to occur.

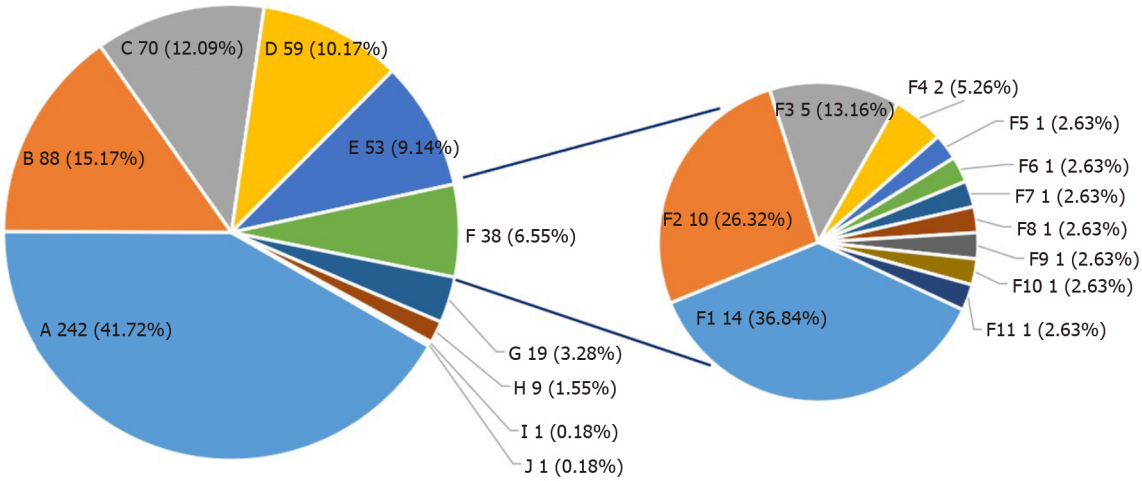

DOI: 10.12998/wjcc.v11.i11.2443

Figure 1 Etiology of severe hyperbilirubinemia. A: Unknown; B: Hemolytic disease of newborn; C: Breast milk jaundice; D: Infection; E: G6PD deficiency; F: Combined factors; G: Extravascular hemorrhage; H: Inadequate feeding; I: Congenital hypothyroidism; J: Polycythemia; F1: Hemolytic disease of newborn + infection; F2: G6PD deficiency + infection; F3: Infection + extravascular hemorrhage; F4: Extravascular hemorrhage + inadequate feeding; F5: Hemolytic disease of newborn + extravascular hemorrhage; F6: Hemolytic disease of newborn + G6PD deficiency; F7: G6PD deficiency + extravascular hemorrhage; F8: G6PD deficiency + inadequate feeding; F9: Inadequate feeding + congenital hypothyroidism; F10: Hemolytic disease of newborn + G6PD deficiency + infection; F11: G6PD deficiency + infection+ polycythemia.

Infection was another cause of severe hyperbilirubinemia (10.17%). Hyperbilirubinemia caused by infection may be due to the imperfect immune function of newborns and lack of mature defense ability, and the neonate is easily to be infected by viruses and bacteria. The destruction of the erythrocyte membrane by the pathogen themselves or secreted toxins, results in hemolysis and increased bilirubin production. At the same time, infection can cause liver dysfunction, inhibit the activity of UGT1A1, and reduce the ability of liver to deal with bilirubin. Hyperbilirubinemia may be the only manifestation of infection[17]. Because of the low positive rate of blood culture, and late diagnosis for infection, the bilirubin may increase and progress to severe hyperbilirubinemia.

Breast milk jaundice is a clinical diagnosis made after excluding the known causes of hyperbilirubinemia. At present, there is still a lack of reliable laboratory testing methods to get this diagnosis. Breast milk jaundice can be divided into early breastfeeding jaundice and late breast milk jaundice[18]. In our study, 9 cases (1.55%) of early breastfeeding jaundice and 70 cases (12.07%) of late breast milk jaundice were identified. Early breast feeding deficiency leads to insufficient calorie intake, reduced intestinal peristalsis, and increased bilirubin enterohepatic circulation, resulting in early hyperbilirubinemia, which is manifested by a weight loss of 10% within one week after birth. Late breast milk jaundice occurs relatively late, and the bilirubin generally peaks on the 7th to 14th days of life. The jaundice can last for 2-3 wk or even 2-3 mo, which may be caused by many factors[19].

The variant of *UGT1A1* c.211G>A was an important cause of breast milk jaundice in newborns, and the serum bilirubin level of breast milk jaundice newborns with this variant was significantly higher than that of breast milk jaundice newborns without this variant[20,21]. This indicated that the presence of *UGT1A1* c.211G>A variant could promote breast milk jaundice. The product encoded by *UGT1A1* gene is bilirubin uridine diphosphate glucuronyltransferase. *UGT1A1* variant make the activity of this enzyme reduced, so that bilirubin cannot combine with glucuronide to form conjugated bilirubin. The unconjugated bilirubin accumulates in the body, and resulting in different degrees of hyperbilirubinemia[22,23].

The *UGT1A1* c.211G>A was a risk factor for neonatal severe hyperbilirubinemia in eastern Guangdong, which might occur with other causes simultaneously. Among the 94 cases with *UGT1A1* variant data, we found that 18 cases were *UGT1A1* gene variant combined with G6PD deficiency, 10 cases were *UGT1A1* gene variant combined with ABO hemolysis. Our previous study found that, in the newborns with hyperbilirubinemia which due to G6PD deficiency, bilirubin level showed an increasing trend with the accumulation of *UGT1A1* c.211G>A variants[10]. Yang *et al*[24] reported that the risk of neonatal severe hyperbilirubinemia increased significantly when ABO hemolytic neonates were combined with *UGT1A1* gene mutation (especially 211A>G homozygous mutation).

The causes for 41.2% of severe hyperbilirubinemia cases were unknown in our study. Previous studies have shown that mutations of other genes, such as heme oxygenase-1, biliverdin reductase A, and solute carrier organic anion transporter family member 1B1 could also affect the serum bilirubin [25]. For severe hyperbilirubinemia neonates with unknown etiology, due to limited conditions, we did not perform gene detection for all cases, resulting in some missing causes. For neonates with unknown etiology, except for *UGT1A1* variants, other gene variants might contribute to increased bilirubin. Pathological jaundice, especially severe jaundice, is often the result of multiple influencing factors.

Detection of bilirubin-related genes such as *G6PD* and *UGT1A1* in neonates can be used as an auxiliary test for clinicians to assess the risk of neonatal severe hyperbilirubinemia, which will benefit for early prevention, etiological exploration and genetic counseling.

CONCLUSION

The main causes of severe hyperbilirubinemia in Chaozhou are neonatal hemolysis and infection. Genetic factors such as *UGT1A1* variant and G6PD deficiency, were also the important risk factors for neonatal severe hyperbilirubinemia. It is very important to clarify the etiology and to treat neonatal severe hyperbilirubinemia timely, which can reduce the occurrence of acute bilirubin encephalopathy and kernicterus.

ARTICLE HIGHLIGHTS

Research background

Neonatal hyperbilirubinemia is one of the common diseases of newborns, the pathogenic factors of neonatal hyperbilirubinemia in eastern Guangdong is not clear.

Research motivation

To understand the etiology for severe neonatal hyperbilirubinemia in Chaozhou.

Research objectives

To analyze the pathological factors contributing to severe hyperbilirubinemia in neonates.

Research methods

The clinical data were retrospectively collected and genetic variants of glucose-6-phosphate dehydrogenase (G6PD) and UGT1A1 were determined by polymerase chain reaction and sequencing.

Research results

Among the causes of severe hyperbilirubinemia, neonatal hemolysis accounted for 15.17%, breast milk jaundice accounted for 12.09%, infection accounted for 10.17%, G6PD deficiency accounted for 9.14%, and the coexistence of multiple etiologies accounted for 6.55%, unknown etiology accounted for 41.72%. ABO hemolysis and G6PD deficiency were the most common causes in the 20 cases with bilirubin encephalopathy. 94 severe hyperbilirubinemia newborns were tested for UGT1A1*6 variant (rs4148323, c.211G>A, p.Arg71Gly), 9 cases were 211 G to A homozygous variant, 37 cases were 211 G to A heterozygous variant, and 48 cases were wild genotypes.

Research conclusions

The main causes for severe hyperbilirubinemia and bilirubin encephalopathy in eastern Guangdong of China were the hemolytic disease of the newborns, G6PD deficiency and infection. *UGT1A1* gene variant was also a high-risk factor for neonatal hyperbilirubinemia.

Research perspectives

Multiple genetic variants may regulate the bilirubin levels in neonate, these gene analysis may contribute to the prognosis and management for neonatal jaundice.

FOOTNOTES

Author contributions: Yang LY conceptualized and designed the study, coordinated and supervised data collection, and reviewed and revised the manuscript; Xu JX analyzed the data, drafted the initial manuscript, and revised the manuscript; Lin F collected the data, did the molecular analysis, and carried out the initial analysis; Chen ZK revised the manuscript; Wu YH and Ma YB participated in the sample and data collection and Wu YH performed the molecular analysis. All authors commented on previous versions of the manuscript. All authors read and approved the final manuscript.

Supported by the Natural Science Foundation of Guangdong Province, No. 2016A030307035; Special Research Plan 2019 of Chaozhou, No. 2020xg01; and High-Level Development Plan of People's Hospital of Yangjiang, No. G2020007.

Institutional review board statement: The study was reviewed and approved by the Ethics Committee of Chaozhou

Central Hospital (No. 2015001).

Informed consent statement: All study participants provided informed written consent prior to study enrollment.

Conflict-of-interest statement: The authors declare that they have no conflict of interest.

Data sharing statement: The datasets used and/or analyzed during the current study are available from the corresponding author on reasonable request.

STROBE statement: The manuscript was prepared and revised according to the STROBE statement.

Country/Territory of origin: China

ORCID number: Jia-Xin Xu 0000-0002-3431-6834; Fen Lin 0000-0001-9614-7776; Yong-Hao Wu 0000-0002-6795-1201; Yu-Bin Ma 0000-0003-4225-4829; Li-Ye Yang 0000-0003-1581-9089.

S-Editor: Zhang H
L-Editor: A
P-Editor: Zhang H

REFERENCES

1 **Kaplan M**, Muraca M, Hammerman C, Rubaltelli FF, Vilei MT, Vreman HJ, Stevenson DK. Imbalance between production and conjugation of bilirubin: a fundamental concept in the mechanism of neonatal jaundice. *Pediatrics* 2002; **110**: e47 [PMID: 12359820 DOI: 10.1542/peds.110.4.e47]
2 **American Academy of Pediatrics Subcommittee on Hyperbilirubinemia**. Management of hyperbilirubinemia in the newborn infant 35 or more weeks of gestation. *Pediatrics* 2004; **114**: 297-316 [PMID: 15231951 DOI: 10.1542/peds.114.1.297]
3 **Bhutani VK**, Vilms RJ, Hamerman-Johnson L. Universal bilirubin screening for severe neonatal hyperbilirubinemia. *J Perinatol* 2010; **30** Suppl: S6-15 [PMID: 20877410 DOI: 10.1038/jp.2010.98]
4 **Chinese Multicenter Study Coordination Group for Neonatal Hyperbilirubinemia**. [Predictive value of hour-specific transcutaneous bilirubin nomogram for neonatal hyperbilirubinemia: a national multicenter study]. *Zhonghua Er Ke Za Zhi* 2015; **53**: 830-834 [PMID: 26758321]
5 **Luzzatto L**, Ally M, Notaro R. Glucose-6-phosphate dehydrogenase deficiency. *Blood* 2020; **136**: 1225-1240 [PMID: 32702756 DOI: 10.1182/blood.2019000944]
6 **Lin F**, Wu J, Yang H, Lin M, Yang L. [Molecular epidemiology of G6PD deficiency in Chaozhou area of eastern Guangdong Province]. *Zhonghua Yi Xue Yi Chuan Xue Za Zhi* 2016; **33**: 26-29 [PMID: 26829728 DOI: 10.3760/cma.j.issn.1003-9406.2016.01.007]
7 **Lin F**, Lou ZY, Xing SY, Zhang L, Yang LY. The gene spectrum of glucose-6-phosphate dehydrogenase (G6PD) deficiency in Guangdong province, China. *Gene* 2018; **678**: 312-317 [PMID: 30077011 DOI: 10.1016/j.gene.2018.07.068]
8 **Bentivegna A**, Santambrogio J, Clerici M. UGT1A1 mutations and psychoses: towards understanding the relationship with unconjugated bilirubin. *CNS Spectr* 2021; **26**: 188-190 [PMID: 31339084 DOI: 10.1017/S1092852919001251]
9 **Wang J**, Yin J, Xue M, Lyu J, Wan Y. Roles of UGT1A1 Gly71Arg and TATA promoter polymorphisms in neonatal hyperbilirubinemia: A meta-analysis. *Gene* 2020; **736**: 144409 [PMID: 32007587 DOI: 10.1016/j.gene.2020.144409]
10 **Xu JX**, Lin F, Chen ZK, Luo ZY, Zhan XF, Wu JR, Ma YB, Li JD, Yang LY. Co-inheritance of G6PD deficiency and 211 G to a variation of UGT1A1 in neonates with hyperbilirubinemia in eastern Guangdong. *BMC Pediatr* 2021; **21**: 564 [PMID: 34895177 DOI: 10.1186/s12887-021-03010-6]
11 **Yang H**, Wang Q, Zheng L, Zheng XB, Lin M, Zhan XF, Yang LY. Clinical Significance of UGT1A1 Genetic Analysis in Chinese Neonates with Severe Hyperbilirubinemia. *Pediatr Neonatol* 2016; **57**: 310-317 [PMID: 26727668 DOI: 10.1016/j.pedneo.2015.08.008]
12 **Zhou J**, Yang C, Zhu W, Chen S, Zeng Y, Wang J, Zhao H, Chen Y, Lin F. Identification of Genetic Risk Factors for Neonatal Hyperbilirubinemia in Fujian Province, Southeastern China: A Case-Control Study. *Biomed Res Int* 2018; **2018**: 7803175 [PMID: 30298137 DOI: 10.1155/2018/7803175]
13 **Mei H**, Dong X, Wu B, Wang H, Lu Y, Hu L, Wang J, Cao Y, Zhang R, Cheng G, Wang L, Li Z, Yang L, Zhou W. Clinical and Genetic Etiologies of Neonatal Unconjugated Hyperbilirubinemia in the China Neonatal Genomes Project. *J Pediatr* 2022; **243**: 53-60.e9 [PMID: 34953813 DOI: 10.1016/j.jpeds.2021.12.038]
14 **Osuorah CDI**, Ekwochi U, Asinobi IN. Clinical evaluation of severe neonatal Hyperbilirubinaemia in a resource-limited setting: a 4-year longitudinal study in south-East Nigeria. *BMC Pediatr* 2018; **18**: 202 [PMID: 29935542 DOI: 10.1186/s12887-018-1174-z]
15 **Christensen RD**, Baer VL, MacQueen BC, O'Brien EA, Ilstrup SJ. ABO hemolytic disease of the fetus and newborn:

thirteen years of data after implementing a universal bilirubin screening and management program. *J Perinatol* 2018; **38**: 517-525 [PMID: 29410540 DOI: 10.1038/s41372-018-0048-4]

16 **Harcke SJ**, Rizzolo D, Harcke HT. G6PD deficiency: An update. *JAAPA* 2019; **32**: 21-26 [PMID: 31609781 DOI: 10.1097/01.JAA.0000586304.65429.a7]

17 **Omar C**, Hamza S, Bassem AM, Mariam R. Urinary tract infection and indirect hyperbilirubinemia in newborns. *N Am J Med Sci* 2011; **3**: 544-547 [PMID: 22363075 DOI: 10.4297/najms.2011.3544]

18 **Gartner LM**. Breastfeeding and jaundice. *J Perinatol* 2001; **21** Suppl 1: S25-9; discussion S35 [PMID: 11803412 DOI: 10.1038/sj.jp.7210629]

19 **Bratton S**, Cantu RM, Stern M. Breast Milk Jaundice. 2022 Sep 12. In: StatPearls [Internet]. Treasure Island (FL): StatPearls Publishing; 2022 [PMID: 30726019]

20 **Maruo Y**, Morioka Y, Fujito H, Nakahara S, Yanagi T, Matsui K, Mori A, Sato H, Tukey RH, Takeuchi Y. Bilirubin uridine diphosphate-glucuronosyltransferase variation is a genetic basis of breast milk jaundice. *J Pediatr* 2014; **165**: 36-41.e1 [PMID: 24650397 DOI: 10.1016/j.jpeds.2014.01.060]

21 **Sato H**, Uchida T, Toyota K, Kanno M, Hashimoto T, Watanabe M, Nakamura T, Tamiya G, Aoki K, Hayasaka K. Association of breast-fed neonatal hyperbilirubinemia with UGT1A1 polymorphisms: 211G>A (G71R) mutation becomes a risk factor under inadequate feeding. *J Hum Genet* 2013; **58**: 7-10 [PMID: 23014115 DOI: 10.1038/jhg.2012.116]

22 **Sarici SU**, Saldir M. Genetic factors in neonatal hyperbilirubinemia and kernicterus. *Turk J Pediatr* 2007; **49**: 245-249 [PMID: 17990575]

23 **Yang LY**. Underestimation of the contribution of 211 G to A variation in UGT1A1 to neonatal hyperbilirubinemia in China. *J Pediatr* 2022; **245**: 251 [PMID: 35346717 DOI: 10.1016/j.jpeds.2022.03.034]

24 **Yang H**, Lin F, Chen ZK, Zhang L, Xu JX, Wu YH, Gu JY, Ma YB, Li JD, Yang LY. UGT1A1 mutation association with increased bilirubin levels and severity of unconjugated hyperbilirubinemia in ABO incompatible newborns of China. *BMC Pediatr* 2021; **21**: 259 [PMID: 34074250 DOI: 10.1186/s12887-021-02726-9]

25 **Lin R**, Wang Y, Fu W, Zhang D, Zheng H, Yu T, Shen M, Lei R, Wu H, Sun A, Zhang R, Wang X, Xiong M, Huang W, Jin L. Common variants of four bilirubin metabolism genes and their association with serum bilirubin and coronary artery disease in Chinese Han population. *Pharmacogenet Genomics* 2009; **19**: 310-318 [PMID: 19238116 DOI: 10.1097/FPC.0b013e328328f818]

World Journal of Clinical Cases

Submit a Manuscript: https://www.f6publishing.com

World J Clin Cases 2023 April 16; 11(11): 2452-2456

DOI: 10.12998/wjcc.v11.i11.2452

ISSN 2307-8960 (online)

CASE REPORT

Aicardi-Goutières syndrome type 7 in a Chinese child: A case report

Shuang-Zhu Lin, Jing-Jing Yang, Tian-Long Xie, Jia-Yi Li, Jia-Qi Ma, Si Wu, Na Wang, Yong-Ji Wang

Specialty type: Genetics and heredity

Provenance and peer review: Unsolicited article; Externally peer reviewed.

Peer-review model: Single blind

Peer-review report's scientific quality classification

Grade A (Excellent): 0
Grade B (Very good): 0
Grade C (Good): C
Grade D (Fair): 0
Grade E (Poor): 0

P-Reviewer: Mirsalehi M, Iran

Received: August 13, 2022
Peer-review started: August 13, 2022
First decision: November 11, 2022
Revised: February 22, 2023
Accepted: March 17, 2023
Article in press: March 17, 2023
Published online: April 16, 2023

Shuang-Zhu Lin, Jing-Jing Yang, Tian-Long Xie, Yong-Ji Wang, Diagnosis and Treatment Center for Children, Affiliated Hospital of Changchun University of Chinese Medicine, Changchun 130021, Jilin Province, China

Jia-Yi Li, Jia-Qi Ma, Si Wu, Na Wang, College of Traditional Chinese Medicine, Changchun University of Chinese Medicine, Changchun 130017, Jilin Province, China

Corresponding author: Yong-Ji Wang, MD, Professor, Diagnosis and Treatment Center for Children, Affiliated Hospital of Changchun University of Chinese Medicine, No. 185 Shenzhen Street, Nanguan Economic and Technological Development Zone, Changchun 130021, Jilin Province, China. 18943188651@189.cn

Abstract

BACKGROUND

IFIH1 is a protein-coding gene. Disorders associated with *IFIH1* include Aicardi-Goutières syndrome (AGS) type 7 and Singleton-Merten syndrome type 1. Related pathways include RIG-I/MDA5-mediated induction of the interferon (IFN)-α/β pathway and the innate immune system. AGS type 7 is an autosomal dominant inflammatory disorder characterized by severe neurological impairment. In infancy, most patients present with psychomotor retardation, axial hypotonia, spasticity, and brain imaging changes Laboratory assessments showed increased IFN-α activity with upregulation of IFN signaling and IFN-stimulated gene expression. Some patients develop normally in the early stage, and then have episodic neurological deficits.

CASE SUMMARY

The 5-year-old girl presented with postpartum height and weight growth retardation, language retardation, brain atrophy, convulsions, and growth hormone deficiency. DNA samples were obtained from peripheral blood from the child and her parents for whole-exome sequencing and test of genome-wide copy number variation. Heterozygous mutations in the *IFIH1* gene were found. Physical examination at admission found that language development was delayed, the reaction to name calling was average, there was no communication with people, but there was eye contact, no social smile, and no autonomous language. However, the child had rich gesture language and body language, could understand instructions, had bad temper. When she wants to achieve something, she starts crying or shouting. Cardiopulmonary examination showed no obvious abnormality, and abdominal examination was normal. Bilateral muscle strength and muscle tone were symmetrical and slightly decreased. Physiological reflexes exist, but pathological reflexes were not elicited.

CONCLUSION
We reported the clinical characteristics of a Chinese child with a clinical diagnosis of AGS type 7, which expanded the mutational spectrum of the *IFIH1* gene.

Key Words: Aicardi-Goutières syndrome type 7; *IFIH1* gene; Children; Case report

Core Tip: We report a 5-year-old girl with Aicardi-Goutières syndrome type 7. The clinical characteristics included postnatal height and weight retardation, delayed language development, brain atrophy, convulsions, and growth hormone deficiency. Whole exome test showed c.1093A>G (p.Lys365Glu) and heterozygous mutation in *IFIH1* gene, and the mutation source was her father. This report provides a molecular basis for etiological diagnosis and treatment of the child, as well as for genetic counseling for the pedigree.

Citation: Lin SZ, Yang JJ, Xie TL, Li JY, Ma JQ, Wu S, Wang N, Wang YJ. Aicardi-Goutières syndrome type 7 in a Chinese child: A case report. *World J Clin Cases* 2023; 11(11): 2452-2456
URL: https://www.wjgnet.com/2307-8960/full/v11/i11/2452.htm
DOI: https://dx.doi.org/10.12998/wjcc.v11.i11.2452

INTRODUCTION

Aicardi-Goutières syndrome (AGS) is a rare, genetically determined early-onset progressive encephalopathy[1-4]. Individuals affected with AGS typically suffer from progressive microcephaly associated with severe neurological symptoms, such as hypotonia, dystonia, seizures, spastic quadriplegia[5,6], and severe developmental delay. On brain imaging, AGS is characterized by basal ganglia calcification, white matter abnormalities, and cerebral atrophy cerebrospinal fluid analyses show chronic lymphocytosis and elevated levels of the interferon (IFN)-α[7] and neopterin. AGS-affected individuals are often misdiagnosed as having intrauterine infections, such as Pseudo-TORCH syndrome[8] (Pseudo-TORCH syndrome is a rare, chronic disorder that is characterised by dimorphic features such as microcephaly, intracranial calcification, seizures, mental retardation, hepatosplenomegaly and coagulation disorders), because of the similarities of these disorders, particularly the intracranial calcifications. AGS type 7 (AGS7) is an autosomal dominant inflammatory disorder characterized by severe neurological impairment. Episodic neurological deficits occur after the onset. Therefore, diseases related to mutations at the genetic locus must be diagnosed in the early phase so as to be treated in timely.

CASE PRESENTATION

Chief complaints

She was 3 years old at the time of her first visit and presented on 16 September 2020 due to language delay. She is 5 years old now.

History of present illness

Since age 6 mo, she had had obvious slow growth in height and weight. Language development was delayed. Her response to name calling was normal but there was no communication with people. Her eyes could not be met and there was no social smile. There was no autonomous language, However, the child had rich gesture language and body language, she could understand instructions, had a short temper, and when she wants to achieve something, she starts crying or shouting. She was thin, with a weight of 9 kg and height of 83 cm.

History of past illness

There was no obvious abnormality at birth, weight 3 kg, height 50 cm. She raised her head at 3 mo, crawled at 7 mo, and walked at 15 mo. She had a history of febrile convulsions twice, each lasting about 2 min, which resolved spontaneously, and a 1-year history of ulcerative colitis.

Personal and family history

Both parents were healthy.

Physical examination

Body temperature was 36.2 °C, heart rate 96 beats/min, breathing 24 beats/min, blood pressure 100/60 mmHg, height 83.0 cm and weight 9 kg. There was no special sick face, and cardiopulmonary and abdominal examinations showed no obvious abnormalities. Bilateral muscle strength and muscle tone were symmetrical and slightly decreased. Physiological reflexes were present but pathological reflexes were not elicited.

Laboratory examinations

Routine blood and urine examinations, myocardial enzymes, lactic acid, liver function, renal function, electrolytes, blood glucose, thyroid function, and hematuria showed no obvious abnormalities. The peak growth hormone challenge test was 5.77 ng/mL.

Imaging examinations

Video electroencephalography showed no abnormalities. Magnetic resonance imaging (MRI) of the brain showed mild atrophy.

FINAL DIAGNOSIS

AGS7 caused by a missense mutation in the *IFIH1* gene.

TREATMENT

Symptomatic nutritional support and rehabilitation were undertaken.

OUTCOME AND FOLLOW-UP

The child was followed up for 1 year and 9 mo. Her weight increased to 12 kg and height to 90 cm. Language ability improved, and simple conversations could be conducted.

DISCUSSION

Our patient presented with growth retardation, language retardation, brain atrophy and convulsions as the main clinical manifestations. Among the various examination indicators of our patient, we particularly noticed that the peak value of growth hormone was decreased, and MRI of the brain showed brain atrophy, Combined with the patient's clinical symptoms and physical and chemical examination results, we considered the possibility of hereditary metabolic disease or genetic disease. Subsequent genetic metabolic screening for hematuria showed no obvious abnormality.

Whole exome analysis showed that the *IFIH1* gene had a c.1093A>G (p.Lys365Glu) heterozygous mutation, and the source of the mutation was her father (Figure 1A-C). *IFIH1* gene can cause two diseases, AGS7, and Singleton-Merten syndrome type 1. According to their clinical manifestations, children are more likely to have AGS7[1]. AGS (MIM 615846) is a rare genetic disorder characterized by aberrant type 1 IFN production and systemic, chronic inflammation. *IFIH1* gene[2-4] may lead to changes in MDA5[7] and type 1 IFN (Mutations in the *IFIH1* gene lead to overproduction of type 1 interferons, resulting in the AGS phenotype). AGS 7 may lead to an increase in type 1 IFN, and there are clinical manifestations caused by elevated type 1 IFN. Our patient had similar manifestations, but due to the patient's clinical conditions, we did not examine the IFN concentration.

It has been reported that the *IFIH1* gene is inherited in an autosomal dominant manner, with high heterogeneity and incomplete penetrance. Our patient had c.1093A>G (p.Lys365Glu) heterozygous mutation, and the pathogenicity of this variant has been reported previously. The clinical manifestations of the child were consistent with the clinical features of AGS7.

CONCLUSION

In summary, we reported the clinical characteristics of a Chinese child with a clinical diagnosis of AGS7, which expanded the mutational spectrum of the *IFIH1* gene.

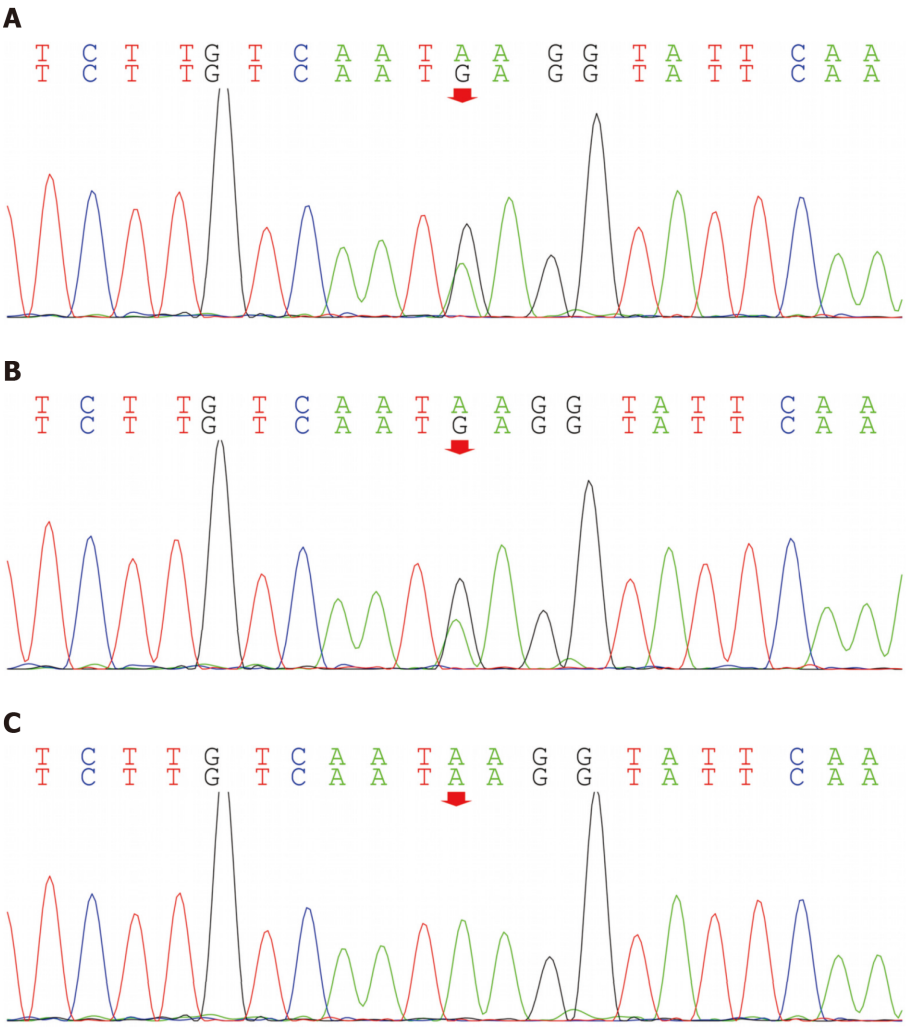

DOI: 10.12998/wjcc.v11.i11.2452

Figure 1 Whole-exome gene sequencing. A: *IFIH1* gene of the patient was found to have c.1093A>G (p.Lys365Glu), and heterozygous mutation. B: The source of mutation was her father. C: The sequencing of the patient's mother.

FOOTNOTES

Author contributions: Lin SZ wrote the manuscript; Yang JJ and Xie TL analyzed the data; Li JY, Ma JQ, Wu S, Wang N contributed to data collation; Wang YJ provided the medical records; all authors approved the final version of the manuscript to be published.

Informed consent statement: Informed consent has been obtained with the support of the child's family.

Conflict-of-interest statement: All the authors report no relevant conflicts of interest for this article.

CARE Checklist (2016) statement: The authors have read the CARE Checklist (2016), and the manuscript was prepared and revised according to the CARE Checklist (2016).

Country/Territory of origin: China

ORCID number: Shuang-Zhu Lin 0000-0001-5333-2138; Jia-Yi Li 0000-0002-7729-4479; Yong-Ji Wang 0000-0001-7222-5645.

S-Editor: Gong ZM
L-Editor: A

P-Editor: Gong ZM

REFERENCES

1 **Oda H**, Nakagawa K, Abe J, Awaya T, Funabiki M, Hijikata A, Nishikomori R, Funatsuka M, Ohshima Y, Sugawara Y, Yasumi T, Kato H, Shirai T, Ohara O, Fujita T, Heike T. Aicardi-Goutières syndrome is caused by IFIH1 mutations. *Am J Hum Genet* 2014; **95**: 121-125 [PMID: 24995871 DOI: 10.1016/j.ajhg.2014.06.007]

2 **Adang LA**, Frank DB, Gilani A, Takanohashi A, Ulrick N, Collins A, Cross Z, Galambos C, Helman G, Kanaan U, Keller S, Simon D, Sherbini O, Hanna BD, Vanderver AL. Aicardi goutières syndrome is associated with pulmonary hypertension. *Mol Genet Metab* 2018; **125**: 351-358 [PMID: 30219631 DOI: 10.1016/j.ymgme.2018.09.004]

3 **Amari S**, Tsukamoto K, Ishiguro A, Yanagi K, Kaname T, Ito Y. An extremely severe case of Aicardi-Goutières syndrome 7 with a novel variant in IFIH1. *Eur J Med Genet* 2020; **63**: 103646 [PMID: 30965144 DOI: 10.1016/j.ejmg.2019.04.003]

4 **Rice GI**, Del Toro Duany Y, Jenkinson EM, Forte GM, Anderson BH, Ariaudo G, Bader-Meunier B, Baildam EM, Battini R, Beresford MW, Casarano M, Chouchane M, Cimaz R, Collins AE, Cordeiro NJ, Dale RC, Davidson JE, De Waele L, Desguerre I, Faivre L, Fazzi E, Isidor B, Lagae L, Latchman AR, Lebon P, Li C, Livingston JH, Lourenço CM, Mancardi MM, Masurel-Paulet A, McInnes IB, Menezes MP, Mignot C, O'Sullivan J, Orcesi S, Picco PP, Riva E, Robinson RA, Rodriguez D, Salvatici E, Scott C, Szybowska M, Tolmie JL, Vanderver A, Vanhulle C, Vieira JP, Webb K, Whitney RN, Williams SG, Wolfe LA, Zuberi SM, Hur S, Crow YJ. Gain-of-function mutations in IFIH1 cause a spectrum of human disease phenotypes associated with upregulated type I interferon signaling. *Nat Genet* 2014; **46**: 503-509 [PMID: 24686847 DOI: 10.1038/ng.2933]

5 **Liu N**, Chen J, Xu C, Shi T, Li J. Hereditary spastic paraplegia associated with a rare IFIH1 mutation: a case report and literature review. *Hereditas* 2019; **156**: 28 [PMID: 31427910 DOI: 10.1186/s41065-019-0104-x]

6 **Crow YJ**, Zaki MS, Abdel-Hamid MS, Abdel-Salam G, Boespflug-Tanguy O, Cordeiro NJ, Gleeson JG, Gowrinathan NR, Laugel V, Renaldo F, Rodriguez D, Livingston JH, Rice GI. Mutations in ADAR1, IFIH1, and RNASEH2B presenting as spastic paraplegia. *Neuropediatrics* 2014; **45**: 386-393 [PMID: 25243380 DOI: 10.1055/s-0034-1389161]

7 **Lamborn IT**, Jing H, Zhang Y, Drutman SB, Abbott JK, Munir S, Bade S, Murdock HM, Santos CP, Brock LG, Masutani E, Fordjour EY, McElwee JJ, Hughes JD, Nichols DP, Belkadi A, Oler AJ, Happel CS, Matthews HF, Abel L, Collins PL, Subbarao K, Gelfand EW, Ciancanelli MJ, Casanova JL, Su HC. Recurrent rhinovirus infections in a child with inherited MDA5 deficiency. *J Exp Med* 2017; **214**: 1949-1972 [PMID: 28606988 DOI: 10.1084/jem.20161759]

8 **Meuwissen ME**, Schot R, Buta S, Oudesluijs G, Tinschert S, Speer SD, Li Z, van Unen L, Heijsman D, Goldmann T, Lequin MH, Kros JM, Stam W, Hermann M, Willemsen R, Brouwer RW, Van IJcken WF, Martin-Fernandez M, de Coo I, Dudink J, de Vries FA, Bertoli Avella A, Prinz M, Crow YJ, Verheijen FW, Pellegrini S, Bogunovic D, Mancini GM. Human USP18 deficiency underlies type 1 interferonopathy leading to severe pseudo-TORCH syndrome. *J Exp Med* 2016; **213**: 1163-1174 [PMID: 27325888 DOI: 10.1084/jem.20151529]

World Journal of Clinical Cases

Submit a Manuscript: https://www.f6publishing.com

World J Clin Cases 2023 April 16; 11(11): 2457-2463

DOI: 10.12998/wjcc.v11.i11.2457

ISSN 2307-8960 (online)

CASE REPORT

Allergic bronchopulmonary aspergillosis with marked peripheral blood eosinophilia and pulmonary eosinophilia: A case report

Xiao-Xi Zhang, Rong Zhou, Chang Liu, Jing Yang, Zi-Han Pan, Cen-Cen Wu, Qiu-Yu Li

Specialty type: Medicine, general and internal

Provenance and peer review: Unsolicited article; Externally peer reviewed.

Peer-review model: Single blind

Peer-review report's scientific quality classification

Grade A (Excellent): 0
Grade B (Very good): 0
Grade C (Good): C
Grade D (Fair): D
Grade E (Poor): 0

P-Reviewer: Routray C, United States; Velázquez-Soto H, Mexico

Received: September 20, 2022
Peer-review started: September 20, 2022
First decision: November 11, 2022
Revised: December 4, 2022
Accepted: March 20, 2023
Article in press: March 20, 2023
Published online: April 16, 2023

Xiao-Xi Zhang, Chang Liu, Department of Emergency Medicine, Beijing Friendship Hospital Affiliated to Capital Medical University, Beijing 100050, China

Rong Zhou, Department of Sleep Medicine, Peking University Sixth Hospital, Beijing 100191, China

Jing Yang, Department of Pathology, Peking University Third Hospital, Beijing 100191, China

Zi-Han Pan, Cen-Cen Wu, Qiu-Yu Li, Department of Respiratory and Critical Care Medicine, Peking University Third Hospital, Beijing 100191, China

Corresponding author: Qiu-Yu Li, MD, Chief Doctor, Department of Respiratory and Critical Care Medicine, Peking University Third Hospital, No. 49 North Garden Rd, Haidian District, Beijing 100191, China. liqiuyu00@bjmu.edu.cn

Abstract

BACKGROUND

Allergic bronchopulmonary aspergillosis (ABPA) is an immune-related pulmonary disease caused by sensitization of airway by *Aspergillus fumigatus*. The disease manifests as bronchial asthma and recurring pulmonary shadows, which may be associated with bronchiectasis. The diagnosis of ABPA mainly depends on serological, immunological, and imaging findings. Pathological examination is not necessary but may be required in atypical cases to exclude pulmonary tuberculosis, tumor, and other diseases through lung biopsy.

CASE SUMMARY

An 18-year-old man presented with recurrent wheezing, cough, and peripheral blood eosinophilia. Chest computed tomography showed pulmonary infiltration. There was a significant increase in eosinophils in bronchoalveolar lavage fluid. There was no history of residing in a parasite-endemic area or any evidence of parasitic infection. Pathologic examination of bronchoalveolar lavage fluid excluded fungal and mycobacterial infections. The patient was receiving medication for comorbid diseases, but there was no temporal correlation between medication use and clinical manifestations, which excluded drug-induced etiology. Histopathological examination of lung biopsy specimen showed no signs of eosinophilic granulomatosis with polyangiitis, IgG4-related diseases, or tumors. The diagnosis of ABPA was considered based on the history of asthma and the significant increase in serum *Aspergillus fumigatus*-specific immunoglobulin (Ig)E. Eosinophil-related diseases were excluded through pathological

biopsy, which showed typical pathological manifestations of ABPA.

CONCLUSION
The possibility of ABPA should be considered in patients with poorly controlled asthma, especially those with eosinophilia, lung infiltration shadows, or bronchiectasis. Screening for serum IgE, *Aspergillus fumigatus*-specific IgE and IgG, and alveolar lavage can help avoid misdiagnosis.

Key Words: Allergic bronchopulmonary aspergillosis; Asthma; Aspergillus; Case report

Core Tip: Clinically, allergic bronchopulmonary aspergillosis should be considered for patients with poorly controlled asthma, especially those with elevated eosinophils, pulmonary infiltrates, or bronchiectasis. Serum total immunoglobulin (Ig)E (IgE), *Aspergillus fumigatus*-specific antibody IgE and IgG detection can help confirm the diagnosis.

Citation: Zhang XX, Zhou R, Liu C, Yang J, Pan ZH, Wu CC, Li QY. Allergic bronchopulmonary aspergillosis with marked peripheral blood eosinophilia and pulmonary eosinophilia: A case report. *World J Clin Cases* 2023; 11(11): 2457-2463
URL: https://www.wjgnet.com/2307-8960/full/v11/i11/2457.htm
DOI: https://dx.doi.org/10.12998/wjcc.v11.i11.2457

INTRODUCTION

Allergic bronchopulmonary aspergillosis (ABPA) is an immune-related pulmonary disease caused by airway sensitization by *Aspergillus fumigatus*, manifesting as bronchial asthma and recurring pulmonary shadows which may be associated with bronchiectasis. The disease is relatively rare and is often misdiagnosed or missed clinically. Early diagnosis and timely treatment with systemic glucocorticoids can control the disease and prevent irreversible lung damage. The estimated prevalence of ABPA in asthma patients worldwide is approximately 2.5%[1]. In the general population, secretory immunoglobulin (Ig)E in the bronchi or IgG in serum normally clears the inhaled Aspergillus spores; however, in patients with asthma or cystic fibrosis, the inhaled Aspergillus spores can colonize the airways, inducing immunity in the bronchi and lung interstitium. Inflammatory reactions, mainly type I and type III hypersensitivity reactions, promote the production of IgE, IgG, and IgA. This inflammatory response is mainly triggered due to the activation of eosinophils mediated by T helper 2 (Th2) cells[2]. The activation of this inflammatory response is mainly due to the activation of eosinophils mediated by Th2 cells[3]. The typical manifestations of ABPA are poorly controlled asthma or repeated pulmonary infiltrates with or without bronchiectasis. Up to one-third of all cases in developing countries are misdiagnosed as pulmonary tuberculosis[3]. In this article, we report a case of ABPA and review the clinical features of ABPA including clinical manifestations and serological, imaging, and pathological findings, which may help improve the diagnosis and treatment of this disease.

CASE PRESENTATION

Chief complaints

An 18-year-old man was admitted to the hospital on February 5, 2021 with a history of intermittent wheezing for the last 15 years, which was aggravated for the last 9 d.

History of present illness

Fifteen years ago, the patient was diagnosed with bronchial asthma. He regularly received salmeterol and ficasone inhalation (50 μg/100 μg or 50 μg/2500 μg, 1 inhalation bid), but acute exacerbations usually occurred 1-2 times every year, typically between the months of October and December. Nine days before admission, the patient developed wheeze but had no fever. His white blood cell count was 10.56×10^9/L, neutrophil percentage was 45.3%, and eosinophil percentage was 17.6%. He was treated with an antibiotic (moxifloxacin) for 3 d, but there was no significant improvement in symptoms. Two days before admission, he had cough with a small amount of white colored sputum. Chest computed tomography (CT) showed consolidation in the anterior basal segment of the right lower lobe, and there

were multiple small nodules with fuzzy margins around the periphery, some of which had merged into small patches of consolidation (Figure 1). Therefore, he was hospitalized for further evaluation and treatment.

History of past illness

The patient's past history included congenital hip dislocation since childhood and developmental deformity of the lower extremities, due to which he was relying on a wheelchair for mobility. The patient was diagnosed with neurogenic bladder 6 years ago due to dysuria and obstructive renal insufficiency due to urinary retention. Cystostomy was performed 5 years ago. Hypertension was diagnosed 5 years ago (systolic blood pressure up to 160 mmHg). His blood pressure was controlled below 130/90 mmHg after treatment with oral fosinopril (10 mg, qd). Scoliosis deformity was discovered 4 years ago. He was also prescribed oral sertraline 50 mg once a night for treatment of depression 4 years ago. Two years ago, he was prescribed oral omeprazole for treatment of reflux esophagitis.

Personal and family history

There was a positive family history of bronchial asthma (the patient's mother and grandmother were both affected).

Physical examination

Physical examination on admission revealed the following: Body temperature, 36.7 °C; pulse, 104 beats/min; respiratory rate, 18 beats/min; blood pressure 131/87 mmHg (1 mmHg = 0.133 kPa). The patient was conscious and had no signs of cyanosis. No dry or wet rales were heard in either lung. Cardiovascular and abdominal examinations were unremarkable.

Laboratory examinations

Laboratory tests after admission revealed the following: White blood cell count, 11.75 × 10^9/L; hemoglobin 159 g/L; platelet count, 201 × 10^9/L; neutrophil percentage 41.7% (absolute value 4.9 × 10^9/L); eosinophil percentage 24% 6% (absolute value 2.89 × 10^9/L); serum procalcitonin 0.056 ng/mL; C-reactive protein 1.43 mg/dL; T-SPOT, G test, GM test, *Mycoplasma pneumoniae* antibody, and *Chlamydia pneumoniae* antibody were all negative; antineutrophil cytoplasmic antibodies and antinuclear antibody profiles were also negative; allergen total IgE > 5000 KU/L; *Aspergillus fumigatus* (m^3) 66.4 (grade 5) KU/L; Aspergillus antibody IgG 276.2 AU/mL (reference value < 80) (Table 1).

Imaging examinations

To further clarify the nature of the lung lesions, bronchoalveolar lavage fluid was examined. On cell count in the bronchoalveolar lavage fluid (Table 1), the proportion of eosinophils was 35%. Further ultrasound-guided percutaneous lung biopsy was performed; histopathological findings (Figure 2) were presence of alveolar structures, mild widening of alveolar septa, and infiltration of a large number of eosinophils and a small amount of scattered lymphoplasmacytic cells in the alveolar septum; interstitium. small amount of eosinophilic exudation was seen in some alveolar spaces, with no signs of necrosis, typical granulomas, or vasculitis. Based on the history of asthma, peripheral blood eosinophilia, significantly increased serum allergen total IgE, and positive *Aspergillus fumigatus*-specific IgE and IgG, a diagnosis of ABPA was established. After 1 mo of prednisone treatment, a routine blood test showed that the white blood cell count was 9.13 × 10^9/L, and the eosinophil percentage was 0.4% (absolute value 0.04 × 10^9/L). Chest CT (Figure 3) showed resorption of shadow in the right lower lobe; only fibrous cords were seen.

FINAL DIAGNOSIS

Based on the history of asthma, peripheral blood eosinophilia, significantly increased serum allergen total IgE, and positive *Aspergillus fumigatus*-specific IgE and IgG, a diagnosis of ABPA was established.

TREATMENT

The patient was prescribed prednisone 20 mg qd orally for 2 mo, which was gradually tapered to 10 mg qd for 6 mo. In addition, he was prescribed antifungal treatment with itraconazole 0.2 g bid for 6 mo to reduce fungal colonization in the airway and the persistent inflammatory reaction caused by fungal antigen stimulation.

Table 1 Laboratory indices

	Test results	Reference range
Peripheral blood eosinophil percentage	28.7%	(0.4-8)%
Absolute value	2.56 ×10^9/L	(0.02-0.52) × 10^9/L
Serum allergen total IgE	> 5000 KU/L	0-60
Serum *Aspergillus fumigatus* (m3) specific IgE	66.4 (5 grade) KU/L	0-0.35
Serum *Aspergillus fumigatus* specific IgG	276.2 AU/mL	< 80
Bronchoalveolar lavage fluid total cells	5.8 × 10^5/mL	
Macrophages	40%	> 85%
Neutrophils	2%	≤ 3%
Lymphocytes	23%	(10-15)%
Eosinophils	35%	≤ 1%

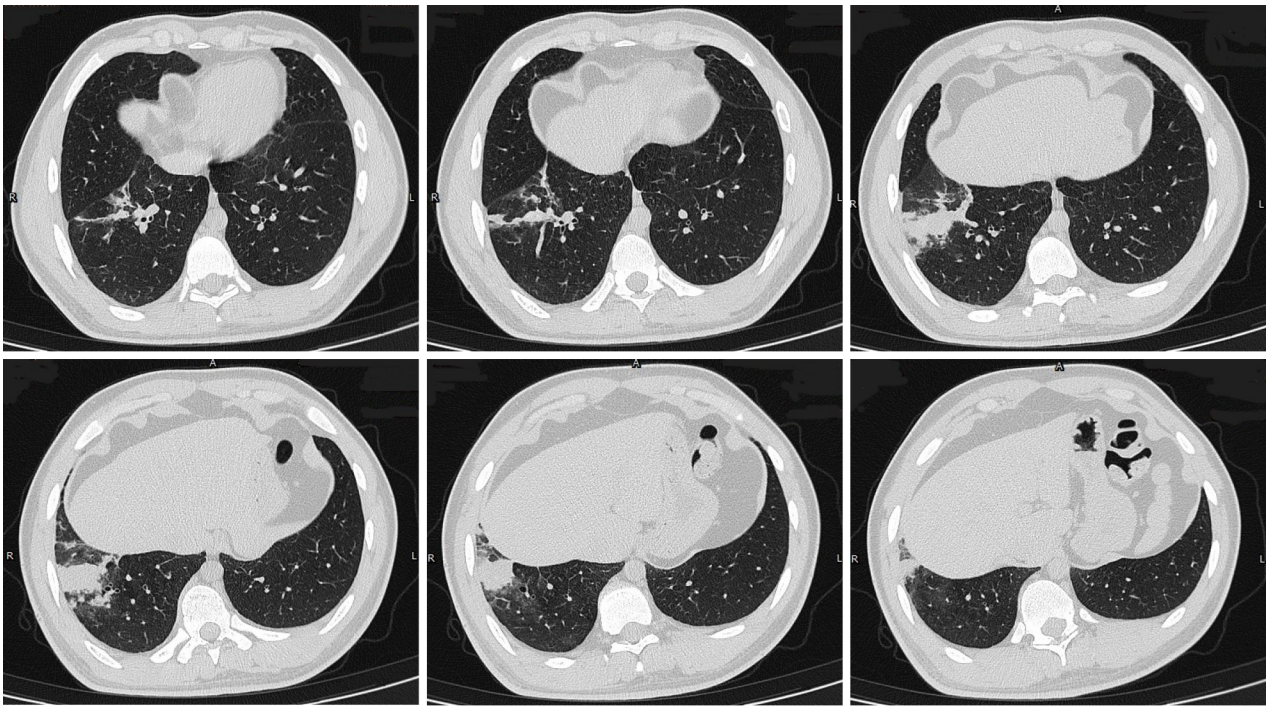

DOI: 10.12998/wjcc.v11.i11.2457

Figure 1 Chest computed tomography images (February 3, 2021) showing consolidation in the anterior basal segment of the right lower lobe, with multiple small nodules surrounded by blurred margins, some of which merged into small patchy consolidations.

OUTCOME AND FOLLOW-UP

After 1 mo of prednisone treatment, the patient's white blood cell count was 9.13 × 10^9/L, and the eosinophil percentage was 0.4% (absolute value 0.04 × 10^9/L). Chest CT (Figure 2) showed resorption of shadow in the right lower lobe; only fibrous cords were seen and the adjacent bronchi were stretched and dilated.

DISCUSSION

The main manifestations of this patient were recurrent wheezing and cough, eosinophilia, pulmonary infiltration shadow, and significantly increased eosinophils in bronchoalveolar lavage fluid. We considered increased eosinophils in bronchoalveolar lavage fluid as the breakthrough point and made differential diagnoses according to pulmonary eosinophilia.

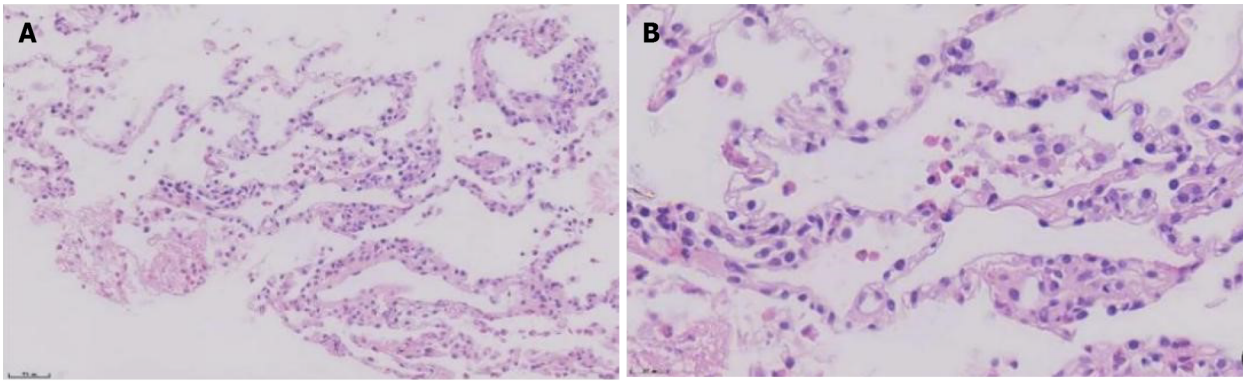

DOI: 10.12998/wjcc.v11.i11.2457

Figure 2 Hematoxylin-eosin-stained sections of lung tissue. A: Magnification × 20; B: Magnification × 40. The alveolar structure can be identified, the alveolar septum is slightly widened, and there are many eosinophils and a small amount of scattered lymphoplasmacytic infiltration in the alveolar septum and interstitium. A small amount of eosinophilic exudation can be seen in some alveolar spaces with no signs of necrosis. No typical granulomas or vasculitis is observed.

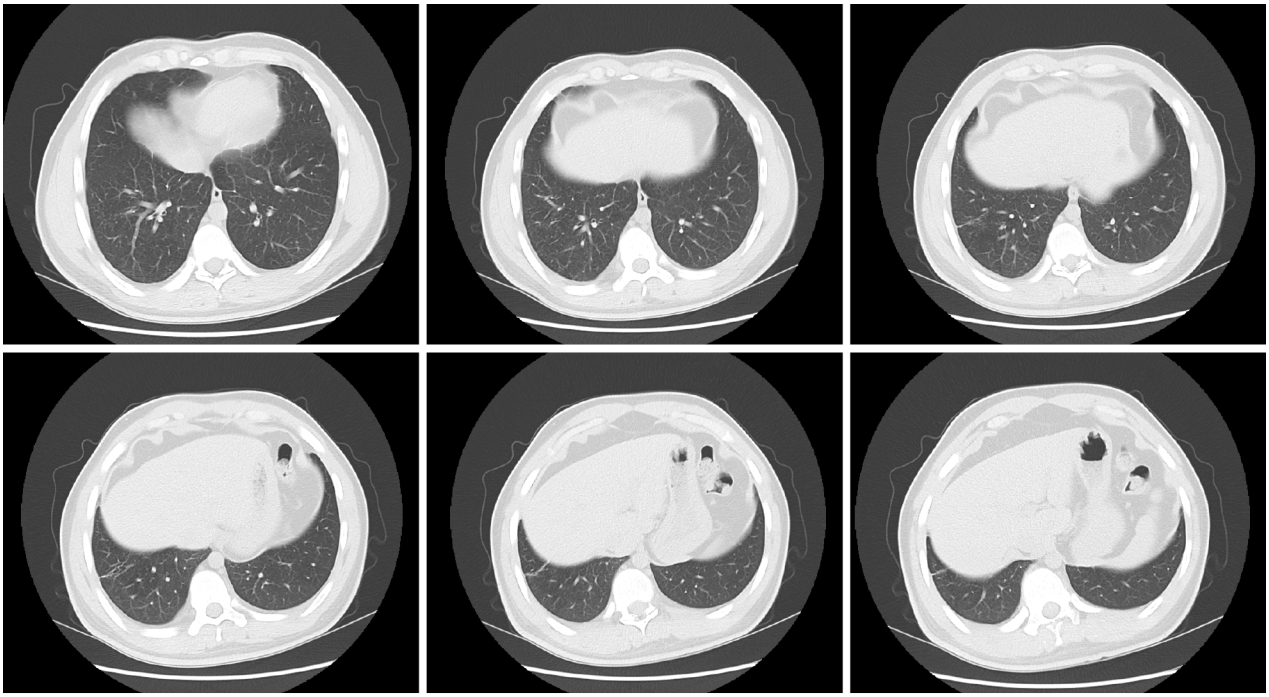

DOI: 10.12998/wjcc.v11.i11.2457

Figure 3 Repeat chest computed tomography performed after 4 wk of glucocorticoid treatment showing resorption of the shadow in the right lower lobe; only a fibrous cord shadow is seen, and the adjacent bronchus is stretched and dilated.

The term pulmonary eosinophilia refers to a group of heterogeneous diseases with common characteristics of abnormal increase in eosinophils in the lung airway and lung parenchyma. The characteristics include: (1) Peripheral blood eosinophilia (absolute eosinophil count ≥ 500/μL) with abnormal pulmonary imaging examination; (2) increased eosinophils in the bronchoalveolar lavage fluid (> 10%); and (3) presence of eosinophils in lung tissue confirmed by bronchopulmonary biopsy or open chest lung biopsy[1]. Pulmonary eosinophilia is classified into secondary and idiopathic. Secondary causes include infectious diseases (including parasitic, fungal, and mycobacterial infections), allergic diseases (related to ABPA, drugs, or toxicants), connective tissue disorders (eosinophilic granulomatosis with polyangiitis, IgG4-related diseases, *etc.*), malignancies (lymphoma, leukemia, solid tumors, *etc.*), and other diseases (bronchial central granulomatosis, interstitial lung disease, lung transplantation, hematopoietic stem cell transplantation, secondary to radiotherapy, *etc.*). Idiopathic pulmonary eosinophilia includes acute eosinophilic pneumonia (AEP), chronic eosinophilic pneumonia (CEP), and idiopathic hypereosinophilic syndrome (IHES).

Our patient had no history of residing in a parasite endemic area or consumption of raw meat, fish, shrimp, or crab, and there was no evidence of parasitic infection. Pathologic examination of bronchoalveolar lavage fluid excluded fungal and mycobacterial infections. The patient was receiving medication

for hypertension, hyperuricemia, depression, and gastroesophageal reflux disease; however, there was no temporal correlation between the medication and the patient's symptoms, eosinophilia, or pulmonary imaging changes. Therefore, any drug-induced etiology was not considered. Pathological examination of lung tissue revealed no signs of eosinophilic granulomatosis with polyangiitis, IgG4-related diseases, or tumors. The diagnosis of ABPA was considered based on the combination of history of asthma and significant increase of serum *Aspergillus fumigatus* IgE.

Elevated serum IgE was another feature of this patient. Serum IgE level can be elevated in many conditions, such as infectious diseases, atopic diseases, immunodeficiencies, inflammatory diseases, neoplasms, and drug-induced conditions; however, significantly elevated serum IgE (> 2000 KU/L or even 5000 KU/L) is seen in ABPA, IgE type multiple myeloma, and hyperimmunoglobulin E syndrome (HIES). IgE type multiple myeloma is extremely rare. Similar to other types of multiple myeloma, the clinical manifestations of IgE type multiple myeloma are anemia, renal dysfunction, hypercalcemia, and bone damage. Bone damage in patients with IgE type multiple myeloma manifests as osteoporosis, osteolytic damage, osteosclerosis, and pathological fracture[4], while osteolytic damage is more common in other types of multiple myeloma. HIES is a rare, primary immunodeficiency distinguished by the clinical triad of atopic dermatitis, recurrent staphylococcal skin infections, and recurrent pulmonary infections. Patients with HIES have characteristic facial features (facial asymmetry, prominent forehead, deep-set eyes, broad nasal bridge, and wide fleshy nasal tip) that appear in early adolescence or late childhood[5]. Our patient had no such symptoms, due to which IgE type multiple myeloma and HIES were excluded.

The diagnosis of ABPA is primarily based on serological, immunological, and imaging findings. Pathological examination is not necessary for diagnosis but may be required in atypical cases to exclude pulmonary tuberculosis, tumor, or other diseases through lung biopsy.

The main therapeutic goal in ABPA is to control asthma, reduce acute exacerbations, and prevent irreversible lung damage such as bronchiectasis and pulmonary fibrosis. The main therapeutic methods include systemic glucocorticoid therapy to suppress immune response, and use of antifungal drugs to reduce the colonization of respiratory tract[3]. At present, there is no clear consensus on the use of antifungal drugs in patients with ABPA, and these are recommended for patients with hormone dependence and relapse after discontinuation of hormone therapy. In addition, studies have also shown that omazumab (a humanized anti IgE monoclonal antibody) can reduce the serum IgE level of patients, the risk of acute exacerbation, and hormone dosage[6]. In terms of treatment follow-up, serum IgE is an important follow-up parameter apart from clinical symptoms and pulmonary imaging. The decrease in serum IgE indicates the effectiveness of treatment. Reducing the IgE to the normal range is often challenging in ABPA patients. Therefore, the goal of treatment is to reduce the IgE level by 35%-50%. In most cases, clinical and imaging improvements will be achieved. There are many published case reports of ABPA. However, there is a paucity of ABPA case reports describing the histopathological findings of lung biopsy. Thus, the present study presents the typical pathological manifestations of ABPA to readers.

CONCLUSION

In clinical practice, for patients with poorly controlled asthma, especially those with elevated eosinophils, lung infiltration shadows, or bronchiectasis, the possibility of ABPA should be considered. Screening of serum IgE, *Aspergillus fumigatus*-specific IgE and IgG, and alveolar lavage should be performed to avoid missed diagnosis and misdiagnosis. Serum total IgE and *Aspergillus fumigatus*-specific IgE and IgG detection can help confirm the diagnosis.

ACKNOWLEDGEMENTS

We thank Sun Yongchang, Zhu Hong and Wang Jianli (Department of Respiratory and Critical Medicine, Peking University Third Hospital), for their guidance on this article.

FOOTNOTES

Author contributions: Zhang XX was responsible for collecting the original data and writing the manuscript; Liu C was responsible for collecting the imaging data; Zhou R and Wu CC were responsible for writing the discussion; Pan ZH and Rong Z were responsible for modifying the format; Yang J was responsible for collecting the pathological pictures; Li QY was responsible for comprehensively designing the case report framework and modifying the logic and language; all authors have read and approved the final manuscript; Li QY and Wu CC, as co correspondents, are responsible for this manuscript.

Supported by the National Natural Science Foundation of China, No. 81900641; the Research Funding of Peking

University, No. BMU2021MX020, No. BMU2022MX008.

Informed consent statement: Informed written consent was obtained from the patient for publication of this report and any accompanying images.

Conflict-of-interest statement: The authors declare that they have no conflict of interest to report.

CARE Checklist (2016) statement: The authors have read the CARE Checklist (2016), and the manuscript was prepared and revised according to the CARE Checklist (2016).

Country/Territory of origin: China

ORCID number: Rong Zhou 0000-0003-3961-5312; Zi-Han Pan 0000-0003-4502-1107; Qiu-Yu Li 0000-0002-8707-5229.

S-Editor: Chang KL
L-Editor: Wang TQ
P-Editor: Chang KL

REFERENCES

1 **Denning DW**, Pleuvry A, Cole DC. Global burden of allergic bronchopulmonary aspergillosis with asthma and its complication chronic pulmonary aspergillosis in adults. *Med Mycol* 2013; **51**: 361-370 [PMID: 23210682 DOI: 10.3109/13693786.2012.738312]
2 **Davidsen JR**, Madsen PH, Laursen CB. Uncontrolled asthma and recurring pulmonary opacities: just asthma? *Case Reports* 2014; bcr2013202428-bcr2013202428 [DOI: 10.1136/bcr-2013-202428]
3 **Agarwal R**, Chakrabarti A, Shah A, Gupta D, Meis JF, Guleria R, Moss R, Denning DW; ABPA complicating asthma ISHAM working group. Allergic bronchopulmonary aspergillosis: review of literature and proposal of new diagnostic and classification criteria. *Clin Exp Allergy* 2013; **43**: 850-873 [PMID: 23889240 DOI: 10.1111/cea.12141]
4 **Wu XB**, Zhou Y, Bao F, Wang X, Yu Y, Chen JX, Li j. IgE multiple myeloma, one case report. *Zhonghua Neike Zazhi* 2020; 59 [DOI: 10.3760/cma.j.cn112138-20200218-00092]
5 **Hashemi H**, Mohebbi M, Mehravaran S, Mazloumi M, Jahanbani-Ardakani H, Abtahi SH. Hyperimmunoglobulin E syndrome: Genetics, immunopathogenesis, clinical findings, and treatment modalities. *J Res Med Sci* 2017; **22**: 53 [PMID: 28567072 DOI: 10.4103/jrms.JRMS_1050_16]
6 **Li JX**, Fan LC, Li MH, Cao WJ, Xu JF. Beneficial effects of Omalizumab therapy in allergic bronchopulmonary aspergillosis: A synthesis review of published literature. *Respir Med* 2017; **122**: 33-42 [PMID: 27993289 DOI: 10.1016/j.rmed.2016.11.019]

World Journal of Clinical Cases

Submit a Manuscript: https://www.f6publishing.com

World J Clin Cases 2023 April 16; 11(11): 2464-2473

DOI: 10.12998/wjcc.v11.i11.2464

ISSN 2307-8960 (online)

CASE REPORT

Late presentation of dural tears: Two case reports and review of literature

Chang Xu, Rong-Peng Dong, Xue-Liang Cheng, Jian-Wu Zhao

Specialty type: Medicine, research and experimental

Provenance and peer review: Unsolicited article; Externally peer reviewed.

Peer-review model: Single blind

Peer-review report's scientific quality classification

Grade A (Excellent): 0
Grade B (Very good): B, B
Grade C (Good): 0
Grade D (Fair): 0
Grade E (Poor): 0

P-Reviewer: Nambi G, Saudi Arabia; Zharikov YO, Russia

Received: January 11, 2023
Peer-review started: January 11, 2023
First decision: February 17, 2023
Revised: February 23, 2023
Accepted: March 21, 2023
Article in press: March 21, 2023
Published online: April 16, 2023

Chang Xu, Department of Orthopedics, Jilin Provincial Armed Police Corps Hospital, Changchun 130000, Jilin Province, China

Rong-Peng Dong, Xue-Liang Cheng, Jian-Wu Zhao, Department of Spinal Surgery, The Second Hospital of Jilin University, Changchun 130012, Jilin Province, China

Corresponding author: Jian-Wu Zhao, MD, PhD, Chief Doctor, Professor, Department of Spinal Surgery, The Second Hospital of Jilin University, No. 218 Ziqiang Street, Changchun 130012, Jilin Province, China. jianwu@jlu.edu.cn

Abstract

BACKGROUND

The late presentation of dural tears (LPDT) has a low incidence rate and hidden symptoms and is easily ignored in clinical practice. If the disease is not treated in time, a series of complications may occur, including low intracranial pressure headache, infection, pseudodural cyst formation, and sinus formation. Here, we describe two cases of LPDT.

CASE SUMMARY

Two patients had sudden fever 1 wk after lumbar surgery. Physical examination showed obvious tenderness in the operation area. The patients were confirmed as having LPDT by lumbar magnetic resonance imaging and surgical exploration. One case was caused by continuous negative pressure suction and malnutrition, and the other was caused by decreased dural ductility and low postoperative nutritional status. The first symptom of both patients was fever, with occasional headache. Both patients underwent secondary surgery to treat the LPDT. Dural defects were observed and dural sealants were used to seal the dural defects, then drainage tubes were retained for drainage. After the operation, the patients were treated with antibiotics and the patients' surgical incisions healed well, without fever or incision tenderness. Both recovered and were discharged 1 wk after the operation.

CONCLUSION

LPDT is a rare complication of spinal surgery or neurosurgery that has hidden symptoms and can easily be overlooked. Since it may cause a series of complications, LPDT needs to be actively addressed in clinical practice.

Key Words: Late presentation of dural tears; Delayed cerebrospinal fluid leakage; Dural

repair; Factors; Clinical management; Case report

Core Tip: Late presentation of dural tears (LPDT) has a low incidence rate and hidden symptoms and is easily overlooked in clinical practice. We describe two cases of LPDT in this paper, and summarize the diagnosis, etiologies and treatment strategies of LPDT through a literature review.

Citation: Xu C, Dong RP, Cheng XL, Zhao JW. Late presentation of dural tears: Two case reports and review of literature. *World J Clin Cases* 2023; 11(11): 2464-2473
URL: https://www.wjgnet.com/2307-8960/full/v11/i11/2464.htm
DOI: https://dx.doi.org/10.12998/wjcc.v11.i11.2464

INTRODUCTION

Dural tears (DT) in the spinal canal often occur before or during surgery, such as spinal trauma, lumbar puncture, removal of intradural tumors, and complications of spinal surgery. According to literature reports, the incidence of DT due to spinal surgery is 1%–17%[1], which is relatively common, especially in patients with ligament ossification, with an incidence as high as 32%. Postoperative cerebrospinal fluid (CSF) leakage is rare, with an incidence of less than 1%[2,3], including unrecognized DT during surgery and late presentation of DT (LPDT). Here, we report two cases of LPDT and provide a comprehensive literature review.

CASE PRESENTATION

Chief complaints

Case 1: A 67-year-old woman complained of headache after continuous vacuum sealing drainage (VSD) for 1 wk.

Case 2: A 61-year-old man complained of headache and fever with a temperature of 38.6 °C 1 wk after lumbar operation.

History of present illness

Case 1: A 67-year-old woman presented to our department with a main complaint of lower back pain and pain in both lower extremities for 2 years. Physical examination showed a body mass index of 21.1 kg/m^2, and a positive (40°) bilateral straight leg elevation test. Lumbar magnetic resonance imaging (MRI) was performed. As the diagnosis was confirmed, posterior lumbar laminectomy, discectomy, bone graft fusion, and internal fixation were performed. After sufficient hemostasis was achieved, unilateral drainage was retained, and the incision was sutured. The patient was administered anti-inflammatory, rehydration, and anti-infection treatments after the operation. The drainage volume gradually decreased three days after the operation. When the drainage volume was less than 50 mL, the drainage was removed. One week later, the patient had chills and high fever. Considering that infection may have occurred in the operation site, debridement, and continuous VSD were performed. Necrotic tissue was found in the muscle layer and the dura was intact. After the operation, the incision was given continuous saline irrigation and negative pressure suction. After continuous VSD for another week, the patient complained of headache, and the integrity of the VSD was damaged.

Case 2: A 61-year-old man was admitted to the hospital with complaints of lower back pain for more than 15 years, numbness of the right lower extremity for 1 year, and aggravation for 10 d. The patient underwent posterior lumbar laminectomy and interbody fusion surgery after diagnosis. After the operation, neurological symptoms and pain improved markedly. On postoperative day 10, the patient complained of headache and fever with a temperature of 38.6 °C.

Personal and family history

Case 1: The patient had a medical history of hypertension, rheumatoid arthritis, hepatitis B, and tuberculosis.

Case 2: The patient denied having a history of hypertension, diabetes, or any other comorbidity.

Physical examination

Case 1: Tenderness was noted over the incision and dark-red blood flowed out after local compression on the incision.

Case 2: Tenderness was noted over the incision.

Laboratory examinations

Case 1: Routine blood tests showed the percentage of neutrophils was significantly increased. Increased C-reactive protein levels suggested the possibility of inflammation in the body. Decreased albumin content indicated that the patient was in a state of low nutrition (Figure 1).

Case 2: Evolution of the patient's nutritional status after hospitalization is presented in Figure 2, which shows that the patient was in a low nutritional state after posterior lumbar interbody fusion surgery.

Imaging examinations

Case 1: As shown in Figure 3, lumbar MRI before the surgery revealed lumbar disc herniation and lumbar spinal stenosis at the L3–S1 level. The MRI after the surgery showed no obvious CSF leakage.

Case 2: Lumbar MRI showed massive long T1 and T2 signals in the soft tissue behind the level of the L3–S1 vertebral body (Figure 4).

FINAL DIAGNOSIS

Both patients were diagnosed with LPDT.

Case 1: In this case, DT was believed to be caused by continuous VSD. The reasons are as follows: The dura mater (dura) was intact after the first debridement, but CSF leakage was found during the second debridement. No sharp protrusions or bone fragments were observed after lamina decompression. The factors of LPDT caused by VSD in this patient were as follows: (1) The patient's low nutritional status, coupled with a history of hepatitis B and tuberculosis, was not conducive to tissue repair; and (2) The fascia layer of the incision was infected, the tissue mass was reduced after debridement, and cavities were easily formed, which reduced tissue and muscle function by isolating and sealing the dura.

Case 2: In this case, the patient had a history of lumbar disease for > 15 years. The protruding disc had been pressing the dural sac posteriorly for a long time, resulting in erosion and adhesion of the dura to the posterior ligament tissue. Postoperatively, the patient presented with malnutrition, which slowed the healing of the soft tissue at the incision site. The tissue behind the dura cannot form an effective protective barrier, which reduces the pressure of the dura against the CSF, resulting in a delayed dural tear.

TREATMENT

Case 1: The third operation was performed to remove the VSD device and explore the operation area of the spine. After the incision was rinsed with saline during the operation, a small amount of clear liquid flowed out of the dural surface. The dura was explored, and no sharp bone fragments or spurs were found. After the fibrin glue was used for sealing the dural defect, the wound was sutured after inserting the indwelling drainage tube. The drainage fluid and the changes of the drainage volume are shown in Figure 5, and the drainage tube was removed 1 wk after the third surgery.

Case 2: Emergency surgical debridement and exploration were performed. After opening the surgical incision, a large amount of clear liquid mixed with blood accumulated in the subcutaneous space. After aspirating the accumulated liquid, damage to the surface of the dorsal dura was observed (Figure 6). We used sutures and dural sealants to treat the dural defects.

OUTCOME AND FOLLOW-UP

The incisions recovered well postoperatively, and the patients were discharged from the hospital. There were no related complications after discharge.

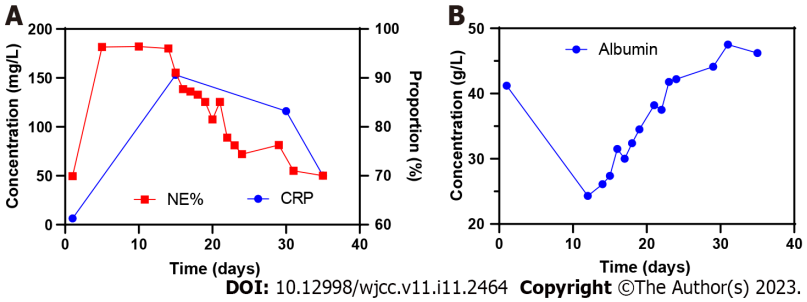

DOI: 10.12998/wjcc.v11.i11.2464

Figure 1 Changes in C-reactive protein level, neutrophils percentage, and albumin level during hospitalization of the first patient. A: Changes in C-reactive protein level, neutrophils percentage; B: Changes in albumin level. CRP: C-reactive protein; NE%: Neutrophils percentage.

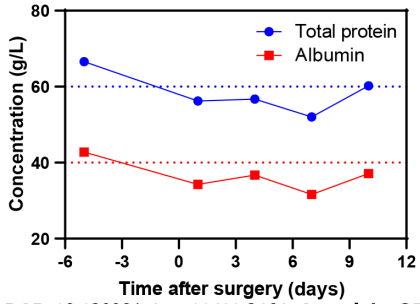

DOI: 10.12998/wjcc.v11.i11.2464

Figure 2 Nutritional status of the second patient during hospitalization.

DISCUSSION

Diagnosis

LPDT can easily be ignored because of its late onset and hidden clinical symptoms. In clinical practice, it is often not detected until pseudocysts and sinuses are formed. The complications of LPDT include delayed wound healing, wound infection, soft tissue swelling in the operative area, persistent positional headache, dural cyst formation, prolonged hospital stay, adhesive arachnoiditis, and secondary surgery. LPDT may also cause pneumonia, urinary tract infections, thrombosis, acute kidney injury, pneumocephalus, and pneumorachis[3-5]. The key elements for LPDT diagnosis are presented in Table 1[4,6-10]. Based on our clinical experience, positional headache is an early symptom of LPDT, and should be treated with caution in clinical practice.

LPDT factors

According to the mechanism of dural damage, LPDT factors can be divided into three categories: Mechanical penetration, decreased dural resistance to CSF pressure, and increased CSF pressure.

Mechanical penetration: For an unidentified DT occurring during the operation, the injury is usually caused by accidental puncture of the dura when using a syringe needle or suture needle. Sharp bone fragments or bone spurs penetrating the dura are common causes of postoperative LPDT[3,4], and accounts for about 40% of all cases[4]. Therefore, during the operation, the operating table should be adjusted to avoid the residual bone surface damaging the dura. Simultaneously, if possible, an ultrasonic osteotome or grinding drill should be used to remove the vertebral lamina and keep the residual bone surface as flat as possible. Traumatic factors also play an important role in the occurrence of LPDT. Kamochi *et al*[11] reported two cases of CSF leakage for more than 10 years after head injury.

Decreased dural resistance to CSF pressure: Many factors influence dural resistance to CSF pressure. First, the integrity of the dura is a direct factor. The dura consists of three layers: The dura propria, arachnoid membrane, and soft membrane. Because CSF remains in the subarachnoid space, CSF leakage does not occur when only the dura is injured during the operation and the arachnoid membrane is intact; however, the ability to resist CSF pressure declines. Second, the duration of the operation also affects the resistance of the dura. Studies have confirmed that a long operation time (more than 250 min) leads to an increase in the incidence of LPDT[3]. This is because the dural exposure time is too long and the light irradiation during the operation is too long, resulting in dehydration of the dura. Eventually, the dura becomes less ductile, making it extremely vulnerable[12,13]. Thirdly, tumor radiotherapy and chemotherapy may also be one of the more common factors leading to LPDT[14,15]. Radiation applied

Table 1 Diagnostic criteria for late presentation of dural tears

Clinical elements	Characteristics
Onset time	5 d after surgery, even up to 3 mo
Symptoms	Headache, dizziness, nausea, and other low intracranial pressure symptoms
Drainage fluids, transudates	Clear or light red
Imaging characteristics	MRI reveals dura damage, CSF outflow, sinus formation
β2-transferrin	+

MRI: Magnetic resonance imaging; CSF: Cerebrospinal fluid.

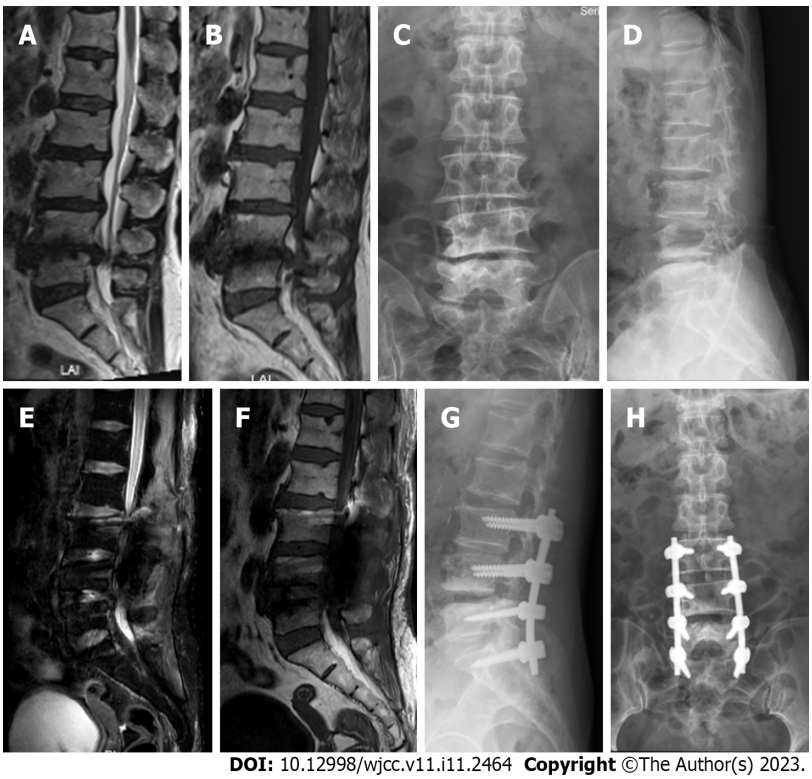

DOI: 10.12998/wjcc.v11.i11.2464

Figure 3 Magnetic resonance imaging and X-ray findings of the first patient. A–D: Preoperative images showing lumbar disc herniation and lumbar spinal stenosis at L3–S1 level; E–H: Images at 1 wk after surgery showing the lack of clear signs of cerebrospinal fluid leakage or pseudocyst formation.

in the course of tumor radiotherapy will cause damage to the dura resulting in thinning or necrosis of the dura. Chemotherapeutic drugs, such as dopamine agonists, may also damage the dura. In addition, Glassman *et al*[16] believe that LPDT is related to bone morphogenetic protein (BMP2), since BMP2 can activate the inflammatory response in vivo, leading to tissue edema. Finally, the patient's condition also affects LPDT. Advanced age is a high-risk factor[17]. At the same time, connective tissue diseases (Marfan's syndrome, Ehlers–Danlos syndrome) can lead to dural expansion, thus affecting the toughness of the dura[18].

Increased CSF pressure: Vigorous activity of the spine after spinal surgery causes significant changes in local CSF pressure. For example, Dannawi *et al*[8] reported an orgasmic dural tear three months after lumbar surgery. Sneezing, coughing, and other factors increase abdominal pressure, which in turn affects CSF pressure. In addition, obvious cavities after spinal surgery may lead to a lack of supporting structures behind the dura, which will affect the pressure balance between the inner and outer dura, and finally show an increase in the local CSF pressure in the cavity[19-21].

Clinical management of LPDT

The treatment of LPDT is often more complicated and difficult than DT that occurs during surgery, because when LPDT is found, sinuses or pseudocysts are generally formed. Initial treatment can be conservative, and surgical repair may be required when the effect is poor[1].

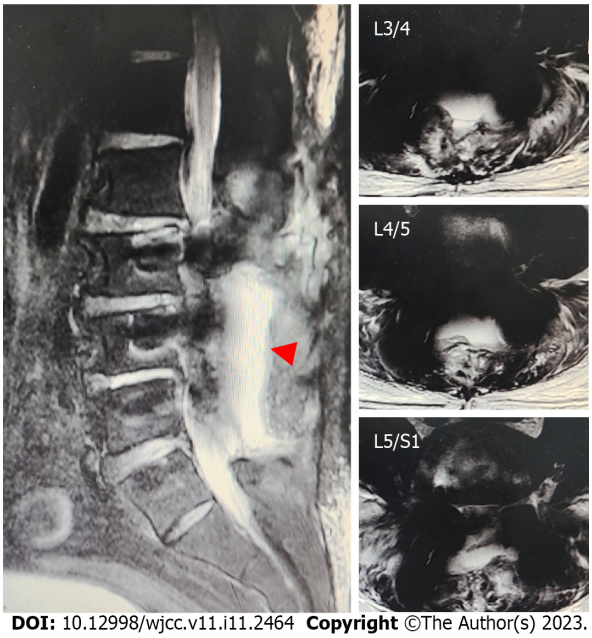

DOI: 10.12998/wjcc.v11.i11.2464

Figure 4 Magnetic resonance imaging findings of the second patient. Red triangle: Exuded cerebrospinal fluid.

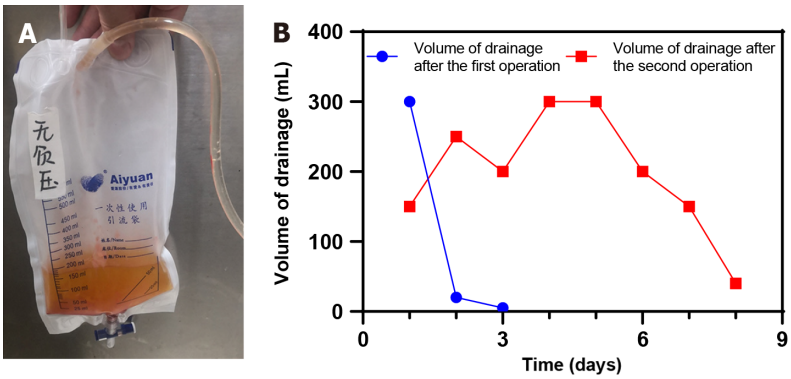

DOI: 10.12998/wjcc.v11.i11.2464

Figure 5 Postoperative drainage of the first patient. A: Drainage fluid after the third operation. The drainage fluid is light red, which is considered as cerebrospinal fluid; B: Changes of postoperative drainage volume.

Conservative treatment: Although the incidence of LPDT is low, it deserves the attention of clinicians, since it affects patient satisfaction with medical treatment and clinical efficacy. When the symptoms are not serious, conservative treatment is preferred, including bed rest, prevention of infection, rehydration, nutrition, and local pressure bandage of the wound, among others[1]. There is currently much debate about the treatment strategy of bed rest, and the results of some studies have revealed that bed rest has little clinical benefit, while increasing medical costs and length of hospital stay. According to literature reports and clinical experience, our research group believes that the necessity and duration of bed rest mainly depend on the size and location of the dural defect and the clinical symptoms of the patient.

Surgical treatment: When conservative treatment fails within three days to a week, surgical treatment is considered necessary, especially in the case of wound infection and sinus and pseudodural cyst formation. There is evidence that successful repair of the dura can effectively reduce the occurrence of complications caused by dural defects[19,22,23]. The main focus of clinical treatment is to effectively and quickly block dural defects. Studies have confirmed that watertight closure is key to the treatment of CSF leakage caused by dural defects[24,25]. The current clinical treatment measures for dural defects vary according to their location and size, mainly including closure with medical sutures or non-penetrating titanium clamps, autologous tissue filling, and sealing with tissue sealants.

Sutures. The traditional treatment philosophy holds that suture closure is the gold standard for the treatment of dural defects[26]. This technique is still one of the main treatment strategies favored by spinal surgeons and neurosurgeons for dural defects, but many difficulties exist: The location of the defect may not be conducive to suturing or cannot be sutured; CSF leakage cannot be avoided in the

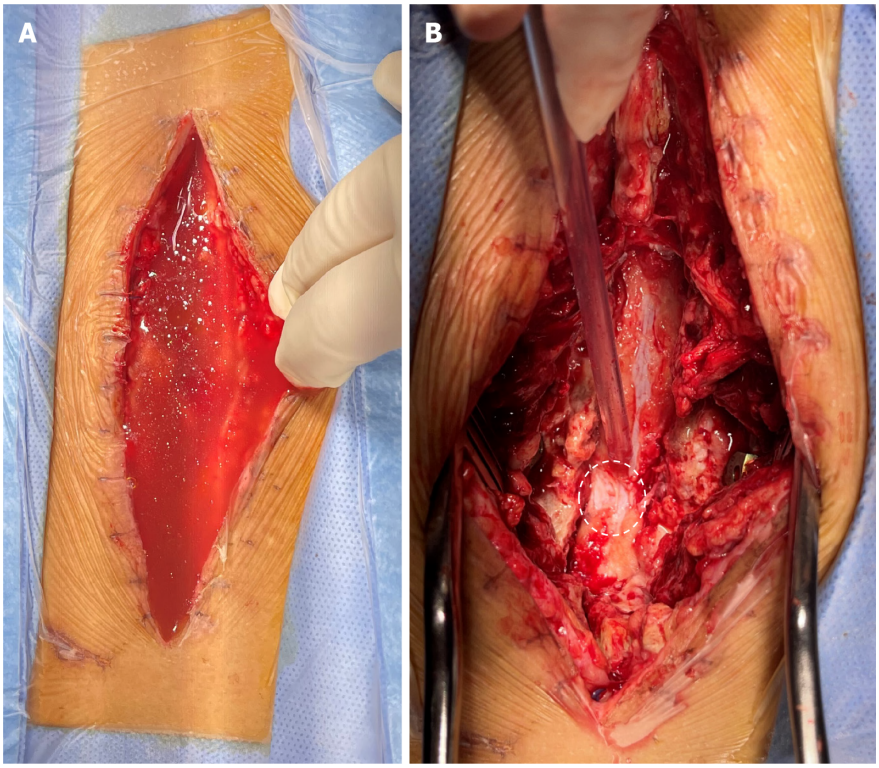

DOI: 10.12998/wjcc.v11.i11.2464

Figure 6 Digital photos of intraoperative exploration of the second patient. A: A large amount of liquid accumulated under the skin; B: Dural defect found during operation. White dotted circle: The size of dura defect.

pinhole left by the suture needle; and it is even possible that the defect area is transformed from a low-pressure area to a high-pressure area because of the suture technique.

Non-penetrating titanium clamp: A non-penetrating titanium clip designed for vascular anastomosis is another option for DT[27-29]. Its clinical use does not produce pinholes, which solves the risk of CSF leakage caused by pinholes. At present, it is considered to have the advantages of a simple operation, rapid process, less postoperative adhesion, less dural exposure and reduced potential risk of CSF leakage. However, because it is made of metal, we must consider metal artifacts that may affect the diagnosis and treatment of the disease in the future. At the same time, issues regarding the use of non-penetrating titanium clips such as clip displacement, inability to be reused during operations, high medical cost, being non-degradable, and subsequent DT also need to be considered.

Autologous tissue: The materials used to fill the dural defect include the periosteum, fascia, fat, muscle, and other tissues. First, the effectiveness of the fascia and other autologous tissues in blocking dural defects was confirmed in animal models[30]. A clinical study of the human body observed the curative effect of repairing dural defects with autologous tissue, and the results confirmed that it can block the dural defect effectively[31-34]. Use of autologous tissue to repair dural defects has the advantages of the lack of infection, rejection, disease transmission, and increase in patient burden. However, additional surgery using local materials increases the surgical trauma, operation time, and adhesion risk. Furthermore, postoperative adhesion is a major factor affecting clinical efficacy.

Sealants: Currently, the commercial synthetic materials used for dural defects are mainly absorbable and degradable materials, which can roughly be divided into three categories: Polyethylene glycol (PEG), hydrogels (such as DuraSeal), fibrin glue (Tissel, Evicel, and Beixiu glue), and hydrogels formed by glutaraldehyde and bovine serum albumin (such as BioGlue surgical adhesives)[35]. According to a multicenter, prospective, and randomized study, PEG hydrogel sealant is not inferior to common dural sealing technology[36]. However, current clinical research has found that PEG hydrogels can cause significant swelling in clinical use, which is extremely unfavorable for the spinal canal or ventricle with limited space[37]; fibrin glue itself can quickly form glue, but it cannot form strong adhesions with the tissue surface, therefore, it cannot resist the fluctuating pressure of CSF at the physiological level; at the same time, the BioGlue adhesive was found to have neurotoxicity. Therefore, more powerful adhesives are expected to be successfully prepared in the future.

Based on the defects of a single treatment strategy, two or a combination of two schemes is often used in the clinic. A Canadian questionnaire showed that, as the size of the defect gradually increases, clinicians gradually adopt a combination of treatment regimens[38].

Perioperative management

The primary role of perioperative management in LPDT is prevention. First, we attempted to choose an operation method that causes less damage to the peridural tissue. The peridural ligaments, lamina, and even posterior muscle groups can provide protection to the dura and reduce the risk of dural damage[3, 39]. Therefore, a treatment strategy for minimally invasive surgery should be preferred if the condition permits. In addition, from the perspective of medical safety and the possibility of LPDT, clinicians should clearly inform patients and their families of the risk when signing the operation before surgery and provide them with a prior understanding of the possible complications. This is because there are many claims of malpractice related to accidental durotomy caused by spinal surgery.

CONCLUSION

LPDT as a rare complication in spinal surgery or neurosurgery, has hidden symptoms and is easily overlooked. If the complication cannot be treated in time, it may cause a series of adverse consequences, including pseudodural cyst and sinus. Therefore, it needs to be actively addressed in clinical practice, through careful examination during surgery and active preventive measures after surgery.

FOOTNOTES

Author contributions: Xu C and Dong RP contributed to manuscript writing and editing, and data collection; Cheng XL and Zhao JW contributed to conceptualization and supervision; all authors have read and approved the final manuscript.

Supported by Jilin Health Science and Technology Capability Improvement Project, No. 2022C107.

Informed consent statement: Informed written consent was obtained from the patient for publication of this report and any accompanying images.

Conflict-of-interest statement: All the authors report no relevant conflicts of interest for this article.

CARE Checklist (2016) statement: The authors have read the CARE Checklist (2016), and the manuscript was prepared and revised according to the CARE Checklist (2016).

Country/Territory of origin: China

ORCID number: Rong-Peng Dong 0000-0001-8585-4344; Xue-Liang Cheng 0000-0001-6285-1175; Jian-Wu Zhao 0000-0003-0574-9742.

S-Editor: Zhao S
L-Editor: A
P-Editor: Zhao S

REFERENCES

1 **Kalidindi KKV**, Bhat MR, Mannem A, Chhabra HS. Conservative Management for Late Presenting Dural Tears After Spine Surgery: An Institutional Experience and Literature Review. *World Neurosurg* 2020; **134**: e82-e92 [PMID: 31542441 DOI: 10.1016/j.wneu.2019.09.067]

2 **Park JS**, Kong DS, Lee JA, Park K. Intraoperative management to prevent cerebrospinal fluid leakage after microvascular decompression: dural closure with a "plugging muscle" method. *Neurosurg Rev* 2007; **30**: 139-42; discussion 142 [PMID: 17221266 DOI: 10.1007/s10143-006-0060-6]

3 **Durand WM**, DePasse JM, Kuris EO, Yang J, Daniels AH. Late-presenting dural tear: incidence, risk factors, and associated complications. *Spine J* 2018; **18**: 2043-2050 [PMID: 29679726 DOI: 10.1016/j.spinee.2018.04.004]

4 **Khazim R**, Dannawi Z, Spacey K, Khazim M, Lennon S, Reda A, Zaidan A. Incidence and treatment of delayed symptoms of CSF leak following lumbar spinal surgery. *Eur Spine J* 2015; **24**: 2069-2076 [PMID: 25711914 DOI: 10.1007/s00586-015-3830-4]

5 **Gupta M**, Kumar Varma KK, Singh Chhabra H. A rare case of concomitant pneumocephalus and pneumorachis after

lumbar spine surgery with late presenting dural leak. *Spinal Cord Ser Cases* 2019; **5**: 86 [PMID: 31700684 DOI: 10.1038/s41394-019-0235-3]
6 **Hawk MW**, Kim KD. Review of spinal pseudomeningoceles and cerebrospinal fluid fistulas. *Neurosurg Focus* 2000; **9**: e5 [PMID: 16859266 DOI: 10.3171/foc.2000.9.1.5]
7 **Epstein NE**. A review article on the diagnosis and treatment of cerebrospinal fluid fistulas and dural tears occurring during spinal surgery. *Surg Neurol Int* 2013; **4**: S301-S317 [PMID: 24163783 DOI: 10.4103/2152-7806.111427]
8 **Dannawi Z**, Lennon SE, Zaidan A, Khazim R. Orgasmic dural tear: an unusual delayed presentation of postural headache following lumbar discectomy. *BMJ Case Rep* 2014; **2014** [PMID: 25432914 DOI: 10.1136/bcr-2014-208071]
9 **Bachmann-Harildstad G**. Diagnostic values of beta-2 transferrin and beta-trace protein as markers for cerebrospinal fluid fistula. *Rhinology* 2008; **46**: 82-85 [PMID: 18575006]
10 **Lauer KK**, Haddox JD. Epidural blood patch as treatment for a surgical durocutaneous fistula. *J Clin Anesth* 1992; **4**: 45-47 [PMID: 1540369 DOI: 10.1016/0952-8180(92)90120-p]
11 **Kamochi H**, Kusaka G, Ishikawa M, Ishikawa S, Tanaka Y. Late onset cerebrospinal fluid leakage associated with past head injury. *Neurol Med Chir (Tokyo)* 2013; **53**: 217-220 [PMID: 23615410 DOI: 10.2176/nmc.53.217]
12 **Narotam PK**, José S, Nathoo N, Taylon C, Vora Y. Collagen matrix (DuraGen) in dural repair: analysis of a new modified technique. *Spine (Phila Pa 1976)* 2004; **29**: 2861-7; discussion 2868 [PMID: 15599291 DOI: 10.1097/01.brs.0000148049.69541.ad]
13 **Kinaci A**, Van Doormaal TPC. Dural sealants for the management of cerebrospinal fluid leakage after intradural surgery: current status and future perspectives. *Expert Rev Med Devices* 2019; **16**: 549-553 [PMID: 31144544 DOI: 10.1080/17434440.2019.1626232]
14 **Ogawa Y**, Tominaga T. Delayed cerebrospinal fluid leakage 10 years after transsphenoidal surgery and gamma knife surgery - case report -. *Neurol Med Chir (Tokyo)* 2007; **47**: 483-485 [PMID: 17965568 DOI: 10.2176/nmc.47.483]
15 **Lee JJ**, Kim HY, Dhong HJ, Chung SK, Kong DS, Nam DH, So YK, Hong SD. Delayed Cerebrospinal Fluid Leakage After Treatment of Skull Base Tumors: Case Series of 9 Patients. *World Neurosurg* 2019; **132**: e591-e598 [PMID: 31442635 DOI: 10.1016/j.wneu.2019.08.067]
16 **Glassman SD**, Gum JL, Crawford CH 3rd, Shields CB, Carreon LY. Complications with recombinant human bone morphogenetic protein-2 in posterolateral spine fusion associated with a dural tear. *Spine J* 2011; **11**: 522-526 [PMID: 20598649 DOI: 10.1016/j.spinee.2010.05.016]
17 **Sin AH**, Caldito G, Smith D, Rashidi M, Willis B, Nanda A. Predictive factors for dural tear and cerebrospinal fluid leakage in patients undergoing lumbar surgery. *J Neurosurg Spine* 2006; **5**: 224-227 [PMID: 16961083 DOI: 10.3171/spi.2006.5.3.224]
18 **Schievink WI**. Spontaneous spinal cerebrospinal fluid leaks and intracranial hypotension. *JAMA* 2006; **295**: 2286-2296 [PMID: 16705110 DOI: 10.1001/jama.295.19.2286]
19 **Wang JC**, Bohlman HH, Riew KD. Dural tears secondary to operations on the lumbar spine. Management and results after a two-year-minimum follow-up of eighty-eight patients. *J Bone Joint Surg Am* 1998; **80**: 1728-1732 [PMID: 9875930 DOI: 10.2106/00004623-199812000-00002]
20 **Papavero L**, Engler N, Kothe R. Incidental durotomy in spine surgery: first aid in ten steps. *Eur Spine J* 2015; **24**: 2077-2084 [PMID: 25735610 DOI: 10.1007/s00586-015-3837-x]
21 **Jito J**, Nitta N, Nozaki K. Delayed cerebrospinal fluid leak after watertight dural closure with a polyethylene glycol hydrogel dural sealant in posterior fossa surgery: case report. *Neurol Med Chir (Tokyo)* 2014; **54**: 634-639 [PMID: 24305019 DOI: 10.2176/nmc.cr2013-0010]
22 **Liang H**, Li C, Gao A, Liang P, Shao Y, Lin T, Zhang X. Spinal duraplasty with two novel substitutes restored locomotor function after acute laceration spinal cord injury in rats. *J Biomed Mater Res B Appl Biomater* 2012; **100**: 2131-2140 [PMID: 22848005 DOI: 10.1002/jbm.b.32778]
23 **Song Y**, Li S, Song B, Zhang Y, Gao W, Li N, Fan K, Ma J. The pathological changes in the spinal cord after dural tear with and without autologous fascia repair. *Eur Spine J* 2014; **23**: 1531-1540 [PMID: 24801575 DOI: 10.1007/s00586-014-3326-7]
24 **Esposito F**, Angileri FF, Kruse P, Cavallo LM, Solari D, Esposito V, Tomasello F, Cappabianca P. Fibrin Sealants in Dura Sealing: A Systematic Literature Review. *PLoS One* 2016; **11**: e0151533 [PMID: 27119993 DOI: 10.1371/journal.pone.0151533]
25 **Ikeme S**, Weltert L, Lewis KM, Bothma G, Cianciulli D, Pay N, Epstein J, Kuntze E. Cost-effectiveness analysis of a sealing hemostat patch (HEMOPATCH) *vs* standard of care in cardiac surgery. *J Med Econ* 2018; **21**: 273-281 [PMID: 29096598 DOI: 10.1080/13696998.2017.1400977]
26 **Cammisa FP Jr**, Girardi FP, Sangani PK, Parvataneni HK, Cadag S, Sandhu HS. Incidental durotomy in spine surgery. *Spine (Phila Pa 1976)* 2000; **25**: 2663-2667 [PMID: 11034653 DOI: 10.1097/00007632-200010150-00019]
27 **Kaufman BA**, Matthews AE, Zwienenberg-Lee M, Lew SM. Spinal dural closure with nonpenetrating titanium clips in pediatric neurosurgery. *J Neurosurg Pediatr* 2010; **6**: 359-363 [PMID: 20887109 DOI: 10.3171/2010.7.PEDS09545]
28 **Marin Laut FM**, Gómez Cárdenas EA, Dormido JR, Molina NM, López López JA. Spinal dural closure without suture: Minimizing the risk of CSF leakage with a flat non-penetrating titanium U-clip. *Neurocirugia (Astur : Engl Ed)* 2019; **30**: 173-178 [PMID: 30782504 DOI: 10.1016/j.neucir.2018.12.002]
29 **Cheng YP**, Lin PY, Huang AP, Cheng CY, Chen CM, Hueng DY. Durotomy repair in minimally invasive transforaminal lumbar interbody fusion by nonpenetrating clips. *Surg Neurol Int* 2014; **5**: 36 [PMID: 24818043 DOI: 10.4103/2152-7806.129161]
30 **Oğretmenoğlu O**, Akyol G. The repair of cerebrospinal fluid rhinorrhea: comparison of histopathologic findings with cadaveric human temporal fascia, dura mater, and autologous fascia in a rabbit model. *Kulak Burun Bogaz Ihtis Derg* 2004; **13**: 1-8 [PMID: 16027484]
31 **Barrientos S**, Leif M, Hon HH, Aizenberg M, Wong S. Duraplasty Using Autologous Fascia Lata and Latissimus Dorsi Free Flap for Chronic Cerebrospinal Fluid Leak. *J Craniofac Surg* 2019; **30**: e671-e674 [PMID: 31574789 DOI: 10.1097/SCS.0000000000005747]

32 **Zha W**, Xu M, Zhang L. [Reparation and restitution of head tissue deletion with fascia lata and local flap]. *Lin Chung Er Bi Yan Hou Tou Jing Wai Ke Za Zhi* 2013; **27**: 1191-1192 [PMID: 24616999]

33 **Fiorindi A**, Gioffrè G, Boaro A, Billeci D, Frascaroli D, Sonego M, Longatti P. Banked Fascia Lata in Sellar Dura Reconstruction after Endoscopic Transsphenoidal Skull Base Surgery. *J Neurol Surg B Skull Base* 2015; **76**: 303-309 [PMID: 26225321 DOI: 10.1055/s-0035-1547364]

34 **Yang HA**, Sun SC, Zheng XR, Ding F, Bie YF. Effect of subdural muscle packing in repairing dura mater after retrosigmoid craniotomy. *J Int Med Res* 2020; **48**: 300060520910299 [PMID: 32223659 DOI: 10.1177/0300060520910299]

35 **Epstein NE**. Dural repair with four spinal sealants: focused review of the manufacturers' inserts and the current literature. *Spine J* 2010; **10**: 1065-1068 [PMID: 21094467 DOI: 10.1016/j.spinee.2010.09.017]

36 **Osbun JW**, Ellenbogen RG, Chesnut RM, Chin LS, Connolly PJ, Cosgrove GR, Delashaw JB Jr, Golfinos JG, Greenlee JD, Haines SJ, Jallo J, Muizelaar JP, Nanda A, Shaffrey M, Shah MV, Tew JM Jr, van Loveren HR, Weinand ME, White JA, Wilberger JE. A multicenter, single-blind, prospective randomized trial to evaluate the safety of a polyethylene glycol hydrogel (Duraseal Dural Sealant System) as a dural sealant in cranial surgery. *World Neurosurg* 2012; **78**: 498-504 [PMID: 22381303 DOI: 10.1016/j.wneu.2011.12.011]

37 **Thavarajah D**, De Lacy P, Hussain R, Redfern RM. Postoperative cervical cord compression induced by hydrogel (DuraSeal): a possible complication. *Spine (Phila Pa 1976)* 2010; **35**: E25-E26 [PMID: 20042944 DOI: 10.1097/BRS.0b013e3181b9fc45]

38 **Oitment C**, Aref M, Almenawar S, Reddy K. Spinal Dural Repair: A Canadian Questionnaire. *Global Spine J* 2018; **8**: 359-364 [PMID: 29977720 DOI: 10.1177/2192568217724132]

39 **Kundu A**, Sano Y, Pagel PS. Case report: delayed presentation of postural headache in an adolescent girl after microscopic lumbar discectomy. *Can J Anaesth* 2008; **55**: 696-701 [PMID: 18835968 DOI: 10.1007/BF03017746]

World Journal of Clinical Cases

Submit a Manuscript: https://www.f6publishing.com

World J Clin Cases 2023 April 16; 11(11): 2474-2481

DOI: 10.12998/wjcc.v11.i11.2474

ISSN 2307-8960 (online)

CASE REPORT

Difficult-to-treat rheumatoid arthritis treated with Abatacept combined with Baricitinib: A case report

Jia-Ping Qi, Huan Jiang, Teng Wu, Yuan Zhang, Wei Huang, Yi-Xuan Li, Jing Wang, Ju Zhang, Zhen-Hua Ying

Specialty type: Medicine, research and experimental

Provenance and peer review: Unsolicited article; Externally peer reviewed.

Peer-review model: Single blind

Peer-review report's scientific quality classification

Grade A (Excellent): 0
Grade B (Very good): B
Grade C (Good): C
Grade D (Fair): 0
Grade E (Poor): 0

P-Reviewer: Dauyey K, Kazakhstan; Primadhi RA, Indonesia

Received: October 20, 2022
Peer-review started: October 20, 2022
First decision: February 7, 2023
Revised: February 19, 2023
Accepted: March 20, 2023
Article in press: March 20, 2023
Published online: April 16, 2023

Jia-Ping Qi, Yuan Zhang, Zhen-Hua Ying, Graduate School, Bengbu Medical College, Bengbu 233030, Anhui Province, China

Jia-Ping Qi, Huan Jiang, Teng Wu, Yuan Zhang, Wei Huang, Yi-Xuan Li, Jing Wang, Ju Zhang, Zhen-Hua Ying, Center for General Practice Medicine, Department of Rheumatology and Immunology, Zhejiang Provincial People's Hospital, Affiliated People's Hospital, Hangzhou 310000, Zhejiang Province, China

Jia-Ping Qi, Huan Jiang, Teng Wu, Yuan Zhang, Wei Huang, Yi-Xuan Li, Jing Wang, Ju Zhang, Zhen-Hua Ying, Zhejiang Provincial Key Laboratory of Traditional Chinese Medicine Cultivation for Arthritis Diagnosis and Treatment, Zhejiang Provincial People's Hospital, Affiliated People's Hospital, Hangzhou Medical College, Hangzhou 310000, Zhejiang Province, China

Huan Jiang, Teng Wu, Yi-Xuan Li, Jing Wang, Zhen-Hua Ying, The Second Clinical Medical College, Zhejiang Chinese Medical University, Hangzhou 310000, Zhejiang Province, China

Corresponding author: Zhen-Hua Ying, MM, Chief Doctor, Professor, Teacher, Center for General Practice Medicine, Department of Rheumatology and Immunology, Zhejiang Provincial People's Hospital, Affiliated People's Hospital, No. 158 Shangtang Road, Hangzhou 310000, Zhejiang Province, China. yingzh2021@163.com

Abstract

BACKGROUND

Sporadic cases of rheumatoid arthritis (RA) due to unsatisfactory responses to Abatacept (ABT) have been reported; however, the rescue therapy has not been finalized. Here, we present a case with difficult-to-treat RA (D2T RA) that was resistant to either a single ABT or a Janus kinase (JAK) inhibitor (Tofacitinib), but improved with a combination of ABT and JAK inhibitor (Baricitinib, BAT).

CASE SUMMARY

A 46-year-old Chinese woman who had RA for ten years that was resistant to Tocilizumab, Etanercept, Adalimumab, and ABT. According to the European League Against Rheumatism definition, the patient was diagnosed with D2T RA. It was then improved with a combination of ABT and a JAK inhibitor BAT.

CONCLUSION

ABT combined with BAT may be an acceptable strategy for treating D2T RA.

Key Words: Difficult-to-treat rheumatoid arthritis; Abatacept; Baricitinib; Combination therapy; Case report

Core Tip: Although the combined use of Abatacept (ABT) and Janus kinase (JAK) inhibitors is not recommended in rheumatoid arthritis (RA) treatment guidelines, inflammatory cytokines have been found to compensate for the inhibitory effect of ABT on co-stimulatory signals, activate T-lymphocytes through the JAK/ Signal Transducers and Activators of Transcription pathway, and promote the inflammatory response. In the treatment of this patient, Baricitinib, as a JAK inhibitor, combined with ABT can be used as a rescue treatment for difficult-to-treat RA, especially for patients with poor responses to single ABT treatment.

Citation: Qi JP, Jiang H, Wu T, Zhang Y, Huang W, Li YX, Wang J, Zhang J, Ying ZH. Difficult-to-treat rheumatoid arthritis treated with Abatacept combined with Baricitinib: A case report. *World J Clin Cases* 2023; 11(11): 2474-2481
URL: https://www.wjgnet.com/2307-8960/full/v11/i11/2474.htm
DOI: https://dx.doi.org/10.12998/wjcc.v11.i11.2474

INTRODUCTION

New disease-modifying anti-rheumatic drugs (DMARDs) have drastically improved rheumatoid arthritis (RA) patients' quality of life[1]. However, 5%-20% of patients continue to show symptoms and clinical signs of autoimmune inflammatory activity despite the continuous treatment with various conventional synthetic, targeted synthetic, and biological DMARDs (cs, ts, and bDMARDs), Such patients are considered as difficult-to-treat RA (D2T RA) population[2,3], according to the European League Against Rheumatism (EULAR) definition of D2T RA (see Table 1 for a complete definition)[4]. D2T RA patients were found to have lower physical function and quality of life, along with substantial fatigue and discomfort than non-D2T RA patients, implying a larger illness load, more significant impairment effects, and early mortality[5]. The current treatment of D2T RA involves a repeated trial process of switching to another b/csDMARD after the first fails, as there are no specific management guidelines for these patients[6]. Therefore, establishing new treatment modalities for this population has become a top priority.

Compared to other b/tsDMARDs, Abatacept (ABT), a novel T-cell costimulation modulator, created compelling clinical benefits and security in patients who did not respond to anti-tumor necrosis factor-α or methotrexate treatment[7,8]. However, ABT is not effective in all patients[9]. The poor response to ABT in D2T RA patients may be linked to inflammatory cytokines; however, the exact pathogenesis remains unknown. According to recent reports, combination therapy with other DMARDs is a more effective management option for patients who do not significantly respond to ABT[9]. Janus kinase (JAK) inhibitors are currently the routine therapy for RA patients on whom csDMARDs are ineffective, and are widely used as an alternative to biologics in patients with no risk factors for venous thromboembolism. Combination therapy has been demonstrated to be clinically and radiologically superior to monotherapy[10]. Although the use of ABT and JAK inhibitors in combination is not suggested in the RA treatment guidelines, it is considered a preliminary experiment because various biologics have been attempted in the past with no notable outcomes. Herein, we present a report of a patient who did not respond to multiple bDMARDs (Tocilizumab, Etanercept, Adalimumab, and ABT) and was successfully treated with a combination therapy of ABT and Baricitinib (BAT).

CASE PRESENTATION

Chief complaints

A 46-year-old woman presented with arthralgia for half a month.

History of present illness

Two years ago, following knee arthroplasty, she experienced profound weariness and stiffness in the morning, with swelling and soreness of several peripheral joints. Quickly, she had trouble moving, and was unable to crouch or rise without assistance. Subsequently, she was admitted to Zhejiang Provincial People's Hospital on October 1, 2020.

Table 1 European League Against Rheumatism definition of difficult-to-treat rheumatoid arthritis

EULAR definition of D2T RA
1 Treatment according to the recommendations of the European League against rheumatism, treatment failure ≥ two biological / tsDMARDs (with different mechanism)[1] after csDMARD treatment failure (unless there are contraindications)[2].
2 Signs indicating active/progressive diseases are defined as ≥ one of them:
(1) At least moderate disease activity (based on validated composite indicators, including joint counts, such as DAS28-ESR > 3.2 or CDAI > 10).
(2) Signs (including acute phase reactants and imaging) and / or symptoms indicating active disease (joint related or other).
(3) No reduction in glucocorticoid treatment (less than 7.5 mg / day prednisone or equivalent).
(4) Rapid radiographic progress (with or without signs of active disease)[3].
(5) According to the above criteria, the disease is well controlled, but there are still RA symptoms, resulting in a decline in the quality of life.
3 Rheumatologists and/or patients believe that there are problems in the management of signs and/or symptoms.

All three standards need to appear in D2T RA.
[1]Unless limited by treatment opportunities due to socioeconomic factors.
[2]If csDMARD treatment is disabled, it is sufficient that ≥ two biologica/tsDMARDs has a different mechanism of action.
[3]Rapid progress in radiographic: the change of van der Heijde-modified Sharp score ≥ five points in a year.
EULAR: European League Against Rheumatism; D2T RA: Difficult-to-treat rheumatoid arthritis; CDAI: Clinical disease activity index; cs: Conventional synthesis; DAS28-ESR: The disease activity score of 28 joints was evaluated by ESR; DMAR: Disease-modifying antirheumatic drug; RA: Rheumatoid arthritis; ts; Targeted synthetic.

History of past illness
The 46-year-old Hangzhou woman developed RA when she was 36 years old. After more than one year of treatment, the disease was nearly controlled.

Personal and family history
The patient had a joint replacement two years ago without a family history.

Physical examination
A body temperature of 37.2°C, a blood pressure of 117/85 mmHg, a heart rate of 83 beats/min, and a respiratory rate of 19 times/min were noted. Swollen and painful joints on both sides of the knuckles, proximal interphalangeal joints, wrist joints and left knee joints.

Laboratory examinations
On presentation to the clinician, the patient had elevated erythrocyte sedimentation rate (ESR) and C-reactive protein (CRP) levels of 118 mm/h (normal range; 0-26 mm/h) and 63.8 mg/L (normal range; 0-8 mg/L), respectively. The levels of rheumatoid factor and anti-cyclic citrullinated peptide antibody increased to 1590.0 IU/mL (normal range; 0-20 IU/mL) and 1351.6 U/mL (normal range; 0-25 U/mL), respectively. Serum immune complex levels, anti-neutrophil cytoplasmic antibody, anti-Sjogren syndrome A antibody (anti-SS-A) and anti-SS-B titers were also significantly increased. Clinical symptoms and serological tests were used to diagnose RA. The disease activity score of 28 joints with ESR (DAS28-ESR) was 6.05 (DAS28-ESR ≤ 2.6, remission; 2.6 < DAS28-ESR ≤ 3.2, mild activity; 3.2 < DAS28-ESR ≤ 5.1, moderate activity, and DAS28-ESR > 5.1, severe activity).

Imaging examinations
Ultrasonic studies revealed a thickened synovial membrane, suprapatellar bursa effusion, and degenerative changes in the left knee joint (Figure 1A and B).

FINAL DIAGNOSIS
Subsequently, the patient was treated with ABT for 3 mo. Although the joint swelling and tenderness improved slightly, the DAS28-ESR decreased from 5.1 to 4.12, and ESR and CRP dropped to 89 mm/h and 64.5 mg/L, respectively, the disease was still in remission. The ultrasound test revealed the development of synovitis and pannus in the articular cavity of the left knee, and blood flow in the articular cavity was more abundant than before (Figure 1C and D). Difficulty in walking, squatting, and upright standing were still present. Comorbidities such as ankylosing spondylitis, psoriatic arthritis, osteoarthritis, lupus, and arthritis caused by other causes were excluded based on laboratory data, joint ultrasonography, and clinical picture. According to the EULAR definition of D2T RA, it was diagnosed

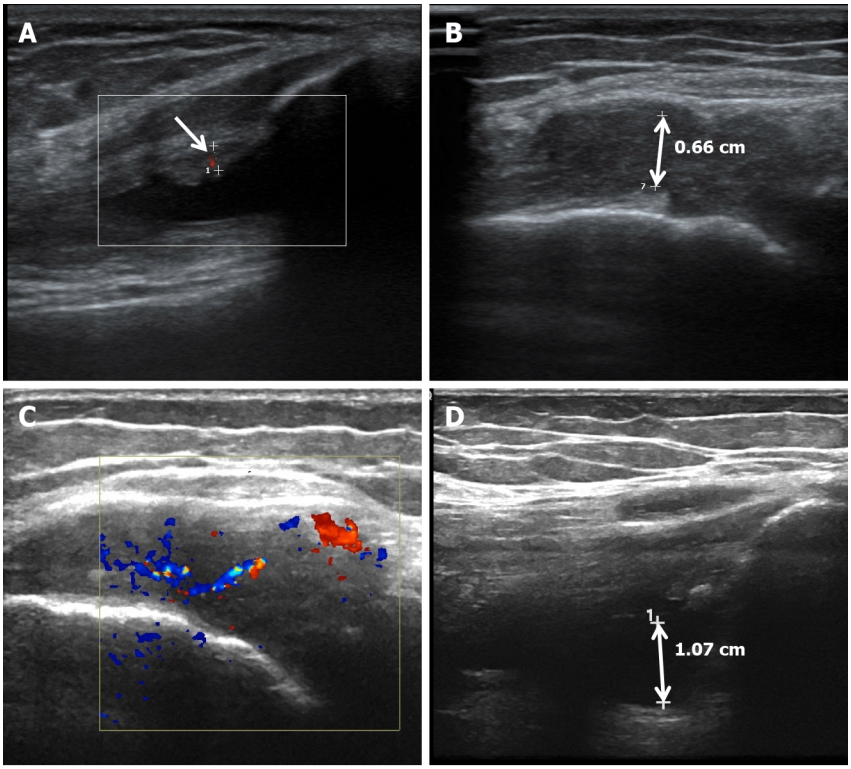

DOI: 10.12998/wjcc.v11.i11.2474

Figure 1 Doppler flow imaging and ultrasonographic pictures. A: Doppler flow imaging shows a few punctate blood flow signals in articular cavity (arrow); B: Ultrasonographic pictures showed that the synovial membrane of the joint was thickened, about 0.66 cm at the thickest point (bidirectional arrow); C: Doppler flow imaging shows abundant blood flow signal in articular cavity. D: Ultrasonographic pictures showed that the synovial membrane of the joint was thickened, about 1.07 cm at the thickest part (bidirectional arrow).

as D2T RA.

TREATMENT

Thereafter, BAT was introduced, considering that the combination of these medications may be successful if the patients do not have any contraindications, such as TB infection or viral hepatitis. After one month, the patient's DAS28-ESR score was 4.08, and ESR and CRP level were 76 mm/h and 10.8 mg/L, respectively. All three indicators constantly remained below this level for the next 3 mo. Furthermore, when compared to the prior time, the ultrasound test revealed that the development of synovitis and pannus in the left knee joint cavity had improved, and blood flow signals were significantly reduced [2021-7 (Figure 2A), 2021-10 (Figure 2B) and 2022-1 (Figure 2C) joint CDFI comparison]. During treatment, no significant side effects were observed.

OUTCOME AND FOLLOW-UP

The patient's ESR and CRP levels were within the normal thresholds (26 mm/h and 3.5 mg/L, respectively) after 3 mo, and DAS28-ESR was 3.26, indicating low-level activity. Moreover, the patients' autonomous walking, squatting, and standing abilities were significantly improved compared to before combination therapy. Entire clinical process and pharmacological dose of the patient is depicted in Figure 2. With the addition of BAT, the patient received effective and continuous treatment for the first time.

DISCUSSION

The pathophysiology of D2T RA is complex, and it is currently categorized into two groups: (1) Multidrug resistance caused by autoimmune disorders and environmental factors in RA patients, such as smoking, pharmacogenetics, or drug immunogenicity; and (2) Difficulties with intensive treatment,

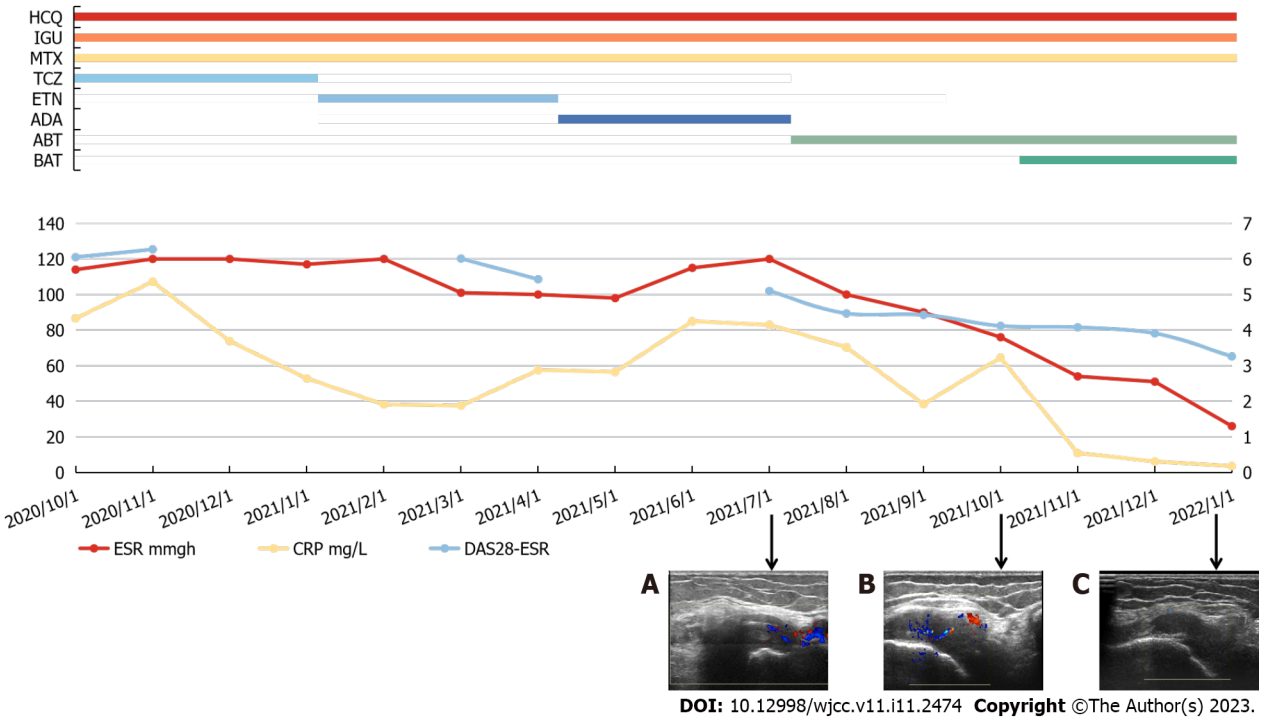

DOI: 10.12998/wjcc.v11.i11.2474

Figure 2 Clinical course of the patient (this statistic does not include tofacitinib because it was only utilized for two weeks). A: Doppler flow imaging showed abundant blood flow signal in the articular cavity in 2021-7-1 (arrow); B: Doppler flow imaging showed abundant blood flow signal in the articular cavity in 2021-10-1 (arrow); C: Doppler flow imaging showed a few punctate blood flow signal in the articular cavity in 2022-1-1 (arrow); HCQ: Hydroxychloroquine, 400 mg/day; IGU: Iguratimod, 50 mg/day; MTX: Methotrexate, 12.5 mg /week; TCZ: Tocilizumab, 400 mg/4 weeks; ETN: Etanercept, 50 mg/week; ADA: Adalimumab, 40 mg/2week; ABT: Abatacept, 250 mg/week; BAT: Bbaricitinib, 2 mg/day; ESR: Erythrocyte sedimentation rate; CRP: C-reactive protein; DAS28-ESR: Disease Activity Score for 28 joints with erythrocyte sedimentation rate.

including comorbidities, poor medication compliance, financial constraints, and reluctance to intensify treatment[11]. Furthermore, from an immunogenetics standpoint, T-lymphocyte pathways play a significant role in inducing and perpetuating chronic relapsing arthritis of D2TRA[12]. Cytotoxic T-lymphocyte-associated protein 4 (CTLA-4) was first identified as an inhibitory signal that is delivered to stop the immune response and has the potential to adversely limit T-lymphocyte activation in various ways[13]. In several research investigations, the prevalence of D2T RA ranged from 5% to 20% of patients with RA[14]. Compared to RA patients, D2T RA patients have more impairment and die sooner. As a result, high-quality evidence is needed to guide D2 TRA patients' management and assist in the formulation of a structured and tailored treatment approach.

CTLA-4 was first identified as an inhibitory signal delivered to stop immune response and has the potential to adversely limit T-lymphocyte activation in a variety of ways[15]. ABT is a soluble, recombinant, completely humanized fusion protein made up of CTLA-4's extracellular domain and IgG1's Fc region. Interacts with co-stimulatory molecules CD80 Antigen and CD80 Antigen on antigen-presenting cells and inhibits T-lymphocyte activation by interfering with CD28 signaling. ABT has been demonstrated to be beneficial in combating a multitude of autoinflammatory disorders, including RA [16,17]. However, several clinical studies have proved that the single CTLA-4 therapy has a limited ability to block T-lymphocyte activation[18,19]. Inflammatory cytokines [Interleukin 6 (IL-6), IL-17, IL-18, and IL-1], which compensate for the loss of costimulatory signals in an inflammatory environment, can enhance the activation of allogeneic T-lymphocytes in a CD28-independent way. By signaling inflammatory cytokines, the JAK/ Signal Transducers and Activators of Transcription (STAT) system plays a vital role in CTLA-4 failure[20].

JAK inhibitors interact with the ATP-binding sites such as JAK1, JAK2, JAK3, and tyrosine kinase 2 (TYK2) to suppress kinase phosphorylation and the JAK/STAT signaling pathway. However, it increases the risk of upper respiratory infections, herpes zoster, hematological abnormalities, and gastrointestinal problems[21]. Four JAK inhibitors are currently approved for RA[22]. As one of them, BAT can effectively inhibit JAK1 and JAK2, and moderately inhibit TYK2. Studies have shown that BAT with safety profiles may be more suitable for RA patients who are resistant to multiple bDMARDs and have a higher American College of Rheumatology (ACR) response rate than Tofacitinib (which mainly inhibits JAK1 and JAK3)[23,24]. It is known that IL-6 signaling is mediated by JAK1 and JAK2, and IL-17 and IL-18 signaling are mainly mediated by JAK2[25-28]. In the treatment of this patient, BAT may have inhibited the signaling of inflammatory cytokines by inhibiting the JAK/STAT pathway, cooperated with the inhibitory effect of ABT on costimulatory signals, and blocked the inflammatory response.

With a more comprehensive exploration of the inflammatory molecules that antagonize CTLA4-Ig and the mechanisms underlying the synergism between BAT and CTLA4- Ig, it will be helpful to identify next-generation JAK inhibitors that will interact with other immunosuppressants more selectively and develop safer and more effective D2T RA management.

We report a case of D2T RA in which the effect was not significant after the replacement of multiple DMARDs, especially ABT, and the combination of ABT and JAK inhibitors was effective. Inflammatory cytokines can compensate for the inhibitory effect of ABT on costimulatory signals, activate T lymphocytes through the JAK/STAT pathway, and promote the inflammatory response. When considering the etiology and treatment of D2T RA patients, especially when the ABT response is not significant, this case can be used as a valuable reference.

CONCLUSION

Inflammatory cytokines can compensate for the inhibitory effect of ABT on co-stimulatory signals, activate T-lymphocytes through the JAK/STAT pathway, and promote the inflammatory response. In the treatment of this patient, BAT, as a JAK inhibitor, combined with ABT can be used as a rescue treatment for D2TRA, especially for patients with poor responses to single ABT treatment.

FOOTNOTES

Author contributions: Qi JP contributed to the intellectual content and drafted the manuscript; Jiang H and Wu T were responsible for the acquisition and interpretation of the data; Huang W and Li YX reconstructed the images, prepared the legends, and updated the literature; Wang J and Zhang J reviewed the data and interpreted the results; Zhang Y was responsible for the acquisition of Color Doppler flow imaging; All authors made a substantial contribution to the preparation of the manuscript, as well as read and approved the final version of the manuscript.

Informed consent statement: Informed written consent was obtained from the patient for the publication of this report and any accompanying images.

Conflict-of-interest statement: The authors declare that they have no conflict of interest to disclose.

CARE Checklist (2016) statement: The authors have read the CARE Checklist (2016), and the manuscript was prepared and revised according to the CARE Checklist (2016).

Country/Territory of origin: China

ORCID number: Zhen-Hua Ying 0000-0002-5443-3675.

S-Editor: Liu GL
L-Editor: A
P-Editor: Liu GL

REFERENCES

1 **de Hair MJH**, Jacobs JWG, Schoneveld JLM, van Laar JM. Difficult-to-treat rheumatoid arthritis: an area of unmet clinical need. *Rheumatology (Oxford)* 2018; **57**: 1135-1144 [PMID: 29029308 DOI: 10.1093/rheumatology/kex349]
2 **Kearsley-Fleet L**, Davies R, De Cock D, Watson KD, Lunt M, Buch MH, Isaacs JD, Hyrich KL; BSRBR-RA Contributors Group. Biologic refractory disease in rheumatoid arthritis: results from the British Society for Rheumatology Biologics Register for Rheumatoid Arthritis. *Ann Rheum Dis* 2018; **77**: 1405-1412 [PMID: 29980575 DOI: 10.1136/annrheumdis-2018-213378]
3 **Buch MH**. Defining refractory rheumatoid arthritis. *Ann Rheum Dis* 2018; **77**: 966-969 [PMID: 29588276 DOI: 10.1136/annrheumdis-2017-212862]
4 **Nagy G**, Roodenrijs NMT, Welsing PM, Kedves M, Hamar A, van der Goes MC, Kent A, Bakkers M, Blaas E, Senolt L, Szekanecz Z, Choy E, Dougados M, Jacobs JW, Geenen R, Bijlsma HW, Zink A, Aletaha D, Schoneveld L, van Riel P, Gutermann L, Prior Y, Nikiphorou E, Ferraccioli G, Schett G, Hyrich KL, Mueller-Ladner U, Buch MH, McInnes IB, van der Heijde D, van Laar JM. EULAR definition of difficult-to-treat rheumatoid arthritis. *Ann Rheum Dis* 2021; **80**: 31-35 [PMID: 33004335 DOI: 10.1136/annrheumdis-2020-217344]

5 **Roodenrijs NMT**, van der Goes MC, Welsing PMJ, Tekstra J, Lafeber FPJG, Jacobs JWG, van Laar JM. Difficult-to-treat rheumatoid arthritis: contributing factors and burden of disease. *Rheumatology (Oxford)* 2021; **60**: 3778-3788 [PMID: 33331946 DOI: 10.1093/rheumatology/keaa860]

6 **Smolen JS**, Landewé RBM, Bijlsma JWJ, Burmester GR, Dougados M, Kerschbaumer A, McInnes IB, Sepriano A, van Vollenhoven RF, de Wit M, Aletaha D, Aringer M, Askling J, Balsa A, Boers M, den Broeder AA, Buch MH, Buttgereit F, Caporali R, Cardiel MH, De Cock D, Codreanu C, Cutolo M, Edwards CJ, van Eijk-Hustings Y, Emery P, Finckh A, Gossec L, Gottenberg JE, Hetland ML, Huizinga TWJ, Koloumas M, Li Z, Mariette X, Müller-Ladner U, Mysler EF, da Silva JAP, Poór G, Pope JE, Rubbert-Roth A, Ruyssen-Witrand A, Saag KG, Strangfeld A, Takeuchi T, Voshaar M, Westhovens R, van der Heijde D. EULAR recommendations for the management of rheumatoid arthritis with synthetic and biological disease-modifying antirheumatic drugs: 2019 update. *Ann Rheum Dis* 2020; **79**: 685-699 [PMID: 31969328 DOI: 10.1136/annrheumdis-2019-216655]

7 **Emery P**, Burmester GR, Bykerk VP, Combe BG, Furst DE, Barré E, Karyekar CS, Wong DA, Huizinga TW. Evaluating drug-free remission with abatacept in early rheumatoid arthritis: results from the phase 3b, multicentre, randomised, active-controlled AVERT study of 24 months, with a 12-month, double-blind treatment period. *Ann Rheum Dis* 2015; **74**: 19-26 [PMID: 25367713 DOI: 10.1136/annrheumdis-2014-206106]

8 **Lundquist LM**, Cole SW, Augustine JM. Critical appraisal of efficacy and safety of abatacept in the treatment of refractory rheumatoid arthritis. *Open Access Rheumatol* 2012; **4**: 9-19 [PMID: 27790008 DOI: 10.2147/OARRR.S16073]

9 **Suzuki M**, Takahashi N, Kida D, Hirano Y, Kato T, Yabe Y, Oguchi T, Fujibayashi T, Hayashi M, Asai S, Ishiguro N, Kojima T. Clinical effectiveness and safety of additional administration of tacrolimus in rheumatoid arthritis patients with an inadequate response to abatacept: A retrospective cohort study. *Int J Rheum Dis* 2019; **22**: 2199-2205 [PMID: 31647174 DOI: 10.1111/1756-185X.13731]

10 **Reddy V**, Cohen S. Role of Janus Kinase inhibitors in rheumatoid arthritis treatment. *Curr Opin Rheumatol* 2021; **33**: 300-306 [PMID: 33767091 DOI: 10.1097/BOR.0000000000000792]

11 **Roodenrijs NMT**, de Hair MJH, van der Goes MC, Jacobs JWG, Welsing PMJ, van der Heijde D, Aletaha D, Dougados M, Hyrich KL, McInnes IB, Mueller-Ladner U, Senolt L, Szekanecz Z, van Laar JM, Nagy G; whole EULAR Task Force on development of EULAR recommendations for the comprehensive management of difficult-to-treat rheumatoid arthritis. Characteristics of difficult-to-treat rheumatoid arthritis: results of an international survey. *Ann Rheum Dis* 2018; **77**: 1705-1709 [PMID: 30194273 DOI: 10.1136/annrheumdis-2018-213687]

12 **Watanabe R**, Hashimoto M, Murata K, Murakami K, Tanaka M, Ohmura K, Ito H, Matsuda S. Prevalence and predictive factors of difficult-to-treat rheumatoid arthritis: the KURAMA cohort. *Immunol Med* 2022; **45**: 35-44 [PMID: 34033729 DOI: 10.1080/25785826.2021.1928383]

13 **Tuncel J**, Holmberg J, Haag S, Hopkins MH, Wester-Rosenlöf L, Carlsen S, Olofsson P, Holmdahl R. Self-reactive T cells induce and perpetuate chronic relapsing arthritis. *Arthritis Res Ther* 2020; **22**: 95 [PMID: 32345366 DOI: 10.1186/s13075-020-2104-7]

14 **Roodenrijs NMT**, Hamar A, Kedves M, Nagy G, van Laar JM, van der Heijde D, Welsing PMJ. Pharmacological and non-pharmacological therapeutic strategies in difficult-to-treat rheumatoid arthritis: a systematic literature review informing the EULAR recommendations for the management of difficult-to-treat rheumatoid arthritis. *RMD Open* 2021; **7** [PMID: 33419871 DOI: 10.1136/rmdopen-2020-001512]

15 **Mitsuiki N**, Schwab C, Grimbacher B. What did we learn from CTLA-4 insufficiency on the human immune system? *Immunol Rev* 2019; **287**: 33-49 [PMID: 30565239 DOI: 10.1111/imr.12721]

16 **Bonelli M**, Scheinecker C. How does abatacept really work in rheumatoid arthritis? *Curr Opin Rheumatol* 2018; **30**: 295-300 [PMID: 29401118 DOI: 10.1097/BOR.0000000000000491]

17 **Hosseini A**, Gharibi T, Marofi F, Babaloo Z, Baradaran B. CTLA-4: From mechanism to autoimmune therapy. *Int Immunopharmacol* 2020; **80**: 106221 [PMID: 32007707 DOI: 10.1016/j.intimp.2020.106221]

18 **Khalifian S**, Raimondi G, Lee WA, Brandacher G. Taming inflammation by targeting cytokine signaling: new perspectives in the induction of transplantation tolerance. *Immunotherapy* 2014; **6**: 637-653 [PMID: 248966314 DOI: 10.2217/imt.14.25]

19 **Vincenti F**, Charpentier B, Vanrenterghem Y, Rostaing L, Bresnahan B, Darji P, Massari P, Mondragon-Ramirez GA, Agarwal M, Di Russo G, Lin CS, Garg P, Larsen CP. A phase III study of belatacept-based immunosuppression regimens versus cyclosporine in renal transplant recipients (BENEFIT study). *Am J Transplant* 2010; **10**: 535-546 [PMID: 20415897 DOI: 10.1111/j.1600-6143.2009.03005.x]

20 **Iglesias M**, Khalifian S, Oh BC, Zhang Y, Miller D, Beck S, Brandacher G, Raimondi G. A short course of tofacitinib sustains the immunoregulatory effect of CTLA4-Ig in the presence of inflammatory cytokines and promotes long-term survival of murine cardiac allografts. *Am J Transplant* 2021; **21**: 2675-2687 [PMID: 333311212 DOI: 10.1111/ajt.16456]

21 **Choy EH**. Clinical significance of Janus Kinase inhibitor selectivity. *Rheumatology (Oxford)* 2019; **58**: 953-962 [PMID: 30508136 DOI: 10.1093/rheumatology/key339]

22 **You H**, Xu D, Zhao J, Li J, Wang Q, Tian X, Li M, Zeng X. JAK Inhibitors: Prospects in Connective Tissue Diseases. *Clin Rev Allergy Immunol* 2020; **59**: 334-351 [PMID: 32222877 DOI: 10.1007/s12016-020-08786-6]

23 **Miyazaki Y**, Nakano K, Nakayamada S, Kubo S, Inoue Y, Fujino Y, Tanaka Y. Efficacy and safety of tofacitinib versus baricitinib in patients with rheumatoid arthritis in real clinical practice: analyses with propensity score-based inverse probability of treatment weighting. *Ann Rheum Dis* 2021; **80**: 1130-1136 [PMID: 33827788 DOI: 10.1136/annrheumdis-2020-219699]

24 **Lee YH**, Song GG. Relative efficacy and safety of tofacitinib, baricitinib, upadacitinib, and filgotinib in comparison to adalimumab in patients with active rheumatoid arthritis. *Z Rheumatol* 2020; **79**: 785-796 [PMID: 320559284 DOI: 10.1007/s00393-020-00750-1]

25 **Taylor PC**. Clinical efficacy of launched JAK inhibitors in rheumatoid arthritis. *Rheumatology (Oxford)* 2019; **58**: i17-i26 [PMID: 30806707 DOI: 10.1093/rheumatology/key225]

26 **Clark JD**, Flanagan ME, Telliez JB. Discovery and development of Janus kinase (JAK) inhibitors for inflammatory diseases. *J Med Chem* 2014; **57**: 5023-5038 [PMID: 24417533 DOI: 10.1021/jm401490p]

27 **Kao CY**, Chen Y, Thai P, Wachi S, Huang F, Kim C, Harper RW, Wu R. IL-17 markedly up-regulates beta-defensin-2 expression in human airway epithelium *via* JAK and NF-kappaB signaling pathways. *J Immunol* 2004; **173**: 3482-3491 [PMID: 15322213 DOI: 10.4049/jimmunol.173.5.3482]

28 **Lee KM**, Kang JH, Yun M, Lee SB. Quercetin inhibits the poly(dA:dT)-induced secretion of IL-18 *via* down-regulation of the expressions of AIM2 and pro-caspase-1 by inhibiting the JAK2/STAT1 pathway in IFN-γ-primed human keratinocytes. *Biochem Biophys Res Commun* 2018; **503**: 116-122 [PMID: 29857000 DOI: 10.1016/j.bbrc.2018.05.191]

World Journal of Clinical Cases

Submit a Manuscript: https://www.f6publishing.com

World J Clin Cases 2023 April 16; 11(11): 2482-2488

DOI: 10.12998/wjcc.v11.i11.2482

ISSN 2307-8960 (online)

CASE REPORT

Anesthesia management in a pediatric patient with complicatedly difficult airway: A case report

Jia-Xiang Chen, Xiao-Li Shi, Chang-Sheng Liang, Xing-Gang Ma, Liang Xu

Specialty type: Anesthesiology

Provenance and peer review: Unsolicited article; Externally peer reviewed.

Peer-review model: Single blind

Peer-review report's scientific quality classification

Grade A (Excellent): 0
Grade B (Very good): 0
Grade C (Good): C, C
Grade D (Fair): 0
Grade E (Poor): 0

P-Reviewer: He YH, China; Wu SH, Taiwan

Received: December 17, 2022
Peer-review started: December 17, 2022
First decision: January 3, 2023
Revised: January 31, 2023
Accepted: March 21, 2023
Article in press: March 21, 2023
Published online: April 16, 2023

Jia-Xiang Chen, Xiao-Li Shi, Chang-Sheng Liang, Xing-Gang Ma, Liang Xu, Department of Anesthesiology, Shenzhen Children's Hospital, Shenzhen 518038, Guangdong Province, China

Jia-Xiang Chen, Department of Anesthesiology, Shenzhen Pediatrics Institute of Shantou University Medical College, Shenzhen 518038, Guangdong Province, China

Corresponding author: Liang Xu, MD, Director, Doctor, Professor, Department of Anesthesiology, Shenzhen Children's Hospital, No. 7019 Yitian Road, Futian District, Shenzhen 518038, Guangdong Province, China. leonnel@msn.com

Abstract

BACKGROUND

Reports on perioperative anesthesia management in pediatric patients with difficult airways are scarce. In addition to relatively more difficulties in the technique of endotracheal intubation, the time for manipulation is restricted compared to adults. Securing the airways safely and avoiding the occurrence of hypoxemia in these patients are of significance.

CASE SUMMARY

A 9-year-old boy with spastic cerebral palsy, severe malnutrition, thoracic scoliosis, thoracic and airway malformation, laryngomalacia, pneumonia, and epilepsy faced the risk of anesthesia during palliative surgery. After a thorough preoperative evaluation, a detailed scheme for anesthesia and a series of intubation tools were prepared by a team of anesthesiologists. Awake fiberoptic intubation is the widely accepted strategy for patients with anticipated difficult airways. Given the age and medical condition of the patient, we kept him sedated with spontaneous breathing during endotracheal intubation. The endotracheal intubation was completed on the second attempt after the failure of the first effort. Fortunately, the surgery was successful without postoperative complications.

CONCLUSION

Dealing with difficult airways in the pediatric population, proper sedation allows time to intubate without interrupting spontaneous breathing. The appropriate endotracheal intubation method based on the patient's unique characteristics is the key factor in successful management of these rare cases.

Key Words: Pediatric anesthesia; Difficult airway; Spastic cerebral palsy; Awake fiberoptic intubation; Case report

Core Tip: A loss of control of the pediatric airway can result in catastrophic consequences if not addressed promptly. Spastic cerebral palsy is often associated with complicated airways in pediatric patients, which can be classified as difficult intubations of anticipated difficult airways. Sedation with spontaneous breathing and fiberoptic bronchoscope-guided endotracheal intubation is a valuable method for such patients. Herein, we describe the entire process of airway management and analyze the failure of the first intubation attempt.

Citation: Chen JX, Shi XL, Liang CS, Ma XG, Xu L. Anesthesia management in a pediatric patient with complicatedly difficult airway: A case report. *World J Clin Cases* 2023; 11(11): 2482-2488
URL: https://www.wjgnet.com/2307-8960/full/v11/i11/2482.htm
DOI: https://dx.doi.org/10.12998/wjcc.v11.i11.2482

INTRODUCTION

The pediatric difficult airway is a massive challenge for anesthesiologists and is one of the main causes of perioperative respiratory complications[1]. Cerebral palsy (CP) comprises a group of permanent disorders affecting the development of movement causing limited activity. Spasticity account for nearly 80% of pediatric CP cases, whereby comorbidities and functional limitations are prevalent and disabling [2]. Life-threatening complications are primarily associated with recurrent chest infections, upper airway obstruction (UAO), and scoliosis leading to progressive lung disease, along with complications of epilepsy[3]. These characteristic features are major risk assessments for anesthesiologists for predicting a difficult airway.

Cases of airway management in spastic CP are infrequently reported worldwide. Herein, we describe anesthesia management in a pediatric case of a difficult airway caused by spastic CP, outlining the detailed process of airway management. We discuss the results of our literature review for evidence related to fiberoptic bronchoscope (FOB)-guided endotracheal intubation, the choice of sedation method, and other management strategies for the pediatric difficult airway, to encourage anesthesiologists to pay more attention to these patients.

CASE PRESENTATION

Chief complaints

A 9-year-old boy (14 kg) was admitted with feeding difficulties after birth caused by spastic CP.

History of present illness

After birth, the patient had persistent feeding difficulties, accompanied by repeated coughing and vomiting after eating. He was diagnosed with spastic CP along with severe malnutrition, thoracic scoliosis, laryngomalacia, pneumonia, and multiple site deformities, including those of the airway, thorax, hip joint, and both hands and feet. In addition to epilepsy and taking clonazepam 1 mg, phenobarbital 25 mg, levetiracetam 150 mg, and sodium valproate oral liquid 5 mL twice daily, he had a history of aspiration pneumonia and copious purulent sputum, for which he was prescribed antibiotics for 9 d. He was scheduled to undergo implantation of an implantable venous access port and gastrostomy to improve feeding and nutrition. This was not a typical elective operation and was difficult to adjust to a conventionally safe state, because the pneumonia was protracted and nursing conditions were limited.

History of past illness

The patient was diagnosed with spastic CP along with severe malnutrition, thoracic scoliosis, laryngomalacia, pneumonia, and multiple site deformities, including those of the airway, thorax, hip joint, and both hands and feet.

Personal and family history

The patient had been abandoned as a toddler, and his birth and family histories were uncertain.

Physical examination

The patient's general physical examination revealed typical facial dysmorphism, thoracic deformities, scoliosis, oxycephaly, and hip dislocation. He showed a Mallampati class IV airway with severely limited neck movement, thyromental distance of fewer than three fingers, and 20-mm-inter-incisor distance. Auscultation indicated an obvious UAO with distinct sputum sounds, and oxygen saturation (SpO_2) was 85%-90% on 3 L/min of supplemental oxygen using a nasal oxygen cannula. Preoperative evaluation exhibited a class III physical status of American Society of Anesthesiologists with a difficult airway.

Laboratory examinations

Routine blood tests showed a hemoglobin (Hb) level of 9.7 g/dL, hematocrit of 33.3%, mean corpuscular volume of 73.9 fL, mean corpuscular Hb of 21.6 pg, and mean corpuscular Hb concentration of 29.2 g/dL. Other blood test results showed no significant abnormalities.

Imaging examinations

Chest radiography demonstrated pneumonia, scoliosis, and right deviation of the trachea (Figure 1). Computed tomography (CT) scans revealed scoliosis, osteoporosis of the spine, significant atrophy of the muscles of the back in the bilateral thoracolumbar region with fat infiltration, and thoracic and tracheal malformation (Figure 2). Lateral cervical spine CT scans displayed laryngomalacia and malformations of the pharynx and cervical spine (Figure 3).

FINAL DIAGNOSIS

The final diagnosis of the present case was spastic CP, along with feeding difficulties, severe malnutrition, laryngomalacia, epilepsy, severe pneumonia, anemia, congenital scoliosis, congenital thoracic deformity, congenital bilateral hip dislocation, and ectrodactyly.

TREATMENT

A series of intubation tools including supraglottic airway devices, video laryngoscope, an FOB, and invasive airway equipment (percutaneous tracheostomy) were utilized and a skilled anesthesiologist was present. In the operating room, the patient was placed in a supine position, and standard monitoring devices for measuring SpO_2, noninvasive blood pressure, and electrocardiogram were installed. Suction device and large suction tubes were ready for sudden regurgitation and aspiration. The patient's position was adjusted to 30°-40° head height and oxygen flow rate was adjusted to 8 L/min. The mask was gently placed on his mouth and nose without additional pressure, and oxygen was continuously inhaled for 5 min. After pre-oxygenation, gradual anesthesia was induced with penehyclidine hydrochloride 0.15 mg, esketamine 8 mg, and midazolam 1.4 mg. The patient was adequately sedated and showed spontaneous breathing. Due to the patient's limited neck motion, narrow inter-incisor distance, and malformed pharynx, we initially attempted a nasotracheal intubation guided by an FOB with a tip diameter of 2.8 mm. The procedure was performed by an anesthesiologist proficient in FOB intubation. Following intranasal administration of xylometazoline, the FOB passed from the nostril to the larynx. Even after making a few adjustments, no view of the epiglottis or the vocal cords was available. This was due to incorrect angles and copious secretions (Figure 4A). As a result, the FOB was removed and pre-oxygenation and aspiration of secretions were immediately commenced. Subsequently, we again tried to pass the FOB from the oral cavity to the pharynx. The assistant gently used a jaw-thrust maneuver to expand the patient's pharyngeal cavity. The glottis could be seen clearly when the forepart advanced from the oropharynx to the pharynx (Figure 4B). Propofol and rocuronium were administrated after confirming that the forepart reached the mid-trachea and the endotracheal anterograde intubation was advanced with FOB view. A cuffed endotracheal tube of size 5.0 was used for the endotracheal intubation. After confirming that the endotracheal tube was in the trachea with a capnograph and auscultation, 20 mg of methylprednisolone was administered to the patient to alleviate airway stress reactions. Anesthesia was maintained with 2% sevoflurane and remifentanil 0.2 μg/kg/min. The operation lasted approximately 4 h and was successful without any incidents. The intraoperative fluid intake was 450 mL and the urine output was 80 mL. After the operation, the patient was sent to the intensive care unit with a tracheal tube inserted for mechanical ventilator support. He was treated with aminomethylbenzoic acid, phenylethylamine for hemostasis, ceftriaxone for infection, and omeprazole for acid inhibition. The patient was successfully extubated after receiving assistance from a mechanical ventilator for 2 d.

DOI: 10.12998/wjcc.v11.i11.2482

Figure 1 Chest radiography demonstrated pneumonia, scoliosis, and right deviation of the trachea.

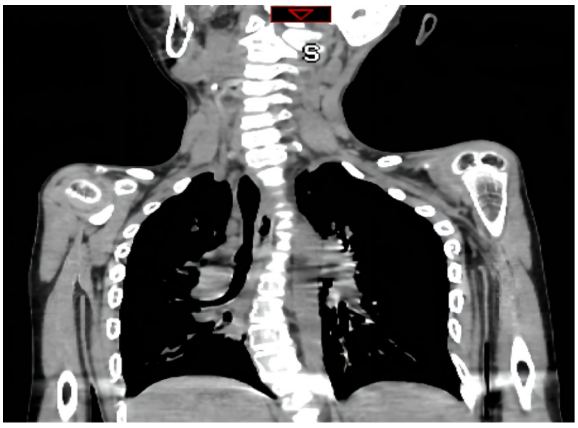

DOI: 10.12998/wjcc.v11.i11.2482

Figure 2 Computed tomography scans revealed scoliosis, osteoporosis of the spine, and thoracic and tracheal malformation.

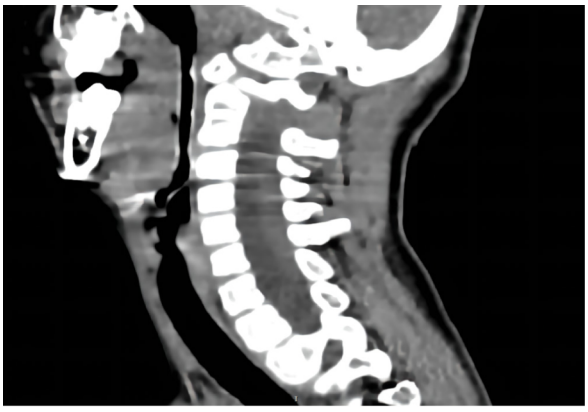

DOI: 10.12998/wjcc.v11.i11.2482

Figure 3 Lateral cervical spine computed tomography scans displayed laryngomalacia, malformations of the pharynx and cervical spine.

OUTCOME AND FOLLOW-UP

The patient was transferred to the general ward on postoperative day 4 and discharged from the hospital 1 wk after surgery without any complications.

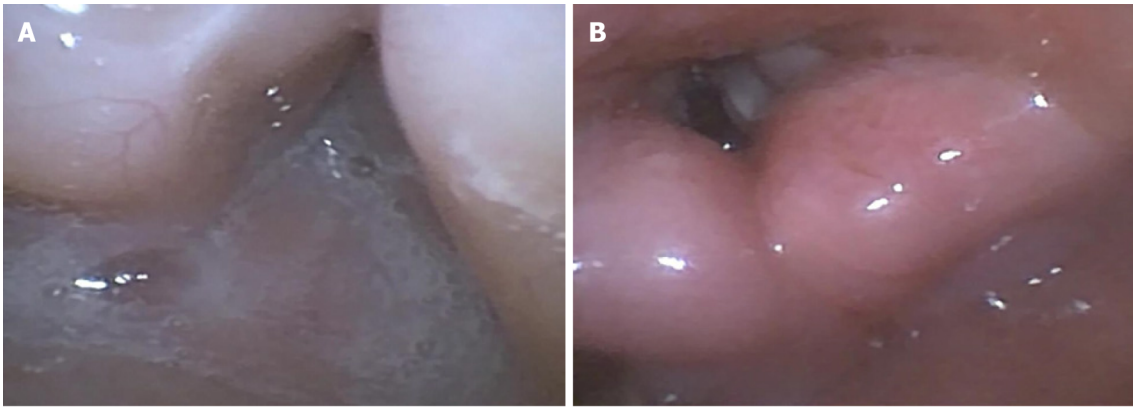

DOI: 10.12998/wjcc.v11.i11.2482

Figure 4 Fiberoptic bronchoscopy. A: There were massive secretions in the nasopharynx; B: The glottis was clearly visible in the transoral approach.

DISCUSSION

Spastic CP is the most common cause of upper motor neuron syndrome among children, accounting for nearly 80% of cases[4]. In patients with spastic CP, motor impairments are often accompanied by seizures and secondary musculoskeletal issues, and abnormalities in sensation, perception, cognition, communication, and behavior[5,6]. The progressive nature of the disorder results in a combination of obstructive and restrictive patterns of pulmonary diseases[7]. The main causes of UAO in patients are abnormal laryngeal structure and muscle hypertonia, tongue prolapsing posteriorly over the larynx, and excessive respiratory secretions, resulting in decreased tidal volume and carbon dioxide accumulation[8]. Moreover, musculoskeletal deformities of the neck result in a severe decrease in neck motion and limited mouth opening, making endotracheal intubation difficult[5]. The resulting pathophysiological alterations pose numerous difficulties for anesthesiologists.

When facing such a case of a pediatric difficult airway, a comprehensive preoperative evaluation is the first and most crucial step of anesthesia management. Unfortunately, no specific scales or suggested measurements for pediatric airway evaluation exist[1]. Despite these limitations, we can evaluate the airway based on previous medical records, facial and jaw features, and anatomical and ultrasonographic measurements[9,10].

An experienced and competent specialist needs to lead the team to formulate an anesthesia plan and discuss alternative strategies before any intervention. Flexible FOB-guided endotracheal intubation is a highly reliable solution for pediatric difficult airways, particularly for difficult or impossible ventilation [11,12]. Studies with observational findings for FOB-guided intubation indicated success rates ranging from 78%-100%[13]. Moreover, FOB-assisted anterograde intubation is almost noninvasive[14]. Unlike adults who can receive FOB-guided endotracheal intubation in the awake state, children require sedation or general anesthesia. Pediatric patients have lower oxygen reserve and higher oxygen consumption during apnea compared to adults[15], so it is better to use appropriate sedation with spontaneous breathing during elective pediatric FOB-aided difficult endotracheal intubation. In this case, we chose esketamine 0.5 mg/kg and midazolam 0.1 mg/kg for sedation, which allowed suitable sedation without interrupting spontaneous breathing. Midazolam provides proper sedation and prevented seizures during the procedure[16]. Esketamine induces a state of dissociative sedation, resulting in strong analgesia, sedation, immobilization, and amnesia whilst maintaining spontaneous respiration and cardiopulmonary stability[17]. Esketamine relatively preserves the protective airway reflexes of patients[18], and is a comparatively safe and effective sedative. However, there is no relevant report on the use of esketamine in the management of pediatric difficult airways. Esketamine produced a good sedative effect that facilitated subsequent procedures in this case. Dexmedetomidine, propofol, fentanyl, and inhalational anesthetic agents are classic sedatives for the management of a difficult airway. Their combinations and dosages need to be adjusted individually to prevent interruption of breathing. If the induction of anesthesia is inappropriate, the airway may turn into a difficult mask ventilation airway or even an emergency airway. Therefore, anesthesiologists should choose the appropriate sedation method according to their experience and the specific patient's situation. Before the procedure began, we also pretreated the nasal cavity with xylometazoline and penehyclidine hydrochloride. Xylometazoline is a topical vasoconstrictor that can reduce nasal bleeding during procedures which may affect the visual field[19]; penehyclidine hydrochloride can inhibit salivary gland and airway gland secretions.

The anesthesiologist team analyzed the reasons for the failure of the first attempt at intubation. Fiberoptic nasotracheal intubation was the first choice owing to the cervical deformity and restricted mouth opening of the patient. However, in the process, despite the use of anticholinergics and full secretion suction before the procedure, the patient had severe respiratory inflammation and constant

copious secretions, which severely affected the visual field. Furthermore, the longer and more curved path from the nasal cavity to the glottis, combined with structural abnormalities in the pharynx, made the adjustment of the anterior end of the FOB more difficult. On the second attempt, we opted for transoral FOB-guided intubation and a jaw-thrust maneuver was performed by the assistant. When the mandible was displaced forward, it pulled the tongue outward, thereby enlarging the pharyngeal cavity and offering more space for the adjustment of the FOB's forepart. There were no adverse events like decreased oxygen saturation, blood pressure, and heart rate during the whole process.

Managing different difficult airways depends on the patient's condition and the individual abilities and habits of the anesthesiologist. A visual laryngoscope can help complete most common intubations, and FOB is a standard protocol for patients who have difficulty with laryngoscope exposure. Awake intubation can be used in adults with a difficult airway, but it is difficult for children to cooperate awake intubation. In the pediatric difficult airway, we need the child to keep sedation with spontaneous breathing to create a suitable operating environment. Midazolam combined with esketamine may be an effective induction regimen.

CONCLUSION

There are only a few articles on the anesthetic management of children with spastic CP. However, patients with spastic CP present several challenges during anesthetic management that may even be fatal on some occasions. When confronted with a pediatric difficult airway, it is essential to have both an experienced specialist and a coordinated team to conduct a complete preoperative evaluation and implement various appropriate management strategies. Under sedation with spontaneous breathing, FOB-guided endotracheal intubation is a standard treatment for a pediatric difficult airway. Anesthesiologists need to individually select the sedation protocol and FOB approach according to the specific patient's situation to reduce the occurrence of respiratory interruption, hypoxemia, drop in blood pressure, and/or other adverse events.

ACKNOWLEDGEMENTS

The authors thank the patient and his guardian for the consent to publish this case.

FOOTNOTES

Author contributions: Chen JX collected the medical records of the patient; Shi XL and Liang CS took responsibility for investigation and data curation; Chen JX, Ma XG, and Xu L drafted and revised the manuscript.

Informed consent statement: Informed written consent was obtained from the patient's guardian for publication of this report and any accompanying images.

Conflict-of-interest statement: All the authors report no relevant conflicts of interest for this article.

CARE Checklist (2016) statement: The authors have read CARE Checklist (2016), and the manuscript was prepared and revised according to CARE Checklist (2016).

Country/Territory of origin: China

ORCID number: Jia-Xiang Chen 0000-0002-4406-6023; Xiao-Li Shi 0000-0002-9775-9392; Chang-Sheng Liang 0000-0001-8549-3032; Xing-Gang Ma 0000-0002-0585-9052; Liang Xu 0000-0002-4108-9043.

S-Editor: Li L
L-Editor: Wang TQ
P-Editor: Li L

REFERENCES

1 **Cook TM**, Woodall N, Frerk C; Fourth National Audit Project. Major complications of airway management in the UK: results of the Fourth National Audit Project of the Royal College of Anaesthetists and the Difficult Airway Society. Part 1: anaesthesia. *Br J Anaesth* 2011; **106**: 617-631 [PMID: 21447488 DOI: 10.1093/bja/aer058]

2 **Novak I**, Morgan C, Adde L, Blackman J, Boyd RN, Brunstrom-Hernandez J, Cioni G, Damiano D, Darrah J, Eliasson AC, de Vries LS, Einspieler C, Fahey M, Fehlings D, Ferriero DM, Fetters L, Fiori S, Forssberg H, Gordon AM, Greaves S, Guzzetta A, Hadders-Algra M, Harbourne R, Kakooza-Mwesige A, Karlsson P, Krumlinde-Sundholm L, Latal B, Loughran-Fowlds A, Maitre N, McIntyre S, Noritz G, Pennington L, Romeo DM, Shepherd R, Spittle AJ, Thornton M, Valentine J, Walker K, White R, Badawi N. Early, Accurate Diagnosis and Early Intervention in Cerebral Palsy: Advances in Diagnosis and Treatment. *JAMA Pediatr* 2017; **171**: 897-907 [PMID: 28715518 DOI: 10.1001/jamapediatrics.2017.1689]

3 **Wilkinson DJ**, Baikie G, Berkowitz RG, Reddihough DS. Awake upper airway obstruction in children with spastic quadriplegic cerebral palsy. *J Paediatr Child Health* 2006; **42**: 44-48 [PMID: 16487389 DOI: 10.1111/j.1440-1754.2006.00787.x]

4 **Skoutelis VC**, Kanellopoulos AD, Kontogeorgakos VA, Dinopoulos A, Papagelopoulos PJ. The orthopaedic aspect of spastic cerebral palsy. *J Orthop* 2020; **22**: 553-558 [PMID: 33214743 DOI: 10.1016/j.jor.2020.11.002]

5 **Graham HK**, Rosenbaum P, Paneth N, Dan B, Lin JP, Damiano DL, Becher JG, Gaebler-Spira D, Colver A, Reddihough DS, Crompton KE, Lieber RL. Cerebral palsy. *Nat Rev Dis Primers* 2016; **2**: 15082 [PMID: 27188686 DOI: 10.1038/nrdp.2015.82]

6 **Morgan C**, Fetters L, Adde L, Badawi N, Bancale A, Boyd RN, Chorna O, Cioni G, Damiano DL, Darrah J, de Vries LS, Dusing S, Einspieler C, Eliasson AC, Ferriero D, Fehlings D, Forssberg H, Gordon AM, Greaves S, Guzzetta A, Hadders-Algra M, Harbourne R, Karlsson P, Krumlinde-Sundholm L, Latal B, Loughran-Fowlds A, Mak C, Maitre N, McIntyre S, Mei C, Morgan A, Kakooza-Mwesige A, Romeo DM, Sanchez K, Spittle A, Shepherd R, Thornton M, Valentine J, Ward R, Whittingham K, Zamany A, Novak I. Early Intervention for Children Aged 0 to 2 Years With or at High Risk of Cerebral Palsy: International Clinical Practice Guideline Based on Systematic Reviews. *JAMA Pediatr* 2021; **175**: 846-858 [PMID: 33999106 DOI: 10.1001/jamapediatrics.2021.0878]

7 **Siriwat R**, Deerojanawong J, Sritippayawan S, Hantragool S, Cheanprapai P. Mechanical Insufflation-Exsufflation Versus Conventional Chest Physiotherapy in Children With Cerebral Palsy. *Respir Care* 2018; **63**: 187-193 [PMID: 29066586 DOI: 10.4187/respcare.05663]

8 **Marpole R**, Blackmore AM, Gibson N, Cooper MS, Langdon K, Wilson AC. Evaluation and Management of Respiratory Illness in Children With Cerebral Palsy. *Front Pediatr* 2020; **8**: 333 [PMID: 32671000 DOI: 10.3389/fped.2020.00333]

9 **Altun D**, Kara H, Bozbora E, Ali A, Dinç T, Sonmez S, Buget M, Aydemir L, Basaran B, Tuğrul M, Çamci E. The Role of Indirect Laryngoscopy, Clinical and Ultrasonographic Assessment in Prediction of Difficult Airway. *Laryngoscope* 2021; **131**: E555-E560 [PMID: 32730647 DOI: 10.1002/lary.28849]

10 **Apfelbaum JL**, Hagberg CA, Connis RT, Abdelmalak BB, Agarkar M, Dutton RP, Fiadjoe JE, Greif R, Klock PA, Mercier D, Myatra SN, O'Sullivan EP, Rosenblatt WH, Sorbello M, Tung A. 2022 American Society of Anesthesiologists Practice Guidelines for Management of the Difficult Airway. *Anesthesiology* 2022; **136**: 31-81 [PMID: 34762729 DOI: 10.1097/ALN.0000000000004002]

11 **Cabrini L**, Baiardo Redaelli M, Ball L, Filippini M, Fominskiy E, Pintaudi M, Putzu A, Votta CD, Sorbello M, Antonelli M, Landoni G, Pelosi P, Zangrillo A. Awake Fiberoptic Intubation Protocols in the Operating Room for Anticipated Difficult Airway: A Systematic Review and Meta-analysis of Randomized Controlled Trials. *Anesth Analg* 2019; **128**: 971-980 [PMID: 30896601 DOI: 10.1213/ANE.0000000000004087]

12 **Yang SZ**, Huang SS, Yi WB, Lv WW, Li L, Qi F. Awake fiberoptic intubation and use of bronchial blockers in ankylosing spondylitis patients. *World J Clin Cases* 2021; **9**: 6705-6716 [PMID: 34447817 DOI: 10.12998/wjcc.v9.i23.6705]

13 **Kaufmann J**, Laschat M, Engelhardt T, Hellmich M, Wappler F. Tracheal intubation with the Bonfils fiberscope in the difficult pediatric airway: a comparison with fiberoptic intubation. *Paediatr Anaesth* 2015; **25**: 372-378 [PMID: 25212815 DOI: 10.1111/pan.12523]

14 **Cui XL**, Wang SY, Xue FS. Fiberoptic and retrograde intubation in difficult pediatric airway: useful suggestions. *J Neurosurg Anesthesiol* 2014; **26**: 257-258 [PMID: 24905031 DOI: 10.1097/ANA.0000000000000022]

15 **Riva T**, Pedersen TH, Seiler S, Kasper N, Theiler L, Greif R, Kleine-Brueggeney M. Transnasal humidified rapid insufflation ventilatory exchange for oxygenation of children during apnoea: a prospective randomised controlled trial. *Br J Anaesth* 2018; **120**: 592-599 [PMID: 29452816 DOI: 10.1016/j.bja.2017.12.017]

16 **Kacar Bayram A**, Yan Q, Isitan C, Rao S, Spencer DD, Alkawadri R. Effect of anesthesia on electrocorticography for localization of epileptic focus: Literature review and future directions. *Epilepsy Behav* 2021; **118**: 107902 [PMID: 33819715 DOI: 10.1016/j.yebeh.2021.107902]

17 **Xin N**, Xu H, Yue C. Comparison between dexmedetomidine and esketamine in pediatric dentistry surgery. *Transl Pediatr* 2021; **10**: 3159-3165 [PMID: 35070829 DOI: 10.21037/tp-21-435]

18 **Patel D**, Talbot C, Luo W, Mulvaney S, Byrne E. The use of esketamine sedation in the emergency department for manipulation of paediatric forearm fractures: A 5 year study. *Injury* 2021; **52**: 1321-1330 [PMID: 33454059 DOI: 10.1016/j.injury.2020.12.033]

19 **Sryma PB**, Mittal S, Tiwari P, Mohan A, Hadda V, Guleria R, Madan K. Topical nasal xylometazoline for flexible bronchoscopy (VAIN): A randomized, double-blind, placebo-controlled trial. *Respir Investig* 2021; **59**: 350-355 [PMID: 33518471 DOI: 10.1016/j.resinv.2020.12.004]

World Journal of Clinical Cases

Submit a Manuscript: https://www.f6publishing.com

World J Clin Cases 2023 April 16; 11(11): 2489-2495

DOI: 10.12998/wjcc.v11.i11.2489

ISSN 2307-8960 (online)

CASE REPORT

Intracranial large artery embolism due to carotid thrombosis caused by a neck massager: A case report

Jie Pan, Jing-Wen Wang, Xiao-Feng Cai, Ke-Feng Lu, Zhen-Zhen Wang, Shun-Yuan Guo

Specialty type: Medicine, research and experimental

Provenance and peer review: Unsolicited article; Externally peer reviewed.

Peer-review model: Single blind

Peer-review report's scientific quality classification

Grade A (Excellent): 0
Grade B (Very good): B
Grade C (Good): C
Grade D (Fair): 0
Grade E (Poor): E

P-Reviewer: Hui P, China; Park HK, South Korea; Sudevan R, India

Received: December 18, 2022
Peer-review started: December 18, 2022
First decision: January 20, 2023
Revised: February 2, 2023
Accepted: March 20, 2023
Article in press: March 20, 2023
Published online: April 16, 2023

Jie Pan, Xiao-Feng Cai, Shun-Yuan Guo, Department of Neurology, Zhejiang Provincial People's Hospital, Hangzhou 310014, Zhejiang Province, China

Jing-Wen Wang, Department of Neurology, Tiantai People's Hospital of Zhejiang Province, Taizhou 317200, Zhejiang Province, China

Ke-Feng Lu, Zhen-Zhen Wang, Department of Ultrasound Medicine, Zhejiang Provincial People's Hospital, Hangzhou 310014, Zhejiang Province, China

Corresponding author: Shun-Yuan Guo, MM, Chief Physician, Doctor, Teacher, Department of Neurology, Zhejiang Provincial People's Hospital, No. 158 Shangtang Road, Gongshu District, Hangzhou 310014, Zhejiang Province, China. gsy9316@126.com

Abstract

BACKGROUND

There are few reported cases of intracranial large artery embolism due to carotid thrombosis caused by a neck massager. Herein we report such a case.

CASE SUMMARY

A 49-year-old woman presented with left limb weakness and dysarthria after a history of neck massage for 1 mo. Neurological examination showed left central facial paralysis and left hemiparesis with a National Institutes of Health Stroke Scale score of 12. Brain magnetic resonance imaging revealed restricted diffusion on diffusion-weighted imaging in the right parietal and temporal lobes. Computed tomography angiography (CTA) indicated M3 segment embolism of the right middle cerebral artery. Neck CTA revealed thrombosis of the bilateral common carotid arteries. Carotid ultrasound showed thrombosis in the bilateral common carotid arteries (approximately 2 cm below the proximal end of the carotid sinus), and contrast-enhanced ultrasound did not suggest enhancement. No hypertension, diabetes, heart disease, vasculitis, or thrombophilia was found after admission. After 1 wk of treatment with aspirin 200 mg and atorvastatin 40 mg, a carotid ultrasound reexamination showed that the thrombosis had significantly reduced.

CONCLUSION

Neck massager may cause carotid artery thrombosis.

Key Words: Neck massager; Carotid thrombosis formed; Intracranial large artery

embolism; Stroke; Endothelial damage; Case report

Core Tip: It has been reported that stroke caused by a neck massager is mainly related to arterial dissection due to the tearing of the inner vessel. Herein we report a rare case of intracranial large artery embolism due to carotid thrombosis caused by a neck massager. Combined with the analysis of the cases indexed in PubMed, only one case of a free thrombus in the carotid artery has been reported, although the etiology is unclear. We found that an intracranial large artery embolism was due to carotid thrombosis caused by a neck massager, which was treated effectively by antiplatelet therapy. In the future, it may be necessary to study further and propose stricter quality management standards for massagers.

Citation: Pan J, Wang JW, Cai XF, Lu KF, Wang ZZ, Guo SY. Intracranial large artery embolism due to carotid thrombosis caused by a neck massager: A case report. *World J Clin Cases* 2023; 11(11): 2489-2495
URL: https://www.wjgnet.com/2307-8960/full/v11/i11/2489.htm
DOI: https://dx.doi.org/10.12998/wjcc.v11.i11.2489

INTRODUCTION

The probability of stroke caused by a neck massager is 1/300–1/400000, which is mostly related to arterial dissection due to the tearing of the vascular inner layer (mainly involving the vertebral artery, followed by the carotid artery)[1-3]. Cerebral infarction caused by arterial embolism after a massager is rare[4,5].

A neck massager stimulates the neck according to the principle of pulsed microcurrents to promote blood circulation and alleviate fatigue. In this report, we describe an intracranial large artery embolism due to carotid thrombosis caused by a neck massager.

CASE PRESENTATION

Chief complaints

Left lower limb weakness for more than 5 h.

History of present illness

More than five hours prior, left lower limb weakness suddenly occurred in a 49-year-old female patient; the left upper limb could move autonomously, but the lower limb could only shift on the bed surface. She had slurred speech, no nausea or vomiting, limb twitching, and urinary incontinence. She was given thrombolytic therapy with alteplase (50 mg) at 11:50 am in another hospital, and her symptoms did not worsen after thrombolytic treatment.

History of past illness

The patient had no history of hypertension, diabetes, hyperlipidemia, heart disease, smoking, or drinking.

Personal and family history

The patient denied any family history of malignant tumors.

Physical examination

The patient's vital signs were: Body temperature, 37.1 °C; blood pressure, 122/82 mmHg; heart rate, 82 beats per min; and respiratory rate, 18 breaths per min. The cardiopulmonary examination was normal. Her cognition seemed normal; her speech was a little vague; the neck showed soft passivity; the Kernig sign was negative; the pupils were symmetrical and 3 mm in diameter; the light reflex was normal; eye movement was normal; there was no nystagmus; bilateral hearing was symmetrical; bilateral nasolabial folds were symmetrical; and the tongue could be stuck out on request in the center.

Her left lower limb muscle strength was level 1, left upper limb muscle strength was level 5, right lower and upper limb muscle strength was level 5, and the tendon reflexes of the extremities were normal; the muscle tone of the extremities was normal; Babinski sign was positive on the left, but negative on the right; and bilateral acupuncture sensations and deep sensations were symmetrical. The

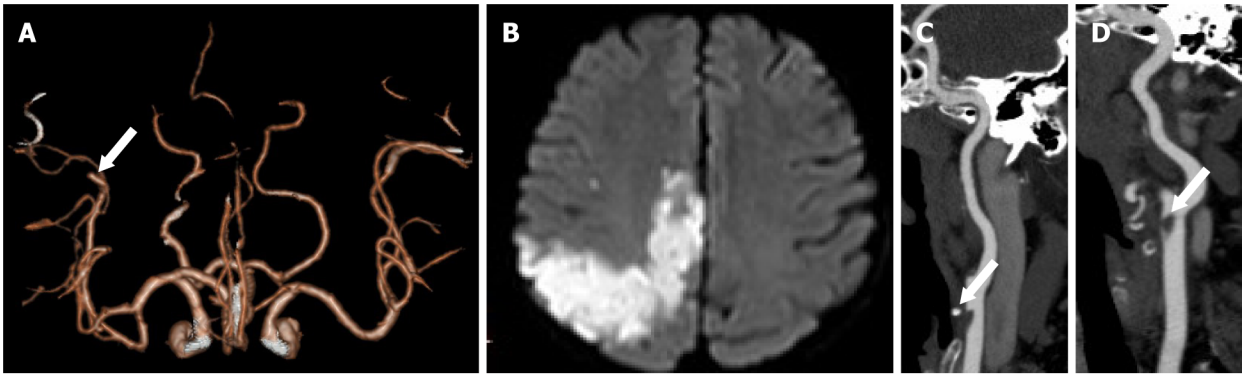

DOI: 10.12998/wjcc.v11.i11.2489

Figure 1 Image of an intracranial major artery embolism due to carotid artery thrombosis caused by a neck massager. A: Computed tomography angiography (CTA) revealed occlusion of the M3 segment of the right middle cerebral artery; B: Magnetic resonance imaging performed 24 h after hospitalization revealed multiple acute infarcts in the cortex of the right cerebral hemisphere; C and D: CTA showed thrombus formation in the distal segment of the right and left sides of the common carotid arteries.

bilateral finger-nose touch, rotation, heel, knee, and tibia tests were stable and accurate, and the closed eyes sign could not be combined. Her initial National Institutes of Health Stroke Scale (NIHSS) score was 4, the modified Rankin Scale (mRS) score was 4, and her water swallow test grade was 2.

Laboratory examinations

Laboratory results were normal except for the D-dimer level at 4410.0 μg/L. In addition, her thrombophilia genes were investigated, and the results suggested two risk factors: A 2 KB heterozygous mutation upstream of PAI-1 (NM_000602.5) and a homozygous missense mutation in MTHFR (NM_005957.5).

Imaging examinations

Computed tomography (CT) of the head showed no brain hemorrhage. CT angiography (CTA) revealed occlusion of the M3 segment of the right middle cerebral artery (MCA) (Figure 1A).

ILLNESS EVOLUTION

Clinical symptoms and signs

The next day, the patient was transferred to the neurology ward; however, the left limb weakness worsened. The NIHSS score was 12, and the mRS was 4. After 4 d of treatment, the left limb weakness improved. At discharge, the patient had improved; her NIHSS score was 2, and her mRS score was 1.

Imaging examinations

Brain magnetic resonance imaging (MRI) showed limited diffusion on diffusion-weighted imaging of the right parietal and temporal lobes (Figure 1B). CTA (Figure 1C and D) and ultrasonography (Figure 2A and B) showed bilateral common carotid artery (CCA) thrombosis. Color Doppler carotid angiography (Figure 2C and D) and high-resolution enhanced MRI (Figure 2E) suggested bilateral CCA local thrombosis. On the eighth (Figure 3A and B) and 21st (Figure 3C and D) day, carotid ultrasound was repeated, which revealed that the thrombosis was reduced in size.

Review of the history

Four months prior, the patient started to use a neck physiotherapy instrument for 1 mo (Figure 4) (twice a day, 15 min each time) because of neck muscle tension. Pulse massager is different from ordinary roller massager, which is simple to relax muscles, while pulse massager is a massage method that simulates electric moxibustion. Pulse electric moxibustion was carried out by electromagnetic frequency of electrode. Deep into the skin of the human body, a pulse massager carries out acupoint massage of the strain points and stimulates the shoulder and neck pain area and acupoints, so as to dredge the cervical vertebra, break up the nodules, dilate blood vessels, promote blood circulation, and improve strain, dizziness, and neck pain.

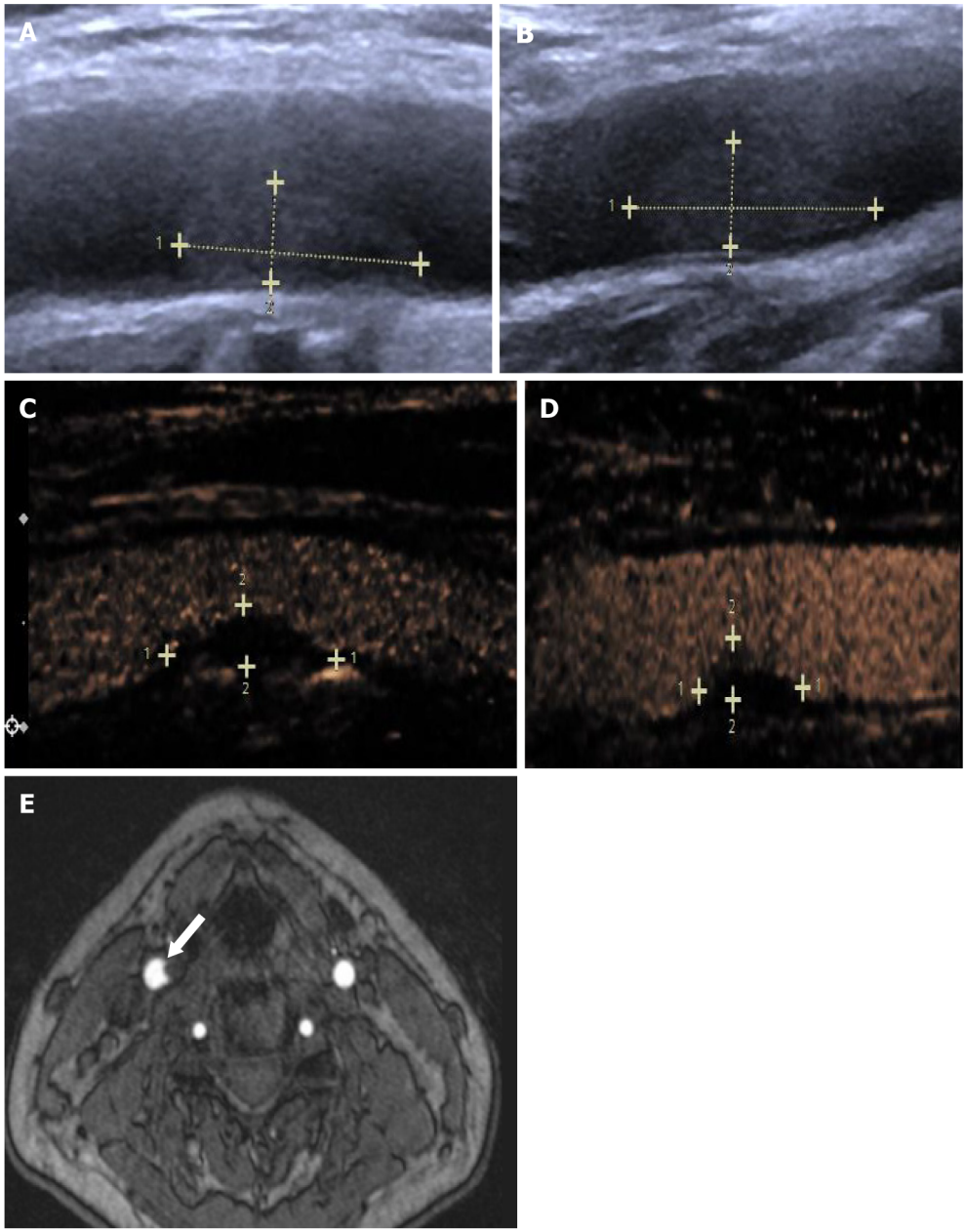

DOI: 10.12998/wjcc.v11.i11.2489

Figure 2 Carotid ultrasound and high-resolution enhanced magnetic resonance imaging of an intracranial major artery embolism due to carotid artery thrombosis caused by a neck massager. A and B: Carotid ultrasound revealed that the right extent was approximately 12.8 mm × 3.8 mm, and the left extent was approximately 14.8 mm × 4.3 mm. Contrast-enhanced ultrasound showed that the thrombus was reduced on the fourth day, with no enhancement; C and D: The right extent was approximately 6.5 mm × 2.1 mm, and the left extent was approximately 6.4 mm × 2.4 mm; E: High-resolution enhanced magnetic resonance imaging of the neck vessels suggested a filling defect in the right common carotid arterie.

FINAL DIAGNOSIS

Intracranial large artery embolism due to carotid thrombosis caused by a neck massager.

TREATMENT

The patient received intensive statin treatment (atorvastatin 40 mg).

Oral aspirin 200 mg and atorvastatin 40 mg daily were prescribed at discharge. After discharge, the aspirin was reduced to 100 mg once a day and the atorvastatin to 20 mg once a day.

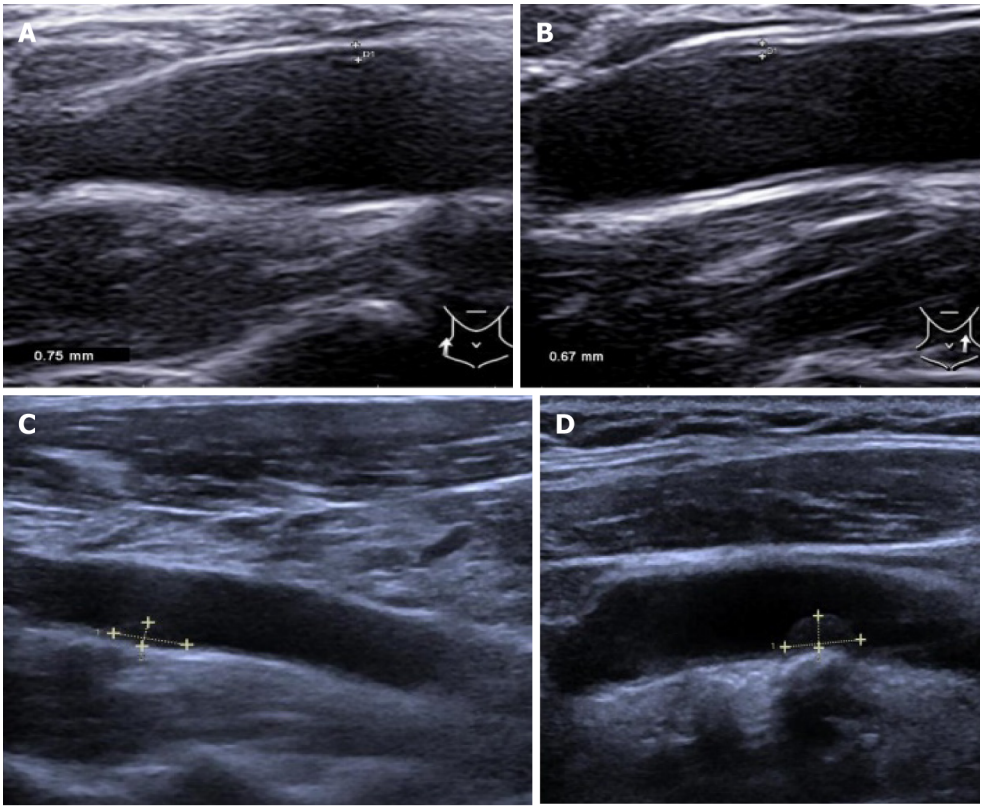

DOI: 10.12998/wjcc.v11.i11.2489

Figure 3 B-ultrasound of carotid thrombus changes after treatment. A and B: On the eighth day, carotid ultrasound showed that the thrombus was further reduced, with an extent of approximately 6.5 mm × 2.4 mm on the right and 5.3 mm × 2.1 mm on the left; C and D: Carotid ultrasound examination performed on the 14th day revealed both right and left side common carotid arteries without thrombosis.

DOI: 10.12998/wjcc.v11.i11.2489

Figure 4 Structure of the neck massager used by the patient.

OUTCOME AND FOLLOW-UP

After 6 mo of follow-up, there was no stroke recurrence, the patient's NIHSS score was 1, and her mRS score was 1. No symptoms were aggravated, no complications occurred, and no adverse events were recorded. The patient is satisfied with the treatment and can now continue with normal life.

DISCUSSION

To our knowledge, this report is the first to document a stroke caused by carotid thrombosis due to a neck massager. The brain MRI of the patient showed multiple acute infarcts in the right cerebral cortex, similar to arterial embolization. The cranial CTA showed that the M3 segment of the upper trunk of the

right MCA was occluded. Carotid ultrasound showed symmetrical thrombosis of the bilateral common carotid arteries. At the same time, other etiologies, such as cardiogenic, immune, infectious, and hematological diseases, were ruled out. After antiplatelet therapy, dynamic reexamination by carotid artery ultrasound showed that the thrombus had significantly reduced and eliminated 21 d after stroke onset. We believe that the neck massager destroyed the vascular endothelial cells in this patient, thus forming carotid artery thrombosis and causing an intracranial arterial embolism.

Cerebral infarction caused by neck massage is often secondary to vascular dissection[1-3]. Only one case of a free thrombus in the carotid artery has been reported, and the specific etiology is unclear[4]. Another case documented vertebral artery dissection after repetitive use of a handheld massage gun[5]. The literature has suggested that massager can make the blood in the carotid artery swirl[6]. Long-term changes in blood flow and acute injury of the artery may lead to changes in the structure of endothelial cells. The lipids exposed after plaque rupture activate platelets and the coagulation system to form thrombi, reducing the blood supply to the brain. In addition, endothelial damage may impact plaques on the arterial wall, causing them to break and fall off. Plaque shedding may lead to distal vascular embolism, which may cause vasospasm, intimal hyperplasia, and accelerated arteriosclerosis, resulting in intracranial arterial embolism[7].

The massager used by the patient in this report is based on the principle of pulsed microcurrents to stimulate local muscles and acupoints by fixing electrodes in the bilateral anterior cervical regions. Carotid and contrast-enhanced ultrasound in this patient suggested that the intima was intact, and the evidence for plaque rupture was insufficient. The possibility of endothelial damage was considered, which may be related to her mutations in MTHFR[8].

The treatment of carotid artery dissection may include antiplatelet therapy, anticoagulation therapy, or surgical treatment according to the incidence, clinical symptoms, and vascular conditions[9]. Emergency endovascular treatment may be selected for patients with acute intracranial large artery occlusion and hypoperfusion[10]. However, the intracranial occlusive segment of this patient was the M3 segment of the MCA, and there was no indication for emergency treatment. Carotid artery thrombosis is usually caused by atherosclerosis or carotid artery dissection; however, there is no clear guidance on drug treatment[11]. The patient's clinical symptoms improved after antiplatelet therapy, and the thrombus disappeared 21 d later, indicating that antiplatelet treatment was effective.

This patient had a stroke after starting to use a neck massager for 1 mo. Bilateral symmetrical thrombus signals occurred at the location of the CCA stimulated by the electric pulse, and the local intima was intact. The thrombus disappeared 21 d after antiplatelet treatment. The development of the thrombus was considered to be related to local endothelial injury after electric pulse stimulation. Different electric pulse frequencies may have varying effects on endothelial cells, and further research is needed to explore a more suitable safety frequency for users and establish a better approach to evaluating the safety of massagers.

The limitation of this case is that although the mechanism of intimal injury is proposed through ultrasound findings, there is no further pathology confirmation. In the future, more research is needed to find a safe massage power and formulate stricter quality management standards.

CONCLUSION

Neck massage may cause carotid artery thrombosis.

ACKNOWLEDGEMENTS

We would like to thank the patient and her family for their informed cooperation and support in our work.

FOOTNOTES

Author contributions: Pan J and Wang JW contributed equally to this work; Pan J, Wang JW, Guo SY, and Cai XF discovered the case; Lu KF and Wang ZZ verified it through B-scan; Pan J and Wang JW analyzed the reason and wrote the manuscript; All authors have read and approved the final manuscript.

Supported by Zhejiang Traditional Chinese Medicine Science and Technology Program, No. 2023ZL259.

Informed consent statement: Informed written consent was obtained from the patient to publish this report and any accompanying images.

Conflict-of-interest statement: All the authors report no relevant conflicts of interest for this article.

CARE Checklist (2016) statement: The authors have read CARE Checklist (2016), and the manuscript was prepared and revised according to CARE Checklist (2016).

Country/Territory of origin: China

ORCID number: Jing-Wen Wang 0000-0002-8720-1109; Shun-Yuan Guo 0000-0003-2945-0366.

S-Editor: Li L
L-Editor: Wang TQ
P-Editor: Li L

REFERENCES

1 **Kaur J**, Singla M, Singh G. Frequent neck massage leading to bilateral anterior cerebral artery infarction. *BMJ Case Rep* 2017; **2017** [PMID: 29103012 DOI: 10.1136/bcr-2017-222169]
2 **Chen WJ**, Qiao HY, Fang GT, Zhong X. Vertebral Artery Dissection Probably Caused by Massage: A Case Report. *Chin Med Sci J* 2019; **34**: 65-68 [PMID: 30961784 DOI: 10.24920/003480]
3 **Dutta G**, Jagetia A, Srivastava AK, Singh D, Singh H, Saran RK. "Crick" in Neck Followed by Massage Led to Stroke: Uncommon Case of Vertebral Artery Dissection. *World Neurosurg* 2018; **115**: 41-43 [PMID: 29653277 DOI: 10.1016/j.wneu.2018.04.008]
4 **Tan AP**, Taneja M, Seah BH, Leong HN, Venketasubramanian N. Acute free-floating carotid artery thrombus causing stroke in a young patient: unique etiology and management using endovascular approach. *J Stroke Cerebrovasc Dis* 2014; **23**: e437-e439 [PMID: 25440371 DOI: 10.1016/j.jstrokecerebrovasdis.2014.05.005]
5 **Sulkowski K**, Grant G, Brodie T. Case Report: Vertebral Artery Dissection After Use of Handheld Massage Gun. *Clin Pract Cases Emerg Med* 2022; **6**: 159-161 [PMID: 35701359 DOI: 10.5811/cpcem.2022.2.56046]
6 **Collins NA**, Higgins GL 3rd. Reconsidering the effectiveness and safety of carotid sinus massage as a therapeutic intervention in patients with supraventricular tachycardia. *Am J Emerg Med* 2015; **33**: 807-809 [PMID: 25907500 DOI: 10.1016/j.ajem.2015.02.047]
7 **Suwaidi JA**, Hamasaki S, Higano ST, Nishimura RA, Holmes DR Jr, Lerman A. Long-term follow-up of patients with mild coronary artery disease and endothelial dysfunction. *Circulation* 2000; **101**: 948-954 [PMID: 10704159 DOI: 10.1161/01.cir.101.9.948]
8 **Çaytemel C**, Topaloğlu Demir F, Büyükbabani N, Türkoğlu Z, Uzuner EG. Multifactorial Painful Leg Ulcers Due to Hyperhomocysteinemia, Plasminogen Activator Inhibitor-1 4G/5G Heterozygote Gene Mutation, and Beta Thalassemia Minor: A Case Report. *Int J Low Extrem Wounds* 2019; **18**: 339-341 [PMID: 31409160 DOI: 10.1177/1534734619861584]
9 **Keser Z**, Chiang CC, Benson JC, Pezzini A, Lanzino G. Cervical Artery Dissections: Etiopathogenesis and Management. *Vasc Health Risk Manag* 2022; **18**: 685-700 [PMID: 36082197 DOI: 10.2147/VHRM.S362844]
10 **Hoving JW**, Marquering HA, Majoie CBLM. Endovascular treatment in patients with carotid artery dissection and intracranial occlusion: a systematic review. *Neuroradiology* 2017; **59**: 641-647 [PMID: 28580530 DOI: 10.1007/s00234-017-1850-y]
11 **Singh RJ**, Chakraborty D, Dey S, Ganesh A, Al Sultan AS, Eesa M, Wong JH, Goyal M, Hill MD, Menon BK. Intraluminal Thrombi in the Cervico-Cephalic Arteries. *Stroke* 2019; **50**: 357-364 [PMID: 30595130 DOI: 10.1161/STROKEAHA.118.023015]

World Journal of Clinical Cases

Submit a Manuscript: https://www.f6publishing.com

World J Clin Cases 2023 April 16; 11(11): 2496-2501

DOI: 10.12998/wjcc.v11.i11.2496

ISSN 2307-8960 (online)

CASE REPORT

Intraductal papillary mucinous neoplasm originating from a jejunal heterotopic pancreas: A case report

Jun-Hao Huang, Wei Guo, Zhe Liu

Specialty type: Medicine, general and internal

Provenance and peer review: Unsolicited article; Externally peer reviewed.

Peer-review model: Single blind

Peer-review report's scientific quality classification

Grade A (Excellent): 0
Grade B (Very good): B
Grade C (Good): 0
Grade D (Fair): 0
Grade E (Poor): E

P-Reviewer: Elkady N, Egypt; Ghazanfar A, United Kingdom

Received: November 28, 2022
Peer-review started: November 28, 2022
First decision: January 19, 2023
Revised: February 1, 2023
Accepted: March 15, 2023
Article in press: March 15, 2023
Published online: April 16, 2023

Jun-Hao Huang, Wei Guo, Zhe Liu, Department of Pancreatic-Biliary Surgery, The First Hospital of China Medical University, Shenyang 110001, Liaoning Province, China

Corresponding author: Zhe Liu, MD, Professor, Surgeon, Department of Pancreatic-Biliary Surgery, The First Hospital of China Medical University, No. 155 Nanjing North Street, Shenyang 110001, Liaoning Province, China. liuzhe4321@126.com

Abstract

BACKGROUND

Intraductal papillary mucinous neoplasm (IPMN) is a rare pancreatic tumor and has the potential to become malignant. Surgery is the most effective treatment at present, but there is no consensus on the site of resection. Heterotopic pancreas occurs in the gastrointestinal tract, especially the stomach and duodenum but is asymptomatic and rare. We report a case of ectopic pancreas with IPMN located in the jejunum.

CASE SUMMARY

A 56-year-old male patient suffered from severe pain, nausea and vomiting due to a traffic accident and sought emergency treatment at our hospital. Contrast-enhanced computed tomography of the whole abdomen suggested splenic congestion, which was considered to be splenic rupture. Emergency laparotomy was performed, and the ruptured spleen was removed during the operation. Unexpectedly, a cauliflower-like mass of about 2.5 cm × 2.5 cm in size was incidentally found about 80 cm from the ligament of Treitz during the operation. A partial small bowel resection was performed, and postoperative pathology confirmed the small bowel mass as heterotopic pancreas with low-grade IPMN.

CONCLUSION

Ectopic pancreas occurs in the jejunum and is pathologically confirmed as IPMN after surgical resection.

Key Words: Heterotopic pancreas; Intraductal papillary mucinous neoplasm; Tumor; Case report; Pathology; Diagnosis

Core Tip: We report a patient who was admitted to the hospital because of splenic rupture caused by vehicle trauma. Exploratory laparotomy, splenectomy, small intestinal tumor resection, abdominal cavity irrigation and drainage were performed. Postoperative pathology confirmed a diagnosis of ectopic pancreas with intraductal papillary mucinous neoplasm.

Citation: Huang JH, Guo W, Liu Z. Intraductal papillary mucinous neoplasm originating from a jejunal heterotopic pancreas: A case report. *World J Clin Cases* 2023; 11(11): 2496-2501
URL: https://www.wjgnet.com/2307-8960/full/v11/i11/2496.htm
DOI: https://dx.doi.org/10.12998/wjcc.v11.i11.2496

INTRODUCTION

The heterotopic pancreas is anatomically separated from the main gland, and there is no continuity of blood vessels and ducts between the two[1]. Heterotopic pancreas usually occurs in the upper gastrointestinal tract, and the stomach, duodenum and proximal jejunum are the most common sites[2]. Although the disease is usually insidious and asymptomatic, some patients may experience abdominal pain, nausea, and vomiting. Heterotopic pancreas is often identified during other abdominal procedures or by accident during imaging examinations or autopsy and is more common in middle-aged males[2,3]. Ectopic pancreatic tissue also has the possibility of malignant transformation[4,5].

Intraductal papillary mucinous neoplasm (IPMN) is a pancreatic cystic tumor. It originates from pancreatic ductal epithelial cells, grows in a papillary pattern and can secrete mucin to form mucus[6,7]. According to epithelial dysplasia and malignant potential, IPMN can be divided into four types: adenoma; borderline carcinoma; carcinoma *in situ*; and invasive carcinoma[8,9]. The average age of onset of IPMN is 64 years, and the prevalence of IPMN is higher in males than in females[10]. IPMN is usually asymptomatic, but some patients may present with abdominal pain, weight instability, new-onset diabetes, pancreatitis and jaundice caused by pancreatic duct obstruction[7]. IPMN has the characteristics of malignant transformation and can eventually transform into invasive carcinoma[11]. Here, we report a rare case of pancreatic heterotopic location in the jejunum and ectopic pancreas pathologically confirmed as low-grade IPMN.

CASE PRESENTATION

Chief complaints

A 56-year-old male patient presented with trauma from a car accident 5 h prior to admission to the hospital.

History of present illness

The patient presented to the emergency department of our hospital with severe abdominal pain accompanied by nausea and vomiting, severe pain in both lower limbs and inability to stand after being hit by a motor vehicle 5 h earlier. Abdominal computed tomography (CT) showed that the shape of the spleen was irregular, and the internal density was uneven. The spleen and stomach had multiple, high-density liquid shadows. It was considered that the spleen might have ruptured because there was perisplenic hemorrhage (Figure 1).

History of past illness

Ten years ago, the patient developed chronic nephritis and urine volume gradually decreased. Uremia developed 1 year later. The patient remained anuria and was treated with hemofiltration three times a week. He regularly took creatinine-lowering medications.

Personal and family history

The patient's personal and family history was not remarkable.

Physical examination

The patient had abdominal tenderness, rebound tenderness and muscle tension.

Laboratory examinations

Laboratory examinations showed abnormalities in white blood cell count 13.64 × 10^9/L (reference range: 3.5 × 10^9-9.5 × 10^9/L), potassium 6.38 mmol/L (reference range 3.5-5.1 mmol/L), creatinine 1027 μmol/L

DOI: 10.12998/wjcc.v11.i11.2496

Figure 1 Computed tomography showed perisplenic fluid accumulation.

(reference range 58-110 μmol/L), urea 30 mmol/L (reference range 3.2-7.1 mmol/L) and hemoglobin 85 g/L (reference range 130-175 g/L).

Imaging examinations

Abdominal CT showed that the shape of the spleen was irregular, its internal density was uneven, and multiple, high-density liquid shadows were seen in the spleen and stomach, which suggested spleen rupture and perisplenic hemorrhage (Figure 1).

FINAL DIAGNOSIS

Under light microscopy, ectopic pancreatic tissue was seen in the muscular layer or submucosa of the intestinal wall, along with normal pancreatic ducts and acinar structures. Some of the ducts were dilated and lined by a single layer of gastric glandular epithelium, and some of the epithelia showed papillary growth with oval nuclei at the base. The cytoplasm was rich with mucus (Figure 2). The resected small intestinal mass suggested ectopic pancreatic tissue with low-grade IPMN. The immunohistochemistry of the tumor cells were diffusely positive for MUC5A, CDX2, CK7, CK20, AB-PAS and Ki67 (Figure 3). The patient was eventually diagnosed with low-grade IPMN, ectopic pancreas, splenic rupture and renal insufficiency.

TREATMENT

The patient underwent emergency laparotomy and splenectomy under general anesthesia. There was a 2.5 cm × 2.5 cm cauliform mass 80 cm from the small intestine to the ligament of Treitz, and partial small bowel resection was performed (Figure 4). During the operation, 100 mL liquid crystal, 2 U white and red blood cell suspension and 200 mL plasma were injected. There was 1500 mL blood loss and anuria. The patient was in critical condition because of severe trauma, blood loss and renal insufficiency. He was transferred to the intensive care unit and was given assisted ventilation, active blood transfusion, fluid replacement and anti-shock and anti-infection treatment. As the patient had a history of chronic renal insufficiency and was in the uremic stage, hemofiltration treatment was given in the intensive care unit.

OUTCOME AND FOLLOW-UP

The patient abandoned treatment.

DISCUSSION

Heterotopic pancreas is usually asymptomatic and < 2 cm, making the diagnosis difficult. The lack of effective and specific detection methods means that many patients may be misdiagnosed before surgery [12,13]. The most common CT finding is a submucosal oval mass with different lobes at the edge[2]. Submucosal tumors are usually seen on endoscopy. However, because they are covered by normal

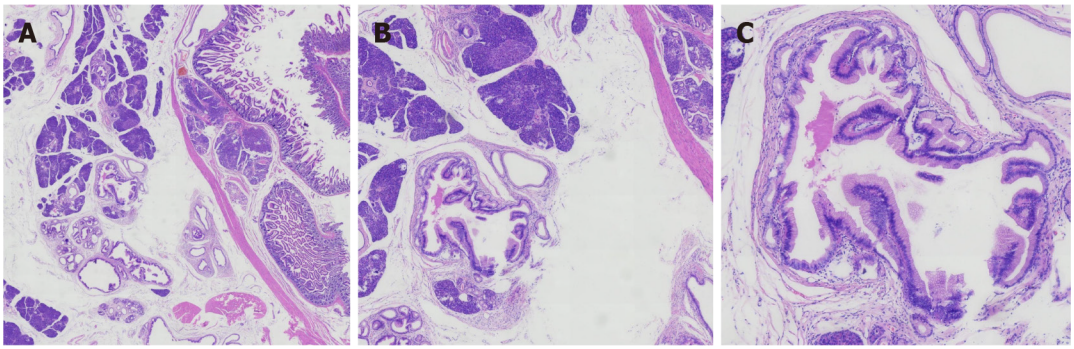

DOI: 10.12998/wjcc.v11.i11.2496

Figure 2 Histopathological analysis of the resected ectopic pancreas. A: × 15 magnification; B: × 40 magnification; C: × 100 magnification.

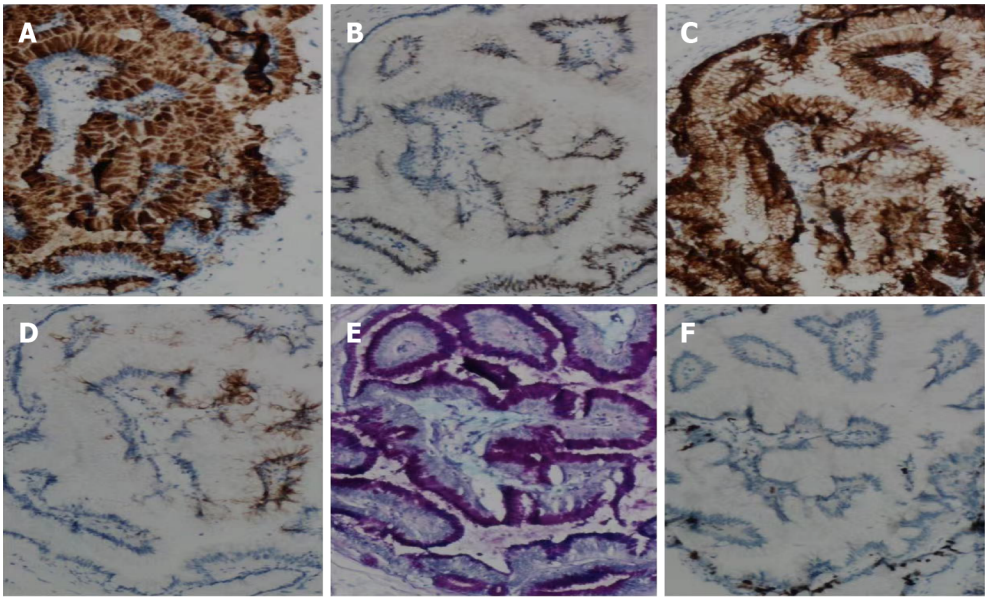

DOI: 10.12998/wjcc.v11.i11.2496

Figure 3 Immunohistochemical examination of the resected ectopic pancreas. A: MUC5A (× 100 magnification); B: CDX2 (× 100 magnification); C: CK7 (× 100 magnification); D: CK20 (× 100 magnification); E: AB-PAS (× 100 magnification); F: Ki67 (× 100 magnification).

mucosa, a valid diagnosis depends on tissue validation of the submucosa[14]. The most widely accepted mechanism of ectopic pancreas is the dislocation theory, in which pancreatic tissue deposits fall into the developing gastrointestinal system and are separated from the main body of the pancreas[15,16].

According to the location of the lesion in the pancreatic duct, IPMN can be classified into three types: main duct; branch duct; and mixed IPMN. The key to differentiating IPMN from other cystic neoplasms of the pancreas, especially from serous and mucinous cystic neoplasms, depends on the location of the tumor in the pancreatic duct[17]. All pancreatic cysts > 10 mm should be examined by CT or enhanced magnetic resonance imaging (MRI) with magnetic resonance cholangiopancreatography (MRCP). MRI/MRCP is the preferred method of examination. In addition, endoscopic ultrasound can be used to perform cyst puncture to detect the content of carcinoembryonic antigen, amylase and other indicators in fluid samples to assist diagnosis or differential diagnosis.

Surgery is the most commonly used treatment, but the consensus guidelines published in 2006 recommended that asymptomatic branch duct IPMN < 30 mm with no solid nodules can be monitored and observed first. Therefore, the choice of treatment depends on the type of IPMN and the nature and size of the tumor[18].

Our patient is a special case of heterotopic pancreas with IPMN. Emergency splenectomy was performed because of the rupture of the spleen. A small intestinal mass was accidentally found during the operation, and small intestinal tumor resection was performed after explaining the condition to the family members during the operation and consent was obtained. Although the nature of the mass was confirmed as heterotopic pancreas with low-grade IPMN by postoperative pathology, we did not take the specimen of the pancreas for pathological examination during the operation as it is difficult diagnosing heterotopic pancreas, which was considered normal when the small intestinal mass was

DOI: 10.12998/wjcc.v11.i11.2496

Figure 4 Resected spleen and ectopic pancreas (located in jejunum). The yellow arrow indicates the resected spleen, and the red arrow indicates the ectopic pancreas.

found. Therefore, more comprehensive considerations about the diagnosis and treatment of the disease are required.

CONCLUSION

Heterotopic pancreas with low-grade IPMN is a rare disease. This case may provide clinicians with a broader vision of heterotopic pancreas or IPMN to provide some new ideas for the diagnosis and differential diagnosis of pancreatic-related diseases.

FOOTNOTES

Author contributions: Huang JH and Guo W wrote the manuscript; Liu Z edited the manuscript; All authors have read and approved the final version.

Informed consent statement: Informed written consent was obtained from the patient for publication of this report and any accompanying images.

Conflict-of-interest statement: The authors declare that they have no conflicts of interest to disclose.

CARE Checklist (2016) statement: The authors have read the CARE Checklist (2016), and the manuscript was prepared and revised according to the CARE Checklist (2016).

Country/Territory of origin: China

ORCID number: Jun-Hao Huang 0000-0001-6501-599X; Wei Guo 0000-0003-0375-0950; Zhe Liu 0000-0003-2950-3966.

S-Editor: Zhang H
L-Editor: Filipodia
P-Editor: Zhang H

REFERENCES

1 **Christodoulidis G**, Zacharoulis D, Barbanis S, Katsogridakis E, Hatzitheofilou K. Heterotopic pancreas in the stomach: a case report and literature review. *World J Gastroenterol* 2007; **13**: 6098-6100 [PMID: 18023108 DOI: 10.3748/wjg.v13.45.6098]

2 **Rezvani M**, Menias C, Sandrasegaran K, Olpin JD, Elsayes KM, Shaaban AM. Heterotopic Pancreas: Histopathologic Features, Imaging Findings, and Complications. *Radiographics* 2017; **37**: 484-499 [PMID: 28287935 DOI:

10.1148/rg.2017160091]
3 **Sandrasegaran K**, Maglinte DD, Cummings OW. Heterotopic pancreas: presentation as jejunal tumor. *AJR Am J Roentgenol* 2006; **187**: W607-W609 [PMID: 17114513 DOI: 10.2214/AJR.05.0555]
4 **Ginori A**, Vassallo L, Butorano MA, Bettarini F, Di Mare G, Marrelli D. Pancreatic adenocarcinoma in duodenal ectopic pancreas: a case report and review of the literature. *Pathologica* 2013; **105**: 56-58 [PMID: 23946982]
5 **Fukumori D**, Matsuhisa T, Taguchi K, Minato M. Ectopic gastric pancreatic cancer: report of a case. *Hepatogastroenterology* 2011; **58**: 740-744 [PMID: 21830381]
6 **Bernard P**, Scoazec JY, Joubert M, Kahn X, Le Borgne J, Berger F, Partensky C. Intraductal papillary-mucinous tumors of the pancreas: predictive criteria of malignancy according to pathological examination of 53 cases. *Arch Surg* 2002; **137**: 1274-1278 [PMID: 12413317 DOI: 10.1001/archsurg.137.11.1274]
7 **Tanaka M**, Fernández-del Castillo C, Adsay V, Chari S, Falconi M, Jang JY, Kimura W, Levy P, Pitman MB, Schmidt CM, Shimizu M, Wolfgang CL, Yamaguchi K, Yamao K; International Association of Pancreatology. International consensus guidelines 2012 for the management of IPMN and MCN of the pancreas. *Pancreatology* 2012; **12**: 183-197 [PMID: 22687371 DOI: 10.1016/j.pan.2012.04.004]
8 **Lahat G**, Lubezky N, Haim MB, Nachmany I, Blachar A, Santo I, Nakache R, Klausner JM. Cystic tumors of the pancreas: high malignant potential. *Isr Med Assoc J* 2011; **13**: 284-289 [PMID: 21845969]
9 **Le Borgne J**, de Calan L, Partensky C. Cystadenomas and cystadenocarcinomas of the pancreas: a multiinstitutional retrospective study of 398 cases. French Surgical Association. *Ann Surg* 1999; **230**: 152-161 [PMID: 10450728 DOI: 10.1097/00000658-199908000-00004]
10 **Rossi RE**, Massironi S. Intraductal papillary mucinous neoplasms of the pancreas: a clinical challenge. *Expert Rev Gastroenterol Hepatol* 2018; **12**: 1123-1133 [PMID: 30264593 DOI: 10.1080/17474124.2018.1530111]
11 **Nagai E**, Ueki T, Chijiiwa K, Tanaka M, Tsuneyoshi M. Intraductal papillary mucinous neoplasms of the pancreas associated with so-called "mucinous ductal ectasia". Histochemical and immunohistochemical analysis of 29 cases. *Am J Surg Pathol* 1995; **19**: 576-589 [PMID: 7726368 DOI: 10.1097/00000478-199505000-00010]
12 **Lin J**, Yu Y, Chen Y, Zheng M, Zhou D. Heterotopic pancreatic cyst in the adrenal gland: A case report and review of literature. *Medicine (Baltimore)* 2018; **97**: e9414 [PMID: 29505516 DOI: 10.1097/MD.0000000000009414]
13 **Sathyanarayana SA**, Deutsch GB, Bajaj J, Friedman B, Bansal R, Molmenti E, Nicastro JM, Coppa GF. Ectopic pancreas: a diagnostic dilemma. *Int J Angiol* 2012; **21**: 177-180 [PMID: 23997566 DOI: 10.1055/s-0032-1325119]
14 **Agale SV**, Agale VG, Zode RR, Grover S, Joshi S. Heterotopic pancreas involving stomach and duodenum. *J Assoc Physicians India* 2009; **57**: 653-654 [PMID: 20214004]
15 **Kim DW**, Kim JH, Park SH, Lee JS, Hong SM, Kim M, Ha HK. Heterotopic pancreas of the jejunum: associations between CT and pathology features. *Abdom Imaging* 2015; **40**: 38-45 [PMID: 24934475 DOI: 10.1007/s00261-014-0177-y]
16 **Shin SS**, Jeong YY, Kang HK. Giant heterotopic pancreas in the jejunal mesentery. *AJR Am J Roentgenol* 2007; **189**: W262-W263 [PMID: 17954622 DOI: 10.2214/AJR.05.1142]
17 **Del Chiaro M**, Verbeke C. Intraductal papillary mucinous neoplasms of the pancreas: reporting clinically relevant features. *Histopathology* 2017; **70**: 850-860 [PMID: 27878841 DOI: 10.1111/his.13131]
18 **Crippa S**, Arcidiacono PG, De Cobelli F, Falconi M. Review of the diagnosis and management of intraductal papillary mucinous neoplasms. *United European Gastroenterol J* 2020; **8**: 249-255 [PMID: 32213017 DOI: 10.1177/2050640619894767]

World Journal of Clinical Cases

Submit a Manuscript: https://www.f6publishing.com

World J Clin Cases 2023 April 16; 11(11): 2502-2509

DOI: 10.12998/wjcc.v11.i11.2502

ISSN 2307-8960 (online)

CASE REPORT

Application of endoscopic retrograde cholangiopancreatography for treatment of obstructive jaundice after hepatoblastoma surgery: A case report

Jun Shu, Hu Yang, Jun Yang, Hong-Qiang Bian, Xin Wang

Specialty type: Medicine, research and experimental

Provenance and peer review: Unsolicited article; Externally peer reviewed.

Peer-review model: Single blind

Peer-review report's scientific quality classification

Grade A (Excellent): 0
Grade B (Very good): B
Grade C (Good): 0
Grade D (Fair): D
Grade E (Poor): 0

P-Reviewer: Amornyotin S, Thailand; Rashid R, Bangladesh

Received: December 2, 2022
Peer-review started: December 2, 2022
First decision: January 5, 2023
Revised: January 14, 2023
Accepted: March 21, 2023
Article in press: March 21, 2023
Published online: April 16, 2023

Jun Shu, Hu Yang, Jun Yang, Hong-Qiang Bian, Xin Wang, Department of General Surgery, Wuhan Children' Hospital, Tongji Medical College, Huazhong University of Science and Technology, Wuhan 430000, Hubei Province, China

Corresponding author: Xin Wang, MD, Surgeon, Department of General Surgery, Wuhan Children' Hospital, Tongji Medical College, Huazhong University of Science and Technology, No. 100 Hong Kong Road, Wuhan 430000, Hubei Province, China.
wangxin20150710@163.com

Abstract

BACKGROUND

We aimed to investigate the effectiveness of endoscopic retrograde cholangiopancreatography (ERCP) for treating obstructive jaundice (OJ) post hepatoblastoma (HB) surgery (post-HB OJ) by analyzing the data of a case and performing a literature review.

CASE SUMMARY

Clinical data of one patient with post-HB OJ treated by ERCP were retrospectively analyzed. Furthermore, clinical characteristics and insights into the diagnosis and treatment of post-HB OJ in children were summarized *via* searching various databases and platforms, such as China National Knowledge Infrastructure, Wanfang database, CQVIP database, PubMed, Ringer Link, and Google Scholar. The patient reported herein underwent five chemotherapy sessions after the diagnosis of HB and right hemihepatectomy after tumor size reduction; these were followed by two postoperative chemotherapy sessions. Three months postoperatively, the patient developed icteric sclera, strong tea-colored urine, and clay-like stools, and showed signs of skin itchiness; blood analysis showed significantly an increased conjugated bilirubin (CB) level (200.3 μmol/L). Following the poor efficacy of anti-jaundice and hepatoprotective treatments, the patient underwent ERCP. Intraoperative imaging showed a dilated bile duct in the porta hepatis with significant distal stenosis. A 5 Fr nasopancreatic tube was placed in the dilated area through the stricture for external drainage, and the patient was extubated on postoperative day 6. Postoperatively, the patient's stool turned yellow, and the CB level decreased to 78.2 μmol/L. Fifteen days later, ERCP was repeated due to unrelieved jaundice symptoms, wherein a 7 Fr nasobiliary drainage tube was successfully placed. Three months post-ERCP, the

jaundice symptoms resolved, and the CB level was reduced to 33.2 μmol/L. A follow-up examination one year postoperatively revealed no jaundice symptoms and normal CB level.

CONCLUSION
Post-HB OJ is rare. Compared to biliary tract reconstruction, ERCP is less invasive and has a better therapeutic effect.

Key Words: Endoscopic retrograde cholangiopancreatography; Hepatoblastoma; Pediatric patients; Obstructive jaundice; Case report

Core Tip: This study aimed to investigate the effectiveness of endoscopic retrograde cholangiopancreatography (ERCP) in the treatment of obstructive jaundice following hepatoblastoma surgery by analyzing the data of a case and performing a literature review. We found that ERCP is less invasive and has a better therapeutic effect compared to biliary tract reconstruction.

Citation: Shu J, Yang H, Yang J, Bian HQ, Wang X. Application of endoscopic retrograde cholangiopancreatography for treatment of obstructive jaundice after hepatoblastoma surgery: A case report. *World J Clin Cases* 2023; 11(11): 2502-2509
URL: https://www.wjgnet.com/2307-8960/full/v11/i11/2502.htm
DOI: https://dx.doi.org/10.12998/wjcc.v11.i11.2502

INTRODUCTION

Hepatoblastoma (HB) is a common malignant, solid tumor that affects children's livers and accounts for approximately two-thirds of all liver malignancies; it has an overall survival rate of 70% to 80%[1]. Presently, a surgery-based multidisciplinary management strategy with chemotherapy is the standard treatment modality for HB. HB-related postoperative complications include obstructive jaundice (OJ), which is rare. OJ is manifested clinically as generalized yellowing of the skin and sclera, skin pruritus, yellow urine, and clay-like stools. Furthermore, perioperative liver function impairment, biliary tract infection, and liver failure are also observed, and they critically affect the patient's postoperative recovery[2]. The effectiveness and safety of endoscopic retrograde cholangiopancreatography (ERCP) in the management of adult biliary and pancreatic diseases are well known; however, its application in children is scarce due to the low incidence of biliopancreatic diseases in children, lack of relevant pediatric instruments, special characteristics associated with pediatric cases, and operational difficulties. This paper reports a case of post-HB surgery OJ (post-HB OJ) treated by ERCP. Moreover, effective diagnosis and treatment methods are explored based on a literature review.

CASE PRESENTATION

Chief complaints

A one-year-old female child presented to a local hospital with an abdominal mass.

History of present illness

The patient presented with icteric sclera and symptoms of itchy skin at 3 mo after a right hemihepatectomy.

History of past illness

The patient was examined and diagnosed with HB for which she underwent five chemotherapy sessions and a right hemihepatectomy after tumor size reduction. These were followed by two postoperative chemotherapy sessions. These were followed by two postoperative chemotherapy sessions.

Physical examination

Strong tea-colored urine and clay-like stools were reported. Blood examinations revealed significantly increased conjugated bilirubin (CB) (200.3 μmol/L) and total bilirubin (293.6 μmol/L) levels.

Laboratory examinations

The patient's gamma-glutamyl transpeptidase (1834 U/L), alanine transaminase (104 U/L), and aspartate aminotransferase (210 U/L) levels were elevated. However, atomolam, inosine, intravenous ornithine aspartate drip, oral ursodeoxycholic acid, and compound glycyrrhizin tablet administered at the local hospital proved ineffective.

Imaging examinations

Magnetic resonance cholangiopancreatography (MRCP) showed a dilated bile duct in the porta hepatis (widest diameter, approximately 12 mm) (Figure 1).

FINAL DIAGNOSIS

The patient underwent ERCP under general anesthesia in our hospital. After routine intubation, MRCP showed a slender common bile duct (2 mm) and contrast agent accumulation in the porta hepatis, and the intrahepatic bile duct and the middle and lower common bile ducts could not be visualized (Figure 2). Pressurized contrast imaging demonstrated a dilated bile duct in the porta hepatis with significant stenosis at its distal terminal. The difficult passage at this site caused the guidewire to bend, leading to a filling defect (Figure 3).

TREATMENT

A 7 Fr nasobiliary drainage tube could not pass through the stricture (Figure 4A), and with great difficulty, a 6 Fr nasobiliary drainage tube was passed through. Subsequently, on poatoperative day 6, a 5 Fr nasopancreatic tube was placed at the dilatation through the stricture for external drainage (Figure 4B) and the patient was extubated. During this time, the patient's stools turned yellow, and the CB level decreased to 78.2 μmol/L. Fifteen days later, ERCP was repeated due to unalleviated jaundice symptoms. Although the imaging results still suggested bile duct dilatation in the porta hepatis, the intrahepatic bile duct, and the lower and middle common bile ducts could not be visualized (Figure 4C), along with balloon dilatation of the stenosis. Finally, a 7 Fr nasobiliary drainage tube was successfully inserted (Figure 4D).

OUTCOME AND FOLLOW-UP

Three months after the second ERCP, the patient's jaundice symptoms mostly resolved; furthermore, the patient's CB level decreased to 33.2 μmol/L. A one-year follow-up revealed that the jaundice symptoms had disappeared and the patient had normal bilirubin level.

China National Knowledge Infrastructure, Wanfang database, CQVIP database, PubMed, Ringer Link, and Google Scholar were searched until April 2022 with the keywords hepatoblastoma, obstructive jaundice, and biliary obstruction. The inclusion criteria for the studies were as follows: (1) Patients with a diagnosis of HB with surgical treatment; (2) Those with postoperative OJ; and (3) Those who underwent treatment of OJ *via* surgical methods, including biliary tract reconstruction and ERCP. Duplicate cases reported by the same author, institute, hospital, and database were excluded.

Five studies that met the requirements were included in the review; two studies were written in English and three in Chinese. A total of six cases were analyzed, of which five met the inclusion criteria. One patient with HB developed post-HB OJ and died of liver failure without surgical treatment and was excluded from the review. Finally, five patients from the retrieved studies and the patients in this case report were included (Table 1). All children presented with post-HB OJ within 14 d to 4 mo postoperatively. Five patients developed OJ due to intraoperative biliary injury; whereas, one patient developed OJ and elevated liver stiffness which was attributed to biliary injury-related bile leakage[3]. Furthermore, one patient developed biliary obstruction due to a postoperatively regenerated liver that compressed the bile duct[4]. Four patients underwent biliary tract reconstruction[3-6] and recovered well postoperatively. One patient developed severe malnutrition post percutaneous transhepatic cholangial drainage (PTCD); however, subsequent biliary tract reconstruction facilitated good recovery [7]. As mentioned previously, the patient in this report was treated by ERCP and recovered well after surgery.

DISCUSSION

Post-HB OJ is a rare complication and is associated with injury or compression of trunk ducts, such as

Table 1 Clinical data of six children with obstructive jaundice after hepatoblastoma operation

Ref.	Case	Age (mo)	Sex	Surgery	Time of postoperative obstructive jaundice	Reason	Solution	Prognosis
Canty[4], 1991	2	6	Male	Right hemihepatectomy	4 mo	Postoperative liver regeneration caused biliary obstruction	Biliary tract reconstruction operation	Good
		2	Male	Right hemihepatectomy	14 d	Postoperative liver regeneration caused biliary obstruction	-	Died of jaundice and liver failure 4 mo after surgery
Murphy *et al*[7], 2012	1	12	Female	Right hemihepatectomy	2.5 mo	Left hepatic duct injury	PTCD failed followed by biliary tract reconstruction operation	Good
Liu *et al* [5], 2015	1	1	–	–	–	Right hepatic duct injury	Biliary tract reconstruction operation	Good
Yao *et al* [6], 2018	1	11	Male	Left hemihepatectomy and VII/VIII section resection	16 d	Right hepatic duct injury	Biliary tract reconstruction operation	Good
Feng *et al* [3], 2020	1	–	–	–	–	Biliary tract injury forms biliary leakage	Biliary tract reconstruction operation	Good
This Study	1	12	Female	Right hemihepatectomy	3 mo	Hepatic duct injury	ERCP	Good

ERCP: Endoscopic retrograde cholangiopancreatography; PTCD: Percutaneous transhepatic cholangial drainage.

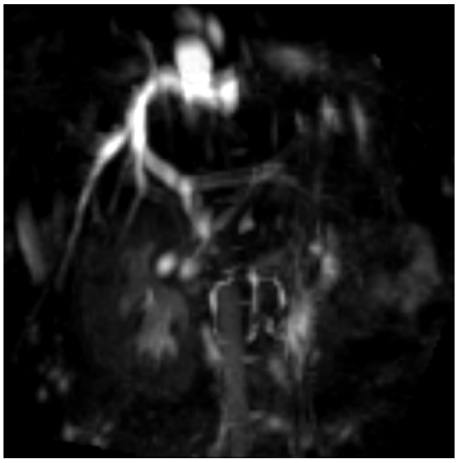

DOI: 10.12998/wjcc.v11.i11.2502

Figure 1 Magnetic resonance cholangiopancreatography examination demonstrating dilatation of the common bile duct in the porta hepatis with the widest diameter of approximately 12 mm.

the right or left hepatic ducts. Incomplete ligation of small bile ducts in the hepatectomy section dislodged ligatures, and necrosis are responsible for bile leakage. In five of the six children included in this review, OJ developed due to injury to the main hepatic duct. Moreover, a rare case of OJ due to postoperative liver regeneration was also noted[4]. Remarkable liver regeneration is observed post hepatectomy, which is typically initiated within a few days postoperatively and is completed within a few months. Rapid macronodular regeneration of the liver leads to stretching, compression, and eventual ischemic fibrosis of the extrahepatic biliary system, resulting in OJ. One child in this review developed postoperative bile leakage due to damage to the main hepatic duct. However, the bile leakage did not resolve after drainage, and local infection and encapsulated effusion were observed. Long-term conservative treatment led to inflammatory scar formation and tissue fragility around the bile leakage site, leading to OJ and increased liver stiffness[3]. However, damage to the main hepatic

DOI: 10.12998/wjcc.v11.i11.2502

Figure 2 Aggregation of contrast in the porta hepatis and non-visualization of the intrahepatic bile duct and the middle and lower common bile ducts.

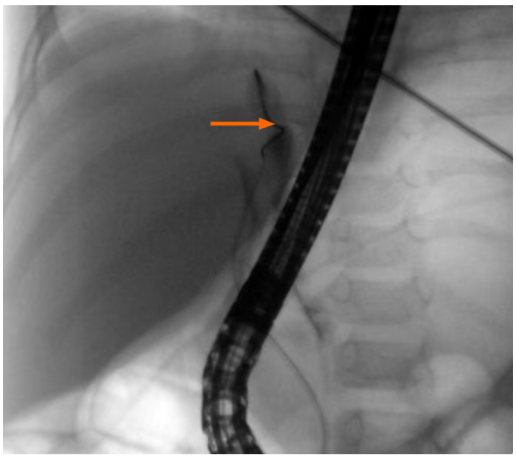

DOI: 10.12998/wjcc.v11.i11.2502

Figure 3 Dilated bile duct in the porta hepatis with significant distal stenosis (arrow), as observed *via* pressurized contrast imaging.

duct does not consistently lead to bile leakage. In one child, the left hepatic duct was ligated extremely close to the common hepatic duct, resulting in a slight angle at the convergence of the right hepatic duct into the common hepatic duct and causing OJ due to poor bile flow[6].

Children with biliary tract infections present with abdominal pain. In addition, children who develop OJ after bile leakage may present with intestinal obstruction, localized and systemic infections, and liver stiffness due to severe abdominal infection. In such cases, hematological tests may demonstrate elevated total bilirubin levels, especially CB levels, with increased transaminases. Ultrasound is the preferred diagnostic modality for biliary obstruction because it is noninvasive, simple, efficient, and economical. However, computed tomography (CT), MPCP, and ERCP are required for confirming the diagnosis. Enhanced CT can demonstrate the tumor's recurrence post-HB surgery, locate the bile duct obstruction site, and determine the degree of bile duct dilatation. Additionally, it can also characterize the morphology and thickness of the bile duct wall. The diagnostic value of MRCP for pancreaticobiliary duct disease is well recognized as it clearly shows the pancreatic-bile duct structure; however, it is not ideal for diagnosing microscopic stones or lesions when pancreaticobiliary duct obstruction and dilatation are not apparent, especially when combined with ascites.

Effective treatments for post-HB OJ include biliary tract reconstruction, PTCD, and ERCP, of which biliary tract reconstruction is the most commonly used method. Despite its definite efficiency, its drawbacks are apparent, including the need for re-laparotomy for choledochojejunostomy and major surgical strikes. PTCD puncture requires a skilled surgeon with expertise in X-ray or ultrasound-guided puncture, and the continuous flow of bile into the abdominal cavity after failed catheterizing leads to acute peritonitis, requiring emergency surgery in severe cases[8]. PTCD is more effective for bile drainage; however, it is prone to complications, such as drainage tube blockage, infection, dislodgement, and bile loss, which cause an imbalance in the internal homeostasis of the body.

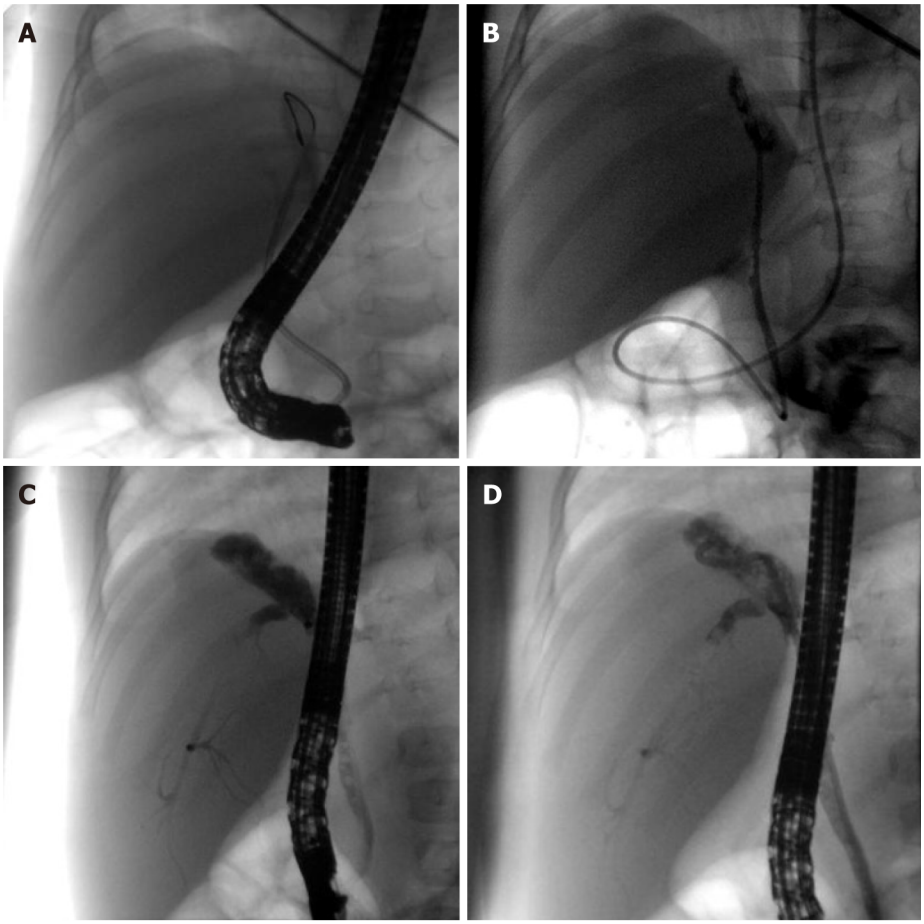

DOI: 10.12998/wjcc.v11.i11.2502

Figure 4 Treatment of the patient. A: Inability and difficulty in passing the stenosis using a 7 Fr nasobiliary drainage tube; B: Smooth passage of a 5 Fr nasopancreatic tube through the stenosis; C: Dilatation of the bile ducts in the porta hepatis with visualization of the intrahepatic bile duct and the middle and lower common bile ducts; D: Smooth placement of a 7 Fr nasobiliary drainage tube.

Furthermore, pediatric care is highly demanding. Despite managing jaundice by external drainage with PTCD, one child developed severe malnutrition; however, the final biliary tract reconstruction facilitated spontaneous recovery[7]. Compared to ERCP, placement of inner support *via* PTCD is a highly traumatic procedure with the formation of a dead zone and is prone to migration into the duodenum, thus possibly triggering intestinal perforation[9].

Biliary stricture is a common complication observed post-liver transplantation and biliary surgery in adults. Its incidence after liver transplantation and due to direct injury during cholecystectomy is approximately 10%-40% and 0.5%, respectively[10,11]. Placement of balloon-dilated stents *via* the ERCP route for biliary strictures is safe, effective, minimally invasive, and the first-line treatment option for benign biliary strictures[12]. ERCP is the preferred treatment modality for simple anastomotic stenosis combined with bile duct calculi and can remarkably improve a patient's clinical symptoms and quality of life; however, patients undergoing ERCP require multiple removals and replacements of plastic stents with poor biocompatibility. Biodegradable biliary stents and tectorial self-expanding metal stents are used clinically and have a longer drainage time and reduce the frequency of stent replacements in a short period. ERCP has a low cure rate in patients with non-anastomotic strictures, especially diffuse strictures combined with calculus; nevertheless, it can provide short-term relief by alleviating the patient's clinical symptoms and improving the general condition. Thus, ERCP can be used as a transitional treatment modality. Moreover, failures of ERCP or poor treatment outcomes do not aggravate the patients' clinical conditions, and PTCD or surgical treatment is still feasible.

The lower frequency of ERCP use as a treatment modality in children compared to adults may be attributed to the relatively low probability of ERCP use in childhood, lack of physicians with extensive relevant experience, and lack of specialized equipment for children[13]. Recent years has witnessed increased use of ERCP for the treatment of pediatric pancreaticobiliary diseases, including congenital pancreaticobiliary diseases, biliary calculi, biliary strictures, pancreas divisum, and acute and chronic pancreatitis in children. This can be attributed to the advancements of duodenoscopic techniques in children and the involvement of adult endoscopists. Although MRCP has become a routine imaging modality for biliary obstructive disease, ERCP remains the gold standard for the diagnosis of biliary obstructive diseases since it allows for simultaneous examination and treatment[14]. The goal of biliary

obstruction treatment is long-term bile duct decompression and maintenance of bile duct patency, and endoscopic balloon dilation followed by placement of stents is one of the primary treatment modalities. Jaundice symptoms of our case disappeared 6 mo after the placement of a 7 Fr nasobiliary drainage tube *via* ERCP, and normal bilirubin levels were observed. In addition, the patient lived normally after extubation. Based on the results of a subsequent follow-up examination of the child, a 9 Fr biliary stent can be considered feasible for dilation and drainage when necessary. Despite the good efficacy of external nasobiliary drainage under ERCP, the tube had to be placed for a long period, remarkably influencing her and her family members. Therefore, placement of a biliary stent under ERCP for internal drainage may be a more optimal option for the treatment of biliary obstruction[15].

We recommend patients who meet the following indications to apply ERCP procedure: (1) Patients who are 10 kg or over or 1 year old or over; (2) A history of hepatectomy which may cause iatrogenic biliary stricture during surgery; and (3) Postoperative clinical findings, laboratory examination, and imaging examination results suggested biliary obstruction.

The effectiveness of ERCP in treating these cases is also affected by the following factors: (1) Scope of the first surgical resection and the degree of bile duct injury; (2) The patient's own ability to repair and regenerate the biliary tract; (3) The patient's degree of adaptation to biliary balloon dilatation; (4) The unobstructed time of the bile stent; and (5) Biliary tract infection and systemic infection of the patient. And the need of multiple ERCP operations is also the limitation of the therapy.

CONCLUSION

In summary, post-HB OJ is rare. ERCP aids in avoiding unnecessary surgical procedures, is less invasive, and shows better treatment outcomes than biliary tract reconstruction.

FOOTNOTES

Author contributions: Wang X and Shu J designed the research study; Wang X and Yang H performed the research; Wang X, Yang J, and Bian HQ analyzed the data and wrote the manuscript; All authors have read and approved the final manuscript.

Informed consent statement: The study received the patient's consent and approval from the hospital's ethics committee.

Conflict-of-interest statement: All the authors report no relevant conflicts of interest for this article.

CARE Checklist (2016) statement: The authors have read CARE Checklist (2016), and the manuscript was prepared and revised according to CARE Checklist (2016).

Country/Territory of origin: China

ORCID number: Xin Wang 0000-0002-0153-953X.

S-Editor: Li L
L-Editor: Wang TQ
P-Editor: Li L

REFERENCES

1 **Hiyama E**, Hishiki T, Watanabe K, Ida K, Yano M, Oue T, Iehara T, Hoshino K, Koh K, Tanaka Y, Kurihara S, Ueda Y, Onitake Y. Mortality and morbidity in primarily resected hepatoblastomas in Japan: Experience of the JPLT (Japanese Study Group for Pediatric Liver Tumor) trials. *J Pediatr Surg* 2015; **50**: 2098-2101 [PMID: 26388131 DOI: 10.1016/j.jpedsurg.2015.08.035]

2 **Saxena P**, Kumbhari V, Zein ME, Khashab MA. Preoperative biliary drainage. *Dig Endosc* 2015; **27**: 265-277 [PMID: 25293587 DOI: 10.1111/den.12394]

3 **Feng J**, Wang HM, Qin H, Yang W, Han W, Cheng HY, Chang XF, Zhu ZY, Han JY. [Diagnosis and treatment of postoperative biliary fistula in children with hepatoblastoma]. *Zhonghua Xiaoer Waike Zazhi* 2020; **19**: 794-799 [DOI:

10.3969/j.issn.1671-6353.2020.09.007]
4 **Canty TG Sr**. Biliary obstruction from hepatic regeneration following extended right hepatectomy for tumor. *J Pediatr Surg* 1991; **26**: 830-833 [PMID: 1654407 DOI: 10.1016/0022-3468(91)90149-n]
5 **Liu GB**, Liu BH, Ma YY, Li K, Dong KR. [Neonatal hepatoblastoma: a report of 8 cases with a literature review]. *Zhonghua Xiaoer Waike Zazhi* 2015; **36**: 269-272 [DOI: 10.3760/cma.j.issn.0253-3006.2015.04.007]
6 **Yao W**, Dong KR, Xiao XM, Zheng JC, Li Km, Liu XQ, Liu BH, Zheng S. [Associating liver partition and portal vein ligation for staged hepatectomy for hepatoblastoma: a report of one case]. *Zhonghua Xiaoer Waike Zazhi* 2018; **39**: 597-603 [DOI: 10.3760/cma.j.issn.0253-3006.2018.08.009]
7 **Murphy AJ**, Rauth TP, Lovvorn HN 3rd. Chronic biloma after right hepatectomy for stage IV hepatoblastoma managed with Roux-en-Y biliary cystenterostomy. *J Pediatr Surg* 2012; **47**: e5-e9 [PMID: 23164033 DOI: 10.1016/j.jpedsurg.2012.06.007]
8 **Du CX**, Li JX, Li DR, Su MB, Ya XQ, Wang WB, Liu JH. [A study comparing PTCD with ENBD on jaundiced patients before laparoscopic pancreaticoduodenectomy]. *Zhonghua Gandan Waike Zazhi* 2022; **28**: 4 [DOI: 10.3760/cma.j.cn113884-20210621-00201]
9 **Sun D**, Liu YG, Yang JQ, Liu S, Zhu GQ. [Therapeutic effect of PTCD in combination with ERCP on malignant obstructive jaundice]. *Zhonghua Gandan Waike Zazhi* 2010; **(4)**: 308-309 [DOI: 10.3760/cma.j.issn.1007-8118.2010.04.023]
10 **Hildebrand T**, Pannicke N, Dechene A, Gotthardt DN, Kirchner G, Reiter FP, Sterneck M, Herzer K, Lenzen H, Rupp C, Barg-Hock H, de Leuw P, Teufel A, Zimmer V, Lammert F, Sarrazin C, Spengler U, Rust C, Manns MP, Strassburg CP, Schramm C, Weismüller TJ; German PSC Study Group. Biliary strictures and recurrence after liver transplantation for primary sclerosing cholangitis: A retrospective multicenter analysis. *Liver Transpl* 2016; **22**: 42-52 [PMID: 26438008 DOI: 10.1002/lt.24350]
11 **Grönroos JM**. Endoscopic management of postcholecystectomy bile duct strictures. *J Am Coll Surg* 2008; **207**: 786-7; author reply 787 [PMID: 18954798 DOI: 10.1016/j.jamcollsurg.2008.08.001]
12 **Kuroda Y**, Tsuyuguchi T, Sakai Y, K C S, Ishihara T, Yamaguchi T, Saisho H, Yokosuka O. Long-term follow-up evaluation for more than 10 years after endoscopic treatment for postoperative bile duct strictures. *Surg Endosc* 2010; **24**: 834-840 [PMID: 19730951 DOI: 10.1007/s00464-009-0673-2]
13 **Jang JY**, Yoon CH, Kim KM. Endoscopic retrograde cholangiopancreatography in pancreatic and biliary tract disease in Korean children. *World J Gastroenterol* 2010; **16**: 490-495 [PMID: 20101777 DOI: 10.3748/wjg.v16.i4.490]
14 **Park ET**. Endoscopic Retrograde Cholangiopancreatography in Bilioenteric Anastomosis. *Clin Endosc* 2016; **49**: 510-514 [PMID: 27838918 DOI: 10.5946/ce.2016.138]
15 **Sun B**, Yu D, Chen J, Tang Y, Wu H. Endoscopic biliary drainage management for children with serious cholangitis caused by congenital biliary dilatation. *Pediatr Surg Int* 2018; **34**: 897-901 [PMID: 29872885 DOI: 10.1007/s00383-018-4296-3]

World Journal of Clinical Cases

Submit a Manuscript: https://www.f6publishing.com

World J Clin Cases 2023 April 16; 11(11): 2510-2520

DOI: 10.12998/wjcc.v11.i11.2510

ISSN 2307-8960 (online)

CASE REPORT

Total removal of a large esophageal schwannoma by submucosal tunneling endoscopic resection: A case report and review of literature

Yu-Zhu Mu, Qi Zhang, Jing Zhao, Yan Liu, Ling-Wei Kong, Zhong-Xiang Ding

Specialty type: Gastroenterology and hepatology

Provenance and peer review: Unsolicited article; Externally peer reviewed.

Peer-review model: Single blind

Peer-review report's scientific quality classification

Grade A (Excellent): 0
Grade B (Very good): B, B
Grade C (Good): C, C
Grade D (Fair): 0
Grade E (Poor): 0

P-Reviewer: Al-Ani RM, Iraq; Hakimi T, Afghanistan

Received: December 23, 2022
Peer-review started: December 23, 2022
First decision: January 3, 2023
Revised: January 14, 2023
Accepted: March 21, 2023
Article in press: March 21, 2023
Published online: April 16, 2023

Yu-Zhu Mu, Department of Radiology, The Fourth School of Clinical Medicine, Zhejiang Chinese Medical University, Hangzhou 310006, Zhejiang Province, China

Yu-Zhu Mu, Ling-Wei Kong, Zhong-Xiang Ding, Department of Radiology, Affiliated Hangzhou First People's Hospital, Zhejiang University School of Medicine, Hangzhou 310006, Zhejiang Province, China

Qi Zhang, Department of Radiology, The First Affiliated Hospital of Zhejiang Chinese Medical University, Hangzhou 310006, Zhejiang Province, China

Jing Zhao, Department of Gastroenterology, The First Affiliated Hospital of Zhejiang Chinese Medical University, Hangzhou 310006, Zhejiang Province, China

Yan Liu, Department of Pathology, The First Affiliated Hospital of Zhejiang Chinese Medical University, Hangzhou 310006, Zhejiang Province, China

Corresponding author: Zhong-Xiang Ding, Doctor, PhD, Professor, Department of Radiology, Affiliated Hangzhou First People's Hospital, Zhejiang University School of Medicine, No. 261 Huansha Road, Hangzhou 310006, Zhejiang Province, China. hangzhoudzx73@126.com

Abstract

BACKGROUND

Primary schwannoma is a rare submucosal tumor of the esophagus, which is most often benign, and surgery is the only effective treatment. So far, only a few cases have been reported. Herein, we reported a single case diagnosed with primary esophageal schwannoma that was totally removed by submucosal tunneling endoscopic resection (STER).

CASE SUMMARY

A 62-year-old man presented to the hospital with a history of resection of a malignant gastric tumor and mild dysphagia. Endoscopic examination revealed a large submucosal elevated lesion in the esophagus 25-30 cm from the incisors. Endoscopic ultrasonography detected a 45 mm × 35 mm × 31 mm hypoechoic lesion; chest computed tomography showed a mass of approximately 55 mm × 35 mm × 29 mm. A preliminary examination showed features suggestive of a stromal tumor. Pathological findings indicated esophageal schwannoma. Next, STER alone was performed to completely resect the mass, and the patient recovered

well post-surgery. Afterward, the patient was discharged and showed no tumor recurrence at 33 mo of follow-up.

CONCLUSION
Endoscopic resection is still an effective treatment for large esophageal schwannomas (> 30 mm) under meticulous morphological evaluation.

Key Words: Esophageal schwannoma; Submucosal tunneling endoscopic resection; S100; Submucosal; Case report

Core Tip: Primary esophageal schwannoma is a rare esophageal submucosal tumor that is usually benign. The final diagnosis requires histopathological and immunohistochemical examinations. The surgical method depends on the morphology and size of the lesion. Submucosal tunneling endoscopic resection appears to be a feasible treatment for a subset of large esophageal schwannomas with large supero-inferior diameter but the smaller antero-posterior diameter and left-right diameters, which may benefit patients intolerant to surgical treatment.

Citation: Mu YZ, Zhang Q, Zhao J, Liu Y, Kong LW, Ding ZX. Total removal of a large esophageal schwannoma by submucosal tunneling endoscopic resection: A case report and review of literature. *World J Clin Cases* 2023; 11(11): 2510-2520
URL: https://www.wjgnet.com/2307-8960/full/v11/i11/2510.htm
DOI: https://dx.doi.org/10.12998/wjcc.v11.i11.2510

INTRODUCTION

Primary esophageal schwannomas are very rare tumors. In most cases, they are benign, while only a few malignant cases have been reported[1,2]. Imaging findings can reveal the specific location of the lesion, blood supply, and the relationship between the mass and the surrounding tissues, which are useful to determine whether the tumor is benign or malignant, and subsequently choose the appropriate treatment[3]. As one of imaging tools, endoscopic ultrasonography (EUS) can clearly display the layers of the esophageal wall[3] as well as reveal the location and origin of lesions[4,5]. Preoperative diagnosis of schwannoma is difficult[6,7], and the final diagnosis requires histopathological and immunohistochemical examinations[7]. Immunohistochemical staining is currently the only reliable diagnostic method and S100 protein is a specific molecular marker of schwannomas[7,8].

Esophageal schwannoma is insensitive to medical treatments such as radiotherapy and chemotherapy. Hence, resection remains the only effective treatment, especially if the tumor is detected in the early stage[8]. The maximum diameter of most endoscopically resected masses over the past 12 years was less than 30 mm[1,2,6-36], but these cases only discussed endoscopic resection according to the maximum diameter of the tumor and did not analyze the three diameter lines of the mass. In this paper, we reported single submucosal tunnel endoscopic resection for an esophageal schwannoma with 55 mm in supero-inferior diameter.

CASE PRESENTATION

Chief complaints

A 62-year-old Asian male presented with mild dysphagia lasting for five months.

History of present illness

The patient suffered from mild dysphagia for five months when swallowing solid food. There was no associated chest pain, nausea, vomiting, or abdominal pain.

History of past illness

The patient underwent Billroth II subtotal gastrectomy six years ago due to the presence of stomach cancer, as well as exploratory laparotomy, intestinal adhesiolysis, and inguinal hernia repair two years ago. The patient also completed eight cycles of XELOX adjunctive therapy. His blood pressure was elevated for about one year, and he regularly took oral nifedipine 10 mg daily.

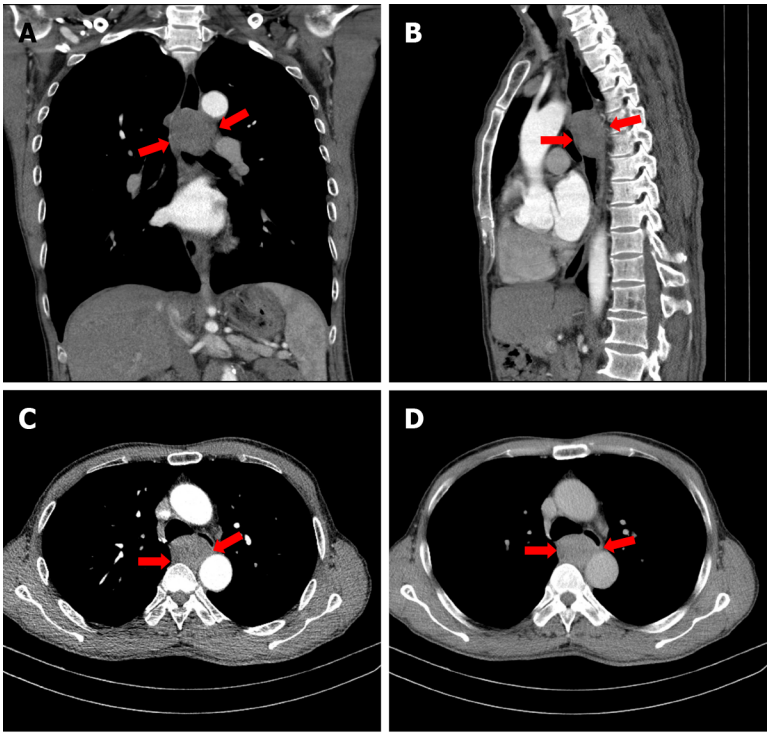

DOI: 10.12998/wjcc.v11.i11.2510

Figure 1 Plain and contrast-enhanced chest computed tomography. A: Coronal view of chest computed tomography (CT) showed that the tumor in the middle and upper esophagus had clear boundaries and homogeneous density; B: Sagittal view of the CT scan revealed the mass was located in the posterior mediastinum, and the upper and lower diameters were larger than the anterior and posterior diameters; C and D: Axial view of CT demonstrated the tumor presented homogeneous enhancement.

Personal and family history

There was no clinically significant family history; the patient had no smoking or drinking habits, and neither did he have a history of exposure to toxic substances.

Physical examination

The patient was 177 cm tall and weighed 63.1 kg. His temperature was 36.1 °C, heart rate was 61 beats per minute, respiratory rate was 17 breaths per minute, and blood pressure was 153/84 mmHg. Lung and abdominal tests were normal. Neurological examination revealed no obvious abnormalities. There was no edema in the bilateral lower limbs.

Laboratory examinations

Levels of anti-thyroid peroxidase antibodies were elevated. Glycosylated hemoglobin level (7.1%), total bilirubin (21.2 μmol/L), and indirect bilirubin (14.2 μmol/L) were increased, while aspartate aminotransferase (11 U/L) was decreased. Tumor markers CYFRA21-13 (40 ng/mL) were elevated. All other laboratory tests were within normal range.

Imaging examinations

Plain and contrast-enhanced chest computed tomography revealed a round lesion of 55 mm × 35 mm × 29 mm in the middle and upper esophagus, with homogeneous enhancement and esophageal lumen stenosis (Figure 1). Upper gastrointestinal endoscopy indicated a lesion in the esophagus about 25-30 cm from the incisor, and the esophageal mucosa was intact (Figure 2A). EUS demonstrated a hypoechoic and homogeneous mass originating from the muscularis propria (MP), with a diameter of about 41 mm. It was provisionally diagnosed as a stromal tumor.

FINAL DIAGNOSIS

Microscopy showed a dense proliferation of spindle cells without mitosis and atypia. In addition (Figure 3A), immunohistochemical staining was positive for S-100 protein (Figure 3D), the expression level of Ki-67 was < 5% (Figure 3B), and negative for CD34, Desmin, CD117 (Figure 3C), DOG-1, and SMA. These findings were strongly suggestive of a benign esophageal schwannoma.

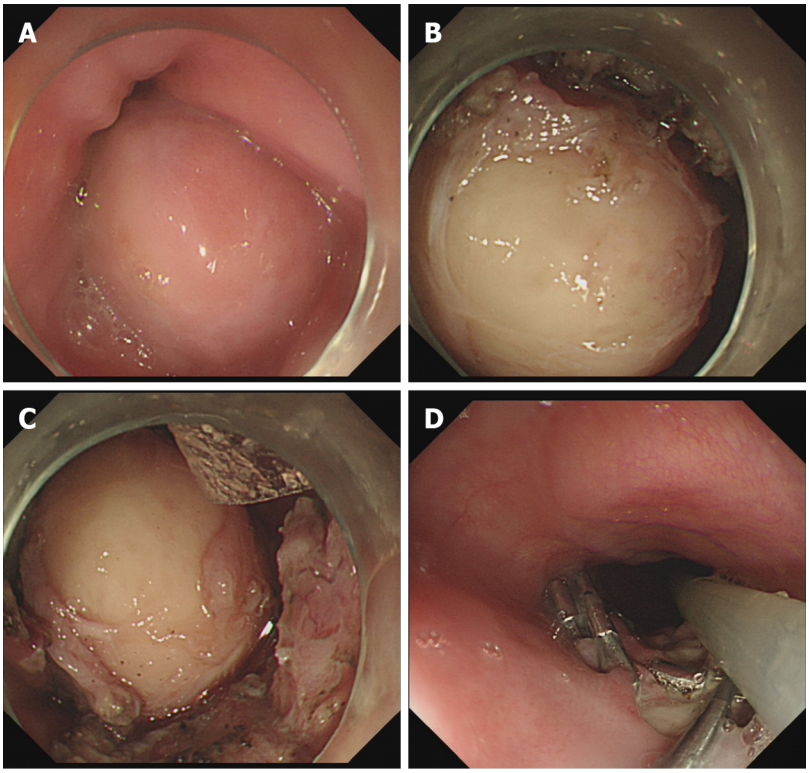

DOI: 10.12998/wjcc.v11.i11.2510

Figure 2 Steps of submucosal tunneling endoscopic resection. A: Upper gastrointestinal endoscopy showing smooth elevated lesion; B: Submucosal tumor; C: Peeling the lesion; D: Closing the mucosal incision site with clips.

TREATMENT

The patient underwent submucosal tunneling endoscopic resection (STER). The tumor with the size of 45 mm × 35 mm × 31 mm was finally resected with the intact fibrous capsule. The entire procedure lasted for about five hours. STER was performed under general anesthesia with intravenous propofol (2 mg/kg). Intraoperative findings showed that the lesion was located in the esophagus about 25-30 cm from the incisor, and the esophageal mucosa was intact (Figure 2A). EUS demonstrated a hypoechoic and homogeneous mass originating from the MP, with a diameter of about 41 mm.

The STER procedure was as follows: after the submucosal injection of glycerol fructose, a submucosal tunnel was created, and a 20 mm longitudinal mucosal incision was made with a Hook knife. Then a submucosal tunnel was created with an IT knife between the mucosal and muscular layers. The tunnel was continued downwards with the dual knife until the tumor was exposed. Within the submucosal tunnel, the tumor was separated from the MP layer as much as possible. Next, circumferential full-thickness MP resection was performed using the IT knife and snare for the tumor involving the deep layer of MP. The tumor was finally resected with the intact fibrous capsule. Hot hemostatic forceps were applied to treat blood vessels in surgical wounds. IT knife was used to incise the mucosal surface of the tumor that was difficult to remove, and multiple snares and stone extractors were used to completely remove the lesion (Figure 2B-D). The mucosal entry incision was closed with 16 vascular clips and 10 tissue clips.

OUTCOME AND FOLLOW-UP

After surgery, the patient's dysphagia disappeared. On follow-up endoscopy at three months, the wound was fully healed. Follow-up did not reveal local tumor recurrence or metastasis at 33 mo post-operation.

DISCUSSION

Primary schwannomas are rare esophageal submucosal tumors accounting for less than 2% of all esophageal tumors[5,7,9]. Most of these tumors are benign, but a few malignant cases have been

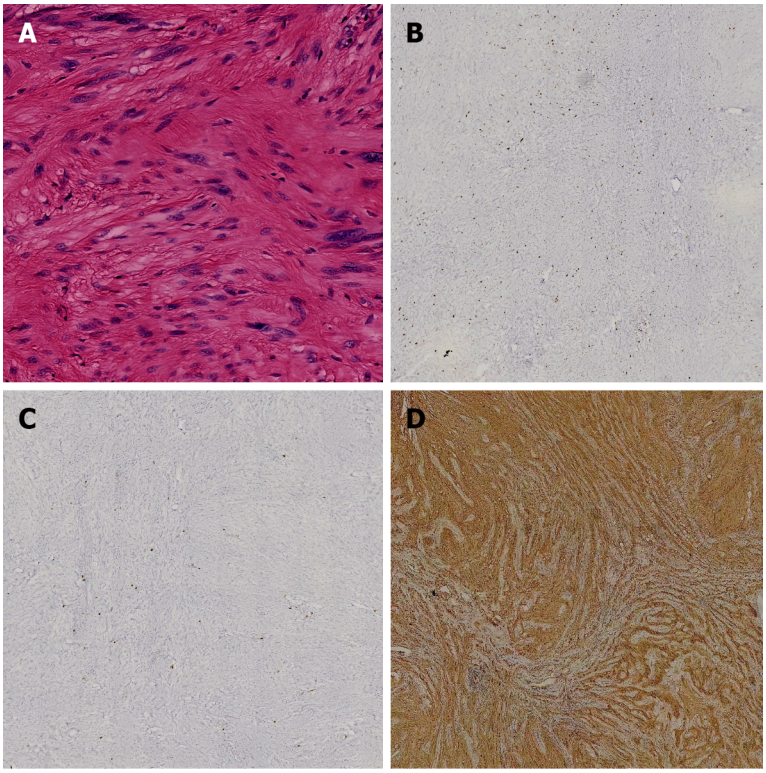

DOI: 10.12998/wjcc.v11.i11.2510

Figure 3 Histology and immunohistochemistry of the tumor. A: Histopathologic findings revealed spindle-shaped cells in a fasciculated and disarrayed architecture, and no pathologic mitosis was observed (hematoxylin and eosin staining; (magnification, × 400); B: The mitotic activity rate was < 5% on Ki-67 staining (magnification, × 80); C: Immunochemical analysis revealed no staining with CD117 (magnification, × 80); D: Immunohistochemical examination revealed S-100 protein positivity (magnification, × 200).

reported[1,2]. Typically, dyspnea and dysphagia are the most common complaints; other reported signs and symptoms include chest pain, stridor, hematemesis, cough, and palpable neck mass[10]. A literature search in the PubMed database identified 40 reported cases[1,2,6-36] published between 2011 and October 2022, which are listed in Table 1. Statistical analysis of baseline information, clinical symptoms, tumor size, and management methods are shown in Tables 2-4.

Tables 1 and 2 show that the mean age of schwannoma patients was 52.92 years, with a standard deviation of 2.17 years, the minimum age was 22 years, and the maximum age was 78 years. The male-to-female ratio was 1:2 in the adult population. Of the 40 esophageal schwannomas, 2 (5%) were malignant, and 38 (95%) were benign. Of these, 28 (70%) tumors were located in the upper or middle esophagus, while 7 (17.5%) were in the lower third of the esophagus. In middle-aged women, tumors were located in the middle and upper esophagus and were mostly benign, in accordance with the description of the esophageal nerve mentioned in the previous literature[11].

The clinical symptoms are summarized in Table 3. Some patients had corresponding clinical symptoms, so we analyzed 40 patients with esophageal schwannoma, 31 (88.6%) of whom had dysphagia, which appears to be the most important symptom that may be caused by the expansive growth of the tumor in the esophagus. Five (14.29%) patients presented with dyspnea, perhaps due to tracheal compression by a tumor, and another patient presented with loss of consciousness. In addition, some patients presented with symptoms of dyspnea, chest pain, palpitation, chest tightness, abdominal distention, *etc.* A sore throat was observed in 2 patients, a cough in 1 patient, and hemoptysis in 1 patient. These findings are consistent with previous reports[10].

Most cases of esophageal schwannoma are found incidentally during a physical examination and are commonly misdiagnosed[6,24]. Previous reports on esophageal schwannoma have failed to correctly diagnose the tumor preoperatively[6,7]. We believe that the two main reasons for the misdiagnosis are the following: first, diagnosing esophageal schwannoma using imaging alone remains a challenging task; the tumor is often misdiagnosed as other submucosal tumors, such as esophageal leiomyoma and esophageal, gastrointestinal stromal tumors. Second, since esophageal schwannomas are very rare, most physicians do not consider it as the first diagnosis or differential diagnosis, highlighting the need to improve doctors' understanding of esophageal schwannoma.

Hence, meticulous radiographic evaluation of esophageal schwannoma is necessary. This can help identify the lesion's specific location, blood supply, relationship with surrounding tissues, and esophageal layer in which the lesion originated, which provide a crucial reference for distinguishing benign from malignant tumors and the choice of surgical methods.

Table 1 Esophageal schwannoma case reports in PubMed during the last 12 years

Case	Ref.	Year	Age	Sex	Location	Tumor size (mm)	Symptoms	Management	Malignant findings
1	Choo *et al*[10]	2011	22	M	Ut	80 × 60 × 30	Cough, dyspnea and dysphagia	Enucleation	Benign
2	Wang *et al*[2]	2011	44	F	Lt	55 × 44	Progressive dysphagia	Surgical enucleation	Malignant
3	Liu *et al*[16]	2013	62	F	NA	90 × 40 × 30	Dysphagia and dyspnea	Partial esophagectomy and esophagogastrostomy	Benign
4	Liu *et al*[17]	2013	NA	NA	NA	< 30	NA	STER	Benign
5	Kitada *et al*[6]	2013	55	F	UM	75 × 57 × 80	Palpitations and dysphagia	Mini thoracotomy	Benign
6	Gu *et al*[18]	2014	39	M	UM	35 × 32 × 12	Obstructive sensation	VATS	Benign
7	Jeon *et al*[19]	2014	63	M	Ut	94 × 89	No symptoms	Thoracotomy	Benign
8	Jeon *et al*[19]	2014	32	F	Ut	60 × 85 × 40	Intermittent chest pain	VATS	Benign
9	Tomono *et al*[20]	2015	59	M	Mt	109 × 72 × 71	Dysphagia, dyspnea, disturbed	Subtotal esophagectomy	Benign
10	Wang *et al*[21]	2015	53	F	NA	NA	NA	Surgical excision	Benign
11	Wang *et al*[21]	2015	52	F	NA	NA	NA	Surgical excision	Benign
12	Zhang *et al*[22]	2015	67	F	NA	NA	Dysphagia	Surgical excision	Benign
13	Mishra *et al*[1]	2016	27	F	Mt	120 × 100 × 101	Dysphagia and palpitations	Surgical enucleation	Malignant
14	Watanabe *et al*[23]	2016	39	F	Ut	55 × 45 × 24	Epigastric pain, difficulty swallowing	Surgical excision	Benign
15	Chen *et al*[24]	2016	46	M	Mt	30 × 20 × 17	Discomfort during swallowing	VATS	Benign
16	Chen *et al*[24]	2016	42	F	Ut	30 × 40 × 40	Dysphagia	Enucleation	Benign
17	Chen *et al*[24]	2016	58	F	Ut	80 × 60 × 60	Dysphagia	Enucleation	Benign
18	Onodera *et al*[12]	2017	47	F	Ut	60	Dysphagia	Thoracoscopic + endoscopic excision	Benign
19	Moro *et al*[25]	2017	66	M	Ut	52 × 40 × 31	Dysphagia	Surgical excision	Benign
20	Zhang *et al*[13]	2018	48	F	Mt	69 × 36	Dysphagia	Robot-assisted enucleation	Benign
21	Iwata *et al*[26]	2018	74	F	Ut	80 × 42	Loss of consciousness	Surgical excision	Benign
22	Zhu *et al*[27]	2019	55	F	Mt	25 × 25 × 20	Dysphagia and chest pain	Left thoracotomy with subtotal esophagectomy	Benign
23	Souza *et al*[28]	2019	43	M	Ut	70	Pharyngitis, odynophagia, hemoptysis	Surgical excision	Benign
24	Ramos *et al*[29]	2019	40	F	Ut	80 × 45 × 20	Pharyngitis, odynophagia, dysphagia	Surgical excision	Benign
25	Degheili *et al*[30]	2019	50	F	Ut	78 × 54 × 105	Dyspnea and dysphagia	Surgical excision	Benign
26	Matteo *et al*[31]	2020	22	M	Lt	37 × 28 × 70	Dysphagia	Subtotal esophagectomy	Benign
27	Wu *et al*[7]	2020	67	F	Ut	61 × 46 × 60	Dysphagia and dyspnea	Surgical excision	Benign
28	Li *et al*[11]	2020	59	M	Lt	14 × 5	Upper abdominal distension	Endoscopic submucosal excision	Benign
29	Li *et al*[11]	2020	51	F	Mt	18 × 20	Heartburn	STER	Benign
30	Li *et al*[11]	2020	49	M	Lt	28 × 22	Dysphagia	STER	Benign

31	Wang *et al*[8]	2021	62	M	Lt	53 × 39 × 50	Severe dysphagia	VATS	Benign
32	Matsui *et al* [32]	2021	50	M	Lt	20	Asymptomatic	VATS	Benign
33	Khalayleh *et al*[33]	2021	61	F	Ut	50 × 30	Dysphagia	VATS	Benign
34	Zackria *et al* [15]	2021	78	F	Ut	30	Dysphagia	FNA	Benign
35	Khan *et al*[34]	2021	60	F	Lt	76 × 46 × 66	Dysphagia	Right-sided VATS	Benign
36	Wang *et al*[35]	2022	70	F	Ut	32 × 40 × 54	Dysphagia	VATS	Benign
37	Froiio *et al*[14]	2022	55	F	Ut	65 × 47	Dysphagia	Robotic enucleation	Benign
38	Gupta *et al*[9]	2022	62	F	Mt	51 × 31	Dysphagia	FNA	Benign
39	Nashed *et al* [36]	2022	72	F	Mt	29 × 29 × 21	Dysphagia	STER	Benign
40	Current article	2022	62	M	Mt	55 × 35	Dysphagia	STER	Benign

NA: Not available; F: Female; M: Male; Ut: Upper thoracic esophagus; Mt: Middle thoracic esophagus; Lt: Lower thoracic esophagus; STER: Submucosal tunneling endoscopic resection; FNA: Fine needle aspiration; VATS: Video-assisted thoracoscopic surgery.

Table 2 Clinical characteristics of schwannomas

Characteristics		*n* (%) s (Total 40)	Characteristics		*n* (%) s (Total 40)	mean ± SD
Location	Upper/middle	28 (70)	Sex	Male	13 (32.5)	
	Lower	7 (17.5)		Female	26 (65.0)	
	NA	5 (12.5)		NA	1 (2.5)	
Malignant findings	Benign	38 (95)	Age (yr)			55.92 ± 2.17
	Malignant	2 (5)				

NA: Not available.

Table 3 Clinical symptoms

Symptoms	*n* (%) s (Total 40)
Dysphagia/odynophagia	31 (88.57)
Epigastric pain/upper abdominal distension	3 (8.57)
Palpitations/chest pain	4 (11.43)
Dyspnea	5 (14.29)
Cough	1 (2.86)
Hemoptysis	1 (2.86)
Loss of consciousness	1 (2.86)
Pharyngitis/pharyngodynia	2 (5.71)
Asymptomatic	2 (5.71)
NA	5 (14.29)

NA: Not available.

Esophageal schwannomas are mainly treated by surgical resection[13]. Literature reports published in the past 12 years (Table 4) revealed that the average maximum diameter of all 40 tumors was 67.25 (± 4.72) mm, of which 29 (72.5%) cases underwent surgical resection or thoracoscopic resection, and the largest diameter reached 120 mm, the smallest was 20 mm, and the average maximum diameter was

Table 4 Management and tumor size

		n (%) s	Maximum diameter (mm)		
Total		40	mean: 67.25 (± 4.72)		
			The largest	The smallest	mean ± SD
Management	Surgical excision/VATS	29 (72.5)	120	20	67.25 ± 4.72
	Endoscopic excision/STER	5 (12.5)	29	14	22.75 ± 3.54
	Current article (STER)	1 (2.5)	55		
	Robot-assisted excision	2 (5)	69	65	
	FNA	2 (5)	51	30	
	Thoracoscopic + endoscopic excision	1 (2.5)	60		

STER: Submucosal tunneling endoscopic resection; FNA: Fine needle aspiration; VATS: Video-assisted thoracoscopic surgery.

67.25 ± 4.72 mm. Five (12.5%) esophageal schwannomas were resected *via* endoscopic surgical approach (including STER), with a maximum diameter of 29 mm, a minimum of 14 mm, a mean maximum diameter of 22.75 ± 3.54 mm, and maximum diameters of these masses were less than 30 mm. In our reported case, complete resection of esophageal schwannoma was performed using STER alone, and the size of this tumor exceeded the maximum size of esophageal schwannomas in all previously reported cases. Only one reported mass with a maximum diameter of 60 mm[12] was larger than our case; however, that case was managed by using thoracoscopy combined with endoscopic surgery rather than endoscopic surgery alone. In addition, there were other management methods, including robot-assisted resection of tumors with maximum diameters of 69 mm[13] and 65 mm[14] in two cases, and no further treatment measures were taken in the other two cases[9,15] after FNA puncture to obtain pathology.

Surgery may be performed by open thoracotomy or video-assisted thoracoscopy[13]. Small lesions in a suitable location can be removed endoscopically by experienced endoscopists using endoscopic submucosal excision or STER[11]. Compared with the first two surgeries, endoscopic resection causes less trauma and fewer complications and reduces the risk of anesthesia, leading to faster recovery and shorter hospitalization[11]. Although no specific cutoff for size could be identified, most tumors > 70 mm were removed by thoracotomy[7,37]. Most of the reported endoscopically resectable submucosal tumors were < 30 mm[11].

However, in all these reports, including cases of esophageal schwannomas treated endoscopically over the past 12 years[11,12,17,36], the size discussed was the maximum diameter of the tumor, while the supero-inferior diameter, antero-posterior diameter, and left-right diameter of the tumor were not analyzed separately. Due to the narrow structure of the esophagus, many schwannomas are limited by the wall of the esophagus and typically have a narrow shape, which often leads to smaller antero-posterior diameter and left-right diameters of the masses although the long diameter is very large, and gives more operating space for endoscopic surgery.

In the present case, the maximum diameter of the lesion was > 50 mm, and postoperative esophageal fistula and pneumothorax may have occurred if endoscopic surgery had been performed. Hence, we recommended thoracoscopic surgery or an open surgical approach[11]. However, the patient refused to undergo surgery again and requested endoscopic minimally invasive resection. After carefully examining the morphology of the mass, we found that this tumor had a large supero-inferior diameter but also smaller antero-posterior and left-right diameters, which meant that the mucosal tunnel only needed to withstand a width of > 30 mm, not 50 mm. Hence, we concluded that there is a certain but controllable risk in treating this patient by endoscopic surgery, and then proposed STER for this patient under the premise of controllable risk and fully considering the possible complications and corresponding solutions.

To the best of our knowledge, this is the first report of using STER alone for the successful removal of an esophageal schwannoma > 30 mm. It is also the first report on the specific analysis of the relationship between the shape of esophageal schwannoma, different diameter lines, and surgical options. Therefore, if the morphological factors of the mass are included, endoscopic treatment could be used for esophageal schwannomas with a maximum diameter of > 30 mm. Hence, risk-controlled STER appears to be a feasible and effective treatment for a subset of large esophageal schwannomas with large supero-inferior diameter but smaller antero-posterior and left-right diameters, which may benefit patients intolerant to surgical treatment.

CONCLUSION

Primary schwannoma is a rare submucosal tumor of the esophagus. Imaging findings can provide useful information, including the location, size, morphology, density, and relationships with the surrounding tissues, particularly the size and morphology, which could influence the treatment choice. We reported a successful resection of the esophageal schwannoma by STER, with a maximum diameter of 55mm and a minimum diameter of 29 mm. In our case, the tumor's small antero-posterior and left-right diameter were important factors for successful removal by STER. Therefore, the morphological features of a mass, especially the three diameters, should be meticulously analyzed. STER appears to be an effective treatment method for a subset of large esophageal schwannomas with large supero-inferior diameter but smaller antero-posterior and left-right diameters, thus benefiting the patients intolerant to surgical treatment.

FOOTNOTES

Author contributions: MU YZ contributed to the data acquisition and analysis, and writing of the manuscript; Zhang Q contributed to the language editing and writing involving the imaging part of the manuscript; Liu Y and Zhao J contributed to the data collection; Ding ZX and Kong LW contributed to the work concept and language editing and important revisions to the manuscript.

Supported by National Natural Science Foundation of China, No. 81871337; and Medical and Health Science and Technology Projects of Zhejiang Province, No. 2019KY117.

Informed consent statement: Informed written consent was obtained from the patient for publication of this report and any accompanying images.

Conflict-of-interest statement: The authors declare that they have no conflict of interest.

CARE Checklist (2016) statement: The authors have read the CARE Checklist (2016), and the manuscript was prepared and revised according to the CARE Checklist (2016).

Country/Territory of origin: China

ORCID number: Yu-Zhu Mu 0000-0002-8794-4703; Qi Zhang 0000-0002-3500-0911; Jing Zhao 0000-0002-4481-9080; Yan Liu 0000-0003-1883-1534; Ling-Wei Kong 0000-0002-3881-0370; Zhong-Xiang Ding 0000-0001-7691-5571.

Corresponding Author's Membership in Professional Societies: Head and Neck Professional Committee of Chinese Society of Radiology.

S-Editor: Yan JP
L-Editor: A
P-Editor: Yan JP

REFERENCES

1 **Mishra B**, Madhusudhan KS, Kilambi R, Das P, Pal S, Srivastava DN. Malignant Schwannoma of the Esophagus: A Rare Case Report. *Korean J Thorac Cardiovasc Surg* 2016; **49**: 63-66 [PMID: 26889451 DOI: 10.5090/kjtcs.2016.49.1.63]
2 **Wang S**, Zheng J, Ruan Z, Huang H, Yang Z. Long-term survival in a rare case of malignant esophageal schwannoma cured by surgical excision. *Ann Thorac Surg* 2011; **92**: 357-358 [PMID: 21718879 DOI: 10.1016/j.athoracsur.2011.01.045]
3 **Karaca C**, Turner BG, Cizginer S, Forcione D, Brugge W. Accuracy of EUS in the evaluation of small gastric subepithelial lesions. *Gastrointest Endosc* 2010; **71**: 722-727 [PMID: 20171632 DOI: 10.1016/j.gie.2009.10.019]
4 **Reddymasu SC**, Oropeza-Vail M, Pakseresht K, Moloney B, Esfandyari T, Grisolano S, Buckles D, Olyaee M. Are endoscopic ultrasonography imaging characteristics reliable for the diagnosis of small upper gastrointestinal subepithelial lesions? *J Clin Gastroenterol* 2012; **46**: 42-45 [PMID: 21778894 DOI: 10.1097/MCG.0b013e318226af8e]
5 **Morales-Maza J**, Pastor-Sifuentes FU, Sánchez-Morales GE, Ramos ES, Santes O, Clemente-Gutiérrez U, Pimienta-Ibarra AS, Medina-Franco H. Clinical characteristics and surgical treatment of schwannomas of the esophagus and stomach: A case series and systematic review. *World J Gastrointest Oncol* 2019; **11**: 750-760 [PMID: 31558979 DOI: 10.4251/wjgo.v11.i9.750]

6 **Kitada M**, Matsuda Y, Hayashi S, Ishibashi K, Oikawa K, Miyokawa N. Esophageal schwannoma: a case report. *World J Surg Oncol* 2013; **11**: 253 [PMID: 24088647 DOI: 10.1186/1477-7819-11-253]

7 **Wu CX**, Yu QQ, Shou WZ, Zhang K, Zhang ZQ, Bao Q. Benign esophageal schwannoma: A case report and brief overview. *Medicine (Baltimore)* 2020; **99**: e21527 [PMID: 32756198 DOI: 10.1097/MD.0000000000021527]

8 **Wang TY**, Wang BL, Wang FR, Jing MY, Zhang LD, Zhang DK. Thoracoscopic resection of a large lower esophageal schwannoma: A case report and review of the literature. *World J Clin Cases* 2021; **9**: 11061-11070 [PMID: 35047619 DOI: 10.12998/wjcc.v9.i35.11061]

9 **Gupta P**, Rana S, Dey P. Cytomorphological and immunocytochemical diagnosis of an oesophageal mass in a 62-year-old female with dysphagia. *Cytopathology* 2022; **33**: 281-284 [PMID: 34525230 DOI: 10.1111/cyt.13059]

10 **Choo SS**, Smith M, Cimino-Mathews A, Yang SC. An early presenting esophageal schwannoma. *Gastroenterol Res Pract* 2011; **2011**: 165120 [PMID: 21687608 DOI: 10.1155/2011/165120]

11 **Li B**, Wang X, Zou WL, Yu SX, Chen Y, Xu HW. Endoscopic resection of benign esophageal schwannoma: Three case reports and review of literature. *World J Clin Cases* 2020; **8**: 5690-5700 [PMID: 33344562 DOI: 10.12998/wjcc.v8.i22.5690]

12 **Onodera Y**, Nakano T, Takeyama D, Maruyama S, Taniyama Y, Sakurai T, Heishi T, Sato C, Kumagai T, Kamei T. Combined thoracoscopic and endoscopic surgery for a large esophageal schwannoma. *World J Gastroenterol* 2017; **23**: 8256-8260 [PMID: 29290662 DOI: 10.3748/wjg.v23.i46.8256]

13 **Zhang Y**, Han Y, Xiang J, Li H. Robot-assisted enucleation of large dumbbell-shaped esophageal schwannoma: a case report. *BMC Surg* 2018; **18**: 36 [PMID: 29871678 DOI: 10.1186/s12893-018-0370-y]

14 **Froiio C**, Berlth F, Capovilla G, Tagkalos E, Hadzijusufovic E, Mann C, Lang H, Grimminger PP. Robotic-assisted surgery for esophageal submucosal tumors: a single-center case series. *Updates Surg* 2022; **74**: 1043-1054 [PMID: 35147859 DOI: 10.1007/s13304-022-01247-z]

15 **Zackria R**, Choi EH. Esophageal Schwannoma: A Rare Benign Esophageal Tumor. *Cureus* 2021; **13**: e15667 [PMID: 34277259 DOI: 10.7759/cureus.15667]

16 **Liu T**, Liu H, Yang C, Zhang X, Xu S, Liu B. Benign esophageal schwannoma compressing the trachea requiring esophagectomy: a case report. *Thorac Cardiovasc Surg* 2013; **61**: 505-506 [PMID: 22791203 DOI: 10.1055/s-0032-1311554]

17 **Liu BR**, Song JT, Kong LJ, Pei FH, Wang XH, Du YJ. Tunneling endoscopic muscularis dissection for subepithelial tumors originating from the muscularis propria of the esophagus and gastric cardia. *Surg Endosc* 2013; **27**: 4354-4359 [PMID: 23765425 DOI: 10.1007/s00464-013-3023-3]

18 **Gu MJ**, Choi JH. Microcystic/reticular schwannoma of the esophagus: the first case report and a diagnostic pitfall. *BMC Gastroenterol* 2014; **14**: 193 [PMID: 25404099 DOI: 10.1186/s12876-014-0193-y]

19 **Jeon HW**, Kim KS, Hyun KY, Park JK. Enucleation of giant esophageal schwannoma of the upper thoracic esophagus: reports of two cases. *World J Surg Oncol* 2014; **12**: 39 [PMID: 24548347 DOI: 10.1186/1477-7819-12-39]

20 **Tomono A**, Nakamura T, Otowa Y, Imanishi T, Tanaka Y, Maniwa Y, Kakeji Y. A Case of Benign Esophageal Schwannoma Causing Life-threatening Tracheal Obstruction. *Ann Thorac Cardiovasc Surg* 2015; **21**: 289-292 [PMID: 25740444 DOI: 10.5761/atcs.cr.14-00171]

21 **Wang YL**, Sun JG, Wang J, Wei WJ, Zhu YX, Wang Y, Sun GH, Xu K, Li H, Zhang L, Ji QH. Schwannoma of the cervical esophagus: Report of 2 cases and a review of the literature. *Ear Nose Throat J* 2015; **94**: E10-E13 [PMID: 26401673]

22 **Zhang Q**, Lu G, Li D. [The resection of the huge mediastinal schwannoma by the jugular approach: one case report]. *Lin Chung Er Bi Yan Hou Tou Jing Wai Ke Za Zhi* 2016; **30**: 329-330 [PMID: 27373047]

23 **Watanabe T**, Miyazaki T, Saito H, Yoshida T, Kumakura Y, Honjyo H, Yokobori T, Sakai M, Sohda M, Kuwano H. Resection of an esophageal schwannoma with thoracoscopic surgery: a case report. *Surg Case Rep* 2016; **2**: 127 [PMID: 27822873 DOI: 10.1186/s40792-016-0256-0]

24 **Chen X**, Li Y, Liu X, Fu H, Sun H, Zhang R, Wang Z, Zheng Y. A report of three cases of surgical removal of esophageal schwannomas. *J Thorac Dis* 2016; **8**: E353-E357 [PMID: 27162699 DOI: 10.21037/jtd.2016.03.41]

25 **Moro K**, Nagahashi M, Hirashima K, Kosugi SI, Hanyu T, Ichikawa H, Ishikawa T, Watanabe G, Gabriel E, Kawaguchi T, Takabe K, Wakai T. Benign esophageal schwannoma: a brief overview and our experience with this rare tumor. *Surg Case Rep* 2017; **3**: 97 [PMID: 28861777 DOI: 10.1186/s40792-017-0369-0]

26 **Iwata Y**, Tanaka C, Komori S, Nagao N, Kawai M, Yoshida K, Kunieda K. Lobulated esophageal schwannoma resected with concurrent approach from the thorax and cervix. *World J Surg Oncol* 2018; **16**: 29 [PMID: 29439724 DOI: 10.1186/s12957-018-1334-5]

27 **Zhu L**, Li W, Zhu Z, Chai Y. Benign esophageal schwannoma: A case report and review of literature. *Niger J Clin Pract* 2019; **22**: 731-733 [PMID: 31089031 DOI: 10.4103/njcp.njcp_142_18]

28 **Souza LCA**, Pinto TDA, Cavalcanti HOF, Rezende AR, Nicoletti ALA, Leão CM, Cunha VC. Esophageal schwannoma: Case report and epidemiological, clinical, surgical and immunopathological analysis. *Int J Surg Case Rep* 2019; **55**: 69-75 [PMID: 30710876 DOI: 10.1016/j.ijscr.2018.10.084]

29 **Sanchez-Garcia Ramos E**, Cortes R, de Leon AR, Contreras-Jimenez E, Rodríguez-Quintero JH, Morales-Maza J, Aguilar-Frasco J, Irigoyen A, Reyes F, Alfaro-Goldaracena A. Esophageal schwannomas: A rarity beneath benign esophageal tumors a case report. *Int J Surg Case Rep* 2019; **58**: 220-223 [PMID: 31102953 DOI: 10.1016/j.ijscr.2019.03.038]

30 **Degheili JA**, Sfeir P, Khalifeh I, Hallal AH. Large esophageal schwannoma: En-bloc resection with primary closure by esophagoplasty. *Int J Surg Case Rep* 2019; **61**: 77-81 [PMID: 31351369 DOI: 10.1016/j.ijscr.2019.07.038]

31 **Matteo MV**, Sassorossi C, Lococo F, Ricci R, Margaritora S, Gasbarrini A, Zileri Dal Verme L. A huge esophageal Schwannoma occurring in a Caucasian young male: a case report. *Eur Rev Med Pharmacol Sci* 2020; **24**: 10703-10707 [PMID: 33155229 DOI: 10.26355/eurrev_202010_23429]

32 **Matsui S**, Yamazaki T, Shiraishi O, Kudo M. Efficacy of endoscopic ultrasound-guided fine-needle aspiration for esophageal schwannoma. *Ann Gastroenterol* 2021; **34**: 597 [PMID: 34276202 DOI: 10.20524/aog.2021.0636]

33 **Khalayleh H**, Mashni I, Bar I, Pines G. Semi-prone position for thoracoscopic resection of a rare oesophageal tumour. *Interact Cardiovasc Thorac Surg* 2021; **33**: 646-648 [PMID: 34000026 DOI: 10.1093/icvts/ivab118]

34 **Khan U**, Simone C, Safieddine N, Gazala S. Video-assisted thoracoscopic resection of a giant esophageal schwannoma: A case report. *Int J Surg Case Rep* 2021; **85**: 106202 [PMID: 34388894 DOI: 10.1016/j.ijscr.2021.106202]

35 **Wang H**, Li Y, Wu M, Cui H. Benign esophageal schwannoma: A case report. *Asian J Surg* 2023; **46**: 1437-1438 [PMID: 36163096 DOI: 10.1016/j.asjsur.2022.09.045]

36 **Nashed B**, Ayas MF, Gharib H, Issa M, Fatouh K, Sebastian F, Backer Z, Mahat K, Barawi M. Esophageal Schwannoma: An Important Differential Diagnosis for Esophageal Subepithelial Lesions. *Cureus* 2022; **14**: e27168 [PMID: 36039243 DOI: 10.7759/cureus.27168]

37 **Kent M**, d'Amato T, Nordman C, Schuchert M, Landreneau R, Alvelo-Rivera M, Luketich J. Minimally invasive resection of benign esophageal tumors. *J Thorac Cardiovasc Surg* 2007; **134**: 176-181 [PMID: 17599505 DOI: 10.1016/j.jtcvs.2006.10.082]

World Journal of Clinical Cases

Submit a Manuscript: https://www.f6publishing.com

World J Clin Cases 2023 April 16; 11(11): 2521-2527

DOI: 10.12998/wjcc.v11.i11.2521

ISSN 2307-8960 (online)

CASE REPORT

SMARCA4-deficient undifferentiated thoracic tumor: A case report

Hee Jung Kwon, Min Hye Jang

Specialty type: Pathology

Provenance and peer review: Unsolicited article; Externally peer reviewed.

Peer-review model: Single blind

Peer-review report's scientific quality classification

Grade A (Excellent): 0
Grade B (Very good): B, B
Grade C (Good): 0
Grade D (Fair): D
Grade E (Poor): 0

P-Reviewer: Moshref L, Saudi Arabia; Vyshka G, Albania; Yang L, China

Received: December 20, 2022
Peer-review started: December 20, 2022
First decision: February 17, 2023
Revised: February 27, 2023
Accepted: March 22, 2023
Article in press: March 22, 2023
Published online: April 16, 2023

Hee Jung Kwon, Min Hye Jang, Department of Pathology, Yeungnam University Medical Center, Daegu 42415, South Korea

Corresponding author: Min Hye Jang, MD, PhD, Assistant Professor, Department of Pathology, Yeungnam University Medical Center, 170, Hyeonchung-ro, Nam-gu, Daegu 42415, South Korea. clodious@ynu.ac.kr

Abstract

BACKGROUND

SMARCA4-deficient undifferentiated tumors (*SMARCA4*-DUTs) present with diverse clinical manifestations and progress to metastasis and even cause death within a few months. This novel subset of undifferentiated tumors occurs in the middle-aged population and is strongly associated with a smoking history. Distinguishing it from other malignancies is challenging.

CASE SUMMARY

A 62-year-old man presented with chest pain for 7 d. The patient had no respiratory symptoms and normal pulmonary function test results. The patient had been a smoker for 8 years and quit smoking 2 years ago. Chest computed tomography revealed a huge mass involving the left upper and lower lung lobes with pericardial invasion and multiple metastases. Tumor samples were obtained using open frozen biopsy, after several unsuccessful attempts. The tumor was composed of sheets of undifferentiated disclosive cells with vesicular nuclei and prominent nucleoli. The differential diagnosis included high-grade lymphoma, germ cell tumor, NUT carcinoma, undifferentiated carcinoma, and sarcoma. The tumor cells were large, arranged in sheets, and did not exhibit glandular or squamous differentiation. Frequent foci of necrosis were noted. There was no evidence of epithelial differentiation on immunohistochemical staining. The SMARCA4 stain showed complete loss of expression of SMARCA4, which is diagnostic.

CONCLUSION

In the present case, thoracic *SMARCA4*-DUT was diagnosed based on clinical features, absence of epithelial differentiation, and negative *SMARCA4* expression.

Key Words: *SMARCA4*; *BRG1*; Deficient; Undifferentiated tumor; Thoracic; Case report

Core Tip: *SMARCA4*-deficient undifferentiated tumors are highly aggressive neoplasms. Here, we report a case of a *SMARCA4*-deficient undifferentiated tumor with characteristic clinical and histological features. The findings of this case could serve as a resource for future studies.

Citation: Kwon HJ, Jang MH. *SMARCA4*-deficient undifferentiated thoracic tumor: A case report. *World J Clin Cases* 2023; 11(11): 2521-2527
URL: https://www.wjgnet.com/2307-8960/full/v11/i11/2521.htm
DOI: https://dx.doi.org/10.12998/wjcc.v11.i11.2521

INTRODUCTION

SMARCA4-deficient undifferentiated tumors (*SMARCA4*-DUTs) are aggressive neoplasms that characteristically involve the thorax. They present with undifferentiated or rhabdoid morphological features with deficiency of Brahma-related gene 1 (*BRG1*) encoded by *SMARCA4*. The newly discovered tumor has recently been included in the World Health Organization Classification of Tumors: Thoracic Tumors. The most frequent sites where this tumor occurs are the mediastinum, pulmonary hilum, lung, pleura, and chest wall[1,2]. Most patients present with lung involvement, including variable metastases, at the time of initial diagnosis. Associated symptoms include dyspnea, pain, weight loss, and symptoms based on the involved organs. This tumor is often diagnosed in middle-aged heavy smokers and leads to death within a few months. Over half of the cases are associated with smoking-related emphysema[2,3]. Most cases occur in the fourth to fifth decades of life with a male predominance. Here, we report a case of thoracic *SMARCA4*-DUT in an older man with a characteristic clinical presentation.

CASE PRESENTATION

Chief complaints

A 62-year-old man presented with pain in the left chest and right flank for 7 d.

History of present illness

The patient had no respiratory symptoms, and pulmonary function test results were normal.

History of past illness

The patient was previously healthy and had no relevant medical history.

Personal and family history

The patient had been a smoker for 8 years (35 pack-years) and quit smoking 2 years earlier.

Physical examination

Physical examination was unremarkable.

Laboratory examinations

A routine blood examination, including tests for white blood cell count, hemoglobin, and other electrolytes, indicated that all levels were within normal range. However, the results of the biochemical tests indicated a slight increase in lactate dehydrogenase (1824 IU/L, with a reference range of 208-450 IU/L) and C-reactive protein (0.885 mg/dL, with a reference range of 0.0-0.5 mg/dL). A polymerase chain reaction test for coronavirus disease 2019 (COVID-19) was conducted, but no evidence of the virus that causes COVID-19 was found.

Imaging examinations

The posteroanterior view of the chest radiograph showed a lesion of dense consolidation in the left lower pericardial area and calcific nodules consistent with an old tuberculosis scar in both upper lobes (Figure 1A). Additional chest computed tomography revealed several enlarged mediastinal lymph nodes (Figure 1B) and a huge mass with necrosis, involving the upper and lower lobes of the left lung, with invasion of the pericardium (Figure 1C). In addition, a low-attenuation lesion was present in the liver, consistent with a metastatic tumor (Figure 1D). Further, multiple lymphadenopathies were found in the bilateral paratracheal, subcarinal, left hilar, left cardiophrenic, internal mammary, and upper abdominal areas. The right lower lung lobe showed small nodules and mild pericardial effusion, also consistent with metastasis. An approximately 9-cm sized lesion in the left lung showed uneven 18F-

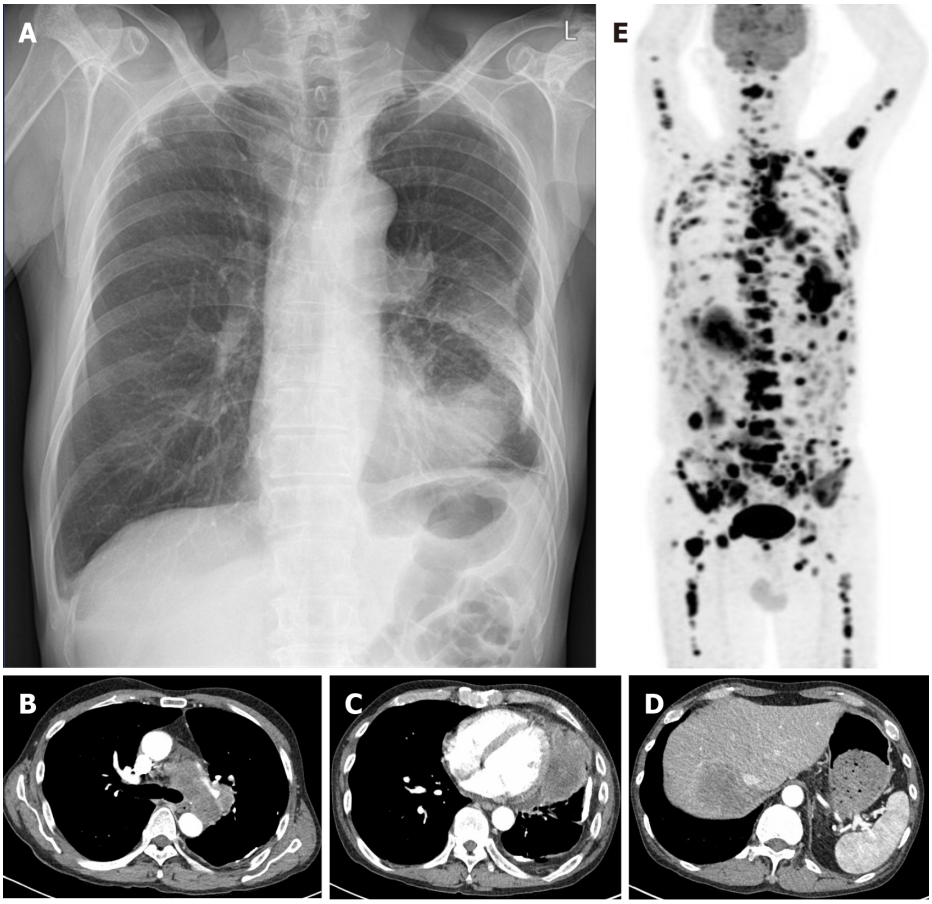

DOI: 10.12998/wjcc.v11.i11.2521

Figure 1 Imaging results. A: The posteroanterior view of the chest radiograph shows a lesion of dense consolidation in the left lower pericardial area and calcific nodules consistent with an old tuberculosis scar in both upper lobes. Computed tomography reveals a huge mass with necrosis involving the upper and lower lobes of the left lung with invasion of the pericardium; B: Several enlarged mediastinal lymph nodes are exhibited; C: Left lung lesion with pericardial invasion is identified; D: Right liver lobe shows a metastatic tumor; E: An approximately 9-cm sized left lung lesion shows uneven 18F-fluorodeoxyglucose uptake on the positron emission tomography (PET) scan. Further, the PET scan shows numerous metastatic lesions involving the mediastinum (left paratracheal, left cardiophrenic, and celiac lymph nodes); liver; bilateral lung lobes; bones of the skull, bilateral humeri, scapula, left clavicle, sternum, vertebras (cervical, thoracic, lumbar), bilateral ribs, pelvis, and bilateral femurs; peritoneum; and retroperitoneum.

fluorodeoxyglucose uptake on positron emission tomography (PET; Figure 1E). Further, PET showed numerous metastatic lesions involving the mediastinum; liver; bilateral lung lobes; bones of the skull, bilateral humeri, scapula, left clavicle, sternum, vertebras (cervical, thoracic, lumbar), bilateral ribs, pelvis, and bilateral femurs; peritoneum; and retroperitoneum.

FURTHER DIAGNOSTIC WORKUP

Despite the large size of the tumor, both endobronchial ultrasound-guided transbronchial lung biopsy and bronchial washing performed twice failed to obtain a sufficient amount of tumor cells. Due to necrosis, tumor cells were insufficient for a definitive diagnosis. Tumor specimens were finally obtained from the mediastinal node using mediastinoscopy and pleural biopsy. The largest biopsy sample, measuring 2.5 cm × 1.8 cm × 0.5 cm in size, was received from the operation theater in the fresh state. The mass had a tan to yellowish cut surface. The representative tissue was fixed in 10% neutral formalin and processed for pathologic examination after a frozen section diagnosis. On hematoxylin and eosin staining, the tumor cells were large, round to epithelioid, arranged in diffuse sheets, and did not exhibit glandular or squamous differentiation (Figure 2). Frequent foci of necrosis were noted on frozen and post fixation tissue sections (Figure 2A and B). The tumor cells showed moderate pleomorphism and had abundant eosinophilic cytoplasm (Figure 2C and D). Nuclei were monotonous and vesicular with conspicuous nucleoli. The mitotic activity was high (Figure 2D). Immunohistochemically, the tumor cells were positive for spalt-like transcription factor 4 (SALL4; Figure 2E), CD34 (Figure 2F), and cytoplasmic p53 (aberrant expression) and negative for CAM5.2, erythroblast transformation-specific-related gene, AE1/AE3 cytokeratin (Figure 2G), thyroid transcription factor-1, p40, CK5/6, nuclear protein in testis (NUT), CD20, and S100 protein. The *SMARCA4* stain showed complete loss of

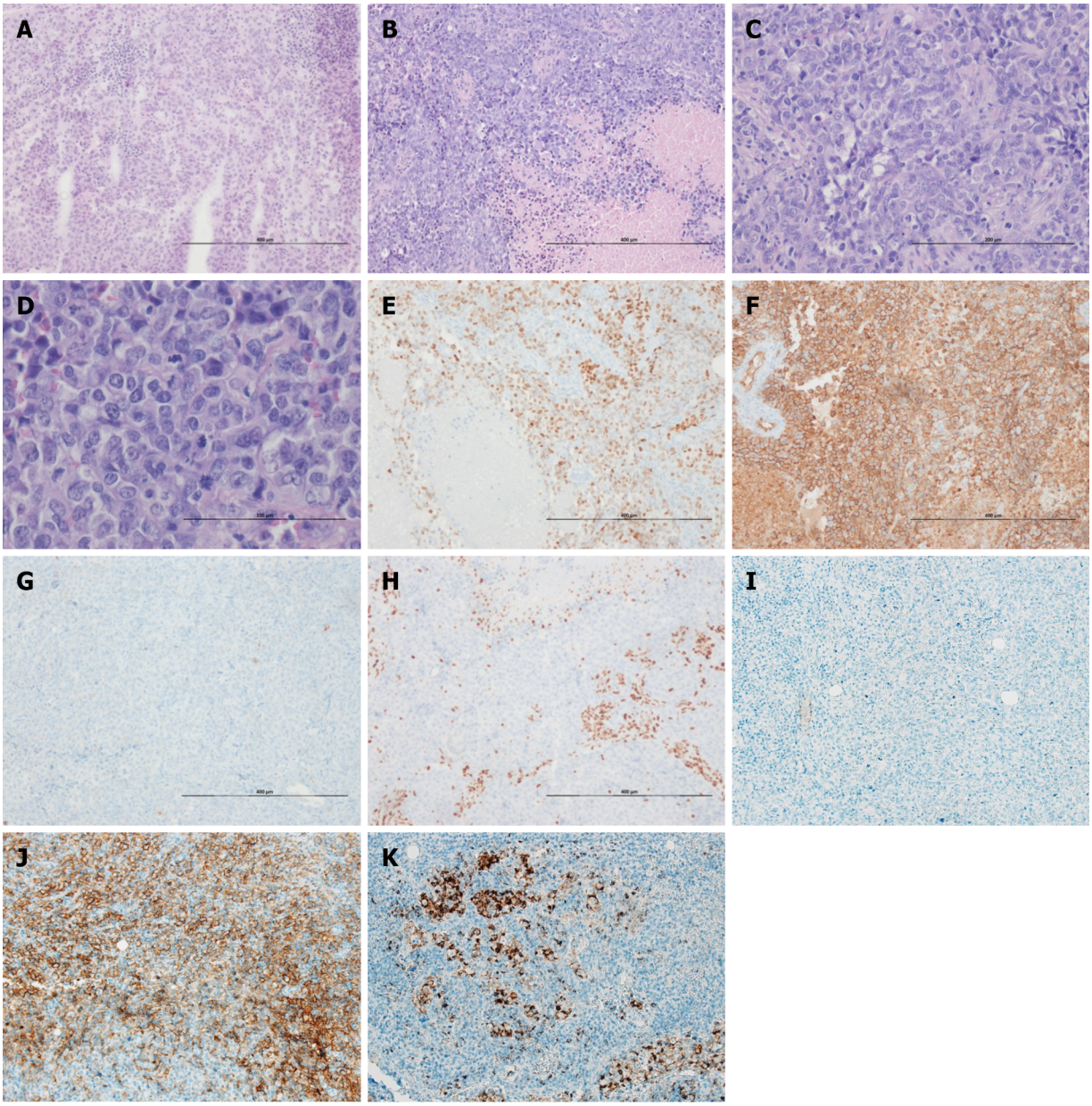

DOI: 10.12998/wjcc.v11.i11.2521

Figure 2 Histological features and immunostaining results of the tumor. A and B: The frozen section shows a diffuse sheet of large round to epithelioid tumor cells on frozen section (A, × 100) and post fixation tissue section (B, × 100). Frequent necrotic foci are seen (B); C: The tumor cells show no glandular or squamous differentiation and exhibit moderate pleomorphism (× 200); D: The nuclei are monotonous and vesicular with conspicuous nucleoli. The tumor has eosinophilic cytoplasm and a markedly increased mitotic activity (× 400); E and F: Immunohistochemical staining for Spalt-like transcription factor 4 (SALL4) (E, × 100) and CD34 (F, × 100) exhibits positive results; G: The ancillary test, such as that for AE1/AE3 cytokeratin confirms the absence of epithelial differentiation (× 100); H: SMARCA4 staining exhibits diagnostic complete loss of expression (× 100); I: Anaplastic lymphoma kinase (ALK) (D5F3) shows negative activity (× 100); J and K: Programmed death-ligand 1 (PDL1) tests exhibit positivity (J, SP263, × 100; K, SP142, × 100). Staining method: Hematoxylin and eosin staining (A-D); polymer method (E-K).

expression, which was diagnostic. (Figure 2H). Anaplastic lymphoma kinase (ALK, D5F3) showed negative activity (Figure 2I). Programmed death-ligand 1 (PDL1) tests showed positivity (Figure 2J, Ventana SP263; Figure 2K, SP142). No epidermal growth factor receptor mutation was detected on pyrosequencing.

FINAL DIAGNOSIS

Histopathology confirmed the diagnosis of *SMARCA4*-DUT.

TREATMENT

After mediastinoscopy and pleural biopsy, the patient was discharged on postoperative day 13 with pain control.

OUTCOME AND FOLLOW-UP

Twenty days after the biopsy, the patient complained of dyspnea on exercise, hoarseness, and a poor general condition. He has not visited the hospital for over 10 mo, thereafter.

DISCUSSION

Thoracic *SMARCA4*-DUT is a newly discovered aggressive malignancy whose pathogenesis remains unclear. The most frequent sites of occurrence of this tumor are the mediastinum, pulmonary hilum, lungs, and pleura or chest wall. *SMARCA4*-DUTs have undifferentiated or rhabdoid morphological features with deficiency of *SMARCA4*. They occur most commonly in young men with a history of heavy smoking, but can occur in patients of any age. In addition to our patient, there have been other reports of the tumor presenting at an advanced age. Associated symptoms include dyspnea, pain, weight loss, and symptoms based on the involved organs. Common sites of metastasis include the lymph nodes, bones, and adrenal glands and rarely the brain[4,5].

The tumor-suppressor role of *SMARCA4* (or *BRG1*) was reported in 2000[6]. Nonsense and frameshift mutations in *SMARCA4* are the dominant oncogenic molecular alterations underlying the pathogenesis of this neoplasm. The hallmark of the diagnosis is loss of *SMARCA4* (*BRG1*) expression on immunohistochemical staining. *SMARCA4* deficiency is found in most cases. However, sequencing of *SMARCA4* alteration is not necessary for the diagnosis, as the truncated protein can occasionally be partially recognized by the antibody, which leads to unstable binding and degradation, explaining the attenuated immunoreactivity in certain cases[7]. Additional molecular tests may help confirm the diagnosis of *SMARCA4*-deficient tumors when immunohistochemistry findings cannot be interpreted with certainty [7].

Concurrent loss of the *SMARCA2* expression and expression of one or more stem cell markers, such as sex determining region Y-box 2, SALL4, or CD34, is common. *SMARCA4* deficiency is a passenger somatic alteration in multiple solid tumors manifesting as focal dedifferentiation and a rhabdoid morphology[8]. *SMARCA4*-DUT and non-small cell lung cancer (NSCLC) with *SMARCA4*-deficiency show considerable overlap in their clinicopathological features, such as male preponderance, association with smoking, pattern of metastasis, rapidly fatal outcomes, immunohistology findings, and molecular alterations[1]. Morphologically, *SMARAC4*-DUT is differentiated from *SMARCA4*-deficient NSCLC by the absence of squamous and solid components[9].

However, the incidence of SMARAC4-DUTs is too low to be included in the differential diagnosis of poorly differentiated tumors. To date, approximately 100 cases of SMARCA4-DUTs have been reported in the literature[10]. Further, SMARAC4-DUTs are commonly located in the thorax, from which only small biopsy samples are usually available. The present patient underwent frozen biopsy after endobronchial ultrasound-guided transbronchial lung biopsy and bronchial washing performed twice failed to obtain sufficient amount of tumor cells because of tumor necrosis. Owing to metastasis, other organs, such as the adrenal gland, may be biopsied first[4]. These issues make it difficult to reach a definitive diagnosis.

SMARCA4-DUTs show an undifferentiated morphology with occasional rhabdoid features. Considering histological findings and clinical presentation, such as significant progression at the time of initial diagnosis, it will not be difficult to include *SMARCA4*-DUT in the differential diagnosis using integrase interactor 1 (INI1) staining in the ancillary test.

SMARCA4-DUTs are rapidly fatal and are refractory to conventional therapies. Although responses vary, immunotherapy is promising. The PDL1 expression appears to be of a poor predictive value. Drugs targeting genetic and epigenetic mechanisms of *SMARCA4* antagonism have therapeutic potential[10].

This case demonstrates the typical clinical presentation and morphological features of *SMARCA4*-DUTs: Diffuse sheets of large round to epithelioid poorly cohesive cells with a high nuclear grade and frequent necrosis on frozen sections. Tumor cell nuclei are typically vesicular, monotonous with moderate pleomorphism, and with a markedly increased mitotic activity. These features were also observed in the frozen sections of the tumor in the present case. A clinicopathologic correlation is crucial for patients' care because of the aggressive behavior of the tumor.

CONCLUSION

We report a case of *SMARCA4*-DUT with characteristic clinical manifestations. This novel subset of tumors should be suspected in patients with rapidly growing mediastinal and pulmonary nodules. The diagnosis can be obtained based on combined clinical features and histopathological features, such as absence of epithelial differentiation and negative *SMARCA4* expression.

FOOTNOTES

Author contributions: Kwon HJ and Jang MH contributed to manuscript writing and editing and data collection; Kwon HJ contributed to data analysis; Jang MH contributed to conceptualization and supervision; all authors have read and approved the final manuscript.

Supported by a grant from Yeungnam University, No. 222A580017.

Informed consent statement: The study protocol was approved by the Institutional Review Board of the Yeungnam University Medical Center with a waiver of informed consent.

Conflict-of-interest statement: The authors declare that they have no conflict of interest to disclose.

CARE Checklist (2016) statement: The authors have read the CARE Checklist (2016), and the manuscript has been prepared and revised according to the CARE Checklist (2016).

Country/Territory of origin: South Korea

ORCID number: Hee Jung Kwon 0000-0002-8800-7690; Min Hye Jang 0000-0002-4270-8897.

S-Editor: Yan JP
L-Editor: A
P-Editor: Yan JP

REFERENCES

1 **Perret R**, Chalabreysse L, Watson S, Serre I, Garcia S, Forest F, Yvorel V, Pissaloux D, Thomas de Montpreville V, Masliah-Planchon J, Lantuejoul S, Brevet M, Blay JY, Coindre JM, Tirode F, Le Loarer F. SMARCA4-deficient Thoracic Sarcomas: Clinicopathologic Study of 30 Cases With an Emphasis on Their Nosology and Differential Diagnoses. *Am J Surg Pathol* 2019; **43**: 455-465 [PMID: 30451731 DOI: 10.1097/PAS.0000000000001188]

2 **Rekhtman N**, Montecalvo J, Chang JC, Alex D, Ptashkin RN, Ai N, Sauter JL, Kezlarian B, Jungbluth A, Desmeules P, Beras A, Bishop JA, Plodkowski AJ, Gounder MM, Schoenfeld AJ, Namakydoust A, Li BT, Rudin CM, Riely GJ, Jones DR, Ladanyi M, Travis WD. SMARCA4-Deficient Thoracic Sarcomatoid Tumors Represent Primarily Smoking-Related Undifferentiated Carcinomas Rather Than Primary Thoracic Sarcomas. *J Thorac Oncol* 2020; **15**: 231-247 [PMID: 31751681 DOI: 10.1016/j.jtho.2019.10.023]

3 **Yoshida A**, Kobayashi E, Kubo T, Kodaira M, Motoi T, Motoi N, Yonemori K, Ohe Y, Watanabe SI, Kawai A, Kohno T, Kishimoto H, Ichikawa H, Hiraoka N. Clinicopathological and molecular characterization of SMARCA4-deficient thoracic sarcomas with comparison to potentially related entities. *Mod Pathol* 2017; **30**: 797-809 [PMID: 28256572 DOI: 10.1038/modpathol.2017.11]

4 **Ashour S**, Reynolds JP, Mukhopadhyay S, McKenney JK. SMARCA4-Deficient Undifferentiated Tumor Diagnosed on Adrenal Sampling. *Am J Clin Pathol* 2022; **157**: 140-145 [PMID: 34463317 DOI: 10.1093/ajcp/aqab101]

5 **Yadav R**, Sun L, Salyana M, Eric M, Gotlieb V, Wang JC. SMARCA4-Deficient Undifferentiated Tumor of Lung Mass-A Rare Tumor With the Rarer Occurrence of Brain Metastasis: A Case Report and Review of the Literature. *J Investig Med High Impact Case Rep* 2022; **10**: 23247096221074864 [PMID: 35356840 DOI: 10.1177/23247096221074864]

6 **Wong AK**, Shanahan F, Chen Y, Lian L, Ha P, Hendricks K, Ghaffari S, Iliev D, Penn B, Woodland AM, Smith R, Salada G, Carillo A, Laity K, Gupte J, Swedlund B, Tavtigian SV, Teng DH, Lees E. BRG1, a component of the SWI-SNF complex, is mutated in multiple human tumor cell lines. *Cancer Res* 2000; **60**: 6171-6177 [PMID: 11085541]

7 **Kuwamoto S**, Matsushita M, Takeda K, Tanaka N, Endo Y, Yamasaki A, Kohashi K, Oda Y, Horie Y. SMARCA4-deficient thoracic sarcoma: report of a case and insights into how to reach the diagnosis using limited samples and resources. *Hum Pathol* 2017; **70**: 92-97 [PMID: 28601660 DOI: 10.1016/j.humpath.2017.05.024]

8 **Chatzopoulos K**, Boland JM. Update on genetically defined lung neoplasms: NUT carcinoma and thoracic SMARCA4-

deficient undifferentiated tumors. *Virchows Arch* 2021; **478**: 21-30 [PMID: 33409598 DOI: 10.1007/s00428-020-03011-3]

9 **Nambirajan A**, Singh V, Bhardwaj N, Mittal S, Kumar S, Jain D. SMARCA4/BRG1-Deficient Non-Small Cell Lung Carcinomas: A Case Series and Review of the Literature. *Arch Pathol Lab Med* 2021; **145**: 90-98 [PMID: 33367658 DOI: 10.5858/arpa.2019-0633-OA]

10 **Nambirajan A**, Jain D. Recent updates in thoracic SMARCA4-deficient undifferentiated tumor. *Semin Diagn Pathol* 2021; **38**: 83-89 [PMID: 34147303 DOI: 10.1053/j.semdp.2021.06.001]

World Journal of Clinical Cases

Submit a Manuscript: https://www.f6publishing.com

World J Clin Cases 2023 April 16; 11(11): 2528-2534

DOI: 10.12998/wjcc.v11.i11.2528

ISSN 2307-8960 (online)

CASE REPORT

Prostate-specific antigen reduction after capecitabine plus oxaliplatin chemotherapy: A case report

Qian Zou, Rui-Lin Shen, Xiao Guo, Chen-Ye Tang

Specialty type: Medicine, research and experimental

Provenance and peer review: Unsolicited article; Externally peer reviewed.

Peer-review model: Single blind

Peer-review report's scientific quality classification

Grade A (Excellent): 0
Grade B (Very good): B, B
Grade C (Good): C
Grade D (Fair): 0
Grade E (Poor): 0

P-Reviewer: Marickar F, India; Sarier M, Turkey

Received: December 21, 2022
Peer-review started: December 21, 2022
First decision: January 20, 2023
Revised: February 1, 2023
Accepted: March 20, 2023
Article in press: March 20, 2023
Published online: April 16, 2023

Qian Zou, Jiaxing University Master Degree Cultivation Base, Zhejiang Chinese Medical University, Hangzhou 310000, Zhejiang Province, China

Rui-Lin Shen, Xiao Guo, Chen-Ye Tang, Department of Urology, The Second Affiliated Hospital of Jiaxing University, Jiaxing 314001, Zhejiang Province, China

Corresponding author: Chen-Ye Tang, Doctor, Department of Urology, The Second Affiliated Hospital of Jiaxing University, No. 1518 Huancheng Bei Lu, Nanhu District, Jiaxing 314001, Zhejiang Province, China. john99233@126.com

Abstract

BACKGROUND

Prostate cancer (PC) is currently the most common malignant tumor of the genitourinary system in men. Radical prostatectomy (RP) is recommended for the treatment of patients with localized PC. Adjuvant hormonal therapy (AHT) can be administered postoperatively in patients with high-risk or locally advanced PC. Chemotherapy is a vital remedy for castration-resistant prostate cancer (CRPC), and may also benefit patients with PC who have not progressed to CRPC.

CASE SUMMARY

A 68-year-old male was admitted to our hospital because of urinary irritation and dysuria with increased prostate-specific antigen (PSA) levels. After detailed examination, he was diagnosed with PC and treated with laparoscopic RP on August 3, 2020. AHT using androgen deprivation therapy (ADT) was performed postoperatively because of the positive surgical margin, extracapsular extension, and neural invasion but lasted only 6 mo. Unfortunately, he was diagnosed with rectal cancer about half a year after self-cessation of AHT, and was then treated with laparoscopic radical rectal resection and adjuvant chemotherapy using the capecitabine plus oxaliplatin (CapeOx) regimen. During the entire treatment process, the patient's PSA level first declined significantly after treatment of PC with laparoscopic RP and ADT, then rebounded because of self-cessation of ADT, and finally decreased again after CapeOx chemotherapy.

CONCLUSION

CapeOx chemotherapy can reduce PSA levels in patients with high-risk locally advanced PC, indicating that CapeOx may be an alternative chemotherapy regimen for PC.

Key Words: Prostate cancer; Chemotherapy; Prostate-specific antigen; Rectal tumor; Androgen deprivation therapy; Case report

Core Tip: Chemotherapy is mainly used for castration-resistant prostate cancer (PC) (CRPC) and may also benefit patients with PC who have not progressed to CRPC. We describe a patient with high-risk locally advanced PC treated with laparoscopic radical prostatectomy plus short-term adjuvant hormonal therapy and rectal cancer treated with laparoscopic radical rectal resection plus adjuvant chemotherapy, and found that prostate-specific antigen declined after the capecitabine plus oxaliplatin chemotherapy.

Citation: Zou Q, Shen RL, Guo X, Tang CY. Prostate-specific antigen reduction after capecitabine plus oxaliplatin chemotherapy: A case report. *World J Clin Cases* 2023; 11(11): 2528-2534
URL: https://www.wjgnet.com/2307-8960/full/v11/i11/2528.htm
DOI: https://dx.doi.org/10.12998/wjcc.v11.i11.2528

INTRODUCTION

Prostate cancer (PC) is the second most commonly diagnosed cancer in men, with 1414259 newly diagnosed cases worldwide in 2020[1]. The treatment of patients with PC differs according to the difference in the overall Gleason score and disease risk, and the main treatment methods include radical surgery (with or without dissection of enlarged lymph nodes), radical radiotherapy, hormone therapy, chemotherapy, and immunotherapy. Chemotherapy for PC is often used in combination with androgen deprivation therapy (ADT) for metastatic castration-resistant prostate cancer (CRPC). Taxanes such as docetaxel plus standard ADT prolong the median overall survival compared to ADT alone[2]. There is no clear conclusion regarding the advantages of chemotherapy after radical surgery for non-androgen-resistant PC, and clinical trials are underway[3].

Capecitabine plus oxaliplatin (CapeOx) is a commonly used chemotherapy regimen for stage III rectal cancer[4]. However, few studies have examined the effect of CapeOx on the recurrence rate in patients after radical prostatectomy (RP). We observed a patient with locally advanced PC treated with laparoscopic RP plus short-term ADT and metastatic rectal cancer treated with laparoscopic radical rectal resection (RRR) plus adjuvant chemotherapy using the CapeOx regimen, and found that the prostate-specific antigen (PSA) level declined after CapeOx chemotherapy in the absence of ADT. This report provides a new approach for the selection of chemotherapy regimens for patients with high-risk locally advanced PC after radical resection.

CASE PRESENTATION

Chief complaints

A 68-year-old male presented with urinary irritation and dysuria for one year and increased PSA levels for one month.

History of present illness

The patient was admitted to our hospital in July 2020 with urinary irritation and dysuria for 1 year, and his total serum PSA level was found to increase to 44.499 ng/mL in a health examination 1 mo prior to admission. The patient had no symptoms of urinary retention, hematuria, abdominal distension, or fever.

History of past illness

The patient had a history of hypertension for 10 years. He was treated with amlodipine besylate and irbesartan hydrochlorothiazide tablets, and his blood pressure was well controlled. Apart from hypertension, the patient had no other significant diseases.

Personal and family history

The patient had no noticeable personal history and no similar family history.

Physical examination

Digital rectal examination (DRE) findings after admission were as follows: The prostate was II degree large, tough, with a shallow central sulcus, and no tenderness; induration was found in the left lobe of the prostate, with no obvious tenderness; the anal sphincter was not loose; there was no blood on the glove, and there were no palpable enlarged lymph nodes in the bilateral inguinal area.

Laboratory examinations

Routine blood and urine tests, blood biochemistry, and coagulation function parameters were all normal, and detection of hepatitis B, hepatitis C, human immunodeficiency virus, and syphilis were all negative. However, the total serum PSA level further increased to 49.689 ng/mL after admission.

Imaging examinations

Ultrasound of the urinary system showed prostate hyperplasia with calcification (full shape of the prostate, approximately 50 mm in left-right diameter, 39 mm in upper-lower diameter, 40 mm in front-back diameter, thickened and uneven echo, imbalance in the ratio of internal and external glands, and multiple strong spots in the prostate). Nuclear magnetic resonance imaging revealed abnormal signals in the left and posterior parts of the peripheral zone of the prostate, suggesting the presence of PC. Therefore, ultrasound-guided needle biopsy was performed. Pathological examination of the left prostate puncture revealed an acinar adenocarcinoma with a Gleason score of 4 + 3 = 7, and examination of the right prostate puncture showed an acinar adenocarcinoma with a Gleason score of 3 + 4 = 7. Positron emission tomography-computed tomography revealed prostatic hyperplasia with calcification and nodular heterogeneous uptake of fluorodeoxyglucose in the peripheral zone.

FINAL DIAGNOSIS

According to the patient's history, DRE findings, relevant imaging examinations, and needle biopsy results, a preoperative diagnosis of PC was confirmed. Postoperative pathology further determined the tumor-node-metastasis stage of PC.

TREATMENT

The patient underwent laparoscopic RP on August 3, 2020. Postoperative pathological examination revealed prostatic acinar adenocarcinoma with a Gleason score of 4 + 3 = 7 and International Society of Urological Pathology grade of 3. The tumor-invasive areas included the bottom, body, and apex of the prostate. Involvement of the extracapsular extension and fibrous integument was also observed. The left and right seminal vesicles did not invade, and intravascular tumor embolus was not detected; however, neural invasion was observed. The left and right vas deferens were not affected, in contrast to the distal and proximal urethral margins. The patient was diagnosed with $T_{3a}N_0M_0$ with a positive margin (R_1) due to extracapsular extension and neural invasion. Therefore, adjuvant hormonal therapy (AHT) was requisite, and oral bicalutamide 50 mg per day plus subcutaneous leuprorelin 3.75 mg per 28 d (maximal androgen blockade) were used for ADT after surgery.

OUTCOME AND FOLLOW-UP

The patient was regularly treated until January 2021 for a total of 6 mo, and ADT was discontinued for personal reasons. In June 2021, the patient underwent an annual health examination, which unexpectedly revealed a rectal mass. Unfortunately, the patient was later diagnosed with rectal cancer *via* colonoscopic biopsy. Therefore, the patient was readmitted to the hospital for rectal cancer treatment, and laparoscopic RRR was performed in July 2021. Postoperative pathology revealed a protruding moderately differentiated adenocarcinoma (about 1.6 cm × 1.1 cm × 0.5 cm in size) with full-thickness invasion, accompanied by intravascular tumor embolus formation, and metastasis in 5 of the 7 resected mesenteric lymph nodes. The rectal cancer stage was $pT_3N_{2a}M_0$, stage IIIB. Therefore, the CapeOx regimen was used for chemotherapy after the operation in August 2021, and the cycle lasted for half a year. At follow-up, we found that the patient's PSA and testosterone levels both declined significantly after treatment of PC with laparoscopic RP and ADT in August 2020, but rebounded after the self-cessation of ADT in January 2021, while the alkaline phosphatase level remained stable (Figure 1). Surprisingly, the PSA level decreased again after CapeOx chemotherapy, eventually falling to zero (Figure 1B). However, a slight increase in PSA was observed in March 2022, the second month following the completion of chemotherapy (Figure 1B).

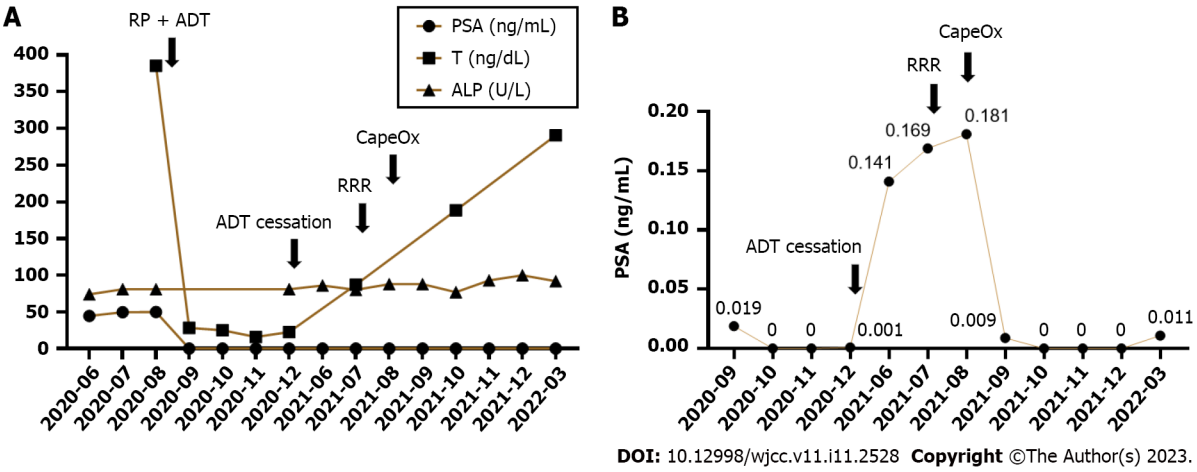

DOI: 10.12998/wjcc.v11.i11.2528

Figure 1 Trends of indicators related to prostate cancer. A: Trends of prostate-specific antigen (PSA), testosterone, and alkaline phosphatase levels during the entire treatment process; B: Variations of PSA level after cessation of androgen deprivation therapy and capecitabine plus oxaliplatin chemotherapy for rectal cancer. PSA: Prostate-specific antigen; T: Testosterone; ALP: Alkaline phosphatase; RP: Radical prostatectomy; ADT: Androgen deprivation therapy; RRR: Radical rectal resection; CapeOx: Capecitabine plus oxaliplatin.

DISCUSSION

According to the EAU-EANM-ESTRO-ESUR-SIOG guidelines on PC, this patient was grouped into the high-risk group before surgery, and there is no unified standard regimen for the treatment of high-risk PC[5]. Either radical surgery or radiotherapy can be chosen, and RP is generally recommended for patients whose tumors do not invade the urethral sphincter or anchor the pelvic wall[5].

Postoperatively, the patient had a positive surgical margin (R_1), extracapsular extension, and neural invasion ($T_{3a}N_0M_0$). Therefore, the patient's diagnosis should be defined as high-risk locally advanced PC, and postoperative pelvic radiotherapy could be selected in this case. Three major randomized controlled trials have addressed the issue of postoperative adjuvant radiotherapy in such patients[6-8]. The current conclusion is that for pT_3pN_0 patients with postoperative PSA level < 0.1 ng/mL, there is a high risk of local recurrence due to a positive surgical margin (the most important factor), extracapsular extension, and/or invasion of the seminal vesicles. At present, there are two options available to patients: (1) Adjuvant radiotherapy to the surgical area immediately after the recovery of urination function; and (2) during close clinical follow-up, starting salvage radiotherapy when PSA exceeds 0.1 ng/mL. However, urinary and gastrointestinal side effects are common during and after radiotherapy, as reported in the EORTC 22991 trial, with approximately 50% of the patients suffering from acute urogenital toxicity of grade 1, 20% of grade 2, and 2% of grade 3; meanwhile, approximately 30% of the patients reported acute gastrointestinal toxicity of grade 1, 10% of grade 2, and less than 1% of grade 3. Common toxic reactions include dysuria, frequent urination, urinary retention, hematuria, diarrhea, rectal bleeding, and proctitis[9]. After communicating with the patient, the second option was finally chosen, and adjuvant radiotherapy was not performed for the time being.

AHT after radical resection of high-risk or locally advanced PC can provide good survival benefits. For patients with a high recurrence risk, a long course of endocrine therapy (2-3 years) can be administered after surgery[10]. The patient was administered ADT postoperatively, after which his PSA and testosterone levels declined rapidly, eventually decreasing to zero for PSA and to less than 50 ng/dL for testosterone. However, after only 6 mo of normative AHT, the patient stopped treatment spontaneously, and both PSA and testosterone levels began to rebound. Subsequently, the patient was diagnosed with rectal cancer approximately half a year after self-cessation of AHT. Because of his condition, adjuvant chemotherapy using the CapeOx regimen was performed after laparoscopic RRR, showing that CapeOx chemotherapy could visibly reduce the PSA level. In other words, CapeOx chemotherapy may effectively control PC progression.

Chemotherapy is primarily used for CRPC. Androgen-targeted therapy prolongs survival in patients with metastatic CRPC; however, most men still face progressive disease and require additional treatment. Taxanes have been shown to improve survival in metastatic CRPC and are first-line chemotherapy drugs for the treatment of PC. Docetaxel is a taxane that can improve the response rates in patients with metastatic CRPC in terms of pain, serum PSA level, quality of life, and overall survival [11]. However, despite a good initial response and survival benefit, almost all patients eventually develop resistance, which is an important barrier to long-term survival[12]. In addition, available studies have shown that platinum-based chemotherapy drugs can benefit patients with CRPC. Dorff *et al*[13] performed re-chemotherapy with oxaliplatin and pemetrexed in men with CRPC that had progressed after one or two cycles of chemotherapy, including taxane, and showed that 47 men received

a median of six cycles of treatment with an overall response rate of 30%, 64% of them had a decrease in PSA, and 74% of them had clinical disease control. Moreover, Lee *et al*[14] treated 33 CRPC patients who had failed docetaxel with intravenous gemcitabine and oxaliplatin combined with oral prednisolone, and showed a PSA response rate of 55%. These two clinical trials suggest that oxaliplatin as the core chemotherapy regimen can be used in patients with CRPC after the failure of taxane-based chemotherapy. In another study, eight of 14 androgen-independent PC patients (57%) treated with CapeOx after first-line docetaxel had a PSA response defined as a 50% reduction from baseline PSA levels. Our findings are consistent with those of this research. Hence, CapeOx chemotherapy may fill the gap in the treatment of CRPC after taxane treatment and become the second- and third-line chemotherapy for patients with CRPC[15].

It is generally believed that platinum drugs are first transported to tumor cells through copper transporter 1. After entering tumor cells, platinum complexes usually undergo the activated step of chloride ligand replacement through water molecules or other small molecules containing sulfhydryl groups. Compared with the extracellular matrix, intracellular chloride concentrations decrease significantly, which promotes the transformation of cation hydrate, and platinum-based chemotherapeutic drugs bind to DNA through the formation of intracellular and interstrand cross-links, changing the DNA structure and causing DNA damage. DNA damage can arrest the cell cycle and induce apoptosis in rapidly proliferating tumor cells[16]. In a mouse model of PC xenograft, compared with mice treated with anti-programmed cell death protein 1 (PD-1) antibody monotherapy alone, mice treated with oxaliplatin combined with anti-PD-1 antibody achieved the best survival rate[17]. In addition, two immunogenic markers, $HMGB_1$ and calreticulin, expressed in oxaliplatin-treated PC cell lines PTEN-CaP_8 and $PNEC_{30}$, were significantly upregulated after 24 h of oxaliplatin treatment[17]. These results indicate that oxaliplatin could activate the immunophenotype of PC cells. Prostate fibroblasts promote the progression of PC by secreting factors that facilitate tumor growth and induce migration and invasion of PC cells. Angiogenin (ANG) can significantly stimulate the invasion of type I collagen in fibroblasts associated with PC[18]. ANG, a member of the secretory ribonuclease superfamily, is upregulated in PC and mediates ribosomal RNA (rRNA) transcription in androgen-stimulated PC cells. Upon androgen stimulation, ANG undergoes nuclear translocation in androgen-dependent PC cells where it binds to the ribosomal DNA promoter and stimulates rRNA transcription. ANG antagonists inhibit androgen-induced rRNA transcription and proliferation in androgen-dependent PC cells[19]. Surprisingly, using a comprehensive multi-technology approach of crystallography, spectroscopy, and spectral analysis, Marzo *et al*[20] demonstrated that oxaliplatin could effectively bind ANG to inhibit the proliferation and migration of the PC cell line PC-3. This finding provides another research direction for the treatment of PC with oxaliplatin.

CONCLUSION

Chemotherapy for PC is mainly used for CRPC, while there are few clinical studies on the use of chemotherapy in patients with common PC after RP. The anticancer mechanism of oxaliplatin mainly causes DNA damage, thereby stopping the cell division cycle. In PC, oxaliplatin has a unique role in immunology and angiogenesis, which may also provide new directions for future studies on the anticancer mechanism of oxaliplatin.

FOOTNOTES

Author contributions: Tang CY conceived the idea; Zou Q collected data and drafted the manuscript; Shen RL and Guo X have reviewed the manuscript; All authors read and approved the final draft of the manuscript.

Supported by Jiaxing Science and Technology Foundation, No. 2021AY30018.

Informed consent statement: Written informed consent was obtained from all the patients.

Conflict-of-interest statement: All the authors report no relevant conflicts of interest for this article.

CARE Checklist (2016) statement: The authors have read the CARE Checklist (2016), and the manuscript was prepared and revised according to the CARE Checklist (2016).

Country/Territory of origin: China

ORCID number: Qian Zou 0000-0001-5646-8153; Chen-Ye Tang 0000-0001-8640-197X.

S-Editor: Fan JR
L-Editor: A
P-Editor: Fan JR

REFERENCES

1 **Sung H**, Ferlay J, Siegel RL, Laversanne M, Soerjomataram I, Jemal A, Bray F. Global Cancer Statistics 2020: GLOBOCAN Estimates of Incidence and Mortality Worldwide for 36 Cancers in 185 Countries. *CA Cancer J Clin* 2021; **71**: 209-249 [PMID: 33538338 DOI: 10.3322/caac.21660]

2 **Sonnenburg DW**, Morgans AK. Emerging Therapies in Metastatic Prostate Cancer. *Curr Oncol Rep* 2018; **20**: 46 [PMID: 29644451 DOI: 10.1007/s11912-018-0692-z]

3 **Ahlgren GM**, Flodgren P, Tammela TLJ, Kellokumpu-Lehtinen P, Borre M, Angelsen A, Iversen JR, Sverrisdottir A, Jonsson E, Sengelov L; Investigators of the Scandinavian Prostate Cancer Study Number 12. Docetaxel Versus Surveillance After Radical Prostatectomy for High-risk Prostate Cancer: Results from the Prospective Randomised, Open-label Phase 3 Scandinavian Prostate Cancer Group 12 Trial. *Eur Urol* 2018; **73**: 870-876 [PMID: 29395502 DOI: 10.1016/j.eururo.2018.01.012]

4 **Liu FQ**, Cai SJ. [Adjuvant and perioperative neoadjuvant therapy for colorectal cancer]. *Zhonghua Wei Chang Wai Ke Za Zhi* 2019; **22**: 315-320 [PMID: 31054544 DOI: 10.3760/cma.j.issn.1671-0274.2019.04.002]

5 **Mottet N**, van den Bergh RCN, Briers E, Van den Broeck T, Cumberbatch MG, De Santis M, Fanti S, Fossati N, Gandaglia G, Gillessen S, Grivas N, Grummet J, Henry AM, van der Kwast TH, Lam TB, Lardas M, Liew M, Mason MD, Moris L, Oprea-Lager DE, van der Poel HG, Rouvière O, Schoots IG, Tilki D, Wiegel T, Willemse PM, Cornford P. EAU-EANM-ESTRO-ESUR-SIOG Guidelines on Prostate Cancer-2020 Update. Part 1: Screening, Diagnosis, and Local Treatment with Curative Intent. *Eur Urol* 2021; **79**: 243-262 [PMID: 33172724 DOI: 10.1016/j.eururo.2020.09.042]

6 **Hackman G**, Taari K, Tammela TL, Matikainen M, Kouri M, Joensuu T, Luukkaala T, Salonen A, Isotalo T, Pétas A, Hendolin N, Boström PJ, Aaltomaa S, Lehtoranta K, Hellström P, Riikonen J, Korpela M, Minn H, Kellokumpu-Lehtinen PL, Pukkala E, Hemminki A; FinnProstate Group. Randomised Trial of Adjuvant Radiotherapy Following Radical Prostatectomy Versus Radical Prostatectomy Alone in Prostate Cancer Patients with Positive Margins or Extracapsular Extension. *Eur Urol* 2019; **76**: 586-595 [PMID: 31375279 DOI: 10.1016/j.eururo.2019.07.001]

7 **Kneebone A**, Fraser-Browne C, Duchesne GM, Fisher R, Frydenberg M, Herschtal A, Williams SG, Brown C, Delprado W, Haworth A, Joseph DJ, Martin JM, Matthews JHL, Millar JL, Sidhom M, Spry N, Tang CI, Turner S, Wiltshire KL, Woo HH, Davis ID, Lim TS, Pearse M. Adjuvant radiotherapy *vs* early salvage radiotherapy following radical prostatectomy (TROG 08.03/ANZUP RAVES): a randomised, controlled, phase 3, non-inferiority trial. *Lancet Oncol* 2020; **21**: 1331-1340 [PMID: 33002437 DOI: 10.1016/S1470-2045(20)30456-3]

8 **Parker CC**, Clarke NW, Cook AD, Kynaston HG, Petersen PM, Catton C, Cross W, Logue J, Parulekar W, Payne H, Persad R, Pickering H, Saad F, Anderson J, Bahl A, Bottomley D, Brasso K, Chahal R, Cooke PW, Eddy B, Gibbs S, Goh C, Gujral S, Heath C, Henderson A, Jaganathan R, Jakobsen H, James ND, Kanaga Sundaram S, Lees K, Lester J, Lindberg H, Money-Kyrle J, Morris S, O'Sullivan J, Ostler P, Owen L, Patel P, Pope A, Popert R, Raman R, Røder MA, Sayers I, Simms M, Wilson J, Zarkar A, Parmar MKB, Sydes MR. Timing of radiotherapy after radical prostatectomy (RADICALS-RT): a randomised, controlled phase 3 trial. *Lancet* 2020; **396**: 1413-1421 [PMID: 33002429 DOI: 10.1016/S0140-6736(20)31553-1]

9 **Matzinger O**, Duclos F, van den Bergh A, Carrie C, Villà S, Kitsios P, Poortmans P, Sundar S, van der Steen-Banasik EM, Gulyban A, Collette L, Bolla M; EORTC Radiation Oncology Group. Acute toxicity of curative radiotherapy for intermediate- and high-risk localised prostate cancer in the EORTC trial 22991. *Eur J Cancer* 2009; **45**: 2825-2834 [PMID: 19682889 DOI: 10.1016/j.ejca.2009.07.009]

10 **Dong BJ**, He DL, Li MZ, Li YH, Li ZH, Liu RR, Liu ZH, Sheng XN, Wang L, Wang XH. [Safety consensus on classical endocrine therapy for prostate cancer]. *Xiandai Miniao Waike Zazhi* 2018; **23**: 248-258 [DOI: 10.3969/j.issn.1009-8291.2018.04.003]

11 **Nader R**, El Amm J, Aragon-Ching JB. Role of chemotherapy in prostate cancer. *Asian J Androl* 2018; **20**: 221-229 [PMID: 29063869 DOI: 10.4103/aja.aja_40_17]

12 **Ruiz de Porras V**, Font A, Aytes A. Chemotherapy in metastatic castration-resistant prostate cancer: Current scenario and future perspectives. *Cancer Lett* 2021; **523**: 162-169 [PMID: 34517086 DOI: 10.1016/j.canlet.2021.08.033]

13 **Dorff TB**, Tsao-Wei DD, Groshen S, Boswell W, Goldkorn A, Xiong S, Quinn DI, Pinski JK. Efficacy of oxaliplatin plus pemetrexed in chemotherapy pretreated metastatic castration-resistant prostate cancer. *Clin Genitourin Cancer* 2013; **11**: 416-422 [PMID: 24099865 DOI: 10.1016/j.clgc.2013.07.011]

14 **Lee JL**, Ahn JH, Choi MK, Kim Y, Hong SW, Lee KH, Jeong IG, Song C, Hong BS, Hong JH, Ahn H. Gemcitabine-oxaliplatin plus prednisolone is active in patients with castration-resistant prostate cancer for whom docetaxel-based chemotherapy failed. *Br J Cancer* 2014; **110**: 2472-2478 [PMID: 24736579 DOI: 10.1038/bjc.2014.204]

15 **Gasent Blesa JM**, Giner Marco V, Giner-Bosch V, Cerezuela Fuentes P, Alberola Candel V. Phase II trial of oxaliplatin and capecitabine after progression to first-line chemotherapy in androgen-independent prostate cancer patients. *Am J Clin Oncol* 2011; **34**: 155-159 [PMID: 20539209 DOI: 10.1097/COC.0b013e3181d6b453]

16 **Zhang C**, Xu C, Gao X, Yao Q. Platinum-based drugs for cancer therapy and anti-tumor strategies. *Theranostics* 2022; **12**: 2115-2132 [PMID: 35265202 DOI: 10.7150/thno.69424]

17 **Zhou J**, Yang T, Liu L, Lu B. Chemotherapy oxaliplatin sensitizes prostate cancer to immune checkpoint blockade therapies *via* stimulating tumor immunogenicity. *Mol Med Rep* 2017; **16**: 2868-2874 [PMID: 28677730 DOI: 10.3892/mmr.2017.6908]

18 **Jones ML**, Ewing CM, Isaacsa WB, Getzenberg RH. Prostate cancer-derived angiogenin stimulates the invasion of prostate fibroblasts. *J Cell Mol Med* 2012; **16**: 193-201 [PMID: 21352472 DOI: 10.1111/j.1582-4934.2011.01283.x]

19 **Li S**, Hu MG, Sun Y, Yoshioka N, Ibaragi S, Sheng J, Sun G, Kishimoto K, Hu GF. Angiogenin mediates androgen-stimulated prostate cancer growth and enables castration resistance. *Mol Cancer Res* 2013; **11**: 1203-1214 [PMID: 23851444 DOI: 10.1158/1541-7786.MCR-13-0072]

20 **Marzo T**, Ferraro G, Cucci LM, Pratesi A, Hansson Ö, Satriano C, Merlino A, La Mendola D. Oxaliplatin inhibits angiogenin proliferative and cell migration effects in prostate cancer cells. *J Inorg Biochem* 2022; **226**: 111657 [PMID: 34784565 DOI: 10.1016/j.jinorgbio.2021.111657]

World Journal of Clinical Cases

Submit a Manuscript: https://www.f6publishing.com

World J Clin Cases 2023 April 16; 11(11): 2535-2540

DOI: 10.12998/wjcc.v11.i11.2535

ISSN 2307-8960 (online)

CASE REPORT

Bilateral carpal tunnel syndrome and motor dysfunction caused by gout and type 2 diabetes: A case report

Gao-Feng Zhang, Cun-Min Rong, Wei Li, Ben-Lei Wei, Ming-Tong Han, Qing-Luan Han

Specialty type: Medicine, research and experimental

Provenance and peer review: Unsolicited article; Externally peer reviewed.

Peer-review model: Single blind

Peer-review report's scientific quality classification

Grade A (Excellent): 0
Grade B (Very good): B
Grade C (Good): C
Grade D (Fair): 0
Grade E (Poor): 0

P-Reviewer: Fazilat-Panah D, Iran; Nguyen B, Viet Nam

Received: December 28, 2022
Peer-review started: December 28, 2022
First decision: February 8, 2023
Revised: February 22, 2023
Accepted: March 15, 2023
Article in press: March 15, 2023
Published online: April 16, 2023

Gao-Feng Zhang, Cun-Min Rong, Wei Li, Ben-Lei Wei, Ming-Tong Han, Qing-Luan Han, Department of Hand and Foot Surgery, Affiliated Hospital of Jining Medical University, Jining 272029, Shandong Province, China

Corresponding author: Wei Li, MD, Chief Doctor, Professor, Department of Hand and Foot Surgery, Affiliated Hospital of Jining Medical University, No.89 Gu Huai Road, Jining 272029, Shandong Province, China. liweimails@163.com

Abstract

BACKGROUND

Carpal tunnel syndrome (CTS) has been associated with gout and type 2 diabetes mellitus (T2DM). However, due to insufficient clinical understanding of gout-related CTS and reliance on the diagnostic importance of elevated serum uric acid levels, such cases are prone to missed diagnosis, misdiagnosis, and delayed treatment. In addition, the effect of T2DM on gout - induced carpal tunnel syndrome has not been reported.

CASE SUMMARY

Herein, we present an unusual case of CTS and motor dysfunction caused by miliary tophaceous gout and T2DM. The patient presented to the hand and foot clinic with paresthesia of the fingers of both hands, especially at night. The patient was diagnosed with type 2 diabetes a month ago. Ultrasonography revealed bilateral transverse carpal ligament thickening with median nerve compression during hospitalization. The patient was successfully treated with carpal tunnel decompression and tendon release. The postoperative pathological examination revealed typical gout nodules. This case suggests that the presence of T2DM could accelerate tophi formation and worsen CTS symptoms, although no definitive proof in this regard has been described previously.

CONCLUSION

Tophi formation may most likely cause the co-occurrence of CTS and flexor dysfunction in gout and incipient diabetes patients.

Key Words: Carpal tunnel syndrome; Motor dysfunction; Tophaceous gout; Type 2 diabetes mellitus; Operate; Case report

Core Tip: The onset of diabetes in patients with a previous history of hyperuricemia would likely accelerate urate deposition and lead to the exacerbation of carpal tunnel syndrome.

Citation: Zhang GF, Rong CM, Li W, Wei BL, Han MT, Han QL. Bilateral carpal tunnel syndrome and motor dysfunction caused by gout and type 2 diabetes: A case report. *World J Clin Cases* 2023; 11(11): 2535-2540
URL: https://www.wjgnet.com/2307-8960/full/v11/i11/2535.htm
DOI: https://dx.doi.org/10.12998/wjcc.v11.i11.2535

INTRODUCTION

Carpal tunnel syndrome (CTS) is the most common form of compressive neuropathy that develops due to the compression of the median nerve in the constrained space of the carpal tunnel. It is typically a chronic and progressive condition, with an incidence of approximately 1%−3% per year[1]. The co-occurrence of CTS and motor dysfunction caused by gout, which has been reported as a cause of CTS in 0.6% of cases, is extremely rare in clinical practice[2]. Herein, we report an unusual case of bilateral CTS associated with tophaceous gout and type 2 diabetes mellitus (T2DM).

CASE PRESENTATION

Chief complaints

A 51-year-old male patient presented to the hand and foot clinic with paresthesia and motor dysfunction of the fingers of both hands for the last 1 mo.

History of present illness

Symptoms started 1 mo with paresthesia and motor dysfunction of the radial fingers of both the hands.

History of past illness

The patient had a history of hyperuricemia for more than 10 years, and his serum uric acid levels were recorded up to 13.44 mg/dL. Accordingly, he was regularly taking febuxostat for two years. One month prior, the patient was found to have elevated blood glucose levels during a physical examination in our hospital and was diagnosed with T2DM, for which he was not receiving treatment.

Personal and family history

The patient's father had a history of diabetes and hyperlipidemia, and the patient denied any family history of hyperuricemia.

Physical examination

Physical examination revealed bilateral thenar muscle atrophy and palmar hypoesthesia on the radial side of both the hands. The wrist flexion test was positive bilaterally, and Tinel's sign was positive on the left and mildly positive on the right.

Laboratory examinations

Laboratory testing showed uric acid levels within the normal range (5.59 mg/dL) and a fasting blood glucose level of 12.0 mmol/L. In addition, the glycosylated hemoglobin was at 10.0%.

Imaging examinations

Ultrasound examination showed narrowing of the bilateral carpal canal as well as median nerve compression, with a diameter of 0.13 cm on the left and 0.17 cm on the right at the narrowest points. Electromyography revealed bilateral median nerve neuropathy, which was more pronounced on the left (Supplementary material). No abnormalities were found in X-rays of both the wrists. During hospitalization, improved electromyography revealed neurogenic lesions in bilateral abductors pollicis brevis. Furthermore, the nerve conduction velocity displayed that the latency of motor branches was prolonged, which confirmed bilateral median nerve damage. Greater severity on the left side was noted.

FINAL DIAGNOSIS

Combined with the patient's medical history, a final diagnosis of bilateral carpal tunnel syndrome was determined.

TREATMENT

Celecoxib and febuxostat were administered to maintain the patient's uric acid at a normal level. Further, dapagliflozin and acarbose were used to adjust the blood glucose level below 11 mmol/L.

Intraoperatively, multiple white calcareous crystals were observed in the bilateral carpal tunnel, and the median nerves were decompressed by excision of tophi from the carpal canal. Bilaterally, there were multiple miliary tophi in the perineurium of median nerve. They were deposited throughout the superficial flexor tendon of the middle finger and the deep flexor tendon of the ring finger of the left hand as well as the deep flexor tendon of the ring and little fingers of the right hand(Figure 1). Longitudinal incisions were made to expose these urate crystals. We cleaned it with a small curette and rinsed the remaining urate crystals with a sodium bicarbonate solution. In addition, we found that sterile sodium bicarbonate solution was more beneficial to rinse urate crystals off than normal saline. Therefore, we suggest that rinsing with sodium bicarbonate solution is necessary. After trimming, those damaged tendon bands were improved with a 5-0 absorbable suture. The postoperative histopathological findings were consistent with gout nodules (monosodium urate crystals), confirming the diagnosis (Figure 2).

OUTCOME AND FOLLOW-UP

Postoperatively, the patient developed a fever despite colchicine and naproxen treatment; however, the fever subsided within 3 d. At the 4-wk follow-up, the hand numbness improved significantly, and the wrist range of motion returned to normal. Three months following the surgery, there was a partial improvement in the thenar muscle atrophy. At the 6-mo follow-up, the numbness was completely resolved, with a marked improvement in the thenar muscle atrophy.

DISCUSSION

The carpal tunnel is an osteoligamentous structure with poor extension ability. It protects the median nerve and nine tendons that act to flex the fingers. The median nerve enters the volar surface of the hand through the carpal tunnel, which runs under the flexor retinaculum. Once the tunnel is narrowed or its content is increased, the median nerve is vulnerable to compression, resulting in the development of CTS.

Gout-related CTS is mainly due to the deposition of tophi on the ligaments or content of the carpal tunnel, such as the tendon surface[3,4]. In 1958, Ward *et al*[5] reported the first case of CTS caused by gout, and suggested that the underlying mechanism could be the deposition of tophi on the wrist flexor tendons that resulted in the compression of the median nerve within the carpal tunnel. In subsequent years, few cases of gout-related CTS have been reported successively. This apparent rarity of the association between gout and CTS is likely to have been fallacious, owing to the failure of recognition and lack of adequate awareness. Our literature search in the PubMed database for articles published in English using the terms "carpal tunnel syndrome," "gout," and "diabetes" showed that the cases of gout-related CTS were reported more frequently in recent decades; however, they remained scarce at large. This suggests that the association between CTS and gout has been gradually discovered over the years and has received increasing attention from doctors. However, the effect of T2DM on gout-induced carpal tunnel syndrome has not been reported.

Gout is a metabolic disorder, and is one of the most common inflammatory arthritic conditions worldwide that is caused by persistent hyperuricemia. The global prevalence of gout is increasing, possibly due to trends in global dietary habits and the increasing gout-associated chronic diseases. Specifically, gout affects more than 41 million worldwide[6]. Both gout and T2DM are metabolic diseases clearly associated with insulin resistance, which generally refers to the reduced role of insulin in the uptake and clearance of glucose from surrounding tissues. T2DM has a promoting effect on the development of gout. A key factor may be that in the proximal convoluted tubules of the glomerulus, glucose and uric acid share the same carriers of reabsorption,with resultant competition between them. In the early stage of T2DM, hyperglycemia and hyperinsulinemia inhibit the urinary excretion of uric acid, thus increasing the blood uric acid level[7,8]. In addition, the microvascular lesions and microcirculation disorder in patients with T2DM accelerate the deposition of urates. The specific anatomical characteristics of the carpal tunnel and the metabolic characteristics of its dense connective tissue make

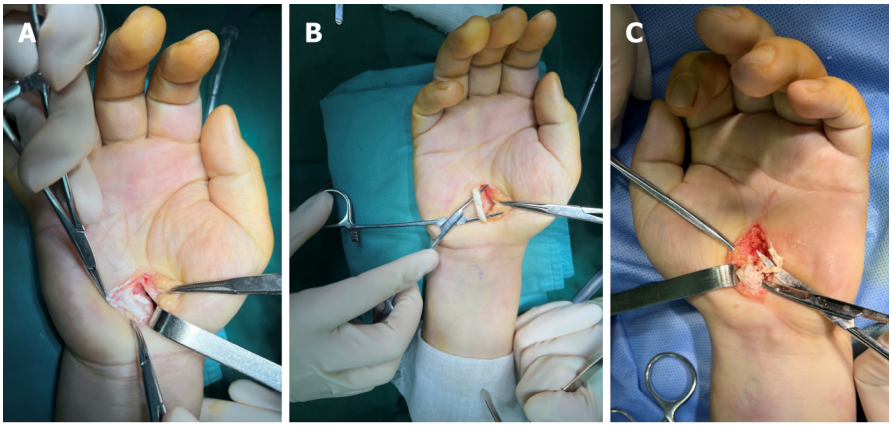

DOI: 10.12998/wjcc.v11.i11.2535

Figure 1 Intraoperative photographs of the surgical field of both hands. A: The median nerve surrounded by miliary tophi in the synovium; B: The deep flexor tendon of the little finger of the right hand thickened by crystals deposited throughout the tendon; C: The deep flexor tendon of the ring finger of the left hand eroded by tophi.

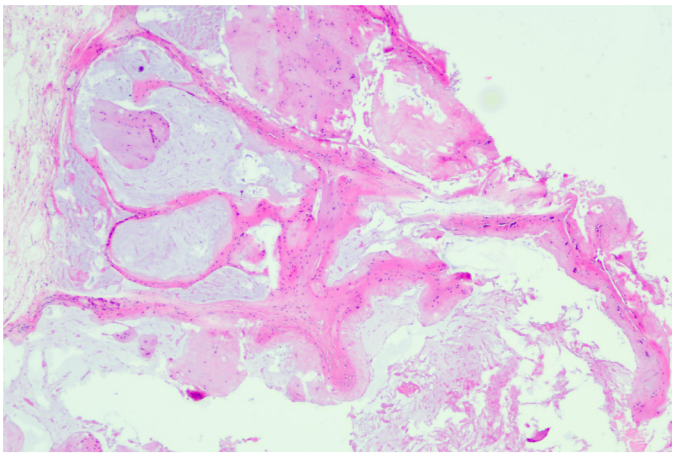

DOI: 10.12998/wjcc.v11.i11.2535

Figure 2 Histopathological findings. Photomicrograph showing gout nodules filled with monosodium urate crystals (hematoxylin and eosin staining, magnification: eyepiece 10 × and objective 4 ×).

the deposition of gout crystals more likely. In our patient, T2DM and CTS appeared successively, which supports that early diabetes is likely to lead to the development of gout associated carpal tunnel syndrome.

Lack of timely medical or surgical treatment of gout can lead to the development of CTS. Reducing the uric acid level within the normal range and anti-inflammatory treatment with allopurinol, probenecid, colchicine or other agents has been shown to alleviate the associated CTS symptoms in patients with gout. Surgical removal of covert tophi and median nerve decompression is another effective option for eliminating CTS symptoms[9]. Jacoulet reported a case in which multiple gout nodules oppressed the median nerve in the carpal canal and the ulnar nerve in the carpal and cubital canals, resulting in severe ulnar nerve palsy[10]. In such cases, standard open tunnel release would not adequately address any of these factors without appropriate medical treatment. Thus, we opted for surgical treatment after the blood glucose and uric acid levels were stabilized within normal ranges.

CONCLUSION

In patients with a history of gout and T2DM, the formation of tophi should be considered the most probable reason for the co-occurrence of CTS and flexor dysfunction. If patients have persistent neurological symptoms, conservative treatment may lead to irreversible neurological damage; therefore, early surgical treatment is recommended. Furthermore, a complete course of uric acid-lowering and anti-inflammatory treatment is necessary to prevent an acute gout attack and irritable nerve syndrome. Based on the patient's history and findings in the present case, we speculate that early-stage T2DM

could accelerate tophi formation and aggravate CTS symptoms, although no definitive proof has been described to date.

ACKNOWLEDGEMENTS

I would like to acknowledge Professors Qing-Luan Han and Wei Li for inspiring my interest in scientific research.

FOOTNOTES

Author contributions: Rong CM contributed to the conception and design of the study; Han MT and Wei BL contributed significantly to the manuscript preparation; Zhang GF obtained information about the cases and wrote the manuscript; Li W and Han QL helped perform the analysis with constructive discussions and provided the final approval for the version of the article to be published.

Supported by Science and Technology Bureau of Jining, No. 2021YXNS115.

Informed consent statement: Informed written consent was obtained from the patient for publication of this report and any accompanying images.

Conflict-of-interest statement: All the authors report no relevant conflicts of interest for this article.

CARE Checklist (2016) statement: The authors have read CARE Checklist (2016), and the manuscript was prepared and revised according to CARE Checklist (2016).

Country/Territory of origin: China

ORCID number: Gao-Feng Zhang 0000000184604968; Wei Li 0000000302312991.

S-Editor: Li L
L-Editor: A
P-Editor: Li L

REFERENCES

1 **Ashworth NL**. Carpal tunnel syndrome, 2022. 2022 Jan 31 [cited 1 March 2023]. Available from: http://emedicine.medscape.com/article/327330-overview
2 **Rich JT**, Bush DC, Lincoski CJ, Harrington TM. Carpal tunnel syndrome due to tophaceous gout. *Orthopedics* 2004; **27**: 862-863 [PMID: 15369009 DOI: 10.3928/0147-7447-20040801-23]
3 **Milandri A**, Farioli A, Gagliardi C, Longhi S, Salvi F, Curti S, Foffi S, Caponetti AG, Lorenzini M, Ferlini A, Rimessi P, Mattioli S, Violante FS, Rapezzi C. Carpal tunnel syndrome in cardiac amyloidosis: implications for early diagnosis and prognostic role across the spectrum of aetiologies. *Eur J Heart Fail* 2020; **22**: 507-515 [PMID: 31975495 DOI: 10.1002/ejhf.1742]
4 **Chuang HL**, Wong CW. Carpal tunnel syndrome induced by tophaceous deposits on the median nerve: case report. *Neurosurgery* 1994; **34**: 919; discussion 920 [PMID: 8052395]
5 **WARD LE**, BICKEL WH, CORBIN KB. Median neuritis (carpal tunnel syndrome) caused by gouty tophi. *J Am Med Assoc* 1958; **167**: 844-846 [PMID: 13549200 DOI: 10.1001/jama.1958.72990240006008b]
6 **Safiri S**, Kolahi AA, Cross M, Carson-Chahhoud K, Hoy D, Almasi-Hashiani A, Sepidarkish M, Ashrafi-Asgarabad A, Moradi-Lakeh M, Mansournia MA, Kaufman JS, Collins G, Woolf AD, March L, Smith E. Prevalence, Incidence, and Years Lived With Disability Due to Gout and Its Attributable Risk Factors for 195 Countries and Territories 1990-2017: A Systematic Analysis of the Global Burden of Disease Study 2017. *Arthritis Rheumatol* 2020; **72**: 1916-1927 [PMID: 32755051 DOI: 10.1002/art.41404]
7 **Lin KC**, Tsai ST, Lin HY, Chou P. Different progressions of hyperglycemia and diabetes among hyperuricemic men and women in the kinmen study. *J Rheumatol* 2004; **31**: 1159-1165 [PMID: 15170930]
8 **Li C**, Hsieh MC, Chang SJ. Metabolic syndrome, diabetes, and hyperuricemia. *Curr Opin Rheumatol* 2013; **25**: 210-216 [PMID: 23370374 DOI: 10.1097/BOR.0b013e32835d951e]
9 **Janssen T**, Rayan GM. Gouty tenosynovitis and compression neuropathy of the median nerve. *Clin Orthop Relat Res* 1987;

203-206 [PMID: 3815949]
10 **Jacoulet P**. [Double tunnel syndrome of the upper limb in tophaceous gout. Apropos of a case]. *Ann Chir Main Memb Super* 1994; **13**: 42-45 [PMID: 7511910 DOI: 10.1016/s0753-9053(05)80356-4]

World Journal of Clinical Cases

Submit a Manuscript: https://www.f6publishing.com

World J Clin Cases 2023 April 16; 11(11): 2541-2548

DOI: 10.12998/wjcc.v11.i11.2541

ISSN 2307-8960 (online)

CASE REPORT

Pregnancy complicated by juxtaglomerular cell tumor of the kidney: A case report

Xian Fu, Gang Deng, Kai Wang, Chang Shao, Li-Ping Xie

Specialty type: Medicine, research and experimental

Provenance and peer review: Unsolicited article; Externally peer reviewed.

Peer-review model: Single blind

Peer-review report's scientific quality classification

Grade A (Excellent): 0
Grade B (Very good): 0
Grade C (Good): C, C
Grade D (Fair): 0
Grade E (Poor): E

P-Reviewer: Ait Addi R, Morocco; Gica N, Romania; Rotondo JC, Italy

Received: December 26, 2022
Peer-review started: December 26, 2022
First decision: January 12, 2023
Revised: January 27, 2023
Accepted: March 17, 2023
Article in press: March 17, 2023
Published online: April 16, 2023

Xian Fu, Gang Deng, Kai Wang, Department of Urology, Affiliated Hangzhou First People's Hospital, Zhejiang University School of Medicine, Hangzhou 310006, Zhejiang Province, China

Chang Shao, Department of Pathology, Affiliated Hangzhou First People's Hospital, Zhejiang University School of Medicine, Hangzhou 310006, Zhejiang Province, China

Li-Ping Xie, Department of Urology, The First Affiliated Hospital, Zhejiang University School of Medicine, Hangzhou 310003, Zhejiang Province, China

Corresponding author: Li-Ping Xie, PhD, Director, Professor, Surgeon, Department of Urology, The First Affiliated Hospital, Zhejiang University School of Medicine, No. 79 Qingchun Road, Shangcheng District, Hangzhou 310003, Zhejiang Province, China. xielp@zju.edu.cn

Abstract

BACKGROUND

Juxtaglomerular cell tumor (JGCT) of the kidney, also known as reninoma, is a rare renal tumor that typically clinically manifests as hypertension, hypokalemia, high renin, and high aldosterone. It is a cause of secondary hypertension. Pregnancy with JGCT is rarer and easily misdiagnosed as pregnancy-induced hypertension, thus affecting treatment.

CASE SUMMARY

A 28-year-old woman presented in early pregnancy with hypertension (blood pressure of 229/159 mmHg), nausea, and occasional dizziness and headache. The patient was diagnosed with pregnancy-induced hypertension, and no relief was found after symptomatic treatment; hence, the pregnancy was terminated by artificial abortion. Her blood pressure remained high following termination of pregnancy. Blood tests suggested hypokalemia (2.997 mmol/L), blood aldosterone measured 613 ng/L, and computed tomography urography showed a tumor in the right kidney. Therefore, laparoscopic partial nephrectomy was performed. After surgery, the patient's blood pressure returned to normal, and blood potassium, aldosterone, and renin normalized. Postoperative pathological examination revealed JGCT. After long-term follow-up, the patient became pregnant again 6 mo after surgery. No hypertension occurred during pregnancy, and the patient delivered a healthy female neonate.

CONCLUSION

Patients with pregnancy complicated by JGCT are difficult to diagnose. Herein,

we advise surgeons on proper handling of such situations.

Key Words: Juxtaglomerular cell tumor; Pregnancy; Hypertension; Hypokalemia; Partial nephrectomy; Case report

Core Tip: Juxtaglomerular cell tumor (JGCT) is a rare endocrine tumor of the kidney. Typical JGCTs are characterized by high serum renin, high aldosterone secretion, severe hypertension, and severe hypokalemia, known as the "three high and one low" phenomenon. The mainstream treatment is surgery. We report an even rarer case of pregnancy complicated with JGCT, who was misdiagnosed with pregnancy-induced hypertension in a primary hospital, and the pregnancy was terminated artificially due to poor response to conservative treatment. The patient was admitted to our hospital for further treatment because her blood pressure remained high after termination of pregnancy and she was diagnosed with JGCT. The patient recovered well after surgery to remove the tumor. In this article, the case is analyzed retrospectively in the context of the literature in an attempt to explore the diagnosis, treatment, and prognosis of this rare disease.

Citation: Fu X, Deng G, Wang K, Shao C, Xie LP. Pregnancy complicated by juxtaglomerular cell tumor of the kidney: A case report. *World J Clin Cases* 2023; 11(11): 2541-2548
URL: https://www.wjgnet.com/2307-8960/full/v11/i11/2541.htm
DOI: https://dx.doi.org/10.12998/wjcc.v11.i11.2541

INTRODUCTION

Juxtaglomerular cell tumor (JGCT) is a very rare renin-secreting tumor of the kidney. The tumor is typically found in young adults, with a peak incidence in the second and third decades of life. It was first reported by Robertson *et al*[1] in 1967, who first described it as a special type of juxtamedullary angiomyocytoma. Subsequently, Kihara reported a second case, calling it the Robertson Kihara syndrome[1,2]. At present, approximately only 100 JGCT cases have been reported worldwide, among which pregnancy complicated by JGCT is even rarer[3]. JGCT can independently secrete large amounts of renin, resulting in excessive secretion of angiotensin and aldosterone, and causing patients to have severe hypertension and hypokalemia that produce a series of symptoms, including headache, dizziness, blurred vision, hypertension-induced nausea and vomiting, muscle weakness, edema, and arrhythmia caused by hypokalemia. Severe target organ damage and cardiovascular disease occur in a short period of time. The severity of these symptoms is independent of tumor size[4,5]. Expression of renin and intracytoplasmatic rhomboid crystals or granules on electron microscopic images are diagnostic features of JGCT. The immunohistochemical profile of JGCT has been recently reported as being immunoreactive for vimentin, focally immunoreactive for smooth muscle actin, and negative for cytokeratin. CD34 and CD117 immunoreactivities have been reported as helpful markers of JGCT[2,6].

JGCT may be associated with hypertension, which may lead to a misdiagnosis as pregnancy-induced hypertension in patients with JGCT during pregnancy, thus affecting treatment[7]. In this article, the clinical data and imaging findings of a patient with pregnancy complicated by JGCT are analyzed retrospectively in the context of the literature in an attempt to explore the diagnosis, treatment, and prognosis of this rare disease.

CASE PRESENTATION

Chief complaints

A 28-year-old pregnant woman was first admitted to Department of Obstetrics of a primary hospital with vaginal bleeding and high blood pressure for 2 d at 7 wk of gestation.

History of present illness

One month previously, the patient presented with vaginal bleeding and high blood pressure of 229/159 mmHg at 7 wk of gestation, with nausea, occasionally accompanied by dizziness and a headache. The primary diagnosis was threatened abortion from pregnancy-induced hypertension. Antihypertensive therapy performed after admission was not beneficial; thus, the pregnancy was terminated by artificial abortion. However, blood pressure remained high (151/110 mmHg). For further treatment, the patient

was admitted to the Department of Cardiology of our hospital. During hospitalization in the Cardiology Department, adrenal-enhanced computed tomography (CT) examination was performed to identify the cause of hypertension. CT examination revealed no adrenal abnormalities, but a tumor of the right kidney was detected, and the patient was referred to our Urology Department for further treatment.

History of past illness

The patient had no history of hypertension, diabetes, cardiovascular or cerebrovascular diseases, and also no history of surgery. The patient had no history of viral or bacterial infection of the urinary system.

Personal and family history

The patient was marriageable, had normal menstruation in the past, and had no history of pregnancy or abortion, and no smoking and drinking habits. Her family history was ordinary, and there was no history of genetic heritability of cancer. The patient had no history of viral or bacterial infection of the urinary system.

Physical examination

No tenderness in the bilateral kidneys, ureters, or bladder was observed on examination. Furthermore, no obvious abnormality was found upon gynecological physical examination, and there was no vaginal bleeding when the patient was transferred to our department.

Laboratory examinations

Laboratory studies showed a blood aldosterone level of 121 ng/L (decubitus reference value, 30-236) and 613 ng/L (orthostatic reference value, 30-353), and the blood renin level was 352.2 mIU/L (decubitus reference value, 2.8-39.9) and 487.9 mIU/L (orthostatic reference value, 4.4-46.1). Meanwhile, serum potassium level was 2.97 mmol/L (reference value, 3.5-5.5). Levels of other hormones, such as adrenaline, dopamine, norepinephrine, and cortisol, were normal. Urine cell analysis and urine culture for bacteria were negative. There were no obvious abnormalities in routine blood tests, coagulation function, hepatitis B, acquired immunodeficiency syndrome, syphilis, liver and kidney function, or other blood biochemical tests.

Imaging examinations

Contrast-enhanced ultrasound of the kidney showed a moderately echogenic mass with low enhancement that was characterized by a "slow in and fast out" pattern (Figure 1A). Both computed tomography urography (CTU) and magnetic resonance imaging (MRI) showed a right upper pole renal mass measuring approximately 3.5 cm × 3 cm × 2.5 cm (endogenic type) in size, without significant abnormalities in the bilateral adrenal glands (Figure 1B and C).

FINAL DIAGNOSIS

The final diagnosis of the presented case was JGCT of the kidney.

TREATMENT

Considering possible malignancy, tumor size and location, experience of the chief surgeon, and will of the patient's family members, retroperitoneoscopic partial nephrectomy of the right kidney was performed. During surgery, laparoscopic ultrasound was used to accurately locate the tumor, which was successfully resected (Figure 2). Both frozen pathological examination and postoperative pathological analyses of the surgical specimen reported JGCT, and immunohistochemistry highlighted the following: CD34 (+), vimentin (+), CK117 (-), and Ki-67 (< 5% positivity) (Figure 3).

OUTCOME AND FOLLOW-UP

The patient was discharged on the seventh day after surgery. One month post-surgery, the patient's blood pressure decreased to normal without dizziness, headache, nausea, vomiting, or other discomfort. Blood potassium, aldosterone, and renin levels normalized after re-examination. Four months post-surgery, contrasted-enhanced CT revealed no tumor recurrence.

After long-term follow-up, the patient became pregnant again 6 mo after surgery; no hypertension occurred during the pregnancy. Eventually, the patient delivered a healthy female neonate.

DOI: 10.12998/wjcc.v11.i11.2541

Figure 1 Imaging examinations. A: Contrast-enhanced ultrasonographic examination of the kidney shows a medium echogenic mass presenting with low enhancement characterized by a "slow in and fast out" pattern; B: Computed tomography (CT) image selected from the enhanced CT urography scan sequence shows an endogenic round-like mass in the upper pole of the right kidney, which is approximately 3 cm in diameter; C: Coronal magnetic resonance imaging shows a right upper pole renal mass (endogenic type) with no significant abnormalities in the bilateral adrenal glands.

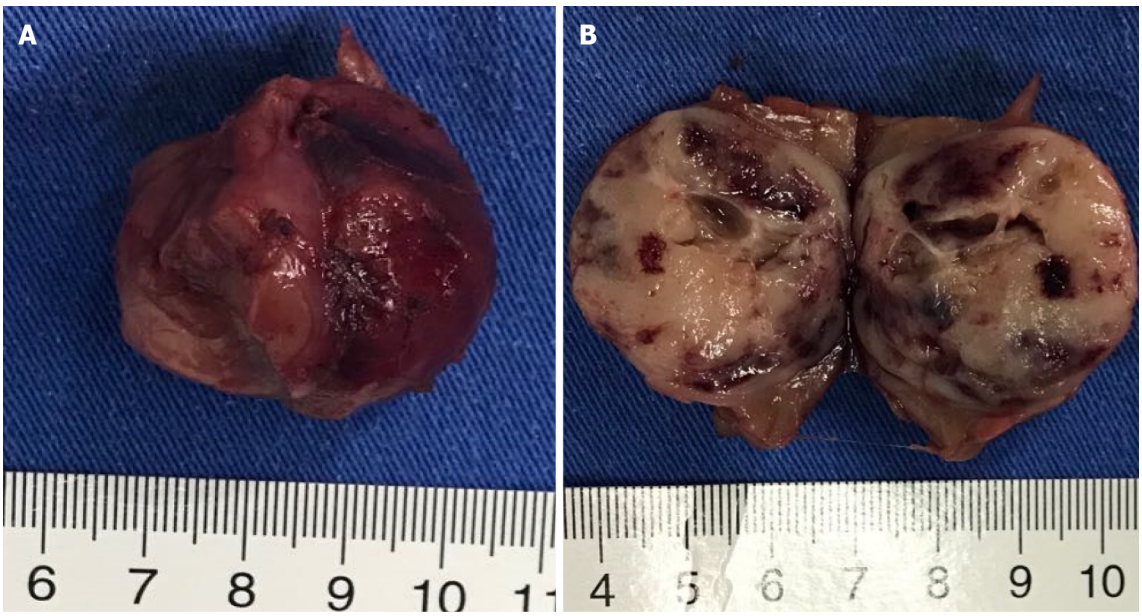

DOI: 10.12998/wjcc.v11.i11.2541

Figure 2 The tumor. A: General view of the tumor after resection; B: Appearance of the tumor after dissection.

DISCUSSION

JGCT, also known as reninoma, is a rare endocrine tumor of the kidney, which causes secondary hypertension. Current studies suggest that JGCT may be associated with an increased number of chromosome 10 and deletion of chromosome 9, X, and the long arm of chromosome 11[8]. Wong *et al*[9] statistically analyzed 89 JGCT cases, and the results showed that these tumors were more common in the 20-30 year age group, with an average age of 27 years, and most occurred in females, with a male-to-female ratio of approximately 1:2[9]. Dong *et al*[10] proposed to divide JGCTs into three categories according to the blood pressure and blood potassium status of the patient: The first category is typical JGCTs, where patients have symptoms of hypertension and hypokalemia; the second type is atypical JGCTs, where patients have one of the two symptoms; the third type is nonfunctional JGCTs, which is confirmed by postoperative pathology despite the absence of both symptoms. Typical renin tumors are the most common type, characterized by high serum renin, high aldosterone secretion, severe hypertension, and severe hypokalemia; this is known as the "three high and one low" phenomenon. Excess renin secreted by JGCT activates the renin-angiotensin-aldosterone system (RAAS), resulting in an abnormal increase of angiotensin II and aldosterone, constriction of peripheral blood vessels, and promotion of water and sodium retention, which often leads to uncontrolled hypertension, accompanied by dizziness, headache, nausea and vomiting, blurred vision, and even fundal hemorrhage, proteinuria, and other manifestations of hypertensive target organ dysfunction. JGCT-induced hypertension often requires the combined use of multiple antihypertensive drugs, mainly

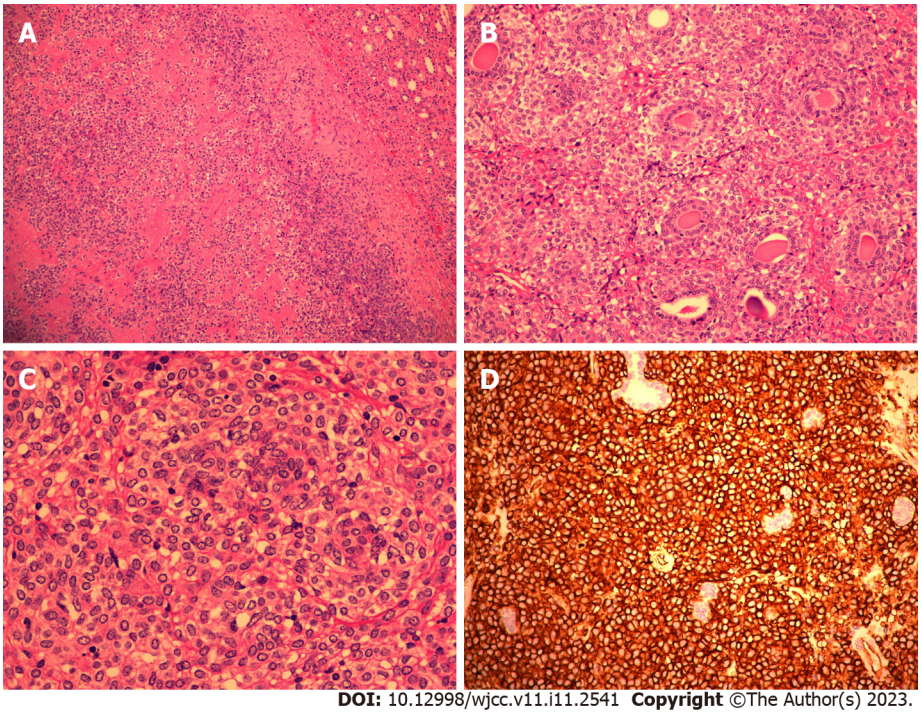

DOI: 10.12998/wjcc.v11.i11.2541

Figure 3 Postoperative pathological and immunohistochemical results confirm juxtaglomerular cell tumor. A: 10 × magnification of tumor cells; B: 10 × magnification of tumor cells; C: 10 × magnification of tumor cells; D: Immunohistochemical results showing that the tumor cells were positive for CD34 and vimentin, and negative for CD117.

angiotensin converting enzyme inhibitors, to effectively control blood pressure[11]. In addition, a secondary increase in aldosterone boosts urinary potassium excretion by promoting exchange of sodium and potassium in the collecting duct of the main cells, leading to hypokalemia, which may lead to limb weakness and other corresponding symptoms[12]. A 24-h urine potassium test is helpful in detecting secondary aldosteronism during the course of the disease.

Consistent with previous observations reported in the literature, our patient was a 28-year-old woman who presented with recurrent hypertension and hypokalemia before surgery-a typical case of JGCT. In our case, preoperative antihypertensive therapy was ineffective, and there was accompanying dizziness, headache, and nausea, with hypokalemia, which was consistent with descriptions in the literature. It should be noted that although the patient's 24-h urine potassium level was within the normal range, abnormal potassium excretion was still present because the patient had been in a low potassium state, under which urinary potassium excretion was reduced, suggesting a secondary increase in aldosterone.

The diagnosis of JGCT should be combined with clinical manifestations, laboratory examination, and imaging examination, such as ultrasonography, CT, and MRI. Serum electrolyte, renin, and aldosterone levels should be tested in cases of suspected JGCT. Patients with typical JGCT present with hypokalemia, high renin, and high aldosterone, with a normal aldosterone-renin ratio (ARR), which can be distinguished from primary aldosteronism (high aldosterone levels, normal or elevated renin levels, and increased ARR) because renin secretion is inhibited by abnormally high aldosterone levels[13]. RAAS inhibitors should be avoided as far as possible before detection, because they may affect the secretion of renin, aldosterone, and other hormones, thus covering up the disease. Comparison of renin activity in bilateral renal venous blood by selective or segmental renal venous blood sampling may be helpful in diagnosing JGCT; however, it is not recommended clinically due to its high false-negative rate. Previous studies have shown that the positive rate of this test was about 62.5%; meanwhile, in a study of 14 cases of JGCTs in China, it was only 21.4%[14]. Our case did not use RAAS inhibitors before the test, and blood test showed hypokalemia, hyperreninemia, and elevated aldosterone; ARR was normal, which was consistent with literature reports. Considering the low positive rate of bilateral renin activity compared to renal venous blood sampling, this test was not performed.

In ultrasonography images, JGCTs mostly present as round masses with low or slightly high echogenicity; however, due to their rarity and typically small volume, they are easily undiagnosed and misdiagnosed on ultrasonography[15]. On a plain CT scan, low to iso-dense circular masses with capsules were mostly found, most of which were located inside the renal parenchyma. Enhanced CT showed no significant enhancement of tumor in the early stage; however, mild to moderate enhancement in delayed stage or portal vein stage was seen. MRI images are characterized by low to equal signal intensity in T1W1 and high signal intensity in T2W2. At present, many experts believe that MRI may lead to misdiagnosis. Compared to MRI, CT scan is more sensitive for JGCT and has more

diagnostic value[16]. However, small JGCTs are sometimes left undiagnosed by CT. Faucon *et al*[17] compared CT and MRI images of ten patients with JGCTs and suggested that MRI examination should be performed for patients with suspected JGCTs if no abnormality was found on CT[17].

A definitive diagnosis of JGCTs requires pathological examination. Microscopically, the tumor tissue shows closely arranged round or polygonal cells, which are rich in small blood vessels. The tumor cells are mostly of the same size and might have focal low-to-moderate atypia. Immunohistochemistry shows that tumor cells are positive for CD34 and vimentin, and CD117 is positive in some cases[18]. Immunohistochemical results of this case were positive for CD34 and vimentin, and negative for CD117, which was consistent with literature reports. Pregnancy complicated by reninoma is rarely reported, and patients are often misdiagnosed as eclamptic or preeclamptic. Mismanagement often leads to premature delivery, abortion, or stillbirth[19]. In the case reported by Ohashi *et al*[20], undiagnosed JGCT caused uncontrolled hypertension. The patient had been diagnosed with pre-eclampsia before termination of pregnancy, and pregnancy was terminated at 25 wk due to congestive heart failure and acute kidney injury. Further examination after termination of pregnancy revealed a tumor in the left kidney, which was confirmed as JGCT on pathological examination after surgical resection[20].

Regarding the relationship between pregnancy and renin tumor development, studies have reported that the change of immune status that occurs during pregnancy makes pregnant women vulnerable to pathogenic infections, including those caused by carcinogenic viruses[21,22]. For example, oncogenic polyomavirus BK can promote the proliferation, invasion, and migration of bladder cancer in immunocompromised patients[23,24]. Regarding Merkel cell polyomavirus, whose DNA sequences have been detected in blood samples from immunocompetent and immunosuppressed patients with kidney disease, pregnant females have been reported to present a decrease in antibody response to this virus [21,25]. Therefore, whether pregnancy complicated by reninoma is associated with viral or bacterial infections is also an aspect to be considered. However, in this case, the pregnant woman had no history of viral or bacterial infection of the urinary system, so we do not believe that the patient's JGCT was related to viral or bacterial infection.

RAAS inhibitors are helpful in relieving hypertension and hypokalemia caused by JGCT, and it has been reported that aliskiren can effectively improve hypertension and hypokalemia in patients before surgery[16]. When the diagnosis of JGCT is confirmed, surgery is the preferred treatment. Previous studies have shown that the average size of JGCTs is approximately 3 cm, and partial nephrectomy can be considered for most small JGCTs to protect renal function as much as possible[16]. Currently, with the advances in laparoscopic technology, laparoscopic partial peritoneal nephrectomy or retroperitoneal partial nephrectomy has been gradually promoted, and studies have shown that the latter has the advantages of lower risk, shorter operation time, faster postoperative recovery, and relatively easy learning compared to the former, thus fast becoming the conventional surgical choice[14], and Da Vinci robot-assisted laparoscopic partial nephrectomy is certain to be more advantageous[26]. According to literature reviews, most JGCTs are endogenous, which may be related to their origin from paraveral cells. In our case, the retroperitoneal approach was adopted. Since the tumor was endogenous, intraoperative ultrasound was used to locate the tumor, which greatly accelerated the surgical progress. JGCTs are mostly benign tumors with a good prognosis, and blood pressure and potassium of patients can return to normalcy after resection; however, a few malignant cases have been reported. In a case reported by Professor Shera *et al*[27] from India, an 8-year-old boy was admitted to the hospital in emergency due to intractable hypertension (blood pressure 210/140 mmHg). Examination revealed an 8 cm × 8 cm mass in the left hilum of the kidney, and pathology after total nephrectomy suggested JGCT. Close follow-up and review after surgery revealed that the patient developed hypertension again a year later, and CT examination revealed a mass about 5 cm × 4 cm in the left renal fossa. Blood pressure returned to normal after another surgical excision. The overall features of the recurrent tumor were suggestive of a malignant and invasive form of JGCT[27]. Therefore, patients with JGCTs should be followed for as long as possible to monitor for tumor recurrence.

CONCLUSION

In the present case, the pregnant woman was initially misdiagnosed with pregnancy-induced hypertension in a primary hospital. As the pregnancy was at an early stage, she opted for induced abortion. Reasons for misdiagnosis were as follows: The patient could not undergo CT because of the pregnancy and doctors in other hospitals did not routinely perform Doppler ultrasound examination of the urinary system. However, the patient's hypertension did not resolve after abortion, which necessitated further CT examination that found the renal tumor. This case reminds us that if refractory hypertension is present during pregnancy, JGCT should be considered, and ultrasonography of the kidney and adrenal gland, MRI scan, or other endocrine hormone examinations need to be completed for further diagnosis. In addition, although most cases of JGCT present as benign tumors of the kidney and are treated with partial nephrectomy or nephrectomy, there are isolated cases of malignant infiltration, and JGCT may also co-exist with other forms of cancer, such as leukemia and breast cancer. JGCT may play a mediating role in these other forms of cancer, for example by regulating renin overex-

pression[28]. Therefore, we should further encourage the study of JGCT related pathological systems.

ACKNOWLEDGEMENTS

The authors thank the patient for allowing us to publish this case report.

FOOTNOTES

Author contributions: Fu X, Wang K, and Deng G performed partial nephrectomy; Fu X and Wang K collected the clinical data and compared the current case with the literature; Fu X and Shao C collected the images; Fu X wrote the manuscript; Xie LP critically revised the manuscript; all authors read and approved the final manuscript.

Supported by Medical and Health Technology Project of Hangzhou, No. A20220540.

Informed consent statement: Informed consent was obtained in both written and verbal format from the patient to publish this case report and any accompanying images.

Conflict-of-interest statement: All the authors report no relevant conflicts of interest for this article.

CARE Checklist (2016) statement: The authors have read the CARE Checklist (2016), and the manuscript was prepared and revised according to the CARE Checklist (2016).

Country/Territory of origin: China

ORCID number: Xian Fu 0000-0002-5128-9305; Gang Deng 0000-0002-8593-4341; Kai Wang 0000-0001-8082-9211; Chang Shao 0000-0002-9059-2382; Li-Ping Xie 0000-0002-3287-5536.

S-Editor: Fan JR
L-Editor: Wang TQ
P-Editor: Fan JR

REFERENCES

1 **Robertson PW**, Klidjian A, Harding LK, Walters G, Lee MR, Robb-Smith AH. Hypertension due to a renin-secreting renal tumour. *Am J Med* 1967; **43**: 963-976 [PMID: 6060417 DOI: 10.1016/0002-9343(67)90256-2]
2 **Kim HJ**, Kim CH, Choi YJ, Ayala AG, Amirikachi M, Ro JY. Juxtaglomerular cell tumor of kidney with CD34 and CD117 immunoreactivity: report of 5 cases. *Arch Pathol Lab Med* 2006; **130**: 707-711 [PMID: 16683889 DOI: 10.5858/2006-130-707-JCTOKW]
3 **Lin SY**, Liu WY, Chen WC, Chen RH. Secondary hypertension due to a renin-secreting juxtaglomerular cell tumor. *J Formos Med Assoc* 2010; **109**: 237-240 [PMID: 20434032 DOI: 10.1016/S0929-6646(10)60047-2]
4 **Conn JW**, Cohen EL, Lucas CP, McDonald WJ, Mayor GH, Blough WM Jr, Eveland WC, Bookstein JJ, Lapides J. Primary reninism. Hypertension, hyperreninemia, and secondary aldosteronism due to renin-producing juxtaglomerular cell tumors. *Arch Intern Med* 1972; **130**: 682-696 [PMID: 4343374 DOI: 10.1001/archinte.130.5.682]
5 **Skarakis NS**, Papadimitriou I, Papanastasiou L, Pappa S, Dimitriadi A, Glykas I, Ntoumas K, Lampropoulou P, Kounadi T. Juxtaglomerular cell tumour of the kidney: a rare cause of resistant hypertension. *Endocrinol Diabetes Metab Case Rep* 2022; **2022** [PMID: 35023474 DOI: 10.1530/EDM-21-0042]
6 **Gupta S**, Folpe AL, Torres-Mora J, Reuter VE, Zuckerman JE, Falk N, Stanton ML, Muthusamy S, Smith SC, Sharma V, Sethi S, Herrera-Hernandez L, Jimenez RE, Cheville JC. Immunohistochemical expression of renin and GATA3 help distinguish juxtaglomerular cell tumors from renal glomus tumors. *Hum Pathol* 2022; **128**: 110-123 [PMID: 35926808 DOI: 10.1016/j.humpath.2022.07.016]
7 **Xue M**, Chen Y, Zhang J, Guan Y, Yang L, Wu B. Reninoma coexisting with adrenal adenoma during pregnancy: A case report. *Oncol Lett* 2017; **13**: 3186-3190 [PMID: 28521424 DOI: 10.3892/ol.2017.5802]
8 **Brandal P**, Busund LT, Heim S. Chromosome abnormalities in juxtaglomerular cell tumors. *Cancer* 2005; **104**: 504-510 [PMID: 15968688 DOI: 10.1002/cncr.21205]
9 **Wong L**, Hsu TH, Perlroth MG, Hofmann LV, Haynes CM, Katznelson L. Reninoma: case report and literature review. *J Hypertens* 2008; **26**: 368-373 [PMID: 18192852 DOI: 10.1097/HJH.0b013e3282f283f3]
10 **Dong D**, Li H, Yan W, Xu W. Juxtaglomerular cell tumor of the kidney--a new classification scheme. *Urol Oncol* 2010; **28**:

34-38 [PMID: 19914097 DOI: 10.1016/j.urolonc.2009.08.003]
11 **Yu ZQ**, Wang JW, Ma LL. [Summary and analysis of diagnostic data of 110 cases of juxtaglomerular cell tumers and introduction of typical cases]. *Zhonghua Gaoxueya Zazhi* 2018; **26**: 693-697 [DOI: 10.5005/jp/books/14145_3]
12 **Kang S**, Chen F, Zhong Y, Han B, Cheng G, Guo A, Tian Y, Tong X, Dou J, Ye H. Preoperative Diagnosis of Juxtaglomerular Cell Tumors in Eight Patients. *J Clin Hypertens (Greenwich)* 2016; **18**: 982-990 [PMID: 27012170 DOI: 10.1111/jch.12810]
13 **Piaditis G**, Markou A, Papanastasiou L, Androulakis II, Kaltsas G. Progress in aldosteronism: a review of the prevalence of primary aldosteronism in pre-hypertension and hypertension. *Eur J Endocrinol* 2015; **172**: R191-R203 [PMID: 25538205 DOI: 10.1530/EJE-14-0537]
14 **Liu K**, Wang B, Ma X, Li H, Zhang Y, Li J, Yao Y, Tang L, Xuan Y, Guo A, Zhang X. Minimally Invasive Surgery-Based Multidisciplinary Clinical Management of Reninoma: A Single-Center Study. *Med Sci Monit* 2019; **25**: 1600-1610 [PMID: 30822300 DOI: 10.12659/MSM.913826]
15 **Osawa S**, Hosokawa Y, Soda T, Yasuda T, Kaneto H, Kitamura T, Kozawa J, Otsuki M, Imagawa A, Okumi M, Miyagawa Y, Nonomura N, Shimomura I. Juxtaglomerular cell tumor that was preoperatively diagnosed using selective renal venous sampling. *Intern Med* 2013; **52**: 1937-1942 [PMID: 23994987 DOI: 10.2169/internalmedicine.52.0395]
16 **Rosei CA**, Giacomelli L, Salvetti M, Paini A, Corbellini C, Tiberio G, Muiesan ML. Advantages of renin inhibition in a patient with reninoma. *Int J Cardiol* 2015; **187**: 240-242 [PMID: 25838223 DOI: 10.1016/j.ijcard.2015.03.280]
17 **Faucon AL**, Bourillon C, Grataloup C, Baron S, Bernadet-Monrozies P, Vidal-Petiot E, Azizi M, Amar L. Usefulness of Magnetic Resonance Imaging in the Diagnosis of Juxtaglomerular Cell Tumors: A Report of 10 Cases and Review of the Literature. *Am J Kidney Dis* 2019; **73**: 566-571 [PMID: 30527885 DOI: 10.1053/j.ajkd.2018.09.005]
18 **Vidal-Petiot E**, Bens M, Choudat L, Fernandez P, Rouzet F, Hermieu JF, Bruneval P, Goujon JM, Flamant M, Vandewalle A. A case report of reninoma: radiological and pathological features of the tumour and characterization of tumour-derived juxtaglomerular cells in culture. *J Hypertens* 2015; **33**: 1709-1715 [PMID: 26132761 DOI: 10.1097/HJH.0000000000000592]
19 **Lachvac L**, Svajdler M, Valansky L, Nagy V, Benicky M, Frohlichova L, Nyitrayova O. Juxtaglomerular cell tumor, causing fetal demise. *Int Urol Nephrol* 2011; **43**: 365-370 [PMID: 20556510 DOI: 10.1007/s11255-010-9782-z]
20 **Ohashi Y**, Kobayashi S, Arai T, Nemoto T, Aoki C, Nagata M, Sakai K. Focal Segmental Glomerulosclerosis Secondary to Juxtaglomerular Cell Tumor during Pregnancy: A Case Report. *Case Rep Nephrol Urol* 2014; **4**: 88-94 [PMID: 24926309 DOI: 10.1159/000362757]
21 **Mazziotta C**, Pellielo G, Tognon M, Martini F, Rotondo JC. Significantly Low Levels of IgG Antibodies Against Oncogenic Merkel Cell Polyomavirus in Sera From Females Affected by Spontaneous Abortion. *Front Microbiol* 2021; **12**: 789991 [PMID: 34970247 DOI: 10.3389/fmicb.2021.789991]
22 **Cheungpasitporn W**, Thongprayoon C, Craici IM, Sharma K, Chesdachai S, Khoury NJ, Ettore AS. Reactivation of BK polyomavirus during pregnancy, vertical transmission, and clinical significance: A meta-analysis. *J Clin Virol* 2018; **102**: 56-62 [PMID: 29502047 DOI: 10.1016/j.jcv.2018.02.015]
23 **Zeng Y**, Sun J, Bao J, Zhu T. BK polyomavirus infection promotes growth and aggressiveness in bladder cancer. *Virol J* 2020; **17**: 139 [PMID: 32928222 DOI: 10.1186/s12985-020-01399-7]
24 **Shen CL**, Wu BS, Lien TJ, Yang AH, Yang CY. BK Polyomavirus Nephropathy in Kidney Transplantation: Balancing Rejection and Infection. *Viruses* 2021; **13** [PMID: 33809472 DOI: 10.3390/v13030487]
25 **Jin HT**, Park SJ, Choi EK, Kim YS. The frequency of Merkel cell polyomavirus in whole blood from immunocompetent and immunosuppressed patients with kidney disease and healthy donors. *Microb Pathog* 2019; **131**: 75-80 [PMID: 30910721 DOI: 10.1016/j.micpath.2019.03.020]
26 **Kweon OJ**, Lim YK, Kim HR, Lee MK, Lee TJ, Won H, Choi SY, Kim JW, Chi BH, Chang IH, Moon YT, Kim KD, Kim TH. Robot-Assisted Partial Nephrectomy for Treatment of Juxtaglomerular Cell Tumor of the Kidney: A Case Report. *J Endourol Case Rep* 2020; **6**: 77-79 [PMID: 32775683 DOI: 10.1089/cren.2019.0066]
27 **Shera AH**, Baba AA, Bakshi IH, Lone IA. Recurrent malignant juxtaglomerular cell tumor: A rare cause of malignant hypertension in a child. *J Indian Assoc Pediatr Surg* 2011; **16**: 152-154 [PMID: 22121315 DOI: 10.4103/0971-9261.86876]
28 **Inam R**, Gandhi J, Joshi G, Smith NL, Khan SA. Juxtaglomerular Cell Tumor: Reviewing a Cryptic Cause of Surgically Correctable Hypertension. *Curr Urol* 2019; **13**: 7-12 [PMID: 31579192 DOI: 10.1159/000499301]

World Journal of Clinical Cases

Submit a Manuscript: https://www.f6publishing.com

World J Clin Cases 2023 April 16; 11(11): 2549-2558

DOI: 10.12998/wjcc.v11.i11.2549

ISSN 2307-8960 (online)

CASE REPORT

Successful treatment of lichen amyloidosis coexisting with atopic dermatitis by dupilumab: Four case reports

Qing Zhu, Bing-Quan Gao, Jin-Fang Zhang, Li-Ping Shi, Guo-Qiang Zhang

Specialty type: Dermatology

Provenance and peer review: Unsolicited article; Externally peer reviewed.

Peer-review model: Single blind

Peer-review report's scientific quality classification

Grade A (Excellent): 0
Grade B (Very good): B
Grade C (Good): C, C
Grade D (Fair): D
Grade E (Poor): 0

P-Reviewer: Sabooniha F, Iran; Sideris N, Greece

Received: December 27, 2022
Peer-review started: December 27, 2022
First decision: January 20, 2023
Revised: February 2, 2023
Accepted: March 22, 2023
Article in press: March 22, 2023
Published online: April 16, 2023

Qing Zhu, Jin-Fang Zhang, Li-Ping Shi, Guo-Qiang Zhang, Department of Dermatology, The First Hospital of Hebei Medical University, Shijiazhuang 050031, Hebei Province, China

Bing-Quan Gao, Department of Burns and Plastic Surgery, The First Hospital of Hebei Medical University, Shijiazhuang 050031, Hebei Province, China

Corresponding author: Guo-Qiang Zhang, MD, Director, Professor, Department of Dermatology, The First Hospital of Hebei Medical University, No. 89 Donggang Road, Shijiazhuang 050031, Hebei Province, China. zlx090702@163.com

Abstract

BACKGROUND

Lichen amyloidosis (LA) is a chronic, severely pruritic skin disease, which is the most common form of primary cutaneous amyloidosis. The treatment of LA has been considered to be difficult. LA may be associated with atopic dermatitis (AD), and in this setting, the treatment options may be more limited. Herein, we report four cases of LA associated with AD successfully treated by dupilumab.

CASE SUMMARY

In this article, we describe four cases of patients who presented with recurrent skin rash accompanied by severe generalized intractable pruritus, diagnosed with refractory LA coexisting with chronic AD. Previous treatments had not produced any apparent improvement. Thus, we administered dupilumab injection subcutaneously at a dose of 600 mg for the first time and 300 mg every 2 wk thereafter. Their lesions all markedly improved.

CONCLUSION

Dupilumab may be a new useful treatment for LA coexisting with AD.

Key Words: Lichen amyloidosis; Atopic dermatitis; Dupilumab; Biologics; Interleukin-31; Case report

Core Tip: Lichen amyloidosis (LA) is a chronic, severely pruritic skin disease, which is the most common subtype of primary cutaneous amyloidosis characterized by deposition of amyloid protein on the skin without visceral involvement. The treatment of LA has been considered difficult, with high relapse rates. In this article, we present four cases of LA associated with atopic dermatitis (AD) treated with dupilumab who achieved remarkable results. Our observations suggested that dupilumab may shed light on the systematic treatment of refractory LA patients with AD.

Citation: Zhu Q, Gao BQ, Zhang JF, Shi LP, Zhang GQ. Successful treatment of lichen amyloidosis coexisting with atopic dermatitis by dupilumab: Four case reports. *World J Clin Cases* 2023; 11(11): 2549-2558
URL: https://www.wjgnet.com/2307-8960/full/v11/i11/2549.htm
DOI: https://dx.doi.org/10.12998/wjcc.v11.i11.2549

INTRODUCTION

Lichen amyloidosis (LA) is the most common subtype of primary cutaneous amyloidosis (PCA) characterized by deposition of amyloid protein in the skin without visceral involvement. PCA is commonly observed in Southeast Asian countries and LA appears to be more prevalent in those of Chinese descent. LA typically presents as persistent hyperkeratotic skin-colored or hyperpigmented papules usually located on the calves and other extensor surfaces, *e.g.*, anterior thighs or forearms, which can then coalesce into corrugated patches that often have a rippled or ridged pattern accompanied by severe itching. At the onset, lesions are usually unilateral, but overtime a bilateral symmetric distribution can develop. Histologically, LA appears as eosinophilic amorphous deposits that are restricted to the upper dermis particularly the papillary dermis with epidermal acanthosis and orthohyperkeratosis. The treatment of LA has been considered difficult, with a high relapse rate. Generally, many medical and physical treatments such as laser and light therapies have been tried with unsatisfactory results. LA associated with atopic dermatitis (AD) has been reported previously. We present four cases of LA associated with AD treated with dupilumab that demonstrated remarkable therapeutic achievements (Table 1).

CASE PRESENTATION

Chief complaints

Case 1: The patient was a 37-year-old man who presented with recurrent skin rash accompanied by severe generalized intractable pruritus for more than 14 years.

Case 2: A 67-year-old man presented with recurrent rashes on his back and limbs, which was most consistent with the characteristics of the nummular variant of AD, with generalized and intense pruritus for 10 years.

Case 3: A 20-year-old man visited our department presenting with multiple pruritic brownish papules that were mostly located on the anterior chest, back, and both thighs for 6 years.

Case 4: A 54-year-old woman presented with skin lesions along with pruritus which appeared 3 years prior to current presentation.

History of present illness

Case 1: The patient had received treatment with a variety of oral antihistamines and topical hormone creams for external use, but without satisfactory result.

Case 2: Prior treatment consisting of halometasone ointment for external use, oral antihistamine, and narrow band ultraviolet B phototherapy showed no benefit, and the rash continued to be worsened.

Case 3: The patient had received treatment with oral epinastine and mometasone furoate for external use, but without obvious effects.

Case 4: The patient had a history of irregular consumption of oral methylprednisolone tablets and epinastine hydrochloride capsules, but without satisfactory effects.

History of past illness

Case 1: The patient had suffered allergic rhinitis for more than 14 years.

Table 1 Clinical features of the four cases

Cases	Age/gender	Duration	Absolute value of eosinophils at baseline	Duration of treatment for absolute value of eosinophils decreased to normal range	Total serum IgE at baseline	Duration of treatment for total IgE decreased to normal range	EASI at baseline	EASI at 16 wk of treatment	VAS at baseline	VAS at 16 wk of treatment	DLQI at baseline	DLQI at 16 wk of treatment
Case 1	37 yr/male	14 yr	6.30 × 10^9/L	6 wk	277.30 IU/mL	10 wk	62	16	10	1	22	3
Case 2	67 yr/male	10 yr	0.10 × 10^9/L	-	54.20 IU/mL	-	36	10	8	0	19	1
Case 3	20 yr/male	6 yr	0.20 × 10^9/L	-	1002 IU/mL	12 wk	16	4	6	0	16	2
Case 4	54 yr/female	5 yr	2.0 × 10^9/L	10 wk	893.60 IU/mL	14 wk	23	8	7	0	17	1

Range of the normal absolute value of eosinophils: 0.00-0.52 (× 10^9/L); Total serum IgE: < 100 IU/mL. EASI: Eczema area and severity index (0-72 scores); VAS: The pruritus visual analog scale (0-10 scores) (with the zero indicating no pruritus and 10 indicates most severe pruritus); DLQI: Dermatology life quality index (0-30 scores).

Case 2: The patient had a past history of allergic rhinitis for 20 years.

Case 3: The patient had suffered allergic rhinitis for 1 year.

Case 4: No significant past history or any illness.

Physical examination

Case 1: A dense distribution of hard and solid confluent plaques and papules was seen throughout the body, covered with dry and thick scales (Figure 1A-D).

Case 2: Cutaneous examination revealed a dense distribution of hard and solid papules and irregular erythematous patches with unclear boundaries distributed in the back and limbs, which were covered with dry scales. Most of the skin was mossy and rough (Figure 2A-D).

Case 3: Upon dermatological examination, a dense distribution of solid and unmixing papules was seen on the back, anterior chest, and both thighs, which were covered with white scales. The skin showed lichenoid changes with a rippled pattern, which were more prominent on the lateral side (Figure 3A-D).

Case 4: A physical examination showed localized discrete brownish papules in association with erythema of different sizes on the neck, trunk, and lower limbs. Lichenoid skin changes and bloody crusts could be seen on the back and lateral aspects of shins. In addition, multiple firm and pigmented papules were symmetrically and densely distributed on the anterolateral surfaces of the calves (Figure 4A-D).

Laboratory examinations

Case 1: Laboratory examination demonstrated a total serum IgE level of 277.30 IU/mL and an absolute eosinophilic value of 6.30 × 10^9/L. The histopathological examination of the specimen obtained from the

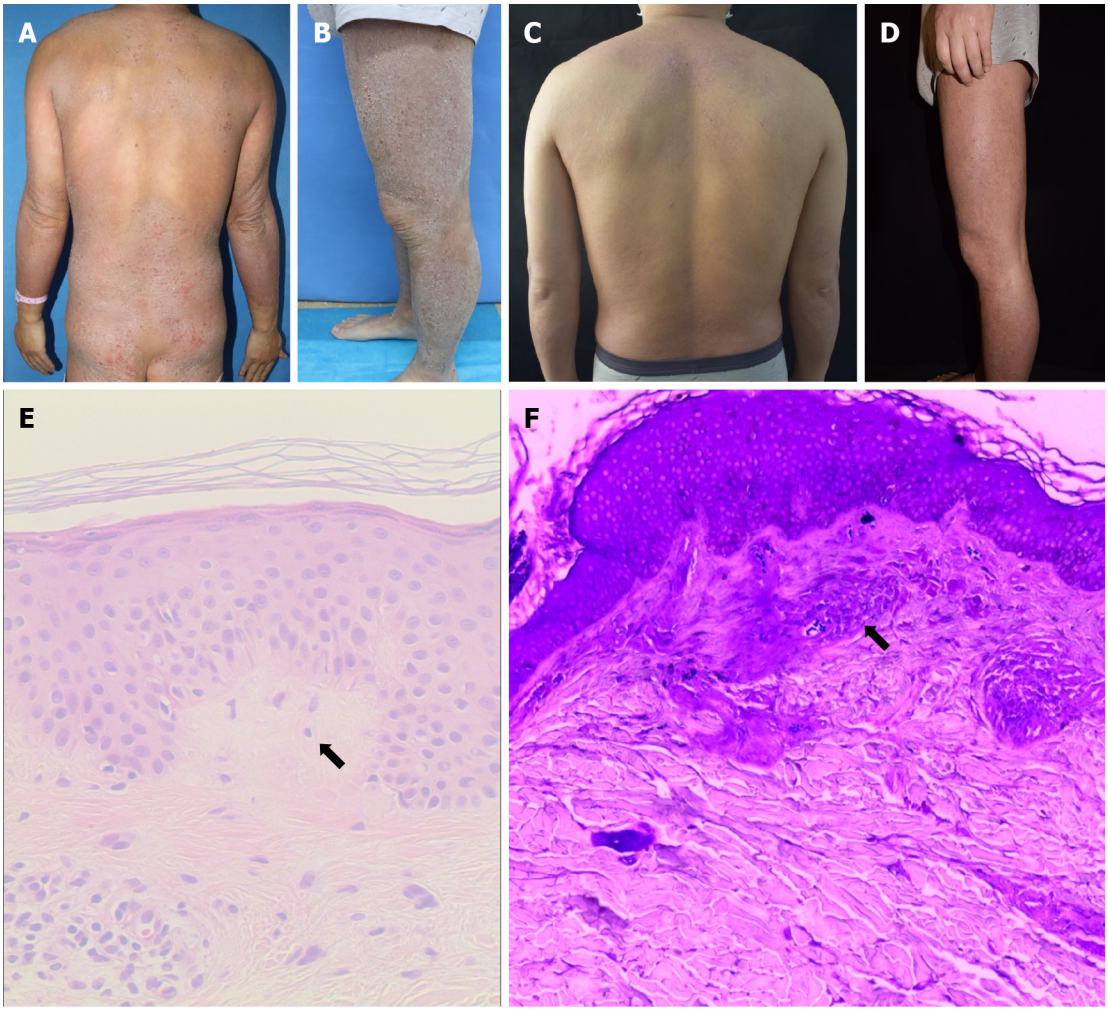

DOI: 10.12998/wjcc.v11.i11.2549

Figure 1 Case 1. A and B: Dense hard brown plaques were seen on the trunk and limbs at baseline; C and D: After 16 wk of treatment with dupilumab, the trunk rash basically subsided, the lower limb rash markedly improved, and the plaques became flat. The remaining lesions on the thigh after treatment, showed a characteristic rippled appearance indicating lichen amyloidosis as a co-existing condition; E: Histopathological examination revealed mild hyperkeratosis of the epidermis, irregular hyperplasia of the spinous layer, and spongy edema, with the dermal papilla and upper dermis showing a uniformly reddish mass that expanded the dermal papillae and displaced the rete ridges laterally (hematoxylin & eosin staining, × 100); F: Crystal violet staining was positive for amyloid deposits in the dermal papillae and upper dermis with characteristic fissures (crystal violet staining, × 400). The arrow indicates amyloid deposits.

back area showed mild hyperkeratosis of the epidermis, irregular hyperplasia of the spinous layer, spongy edema, complete basal cells, an equal number of lymphocytes, and histocytes infiltrating into the blood vessels in the superficial dermis. The dermal papilla and superficial dermis also showed uniformly reddish masses stained with crystal violet confirming amyloid deposits (Figure 1E and F).

Case 2: The biopsy of the right leg revealed epidermal hyperkeratosis, irregular hyperplasia of the spinous layer, increased basal pigment cells, red mass material deposition in the dermal papilla, and superficial perivascular lymphatic and histiocytic infiltration. Crystal violet staining was positive for amyloid bodies (Figure 2E and F).

Case 3: The LA lesions are usually located primarily on the shins or other extensor aspects of the extremities; the thighs, the upper back, abdominal area, and chest wall may also be involved[1,2]. While LA is often limited to localized areas of the body, it can present in a generalized fashion[3]. Due to the atypical presentation and the lack of age-specific distribution of lesions for the diagnosis of AD, a skin biopsy was performed on the back skin to aid in the diagnosis. Pathological findings included hyperkeratosis with incomplete keratosis and irregular hyperplasia of the spinous layer. Moreover, a pink, amorphous material can be seen in the dermal papilla. Crystal violet staining was positive for amyloid deposits (Figure 3E and F).

Case 4: A biopsy specimen obtained from a papular lesion of the right shin revealed hyperkeratotic and hyperplastic epidermis and homogeneous pinkish materials in the dermal papilla. Crystal violet staining was positive for amyloid deposits (Figure 4E and F).

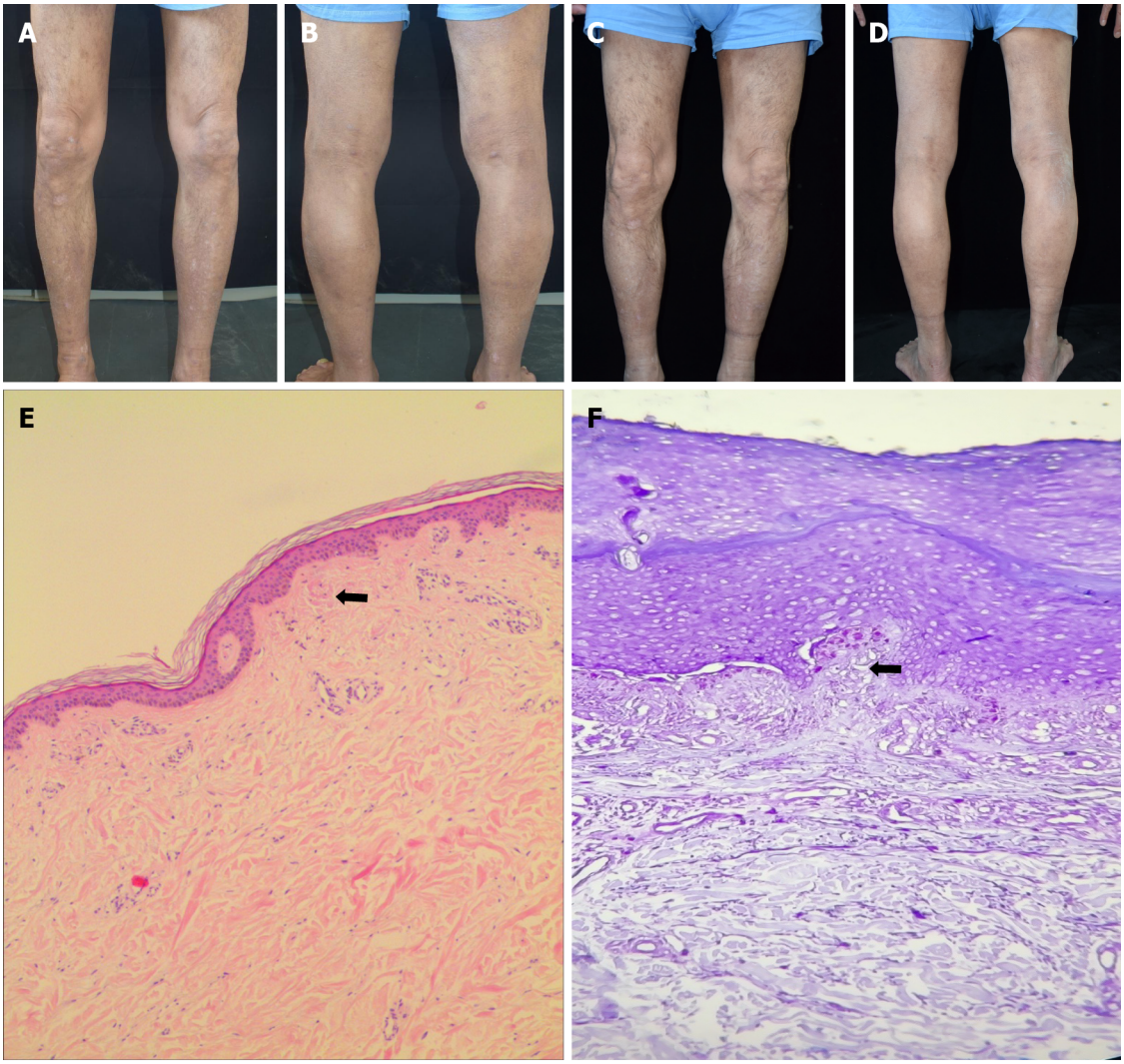

DOI: 10.12998/wjcc.v11.i11.2549

Figure 2 Case 2. A and B: Dense distribution of hard brown papules was observed on both lower limbs, with scales on the surface and dry and rough skin at baseline. Moreover, post-inflammatory hypopigmentation was evident on the anterior aspects of the calves; C and D: After 16 wk of treatment, the rash on both lower limbs was markedly reduced, the papules became flat, the scales were reduced, and the skin became smooth. Furthermore, the rippled appearance of the lesions of the posterior thighs has considerably diminished after the treatment, suggesting a decreased burden of amyloid deposits; E: Histopathological examination revealed epidermal hyperkeratosis, irregular hyperplasia of the spinous layer, increased basal pigmented cells, and red mass material deposition in the dermal papilla (hematoxylin & eosin staining, × 100); F: Crystal violet staining was positive for amyloid bodies (crystal violet staining, × 400). The arrow indicates amyloid deposits.

Initial diagnosis

Case 1: The patient had the following essential features for the diagnosis of AD based on the American Academy of Dermatology (AAD) diagnostic criteria 2014 including: Pruritus and a history of chronic and relapsing eczema. Besides, supporting features for the diagnosis of AD consisted of a personal history of allergic rhinitis, immunoglobulin E reactivity, and xerosis. The lesions among AD adults are frequently localized to the extremities; however, the lesions of this patient were generalized and involved the whole body. According to the eczema area and severity index, the severity of AD in this patient was estimated to be very severe, with a score between 7.1 and 21 denoting moderate, 21.1 to 50 indicating severe, and 50.1 to 72 designating very severe. Thus, the patient was considered to have concurrent refractory LA and AD.

Case 2: The patient had the following essential features for the diagnosis of AD based on the AAD diagnostic criteria 2014: Pruritus and a history of a chronic and relapsing eczema, with typical morphology and age-specific patterns. In addition, supportive features included a personal history of allergic rhinitis and xerosis. Thus, a diagnosis of LA coexisting with chronic AD was made.

Case 3: Important supportive features included a personal history of allergic rhinitis, early age of onset, immunoglobulin E reactivity, and "goose bump" appearance on thighs and xerosis. A diagnosis of LA associated with chronic AD was made based on the clinical and histopathological findings.

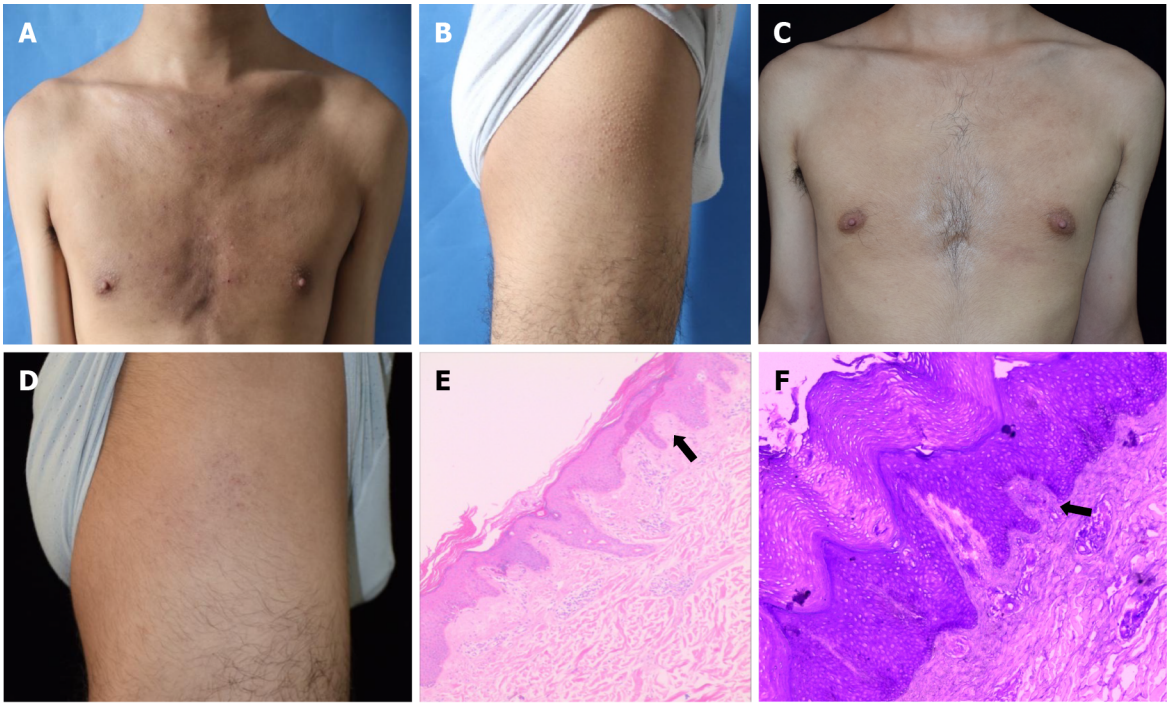

DOI: 10.12998/wjcc.v11.i11.2549

Figure 3 Case 3. A and B: Dense distribution of hard brown papules was observed on the chest plus papules on the thighs, with a "goose bump" appearance presenting at baseline, suggestive of atopic dermatitis; C and D: After 16 wk of treatment, the rash on the lower limbs markedly improved, and the papules were reduced and became flat; E: Histopathology revealed hyperkeratosis with incomplete keratosis and irregular acanthosis. Further, a pink amorphous material can be seen in the dermal papilla (hematoxylin & eosin staining, × 100); F: Crystal violet staining was positive for amyloid (crystal violet staining, × 400). The arrow indicates amyloid deposits.

Case 4: The patient had the following essential features: Pruritus and a history of chronic and relapsing eczema, with typical morphology and age-specific patterns. Other important characteristics were a family history of allergic conjunctivitis and xerosis. Based on these findings, the patient was diagnosed with LA associated with chronic AD.

FINAL DIAGNOSIS

LA coexisting with AD.

TREATMENT

Case 1

Previous treatments with topical corticosteroids and an antihistamine had not produced any apparent improvement; thus, we administered dupilumab injection subcutaneously at a dose of 600 mg for the first time and 300 mg every 2 wk thereafter.

Case 2

Treatment was then initiated with dupilumab at a dose of 600 mg, which was injected subcutaneously, and continued at a dose of 300 mg every 2 wk thereafter.

Case 3

The patient started on subcutaneous injection of dupilumab at a dose of 600 mg for the first time and 300 mg every 2 wk thereafter.

Case 4

We decided to treat the patient's lesions with subcutaneous injections of dupilumab at a dose of 600 mg initially, which was continued at a dose of 300 mg every 2 wk thereafter.

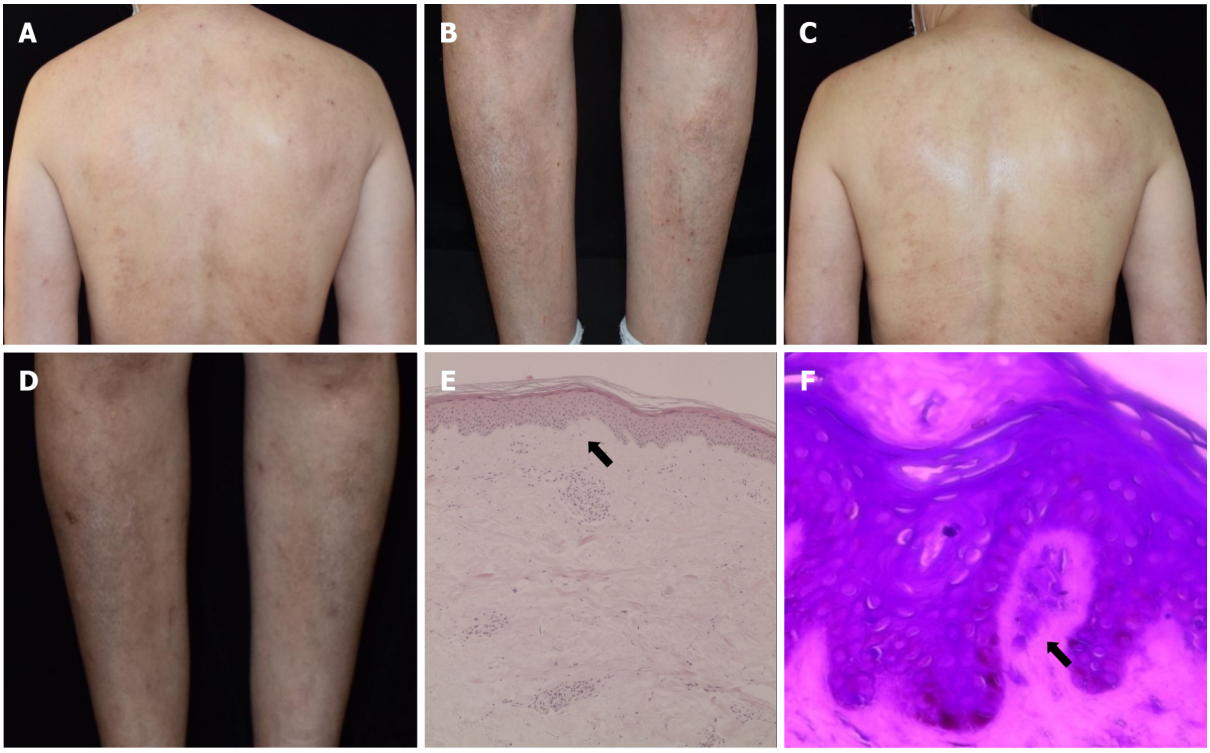

DOI: 10.12998/wjcc.v11.i11.2549

Figure 4 Case 4. A and B: Erythema and a dense distribution of hard brown papules were seen on the patient's back. Both calves showed a characteristic rippled pattern, which was most prominent on the anterolateral aspect of the right calf; C and D: After 16 wk of treatment, the papules on both calves became flat and the wavy pattern markedly disappeared, suggestive of diminished amyloid burden; E: Hyperkeratotic and hyperplastic epidermis as well as homogeneous pinkish materials in the dermal papilla were seen (hematoxylin & eosin staining, × 100); F: Crystal violet staining was positive for amyloid deposits (crystal violet staining, × 400). The arrow indicates amyloid deposits.

OUTCOME AND FOLLOW-UP

Case 1

After 16 wk of treatment, the plaques steadily flattened and decreased in size and number, and the skin became smooth. The itching continued to improve without any obvious adverse reactions. The patient continues to receive dupilumab maintenance therapy by injection of 300 mg every 4 wk.

Case 2

After 16 wk of treatment, the patient had experienced complete resolution of pruritus. He had visual clinical improvement of his skin lesions with steadily flattening and lightening of the papules and plaques. No obvious adverse reactions were observed.

Case 3

At week 16, the patient showed a marked reduction of pruritus, and subsequent progressive improvement of both AD and LA.

Case 4

After 16 wk of treatment, the papules steadily flattened and decreased in number, and the itching disappeared. Moreover, no obvious adverse reactions were observed. She is still under treatment.

DISCUSSION

LA has been implicated to be associated with other skin conditions including lichen planus and especially AD[4]. It is also associated with HIV, Type A multiple endocrine tumor, vascular lymphoid hyperplasia with eosinophilia, ankylosing spondylitis, autoimmune thyroiditis, hyperthyroidism, and other autoimmune disorders[5-7]. LA treatment is generally directed to relieve pruritus and inflammation, such as low doses of systemic cyclosporine, topical corticosteroids, and oral retinoids such as acitretin. Owing to the drying effects of retinoid on the skin and thereby the potential for exacerbation of AD, the therapeutic options for treating co-existing LA and AD are more limited than those for LA alone

[8]. Successful treatment of AD-associated LA with oral cyclosporine and subsequent narrow band ultraviolet B therapy has been reported[9]. Three cases of LA with AD have also been successfully treated with CO_2 laser[10]. Koh *et al*[8] also reported a case of LA with AD successfully treated with alitretinoin, which has lower mucocutaneous side-effects, as compared to other vitamin A derivatives.

Aoki *et al*[11] reported a case of generalized LA with AD in a female patient, whose intractable pruritus decreased within 4 wk after treatment with dupilumab, her eczematous lesions significantly improved, and the LA papules flattened and decreased after 3 mo of treatment. Humeda *et al*[12] reported a case of generalized PCA in a male patient without an atopic disease history who had a 4-year history of severe itching. After treatment with dupilumab, both itching and rash were markedly improved. An excellent response to dupilumab was observed in the treatment of extensive LA associated with AD in our patients. No adverse effect or relapse till date was observed. Thus, dupilumab should be considered more often in the treatment of extensive, recalcitrant cases of LA associated with AD. The pathogenesis of PCA is still not clearly established, but it is considered to involve both genetic and environmental factors. Frictional epidermal damage, apoptosis, viral infection, and other triggers have been implicated in the disease etiology in previous reports. Chronic irritation, itching, and scratching causing prolonged epidermal trauma may lead to dermal amyloid deposition by inducing degradation of keratinocytes, thereby leading to amyloid formation by dermal macrophages and fibroblasts through conversion of keratin peptides to amyloid fibrils that react with antikeratin antibodies[13,14]. Thus, scratching seems to be the most important step in its pathogenesis. Hence, treatment modalities should be centered on minimizing skin trauma and relieving pruritus. A previous study has suggested that small fiber neuropathy and interleukin (IL)-31 receptor overexpression may play a role in the intense pruritus associated with PCA[11]. IL-31, a key mediator of pruritus, signals through a receptor composed of two subunits, IL-31 receptor A and oncostatin M receptor β (OSMR β). A familial study of some cases of PCA has revealed mutations in both genes encoding the subunits of IL-31 receptors (IL31RA and OSMR β)[15]. It has been demonstrated that IL-4, IL-13, and IL-31 are associated with sensory nerve sensitization and itching in AD patients, leading to scratching that further exacerbates inflammation and barrier dysfunction[16]. IL-31 is significantly overexpressed in the skin samples of patients with AD. Thus, it is possible that the IL-31 signaling pathway is involved in the pathogenesis of both PCA and AD, and patients with abnormalities in this pathway may show phenotypes of both diseases[7].

Dupilumab, a human anti-IL-4 receptor-α monoclonal antibody that blocks signaling of both IL-4 and IL-13[17], has been approved by the Food and Drug Administration for use in the treatment of adult patients with moderate-to-severe AD whose disease is not adequately controlled with topical medications or when those therapies are not advisable. Previous analyses have shown that treatment with dupilumab normalizes the AD transcriptome by downregulating markers of type 2 inflammation such as IL-13 and IL-3. It effectively treats itching by directly blocking IL-4 and IL-13 on sensory neurons and indirectly through inhibition of IL-31 production by T2-helper cells by blocking IL-4[18]. We hypothesized that dupilumab may also be effective in treating LA with AD. In our four cases of LA with AD, we observed a convincing antipruritic effect and improvement of skin lesions after injection of dupilumab. The advantages of this treatment are practicability, convenience, and low side-effects. In general, AD symptomatology and distribution depend on the patient's age at the time of presentation. Adults may present with dry and scaly patches on the extremities[19]. Our cases demonstrated that dupilumab may be a good therapy for LA coexisting with AD regardless of the generalized eczema type or typical age-specific patterns of clinical phenotypes of adult AD.

CONCLUSION

Dupilumab may shed light on the systematic treatment of refractory LA patients associated with AD but further case studies are required to evaluate the effectiveness of this drug for these cases. Meanwhile, the mechanism by which dupilumab improves LA remains elusive but it seems that the interruption of the vicious cycle of pruritus and skin trauma as well as its direct and indirect effects on the cytokines involved in the pathophysiology of this disorder are all implicated.

FOOTNOTES

Author contributions: Gao BQ and Zhang JF performed the pathological studies, laboratory testing, and clinical data collection; Zhu Q and Shi LP were responsible for patient care and drafted this manuscript; Zhang GQ revised the manuscript critically for important intellectual content; all authors contributed to the article and approved the submitted version.

Informed consent statement: Written Informed consent was obtained from all patients for the publication of this case report.

Conflict-of-interest statement: The authors declare that they have no conflict of interest to disclose.

CARE Checklist (2016) statement: The authors have read the CARE Checklist (2016), and the manuscript was prepared and revised according to the CARE Checklist (2016).

Country/Territory of origin: China

ORCID number: Qing Zhu 0000-0002-7075-7696; Guo-Qiang Zhang 0000-0002-4132-1690.

S-Editor: Yan JP
L-Editor: Wang TQ
P-Editor: Yan JP

REFERENCES

1 **Dousset L**, Seneschal J, Boniface K, Charreau S, Ezzedine K, Milpied B, Mossalayi MD, McGrath JA, Lecron JC, Taïeb A. A Th2 cytokine interleukin-31 signature in a case of sporadic lichen amyloidosis. *Acta Derm Venereol* 2015; **95**: 223-224 [PMID: 24573820 DOI: 10.2340/00015555-1829]
2 **Panchaprateep R**, Tusgate S, Munavalli GS, Noppakun N. Fractional 1,550 nm Ytterbium/Erbium fiber laser in the treatment of lichen amyloidosis: clinical and histological study. *Lasers Surg Med* 2015; **47**: 222-230 [PMID: 25771782 DOI: 10.1002/lsm.22338]
3 **Tursen U**, Kaya TI, Dusmez D, Ikizoglu G. Case of generalized lichen amyloidosis. *Int J Dermatol* 2003; **42**: 649-651 [PMID: 12890115 DOI: 10.1046/j.1365-4362.2003.01949_2.x]
4 **Hongcharu W**, Baldassano M, Gonzalez E. Generalized lichen amyloidosis associated with chronic lichen planus. *J Am Acad Dermatol* 2000; **43**: 346-348 [PMID: 10901719 DOI: 10.1067/mjd.2000.100966]
5 **Gönül M**, Cakmak SK, Kayaçatin S. Generalized lichen amyloidosis and hyperthyroidism: coincidence or association. *Postepy Dermatol Alergol* 2013; **30**: 265-267 [PMID: 24278086 DOI: 10.5114/pdia.2013.37039]
6 **Akar A**, Taştan HB, Demiriz M, Erbil H. Lack of effect of cyclosporine in lichen amyloidosis associated with atopic dermatitis. *Eur J Dermatol* 2002; **12**: 612-614 [PMID: 12459544]
7 **Lee DD**, Huang CK, Ko PC, Chang YT, Sun WZ, Oyang YJ. Association of primary cutaneous amyloidosis with atopic dermatitis: a nationwide population-based study in Taiwan. *Br J Dermatol* 2011; **164**: 148-153 [PMID: 21070198 DOI: 10.1111/j.1365-2133.2010.10024.x]
8 **Koh WS**, Oh EH, Kim JE, Ro YS. Alitretinoin treatment of lichen amyloidosis. *Dermatol Ther* 2017; **30** [PMID: 28906049 DOI: 10.1111/dth.12537]
9 **Kang MJ**, Kim HS, Kim HO, Park YM. A case of atopic dermatitis-associated lichen amyloidosis successfully treated with oral cyclosporine and narrow band UVB therapy in succession. *J Dermatolog Treat* 2009; **20**: 368-370 [PMID: 19954395 DOI: 10.3109/09546630802691325]
10 **Chu H**, Shin JU, Lee J, Park CO, Lee KH. Successful treatment of lichen amyloidosis accompanied by atopic dermatitis by fractional CO(2) laser. *J Cosmet Laser Ther* 2017; **19**: 345-346 [PMID: 28535110 DOI: 10.1080/14764172.2017.1326612]
11 **Aoki K**, Ohyama M, Mizukawa Y. A case of lichen amyloidosis associated with atopic dermatitis successfully treated with dupilumab: A case report and literature review. *Dermatol Ther* 2021; **34**: e15005 [PMID: 34037298 DOI: 10.1111/dth.15005]
12 **Humeda Y**, Beasley J, Calder K. Clinical resolution of generalized lichen amyloidosis with dupilumab: a new alternative therapy. *Dermatol Online J* 2020; **26** [PMID: 33423428 DOI: 10.5070/D32612051364]
13 **Kobayashi H**, Hashimoto K. Amyloidogenesis in organ-limited cutaneous amyloidosis: an antigenic identity between epidermal keratin and skin amyloid. *J Invest Dermatol* 1983; **80**: 66-72 [PMID: 6184423 DOI: 10.1111/1523-1747.ep12531130]
14 **He A**, Zampella JG, Kwatra SG. Interleukin-31 receptor and pruritus associated with primary localized cutaneous amyloidosis. *Br J Dermatol* 2016; **175**: 433 [PMID: 26941119 DOI: 10.1111/bjd.14510]
15 **Tanaka A**, Arita K, Lai-Cheong JE, Palisson F, Hide M, McGrath JA. New insight into mechanisms of pruritus from molecular studies on familial primary localized cutaneous amyloidosis. *Br J Dermatol* 2009; **161**: 1217-1224 [PMID: 19663869 DOI: 10.1111/j.1365-2133.2009.09311.x]
16 **Haddad EB**, Cyr SL, Arima K, McDonald RA, Levit NA, Nestle FO. Current and Emerging Strategies to Inhibit Type 2 Inflammation in Atopic Dermatitis. *Dermatol Ther (Heidelb)* 2022; **12**: 1501-1533 [PMID: 35596901 DOI: 10.1007/s13555-022-00737-7]
17 **Shirley M**. Dupilumab: First Global Approval. *Drugs* 2017; **77**: 1115-1121 [PMID: 28547386 DOI: 10.1007/s40265-017-0768-3]
18 **Miake S**, Tsuji G, Takemura M, Hashimoto-Hachiya A, Vu YH, Furue M, Nakahara T. IL-4 Augments IL-31/IL-31 Receptor Alpha Interaction Leading to Enhanced Ccl 17 and Ccl 22 Production in Dendritic Cells: Implications for Atopic

Dermatitis. *Int J Mol Sci* 2019; **20** [PMID: 31434203 DOI: 10.3390/ijms20164053]

19 **Frazier W**, Bhardwaj N. Atopic Dermatitis: Diagnosis and Treatment. *Am Fam Physician* 2020; **101**: 590-598 [PMID: 32412211]

World Journal of Clinical Cases

Submit a Manuscript: https://www.f6publishing.com

World J Clin Cases 2023 April 16; 11(11): 2559-2566

DOI: 10.12998/wjcc.v11.i11.2559

ISSN 2307-8960 (online)

CASE REPORT

Successful treatment of breast metastasis from primary transverse colon cancer: A case report

Xin Jiao, Fang-Zhou Xing, Mi-Mi Zhai, Peng Sun

Specialty type: Medicine, research and experimental

Provenance and peer review: Unsolicited article; Externally peer reviewed.

Peer-review model: Single blind

Peer-review report's scientific quality classification

Grade A (Excellent): 0
Grade B (Very good): 0
Grade C (Good): C, C
Grade D (Fair): D, D, D
Grade E (Poor): 0

P-Reviewer: Dambrauskas Z, Lithuania; Faraji N, Iran; Pattarajierapan S, Thailand

Received: January 18, 2023
Peer-review started: January 18, 2023
First decision: February 7, 2023
Revised: February 13, 2023
Accepted: March 23, 2023
Article in press: March 23, 2023
Published online: April 16, 2023

Xin Jiao, Fang-Zhou Xing, Peng Sun, Department of Gastrointestinal Surgery, Affiliated Hospital of Weifang Medical University, Weifang 261041, Shandong Province, China

Mi-Mi Zhai, Department of Digestive System, Weifang People's Hospital, Weifang 261041, Shandong Province, China

Corresponding author: Peng Sun, PhD, Doctor, Department of Gastrointestinal Surgery, Affiliated Hospital of Weifang Medical University, No. 2428 Yuhe Road, Kuiwen District, Weifang 261041, Shandong Province, China. 1105031456@qq.com

Abstract

BACKGROUND

The incidence of colon cancer is increasing worldwide. Treatments for colon cancer include surgery and surgery combined with chemotherapy and radiotherapy, but the median survival rate is still poor. Colon cancer most commonly metastasizes to the lymph nodes, lungs, liver, peritoneum, and brain, but breast metastasis is rare. There is no agreement on its treatment.

CASE SUMMARY

A 23-year-old woman was admitted to our hospital for further treatment with a history of acute abdominal pain, nausea, and vomiting. Her physical examination and computed tomography scan revealed an abdominal tumor. Transverse colectomy was successfully performed. Histopathological examination revealed that the tumor was a mucosecretory adenocarcinoma with signet ring cells. The patient inadvertently found a mass in the outer upper quadrant of the right breast after four cycles of XELOX chemotherapy [oxaliplatin 130 mg/m^2, d1, intravenous (iv) drip for 2 h; capecitabine 1000 mg/m^2, po, bid, d1–d14]. After discussion with the patient, we performed a lumpectomy and frozen biopsy. The latter revealed that the breast tumor was intestinal metastasis. Genetic testing showed wild-type *RAS* and *BRAF*. So we replaced the original chemotherapy with FOLFIRI [irinotecan 180 mg/m^2, d1, iv drip for 3–90 min; leucovorin 400 mg/m^2, d1, iv drip for 2 h; 5-fluorouracil (5-FU) 400 mg/m^2, d1 and 5-FU 1200 mg/(m^2 d) × 2 d, continuous iv drip for 46–48 h] + cetuximab (500 mg/m^2, d1, iv drip for 2 h). Serum levels of tumor markers returned to normal after several treatment cycles, and there was no evidence of tumor recurrence or metastasis.

CONCLUSION

Breast metastasis from colon cancer is rare. Radical breast surgery should be avoided unless needed for palliation. Chemotherapy combined with targeted

therapy should be the first choice.

Key Words: Colon cancer; Breast metastasis; Tumor markers; FOLFIRI; Cetuximab; Prognosis; Case report

Core Tip: Breast metastasis from colon cancer is rare. The prognosis is poor and conservative treatment is mainly adopted. We present a rare case of breast metastasis from colon cancer in a young patient who received chemotherapy (FOLFIRI) combined with targeted therapy (cetuximab) after undergoing transverse colectomy and lumpectomy. There was no recurrence or metastasis during the 16-mo follow-up after lumpectomy, and the treatment effect was good.

Citation: Jiao X, Xing FZ, Zhai MM, Sun P. Successful treatment of breast metastasis from primary transverse colon cancer: A case report. *World J Clin Cases* 2023; 11(11): 2559-2566
URL: https://www.wjgnet.com/2307-8960/full/v11/i11/2559.htm
DOI: https://dx.doi.org/10.12998/wjcc.v11.i11.2559

INTRODUCTION

Colon cancer is the third most common type of cancer worldwide and the fourth leading cause of cancer mortality[1]. Approximately 25% of patients with colon cancer have been diagnosed as having stage IV cancer, and the five-year survival rate for patients with stage IV tumors is less than 10%[2]. The metastatic pathways of colon cancer are similar to those of other malignancies, and include lymphatic, hematogenous, and distant metastases. Breast metastasis is rare, with an incidence of 0.5%–3%[3], and is especially rare from colon carcinoma. Since the first case reported in 1976[4], only no more than 30 cases have been reported[5,6]. Hsieh and Hsu[7] summarized 45 cases that were previously reported, and we found that about 60 studies have reported this rare case so far by searching the literature in the *Reference Citation Analysis* (https://www.referencecitationanalysis.com/) database, PubMed, and Embase. Prognosis is poor because it is usually indicative of disseminated disease. It is important to distinguish breast metastasis from primary breast carcinoma in order to plan the most suitable treatment[8]. Treatment experience is uncomfortable due to the rarity of the metastatic pattern. We report a new case of breast metastasis from colon carcinoma.

CASE PRESENTATION

Chief complaints

A 23-year-old woman was admitted to our hospital in February 2021 for further treatment with a history of acute abdominal pain, nausea, and vomiting.

History of present illness

The patient suddenly suffered from abdominal pain, nausea, and vomiting, without fever, chills, fatigue, melena, haematemesis, hematochezia, or other discomforts.

History of past illness

The patient had no previous medical history.

Personal and family history

There was no personal or family history of acute or chronic disease. There was no family history of tumors.

Physical examination

Physical examination revealed abdominal tension, pressing pain, and rebound pain. There was a large abdominal mass with hard texture, unclear boundary, and uncertain size, and tenderness of the left abdomen.

Laboratory examinations

Laboratory examination showed a significant increase in serum levels of tumor markers: Carcinoem-

bryonic antigen (CEA), 697.90 ng/mL (normal range: 0–10 ng/mL); carbohydrate antigen (CA)125, 104.20 U/mL (normal range: 0–35 U/mL); and CA72-4, > 300.0 U/ mL (normal range: 0–6.9 U/mL). The level of CA19-9 (3.49 U/mL) was normal (normal range: 0–27 U/mL).

Imaging examinations

Computed tomography (CT) and abdominal enhanced CT showed that the abdominal tumor measured 7.5 cm × 10.9 cm, with uneven density, and unclear boundary between the tumor and surrounding tissues (Figure 1A). There were swollen lymph nodes in the mesentery. Abdominal enhanced CT was highly suspicious for gastrointestinal stromal tumors, and abdominal and retroperitoneal lymph nodes were swollen. Preoperative chest CT showed no abnormalities.

Surgical exploration and pathological diagnosis

We performed exploratory laparotomy. A tumor with hard texture was located in the middle of the transverse colon, causing peritonitis because of perforation. The diameter of the tumor was approximately 10 cm. Transverse colectomy was successfully performed. The lymph nodes around the transverse colon were cleared, but the retroperitoneal lymph nodes could not be removed. The favorable recovery period for the patient was approximately 2 wk. Immunohistochemistry was negative for CD20 and CD117, but positive for CK20, caudal-related homeobox transcription factor 2 (CDX-2) (Figure 2A), mucin 2 (Figure 2B), villin (Figure 2C), delay of germination 1, leukocyte common antigen, and CD3. Histopathological examination revealed that the tumor was a mucosecretory adenocarcinoma with signet ring cells (Figure 2D and E). Lymph node metastasis was evident (of the 24 detected lymph nodes, 23 were metastatic lymph nodes), but no distant metastasis was detected. The pathological stage was IIIC.

Disease evolution

The patient received chemotherapy according to the National Comprehensive Cancer Network guidelines for colorectal cancer. We retested the serum tumor markers after surgery in March 2021, which revealed significant changes: CEA, 44.65 ng/mL (normal range: 0–10 ng/mL); CA125, 7.33 U/mL (normal range: 0–35 U/mL); and CA72-4, 68.0 U/mL (normal range: 0–6.9 U/mL). The level of CA19-9 was normal (< 0.6 U/mL; normal range: 0–27 U/mL). The effect of tumor resection was remarkable. The patient inadvertently found a mass in the outer upper quadrant of the right breast after receiving four cycles of chemotherapy (XELOX: Oxaliplatin 130 mg/m^2, d1, iv drip for 2 h; capecitabine 1000 mg/m^2, po, bid, d1–d14). Physical examination revealed that the breast mass was 1.5 cm × 2 cm in size, with hard texture, and clear boundary between the mass and surrounding tissues. Further examination was performed. Breast ultrasound showed a tumor of 2.1 cm × 1.5 cm × 1.3 cm, with unclear boundary and echo heterogenicity. Color Doppler flow imaging showed blood flow signal (Figure 1B). Axillary lymph nodes were normal. It was not clear whether the breast tumor was a primary cancer or metastasis from colon cancer. There were slight elevations in serum tumor markers: CEA, 76.7 ng/mL (normal range: 0–10 ng/mL); CA125, 7.66 U/mL (normal range: 0–35 U/mL); and CA72-4, 43.20 U/mL (normal range: 0–6.9 U/mL). The level of CA19-9 (8.83 U/mL; normal range: 0–27 U/mL) was still normal. After discussion with the patient, we decided to perform a lumpectomy and frozen biopsy in June 2021. Frozen biopsy revealed that the breast tumor was intestinal metastasis. Routine hematoxylin and eosin staining of the breast tumor revealed breast metastasis from mucosecretory adenocarcinoma possibly of colonic origin (Figure 2F and G). The tumor was negative for estrogen receptor, progesterone receptor, GATA binding protein-3 (GATA3) (Figure 2H), gross cystic disease fluid protein, human epidermal-growth factor receptor-2, and CK7, but positive for CDX-2, villin, and special AT-rich binding protein (SATB). GATA3 is an important indicator of primary breast cancer; however, CDX-2, villin, and SATB are important indicators of enterogenous breast cancer. The disease was considered to be disseminated.

FINAL DIAGNOSIS

Based on the pathological findings and clinical results, the final diagnosis was breast metastasis from transverse colon carcinoma.

TREATMENT

Genetic testing showed that *RAS* and *BRAF* were wild type. According to the treatment guidelines for distant metastasis of colon cancer, we replaced the original chemotherapy with FOLFIRI + cetuximab [irinotecan 180 mg/m^2, d1, iv drip for 30–90 min; leucovorin 400 mg/m^2, d1, iv drip for 2 h; 5-fluorouracil (5-FU) 400 mg/m^2, d1 and 5-FU 1200 mg/(m^2 d) × 2 d, continuous iv drip for 46–48 h; cetuximab 500 mg/m^2, d1, iv drip for 2 h]. The serum levels of tumor markers were significantly reduced in July 2021 after one treatment cycle: CEA, 26.20 ng/mL (normal range: 0–10 ng/mL); CA125,

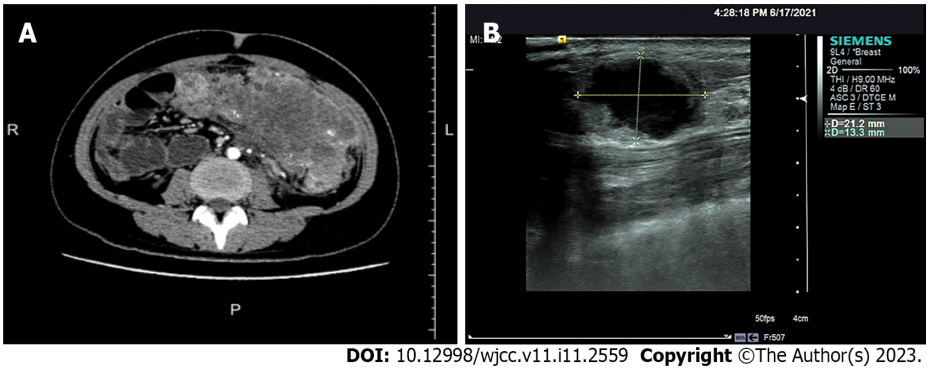

DOI: 10.12998/wjcc.v11.i11.2559

Figure 1 Imaging findings of the abdominal tumor and breast tumor. A: Abdominal computed tomography showed that the abdominal tumor measured 7.5 cm × 10.9 cm, with uneven density, and the boundary between the tumor and the surrounding tissues was unclear; B: Breast ultrasound clearly showed the breast tumor measuring 2.1 cm × 1.5 cm × 1.3 cm, with an unclear boundary and echo heterogenicity. Color Doppler flow imaging showed short rod blood flow signal.

2.84U/mL (normal range: 0–35 U/mL); and CA72-4, 5.96 U/mL (normal range: 0–6.9 U/mL). The level of CA19-9 (7.76 U/mL; normal range: 0–27 U/mL) was still normal. The patient received 10 cycles of FOLFIRI + cetuximab. The serum levels of tumor markers (CEA, CA12-5, CA72-4, and CA19-9) were normal, and there was no evidence of tumor recurrence or metastasis. The patient has been reviewed regularly without further treatment.

OUTCOME AND FOLLOW-UP

The patient did not receive further treatment after 10 cycles of FOLFIRI + cetuximab. During the whole treatment process, the patient underwent chest and abdominal CT examinations every 3 mo, and there was no evidence of distant metastasis. The serum levels of tumor markers (CEA, CA12-5, CA72-4, and CA19-9) were normal (Figure 3). The patient is in no evidence of disease state.

DISCUSSION

Breast metastasis from colon cancer without liver metastasis, lung metastasis, or peritoneal dissemination is extremely rare. The prognosis for metastatic breast cancer remains poor overall, due to disseminated disease. The breast lump can be mistaken for primary breast cancer[9]. Histopathological examination revealed that the tumor in the present case was a mucosecretory adenocarcinoma with signet ring cells, which is a type of colon cancer with poor prognosis. In addition, there was a large number of lymph node metastases. Metastatic breast cancer appeared about 4 mo after surgery.

In the present case, rapid growth of the breast mass indicated high malignancy of the colon tumor. Signet ring cells were found in the colon and breast tumors. Typically, colorectal carcinoma is positive for CK20, whereas this is exceptional in primary breast carcinoma. Metastatic breast cancer is usually negative for estrogen and progesterone receptors. Aspiration and excision biopsies are feasible for diagnosis of breast metastases. Previously, some authors have advised against extensive resection of metastatic breast tumor[5]. Thus, surgical treatment of metastatic breast tumor should be both diagnostic and palliative. However, when the tumor is large or painful, mastectomy is sometimes required.

Breast metastasis from colon cancer should be considered as systemic metastasis, although the metastatic pathway is not clear. The most common forms of metastasis of colon cancer are lymph node and hematogenous metastases[10]. The lymphatic network of the breast is rich, with a large distribution of lymph flowing to the axillary lymph nodes. The lymphatic drainage of the breast can flow to the parasternal lymphatic vessels through the intercostal lymphatic vessels, or it can flow back to the abdominal organs along the rectus abdominis sheath[11]. Therefore, we consider that there may be two possible pathways for metastasis to the breast from colon carcinoma. The first possibility is that colon cancer cells invade the blood circulation, and tumor cells are planted in the breast and grow into a mass similar to primary breast cancer. Another possibility is that colon cancer cells invade the lymphatic vessels of the abdominal wall and communicate with the lymphatic vessels of the breast along the intercostal lymphatic vessels or along the rectus abdominis sheath. In the present case, we prefer the second explanation. Previous reports have hardly mentioned the route of breast metastasis of colon cancer.

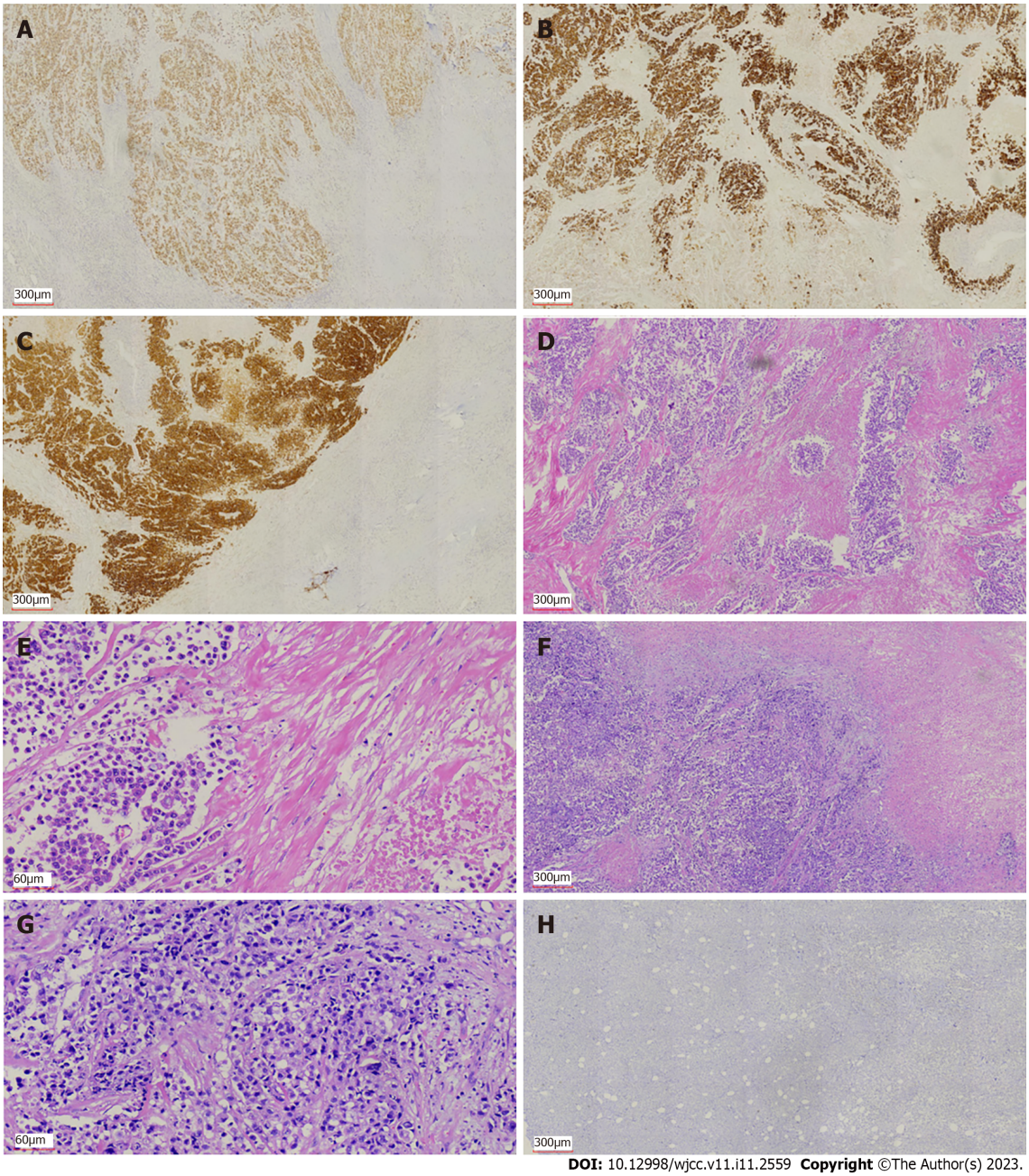

DOI: 10.12998/wjcc.v11.i11.2559

Figure 2 Immunohistochemical and histological features of the primary colon cancer and breast metastasis from colon cancer. A-C: Immunohistochemical staining showed expression of caudal-related homeobox transcription factor 2 (A), mucin-2 (B), and villin (C) in colon cancer; D and E: Hematoxylin and eosin (H&E) staining showed intracellular mucus in colon cancer (D, 40 ×; E, 200 ×); F: H&E staining showed breast metastasis from colon cancer (40 ×); G: H&E staining showed adenocarcinoma cells in the breast metastasis (200 ×); H: Immunohistochemical staining showed negative expression of GATA binding protein-3 in breast metastasis from colon cancer.

Because of early diagnosis and new therapeutic methods, the overall incidence and mortality of colorectal cancer have declined significantly[12,13]. However, metastasis remains a significant challenge in prolonging survival. In particular, we have no experience in the treatment of breast metastasis from colon cancer, and there is no clear statement in the relevant guidelines. For the treatment of metastatic colorectal cancer, *KRAS*, *NRAS*, *RAS*, and *BRAF* should be tested first by genetic testing, which is the basis for treatment with cetuximab or bevacizumab. We selected cetuximab according to the results of genetic testing (wild-type *KRAS*, *NRAS*, *RAS*, and *BRAF*). After we replaced FOLFIRI + cetuximab with XELOX, the serum levels of CEA, CA125, and CA72-4 decreased dramatically. According to the treatment guidelines for distant metastasis of colon cancer, there is no mistake in giving chemotherapy and targeted treatment. Diagnosis of breast metastasis from colon cancer has been reported, but there are few reports on treatment and metastasis route[14,15]. The prognosis of such patients is poor. Barthelmes reported a case of breast metastasis from colon cancer who died 4 mo later from advanced intra-abdominal carcinomatosis[5]. In our case, the patient survived for 16 mo after receiving lumpectomy, which was due to the application of chemotherapeutic and targeted drugs, especially

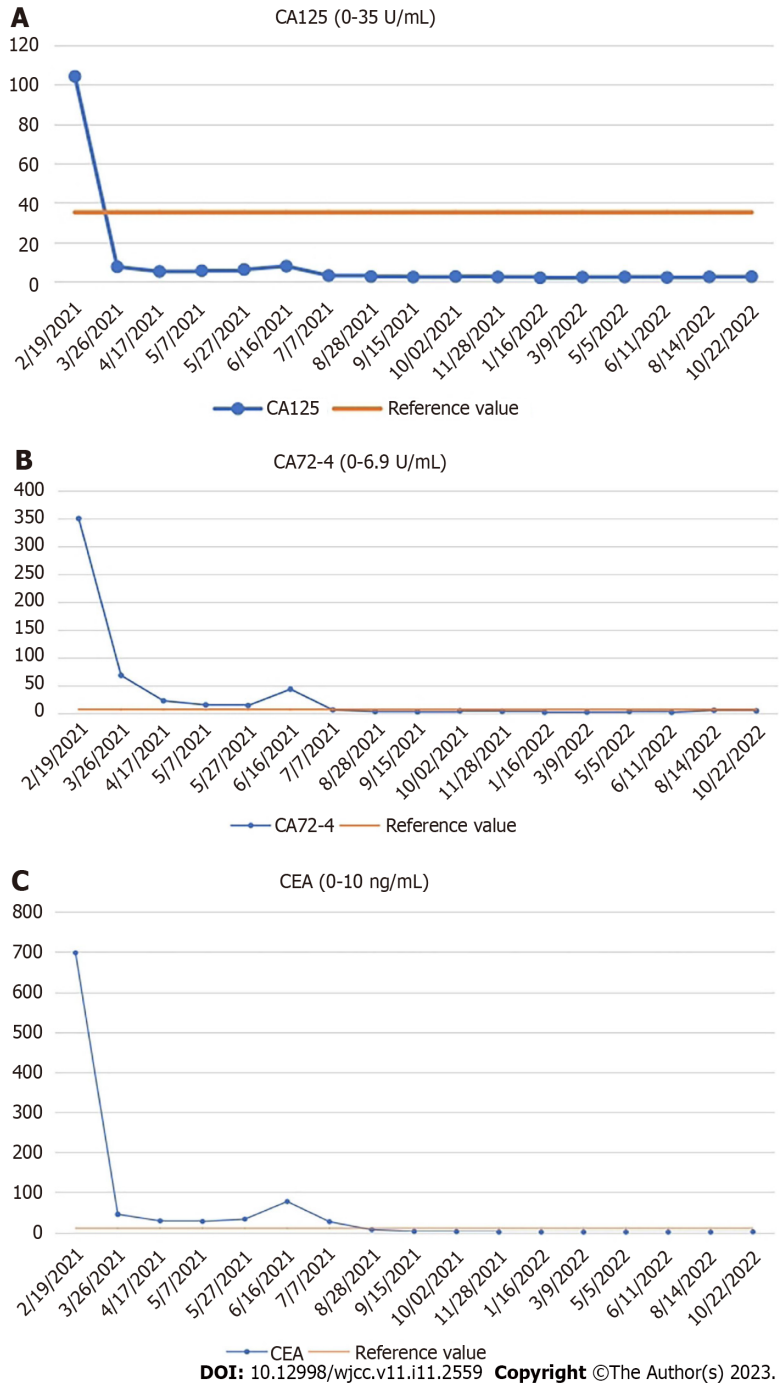

DOI: 10.12998/wjcc.v11.i11.2559

Figure 3 Changes in serum levels of carcinoembryonic antigen, carbohydrate antigen 72-4, and carbohydrate antigen 125. A: Carbohydrate antigen (CA) 125 (0-35 U/mL); B: CA72-4 (0-6.9 U/mL); C: Carcinoembryonic antigen (0-10 ng/mL). CA: Carbohydrate antigen; CEA: Carcinoembryonic antigen.

cetuximab. Cetuximab is used for the treatment of metastatic colorectal cancer with overexpression of epidermal growth factor (EGF) receptor and resistance to irinotecan-based chemotherapy. Cetuximab is an immunoglobulin G1 monoclonal antibody against EGF receptor. After specific binding, the two antibodies block the intracellular signal transduction pathway by inhibiting the binding of ligands to EGF receptor, resulting in inhibition of proliferation of cancer cells, inducing apoptosis of cancer cells, and reducing the production of matrix metalloproteinase and vascular endothelial growth factor[16]. Wang *et al*[6] performed treatment with XELOX chemotherapy regimen in combination with bevacizumab in a patient with breast metastasis from colon cancer for 8 cycles, increasing successful treatment experience for patients with this rare metastasis. This is similar to our research. In addition, most of the other reports only reported the diagnosis of this rare metastasis. The average survival time is 14.9 mo according to the literature[6]. Only one case had a more than 5-year overall survival with colon cancer metastasis to the breast[6]. The patient had a 16-mo disease-free survival in our case, which has exceeded the average level, indicating that our treatment is effective.

Our patient received chemotherapy and targeted therapy after surgery. At the same time, the patient was regularly reviewed, including chest and abdominal CT, and gastrointestinal tumor markers. The dramatic decrease in tumor markers (CEA, CA125, and CA72-4) was due to the removal of colon tumor after transverse colectomy. When breast metastasis occurs, tumor markers begin to increase. However, in our case, the levels of tumor markers (CEA, CA125, and CA72-4) decreased and remained within the normal range after treatment with FOLFIRI + cetuximab. CEA is usually highly expressed in digestive system tumors, especially in some patients with advanced gastric cancer and colorectal cancer[17]. As a specific tumor marker, CA72-4 is used to monitor the recurrence and prognosis of gastric cancer. CA125 is a sensitive marker for ovarian cancer[18], and is also elevated in gastrointestinal tumors. CA125 seems to be a better tumor marker than CEA for predicting progressive disease in colorectal cancer in both men and women[19]. The changes of CEA, CA125, and CA72-4 reflected disease progression and effect of treatment in our patient. These three tumor markers play an important role in evaluating disease status, tumor recurrence, tumor metastasis, and prognosis of gastrointestinal cancer patients. They also indicate postoperative follow-up of patients with gastrointestinal tumors. We will continue to evaluate the condition of the patient by monitoring the levels of tumor markers and CT changes, which are beneficial for treatment planning.

Breast metastasis from colon cancer is a manifestation of advanced cancer. There are a variety of treatment methods, but they are complex and difficult. In addition to chemotherapy and targeted therapy, immunotherapy may also become a new choice, which needs further clinical research. For this patient, we will continue to observe the effect of treatment by follow-up and decide whether to give further treatment according to the review results.

CONCLUSION

Breast metastasis from colon cancer is rare. Typically, it has a poor prognosis because it is associated with disseminated metastatic disease. Radical breast surgery should be avoided unless needed for palliation. The surgical treatment of a metastatic breast tumor should be both diagnostic and palliative. Chemotherapy combined with targeted therapy should be the first choice. The mechanism of metastasis and better treatment need to be studied.

FOOTNOTES

Author contributions: Jiao X reviewed the literature and contributed to manuscript drafting; Xing FZ was the patient's primary doctor and substantially contributed to the conception and design of the study and acquisition of the data; Zhai MM substantially contributed to the data acquisition; Sun P was responsible for the revision of the manuscript for important intellectual content.

Informed consent statement: Informed written consent was obtained from the patient for the publication of this case report.

Conflict-of-interest statement: All the authors report no relevant conflicts of interest for this article.

CARE Checklist (2016) statement: The authors have read the CARE Checklist (2016), and the manuscript was prepared and revised according to the CARE Checklist (2016).

Country/Territory of origin: China

ORCID number: Xin Jiao 0000-0002-4153-7870; Fang-Zhou Xing 0000-0002-0451-416X; Mi-Mi Zhai 0000-0002-6909-9685; Peng Sun 0000-0002-7276-7724.

S-Editor: Zhao S
L-Editor: Wang TQ
P-Editor: Zhao S

REFERENCES

1 **Taieb J**, Karoui M, Basile D. How I treat stage II colon cancer patients. *ESMO Open* 2021; **6**: 100184 [PMID: 34237612 DOI: 10.1016/j.esmoop.2021.100184]
2 **Wang Z**, Song J, Azami NLB, Sun M. Identification of a Novel Immune Landscape Signature for Predicting Prognosis and Response of Colon Cancer to Immunotherapy. *Front Immunol* 2022; **13**: 802665 [PMID: 35572595 DOI: 10.3389/fimmu.2022.802665]
3 **Tsung SH**. Metastasis of Colon Cancer to the Breast. *Case Rep Oncol* 2017; **10**: 77-80 [PMID: 28203167 DOI: 10.1159/000455225]
4 **McIntosh IH**, Hooper AA, Millis RR, Greening WP. Metastatic carcinoma within the breast. *Clin Oncol* 1976; **2**: 393-401 [PMID: 1024766]
5 **Arnaout K**, Hawa N, Agha S, Kadoura L, Aloulou M, Ayoub K. A case report of multiple bilateral breast metastases after colorectal cancer. *Int J Surg Case Rep* 2021; **81**: 105759 [PMID: 33743246 DOI: 10.1016/j.ijscr.2021.105759]
6 **Wang X**, Zhang H, Lu Y. Breast metastasis of signet ring cell carcinoma from the colon: a case report. *World J Surg Oncol* 2022; **20**: 376 [PMID: 36451153 DOI: 10.1186/s12957-022-02840-7]
7 **Hsieh TC**, Hsu CW. Breast metastasis from colorectal cancer treated by multimodal therapy: Case report and literature review. *Medicine (Baltimore)* 2019; **98**: e18016 [PMID: 31860952 DOI: 10.1097/MD.0000000000018016]
8 **Fernández de Bobadilla L**, García Villanueva A, Collado M, de Juan A, Rojo R, Pérez J, Lisa E, Aguilera A, Mena A, González-Palacios F. Breast metastasis of primary colon cancer. *Rev Esp Enferm Dig* 2004; **96**: 415-7; 418 [PMID: 15230671 DOI: 10.4321/s1130-01082004000600007]
9 **Taccogna S**, Gozzi E, Rossi L, Caruso D, Conte D, Trenta P, Leoni V, Tomao S, Raimondi L, Angelini F. Colorectal cancer metastatic to the breast: A case report. *World J Gastrointest Oncol* 2020; **12**: 1073-1079 [PMID: 33005300 DOI: 10.4251/wjgo.v12.i9.1073]
10 **Gallagher DJ**, Kemeny N. Metastatic colorectal cancer: from improved survival to potential cure. *Oncology* 2010; **78**: 237-248 [PMID: 20523084 DOI: 10.1159/000315730]
11 **Lane K**, Worsley D, McKenzie D. Exercise and the lymphatic system: implications for breast-cancer survivors. *Sports Med* 2005; **35**: 461-471 [PMID: 15974632 DOI: 10.2165/00007256-200535060-00001]
12 **Siegel RL**, Miller KD, Jemal A. Cancer statistics, 2015. *CA Cancer J Clin* 2015; **65**: 5-29 [PMID: 25559415 DOI: 10.3322/caac.21254]
13 **Zhao L**, Xu J, Liang F, Li A, Zhang Y, Sun J. Effect of Chronic Psychological Stress on Liver Metastasis of Colon Cancer in Mice. *PLoS One* 2015; **10**: e0139978 [PMID: 26444281 DOI: 10.1371/journal.pone.0139978]
14 **Mihai R**, Christie-Brown J, Bristol J. Breast metastases from colorectal carcinoma. *Breast* 2004; **13**: 155-158 [PMID: 15019699 DOI: 10.1016/S0960-9776(03)00125-5]
15 **Wakeham NR**, Satchithananda K, Svensson WE, Barrett NK, Comitis S, Zaman N, Ralleigh G, Sinnett D, Shousha S, Lim AK. Colorectal breast metastases presenting with atypical imaging features. *Br J Radiol* 2008; **81**: e149-e153 [PMID: 18440938 DOI: 10.1259/bjr/62391254]
16 **Kopetz S**, Guthrie KA, Morris VK, Lenz HJ, Magliocco AM, Maru D, Yan Y, Lanman R, Manyam G, Hong DS, Sorokin A, Atreya CE, Diaz LA, Allegra C, Raghav KP, Wang SE, Lieu CH, McDonough SL, Philip PA, Hochster HS. Randomized Trial of Irinotecan and Cetuximab With or Without Vemurafenib in BRAF-Mutant Metastatic Colorectal Cancer (SWOG S1406). *J Clin Oncol* 2021; **39**: 285-294 [PMID: 33356422 DOI: 10.1200/JCO.20.01994]
17 **Zheng TH**, Zhao JL, Guleng B. Advances in Molecular Biomarkers for Gastric Cancer. *Crit Rev Eukaryot Gene Expr* 2015; **25**: 299-305 [PMID: 26559090 DOI: 10.1615/critreveukaryotgeneexpr.2015014360]
18 **Bast RC Jr**, Feeney M, Lazarus H, Nadler LM, Colvin RB, Knapp RC. Reactivity of a monoclonal antibody with human ovarian carcinoma. *J Clin Invest* 1981; **68**: 1331-1337 [PMID: 7028788 DOI: 10.1172/jci110380]
19 **Huang CJ**, Jiang JK, Chang SC, Lin JK, Yang SH. Serum CA125 concentration as a predictor of peritoneal dissemination of colorectal cancer in men and women. *Medicine (Baltimore)* 2016; **95**: e5177 [PMID: 27893659 DOI: 10.1097/MD.0000000000005177]

World Journal of Clinical Cases

Submit a Manuscript: https://www.f6publishing.com

World J Clin Cases 2023 April 16; 11(11): 2567-2575

DOI: 10.12998/wjcc.v11.i11.2567

ISSN 2307-8960 (online)

CASE REPORT

Different endodontic treatments induced root development of two nonvital immature teeth in the same patient: A case report

Rong Chai, Xiu Yang, An-Sheng Zhang

Specialty type: Medicine, research and experimental

Provenance and peer review: Unsolicited article; Externally peer reviewed.

Peer-review model: Single blind

Peer-review report's scientific quality classification

Grade A (Excellent): 0
Grade B (Very good): B, B
Grade C (Good): 0
Grade D (Fair): 0
Grade E (Poor): 0

P-Reviewer: He YH, China; Sekhar P, India

Received: January 20, 2023
Peer-review started: January 20, 2023
First decision: February 20, 2023
Revised: March 1, 2023
Accepted: March 22, 2023
Article in press: March 22, 2023
Published online: April 16, 2023

Rong Chai, Xiu Yang, An-Sheng Zhang, Department of Stomatology, Xi'an International Medical Center Hospital Affiliated to Northwest University, Xi'an 710061, Shaanxi Province, China

Corresponding author: An-Sheng Zhang, MD, Associate Chief Physician, Department of Stomatology, Xi'an International Medical Center Hospital Affiliated to Northwest University, No. 777 Xitai Road, Hightech District, Xi'an 710061, Shaanxi Province, China.
zhang.ansheng@000516.cn

Abstract

BACKGROUND

Pulp revascularization is a novel way to treat immature teeth with periapical disease, and the technique has become increasingly well established in recent years. By puncturing the periapical tissue, bleeding is induced, and a blood clot is formed in the root canal. The blood clot acts as a natural bioscaffold onto which mesenchymal stem cells from periapical tissue can be seeded and restore pulp vascularity, thus promoting root development as well as apical closure. Although the effect of pulp revascularization is ideal, there are certain requirements for the apical condition of the teeth. The apical barrier technique and apexification are still indispensable for teeth that cannot achieve ideal blood clot formation. In addition, a meta-analysis of several clinical studies concluded that pulp revascularization has no significant advantages over other treatments.

CASE SUMMARY

A 10-year-old girl complained of pain in the right upper and lower posterior teeth for 2 d. Clinical and radiological examinations revealed that both the right maxillary and mandibular second premolars were immature with periapical radiolucency. The right maxillary second premolar was treated by pulp revascularization, while the right mandibular second premolar was treated by conventional apical barrier surgery after revascularization failed. The purpose of this report is to compare the different root maturation processes induced by the pulp revascularization and apical barrier techniques in the same patient in homonymous teeth from different jaws. Twelve months of follow-up showed that the apical foramen of both teeth presented a clear tendency to close; however, the tooth treated with pulp revascularization showed a significant increase in root length as well as root canal wall thickness.

CONCLUSION

For the treatment of nonvital immature teeth, pulp revascularization showed a

superior therapeutic effect in comparison with the apical barrier technique.

Key Words: Nonvital immature tooth; Central cusp deformity; Pulp revascularization; Apical barrier technique; Root canal; Case report

Core Tip: This report presents a case where pulp revascularization and the apical barrier technique were performed in the right maxillary and mandibular premolars. Twelve months of follow-up showed that both teeth were asymptomatic; however, the tooth treated with pulp revascularization showed a better outcome in root development.

Citation: Chai R, Yang X, Zhang AS. Different endodontic treatments induced root development of two nonvital immature teeth in the same patient: A case report. *World J Clin Cases* 2023; 11(11): 2567-2575
URL: https://www.wjgnet.com/2307-8960/full/v11/i11/2567.htm
DOI: https://dx.doi.org/10.12998/wjcc.v11.i11.2567

INTRODUCTION

Young permanent teeth take 3-5 years to complete root development and form the apical foramen after eruption. During this process, pulp or periapical tissue disease caused by infection or trauma may hinder or even stop root development. Flared and wide apical foramens have always been a great challenge for dental clinicians. Pulp revascularization is a novel therapeutic method that has been proven to be a clinically successful application of regenerative medicine. Numerous reports in recent years have demonstrated that revascularization is undoubtedly an ideal treatment for nonvital teeth with wide-open apexes. Sterilized drug irrigation replaces the conventional mechanical root canal preparation and maximizes the preservation of root apical tissue to provide conditions for subsequent tissue regeneration in the root canal. Previous studies have suggested that secondary hard tissue may be derived from residual pulp tissue at the root apex, Hertwig's epithelial root sheath cells and periapical stem cells[1]. These cells adhere to the autologous scaffold formed by the blood clot in the root canal; induce the formation of hard tissues, such as reparative dentin, cementoid tissue and bone-like tissue at the root apex; or directly induce the ingrowth of periapical hard tissue[2-5]. In this report, we describe a case of pulp revascularization use for the treatment of apical periodontitis in a young permanent tooth with a wide-open apex. After revascularization, the apical foramen closed, and the thickness of the dentinal wall increased significantly.

Although the therapeutic effect of pulp revascularization is satisfactory, if the apical blood supply of the affected tooth is poor, sufficient blood cannot be delivered during the treatment, which makes it difficult to conduct blood-clot induced revascularization. In our report, pulp revascularization was successfully performed on the maxillary second premolar, but microscopy did not reveal obvious blood inflow into the root canal of the mandibular second premolar, so we resorted to the use of the apical barrier technique. Both techniques are important treatments for nonvital teeth with wide-open apexes, and this case was a rare opportunity to evaluate and compare the therapeutic effect of pulp revascularization and the apical barrier technique in the same individual. A case report is presented to compare the different root maturation processes of pulp revascularization and the apical barrier technique in the same patient in homonymous teeth from different jaws.

CASE PRESENTATION

Chief complaints

A 10-year-old girl complained of pain in the right upper posterior teeth for 2 d before visiting; four months later, she visited again and complained of pain in the right lower posterior teeth for 2 d.

History of present illness

The patient reported that she felt discomfort in the right maxillary posterior region two days prior to visiting our department and went to see a dentist in another clinic. The diagnosis was central cusp deformity in the right maxillary and mandibular second premolars. The central cusps were partly ground off during the visit. The next day, she felt severe spontaneous pain in the right maxillary posterior region accompanied by swelling of the right maxillofacial area. Approximately 4 mo later, she

complained of paroxysmal pain in the right mandibular posterior region, and the next day, the pain became persistent.

History of past illness

The patient denied any history of previous disease.

Personal and family history

The patient denied a personal or family history of any systemic disease.

Physical examination

When the patient presented with pain in the right upper posterior teeth, the extraoral examination revealed mild swelling of the right maxillofacial region. Intraoral examination showed that the buccal gingiva around the apical region of the right maxillary premolars was swollen, the vestibular sulcus was shallow, and the residual partial central cusp deformity was visible on the occlusal surface (Figure 1A). The right maxillary second premolar was moderately loose and had a severe response to percussion.

When the patient presented with pain in the right lower posterior teeth, extraoral examination showed bilateral maxillofacial symmetry and no obvious swelling. Intraoral examination showed that the buccal gingiva around the apical area of the right mandibular premolars was red and slightly swollen. The right mandibular second premolar was slightly loose and had a severe response to percussion.

Laboratory examinations

No laboratory examination was performed.

Imaging examinations

Intraoral radiographic examination revealed a hypodense area around the apex of the right maxillary second premolar, and the root was incompletely developed with an open apex (Figure 1B).

Periapical X-ray examination showed a hypodense area around the apex of the right mandibular second premolar with an open apex (Figure 1C).

FINAL DIAGNOSIS

Based on the patient's history as well as clinical and radiographic examinations, a diagnosis of chronic apical periodontitis was made for the right maxillary second premolar and the right mandibular second premolar.

TREATMENT

Treatment options, including the use of the pulp revascularization technique and the apical barrier technique, were offered to the patient. After fully understanding the advantages and disadvantages of the two techniques, the patient chose pulp revascularization. The timelines of the treatment of the affected teeth are presented in Tables 1 and 2.

Treatment of the right maxillary second premolar

First treatment visit: Local anesthesia was performed with 2% lidocaine hydrochloride. A rubber dam was used to isolate the affected tooth. Under a microscope, pulp chamber access was performed with a diamond bur. A large amount of pus was seen in the pulp chamber. The root canal was irrigated alternately with 1.5% sodium hypochlorite solution (Longly Biotechnology, Wuhan, China) and 17% ethylene diamine tetraacetic acid (EDTA) solution (Longly Biotechnology, Wuhan, China) for five minutes. After drying the canal with sterile paper tips, calcium hydroxide paste (ApexCal®, Ivoclar Vivadent, Liechtenstein) was placed into the root canal; a sterile cotton pellet was placed in the pulp chamber, and the access cavity was sealed with a temporary sealing paste (Cavit-G, 3M ESPE, St. Paul, MN, United States).

Second treatment visit: Two weeks later, the affected tooth had no percussion pain or abnormal mobility. Local anesthesia was performed with 2% lidocaine hydrochloride, and a rubber dam was used to isolate the affected tooth. Under a microscope, the temporary sealing material was removed, and the root canal was washed with an ultrasonic apparatus (Satelec P5 Newtron XS, Acteon, France). After copious irrigation with 17% EDTA solution (Longly Biotechnology, Wuhan, China) for five minutes, the root canal was dried with sterile paper tips. The periapical tissue was penetrated with a #20 K-file to induce bleeding until blood filled the root canal (Figure 2A). The coronal third of the root canal was sealed with iRoot BP plus (iRoot® BP+, Innovative BioCeramix, Canada) (Figure 2B). The access cavity

Table 1 Timeline of the treatment of the right maxillary second premolar

Timeline	Events	
March 11, 2021	First treatment visit	Root canal irrigation and intracranial medication with calcium hydroxide paste
March 26, 2021	Second treatment visit	Penetration of the periapical tissue to induce bleeding, sealing of the coronal third of the root canal with iRoot BP plus
June 29, 2021	3-mo follow-up	Significant reduction of the periapical hypodense area and obvious closure of the apex
September 28, 2021	6-mo follow-up	Complete healing of the periapical lesion and slight increase in dentinal wall thickness
April 1, 2022	12-mo follow-up	Significant thickening of the dentinal wall and obvious narrowing of the root canal

Table 2 Timeline of the treatment of the right mandibular second premolar

Timeline	Events	
July 19, 2021	First treatment visit	Root canal irrigation and intracranial medication with calcium hydroxide paste
July 30, 2021	Second treatment visit	Penetration of the periapical tissue without obvious bleeding
August 6, 2021	Third treatment visit	Penetration of the periapical tissue for a second time without obvious bleeding and performance of the apical barrier technique
August 13, 2021	Fourth treatment visit	Filling of the middle and coronal third of the root canal with hot gutta-percha and filling of the access cavity with light-cured composite resin
November 10, 2021	3-mo follow-up	Significant decrease in size of the periapical hypodense area
February 11, 2022	6-mo follow-up	Complete healing of the periapical hypodense area
August 25, 2022	12-mo follow-up	Narrowing of the periodontal ligament and complete closure of the apex

DOI: 10.12998/wjcc.v11.i11.2567

Figure 1 Preoperative photos of the right maxillary second premolar and the right mandibular second premolar. A: Preoperative intraoral photo of the right maxillary second premolar. Note that the central cusp deformity had been polished during the patient's last visit in another clinic, and a residual part was still visible (white arrow); B: Preoperative periapical radiograph of the right maxillary second premolar. Note that the apex of the root is open (white arrow), the root canal is wide, the dentinal wall is relatively thin (black arrow), and there is a hypodense area around the root apex; C: Preoperative periapical radiograph of the right mandibular second premolar. Note that the apex of the root is not closed (white arrow), the root canal is wide, the dentinal wall is thin (black arrow), and there is a hypodense area around the root apex.

was temporarily restored with glass ionomer cement (Fuji IX GP, GC, Japan) (Figure 2C). A postoperative periapical radiograph of the right maxillary second premolar was performed (Figure 2D).

Treatment of the right mandibular second premolar

First treatment visit: Local anesthesia was performed with 2% lidocaine hydrochloride. A rubber dam was used to isolate the affected tooth. Under a microscope, pulp chamber access was performed with a diamond bur. The root canal was irrigated alternately with 1.5% sodium hypochlorite solution (Longly Biotechnology, Wuhan, China) and 17% EDTA solution (Longly Biotechnology, Wuhan, China) for five minutes. After drying the canal with sterile paper tips, calcium hydroxide paste (ApexCal®, Ivoclar Vivadent, Liechtenstein) was placed into the root canal; a sterile cotton pellet was placed in the pulp

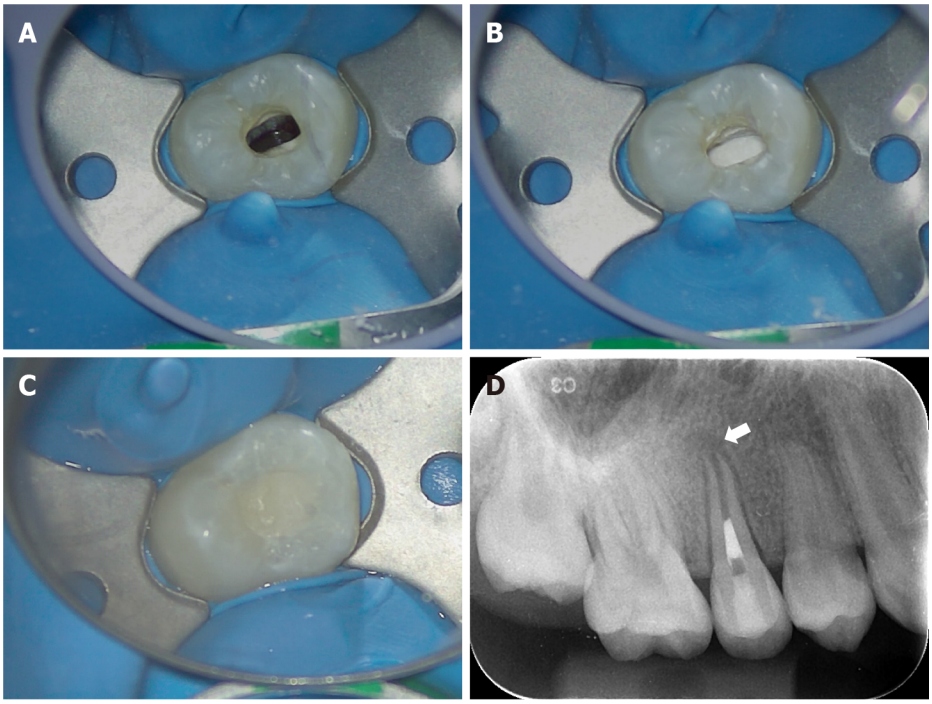

DOI: 10.12998/wjcc.v11.i11.2567

Figure 2 Treatment process of revascularization in the right maxillary second premolar. A: Blood filled in the root canal space after penetration of the periapical tissue by a #20 K-file; B: The coronal third of the root canal was sealed with iRoot BP plus; C: The access cavity was temporarily restored with glass ionomer cement; D: Postoperative periapical radiograph of the right maxillary second premolar. Note the obvious hypodense area around the root apex and the wide-open apex (white arrow); the root canal is wide, and the dentinal wall is relatively thin.

chamber, and the access cavity was sealed with a temporary sealing paste (Cavit-G, 3M ESPE, St. Paul, MN, United States).

Second treatment visit: After two weeks, the affected tooth had no percussion pain or abnormal mobility. Local anesthesia was performed with 2% lidocaine hydrochloride, and a rubber dam was used to isolate the affected tooth. Under a microscope, the temporary sealing material was removed, and the root canal was washed with an ultrasonic apparatus (Satelec P5 Newtron XS, Acteon, France). After copious irrigation with 17% EDTA solution (Longly Biotechnology, Wuhan, China) for five minutes, the root canal was dried with sterile paper tips. The periapical tissue was penetrated with a #20 K-file to induce bleeding. However, after multiple attempts, there was no significant bleeding. The root canal was irrigated with 1.5% sodium hypochlorite solution (Longly Biotechnology, Wuhan, China) and then filled with calcium hydroxide paste (ApexCal®, Ivoclar Vivadent, Liechtenstein); a sterile cotton pellet was placed in the pulp chamber, and the access cavity was sealed with a temporary sealing paste (Cavit-G, 3M ESPE, St. Paul, MN, United States).

Third treatment visit

A week later, local anesthesia was performed with 2% lidocaine hydrochloride, and a rubber dam was used to isolate the affected tooth. Under a microscope, the temporary sealing material was removed, and the root canal was washed with an ultrasonic apparatus (Satelec P5 Newtron XS, Acteon, France). After copious irrigation with 17% EDTA solution (Longly Biotechnology, Wuhan, China) for five minutes, the root canal was dried with sterile paper tips. The periapical tissue was penetrated again with a #20 K-file to induce bleeding. After several attempts, there was still no obvious bleeding (Figure 3A). After discussion with the patient's parents, we decided to switch the treatment plan to the apical barrier technique. Under a microscope, an appropriate amount of iRoot BP plus was placed into the root canal and pressed repeatedly to form an apical barrier with a thickness of approximately 4 mm at the root tip (Figure 3B and C). A moist sterile cotton pellet was placed in the pulp chamber, and the access cavity was sealed with a temporary sealing paste (Cavit-G, 3M ESPE, St. Paul, MN, United States).

Fourth treatment visit

After one week, a rubber dam was used to isolate the affected tooth. Under a microscope, the temporary sealing material was removed, and the root canal was washed with an ultrasonic apparatus (Satelec P5 Newtron XS, Acteon, France). After drying with sterile paper tips, the coronal and middle third of the root canal was filled with hot gutta-percha (Figure 3D and E), and the access cavity was restored with a

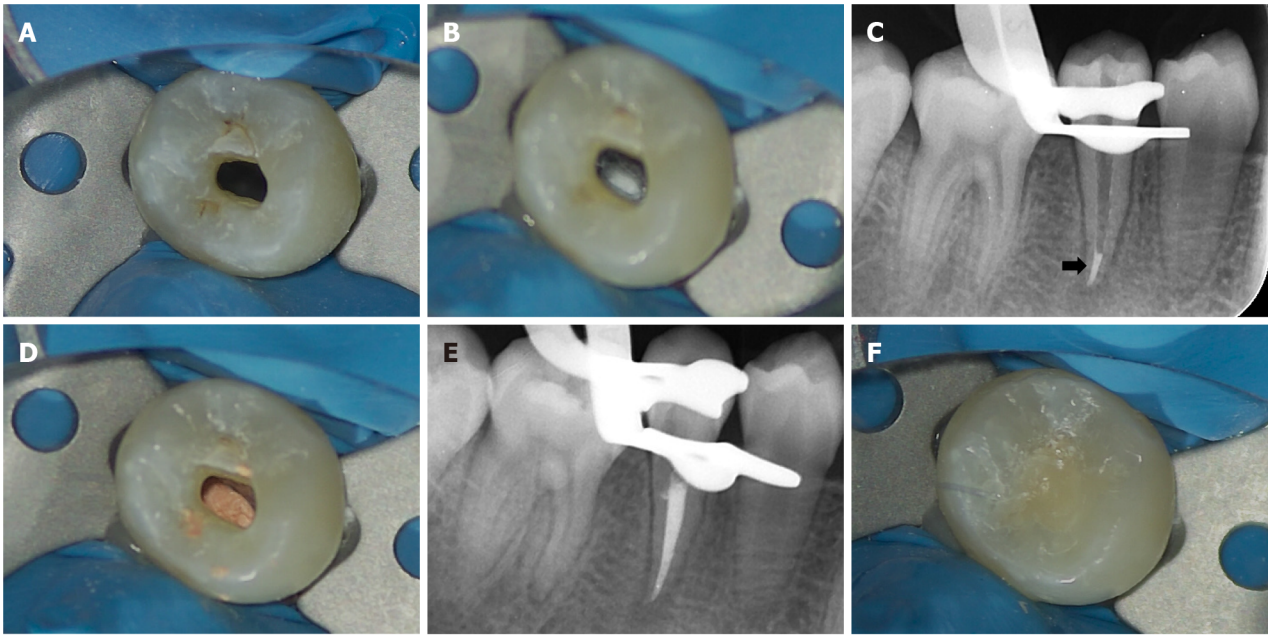

DOI: 10.12998/wjcc.v11.i11.2567

Figure 3 Treatment process of the right mandibular second premolar. A: There was no obvious blood in the root canal after penetration of the periapical tissue by a #20 K-file; B: iRoot BP plus was placed in the apical third of the root canal and pressed tightly to form an apical barrier; C: Intraoral radiograph of the right mandibular second premolar after the placement of iRoot BP plus at the apical third of the root canal (black arrow); D and E: The coronal and middle third of the root canal was filled with hot gutta-percha; F: The access cavity was restored with light-cured composite resin.

flowable light-cured resin base (Z350XT Flowable, 3M™ Filtek™, United States) and light-cured composite resin (Z350XT, 3M™ Filtek™, United States) (Figure 3F).

OUTCOME AND FOLLOW-UP

Follow-up of the right maxillary second premolar

At the 3-mo follow-up, the periapical radiograph revealed that the hypodense area around the root apex had significantly diminished, and the apex had obviously closed (Figure 4A). The glass ionomer cement was replaced by a flowable light-cured resin base (Z350XT Flowable, 3M™ Filtek™, United States) and light-cured composite resin (Z350XT, 3M™ Filtek™, United States).

At the 6-mo follow-up, there was complete healing of the periapical lesion. The thickness of the dentinal wall slightly increased, and there seemed to be some scattered calcifications in the root canal (Figure 4B).

At the 12-mo follow-up, the root canal had obviously narrowed, and the thickness of the dentinal wall had increased significantly (Figure 4C).

The affected tooth showed no response to cold, heat or electric stimulations.

Follow-up of the right mandibular second premolar

At the 3-mo follow-up, the periapical radiolucency area was significantly reduced (Figure 5A).

At the 6-mo follow-up, the periapical radiolucency area had completely healed (Figure 5B).

At the 12-mo follow-up, the periodontal ligament had narrowed, and complete closure of the apex was observed, with an obvious calcification layer generated just around the apical barrier materials (Figure 5C).

DISCUSSION

In the present case report, we described the maturation processes of homonymous teeth from different jaws after applying dental pulp revascularization and the apical barrier technique in the same patient. This was a valuable opportunity to observe the differences in the therapeutic effects between the two techniques. After 12 mo of follow-up, both teeth were asymptomatic; however, the different statuses of the roots indicated that pulp revascularization showed several advantages over the apical barrier technique. Pulp revascularization can stimulate the regeneration potential of periapical tissues, thereby promoting further development of the root, including root canal wall thickening, root elongation, and

DOI: 10.12998/wjcc.v11.i11.2567

Figure 4 Follow-up of the right maxillary second premolar. A: 3-mo follow-up. The hypodense area around the root apex was significantly diminished, and the apex was obviously closed (white arrow); B: 6-mo follow-up. There was complete healing of the periapical hypodense area (white arrow). The thickness of the dentinal wall was slightly increased, and there seemed to be some scattered calcifications in the root canal (black arrow); C: 12-mo follow-up. The root canal was obviously narrowed, and the thickness of the dentinal wall was increased significantly (black arrow).

DOI: 10.12998/wjcc.v11.i11.2567

Figure 5 Follow-up of the right mandibular second premolar. A: 3-mo follow-up. The hypodense area around the root apex was significantly diminished (white arrow); B: 6-mo follow-up. The periapical hypodense area was completely healed (white arrow); C: 12-mo follow-up. The periodontal ligament was narrowed (white arrow). Complete closure of the apex was observed, and there was an obvious calcification layer generated just around the apical barrier materials (black arrow).

closure of the apical foramen[6,7]. In this way, the fragile and blunderbuss-like root can be rescued, and the incidence of tooth fracture and crown-to-root ratio incompatibility can be further reduced. In addition, after pulp revascularization, the tooth does not need root canal therapy, avoiding the risk of reinfection caused by reopening the pulp cavity.

Even if pulp revascularization fails, apexification and the apical barrier technique are alternative options. Traditionally, the procedure indicated for teeth with incomplete root formation is apexification; this technique is mainly performed by placing calcium hydroxide paste into the root canal for a certain time period to induce the formation of a calcified barrier[8]. Currently, apexification is regarded as the most classical treatment; however, long-term intracanal medication may decrease root strength due to the hygroscopic and proteolytic properties of calcium hydroxide[9,10]. The key to the apical barrier technique is to seal the wide-open apex tightly with bioceramic materials, such as iRoot BP plus or mineral trioxide aggregate[11], to prevent further infections. It is often a substantial technical challenge for dentists, and if the treatment fails, it is difficult to address[12]. The current view is that the root length and dentinal wall thickness will not change after treatment; thus, this technique does not considerably enhance the strength of the root. Therefore, with a comprehensive analysis of the pros and cons of apexification and the apical barrier technique, in this case, after the failure of revascularization, we resorted to the apical barrier technique to treat the mandibular second premolar. At the 6-mo follow-up, the hypodense area around the root apex had completely healed, demonstrating that successful application of the apical barrier technique can effectively control root canal infection and promote the healing of the periapical tissue. At the 12-mo follow-up, complete closure of the apex was observed, and there was an obvious calcification layer generated just around the apical barrier materials, likely due to the mineralization induction capacity of iRoot BP plus[13].

In this case, the different maturation processes of the two teeth demonstrated that pulp revascularization showed a superior therapeutic effect in nonvital young permanent teeth because pulp revascularization offers the possibility of additional tooth development rather than simple hard tissue deposition, which may greatly reduce the incidence of future tooth fractures. According to studies in regenerative medicine, therapeutic angiogenesis is a key factor in tissue regeneration[14-16]. Both the American Association of Endodontics and the European Society of Endodontology agree that pulp

revascularization is the preferred treatment for teeth with incomplete root formation[17,18]. The blood clot-induced revascularization used in this study is the most commonly used, well-established technique. With the continuous development of regenerative medicine, revascularization can also be induced by, for example, platelet-rich fibrin, platelet-rich plasma, angiogenic peptide hydrogels, and buccal fat grafts[19-21]. Although pulp revascularization is highly recommended by many clinicians, its shortcomings, such as discoloration of the crown and root canal blockage, cannot be ignored[22-24]. Nicoloso *et al*[25] conducted a meta-analysis of several clinical studies and concluded that pulp revascularization has no significant advantages over other treatments. The optimal treatment for nonvital immature teeth remains uncertain. In the future, we need to pay close attention to new trends in regenerative medicine to create more innovative points for root regeneration; we also need to carefully analyze the condition of the affected teeth in clinical practice, balance the advantages and disadvantages of various treatment methods, and try to provide the most suitable choice for patients.

CONCLUSION

In this case, pulp revascularization showed a superior outcome of inducing root development in comparison with the apical barrier technique. However, more attention should be given to regenerative endodontics to optimize treatment for nonvital immature teeth.

FOOTNOTES

Author contributions: Chai R performed the treatment, collected data, and wrote the manuscript; Yang X contributed to data collection; Zhang AS conceived the study, provided financial support, and reviewed the manuscript; and all authors read and approved the manuscript.

Supported by The Natural Science Foundation of Shaanxi Province, China, No. 2022JM-447.

Informed consent statement: Informed written consent was obtained from the patient for publication of this report and any accompanying images.

Conflict-of-interest statement: All the authors report no relevant conflicts of interest for this article.

CARE Checklist (2016) statement: The authors have read the CARE Checklist (2016), and the manuscript was prepared and revised according to the CARE Checklist (2016).

Country/Territory of origin: China

ORCID number: An-Sheng Zhang 0000-0003-3268-7620.

S-Editor: Hu YR
L-Editor: A
P-Editor: Hu YR

REFERENCES

1 **Chueh LH**, Huang GT. Immature teeth with periradicular periodontitis or abscess undergoing apexogenesis: a paradigm shift. *J Endod* 2006; **32**: 1205-1213 [PMID: 17174685 DOI: 10.1016/j.joen.2006.07.010]
2 **Torabinejad M**, Alexander A, Vahdati SA, Grandhi A, Baylink D, Shabahang S. Effect of Residual Dental Pulp Tissue on Regeneration of Dentin-pulp Complex: An In Vivo Investigation. *J Endod* 2018; **44**: 1796-1801 [PMID: 30477665 DOI: 10.1016/j.joen.2018.09.005]
3 **Zhu X**, Wang Y, Liu Y, Huang GT, Zhang C. Immunohistochemical and histochemical analysis of newly formed tissues in root canal space transplanted with dental pulp stem cells plus platelet-rich plasma. *J Endod* 2014; **40**: 1573-1578 [PMID: 25260728 DOI: 10.1016/j.joen.2014.05.010]
4 **Lui JN**, Lim WY, Ricucci D. An Immunofluorescence Study to Analyze Wound Healing Outcomes of Regenerative Endodontics in an Immature Premolar with Chronic Apical Abscess. *J Endod* 2020; **46**: 627-640 [PMID: 32139263 DOI: 10.1016/j.joen.2020.01.015]

5 **Becerra P**, Ricucci D, Loghin S, Gibbs JL, Lin LM. Histologic study of a human immature permanent premolar with chronic apical abscess after revascularization/revitalization. *J Endod* 2014; **40**: 133-139 [PMID: 24332005 DOI: 10.1016/j.joen.2013.07.017]

6 **Zhou R**, Wang Y, Chen Y, Chen S, Lyu H, Cai Z, Huang X. Radiographic, Histologic, and Biomechanical Evaluation of Combined Application of Platelet-rich Fibrin with Blood Clot in Regenerative Endodontics. *J Endod* 2017; **43**: 2034-2040 [PMID: 29032818 DOI: 10.1016/j.joen.2017.07.021]

7 **Nawal RR**, Utneja S, Sharma V, Yadav S, Talwar S. Long-term follow-up of traumatized immature necrotic permanent teeth treated with regenerative endodontic protocol using platelet-rich fibrin: A prospective case series. *J Conserv Dent* 2020; **23**: 417-421 [PMID: 33623247 DOI: 10.4103/JCD.JCD_460_20]

8 **Shaik I**, Dasari B, Kolichala R, Doos M, Qadri F, Arokiyasamy JL, Tiwari RVC. Comparison of the Success Rate of Mineral Trioxide Aggregate, Endosequence Bioceramic Root Repair Material, and Calcium Hydroxide for Apexification of Immature Permanent Teeth: Systematic Review and Meta-Analysis. *J Pharm Bioallied Sci* 2021; **13**: S43-S47 [PMID: 34447040 DOI: 10.4103/jpbs.JPBS_810_20]

9 **Arruda MEF**, Neves MAS, Diogenes A, Mdala I, Guilherme BPS, Siqueira JF Jr, Rôças IN. Infection Control in Teeth with Apical Periodontitis Using a Triple Antibiotic Solution or Calcium Hydroxide with Chlorhexidine: A Randomized Clinical Trial. *J Endod* 2018; **44**: 1474-1479 [PMID: 30144986 DOI: 10.1016/j.joen.2018.07.001]

10 **Guerrero F**, Mendoza A, Ribas D, Aspiazu K. Apexification: A systematic review. *J Conserv Dent* 2018; **21**: 462-465 [PMID: 30294103 DOI: 10.4103/JCD.JCD_96_18]

11 **Plascencia H**, Díaz M, Gascón G, Garduño S, Guerrero-Bobadilla C, Márquez-De Alba S, González-Barba G. Management of permanent teeth with necrotic pulps and open apices according to the stage of root development. *J Clin Exp Dent* 2017; **9**: e1329-e1339 [PMID: 29302286 DOI: 10.4317/jced.54287]

12 **Asgary S**, Fayazi S. Endodontic Surgery of a Symptomatic Overfilled MTA Apical Plug: A Histological and Clinical Case Report. *Iran Endod J* 2017; **12**: 376-380 [PMID: 28808469 DOI: 10.22037/iej.v12i3.17689]

13 **Zhang J**, Zhu LX, Cheng X, Lin Y, Yan P, Peng B. Promotion of Dental Pulp Cell Migration and Pulp Repair by a Bioceramic Putty Involving FGFR-mediated Signaling Pathways. *J Dent Res* 2015; **94**: 853-862 [PMID: 25724555 DOI: 10.1177/0022034515572020]

14 **Carmeliet P**, Jain RK. Molecular mechanisms and clinical applications of angiogenesis. *Nature* 2011; **473**: 298-307 [PMID: 21593862 DOI: 10.1038/nature10144]

15 **Sarkar B**, Nguyen PK, Gao W, Dondapati A, Siddiqui Z, Kumar VA. Angiogenic Self-Assembling Peptide Scaffolds for Functional Tissue Regeneration. *Biomacromolecules* 2018; **19**: 3597-3611 [PMID: 30132656 DOI: 10.1021/acs.biomac.8b01137]

16 **Mastrullo V**, Cathery W, Velliou E, Madeddu P, Campagnolo P. Angiogenesis in Tissue Engineering: As Nature Intended? *Front Bioeng Biotechnol* 2020; **8**: 188 [PMID: 32266227 DOI: 10.3389/fbioe.2020.00188]

17 **Galler KM**, Krastl G, Simon S, Van Gorp G, Meschi N, Vahedi B, Lambrechts P. European Society of Endodontology position statement: Revitalization procedures. *Int Endod J* 2016; **49**: 717-723 [PMID: 26990236 DOI: 10.1111/iej.12629]

18 **American Association of Endodontists**. AAE Clinical Considerations for a Regenerative Procedure. 2016. Available from: https://www.aae.org/specialty/clinical-resources/guide-clinical-endodontics/

19 **Nicoloso GF**, Pötter IG, Rocha RO, Montagner F, Casagrande L. A comparative evaluation of endodontic treatments for immature necrotic permanent teeth based on clinical and radiographic outcomes: a systematic review and meta-analysis. *Int J Paediatr Dent* 2017; **27**: 217-227 [PMID: 27529749 DOI: 10.1111/ipd.12261]

20 **Siddiqui Z**, Sarkar B, Kim KK, Kadincesme N, Paul R, Kumar A, Kobayashi Y, Roy A, Choudhury M, Yang J, Shimizu E, Kumar VA. Angiogenic hydrogels for dental pulp revascularization. *Acta Biomater* 2021; **126**: 109-118 [PMID: 33689817 DOI: 10.1016/j.actbio.2021.03.001]

21 **Khazaei S**, Khademi A, Torabinejad M, Nasr Esfahani MH, Khazaei M, Razavi SM. Improving pulp revascularization outcomes with buccal fat autotransplantation. *J Tissue Eng Regen Med* 2020; **14**: 1227-1235 [PMID: 32610370 DOI: 10.1002/term.3094]

22 **Bezgin T**, Yilmaz AD, Celik BN, Kolsuz ME, Sonmez H. Efficacy of platelet-rich plasma as a scaffold in regenerative endodontic treatment. *J Endod* 2015; **41**: 36-44 [PMID: 25459571 DOI: 10.1016/j.joen.2014.10.004]

23 **Kim JH**, Kim Y, Shin SJ, Park JW, Jung IY. Tooth discoloration of immature permanent incisor associated with triple antibiotic therapy: a case report. *J Endod* 2010; **36**: 1086-1091 [PMID: 20478471 DOI: 10.1016/j.joen.2010.03.031]

24 **Gelman R**, Park H. Pulp revascularization in an immature necrotic tooth: a case report. *Pediatr Dent* 2012; **34**: 496-499 [PMID: 23265169]

25 **Nicoloso GF**, Goldenfum GM, Pizzol TDSD, Scarparo RK, Montagner F, de Almeida Rodrigues J, Casagrande L. Pulp Revascularization or Apexification for the Treatment of Immature Necrotic Permanent Teeth: Systematic Review and Meta-Analysis. *J Clin Pediatr Dent* 2019; **43**: 305-313 [PMID: 31560588 DOI: 10.17796/1053-4625-43.5.1]

World Journal of Clinical Cases

Submit a Manuscript: https://www.f6publishing.com

World J Clin Cases 2023 April 16; 11(11): 2576-2581

DOI: 10.12998/wjcc.v11.i11.2576

ISSN 2307-8960 (online)

CASE REPORT

Autoimmune encephalitis after surgery for appendiceal cancer: A case report

Yan-Hui Mao, Lu Li, Li-Ming Wen, Jia-Min Qin, Ya-Ling Yang, Li Wang, Fan-Rong Wang, Yi-Zhou Zhao

Specialty type: Medicine, research and experimental

Provenance and peer review: Unsolicited article; Externally peer reviewed.

Peer-review model: Single blind

Peer-review report's scientific quality classification

Grade A (Excellent): 0
Grade B (Very good): B, B
Grade C (Good): 0
Grade D (Fair): 0
Grade E (Poor): 0

P-Reviewer: Glumac S, Croatia; Rocha R, Brazil

Received: February 19, 2023
Peer-review started: February 19, 2023
First decision: February 28, 2023
Revised: March 7, 2023
Accepted: March 17, 2023
Article in press: March 17, 2023
Published online: April 16, 2023

Yan-Hui Mao, Lu Li, Li-Ming Wen, Jia-Min Qin, Ya-Ling Yang, Li Wang, Department of Gastroenterology, Sichuan Mianyang 404 Hospital, Mianyang 621000, Sichuan Province, China

Fan-Rong Wang, Department of Pathology, Sichuan Mianyang 404 Hospital, Mianyang 621000, Sichuan Province, China

Yi-Zhou Zhao, Department of Medical Imaging, Sichuan Mianyang 404 Hospital, Mianyang 621000, Sichuan Province, China

Corresponding author: Li-Ming Wen, MD, Chief Doctor, Department of Gastroenterology, Sichuan Mianyang 404 Hospital, No. 56 Yuejin Road, Mianyang 621000, Sichuan Province, China. scmy404yy@sina.com

Abstract

BACKGROUND

Primary cancer of the appendix is rare and often difficult to diagnose preoperatively due to the lack of specific clinical symptoms. Autoimmune encephalitis (AIE) is the most common cause of non-infectious encephalitis. The etiologies of AIE include tumors (paraneoplastic), infections (parainfections), or recessive infections. The tumors that have been reported to cause AIE include thymomas, ovarian teratomas, lung cancers, and breast cancers. However, there are no reports of AIE occurring after surgery for appendiceal cancer. This report describes the diagnosis and treatment of a patient with an appendiceal cancer and postoperative AIE.

CASE SUMMARY

We report the case of a 47-year-old man who was transferred to our hospital due to a recurrent low intestinal obstruction. Abdominal enhanced computed tomography was used to consider the possibility of a terminal ileal tumor with serous infiltration and lymph node metastasis. A right hemi-colectomy was performed under general anesthesia with an ileo-transcolon anastomosis and laparoscopic exploration. The postoperative pathologic evaluation revealed a high-grade goblet cell carcinoma of the appendix, accompanied by mesangial and abdominal lymph node metastases, and neural tube and vascular infiltration. The operation was completed without complication. The patient developed restlessness on postoperative day 4, and gradually developed a disturbance of consciousness on postoperative day 6. He was transferred to West China Hospital of Sichuan University and diagnosed with AIE.

CONCLUSION
Albeit rare, the occurrence of neurologic and psychiatric symptoms in patients with an appendiceal cancer postoperatively suggests the possibility of AIE.

Key Words: Appendiceal cancer; Goblet cell carcinoma; Repeated ileus; Postoperative; Autoimmune encephalitis; Case report

Core Tip: Tumors (paraneoplastic) are one of the etiologies of autoimmune encephalitis (AIE). However, there are no reports of AIE occurring after surgery for appendiceal cancer. This report we describes a 47-year-old man who was transferred to our hospital due to a recurrent low intestinal obstruction and a right hemi-colectomy was performed with an ileo-transcolon anastomosis and laparoscopic exploration. But he developed a disturbance of consciousness on postoperative day 6, and diagnosed with AIE at last. We report this case in the hope of giving some guidance to clinicians with similar challenging cases.

Citation: Mao YH, Li L, Wen LM, Qin JM, Yang YL, Wang L, Wang FR, Zhao YZ. Autoimmune encephalitis after surgery for appendiceal cancer: A case report. *World J Clin Cases* 2023; 11(11): 2576-2581
URL: https://www.wjgnet.com/2307-8960/full/v11/i11/2576.htm
DOI: https://dx.doi.org/10.12998/wjcc.v11.i11.2576

INTRODUCTION

Primary appendiceal cancer is rare and an incidental finding after an appendectomy for acute appendicitis in most cases[1]. Autoimmune encephalitis (AIE) is considered one of the most common causes of non-infectious acute encephalitis[2]; however, AIE after an appendectomy has not been reported. In this case report, a 47-year-old man with appendiceal cancer developed a disturbance of consciousness postoperatively and was diagnosed with AIE. The purpose of this report was to detail the evolution and diagnosis of the patient.

CASE PRESENTATION

Chief complaints

A 47-year-old male was admitted to our hospital for evaluation of abdominal distension, and difficulty exhaling and defecating for > 1 mo.

History of present illness

The patient had repeated intestinal obstruction for > 1 mo. Plain abdominal radiographs and an enhanced abdominal computed tomography (CT) indicated a low intestinal obstruction. A gastroendoscopy did not reveal abnormal findings. The patient was treated with fasting, fluid rehydration, and enemas. The symptoms improved and the patient was discharged to home; however, the symptoms recurred again 1 wk before admission in addition to vomiting. The patient was re-admitted to our hospital for further evaluation and treatment. The patient underwent a right hemi-colectomy under general anesthesia with an ileointestine-transverse colon anastomosis and laparoscopic exploration. The operation was completed without complications. On day 4 postoperatively the patient developed restlessness and gradually exhibited a disturbance of consciousness on day 6 postoperatively. Laboratory testing and imaging studies did not reveal the underlying cause. Based on our experience and a review of the literature, this case appeared to be unique.

History of past illness

The medical history was negative for cancer, surgery (other than the right hemi-colectomy with ileointestine-transverse colon anastomosis), hypertension, diabetes, and hyperlipidemia.

Personal and family history

The patient admitted to smoking five cigarettes daily for > 20 years. The remaining personal and family histories were non-contributory.

Physical examination

The abdomen was flat and no peristaltic wave was observed. The right lower abdomen was tender without rebound pain or muscle tension. No obvious air or water sounds were heard during auscultation; the bowel sounds were approximately 6 times/min.

Laboratory examinations

The routine hematologic and biochemistry profiles, and the tumor marker, carcinoembryonic antigen, were all in the normal range. The gamma interferon release test results were as follows: McCl-ifn (N): 24.52 pg/mL; McCl-ifn (T): 39.6 pg/mL; McCl-ifn (P): 5000 pg/mL; γ-interferon (IFN) (T-N): 15.08 pg/mL; γ-IFN (P-N): 4975.48 pg/mL; TB-TGRA (+); PPD (-); and TB antibody (-). On day 2 postoperatively, routine hematologic testing revealed the following: White blood cell, 12.38 × 10^9; and neutrophils, 85%. The blood gas analysis and electrolytes were normal. On day 4 postoperatively, electroencephalogram (EEG) with epileptic or slow-wave activity involving the temporal lobes.

When transferred to West China Hospital of Sichuan University, antibodies against intraneuronal antigens (INAab), a well-characterized autoantibodies was found in cerebrospinal fluid (CSF).

Imaging examinations

Colonoscopy revealed no abnormalities in the ileocecum (Figure 1A), but multiple ulcers were noted in the distal ileum (Figure 1B), consistent with inflammation on pathologic evaluation. A whole-abdominal enhanced CT indicated that the wall of the distal ileum was thickened with abnormal enhancement with multiple enlarged lymph nodes (Figure 1C). The possibility of neoplastic lesions involving the serous surface and the fat space were considered (Figure 1D).

The postoperative pathologic evaluation indicated high-grade goblet cell adenocarcinoma of the appendix, invasion of the mesangium of the appendix, and involvement of the cecum wall. Metastases were noted in six of 21 peri-ileal lymph nodes and one of two peri-ileocecal lymph nodes (Figure 1E). The terminal ileum was characterized by chronic active inflammation, necrosis, granulation tissue hyperplasia, and chronic ulcer formation (Figure 1F). A cranial CT scan showed no abnormalities. A cranial magnetic resonance imaging (MRI) indicated abnormal symmetric signals of the bilateral paramedian thalamus, and midbrain aqueduct and brain stem adjacent to the fourth ventricle, which was consistent with a metabolic encephalopathy; however, the cranial CT and MRI did not fully explain the consciousness disorder.

FINAL DIAGNOSIS

The final diagnosis was therefore a goblet cell adenocarcinoma of the appendix with multiple metastases (T4N2Mx), AIE, incomplete ileus, and multiple ulcers in the terminal ileum.

TREATMENT

Based on the patient signs and symptoms, physical examination, medical history, and auxiliary examinations, the patient underwent a right hemi-colectomy under general anesthesia with an ileointestine-transverse colon anastomosis and laparoscopic exploration. The operation was completed without complication. On postoperative day 2, the blood gas analysis and electrolyte levels were normal. A routine hematologic profile showed white blood cell count of 12.38 × 10^9 with 85% neutrophils. Despite no symptoms suggestive of an infection, such as a fever, anti-infection treatment was initiated. The hematologic profile returned to normal after the follow-up review. The patient had no specific complaints, but was uncomfortable. On postoperative day 4, the patient became noticeably restless. A complete cranial CT showed no abnormalities. A neurology consultation was obtained to rule out epilepsy; a sedative was administered. After brief improvement, the symptoms worsened until postoperative day 6 when the patient appeared to have a disorder of consciousness. The postoperative pathologic evaluation indicated a high-grade goblet cell adenocarcinoma of the appendix, invasion of the mesangium of the appendix, and involvement of the cecum wall. Metastases were noted in 6 of 21 peri-ileal lymph nodes and 1 of 2 peri-ileocecal lymph nodes. The terminal ileum revealed chronic active inflammation, necrosis, granulation tissue hyperplasia, and chronic ulcer formation. After a multidisciplinary meeting, it was concluded that encephalitis, metabolic encephalopathy, and tumor brain metastases could not be excluded. Thus, a CSF examination and EEG were recommended; however, the patient and the patient's family requested further treatment at a higher authority hospital. After the patient was transferred to West China Hospital, antibodies against INAab, a well-characterized autoantibodies was found in CSF, the diagnosis of AIE was confirmed. The patient received methylprednisolone (1 g × 5 d) and immunoglobulin (0.4 g/kg/day × 5 d).

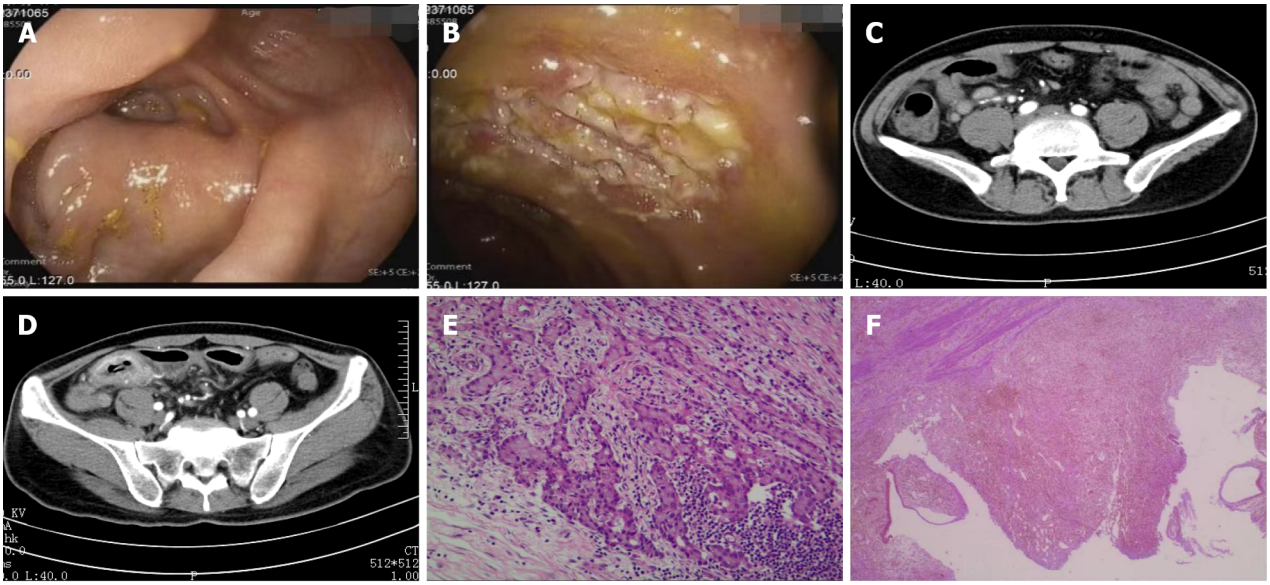

DOI: 10.12998/wjcc.v11.i11.2576

Figure 1 Preoperative colonoscopy, computed tomography and postoperative pathological images. A: Ileocecum with poor exposure of the appendiceal foramen; B: Multiple ulcers in the terminal ileum; C: Multiple enlarged lymph nodes in the abdomen; D: The wall of the distal ileum was thickened with abnormal enhancement, and multiple adjacent, enlarged lymph nodes; E: Postoperative pathologic evaluation indicated high-grade goblet cell adenocarcinoma of the appendix (original magnification × 400); F: The terminal ileum indicated chronic active inflammation (original magnification × 400).

OUTCOME AND FOLLOW-UP

At the West China Hospital, the patient's level of consciousness returned to baseline, but functional limitations persisted. Due to financial reasons, further review and chemotherapy were not performed. The patient died 10 mo later.

DISCUSSION

Primary appendiceal cancer is rare and most often an incidental finding on a surgical specimen from an appendectomy for acute appendicitis[1]. The 5-year survival rate of appendiceal cancer is 57.0%-64.0%; the prognosis is slightly worse than the prognosis for colon and rectal cancers[3]. The prognosis for primary appendiceal cancer mainly reflects the lack of specific clinical symptoms and early diagnostic methods. Indeed, primary appendiceal cancer is not easy to diagnose in the early stage or even preoperatively, and the symptoms are similar to acute appendicitis. The clinical manifestations of appendicitis account for 37.2% of patients with appendiceal cancer, and 23% of patients with appendiceal cancer are diagnosed after surgery[4]. Second, due to the anatomic characteristics of the appendix, the local muscular layer and submucosa are thin and rich in lymphatic tissue, which may lead to early lymph node metastases[5]. Appendiceal cancer can be classified into four subtypes: Colonic-type adenocarcinoma; mucinous neoplasms; goblet cell carcinoma (GCC); and neuroendocrine neoplasm[1]. GCC occurs almost exclusively in the appendix and is characterized by epithelial (adenocarcinoma) and neuroendocrine components containing goblet cells. GCC produces neuroendocrine markers and mucin. GCC is often asymptomatic and is often an incidental finding during the routine management of acute appendicitis. The clinical presentation is variable and can be an acute right fossa iliac syndrome or a more chronic abdominal pain syndrome with a palpable pelvic mass[6]. In the present case, repeated ileus was the main manifestation, which has not been reported previously.

Endoscopy is not expected to be sufficient for detection of early appendiceal cancer. It has been reported that there is a low detection rate of 11% for appendiceal abnormalities and 19% for cecal abnormalities in patients with appendiceal cancer[7]. CT findings of appendiceal cancer include appendiceal enlargement ≥ 15 mm, wall thickening, a soft tissue mass, and peri-appendiceal fat[8]. When a possibly submucosal invasive tumor is noted in the cecum, it is important to carefully observe around the appendix orifice. In the present case, multiple ulcers were observed in the terminal ileum during endoscopy. A neoplastic lesion was considered based on CT findings. The endoscopic findings were consistent with the CT findings, so we initially suspected a terminal ileal tumor. A retrospective review of the endoscopic and CT images showed swelling around the appendiceal foramen (Figure 1A and C); however, careful inspection of the appendiceal orifice was not performed. Some endoscopists do not pay attention to the appendiceal orifice drawing, which should be noted in future work.

AIE is one of the most common causes of non-infectious encephalitis. Suggested mechanisms that may trigger AIE include tumors (paraneoplastic), infections (parainfectious), or cryptogenic infections [8], which predominantly affects children and young females. Studies have shown that tumor-induced AIE is likely due to the production of antibodies against INAab, which are probably not directly pathogenic, but an epiphenomenon of a T-cell-mediated immune response[9]. The tumors that induce AIE which have been reported in the literature include thymomas, ovarian teratomas, lung cancer, and breast cancer; however, AIE induced by appendiceal cancer has not been reported. Experts agree that if relevant tumors are found, tumor treatment (chemotherapy or tumor resection) is essential, and all patients with AIE should be screened for tumors at the time of disease onset[9]. This patient subsequently discontinued chemotherapy; it is possible that chemotherapy can prolong survival. Unlike cases, the patient described herein developed AIE after radical tumor resection. The underlying mechanism is unclear, perhaps because the tumor was removed, while some cytokines were released into the blood during the process, thus inducing an immune chain effect. This possible explanation warrants further analysis with a large-scale corollary study. We report this case in the hope of giving some guidance to clinicians with similar challenging cases.

CONCLUSION

Albeit rare, the occurrence of neurologic and psychiatric symptoms in patients with an appendiceal cancer postoperatively suggests the possibility of AIE. The underlying mechanism of AIE in this patient after radical tumor resection is unclear, and that's what we need to figure out in the future.

FOOTNOTES

Author contributions: Mao YH followed-up the patient and wrote the paper; Li L participated in the treatment and management of patient; Wang FR, Zhao YZ and Wang L collected the data; Qin JM and Yang YL helped to correct the article; Wen LM conceptualized the idea and finalized the manuscript; All authors have read and approve the final manuscript.

Informed consent statement: Since the patient is deceased, informed written consent was obtained from the relatives of patient for publication of this report and any accompanying images.

Conflict-of-interest statement: All the authors report no relevant conflicts of interest for this article.

CARE Checklist (2016) statement: The authors have read the CARE Checklist (2016), and the manuscript was prepared and revised according to the CARE Checklist (2016).

Country/Territory of origin: China

ORCID number: Yan-Hui Mao 0000-0003-0133-8516; Lu Li 0009-0004-9709-4337; Li-Ming Wen 0000-0003-3857-2138; Jia-Min Qin 0000-0002-3692-6353; Ya-Ling Yang 0000-0001-9298-7452; Li Wang 0000-0001-7627-5973; Fan-Rong Wang 0009-0001-8304-189X; Yi-Zhou Zhao 0009-0005-2051-066X.

Corresponding Author's Membership in Professional Societies: Chinese Society of Gastroenterology.

S-Editor: Fan JR
L-Editor: A
P-Editor: Fan JR

REFERENCES

1 **Van de Moortele M**, De Hertogh G, Sagaert X, Van Cutsem E. Appendiceal cancer : a review of the literature. *Acta Gastroenterol Belg* 2020; **83**: 441-448 [PMID: 33094592 DOI: 10.5840/augustinus19762183/8420]
2 **Dutra LA**, Abrantes F, Toso FF, Pedroso JL, Barsottini OGP, Hoftberger R. Autoimmune encephalitis: a review of diagnosis and treatment. *Arq Neuropsiquiatr* 2018; **76**: 41-49 [PMID: 29364393 DOI: 10.1590/0004-282X20170176]
3 **Ko YH**, Park SH, Jung CK, Won HS, Hong SH, Park JC, Roh SY, Woo IS, Kang JH, Hong YS, Byun JH. Clinical

characteristics and prognostic factors for primary appendiceal carcinoma. *Asia Pac J Clin Oncol* 2010; **6**: 19-27 [PMID: 20398034 DOI: 10.1111/j.1743-7563.2010.01276.x]

4 **Benedix F**, Reimer A, Gastinger I, Mroczkowski P, Lippert H, Kube R; Study Group Colon/Rectum Carcinoma Primary Tumor. Primary appendiceal carcinoma--epidemiology, surgery and survival: results of a German multi-center study. *Eur J Surg Oncol* 2010; **36**: 763-771 [PMID: 20561765 DOI: 10.1016/j.ejso.2010.05.025]

5 **Katayama R**, Aoki T, Tomioka K, Tashiro Y, Fujimasa K, Ono K, Kitajima T, Yoshizawa S, Ozawa Y, Matsuda K, Kusano T, Koizumi T, Watanabe M, Murakami M. A rare case of synchronous appendiceal and cecal cancer. *Clin J Gastroenterol* 2021; **14**: 1443-1447 [PMID: 34264499 DOI: 10.1007/s12328-021-01479-3]

6 **Vincenti L**, Andriola V, Cazzato G, Colagrande A, Fiore F. Goblet Cell Carcinoma of the Appendix with Synchronous Adenocarcinoma of the Cecum: Distinct or Related Entities? *Diseases* 2022; **10** [PMID: 36278575 DOI: 10.3390/diseases10040077]

7 **Trivedi AN**, Levine EA, Mishra G. Adenocarcinoma of the appendix is rarely detected by colonoscopy. *J Gastrointest Surg* 2009; **13**: 668-675 [PMID: 19089515 DOI: 10.1007/s11605-008-0774-6]

8 **Chiou YY**, Pitman MB, Hahn PF, Kim YH, Rhea JT, Mueller PR. Rare benign and malignant appendiceal lesions: spectrum of computed tomography findings with pathologic correlation. *J Comput Assist Tomogr* 2003; **27**: 297-306 [PMID: 12794590 DOI: 10.1097/00004728-200305000-00001]

9 **van Coevorden-Hameete MH**, de Graaff E, Titulaer MJ, Hoogenraad CC, Sillevis Smitt PA. Molecular and cellular mechanisms underlying anti-neuronal antibody mediated disorders of the central nervous system. *Autoimmun Rev* 2014; **13**: 299-312 [PMID: 24225076 DOI: 10.1016/j.autrev.2013.10.016]

Published by **Baishideng Publishing Group Inc**
7041 Koll Center Parkway, Suite 160, Pleasanton, CA 94566, USA
Telephone: +1-925-3991568
E-mail: bpgoffice@wjgnet.com
Help Desk: https://www.f6publishing.com/helpdesk
https://www.wjgnet.com